University of Pretoria

QHW Shaw

PhD Thesis:

A New Understanding of the Early Behaviour of Roller Compacted Concrete in Large Dams

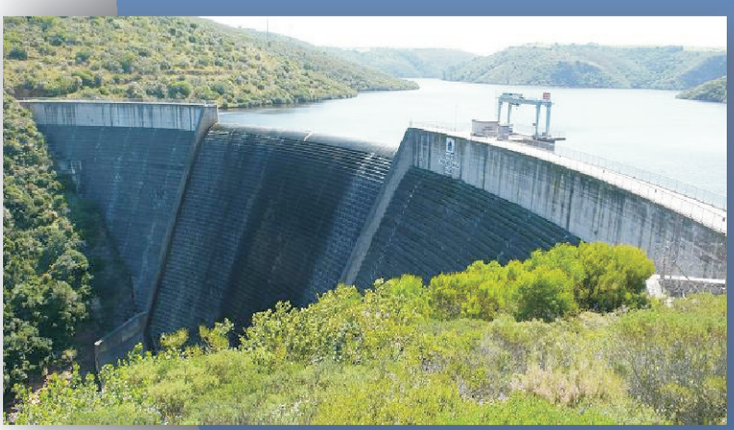

University of Pretoria

A NEW UNDERSTANDING OF THE EARLY BEHAVIOUR OF ROLLER COMPACTED CONCRETE IN LARGE DAMS

by

QUENTIN HENRY WENHAM SHAW

Submitted in partial fulfilment of the requirements for the degree of Philosophiae Doctor (Civil Engineering) in the Faculty of Engineering, Built Environment and Information Technology, University of Pretoria, Pretoria.

Supervisor: Professor BWJ van Rensburg

Co-supervisor: Professor RJ du Preez

Department: Faculty of Engineering, Built Environment and Information Technology.

University: University of Pretoria, Pretoria.

Submitted: **10th August 2010**

University of Pretoria

Title: ***A New Understanding of the Early Behaviour of Roller Compacted Concrete in Large Dams***

by Quentin Henry Wenham Shaw

Supervisor: Professor BWJ van Rensburg

Co-supervisor: Professor RJ du Preez

Department: Faculty of Engineering, Built Environment and Information Technology.

University: University of Pretoria, Pretoria.

Degree: Philosophiae Doctor (Civil Engineering).

Date: 10th August 2010.

Key Terms: Roller compacted concrete (RCC), early behaviour, hydration cycle, thermal effects, autogenous shrinkage, drying shrinkage, stress relaxation creep, dams, arch dams, finite element analysis, instrumentation.

Summary

In respect of autogenous and drying shrinkage and the effects of relaxation creep during the hydration cycle, roller compacted concrete in dams has to date been universally assumed to behave in the same manner as conventional mass concrete,

despite notional evidence to the contrary on prototype dam structures, particularly in respect of high-paste RCC.

While the results of laboratory materials testing and associated early behaviour analyses for RCC have been published, no conclusive example exists in the public domain whereby predicted behaviour is confirmed through measured behaviour on a comprehensively-instrumented prototype dam structure.

In his PhD thesis, Quentin Shaw presents evidence to indicate that the early behaviour of RCC, and particularly high quality, high-paste RCC in dams, is quite different to that of CVC. Referring to instrumentation records from Wolwedans and Knellpoort dams in South Africa, Çine Dam in Turkey, Wadi Dayqah Dam in Oman and Changuinola 1 Dam in Panama, indications of less than expected shrinkage and stress relaxation creep during the hydration cycle in the constituent RCC are documented.

Taking the comprehensively-instrumented and monitored Wolwedans Dam, the actual materials behaviour of the constituent RCC is evaluated through the replication of the prototype behaviour on a finite element model. Through this analysis, it is clearly demonstrated that the level of shrinkage and stress relaxation creep that would be traditionally assumed in RCC simply did not occur. In fact, the analyses suggested that no shrinkage, or creep was apparent.

The reasons for the different behaviour of high-paste RCC compared to CVC are subsequently explored. With Wadi Dayqah Dam as the only example evaluated where some drying shrinkage and/or stress relaxation creep was obviously apparent, the evident susceptibility of this lean RCC mix, with a high w/c ratio, a high content of non-cementitious fines, natural gravel aggregates, a high aggregate water absorption and placement in a very dry environment, is noted. However, it is considered to be the combination of a strong aggregate skeletal structure developed through roller compaction and a low w/c ratio that results in a particularly resilience in high-paste RCC to early shrinkage and creep. It is also recognised that temperature and gravity effects in an arch dam structure will tend to limit, or even eliminate containment stresses in the critical load-carrying upper section and that this will reduce the risk and impact of stress relaxation creep.

Consequently, a new understanding of the early behaviour of RCC in large dams is presented, suggesting that a high quality RCC mix in an arch dam can be designed for a cumulative shrinkage and stress relaxation creep under the hydration cycle of

approximately 20 microstrain, compared with a more traditionally accepted value of between 125 and 200 microstrain.

The implications of these findings on the design of large RCC dams are demonstrated to be significant, particularly in respect of RCC arch dams. In addition, suggestions are made for the requirements in respect of RCC mix design for negligible shrinkage and creep, while an approach to combine the use of field measurement with structural modelling to predict and demonstrate actual RCC behaviour is briefly discussed.

TABLE OF CONTENTS

Page No.:

Page No.:

CHAPTER 2:

RCC CONSTRUCTION, RCC INSTRUMENTATION, RCC DAMS STUDIED & RCC MIXES

Page No.:

CHAPTER 3:

LITERATURE AND REFERENCE: THE TRADITIONAL APPROACH TO DAM DESIGN IN RESPECT OF EARLY CONCRETE BEHAVIOUR AND TEMPERATURE LOADS AND THE ASSOCIATED APPLICATION FOR RCC DAMS

Page No.:

Page No.:

Page No.:

Page No.:

Page No.:

Page No.:

Page No.:

LIST OF ABBREVIATIONS AND ACRONYMS

CBD	Compacted Bulk Density
CVC	Conventional Vibrated Concrete (Mass Concrete compacted with an immersion vibrator)
COSMOS	COSMOS Finite Element Analysis Computer Software
E	Elastic (or deformation) Modulus
FE	Finite Element
FSL	Full Supply Level
H	Height (m)
High-Paste RCC	RCC Containing > 150 kg/m^3 cementitious materials
ICOLD	International Commission on Large Dams
LBSGTM	Long-Base-Strain-Gauge-Temperature-Meter
Lean RCC	RCC Containing < 100 kg/m^3 cementitious materials
mASL	m Above Mean Sea Level
NOC	Non Overspill Crest
RCC	Roller Compacted Concrete
RL	Reduced Level (m)
RMC	Rubble Masonry Concrete
SANCOLD	South African National Committee on Large Dams
Temperatures:	
T1	Concrete Placement (^{o}C)
T2	Maximum Hydration Temperature (^{o}C)
T3	Natural Closure, or Zero Stress Temperature (^{o}C)
T4	Minimum long-term Equilibrium Temperature (^{o}C)
USACE	United States Army Corps of Engineers
USBR	United States Department of the Interior. Bureau of Reclamation
Ø	Angle of internal friction

Stress Sign Convention:

-ve = Compression

+ve = Tension

TERMINOLOGY:

Axis

The "Axis" of a dam is taken as a line parallel to the upstream face. Induced Joints in an RCC dam are inserted on an alignment perpendicular to the axis.

Conventional Analysis Techniques

"Conventional Analysis Techniques" refers to the design approach generally accepted as state of the art practice and adopted by dam engineers worldwide.

Creep

According to Fulton's *Concrete Technology* (9th Edition). 2009[1], "Creep is defined as the time-dependent increase in strain of a solid body under constant stress. Creep may also be manifested as a relaxation of stress under constant strain." In respect of the behaviour of RCC under early heat development and dissipation, it is the latter "relaxation" form of Creep to which the text of this work refers.

Early Behaviour

"Early Behaviour" is taken to mean the shrinkage/creep behaviour that occurs after placement and before the hydration heat is fully dissipated and gives rise to an effective volume reduction in the RCC. In a dam, the hydration heat can take several years to fully dissipate and consequently an evaluation of the impact of the "Early Behaviour" is often only possible on a prototype dam after a substantial delay, but the significant part of this behaviour undoubtedly occurs during the first month, or two after placement, before the concrete has gained significant strength.

Materials Model

In this Thesis, the term "materials model" is taken as the definition of expected materials properties and behaviour for RCC as a construction material.

"New" RCC materials model is an abbreviation occasionally applied for the New Understanding of the Early Behaviour of RCC.

"Traditional RCC Materials Model" describes the assumed behaviour for RCC generally accepted for RCC to date by designers.

Zones: Surface (External) & Core

Figure 7.1 of the USBR's *Design of Arch Dams.* 1977[2] indicates that seasonal temperature variations experienced in a mass concrete (CVC) block will be reduced to 10% at a depth of 2.4 m and 1% at a depth of 24 m, compared to the variations experienced on the surface. For the purposes of this Thesis, the terms "surface", or "external" zone is accordingly used to describe the concrete within approximately 2 to 3 m of the external/exposed surface. The "core" zone consequently refers to all concrete at greater depth than the "surface" zone. Occasionally, reference is made to an "intermediate" zone and this is defined as the concrete between 2.5 and 5 m from the external surface.

CHAPTER 1

1. BACKGROUND, INTRODUCTION, METHODOLOGY & OBJECTIVES

1.1. INTRODUCTION

In this Chapter, the author discusses the background and motivation for the work addressed in this PhD thesis. In addition, the approach to the investigations and analysis and the structure of the thesis document are outlined.

The title of the work presented is "A New Understanding of the Early Behaviour of Roller Compacted Concrete in Large Dams" and the behaviour in question is the effective volume reduction that occurs as a consequence of shrinkage and creep during the period that the concrete temperature is elevated by hydration heat. While the impact of this volume change may only become evident once the hydration heat has dissipated, which can take several years in the case of a large dam, the majority of the associated shrinkage and creep will probably occur within the first month, or two of placement.

1.2. BACKGROUND & MOTIVATION

1.2.1. BACKGROUND

Much has been published addressing the design and the thermal analysis of RCC dams, but no work has been published in the public domain to date to quantitatively compare the predicted early behaviour of RCC with the actual performance on a prototype structure. The scale and cost of any verification work of this nature are obvious and it must always be borne in mind that it is very difficult to motivate expenditure on the investigation of something that is in fact functioning quite satisfactorily and quite possibly even better than anticipated. Furthermore, the period over which performance data must be collected on a large prototype structure, with a hydration heat dissipation period of many years, or even decades, significantly complicates the achievement of a conclusive investigation.

As will be discussed in Chapter 3, the "Traditional" materials model and the "Conventional" analysis techniques generally applied to date have assumed that RCC behaves in the same manner as conventional mass concrete (CVC) during the hydration heating and cooling cycle, with consequential shrinkage and creep resulting in a net reduction in volume compared to placement typically in the range of 125 to 200 microstrain. In the case of a gravity dam, applying these assumptions is conservative, consequently adding an unquantified factor of safety into the design

process. In respect of an arch dam, however, adopting such an approach may not necessarily be conservative (*see Chapter 7*), while it may also unnecessarily compromise the technical feasibility of such dam types. With only a small proportion of the world's RCC dams constructed to date being arch, or arch/gravity dam types, this issue has not been of particular significance in the past.

Furthermore, the construction of very high RCC dams (> 150 m) is something of a recent development and accordingly, a conservative approach of favouring gravity-type dams on this scale has so far generally been applied. It must of course be borne in mind that most of these large RCC structures remain decades away from reaching a condition of thermal equilibrium. However, with very high quality concrete now being generally produced by roller compaction, arch-type RCC dams are seen, with increasing frequency, to be the favoured solution at numerous sites and consequently the need for a more precise knowledge of the early behaviour of RCC is becoming critical.

1.2.2. MOTIVATION

The experience of the author has repeatedly suggested that high-paste RCC does not suffer to the same extent as CVC from early shrinkage and creep effects during the hydration cycle. Without quantitative investigation and analysis, however, these subjective observations are of no material value and the consequential need for a detailed investigation was obvious.

Experience in South Africa[3 & 4] and China[5] has demonstrated that the construction of arch dams in RCC is both possible and economically advantageous. For a topographically and geotechnically suitable site, where simplicity and access allow efficient construction, an RCC arch dam type will represent a highly efficient solution. With the production of high quality concrete through roller compaction now widely acknowledged, the application of RCC in arch dams is accordingly likely to become more prevalent.

Many issues related to the construction of arch dams in RCC have been resolved through construction experience and development. Adequate inter-layer bond can be achieved with the correct RCC mix, placement approach and layer surface treatment, while the inducing and directing of joints can now consistently be achieved with confidence. Although the realities of installing effective systems for induced joint grouting are not generally acknowledged, or understood, appropriate solutions have been developed and these will undoubtedly continue to undergo ongoing improvement through future application.

In order to ensure that arch dams can be confidently and efficiently designed and constructed in RCC, however, certain inter-related issues of particular importance must be given specific attention. These can be summarized as follows:

- The early behaviour of RCC under thermal loads.
- The management of hydration heat and joint grouting.
- The ongoing development of efficient induced joint grouting systems.

To facilitate the effective design of hydration heat management and induced joint grouting, it is of fundamental importance that the early behaviour of particularly high-paste RCC, in respect of shrinkage and creep, be better understood.

For a dam designer, the findings presented subsequently in this thesis are of very significant impact. It is not realistically possible to design an RCC arch dam for a shrinkage strain from placement of 200 microstrain. Such a dam would have to cool and be grouted before loading, as is the case for a conventional concrete dam. Otherwise, the stresses would be so high as to be at a level of potential failure. In the case of an RCC arch, the requirement for post-cooling and/or the necessity to delay loading would give rise to the loss of many of the benefits otherwise associated with RCC construction, particularly in the case of a large dam.

If the net shrinkage strain is limited to approximately 50 microstrain, however, it is quite possible to design a dam that can be loaded before it cools. In the case of large gravity dams, the findings imply a reduced sensitivity to cracking parallel to the dam axis and/or a reduced requirement for RCC pre-cooling and restrictive placement temperature specifications.

The foregoing implies that this work makes a very meaningful contribution to the state of the art of RCC dam engineering and will result in real cost savings on large dam construction. With a proven ability to design RCC mixes for significantly reduced shrinkage and creep during the hydration cycle, a complete change in approach and mix testing requirements for the design of RCC arch dams will result.

1.3. RESEARCH OBJECTIVES

1.3.1. THESIS OBJECTIVES

The purpose of this study is to demonstrate that high-paste RCC in large dams does not necessarily behave in the same manner as CVC, or need not behave in the same manner if appropriately designed, under the early hydration heating and cooling cycle. On the basis of observation, interpreted and evaluated by modelling, the investigation provides evidence of the actual manner in which the behaviour of RCC differs from the assumptions traditionally applied for dam design and attempts to establish the associated reasons behind these differences.

1.3.2. KEY RESEARCH QUESTIONS

The traditional “early behaviour model” for RCC dam design assumes the same materials properties and behaviour characteristics as conventional mass concrete in respect of shrinkage and creep. The associated design approach equates the consequential reduction in volume from placement to a thermal shrinkage, approximately equivalent to the adiabatic hydration temperature rise, or typically 125 to 200 microstrain. Recorded behaviour from several dams suggests that this approach is not appropriate and significantly overstates the total “shrinkage” experienced in high-paste RCC. The key research question addressed in this work can

accordingly be stated as; "Is the traditional design approach that accounts for early shrinkage and creep in concrete dams valid in the case of high-paste RCC dams?"

1.3.3. RESEARCH APPROACH AND FOCUS

The above objectives should be seen in the light of certain realities related to the scale and nature of a dam that will frustrate the absolute accuracy of the comparative analyses. For example, as a consequence of the indeterminate degree of restraint and the variability of the elastic and inelastic properties of concrete and the materials of a foundation rockmass, an evaluation of the stresses induced in mass concrete structures by temperature changes can be considered an estimation at best[2]. Consequently, a parametric approach is required in a process of homing in on the set of behaviour characteristics for the RCC in question that most closely represents its actual performance within the prototype dam.

The study uses measured data from prototype structures to evaluate and quantify the observed early behaviour of high-paste RCC in large dams. By simulating the measured performance of a prototype structure through FE modelling, the study seeks to develop a meaningful picture of the actual behaviour of the constituent RCC, on the scale applicable within a large dam, during the process of hydration and subsequent cooling.

While thermal analyses for RCC dams have generally applied a high level of assumption in respect of the shrinkage and creep performance characteristics of the material, the work addressed in this study stands apart in presenting a meaningful comparison of assumed behaviour and actual measured performance.

1.3.4. VALUE OF RESEARCH FINDINGS

In comparing the actual structural behaviour of a high quality, high-paste RCC mix, in the context of a prototype dam, with a number of possible behaviour models, a new, and quite different picture of the early behaviour of RCC in large dams emerges. The introduction of this new understanding of the materials behaviour of high quality RCC will add another dimension into the design of large RCC dams and most particularly RCC arch-type dams.

1.4. SCOPE OF STUDY

The investigation presented herein evaluates the instrumentation data for four large prototype RCC dams and discusses preliminary construction instrumentation data from a fifth dam. On the basis of the observations made through measurement, the study goes on to review the associated behaviour of the RCC in each dam. To enable a quantitative evaluation of the behaviour of RCC, FE models are subsequently developed and analysed in an effort to reproduce, as accurately as possible, measured behaviour on a prototype structure.

Combining the temperature, strain and deformation data available for Wolwedans Dam over a period of over 15 years with the fact that the structure functions three-

dimensionally provided a unique opportunity to quantitatively investigate the early behaviour of the constituent RCC, specifically in respect of the total apparent volume reduction assumed to be associated with autogenous shrinkage and creep.

Having demonstrated the assumptions in respect of autogenous shrinkage and creep traditionally applied for RCC dam design to be exaggerated in the case of a high-paste RCC, the associated reasons are explored.

A new understanding for the early behaviour of high-paste RCC is consequently proposed and the implications of this materials model on the future design of both gravity and arch-type RCC structures are discussed.

Due to the fact that the hydration heat will take several decades to be fully dissipated from a very large dam, the availability of data in respect of the performance of RCC under long-term temperature load in large dams is limited. Wolwedans and Knellpoort Dams in South Africa have been in operation for almost 2 decades and, as a result of their relatively modest size, all of the hydration heat has long since been dissipated, allowing analysis of the long-term thermal effects. In the case of Çine Dam in Turkey, its large size implies that very little of the hydration heat has yet been lost, while Wadi Dayqah Dam in Oman was only very recently completed. As a consequence, it is not yet possible to review the performance of the latter two dams during the heat dissipation cycle phase.

Due to the fact that only strain, and not stress, can realistically be measured in RCC, it is very difficult to establish when creep is occurring under stress. Furthermore, dam instruments do not always function particularly predictably; one gauge might indicate one reading in a particular location, while another might indicate something quite different, despite the fact that conditions are similar.

There are also many factors of influence to assimilate when reviewing dam instrumentation data. Poorly installed, or located instruments and incomplete data will often result in the emergence of a complex picture, which requires detailed consideration in order to identify meaningful trends. Dams are complex, three-dimensional structures constructed on rockmasses with divergent and variable properties and the evaluation of instrument measurements can often involve resolving conflicting data and the development of explanations for identified anomalies.

1.5. LITERATURE & PUBLICATIONS IN DAM ENGINEERING

1.5.1. GENERAL

Dam engineering is unlike other forms of engineering in that many decisions on important aspects are left to the judgement of the dam engineer. For this reason, many countries require that the experience and competence of practitioners be reviewed before they may be approved for work on dams of a certain size and importance. In South Africa, before an engineer may take responsibility for a certain task of work on a particular dam, his experience and qualifications for that task must

be reviewed by a sub-committee of the Engineering Council and a recommendation made to the Minister of Water Affairs, in terms of Government notice R.1560 of 1986.

Furthermore, the state of the art of technology in dam engineering is maintained by ICOLD, the International Committee on Large Dams, and its national member committees, such as SANCOLD. The triennial Congress on Large Dams is recognised as the forum at which new developments in dam engineering are discussed and endorsed and the volumes of papers published at that forum are regarded as validated technology. Through its sub-committees and national committees, ICOLD also publishes bulletins on specific aspects of dam engineering. These, again, are considered to present the accepted state of the art in relation to any particular technology. The last bulletin on RCC, Bulletin 126, was published in 2003.

In view of the fact that RCC dam technology remains in the process of development, the Chinese and Spanish national committees of ICOLD organise a four-yearly Symposium at which the latest developments and trends in the technology are presented and discussed. Again, this forum is considered to record the state of the art in RCC dam technology. An early paper by the author on the subject of this thesis was considered of such importance that it was selected for presentation as one of the Keynote lectures for the RCC Symposium of November 2007, while Wolwedans Dam was recognised as one of the ten RCC milestone dams on the same occasion.

For a number of years, the United States Army Corps of Engineers (USACE) has published engineering manuals and technical letters on all manner of issues in engineering and their publications on dam engineering are recognised as the leading guidelines in respect of the design and analysis of dams. While regular peer review throughout the duration of a project, in the form of an external panel of experts, has become a matter of course in respect of large dams, probably the most used form of reference in such reviews would be the USACE publications.

Specialist journals that routinely cover dam engineering topics are realistically limited to the following publications:

- The International Journal of Hydropower & Dams. Aqua-Media International Ltd. (Wallington, UK);
- International Water Power & dam Construction. Progressive Media Markets Ltd (Sidcup, UK);
- Hydroworld - HRW. HCI Publications. (Kansas, USA).
- Dam Engineering. British Institution of Civil Engineers. (London, UK).

1.5.2. AVAILABLE REFERENCES

As a consequence of the above, the available references with specific relevance to the investigations addressed in this study are generally guidelines issued by the USACE and papers published at ICOLD congresses and the RCC Symposia. Furthermore, as a consequence of the nature of the work addressed, the period over which data needs to be recovered from a prototype structure, the complications of scale in respect of testing, the specialist nature of the problem in question, the stage of development of RCC technology and the developing relevance of the subject in question, very little work of a similar nature exists for reference and comparison. A review and evaluation of the available literature relating to the investigations in question is presented in Chapter 3 of this Thesis.

1.6. INVESTIGATION METHODOLOGIES

1.6.1. GENERAL

The investigations presented in this study are the work of a practising RCC dam engineer, with extensive experience in the design and construction of RCC dams and the use of Finite Element structural analysis techniques. The investigations start from the point of macro-scale observation, move through an analytical process of comparing and analysing modelled and prototype performance by Finite Element analysis and finally hypothesise and motivate the cause of the apparent behavioural differences of high paste RCC and CVC.

With data from four prototype RCC dams being analysed and evaluated, the apparent behaviour is repeatedly compared with what might have been anticipated on the basis of conventionally assumed behaviour. When induced joints do not open to the extent predicted, however, the installed instrumentation is generally not adequate to allow the cause of such behaviour to be isolated with certainty. The level of residual stress across un-opened induced joints and between the induced joints, for example, cannot be known, while the impact of the foundation restraint and various other factors cannot be definitively ascertained.

1.6.2. MODELLING & ANALYSIS

Simulating measured induced joint openings and crest displacements on a three-dimensional structure through FE modelling allows as real a picture of actual prototype performance and constituent materials behaviour as is ever likely to be possible on a structure with as many factors of influence as a large dam. Applying RCC behaviour characteristics that do not correspond with reality will quickly be demonstrated to cause the modelled structure to behave significantly differently to the

prototype. Isolating the actual materials behaviour, it should be possible to simulate the prototype performance with a reasonable level of accuracy.

Essentially two specific performance characteristics of the prototype structure are used for comparison with the FE model; the joint opening at approximately mid-dam height and the crest displacements. The relative simplicity of the model and the applied materials properties with which it was possible to demonstrate that the traditional assumptions in respect of RCC behaviour are flawed is considered as important as the nature of the materials behaviour model itself.

The COSMOS FE analysis software was used for all structural and thermal modelling, with ten-noded solid tetrahedral elements in a high-density mesh. The model simulated the dam and a large section of the foundation, with each radial dam block between induced joints being developed as a separate part, joined to the adjacent blocks with Gap elements, which simply associated adjacent nodes with a friction factor when in contact. For analyses in which induced joints were not allowed to open, replicating the fact that these joints had not opened on the prototype, the Gap elements were simply omitted.

To simulate the effective reduction in concrete volume caused by a range of autogenous shrinkages and creep, which may have occurred during the hydration cycle, equivalent temperature drop loads were applied to the dam structure, using a linear thermal shrinkage/expansion coefficient. Initially, it was foreseen that it would be necessary to apply complex, non-linear materials properties for the dam structure, but the initial analyses, which used elastic properties for both the dam concrete and the foundation, proved quite adequate to accurately reproduce the actual performance measured on the prototype and consequently, all analyses were completed using linear-elastic materials properties.

1.6.3. NEW MODEL APPLICATION

In order to illustrate the impact and importance of the new materials understanding for the early behaviour of high paste RCC, various aspects of the design of the 105 m Changuinola 1 RCC arch/gravity Dam are presented by way of an example. Using the COSMOS FE software, a comparison is made of an appropriate joint spacing design on the basis of the traditional RCC behaviour assumptions and the proposed new understanding. Similarly, the significant impact of the new understanding on the arch design of the same dam is discussed and illustrated.

1.7. RCC DAMS & THE NEED FOR RESEARCH

1.7.1. GENERAL

Over the past two decades the construction of concrete dams by roller compaction has advanced significantly and it is now possible to produce a broad range of concrete qualities by roller compaction. While lower strength, lower deformation modulus and higher permeability RCC is applied for smaller gravity dams (< 100 kg/m^3 cementitious materials), generally in conjunction with an impermeable, upstream face PVC membrane, the preferred approach for most RCC dam construction now applies higher cementitious materials contents (> 150 kg/m^3 cementitious materials) to produce dense, impermeable, high strength mass concrete, as demonstrated by the continuous, bonded concrete cores routinely extracted during quality control testing.

Plate 1.1: Çine RCC

Roller Compacted Concrete (RCC) was first used in dam construction in South Africa in 1984 and at the time, the country was recognized as one of the pioneers of the technology. After the completion of just two significant gravity dams, South Africa's Department of Water Affairs felt sufficiently confident to apply RCC for the construction of arch dams and the design of the 70 m high Wolwedans and the 50 m high Knellpoort dams was initiated. Although Knellpoort is recorded as the first RCC arch/gravity dam in the world, arch action is only incurred during unusual and extreme loading. In the case of Wolwedans Dam, however, arching is initiated once the impounded water exceeds approximately 70% of full capacity.

1.7.2. RCC ARCH DAMS & EARLY RCC BEHAVIOUR

To date, the accommodation of early temperature loads in RCC dams has effectively been limited to the inclusion of induced transverse joints, while the approach to design has generally assumed that RCC behaves in a similar manner to conventional mass concrete (CVC) under hydration temperature rise and post-hydration cooling[6].

Although the above approach has been quite adequate for RCC gravity dam structures, the situation in respect of dams that rely on three-dimensional arching for stability is quite different.

In CVC arch dams, construction in vertical monolithic blocks with groutable joints in between (see **Plate 1.2**) and the inclusion of cooling pipes to remove hydration heat and cool the concrete to a suitable temperature for joint grouting together facilitate the management of the otherwise structurally problematic temperature impacts. Grouting the joints at a suitably depressed temperature consequently effectively eliminates significant temperature drop shrinkage as a loading condition. This approach essentially accommodates all of the volume reduction in the concrete that is

experienced after placement, i.e. autogenous shrinkage, drying shrinkage, stress relaxation creep and thermal shrinkage.

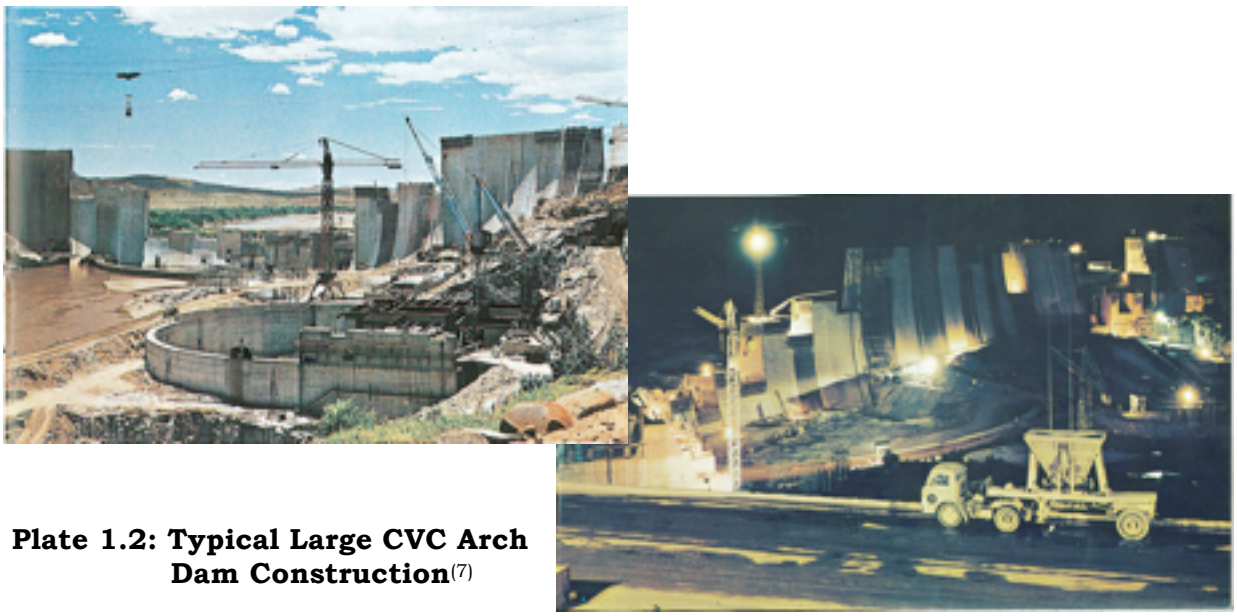

Plate 1.2: Typical Large CVC Arch Dam Construction(7)

In the case of RCC, however, vertical joints must be induced, while the installation of an extensive network of embedded cooling pipes is realistically impractical. Consequently, long-term shrinkage becomes an issue of greater significance in the case of an RCC arch dam and a comprehensive understanding of the behaviour of RCC under applicable early thermal loading takes on a particular importance.

1.7.3. THE NEED FOR RESEARCH

In view of the relatively untested status of RCC technology at the time at which construction at Wolwedans Dam was initiated, it was considered appropriate to install a very comprehensive system of monitoring instrumentation, as described in Chapter 2.

During the course of ongoing monitoring of the installed instrumentation at Wolwedans Dam, a picture started to emerge that demonstrated lower levels of displacement and smaller induced joint openings than had been anticipated in the dam design. In view of the fact that these observations suggested better than expected performance, however, no specific efforts were made to investigate the causative RCC behaviour.

Evaluating the possible origins of this anomalous behaviour, it appeared that significantly less creep than typically occurs in large-scale mass concrete (CVC) during the process of hydration heat development and dissipation might in fact have occurred in the RCC at Wolwedans. This would contradict conventional wisdom, which assumes that RCC behaves in a similar manner to CVC in respect of early shrinkage and creep. Undertaking a quantitative evaluation of this hypothesis, however, was not a straightforward matter, particularly as a consequence of the fact that the dam structure was under load before the effects of the hydration heat had been fully

dissipated, the fact that it is not realistically possible to measure stress within RCC and the fact that the three dimensional structural action caused it to be impossible to isolate temperature-specific joint openings.

With instrumentation in later RCC dams suggesting similar patterns of behaviour, it has been the author's long held ambition to undertake an appropriate programme of research, modelling and analysis, with the objective of investigating more thoroughly the actual shrinkage and creep behaviour of high quality RCC under early hydration temperature development and dissipation.

1.8. ORGANISATION OF THE REPORT

CHAPTER 1: INTRODUCTION

Chapter 1 describes the background, motivation and objectives of the investigations undertaken. The approach, scope and structure of the work presented are also discussed.

CHAPTER 2: RCC DAMS INSTRUMENTED, RCC CONSTRUCTION ISSUES AND APPLIED INSTRUMENTATION

In Chapter 2, the dams that form the basis of this thesis are introduced and a brief description of the respective instrumentation installed is provided. In addition, RCC dam construction is described, with particular reference to the methods applied to induce joints and how these influence deformation and strain measurement. The instruments installed to measure strain and joint opening are described and comments are made on respective reliability and accuracy.

CHAPTER 3: LITERATURE AND REFERENCE: THE TRADITIONAL APPROACH TO DAM DESIGN IN RESPECT OF EARLY CONCRETE BEHAVIOUR AND TEMPERATURE LOADS AND THE ASSOCIATED APPLICATION FOR RCC DAMS

In Chapter 3, the state of the art in respect of the early behaviour of concrete in dams is explored through reference, with particular attention to shrinkage and creep and the methods applied to address these issues in dam design. The associated design approach generally applied for RCC is discussed and the compositional differences between RCC and CVC in dams are explored.

CHAPTER 4: STUDYING THE INSTRUMENTATION DATA FOR WOLWEDANS, KNELLPOORT, ÇINE, WADI DAYQAH & CHANGUINOLA 1 DAMS

In Chapter 4, the author presents instrumentation data from the Wolwedans and Knellpoort Dams in South Africa, Çine Dam in Turkey, Wadi Dayqah Dam in Oman and Changuinola 1 Dam in Panama. The indicated performance and behaviour are reviewed and discussed and indications that suggest a possible different behaviour pattern for RCC compared to CVC under hydration heat development and subsequent cooling are highlighted.

CHAPTER 5: SIMULATING PROTOTYPE MATERIALS BEHAVIOUR THROUGH FINITE ELEMENT MODELLING FOR WOLWEDANS DAM

In Chapter 5, the comparative evaluation of the behaviour of the constituent RCC of Wolwedans Dam is described through a series of parametric Finite Element Analyses. In addition, preliminary observations of early RCC behaviour at Changuinola 1 Dam are compared with predictions derived from the Thermal analysis.

The Chapter comprises four sections; the first three addressing a progressive development of the Wolwedans FE analysis. The first analysis seeks to develop a better understanding of the surprisingly small induced joint openings at mid-height, while the second reviews the joint opening profile and the differential temperature drop variations and loads across the dam section and the third reproduces measured joint openings and crest displacements in an effort to establish the order of total shrinkage experienced. The fourth section of Chapter 5 describes briefly the Thermal Analysis for Changuinola 1 Dam and compares the predicted performance with observations and measurements to provide indications of the apparent early RCC behaviour.

CHAPTER 6: DEVELOPING A NEW UNDERSTANDING OF THE EARLY BEHAVIOUR OF RCC IN LARGE DAMS

In Chapter 6, the indicated behaviour demonstrated through the earlier analyses is reviewed and discussed and conclusions are presented. Applying typical Elastic modulus development models and creep models, the creep levels that might be expected to have been evident in the RCC at Wolwedans Dam are compared with the values apparent from the analyses.

In view of the fact that these conclusions suggest that the total shrinkage and creep experienced in the RCC of Wolwedans during the time that the temperature was elevated by hydration heat were substantially lower than would have been expected for CVC, or a low quality RCC, the associated reasons and potential behaviour mechanisms are discussed.

CHAPTER 7: THE INFLUENCE OF THE BENEFICIAL BEHAVIOUR OF HIGH-PASTE RCC ON DAM DESIGN

In Chapter 7, the impact of the better early behaviour of high-paste RCC on dam design is illustrated through the induced joint spacing design, the thermal study, the maximum allowable RCC placement temperature and the arch performance of the 105 m Changuinola 1 arch/gravity dam currently under construction in Panama.

The most significant relevance of a better early behaviour of high-paste RCC will relate to the design of RCC arch dams and the consequential differences in design approach compared to conventionally assumed behaviour are discussed in this Chapter.

CHAPTER 8: STUDY SUMMARY & CONCLUSIONS

In the concluding Chapter, the work presented is summarized, the application of the study findings is discussed and the need for ongoing industry involvement and contribution is highlighted. A summary of the New Understanding of the Early Behaviour of RCC in Large Dams is presented and the methodology for its application in the design of RCC dams is motivated.

1.9. ACKNOWLEDGEMENTS

1.9.1. WOLWEDANS & KNELLPOORT DAMS

For its diligent efforts in monitoring instrumentation and their assistance in making data available for Wolwedans and Knellpoort Dams, the South African Department of Water Affairs is gratefully acknowledged.

1.9.2. ÇINE DAM

The Turkish State Hydraulic Works (DSI) is thanked for its permission to use instrumentation data measured at Çine Dam.

1.9.3. WADI DAYQAH DAM

The Ministry of Regional Municipalities, Environment and Water Resources of the Sultanate of Oman is thanked for its permission to use instrumentation data measured at Wadi Dayqah Dam.

1.9.4. CHANGUINOLA 1 DAM

CCWJV of Changuinola of Panama is thanked for its permission for the author to refer to the structural and thermal analyses for Changuinola 1 Dam.

1.10. REFERENCES

[1] Owens, G. *Fulton's Concrete Technology.* Chapter 8. Ninth Edition. Cement & Concrete Institute. Midrand. RSA. 2009.

[2] United States Department of the Interior. Bureau of Reclamation. *Design of Arch Dams.* US Government Printing Office. Denver. 1977.

[3] Oosthuizen C. *Behaviour of Roller Compacted Concrete in Arch/Gravity Dams.* Proceedings. International Workshop on Dam Safety Evaluation. Grindelwald, Switzerland. April 1993.

[4] Oosthuizen C. *Performance of Roller Compacted Concrete in Arch/Gravity Dams.* Proceedings. 2nd International Symposium on Roller Compacted concrete Dams. Santander, Spain. pp 1053-1067. 1995.

[5] Shengpei W. *The Technology Development of RCC Dam Construction in China.* Proceedings. 5th International Symposium on Roller Compacted Concrete Dams. Guiyang, China. pp 41-52. 2007.

[6] United States Army Corps of Engineers. *Thermal Studies of Mass Concrete Structures.* Engineering Technical Letter, ETL 1110-2-542. Washington. May 1997.

[7] The Department of Water Affairs & Escom. *Hendrik Verwoerd Dam – SA Water Giant.* Information Brochure. New Graphis, Johannesburg. 1972.

CHAPTER 2

2. RCC CONSTRUCTION, RCC MIXES, RCC INSTRUMENTATION & RCC DAMS STUDIED

2.1. INTRODUCTION

The research and investigations addressed in this Thesis relate entirely to the behaviour and performance of Roller Compacted Concrete in dams. In view of the fact that many of the observations made and the hypotheses presented relate to the nature of RCC as a material and the methods applied for construction, it is considered appropriate to provide the reader with some background on RCC in these areas. Consequently, Chapter 2 presents a background for RCC construction, describing the typical composition of RCC, isolating specifically the "high-paste" RCC that is of particular interest, the methods applied for construction and their influence on instrumentation readings and the instruments installed.

Each of the five dams whose instrumentation data are investigated during the course of this study is subsequently introduced.

2.2. RCC DAM CONSTRUCTION

2.2.1 BACKGROUND

The following description of RCC is partly extracted from *Fulton's Concrete Technology*. (Ninth Edition). 2009[1], Chapter 24, RCC for Dams, which was written by the author of this Thesis.

The term Roller Compacted Concrete (RCC) is used to describe a concrete used in the construction of dams (and pavements), which combines the economical and rapid placement techniques used for fill dams with the strength and durability of concrete. As a consequence of the application of high capacity plant and equipment, it is most suited to use in large-scale construction and for mass concrete works. Since the early 1980s, RCC has gained general acceptance as an appropriate material and method for the construction of dams and by the end of 2009, more than 350 large RCC dams had been completed worldwide.

In the early days, RCC was perceived as a low quality, low strength mass material. It has since become possible to produce a range of concrete qualities by roller compaction, with the most common product being a dense, high quality and relatively high strength concrete.

In principle, RCC is placed and compacted in 300 mm deep horizontal layers, at rates often exceeding 3000 m^3 per day, allowing construction progress commonly of around 10 m in height per month. The main benefits of RCC for dam construction are increased economy and more rapid implementation.

To minimise cementitious materials contents and to take advantage of the fact that the critical zones of a large dam do not generally experience load for an extended period after placement, characteristic strengths for RCC are specified at ages of up to 1 year, and commonly not less than 90 days age.

2.2.2 MODERN RCCS

Modern RCCs are primarily designed in accordance with two different approaches[2]:

- The "overall" approach, which relies on the dam body for water-tightness through high quality concrete and treatment to ensure well-bonded layer and lift joints.
- The "separate" approach, which relies on an independent impervious barrier, which is usually placed on the upstream face.

The majority of RCC dams contain mineral admixtures, most commonly fly ash, as an active constituent of the concrete.

Beyond the basic requirements of strength, a modern RCC mix is defined by the paste/mortar (p/m) and the sand/aggregate (s/a) ratios, the maximum size aggregate (MSA) and the modified Vebe time. These parameters essentially relate to the achievable density (and impermeability), the achievable compaction ratio and the tendency of the constituent materials to segregate during handling. Under construction conditions, the aforementioned properties determine workability and the difference between permeable, stoney RCC, with planes of weakness and a cohesive, seamless watertight and dense RCC. For the "overall" approach, mixes are designed for maximum density, with a paste/mortar ratio of at least 0.37 being required to achieve a density of 98.5% of the theoretical maximum solid density.

In modern RCC practice, a tendency to use a MSA of 37.5, or 40 mm has developed, as larger sizes demonstrate a tendency to segregate in an RCC mix during handling operations. While early RCC testing suggested that a lower sand/aggregate ratio was optimal for RCC, compared to conventional vibrated concrete (CVC), practical experience in the interim has demonstrated that quality control and the maintenance of RCC consistency is much more realistically achieved in an RCC with a sand/aggregate ratio exceeding 0.35.

The workability of RCC is determined by testing with the Vebe apparatus, which is modified to include a surcharge mass of 19.1 kg. For workable RCC, the modified Vebe time should lie between 10 and 20 seconds. For high-workability RCC, a modified vebe time of 8 to 15 seconds is usually specified. In the case of lean RCC, the modified Vebe time generally exceeds 30 seconds.

With a very significant number of approaches attempted during the early years of development, three primary concepts emerged for the design and construction of RCC dams:

- The lean RCC dam; for which the cementitious materials content is < 100 kg/m^3. For such mixes, often only Portland cement is used without mineral admixtures, or pozzolanic material.
- The RCD method (roller compacted dam) unique to Japan; for which the cementitious materials content is generally 125 kg/m^3, but only the hearting zone of the dam is RCC.
- The high-paste RCC dam; for which the cementitious materials content is > 150 kg/m^3.

In the case of high-paste RCC, the RCC material itself provides the watertight barrier and must be designed for an in-situ permeability equivalent to that of traditional dam mass concrete. The RCC and the associated construction methods must further be designed to ensure effective bond between layers. Various facing systems are applied for high-paste RCC dams, but with the simple objective of creating a good and durable surface finish. Transverse joints are induced at pre-determined intervals, which are generally wider than is the case on a conventional vibrated mass concrete dam.

In early RCC dam construction, a particular problem was recognised as low bond between successive placement layers. Whilst a relatively high shear friction angle could generally be assured between layers under all circumstances, low cohesion and tensile strengths were compounded by high permeability when a new layer was placed on an excessively mature existing layer. Development in the interim has included the use of set retarding admixtures and the use of sloped and non-continuous layer placement methods to ensure the freshness of the underlying RCC layer when the subsequent layer is placed. While such practices are only implemented where required as part of the dam design, the result is a seamless bond between successive RCC placement layers, with joint properties equivalent to the parent RCC properties.

2.2.3 RCC Mix Composition

In the case of lean RCC, the material itself is not designed for impermeability and consequently the requirements for aggregate gradings are not necessarily as prescriptive as would be the case for CVC, although density is always important in the case of a dam.

Lean RCC is also often referred to as a dry consistency mix RCC. With similar water contents to high-paste RCC, i.e. 100 – 125 litres/m^3, aggregate contents are obviously relatively high. To ensure consistency and ease of compaction under construction conditions, lean mix RCC often contains a high proportion of aggregate fines (often around 8% of the total aggregate content)[3] that form part of the paste fraction.

A typical lean RCC comprises the following materials proportions:

Constituents	Portland Cement	Fly Ash	Water	Coarse Aggregate	Fine Aggregate	Air
By Mass (kg/m³)	60 - 70	0 - 40	100 - 125	1500	825	0
By Volume (litres/m³)	21	9	113	545	300	12

Ignoring the aggregate fines, the typical lean mix above would contain approximately 140 litres of paste per m³ of concrete. Including 8% fines in the aggregates, the total paste would be of the order of 200 litres.

In view of the fact that high-paste RCC is designed for impermeability, maximum density is important and consequently a continuous aggregate grading is applied. For the latest high-workability RCC mixes, more restrictive aggregate specifications than required for CVC are applied, with lower compacted void ratios and tighter restrictions in respect of aggregate shaping and flakiness. For all high-paste RCC, aggregates of suitable quality for use in a 30 MPa concrete are required.

A typical high-paste RCC comprises the following materials proportions:

Constituents	Portland Cement	Fly Ash	Water	Coarse Aggregate	Fine Aggregate	Retarder
By Mass (kg/m³)	60 - 70	140 - 150	100 - 125	1400	800	3
By Volume (litres/m³)	21	63	113	510	290	3

While it is common to allow relatively high percentages of sand fines in RCC to increase the paste volume, ignoring this component, a high paste RCC will comprise approximately 200 litres of paste and 800 litres of aggregates per m³ of concrete.

2.2.4 RCC CONSTRUCTION

A number of different approaches exist for RCC placement, but the essential principle is to place and compact 300 mm (compacted) layers as rapidly as practically possible, creating a monolithic mass either by placing successive layers before the first set of the previous layer, or by binding layers together with a bedding mortar, or concrete. RCC is generally placed continuously between upstream and downstream formwork and the abutments, with no expansion joints and with induced joints at predetermined intervals to accommodate long-term shrinkage and creep and thermal contraction due to temperature drop loads.

While it is optimal to place RCC as continuously as possible, without interruptions, practical circumstances and breakdowns often necessitate breaks, when a “cold’ joint is formed and the compacted RCC surface must be “green-cut” and treated with mortar, or grout before placement above is resumed.

Plate 2.1: RCC Construction- Dumping, Spreading & Compaction

Plate 2.2: RCC Compaction

Compaction is achieved with 10 to 15 tonne, single-drum vibratory rollers generally applying 4 passes in either direction to achieve the target compaction. The behaviour of lean RCC and high-paste RCC under vibratory compaction are quite different; with the former consolidating to form a hard and flat surface and the latter producing a "live" surface, particularly when the set is retarded, into which the passage of trucks, etc, can make an impression. While lean, or dry consistency mix RCC simply consolidates in the same manner as a fill under compaction, consolidation causes paste to be squeezed through the aggregate structure and to rise to the surface in high-paste (and particularly high-workability) RCC.

Plate 2.3: High Workability RCC

2.2.5 INDUCED JOINTS IN RCC

Joints are induced in RCC at specific cross-sections by de-bonding placement by between 25 and 100% and thereby creating a localized weakness that will concentrate cracking consequential to long term temperature drop shrinkage at a pre-determined location, where it can be isolated with a waterstop. While South African practice has to date inserted a de-bonding mechanism in every fourth layer (see **Figure 2.1**), international practice generally applies de-bonding in every layer. The early practice of inserting de-bonding systems into the RCC during placement (see **Plate 2.4** and **Figure 2.2**), but before compaction, has almost universally been replaced by driving de-bonding systems into compacted RCC (see **Figure 2.3** and **Plate 2.5**).

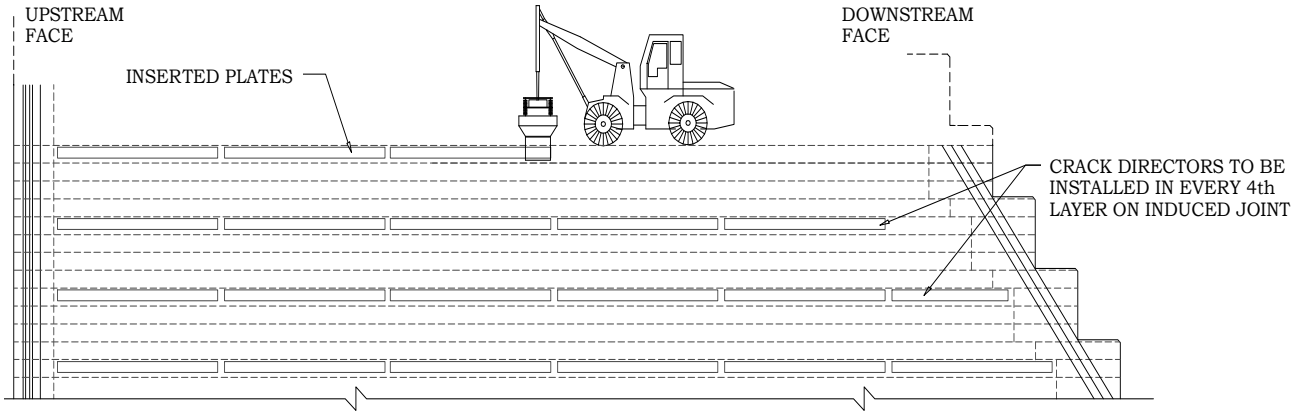

Figure 2.1: Induced Joints Cut into RCC every 4th Layer

Plate 2.4: Induced Joints Inserted into RCC with Placement(3)

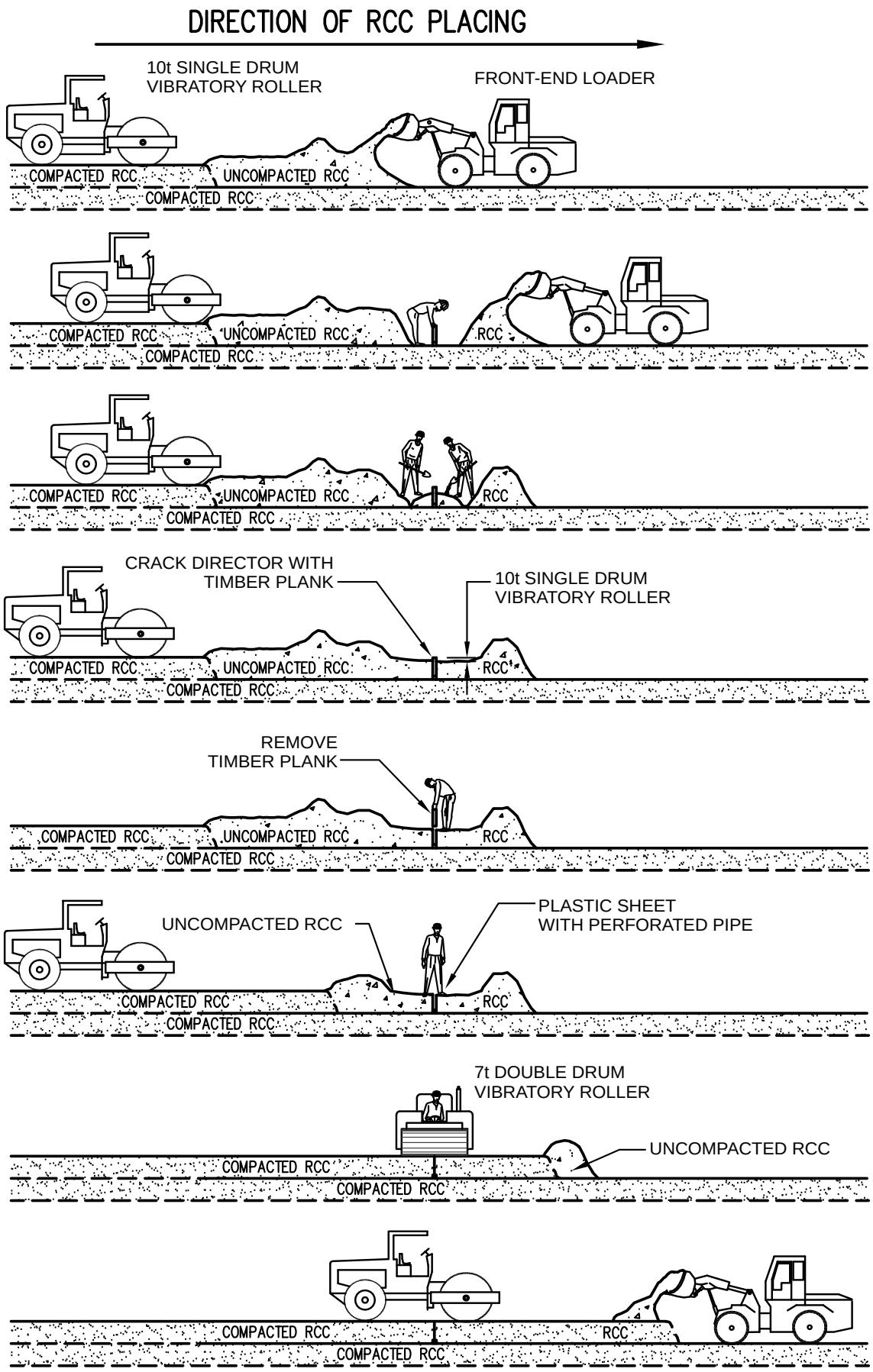

Figure 2.2: Induced Joint Inserted with RCC Placement[3]

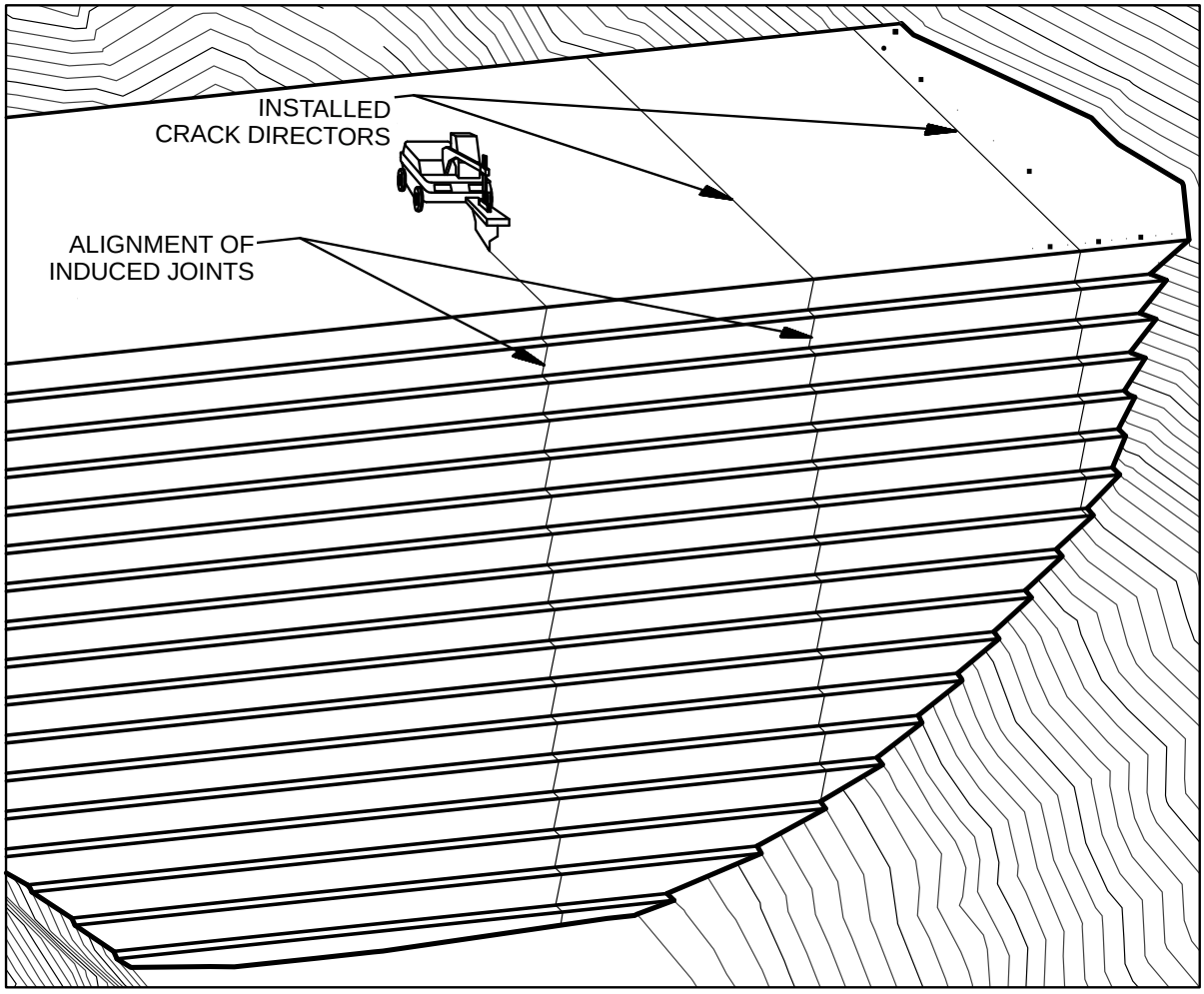

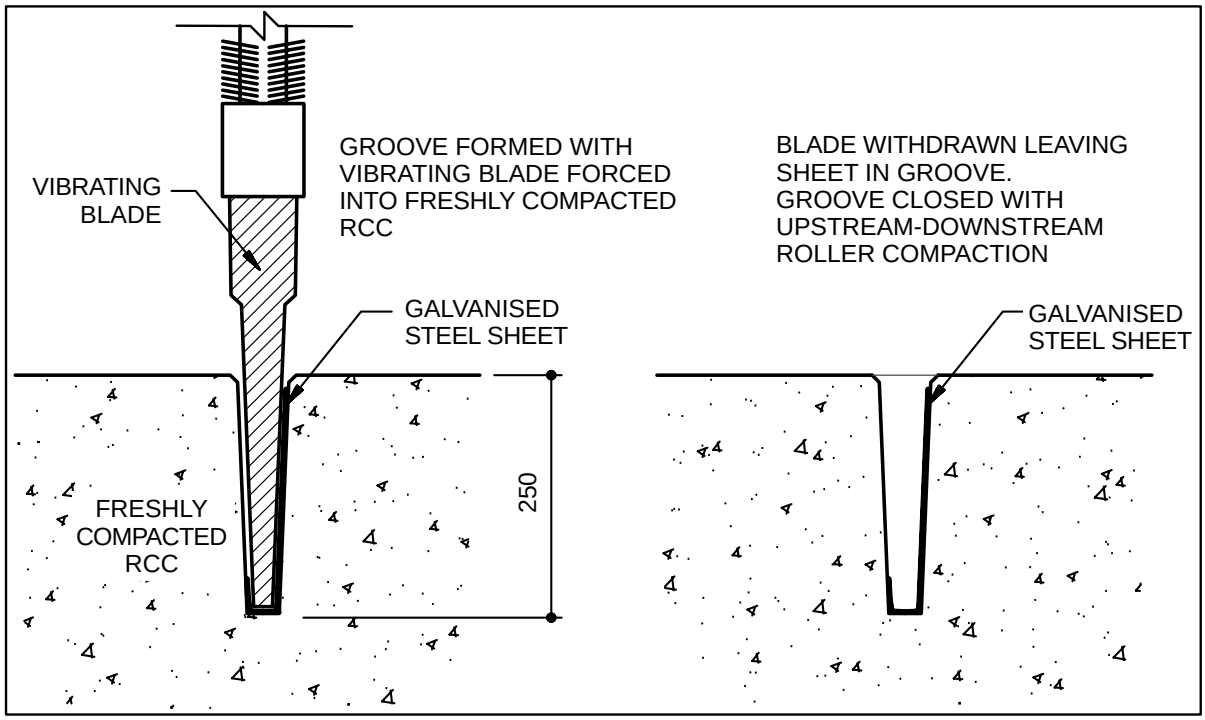

Figure 2.3: Induced Joint Inserted into Compacted RCC

Plate 2.5: Induced Joint Inserted into Compacted RCC

Although several methods and systems are used for de-bonding RCC to create an "induced joint", all result in an increased compressibility on the induced joint, compared to the adjacent RCC. While the construction process causes a disturbance of the RCC on either side of the induced joint, the insertion of folded plastic sheeting, geotextile material, or a folded galvanized steel sheet, implies that the aggregate-to-aggregate contact within the RCC is broken. As the presence of the de-bonding system implies that the RCC structure cannot be as effectively redeveloped during the subsequent re-compaction, the increased compressibility is undoubtedly not only the consequence of a compressible joint filler, but also a slightly more open structure within the concrete on either side.

A consequence of the evident compressibility of the de-bonded areas of the induced joints is local exaggerated movement/closure during thermal expansion of the RCC. As the temperature of the RCC rises with the evolution of hydration heat, it will experience expansion, which will be restrained by the continuity of the placement in a direction parallel to the dam axis (left to right bank direction). Due to the fact that

joint inducers are only installed in every second, or fourth layer in the dams investigated as part of this study, their presence will not reduce the overall resistance of the RCC mass to thermal expansion, nor will it cause any perceptible increase in the overall compressibility of the full joint, but it will undoubtedly give rise to increased local compression across the actual de-bonded section of the joint

2.3. RCC INSTRUMENTATION

2.3.1 GENERAL

The instrumentation installed in the dams addressed in this study was designed to fulfil two specific purposes; to monitor the overall performance of the dam structure with a view to ensuring continued dam safety and to monitor the behaviour of the constituent RCC. The dam safety instrumentation comprised pendulums, displacement survey systems, load cells, pore pressure meters and seepage measurement weirs, while the RCC-specific instrumentation comprised long-base-strain-gauge-temperature-meters (LBSGTMs), strain gauges, temperature gauges and thermocouples.

Instrumentation installed in RCC was generally developed for use in soils and for monitoring geotechnical structures, etc. Accordingly, it is of a robust construction and only instruments and measurement systems that have proved accurate and reliable in conditions in which heavy equipment operates are installed in RCC dams.

2.3.1 THE INSTRUMENTS

The Long-Base-Strain-Gauge-Temperature-Meters (LBSGTMs) and the strain gauges installed at all of the dams addressed in this study were vibrating-wire type gauges, a system that is acknowledged for its long-term stability and accuracy[5].

A long-base-strain-gauge-temperature-meter is essentially a long strain, or deformation gauge that is installed across (perpendicular to) the alignment of an induced joint. These instruments are correspondingly aligned parallel to the axis of the dam structure. The LBSGTM was developed by Geokon for use in RCC dam construction on the request of the South African Department of Water Affairs (DWA). The gauge is a vibrating wire meter that measures deformation across a distance of between 600 mm and 1 m. The long-base was considered necessary to ensure that the crack on the induced joint passes between the flanged end plates of the gauge. Initially, a gauge length of 1 m was considered necessary, but it has since become evident that 600 – 700 mm is quite adequate. The Geokon Model 4430 gauge is specified for a measurement sensitivity of 0.01 mm and an accuracy of ± 0.05 mm. The gauge measures temperature, as well as deformation, and the indicated deformations must be adjusted for temperature.

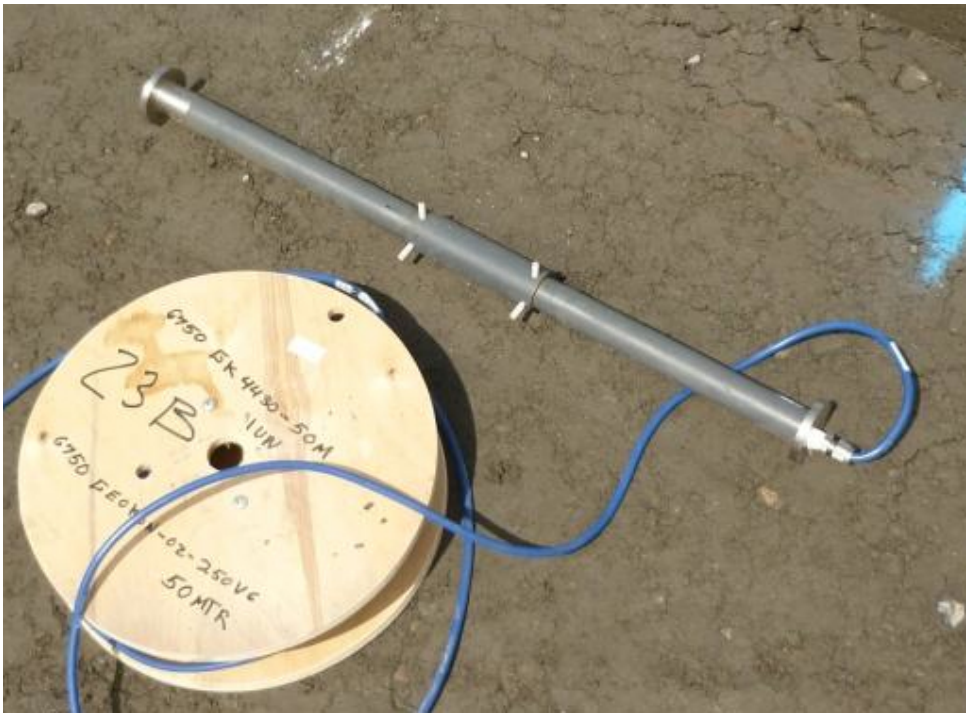

Plate 2.6: Long-Base-Strain-Gauge- Temperature-Meter (LGSGTM)

The first gauges used by DWA were tested under the direct action of a 10 tonne vibratory roller[6] and were demonstrated to remain operational and to continue providing accurate measurement no matter how roughly they were treated. The continued operation of the vast majority of these gauges at Wolwedans Dam after some 20 years is testament to their robustness.

The Geokon Model 4210 gauge used for measuring strain is a particularly robust, all-stainless steel-cased instrument that is designed for direct installation into concrete with large aggregate and indicates a measurement sensitivity of 0.4 microstrain and an accuracy of ± 1%. The gauge also measures temperature and the gauge readings must be adjusted to indicate actual concrete strain.

Plate 2.7: Strain Gauge

2.3.2 INSTRUMENT INSTALLATION

For simplicity and to ensure minimum interruption to RCC placement, instrumentation to monitor RCC behaviour is generally installed at a number of specific elevations over the height of an RCC dam, ideally when planned stoppages will anyway occur for galleries, etc. Stoppages generally correspond with "cold" lift joints, where the RCC is allowed to set fully. A number of methods have been used to create trenches and slots in the RCC surface for the instrumentation and associated cabling and this has sometimes been done by excavation after completion of the layer and other times by cutting slots with a vibrating blade during the process of completing the layer surface. In either case, the cabling is laid out, the instruments are installed and the trenches and slots are backfilled with a structural concrete. Resumption of RCC placement above can often be delayed for a further number of days, but critical data collection starts as soon as the respective gauge is covered with a layer of RCC.

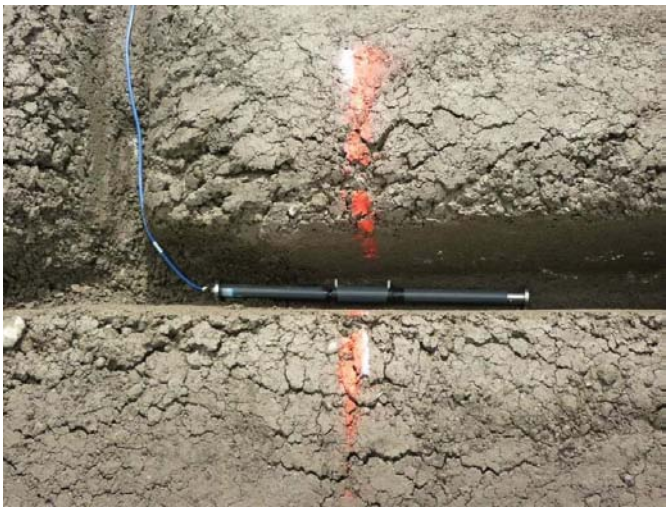

Plate 2.8: LBSGTM in Slot

Plate 2.9: Instrumentation Cable Trench

LBSGTMs are installed in, or immediately above, the layer in which the induced joint de-bonding medium is installed, to ensure that the crack occurs relatively centrally on the gauge.

As a consequence of locating the LGSTMs immediately above an induced joint de-bonding mechanism, the initial deformation readings during the build up in temperature due to hydration reflect the compressibility of the joint inducer system installed. While this will result in a distortion and will not provide a true representation of the actual strain within the continuous RCC in compression above and below the de-bonding system while the temperatures are elevated, the related impact will dissipate once the joint experiences any tension and/or cracking.

2.4. THE RCC DAMS STUDIED

The central focus of the work presented in this Thesis is the data recovered from instrumentation installed in the Wolwedans and Knellpoort Dams in South Africa, Çine Dam in Turkey and Wadi Dayqah Dam in Oman. On the basis of the interpretation of this data, the behaviour of the constituent RCC is observed over periods varying from several months to several years. Behavioural observations from Changuinola 1 Dam, currently under construction in Panama, are also addressed herein.

2.5. WOLWEDANS DAM

2.5.1. INTRODUCTION

Wolwedans Dam was completed in early 1990 and was the first RCC dam in the world to rely fully on three-dimensional arch action for stability. The dam is 70 m high, has a crest length of 270 m, an upstream face arch radius of 135 m and comprises approximately 200 000 m^3 of concrete. The dam was constructed with induced joints at 10 m spacings, de-bonding every 4^{th} layer with inducers installed during placement and the RCC was placed in October and November of 1988 and between May and November of 1989. The first season involved the placement of the bottom 15 m of the dam, while the second encompassed the placement of the remaining 55 m. RCC placement for Wolwedans was achieved over a total period of approximately 7.5 months, with a peak daily rate of 2994 m^3 [7].

The dam first filled to capacity during 1992 and the induced joints were grouted during late winter in 1993. With a full storage volume of 64% of the Mean Annual Runnoff (MAR), a high supply assurance requirement and a relatively high catchment rainfall, Wolwedans Dam is subject to consistently high water levels. The dam has spilt on several occasions to date and discharged a relatively large flood just two years after completion.

The composition of the high-paste Wolwedans RCC mix was as follows[7]:

Constituents	Portland Cement	Fly Ash	Water	Coarse Aggregate	Fine Aggregate	Air
By Mass (kg/m^3)	58	136	100	1510	625	0
By Volume ($litres/m^3$)	18.5	63.5	100	565	240	13

Ignoring aggregate fines, the Wolwedans RCC comprised 182 litres of paste and 805 litres of aggregates. The blend of 75% crusher and 25% pit sand contained only 1.3% of fines and accordingly, the paste volume was only increased by 3 $litres/m^3$. With a low sand/aggregate ratio of just 0.3, the paste/mortar ratio was correspondingly high, at almost 0.44.

A basic layout of Wolwedans Dam is provided in **Figure 2.4**.

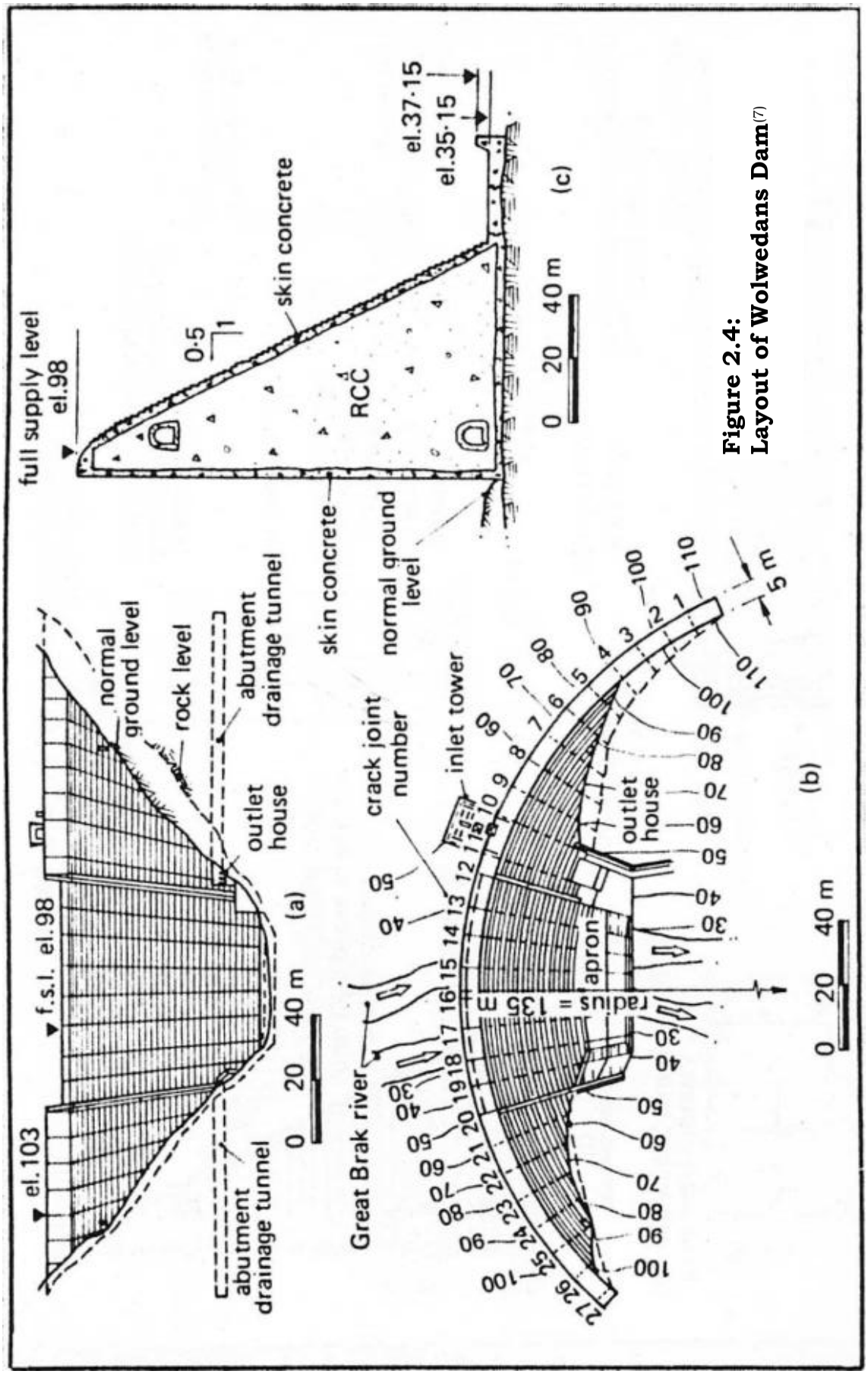

Figure 2.4:
Layout of Wolwedans Dam[7]

2.5.2. WOLWEDANS INSTRUMENTATION

Being one of the first two structures of its type and dependent on arching for stability, a very comprehensive network of structural and thermal monitoring instrumentation was installed within the body of Wolwedans Dam (see **Figure 2.11** at the end of this Chapter and **Figures C1** to **C4** in **Appendix C**). Virtually all of the instrumentation installed during construction is still functional and a central, remotely interrogated control system allows real-time monitoring of the dam's performance and behaviour.

LBSGTMs were installed across all induced joints at four different levels and these instruments formed the core of the system for monitoring the thermal/structural behaviour of the dam structure. With a lowest foundation elevation of RL 33 m and a NOC elevation of RL 103 m, instrumentation was installed at elevations RL 40.25 m, RL 52.25 m, RL 66.25 m and RL 84.25 m.

The lowest level of instrumentation was installed approximately at mid-height of the first RCC cast during October and November 1988. The second level of instrumentation was installed just 4.25 m above the bottom level of the RCC placed during 1989. The third level of instrumentation was installed at approximately mid height, 33 m above lowest foundation level. The top level of instrumentation was installed at the level of the top gallery, implying that instruments were installed 2 m from an external surface on one side and 2.75 m from the gallery on the other.

Plate 2.10: Wolwedans Dam

2.5.3. IMPORTANT INFLUENCES ON RECORDED BEHAVIOUR

In view of the fact that the dam structure at Wolwedans was constructed in two distinct parts[7], separated by a substantial break, it is not considered that the full structure behaves entirely monolithically with respect to temperature and hydration

heat dissipation. Two specific issues are considered of importance in this regard; construction of the first part during the summer months and initiation of the latter part in winter and the fact that the instrumentation installed at elevation RL 40.25 m suggests that almost all of the hydration heat from the bottom section had been dissipated by the time that the construction of the upper section was initiated. Correspondingly, the instrumentation data at elevations RL 40.25 m and RL 52.25 m are likely to have been influenced significantly by the extended interruption in construction that occurred at RL 48 m.

With only 2 rows of LBSGTMs and surface cover of just 2 m to the outside and 2.75 m to the gallery, it is considered that the readings in the highest level of instrumentation (RL 84.25 m) will substantially reflect surface zone temperatures and effects. In the third level of instrumentation (RL 66.25 m), however, foundation restraint will not be a significant influence, while the dam wall thickness is approximately 21 m, which the instrumentation records demonstrated to be sufficient to limit the core temperature variation over a typical annual cycle to approximately 2°C, while still allowing all of the hydration heat to be dissipated within 2 years after dam completion.

The induced joints at Wolwedans Dam were grouted in two phases, between July and November 1993. With the impounded water level dropped by 8 m during the latter part of the period, grouting to mid dam height (RL 66.25 m) was completed over the winter months of June to August. With the dam filled to capacity once more, the top half of the structure was subsequently grouted over the Spring and early Summer months of September to November. It is significant to note that while a net upstream crest movement of the order of 2.5 mm was recorded when the water level was drawn down, equivalent displacements in the upper gallery were of the order of only 0.5 mm and no associated movement was really apparent on any of the induced joint instruments. At the time that the induced joints were grouted, it is apparent from the displacement data records that the dam crest was displaced downstream by a maximum of well over 10 mm, indicating that the structure was already subject to a significant temperature drop and that the grouting merely filled open joints and did not serve a significant purpose in alleviating the impact of long-term temperature-related loading.

2.6. KNELLPOORT DAM

2.6.1. INTRODUCTION

Knellpoort Dam is also in South Africa and was designed in parallel with Wolwedans, but construction was initiated earlier and completed over a shorter period, as concrete volumes were relatively small. Although this 50 m high dam is defined as an arch/gravity structure, arching is only incurred under extreme loading conditions and, as an off-channel storage dam, with a large capacity compared to the natural catchment inflow, hydrostatic loadings are generally low.

The main part of the dam is aligned on a circular arch and has a vertical upstream face and a downstream face sloped at 0.6 horizontal to 1 vertical. The left flank comprises a straight conventional gravity structure. The combined crest length measures 200 m.

The 60 000 m^3 of concrete comprising Knellpoort Dam was placed over a single winter season during 1988. Induced joints were aligned radially at a 10 m spacing on the upstream face, de-bonding every 4th layer with inducers installed during RCC placement.

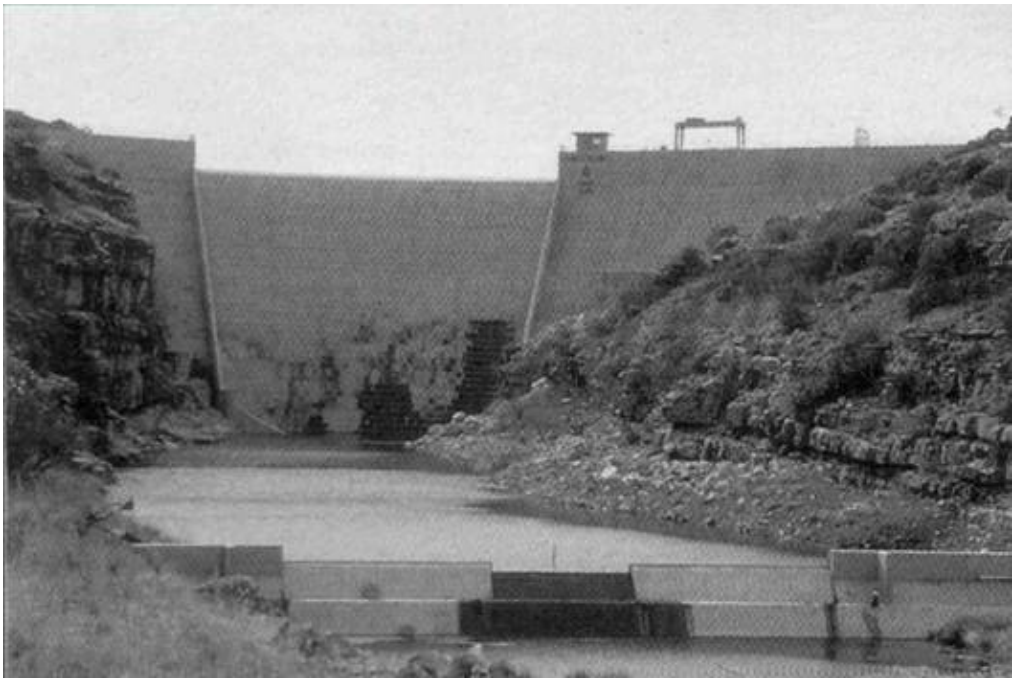

Plate 2.11: Knellpoort Dam[8]

The composition of the RCC mix placed at Knellpoort Dam was as follows[8]:

Constituents	Portland Cement	Fly Ash	Water	Coarse Aggregate	Fine Aggregate	Air
By Mass (kg/m^3)	61	142	108	1610	685	0
By Volume (litres/m^3)	19.5	66	108	555	245	6.5

Ignoring aggregate fines, the Knellpoort RCC comprised approximately 195 litres of paste and 800 litres of aggregates. Again, a low sand/aggregate ratio of just 0.3 gives rise to a high paste/mortar ratio of 0.44.

A basic layout of Knellpoort Dam is provided in **Figure 2.5**.

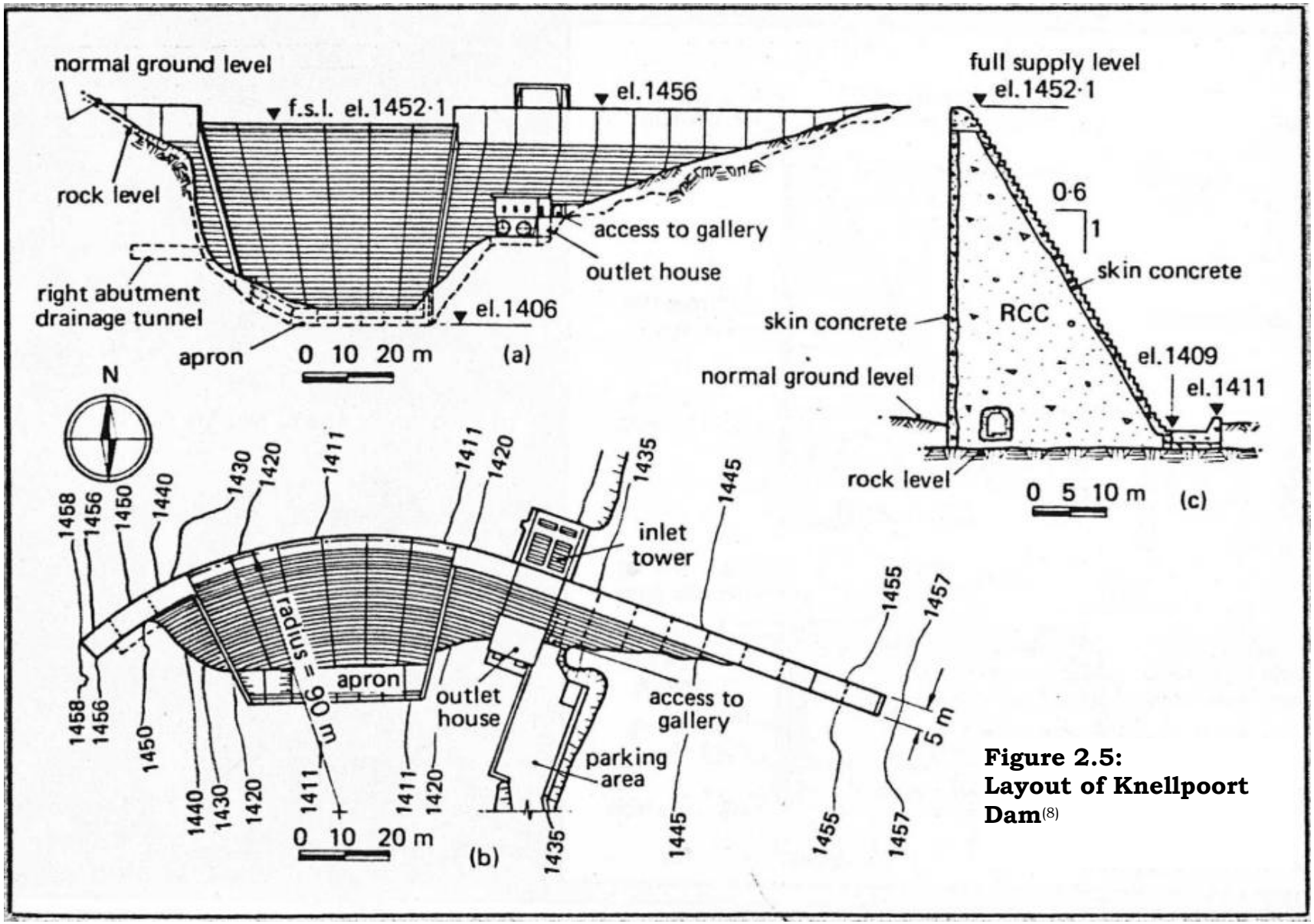

Figure 2.5: Layout of Knellpoort Dam[8]

2.6.2. KNELLPOORT INSTRUMENTATION

The instrumentation installed at Knellpoort Dam was essentially identical to that installed at Wolwedans. Despite the lower dam height, the reduced dependence on arching and the inclusion of only a single gallery, instrumentation was installed on four separate levels. However, unlike Wolwedans Dam, Knellpoort was constructed largely during a particularly cold winter, with built-in temperatures frequently below 15°C.

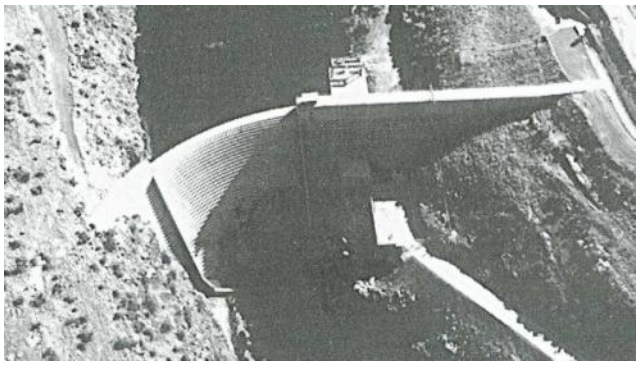

Plate 2.12: Knellpoort Dam[9]

2.6.3. IMPORTANT INFLUENCES ON RECORDED BEHAVIOUR

Knellpoort Dam was constructed primarily over a particularly cold winter in 1988. The temperature at which the RCC at any particular location in the dam body was placed, or effectively insulated by RCC placed above, was frequently below 15°C. In view of the fact that the long-term temperature at the core of the dam structure varies seasonally between 13 and 16°C, the difference between the average long-term core temperature and the average "built-in" temperature is minimal, as indicated in **Figure 2.6**.

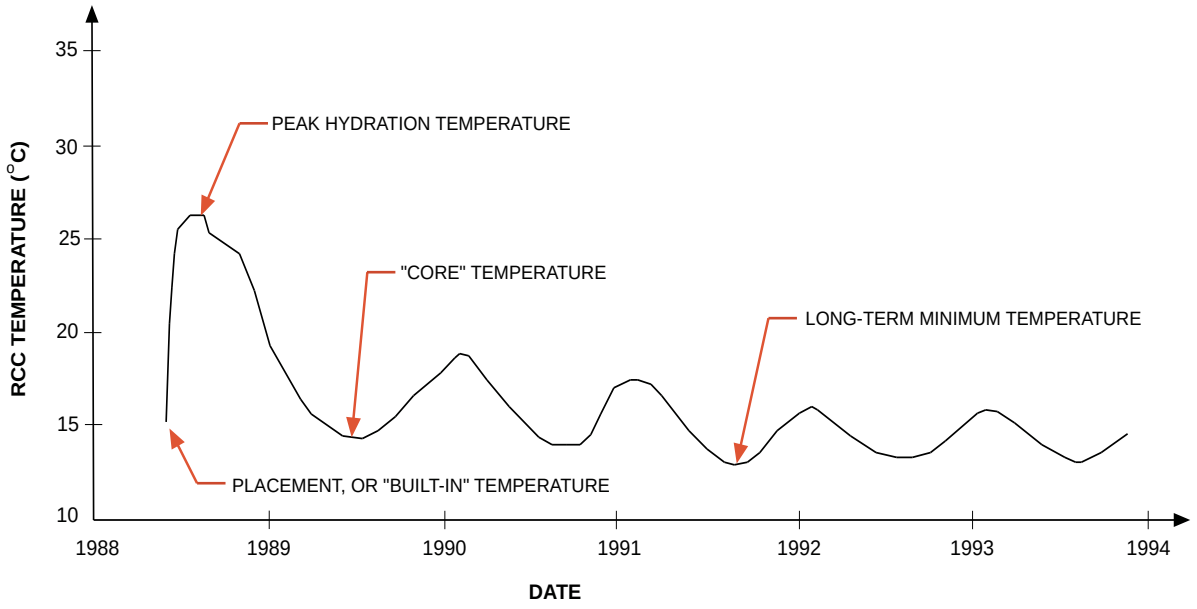

Figure 2.6: Typical RCC Temperature History for Knellpoort Dam[8]

2.7. ÇINE DAM

2.7.1. INTRODUCTION

Çine Dam is currently under construction in south-western Turkey. Placement of RCC is restricted to the winter months of the year and limited each year on the basis of available State fund allocations. By April 2009, almost 1.4 million m³ of the required total of 1.65 million m³ of RCC had been placed. The dam is a gravity structure with a maximum height of 136.5 m and a crest length of approximately 300 m. While the topography could accommodate an arch structure, the foundation rockmass conditions were not considered suitable. As a consequence of the dam's location in an area of relatively high seismic risk, the structure has a wide base and the RCC strength characteristics are determined by the related requirements under seismic loading.

Plate 2.13: Çine Dam

Induced joints at Çine Dam were installed in the compacted RCC at intervals of 24 m along the length of the main body of the wall, de-bonding every 4th layer. On the extremes of the flanks, where the dam height reduces, a closer joint spacing was applied. The RCC for Çine Dam is zoned, with the an upstream "impermeable" zone containing 85 kg/m³ cement and 105 kg/m³ fly ash and the remaining bulk of the wall structure containing 75 kg/m³ cement and 95 kg/m³ fly ash.

The compositions of the two RCC mixes placed at Çine Dam were as follows[10]:

Constituents	Portland Cement	Fly Ash	Water	Coarse Aggregate	Fine Aggregate	Air
D10 Mix						
By Mass (kg/m³)	85	105	115	1406	791	0
By Volume (litres/m³)	27	46	115	516	290	6
Net Paste (*l*/m³)	Fines (*l*/m³)	Aggregate (*l*/m³)	Paste/ Mortar	Sand/ Aggregate		
193	49	806	0.40	0.36		

Constituents	Portland Cement	Fly Ash	Water	Coarse Aggregate	Fine Aggregate	Air
D05 Mix						
By Mass (kg/m³)	75	95	120	1590	586	0
By Volume (litres/m³)	24	41	120	586	218	11
Net Paste (l/m³)	Fines (l/m³)	Aggregate (l/m³)	Paste/ Mortar	Sand/ Aggregate		
185	36	804	0.46	0.27		

A basic plan layout of Çine Dam is provided in **Figure 2.7**.

2.7.2. ÇINE INSTRUMENTATION

A comprehensive network of monitoring instrumentation was installed in Çine Dam, including 200 LBSGTMs, 50 separate temperature gauges, 3 pendulum lines, 30 strain gauges, 30 surface crack meters, 13 piezometers and 6 seepage measurement sites. The dam contains 3 separate, horizontal galleries at elevations 147.5 mASL, 185 mASL and 232 mASL and instrumentation was installed at each of these levels, as well as at elevation 210 mASL.

For the purposes of evaluating the thermal performance of the RCC at Çine Dam, data from the LBSGTMs, the strain gauges and the various temperature meters were analysed. The LBSGTMs were ascribed an SGT designation, while the strain gauges were ascribed an SGA designation. **Figure 2.12** at the end of this Chapter and **Figures C5** to **C7** illustrate the basic layout of the installed instrumentation on a typical induced joint. The SGA strain gauges installed at Çine Dam were aligned in an array in an upstream-downstream direction to measure strain perpendicular to the dam axis.

2.7.3. IMPORTANT INFLUENCES ON RECORDED BEHAVIOUR

As previously mentioned, the RCC for Çine Dam was placed between October and April of each year from 2004. Each season saw the placement of approximately 300 000 m³ of RCC, with the levels listed in **Table 2.1** being achieved at the end of each placement in April. The surface of the RCC at this level was subsequently exposed to the elements, until placement resumed the following October.

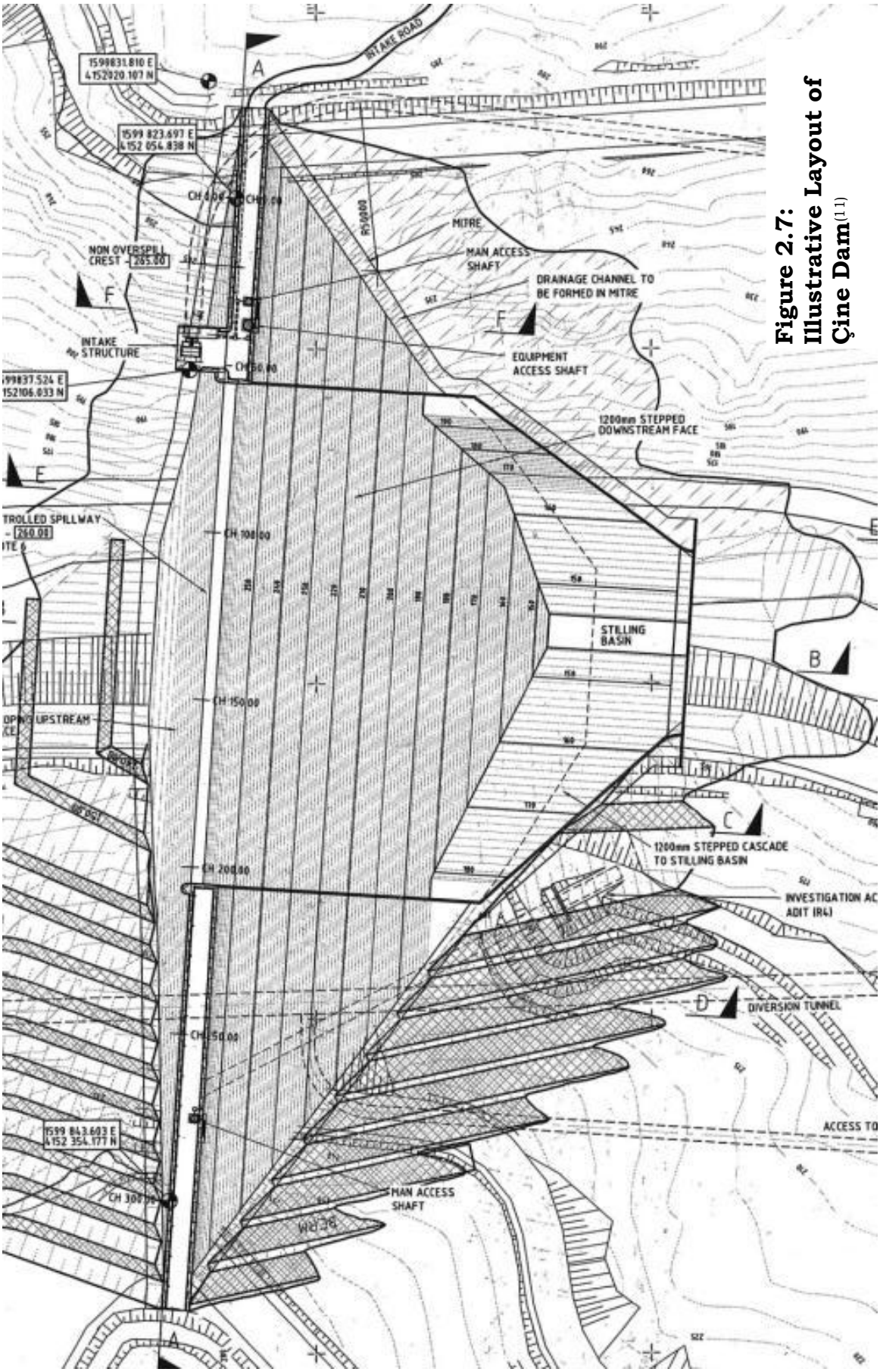

Figure 2.7: Illustrative Layout of Çine Dam[11]

The dam structure, constructed in accordance with the actual construction programme, was consequently the subject of a detailed thermal analysis, undertaken to establish whether any consequential deleterious thermal stresses might be developed and to establish whether any RCC cooling and/or thermal insulation may be required.

This thermal analysis will not be addressed in detail in this study, as the related results have no specific relevance. However, it is important to note that a very good correlation was evident between the temperatures within the dam predicted by the finite element thermal model and those measured on the prototype structure and this is illustrated in Chapter 4.

Table 2.1: RCC Progress at Çine Dam

Placement Period		**Level Achieved** (m ASL)
1	October 2004 – April 2005	147.50
2	October 2005 – April 2006	166
3	October 2006 – April 2007	187
4	October 2007 – April 2008	208.25
5	October 2008 – April 2009	232
6	October 2009 – October 2010	265 (completed)

Figure 2.8: Çine Dam Construction Progress

Figure 2.8: Çine Dam Construction Progress *continued*

2.8. WADI DAYQAH DAM

2.8.1. INTRODUCTION

Construction of Wadi Dayqah Dam in Oman was recently completed (2009). The dam comprises an 80 m high RCC gravity structure and a 40 m high rockfill saddle embankment. With a crest length of a little under 400 m, the RCC structure comprises a total concrete quantity of approximately 650 000 m^3 and the RCC was essentially placed between February and December 2008. The dam is aligned on a curve, with a radius of 500 m to the upstream face and induced joints are arranged

radially, generally at a spacing of 15 m measured on the upstream face. Induced joints were installed in every 2nd layer of RCC after compaction.

Plate 2.14: Wadi Dayqah Dam

The RCC for Wadi Dayqah Dam was zoned, with an upstream "impermeable" 15 MPa RCC zone containing 126 kg/m³ cement and 54 kg/m³ ground Limestone and the remaining bulk of the wall structure (12 MPa RCC) containing 112 kg/m³ cement and 48 kg/m³ ground Limestone.

The compositions of the two RCC mixes placed at Wadi Dayqah were as follows[12]:

Constituents	Portland Cement	Ground Limestone	Water*	Coarse Aggregate	Fine Aggregate	Retarder
Zone 1 - 15 MPa Mix						
By Mass (kg/m³)	126	54	137	1200	944	1.76
By Volume (litres/m³)	41	21	103	455	378	1.5
Net Paste (*l*/m³)	Fines (*l*/m³)	Aggregate (*l*/m³)	Paste/ Mortar**	Sand/ Aggregate		
166.5	51	833	0.31	0.45		

* - the free water content was 103 litres/m³, but an additional quantity of 34 litres was required due to aggregate absorption.

** - including aggregate fines increases the paste to 217.5 litres/m³ and the p/m to 0.40.

Constituents	Portland Cement	Ground Limestone	Water*	Coarse Aggregate	Fine Aggregate	Retarder
Zone 2 – 12 MPa Mix						
By Mass (kg/m³)	112	48	131	1227	960	1.76
By Volume (litres/m³)	37	19	96	463	384	1.5
Net Paste (l/m³)	Fines (l/m³)	Aggregate (l/m³)	Paste/ Mortar**	Sand/ Aggregate		
153.5	52	847	0.29	0.45		

* - the free water content was 96 litres/m³, but an additional quantity of 35 litres was required due to aggregate absorption.

** - including aggregate fines increases the paste to 205.5 litres/m³ and the p/m to 0.38.

2.8.2. WADI DAYQAH INSTRUMENTATION

The instrumentation installed in Wadi Dayqah RCC gravity dam in Oman was less comprehensive than was the case for the previous examples. With the same types of instruments, only a single LBSGTM was installed across each of the induced joints in the centre of the section at two elevations, namely 135 mASL and 150 mASL. Five levels of concrete temperature meters and external temperature gauges were also installed on three specific cross sections; one in the spillway section and one on the non-overspill section on either flank. The typical layouts of the temperature meters and the LBSGTMs are illustrated on **Figures 2.13** and **2.14** at the end of this Chapter.

2.8.3. IMPORTANT INFLUENCES ON RECORDED BEHAVIOUR

Placement of the RCC for Wadi Dayqah Dam took place between February 2008 and July 2009 in temperatures varying between 25 and 45°C. However, as a consequence of the dam having a spillway with Robert's crest splitters, a substantial slowing in the pace of construction occurred once the base of the spillway crest was reached in November 2008. The vast majority of the RCC comprising the dam was accordingly placed in just 10 months.

With a better picture of the behaviour expectations of the RCC and a relatively small budget for instrumentation, it was considered most appropriate to install a single LBSGTM across all joints in the centre of the dam section at two levels. With this configuration, it was understood that only the behaviour of the "core" zone RCC would be monitored.

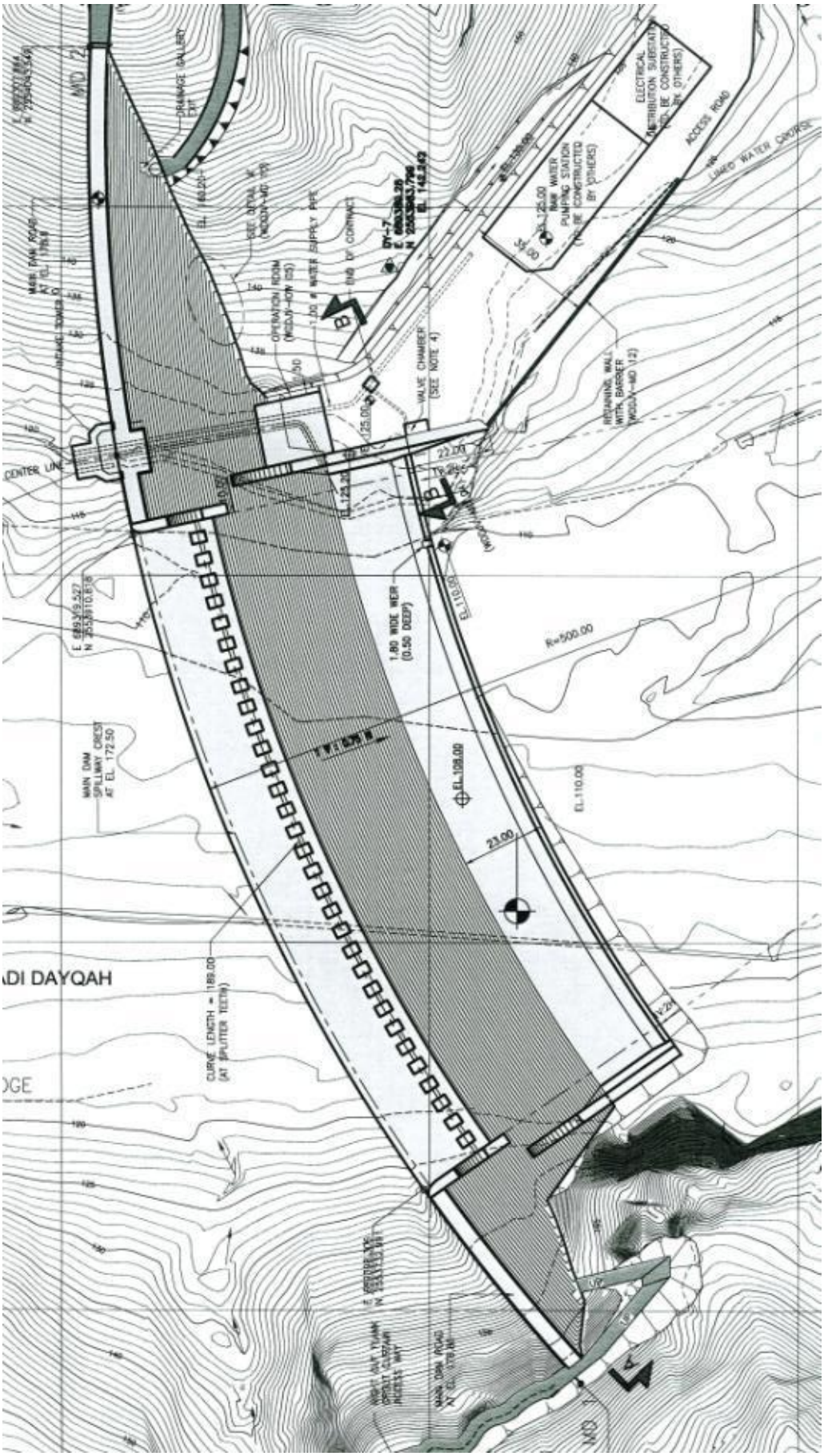

Figure 2.9: Illustrative Layout of Wadi Dayqah Dam[13]

Whereas all of the other dams for which instrumentation data were reviewed contain high-paste RCC for which a relatively high proportion of fly ash was used, the RCC of Wadi Dayqah comprised a relatively low cement content (112 kg/m^3) in combination with a ground limestone filler (48 kg/m^3) and a 0.44 sand/aggregate ratio. Furthermore, 34% of the sand fraction comprised crushed limestone. As a consequence, the final RCC contained over 13% fines.

Three further factors are considered of importance in respect of the measured behaviour of the RCC at Wadi Dayqah Dam and these are the rounded particle shape of the natural gravel coarse aggregate, the high water absorption characteristics of the aggregates (approximately 35 litres/m^3) and the fact that the RCC temperature was artificially cooled by approximately 15°C before placement.

Plate 2.15: Wadi Dayqah Dam January 2009

2.9. CHANGUINOLA 1 DAM

2.9.1. INTRODUCTION

Placement of the RCC for Changuinola 1 Dam in Panama commenced in December 2009, with completion scheduled for February/March 2011. The dam is a 105 m arch/gravity structure comprising approximately 890 000 m^3 of RCC. The upstream face arch radius is 525 m, the induced joints are spaced at 20 m intervals, with

inducers installed in every 2nd layer after compaction and the downstream face slope varies from 0.5 H to 1 V in the centre to 0.7 H to 1 V on the flanks.

For Changuinola 1, a high-workability RCC is being applied, with a first set retarded typically to 20 hours. The mix strength requirements are determined primarily by a target direct vertical tensile strength of 1.2 MPa and peak RCC placement rates should exceed 120 000 m³ per month.

The composition of the high-workability RCC mix applied for Changuinola 1 is follows:

Constituents	Portland Cement	Fly Ash	Water	Coarse Aggregate	Fine Aggregate	Retarder
By Mass (kg/m³)	70	145	119	1282	888	3.44
By Volume (litres/m³)	22	60	119	462	334	3
Net Paste (l/m³)	Fines (l/m³)	Aggregate (l/m³)	Paste/ Mortar	Sand/ Aggregate		
201	35	799	0.375	0.42		

Including the aggregate fines within the paste increases the p/m to 0.44.

2.9.2. CHANGUINOLA 1 INSTRUMENTATION

The instrumentation to be installed in Changuinola 1 Dam is very similar to the arrangements described above. At the time of writing, however, only one level of instruments had been installed and the while these were indicating the same patterns as for Wolwedans and Knellpoort, the record was of not of adequate length to be used for the purposes of the work addressed herein.

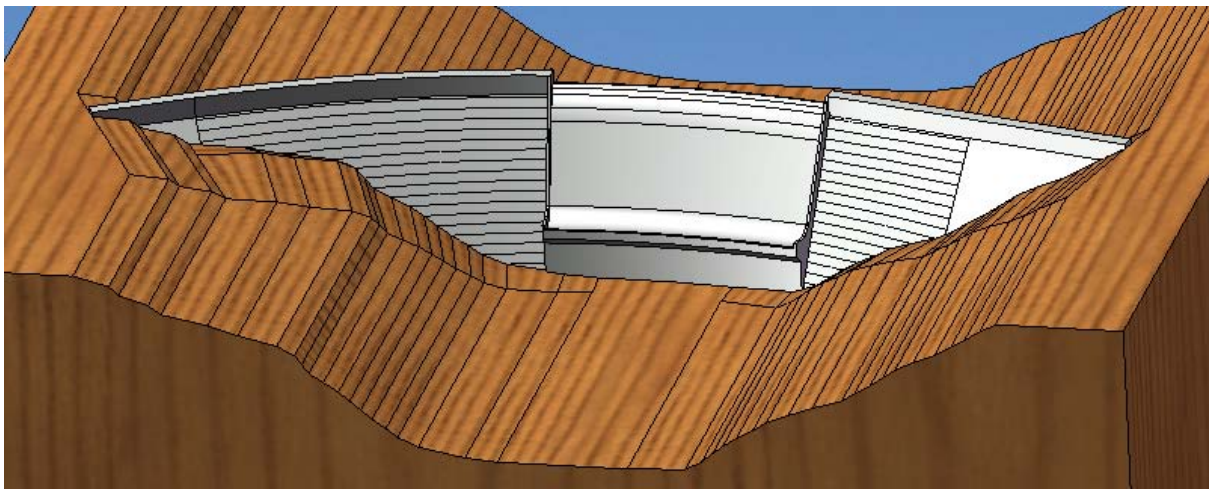

Figure 2.10: Changuinola FE Model Illustrating Final Layout

2.9.3. IMPORTANT INFLUENCES ON RECORDED BEHAVIOUR

With almost 3 m of rainfall per annum on site and a wet month containing 25 days of rain and a dry month 16 days, the weather conditions on site represent a very significant factor in relation to the construction of Changuinola 1 Dam. While RCC dam construction offered very significant advantages in respect of the river diversion, compared to other dam types, the final programme and the shear size of the river implied that the structure was constructed to approximately 40 m height in two sections, with a formed joint in between (see **Plate 2.16**). Another factor of specific relevance in the case of Changuinola 1 Dam is the temperate climatic conditions, with average monthly temperatures varying only by 4°C year-round.

Plate 2.16: Construction Progress at Changuinola 1 Dam on 25th June 2010

2.10. INSTRUMENTATION LAYOUTS

2.10.1. WOLWEDANS DAM

Figure 2.11 illustrates the typical layout of the instrumentation installed in Wolwedans Dam. Additional plan layouts of each of the instrumentation levels are provided for illustration on **Appendix C**.

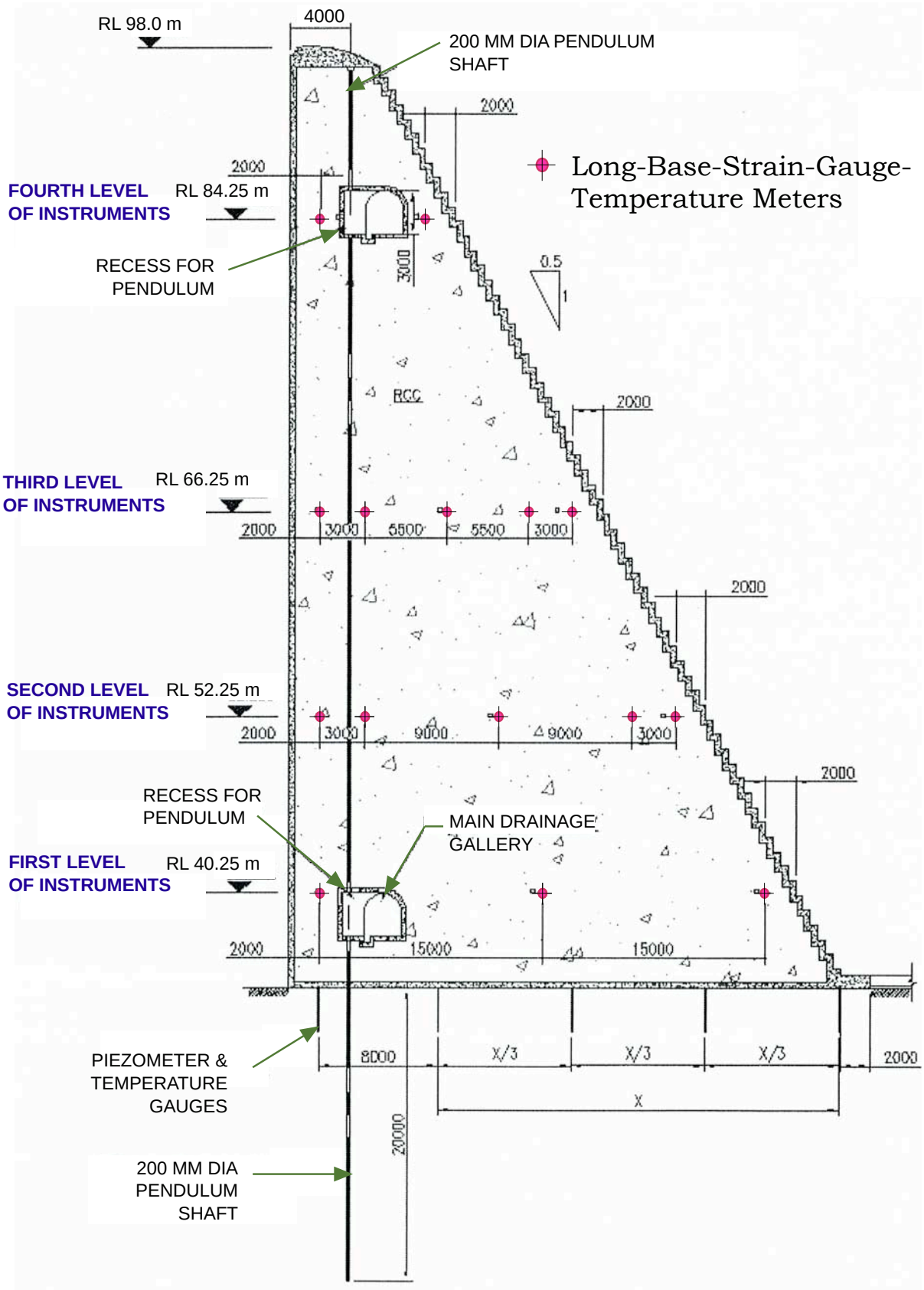

Figure 2.11: Illustrative Section Indicating Instrumentation[7]
(from 1987/88 Hand Drawn Plan)

2.10.2. ÇINE DAM

Figure 2.12 illustrates the typical instrumentation installed in Çine Dam. The layouts for the instrumentation at El 147.5 mASL, El 184.25 mASL & El 208.5 mASL are included in **Appendix C**.

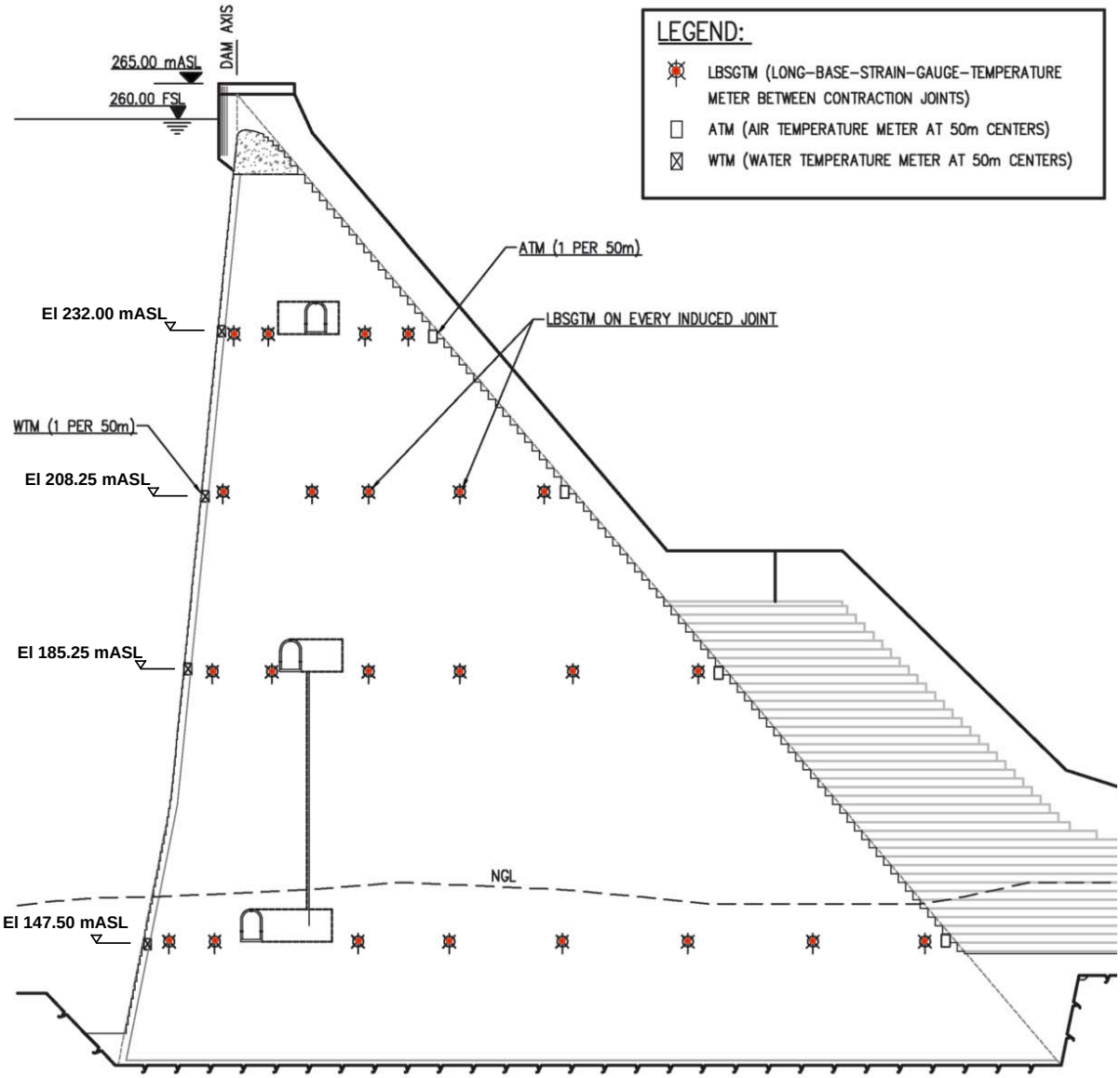

FIGURE 2.12: Typical Instrumentation Installed in Çine Dam(11)

2.10.3. WADI DAYQAH DAM

Figures 2.12 and **2.14** illustrate the typical instrumentation installed in Wadi Dayqah Dam.

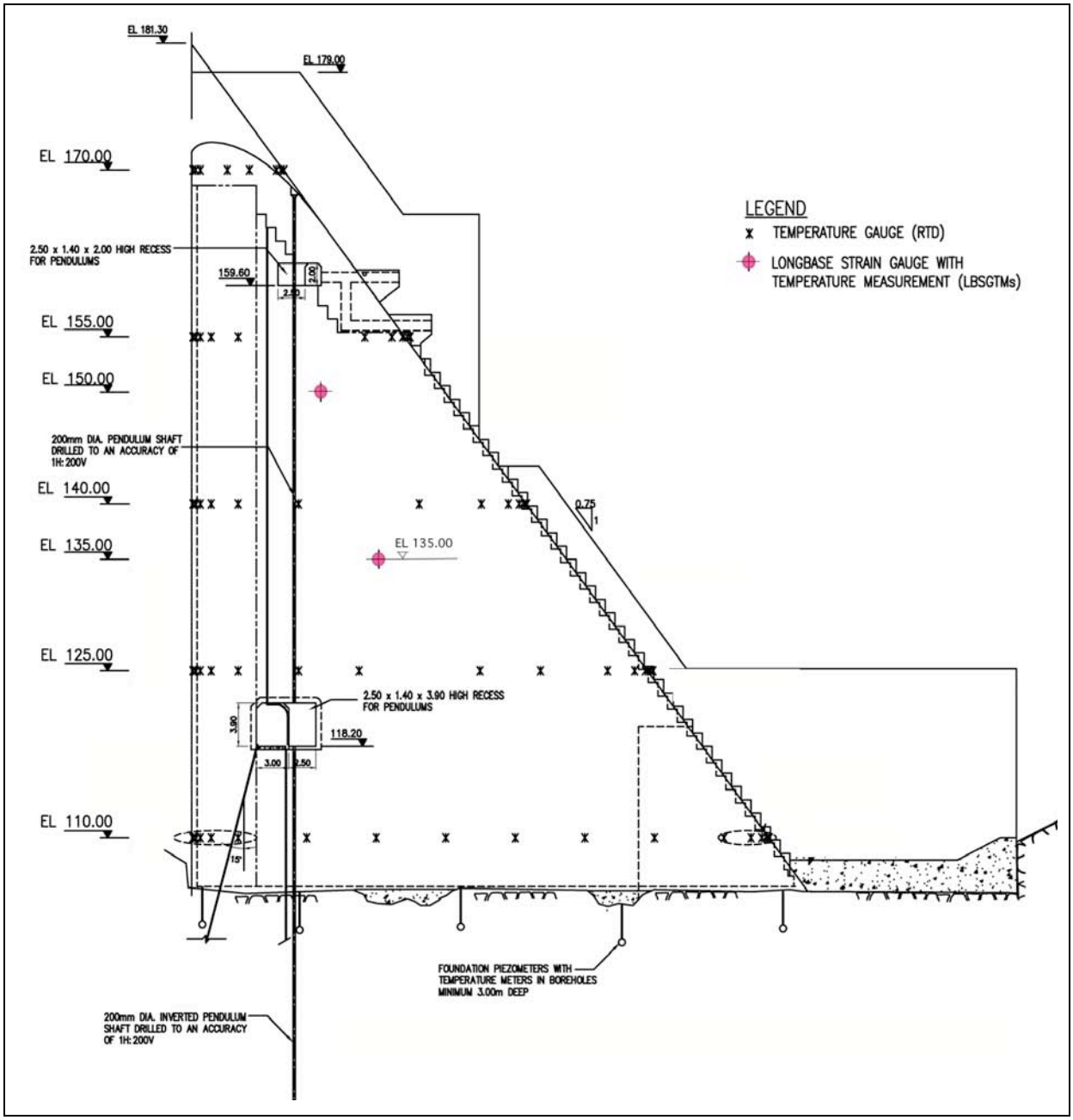

Figure 2.13: Typical Instrumentation - Spillway Section – Wadi Dayqah Dam[13]

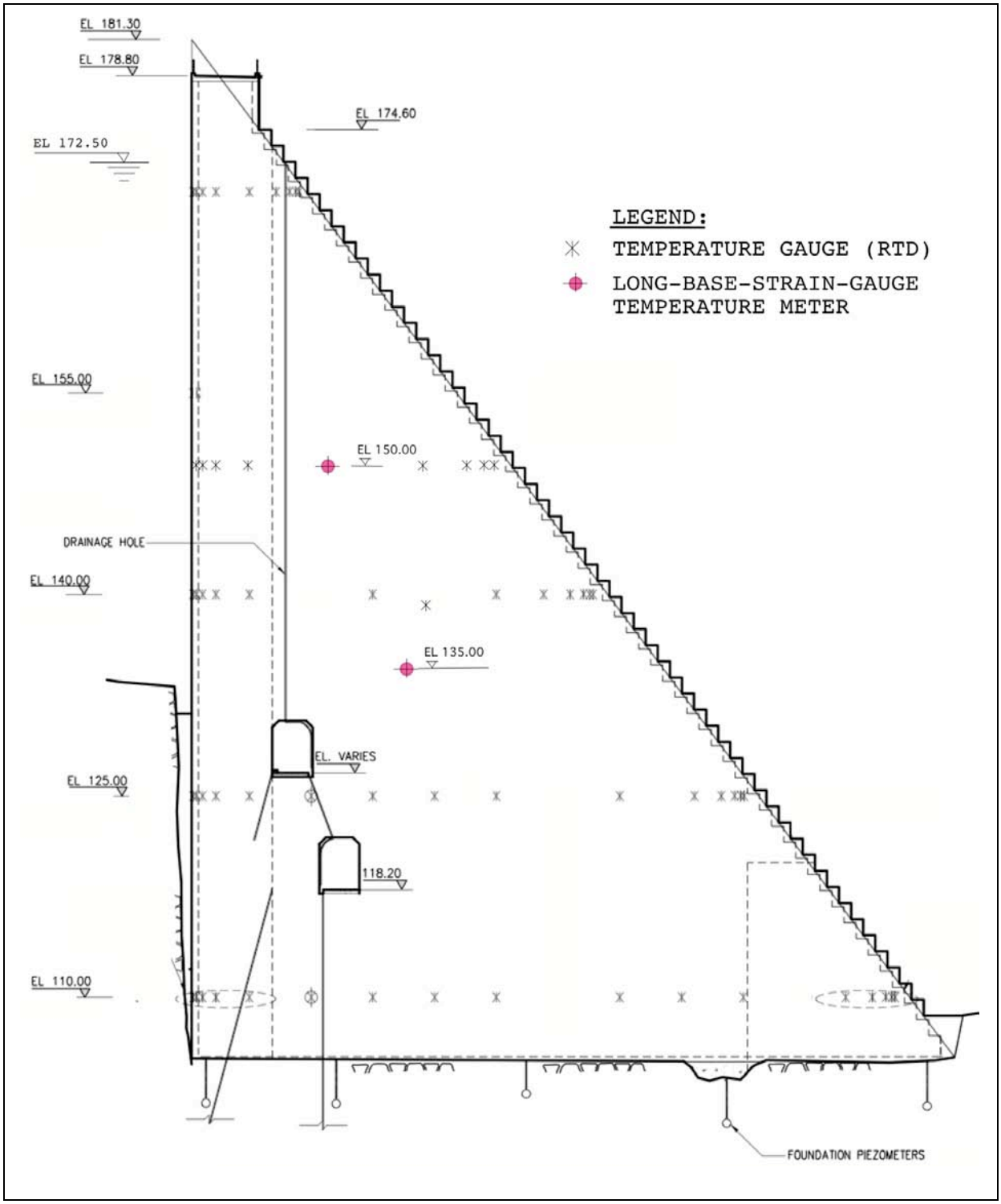

Figure 2.14: Typical Instrumentation - NOC Section – Wadi Dayqah Dam[13]

2.11. REFERENCES

[1] Owens, G. *Fulton's Concrete Technology.* Chapter 8. Ninth Edition. Cement & Concrete Institute. Midrand. RSA. 2009.

[2] ICOLD. Committee on Concrete for Dams. *Roller Compacted Concrete Dams. State of the Art and Case Histories.* ICOLD Bulletin 126. 2003.

[3] Schrader, EK. *Roller Compacted Concrete.* Chapter 20. Concrete Construction Engineering Handbook. Second Edition. Edited by Nawy, EG. CRC Press. New Jersey. 2008.

[4] Shaw, QHW. *DWS 740. Standard Specification. Roller Compacted Concrete for Dams.* Department of Water Affairs & Forestry. Second Edition. August 2005.

[5] McRae, JB & Simmonds, T. *Long-Term Stability of Vibrating Wire Instruments: One Manufacturer's Perspective.* Proceedings of 3rd International Symposium on Field Measurements in Geotechnics. Field Measurements in Geomechanics. Oslo. September 1991.

[6] Shaw QHW, & Maartens, W.W. Department of Water Affairs Internal Report. *Construction and Grouting of the Wolwedans Dam Test Section.* Un-numbered DWAF Report No. Mossel Bay. October 1988.

[7] Shaw QHW, Geringer JJ & Hollingworth F. Department of Water Affairs Internal Report. *Wolwedans Dam Completion Report.* DWAF Report No. K200/02/DE01. Pretoria. April 1993.

[8] The Department of Water Affairs & Forestry Internal Report. *Knellpoort Dam Completion Report.* Information Report No. D203/39/DD04. DWAF, Pretoria. 1991.

[9] SANCOLD. *Large Dams and Water Systems in South Africa.* SANCOLD. CTP-Book Printers. Cape Town, South Africa. 1994.

[10] Özkar Construction Internal Report. *Work Reports. Quality Control Unit.* Ankara, Turkey. July 2005 – February 2008.

[11] Geoconsult. Gibb. ARQ. *Çine RCC Dam. Phase 2 Design Report.* Vol.4 of 4. Drawings. Özkar Construction. Ankara, Turkey. January 2000.

[12] Vinci & CCC Construction JV. Wadi Dayqah Dam. *Quality Control Records.* Quriyat, Oman. February 2008.

[13] Wadi Dayqah Dam JV. *Wadi Dayqah Dam. Drawings for Construction.* Sultanate of Oman. M.R.M.E.W.R. Muscat, Oman. August 2006.

CHAPTER 3

3. LITERATURE AND REFERENCE:

THE TRADITIONAL APPROACH TO DAM DESIGN IN RESPECT OF EARLY CONCRETE BEHAVIOUR AND TEMPERATURE LOADS AND THE ASSOCIATED APPLICATION FOR RCC DAMS

3.1. INTRODUCTION

On the basis of referenced literature, the state of the art in respect of typical design approaches and RCC behaviour in dams, with particular reference to early shrinkage and creep, is presented in Chapter 3.

The literature review is presented in four distinct parts. The first part addresses the accepted approach with which shrinkage and creep are accommodated in CVC dam design and quotes guidelines and other references that have applied the same approach for RCC dams. The second part addresses earlier investigations and laboratory testing that suggest that shrinkage and creep in RCC are similar to that typically expected in CVC. The third part presents notional evidence that supports a view of reduced shrinkage and creep in RCC compared to CVC. The fourth part addresses the characteristics of concrete that increase susceptibility to shrinkage and creep and presents a review of the properties of lean and high-paste RCC in relation to these characteristics.

3.2. BACKGROUND

In setting the scene for the studies undertaken as part of this investigation, it is considered of value to describe the state of the art understanding and practice in respect of managing the early behaviour of concrete and RCC in large dams. In order to promote a better understanding of the need for the work addressed herein, it is considered beneficial to define the early heat development and dissipation processes that impact mass concrete, to discuss how these are managed in conventional mass concrete and to illustrate how the related problems are more complex in the case of Roller Compacted Concrete.

Dam engineering technology applies temperature drop loads to make provision for early concrete shrinkage and creep effects and a particular effort will be made to describe the actual behaviour for which simplified assumptions are made in design.

It is considered particularly relevant to note that 28 of the 118 papers included in the proceedings of the 5th International Symposium on RCC (titled New Progress on RCC Dams) held in Guiyang, China in November 2007, directly addressed the issue

of temperature in RCC dams. This can be compared with 9 out of the submitted 154 papers of the 4th International Symposium on RCC held in Madrid in 2003, indicating the increasing perceived importance of thermal impacts on RCC dams. Also of interest is the fact that while only 4 papers addressed RCC arch dams in 2003, that number increased to 10 in 2007.

PART I: DESIGN FOR EARLY THERMAL EFFECTS IN CVC DAMS

3.3. EARLY CONCRETE BEHAVIOUR IN LARGE DAMS

3.3.1. LITERATURE

The issues of autogenous and drying shrinkage and stress relaxation creep are not specifically addressed in dam design literature, with the consequential shrinkage rather treated as a thermal contraction. The ever-increasing trend towards the almost exclusive use of RCC for the construction of concrete-type dams has, however, resulted in a growing focus on prediction of the early thermal behaviour, as derived through analysis.

The United States Army Corps of Engineers (USACE) has published three guidelines that address the necessary analysis of the early thermal behaviour of RCC dams and the appropriate approach to dam design for long-term temperature loads; *Thermal Studies of Mass Concrete Structures.* 1997[1], *Roller Compacted Concrete.* 2000[2] and *Gravity Dam Design.* 1995[3]. In addition, the USACE's Engineering Manual *Arch Dam Design.* 1994[6] addresses the requirements of thermal design for CVC arch dams. The United States Department of the Interior, Bureau of Reclamation (USBR) *Design of Arch Dams.* 1977[5] includes a chapter on Temperature Studies for Dam Design.

The above literature comprised the primary sources of the subsequent discussion on the manner in which early thermal effects and shrinkage and creep behaviour are traditionally addressed in concrete dam design and how this approach has been applied for RCC dam design.

3.3.2. GENERAL

Thermal issues for large-scale concrete pours can be divided into two specific categories[1]; Surface Gradient and Mass Gradient effects. In principle, Surface Gradient effects are relatively short term in duration and are more critical in the case of CVC than RCC, due to the higher hydration heats generally prevalent in the former concrete type. Mass Gradient effects occur later, as the retained hydration heat is slowly dissipated and are more critical in the case of RCC, in which contraction joints must be induced and for which grouting of contraction joints is a more complex issue. In very large mass concrete dams, the hydration heat can take more than 50 years to be fully dissipated from the dam core.

The intensity of the impact of both surface and mass gradient effects is determined by the magnitude of the hydration heat developed, the placement temperatures and the relative extremities of external temperatures. As a short-term issue, surface gradient effects are generally more intense during winter, while mass gradient effects are largely determined by the overall regional climate.

Due to the fact that hydration heat is evolved early during the strength development process, the consequential thermal expansion is generally accompanied by significant levels of creep. External zones from which hydration heat is quickly dissipated experience lower maximum temperatures and consequently less creep and accordingly, a complex stress field is developed across the structure. Early thermal effects in large-scale mass concrete consequently relate to thermal gradients and the differential development of creep across the structure.

Figure 3.1 illustrates the typical short and longer-term stress development patterns as a consequence of hydration heat development and dissipation within a large concrete body.

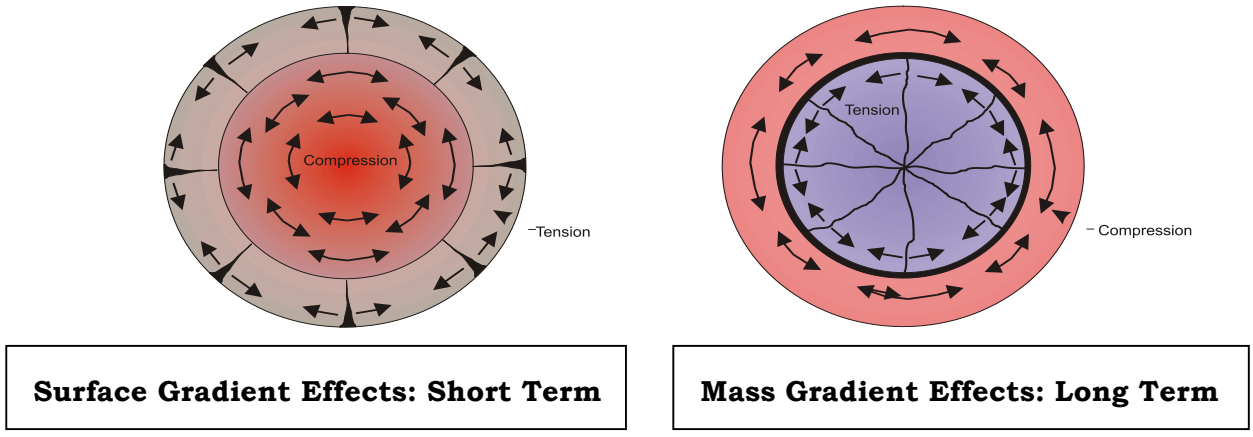

Figure 3.1: Thermal Gradient Stress Development

In a large concrete body, the evolution of hydration heat will cause the body to become significantly warmer than its immediate environment. As the temperature increases, heat will be dissipated relatively rapidly from the surface zone into the cooler external environment and a temperature gradient will develop between the core and the surface of the structure. While in this hot, expanded state, the internal, immature core concrete can experience significant creep, particularly manifested in the form of stress relaxation when thermal expansion is constrained. The surface zones, on the other hand, are never exposed to such high levels of temperature and consequently will not be subjected to the same levels of compressive stress and accordingly, little or no creep is consequently incurred. In this process of heat development and dissipation, two effects are experienced. The first relates to a warmer, expanded core and a cooler surface, which gives rise to core compression and surface tension that can result in cracking. The second

effect occurs later as the core cools and shrinks more than the surface zone as a consequence of the creep experienced and the greater cooling range applicable. This effect results in compression in the surface and tension in the core, potentially giving rise to cracking in the core zone.

The intensities of the surface and mass gradient effects are obviously directly related to the temperature gradients experienced between the core and the surface, during the processes of heating and cooling. The first effect will usually be most pronounced when the internal temperature is at its highest and accordingly the related consequences are usually experienced during the construction period. The second effect will occur later, as the body of the dam cools. As a consequence of the immaturity of the concrete at the time that the highest core temperatures are experienced in a large concrete dam wall, creep will partly mitigate the impact of surface gradient effects. As a consequence of a significantly greater concrete maturity at the later time of occurrence of the mass gradient effects, less creep will occur in mitigation and a higher susceptibility to cracking is developed.

To provide some perspective to any quantitative analysis in respect of the above effects, it is interesting to quote the USBR's *Design of Arch Dams.* 1994[6] as follows:

> *Unlike ordinary structural members undergoing temperature change, the stresses induced in mass concrete structures by temperature changes are not capable of being defined with any high degree of accuracy. The indeterminate degree of restraint and the varying elastic and inelastic properties of the concrete, particularly during the early age of the concrete, make such an evaluation an estimate at best.*

3.3.3. MANAGING EARLY THERMAL GRADIENT EFFECTS IN CVC

While higher cement contents give rise to greater total hydration heat development in the case of CVC, various factors make management of the consequential problems more straightforward than is the case for RCC. Construction in vertical monolithic blocks of limited size (see **Plate 3.1**) and separated from each other with contraction joints, the use of ice and chilled water in the mix and the circulation of cooling water through the placed concrete serve to minimise the thermal tension stresses developed[1]. With higher water contents in CVC than RCC, replacement of water with ice in the mix is more effective in reducing the maximum concrete temperature experienced during hydration, while the circulation of chilled water through steel pipe loops in CVC is effective in drawing out heat and reducing the maximum temperatures experienced in the core zone.

A general rule of thumb[1] for mass concrete suggests maximum internal/external concrete zone temperature differences of 20°C to prevent surface cracking and 15°C to prevent internal cracking.

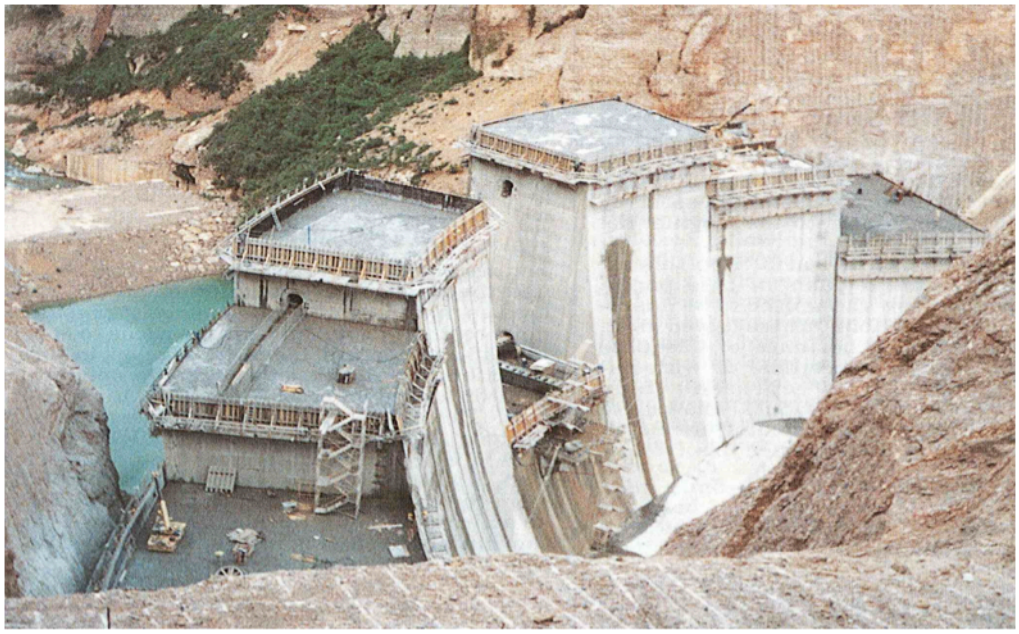

Plate 3.1: CVC Dam Construction in Vertical Monoliths

3.3.4. MANAGING EARLY THERMAL GRADIENT EFFECTS IN RCC

While the author has no knowledge of internal core cracking in RCC having yet been caused by short-term temperature gradient effects, numerous examples exist where surface cracking has been developed. Furthermore, although the total hydration heat development in RCC is typically lower than is the case for CVC, the reduced water content implies that ice is less effective in restricting the maximum temperatures experienced, while the inclusion of cooling pipes is of significantly greater impact on the construction process and realistically impractical.

The management of early thermal gradient effects in large RCC dam construction has to date consequently been achieved primarily by limiting the maximum temperature experienced within the core zone. For typical RCC adiabatic hydration temperature rises of 10 to 18°C, limiting thermal gradients from core to surface to approximately 20°C is relatively straightforward.

In the case of high-workability RCC, the maximum hydration temperature rise can exceed 20°C and pre-cooling of the RCC is consequently usually required in order to maintain acceptable thermal gradients.

In a temperate climate, sensible control of the temperature of each of the constituent materials and sometimes avoiding placement during the warmer parts of the summer season are usually quite adequate to avoid the development of dangerous thermal gradients. In less temperate climates, the use of chilled water and ice is usually required, together with wet-belt cooling of the coarse aggregates,

while in more extreme climates, seasonally restricted placement will be enforced in tandem with an appropriate combination of the previously mentioned measures augmented with others, such as fogging of the placement area.

3.4. INTERMEDIATE THERMAL EFFECTS IN LARGE MASS CONCRETE DAMS

3.4.1. GENERAL

Notwithstanding the importance of the surface gradient thermal effects, it is, however, the longer term cooling of the internal zone of the dam wall that is of most interest in respect of the structural action of an arch dam and in respect of the potential development of cracking parallel to the axis in a large gravity dam. The applicable long-term temperature drop is the difference between the "zero thermal stress temperature" experienced during the hydration cycle and the final equilibrium core temperature, experienced once all of the hydration heat has been dissipated. The consequential thermal shrinkage is accommodated parallel to the axis in RCC dams through the provision of transverse induced joints and perpendicular to the axis by limiting tensile stress through placement temperature restrictions.

Referring to **Figure 3.2** below to illustrate the longer term temperature history typical at the core of a large RCC dam, it can be seen that the maximum macro effects of hydration heat dissipation are only likely to be at their worst long after construction completion.

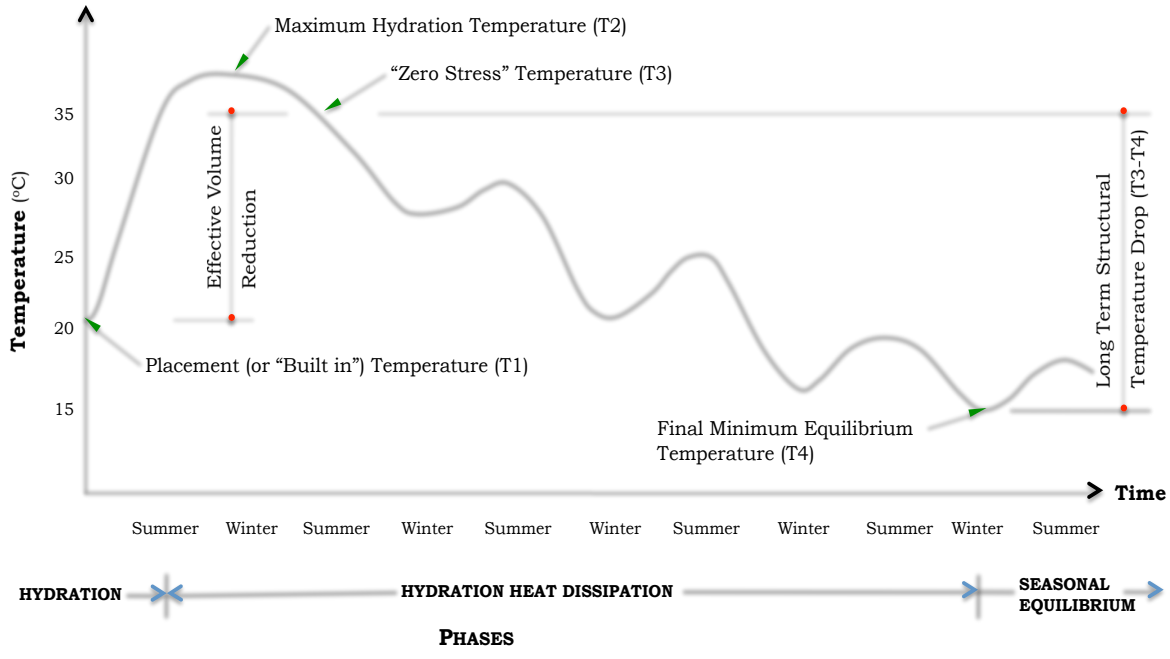

Figure 3.2: Typical Long-term Thermal History

While the maximum temperature within the RCC is generally experienced within a month of placement, the minimum temperatures that determine the maximum temperature drop load will only be experienced during a particularly cold winter after the hydration heat has fully dissipated. In the case of a very large dam, this could be 50 years after completion.

The critical long-term structural temperature drop can accordingly be defined as the difference between the "zero stress" temperature and the lowest temperature experienced once the hydration heat has fully dissipated, towards the end of a particularly cold winter. With the dam wall stress state and volume effectively at equilibrium at the "zero stress" temperature, the restrained shrinkage that will occur with reducing temperature will develop tensions that will give rise to cracking where the concrete tensile strength is exceeded.

In accordance with the indicated design approach, the effective volume reduction in the concrete associated with autogenous and drying shrinkage and stress relaxation creep is correspondingly equated to a thermal contraction consequential to a temperature drop equivalent to the difference between the "Zero Stress" Temperature and the Placement (or "Built in") Temperature.

3.5. DEFINING THE LONG-TERM TEMPERATURE DROP LOAD

3.5.1. TRADITIONALLY ACCEPTED APPROACH

In relating the applicable early structural temperature loadings, the USACE Engineering Manual on *Arch Dam Design* (EM 1110-2-2201)[4] defines a series of key temperature values, T1 to T4, on a temperature history for artificially cooled concrete, as indicated on **Figure 3.3**.

T1 represents the initial placement temperature, T2 the peak temperature experienced as a result of hydration, T3 the natural closure temperature and T4 the design closure temperature, or the contraction joint grouting temperature. Direct comparisons can be made between the temperatures represented by T1, T2 and T4 and those indicated on **Figure 3.2**; T1 being equivalent to the "built in" temperature, T2 being the peak hydration temperature and T4, the final minimum equilibrium temperature. T3, the "zero stress" temperature, is more difficult to define and will depend on the extent of shrinkage and creep that occurred in the green concrete during the heating and cooling cycle.

While T4 represents an artificially cooled temperature, the typical approach is to set the T4 temperature close to the long-term minimum anticipated temperature. If T4 is below the long-term minimum temperature, temperature drop loading on the dam will never be experienced, but arch compressions will be increased during warmer periods. If T4 is above the long-term minimum temperature, the structure needs to be designed for an equivalent temperature drop.

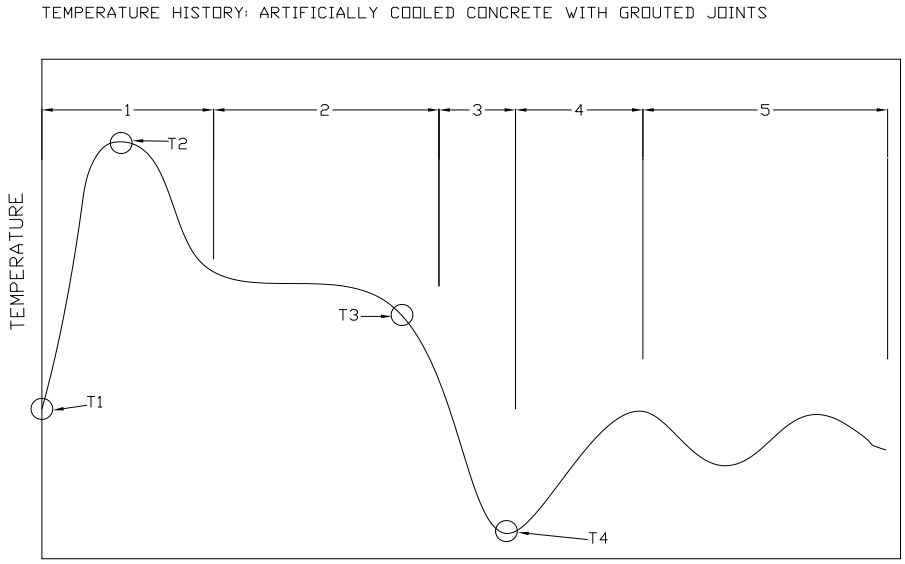

1. Initial cooling period.
2. Period of no pipe cooling. Period can vary from 1 or 2 months to about 1 year, depending on the grouting programme.

3. Intermediate and final cooling periods.
4. Stabilisation period. Requires from 2 to 3 years to 20 years depending on the amount of subcooling and dam dimensions.
5. Final annual temperature cycle.

T1 – Initial placement temperature.
T2 – Peak temperature.
T3 – Natural closure temperature.
T4 – Design closure temperature (grouting temperature).

Figure 3.3: Typical Temperature History for Dam with Grouted Joints[2]

In instances when it is possible to achieve a T3 (natural closure) temperature below the long-term minimum, as illustrated on **Figure 3.4**, no grouting of the contraction joints is necessary and no temperature drop loading will be applicable.

For a conventional mass concrete dam, the long-term structural temperature drop before grouting is accordingly T3 – T4. If T4 is equivalent to the long-term minimum core concrete temperature experienced, T3 – T4 would also represent the structural temperature drop to be accommodated, should the dam wall not be grouted. With T1, T2 and T4 relatively easily measured, the more difficult issue is to establish T3.

In the case of conventional concrete, it is assumed that most of the compression experienced during hydration heat development is dissipated through creep[4] and, while it is dependent on the placement lift height, the “zero thermal stress temperature”, or T3, is taken as 1.5 - 3°C below the maximum temperature experienced during the process of hydration (T2).

The implied design approach accordingly assumes that the long-term thermal cooling that causes shrinkage is incurred by a temperature drop from either the maximum temperature experienced during hydration, or a temperature only slightly lower, down to the lowest core temperature experienced during a particularly cold winter, at some future date[1, 2, 4, 5 & 6]. For a conventional mass concrete, with a total hydration heat temperature rise of perhaps 20°C, this temperature drop (T3 – T4) can accordingly easily exceed 30°C.

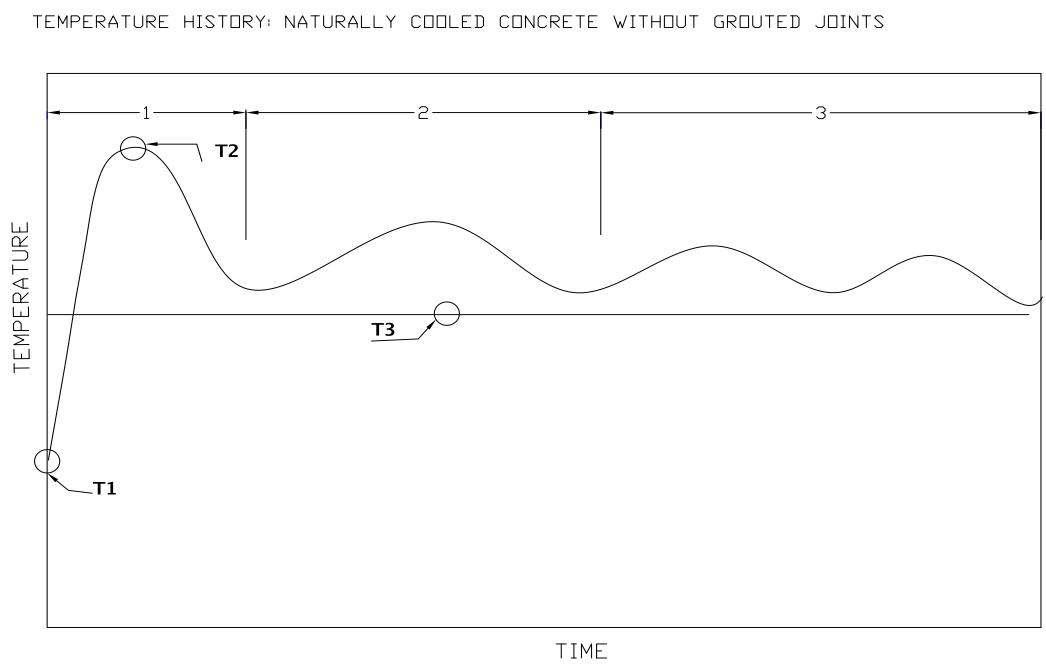

Figure 3.4: Typical Temperature History for Dam without Grouted Joints[2]

The same principles as applied for the "temperature drop" design in the USACE Engineering Manual on *Arch Dam Design*. 1994[4] are repeated in the USBR's *Design of Arch Dams*. 1977[6]. The latter publication indicates that experience has demonstrated that an effective volume reduction of between 125 and 200 microstrain typically occurs for CVC in mass dam pours for arch dams when post-cooling is applied to reduce the maximum hydration temperature by between 5 and 15°C.

3.6. EXAMPLES OF CVC DESIGN MODEL APPLIED FOR RCC

3.6.1. LITERATURE

To confirm the generally accepted application of the above CVC dam design approach to RCC dams, the following examples from referenced literature are provided.

The USACE publication on *Thermal Studies of Mass Concrete Structures* (ETL 1110-2-542). 1997[1] assumes a value for T3 equal to that of T2 in the example thermal analysis presented for the RCC gravity Cache Creek Detention Basin Weir. For the example analysis of a 146 m high RCC gravity dam, T1 is assumed as the temperature in the RCC at the age of 1 day, while T3 is again equated to T2.

In their 2003 paper on thermal stresses in RCC dams, Noorzaei et al[7] stated that the "reference temperature" (T3) is generally established at concrete ages of 0.25, 0.5 or 21 day. However, they considered that the temperature at an age of 30 days, in fact, to be more representative. In the case of mass RCC in a large dam, this temperature would essentially be the maximum experienced during hydration (T2), again suggesting that all of the expansion compression stress is lost to creep.

Zhu[8] describes the thermal issues addressed in the design of a number of RCC arch dams in China, confirming again that conventional CVC behaviour through the hydration cycle is assumed for RCC. While post-cooling has successfully been used prior to the grouting of the induced joints on a number of Chinese dams, the maximum hydration temperature is assumed as the "zero stress" temperature. Unfortunately, no correlation has apparently yet been made in China between the assumed early RCC behaviour and that measured on prototype dam structures.

In their analyses of early RCC stress development during the hydration cycle, Kaitao X & Yun[9] applied creep models developed for conventional concrete, while Carvera et al[10 & 11] used an aging model for a variety of RCC properties and a "solidification theory" creep model, also developed for conventional concrete.

Chen et al [12] varied elastic modulus with time and temperature, whilst applying a CVC model for creep effects, to estimate the structural consequences of hydration heat development and dissipation within a large RCC dam structure. Lackner & Mang[13] proposed a chemoplastic materials behaviour model for RCC to simulate cracking under early thermal effects. While this model was developed for CVC, no comparisons with measured RCC behaviour were included as part of this study.

It is of particular significance to observe that all of the above studies that address the early behaviour of RCC in dams and the consequences thereof failed to compare the predicted behaviour with that actually realised on the prototype structure. Often, it is simply assumed that RCC behaves in the same manner as CVC under the early hydration temperature rise and subsequent dissipation and various models developed for CVC are applied for RCC without any form of verification. No

literature reference seems to exist that evaluates the validity of an assumed CVC behaviour model through comparative measurement on a prototype RCC structure.

PART II: INVESTIGATIONS INTO THE SHRINKAGE & CREEP BEHAVIOUR OF RCC

3.7. INVESTIGATING SHRINKAGE & CREEP BEHAVIOUR OF RCC

3.7.1. LITERATURE

3.7.1.1. Creep

When it comes to establishing the applicable levels of creep in young RCC, conflicting opinions, conflicting approaches and conflicting test data are found in literature. The following references provide evidence to support the contention that RCC will often indicate creep equivalent to, or exceeding that of CVC.

Andriolo[14] states that creep in young concrete is mainly affected by the aggregate modulus of elasticity and the filler material in the mix. Due to the fact that the mortar content of an RCC mix will almost always be higher than an equivalent CVC mix, RCC will indicate a higher level of creep than CVC comprising the same aggregates. Generally, aggregates with a low modulus of elasticity will produce concrete with high creep.

In laboratory testing for their thermal and stress analysis of the Cana Brava Dam in Brazil, Calmon et al[15] found values of creep that were typically 20% higher for a low strength RCC (9 MPa at 90 days) than for a slightly higher strength CVC (12 MPa at 90 days).

In their thermal analysis for Mujib Dam in Jordan, Husein Malkawi et al[16] used age-dependent elasticity moduli curves to evaluate stress levels during the early hydration heat development cycle, concluding that these gave rise to a more realistic estimation of stress within the dam structure. Creep was not addressed beyond acknowledging that non-linear behaviour occurs in RCC during early hydration heat-related expansion and that consequently the "zero stress" temperature will be increased above the placement temperature.

To determine creep values for the thermal analysis of Dahuashui RCC arch dam, Penghui et al[17] applied time and stress dependent coefficients, in a multi-term expression, whereby certain constants were apparently derived through testing to an accuracy of 6 decimal places. Unfortunately, no consequential values for creep, or the consequential impact thereof are presented.

Investigations published by Conrad et al[18] discussed the installation and monitoring of modified stress measurement gauges in the CVC facing and RCC close to the upstream face at the Mujib Dam in Jordan. These gauges require RCC with the same characteristics and age as that simultaneously placed on the dam to be compacted within a 400 mm long x 56 mm diameter steel pipe. From the results of these gauges, the study concluded that the zero stress (T3) temperature for the CVC was only marginally beneath the peak temperature experienced during hydration, while the zero stress temperature for the RCC was approximately 3.5°C below the hydration peak. In the case of the CVC, the data suggested that at least 18°C of the effective hydration temperature rise had been lost to shrinkage and creep. In the case of the RCC, the interpretation of the results suggested that approximately 2/3 (or 7°C) of the hydration temperature rise was lost to shrinkage and creep.

While the Stress/Time graph presented for the surface CVC already indicated tension approximately 1 day after placement and the formation of a crack once a tension of 2.1 MPa was reached, the same graph for the RCC indicated very minor levels of tension developing after approximately 4 months and contradictory levels of stress during the subsequent two summer seasons. With a temperature of 37.1°C corresponding to the first incidence of zero stress on the gauge, Conrad interpreted this to be the zero stress temperature for the RCC. Despite never subsequently experiencing a temperature above 37°C, however, compressions of up to 1.1 MPa and maximum tensions of just 0.2 MPa are paradoxically subsequently experienced over the following two years. Observed seasonal temperature variations over this period from approximately 24°C to 37°C correspond with stress variations between 0 and 1 MPa compression. This data would suggest an apparent zero stress temperature of approximately 25°C (rather than 37.1°C), which is below the placement temperature of 30°C. While it may be that the relief of tensile stresses elsewhere through cracking changed the stress state at the gauge in question, there is no direct evidence of such an occurrence and at least the indicated pattern is considered to compromise the certainty with which the zero stress value at the gauge can be defined as 37.1°C. The increasing compression indicated on the surface gauge in question is actually considered to be a reflection of the ongoing shrinkage (thermal and possibly creep) of the internal core RCC.

3.7.1.2. Thermal Modeling

A number of studies have been published that compare the predicted temperatures in RCC dams with measurements on the applicable prototypes[19, 20, 21, 22 & 23] and the technology of temperature prediction has been demonstrated through monitoring to be accurate and reliable. Several of these thermal studies have translated temperatures into the prediction of stress states and while Conrad et al[21] and Yi et al[23] used such studies to back-analyse stress states, only Conrad et al[18] actually

attempted to verify predictions through measurement on a prototype structure, as discussed above.

3.7.2. DISCUSSION

When reviewing the results of the Mujib investigations[18] in respect of the RCC behaviour, it is important to consider a variety of influencing factors, as follows:

- The location of the monitoring point relatively close to the surface can significantly influence the findings. For example, while the hydration heat at the gauge may have been dissipated sufficiently quickly to allow the temperature to follow the ambient cycle very quickly, the core temperature will almost certainly have remained elevated for a number of years further, influencing the stress state at the surface.

- Experience has demonstrated that confirmatory data from a number of instruments are realistically necessary before any quantitative evaluations can realistically be made.

- Bearing in mind the problems associated with the manufacture of RCC cubes and cylinders, it would be reasonable to question whether it is possible to create RCC within a 56 mm diameter pipe with the same characteristics as RCC placed in the dam.

- Presumably as a result of the use of pure cement, without pozzolans, the RCC appears to have experienced a peak hydration temperature, and correspondingly expansion, within only a few days of placement while consequently still of very low strength.

The RCC of Mujib Dam, in which the above instrumentation was installed, was a low strength, lean mix material, with a low cementitious materials content (85 kg/m^3) and a high water content (137 l/m^3 & w/c = 1.61). In such a mix, no excess paste would be available and accordingly, lower densities would be anticipated. The high apparent water content would have been designed to allow a reasonable modified Vebe time and consequently, more moisture would have been provided than required for the hydration process, resulting in an increased tendency for drying shrinkage and an increased susceptibility to creep. While it is not considered possible to draw any specific conclusions on the basis of the limited data available, the nature of the RCC of Mujib Dam is such that some autogenous shrinkage and creep would be expected.

Furthermore, it is considered particularly significant to note of the fact that all of the above studies that indicate equivalent, or greater creep and shrinkage compared to CVC refer specifically to lean, or low cementitious materials content RCC.

3.7.3. APPLYING TYPICAL ANTICIPATED RCC BEHAVIOUR

In the core of a large RCC dam with a mix including a large proportion of pozzolan, the hydration heat builds up to a maximum over a period typically of approximately 90 days, with perhaps 85% of the peak temperature achieved within 30 days of placement[6 & 24]. According to the various literature for which creep testing is referenced[25, 26 & 15], RCC that is loaded at an age of say 15 days, and which loading is sustained for 365 days, will creep at a rate of between 50 to 100 x 10^{-6} per MPa stress. For a temperature rise of approximately 15°C, an average (sustained) elastic modulus of say 10 GPa and a thermal expansion coefficient of say 10 x 10^{-6}/°C, a consequential compressive stress of 1.5 MPa would be developed as a result of the hydration temperature rise. Consequently, creep of the order of 75 to 150 x 10^{-6} would be anticipated. Such creep would effectively increase the reference, or zero stress temperature in the RCC by between 7.5 and 15°C. On the basis of this type of calculation, it can clearly be seen why it would be considered appropriately conservative to set the reference temperature equal to the maximum hydration temperature (T2).

Applying Schrader's[27] graphical relationship between strength at the time of initial loading, and creep and assuming an effective initial strength of 5 MPa at loading, would indicate a 365 day creep of approximately 70 microstrain per 1 MPa containing stress. For a sustained temperature rise of 15°C in the centre of a large dam, the containing stress may be approximately 1.5 MPa, for which a total creep of approximately 105 microstrain would accordingly be anticipated. This is of a similar order to other indications.

PART III: EVIDENCE TO SUPPORT REDUCED SHRINKAGE & CREEP IN RCC

3.8. NOTIONAL EVIDENCE OF SHRINKAGE & CREEP BEHAVIOUR OF RCC

3.8.1. LITERATURE

3.8.1.1. Drying Shrinkage

The USACE's Engineering Manual *Roller Compacted Concrete*. 2000[2] states that while drying shrinkage is governed primarily by the water content and the mixture and characteristics of the aggregates, RCC drying shrinkage is similar, but generally lower than CVC, as a consequences of the lower moisture contents. However, the effects of drying shrinkage are usually considered to be negligible and are consequently ignored for mass concrete in dams, as moisture cannot escape from

the interior and only surface zones are accordingly likely to experience any drying shrinkage.

Laboratory investigations by Xia et al[25] and Kaitao[8] suggested that RCC indicates typical drying shrinkage of the order of 50 to 75% of that applicable for the equivalent CVC. Dependent on the aggregates used, a total 90 day drying shrinkage of 100 to 300 microstrain can be anticipated. While drying shrinkage in RCC appears to continue for approximately 5 months after compaction, the majority has occurred within the first 90 days.

In the ICOLD Bulletin 126, *Roller-Compacted Concrete Dams.* 2003[29], it is stated that drying shrinkage is limited to the exposed surfaces of the RCC mass.

3.8.1.2. Autogenous Shrinkage

The USACE's Engineering Manual *Roller Compacted Concrete.* 2000[2] states that autogenous shrinkage can be a significant factor for all mass concrete and is particularly dependent on the proportions of the mix and particularly the content and type of aggregates. Autogenous shrinkage occurs over a significantly longer period than drying shrinkage, but can be negligible, or even take the form of an expansion.

In Chapter 20 of the *Concrete Construction Handbook.* 2008[27], Schrader briefly discusses autogenous volume changes, stating that this cannot be reliably estimated in RCC, or CVC in mass dams. However, in some RCC, early expansion has been followed by later contraction, while the reverse has also been observed.

The ICOLD Bulletin 126, *Roller-Compacted Concrete Dams.* 2003[29] states that autogenous changes in volume are normally inconsequential.

3.8.1.3. Creep

Testing on a number of RCCs and CVCs by Zhu et al[26] indicated a general pattern of substantially lower creep in RCC than CVC. Testing by Xia et al[25] for the Yantan coffer dam suggested very similar levels of creep for RCC and CVC, with fractionally higher creep in RCC loaded at a very early age and significantly higher creep in CVC loaded at an age of 1 year. This work would seem to be confirmed by testing by Conrad et al[18], which indicated a lower early elastic modulus and a higher long-term modulus for low-cementitious RCC, when compared with an equivalent CVC.

In Chapter 20 of the *Concrete Construction Handbook.* 2008[27] Schrader states that a very high creep rate, with dramatic reductions in stress over time, is possible with low-cementitious-content RCC mixtures. This characteristic is seen as beneficial in respect of improving the crack resistance of massive placements subject to thermal stress by reducing the sustained deformation modulus (E value). Schrader[27] goes on to state that assuming creep in tension is equivalent to creep in compression

can be conservative, particularly for mixtures containing a relatively high content of coarse aggregates and that aggregate-to-aggregate contact can decrease creep in compression. Comparing creep measured across a large number of RCC samples, Schrader observed that specific creep does not increase significantly for RCC with a compressive strength greater than 15 MPa at first loading. The same graph (Figure 20.34) suggests that RCC of higher strength tends to indicate lower creep than equivalent strength CVC. For RCC of a lower strength than 5 MPa at first loading, however, creep increases exponentially with reducing strength.

Testing for the Miel Dam in Columbia, López et al[28] demonstrated a very significant decrease in creep with increasing cement content. Loading the specimens at 7, 28 and 90 days, the reduction in creep with increasing cement content was progressively more pronounced the earlier the initial loading.

3.8.1.4. Total Shrinkage

The USACE EM 1110-2-2006 guideline on *Roller Compacted Concrete*. 2000.[2] observes that typical maximum joint openings on RCC dams generally vary between 1 and 3 mm, for typical induced joint spacings of between 15 and 40 m. These observations are in stark contrast with the extent of joint openings predicted on the basis of the characteristics apparent through the referenced laboratory testing and analysis. For joint spacings of 15 to 40 m, “accepted theory” would anticipate maximum joint openings of between 5 and 15 mm.

The ICOLD Bulletin 126, *Roller-Compacted Concrete Dams*. 2003[29] states that induced joints are usually spaced at greater distances than typically applied for CVC dams.

The weight of notional evidence of reduced shrinkage in respect of RCC compared to CVC is particularly strong at the De Hoop Dam[30], which is an 85 m high RCC gravity dam currently under construction on the Steelpoort River in Mpumulanga. At De Hoop Dam, cracking has been observed in a number of the CVC concrete pours, including the mass concrete outlet block. The boat slipway, on the other hand, which was cast as part of the final RCC trials, demonstrates an RCC placement of several hundred metres in length, manufactured with the same materials, without a single trace of cracking. While no RCC placement lifts exceeding 2.4 m have yet been achieved, no cracking at all is evident on the various stretches of RCC placed to date on the dam wall.

While the related investigations and the associated Thermal studies are described in more detail in Chapters 4 and 5, important observations of the apparent early behaviour of the RCC can be made at Changuinola 1 Dam. Cracking in the surface of the RCC has been observed on all large blocks left exposed for periods exceeding approximately 3 weeks. Simulation through the Thermal study reveals these cracks to form as a result of excessive temperature gradients and the associated differential expansion of the RCC mass, compared with the surface. Applying a

scenario with no creep to represent the worst-case situation, the development of these cracks was predicted with some accuracy. Applying internal creep (or total shrinkage) of just 25 microstrain in the Thermal analysis was sufficient to substantially reduce the likelihood of these cracks forming during the first three months after placement.

3.8.2. DISCUSSION

The general literature discussion on the subject suggests that creep in RCC under early thermal load is beneficial in reducing the stresses developed through temperature gradients[2 & 27]. In more extreme climates and in the case of RCC mixes with a relatively high heat of hydration, this is undoubtedly true. However, what might be a beneficial effect in mitigating stresses developed through short-term thermal gradients, is in fact disadvantageous in increasing the effective long-term temperature drop.

To illustrate this point quantitatively, it is considered of value to review the impacts of the autogenous shrinkage and creep typically assumed in accordance with a "Traditional RCC Materials Model", which might assume a "typical" total volume reduction of 150 microstrain to account for the combined impacts of autogenous shrinkage and stress relaxation creep during thermal expansion. For a further temperature drop of the order of 8°C to the long-term average core body temperature and a coefficient of thermal expansion of 10 x 10^{-6}/°C, total shrinkage of the order of 230 microstrain might be anticipated for RCC in the core of a large dam. Assuming RCC with a sustained elastic modulus of 15 GPa, total strain of this order would develop tensions of 3.45 MPa, well in excess of the tensile strength capacity of any RCC.

For transverse joints spaced at say 20 m centres, such shrinkage would suggest joint openings of 4.6 mm. Over a dam wall length of 270 m, as is the case for Wolwedans Dam, total concrete "shrinkage" would equate to approximately 62 mm.

In the cases of all of the dams for which the author of this work has data, no evidence is available to suggest a shrinkage, or net volume reduction, approaching the levels predicted by the traditional theory. In fact, quite the opposite and the data to be presented as part of this thesis firmly contradict the theoretical behaviour of RCC, suggesting substantially lower levels of autogenous shrinkage and creep under early thermal loading.

PART IV: A COMPARISON OF THE MATERIALS CHARACTERISTICS OF HIGH-PASTE RCC COMPARED TO CVC IN DAMS

3.9. A LITERATURE REVIEW OF SHRINKAGE & CREEP IN CONCRETE

3.9.1. GENERAL

Before going on to review RCC in dams against those characteristics that make a concrete more, or less susceptible to shrinkage and creep, it is first worth briefly reviewing and discussing the phenomena of shrinkage and creep in concrete. In the process of a literature review, it is possible to develop a greater understanding of the associated differences in behaviour between RCC and CVC. Consequently, it is also possible to isolate those characteristics of an RCC mix that should be given specific attention in design when it is important to minimise shrinkage and creep.

Shrinkage and creep in concrete are very similar[31], inter-related effects and the susceptibility of concrete to both of these phenomena relates to the nature of its composition and the manner in which it is formed and develops strength. As the cementitious materials in concrete hydrate, they form a gel, which has a smaller volume than its constituents. As the cement paste shrinks in this process, the bond between the paste and the aggregates and the structure between the different sized and shaped aggregate particles serve to resist a general shrinkage of the concrete. The net result is a structure with internal residual shrinkage stresses and micro-cracks.

To complicate this situation further, the matrix experiences expansion stresses as a consequence of the heat evolved during the exothermic reaction of hydration. As a result, hardened concrete is actually a complex network of micro-structures, internal stresses and micro-cracking, whose consequential susceptibility to creep under load is obvious.

The extents of early autogenous/drying shrinkage and creep in concrete are dependent on a number of factors, primarily related to the paste content and the characteristics of the mortar sand[31 & 38].

In the following sections, shrinkage, creep and the typical early behaviour of concrete are discussed.

3.9.2. SHRINKAGE

Shrinkage in concrete comprises two components; autogenous shrinkage, which develops immediately after setting, and drying shrinkage, which is a consequence of the long-term loss of moisture. Autogenous shrinkage is caused by the consumption of water in the hydration process, or could be perceived as a consequence of the gel formed through hydration being of a reduced volume than its constituent components, of cementitious materials and water.

Conventional concrete will usually contain more water than can chemically be combined with the cement, with the consequence that, in a normal environment, water will eventually be lost from the concrete, resulting in drying shrinkage. Autogenous shrinkage experienced and measured in concrete is a small fraction of that which occurs in the cement itself[33]. The aggregate particles in concrete dilute the effect of the cement shrinkage and the bond between the aggregates and the cement paste causes a restraining effect on the overall shrinkage.

The lower the w/c ratio in concrete and the greater the degree of hydration, the greater the volume of the hydration product (gel) and the greater the ratio of gel pore to capillary pore volume. As the paste dries, it loses capillary water first, then absorbed water and then gel-pore water. As a consequence, low cementitious materials content concretes demonstrate a greater tendency for both autogenous and drying shrinkage.

The chemical composition of cements used in concrete influences the extent of shrinkage that can be expected, with the tri-calcium aluminate phase and the gypsum content being of specific importance[33]. An optimum sulphate content appears to exist for minimum shrinkage, while higher alkali cements indicate higher shrinkages.

Investigations by the National Building Research Institute (NBRI)[33] demonstrated that a relatively good correlation exists between the shrinkage of mortar and the specific surface of the mortar and its constituent aggregates. Furthermore, aggregate properties such as size and grading affect shrinkage of concrete indirectly as a consequence of their influence on the mix water requirements[32].

The use of aggregates that themselves demonstrate drying shrinkage can increase concrete shrinkage very substantially.

3.9.3. CREEP

Creep in concrete is associated with the presence of mobile water in the paste and accordingly, the greater the moisture content, the greater the creep[31] and the greater the component of the moisture that is not consumed in the hydration process, the greater the susceptibility to creep.

Normal density aggregates of hard gravel or crushed rock do not usually exhibit creep at the stress levels typical of normal concrete and particularly mass concrete. On the other hand, aggregate grading and volume concentration have a significant, if indirect, influence on concrete creep, with a higher aggregate content resulting in less creep. This is unsurprising, as the higher the concentration and elastic modulus of the aggregate, the higher the restraint against creep exerted on the paste.

The impact of admixtures on concrete creep has demonstrated some significant variability, with the effects apparently varying dependent on the specific conditions and the specific methods of testing. Various testing work in South Africa has

demonstrated a substantial influence of aggregate type on creep[32]. While this work also took into account the water demand of the aggregates, creep was found to be a variable phenomenon that necessitated specific laboratory testing in critical cases.

The intensity and rate of drying of concrete have been found to be of specific influence on the extent of creep subsequently observed[34]. Work by Grieve[35] found that fly ash has a benefit in reducing creep in concrete, while Ground Granulated Blastfurnace Slag (GGBS), on the other hand, can sometimes result in increased creep[33].

A significant amount of experimental work has been undertaken on the creep behaviour of conventional concrete and a number of algorithms have been developed to predict creep at various ages[31 & 33]. In view of the fact that all such work is based on empirical observation, the documented observed differences in the early behaviour of RCC compared to CVC must compromise the value of any of these approaches in respect of RCC.

3.9.4. PROPERTIES OF CONCRETE WITH PARTICULAR INFLUENCE ON SHRINKAGE & CREEP

In summary of the above, factors that have been demonstrated to impact shrinkage and creep in concrete include the following:

- A high w/c ratio, as this tends to imply that more moisture is present than required for hydration and this will eventually be lost with consequential drying shrinkage,
- Excess water not consumed in the hydration process increases the susceptibility of concrete to creep,
- A dry environment and direct exposure to the atmosphere increase drying shrinkage,
- The rate of drying of concrete increases creep,
- A high aggregate content reduces shrinkage and creep,
- A smooth aggregate surface (rounded gravels) reduces the aggregate/paste bond and accordingly gives rise to increased shrinkage and creep,
- A high proportion of fine aggregates and particularly non-cementitious fines increases shrinkage, and
- The use of fly ash in concrete decreases shrinkage and creep.

3.9.5. OTHER IMPORTANT INFLUENCES

Techniques for the manufacture of mortar and conventional concrete test samples relatively accurately replicate the process applied in full-scale construction. The methods used for the manufacture of RCC cubes and cylinders, on the other hand do not particularly accurately replicate the effect of roller compaction applied on full-scale construction. Furthermore, the difficulties inherent to the manufacture of RCC samples on a laboratory scale give rise to a comparatively broad spread of test results. In comparison to CVC, for which many more years of technological development and a significantly broader range of utilisation exist, these problems, limited experience in a developing technology and a use generally limited to dam construction can be seen to have compromised the level of understanding of the early shrinkage and creep behaviour of RCC developed to date.

Drying shrinkage is measured in the laboratory in a mortar form, while creep is measured on concrete moulded in cylinders with the > 50 mm aggregate removed. Creep is typically tested at loads up to 40% of the compressive strength of the sample at the start of testing[37]. Neither of these testing conditions replicate the insulated, contained and relatively low stress environment typical of the core of a dam.

Conrad et al[38] investigated the stress-strain behaviour of low strength RCC of between 6 hours and 365 days age. While the RCC mix used for this research was of a low cementitious materials content (85 kg/m^3) and a very high w/c ratio (1.61), the complexity of the RCC moulding process was also recognised as a factor that gave rise to a more pronounced variability in the results recorded across a number of samples of the same material. The investigations found that the development of the deformation modulus in RCC was quite different to that of CVC and concluded that common approaches for the temporal evolution of the modulus of deformation of concrete in compression are not applicable for low-cementitious RCC. This testing, however, suggested that the deformation modulus for a low-cementitious materials content RCC would be lower than that of an equivalent CVC at early ages, but higher at later ages.

3.10. HIGH-PASTE RCC IN LARGE DAMS

In respect of a high-paste RCC within a large dam body, the conditions are perhaps ideal, as the factors that tend to increase the tendency of concrete to shrink and creep are not generally evident. The following factors are important:

- In a high-paste RCC, the w/c ratio will be low (0.5 to 0.65) and all available moisture will be consumed in the hydration process,
- In a large dam body, the RCC is well protected against rapid and surface drying and any form of drying shrinkage is unlikely to be a factor at the core of a dam,

- Even high paste RCC mixes contain a high aggregate content compared to a high strength structural concrete, and
- Fly ash, or an active pozzolan, is often used in high paste RCC.

Sembenelli & Shengpei[39] also considered that the slower rate of hydration heat evolution of RCC compared to CVC would imply a comparatively higher modulus in the case of RCC at the time of maximum temperature-induced compressive stress. Suggesting that the peak hydration temperature in mass CVC is usually reached within 3 to 7 days of placement, compared to 28 days or more in the case of RCC containing a high percentage of pozzolanic materials, it was considered that the modulus of elasticity in the case of RCC would be higher by the time the peak hydration temperature was reached. As a result, RCC should be less susceptible to creep under the associated contained expansion (compressive) stress. Putting this supposition into the context of the findings of the investigations addressed in this study, the records for the dams studied suggest that approximately 70% of the hydration temperature rise in RCC is typically evident within 3 to 5 days of placement. Consequently, it can be stated that while RCC may gain some benefit due to a slower and lower hydration heat development, that benefit is not likely to be particularly significant in respect of reducing its susceptibility to creep under contained expansion stresses.

It is considered likely that fly ash in an RCC mix adds significant benefits, through increasing the mobility of the paste and slowing the rate of moisture loss by reducing permeability. In view of the fact that fly ash has been demonstrated to reduce creep in concrete[35], it is considered likely that the autogenous shrinkage of cementitious paste is reduced when fly ash is used in relatively large proportions.

As a result of the various factors listed, however, it is considered un-surprising that shrinkage and creep effects in high-paste RCC are in fact not as prevalent as is the case in an equivalent CVC.

It is also considered that the method of compaction is likely to decrease the susceptibility of RCC to shrinkage and creep. If it can be stated that the skeletal structure formed by the aggregates in concrete acts to restrain the shrinkage of the paste during hydration, the compaction energy exerted on RCC undoubtedly ensures that

Plate 3.2: A Modern RCC at De Hoop Dam

this skeletal structure is better developed, with inter-aggregate particle contact, and stronger than will be the case for immersion vibrated compaction.

3.11. CONCLUSIONS

3.11.1. SUMMARY

On the basis of the foregoing literature study, the following indications in respect of the early shrinkage and creep behaviour of RCC can be deduced:

- In terms of dam design, RCC is often assumed to behave in the same manner as CVC, in terms of shrinkage and creep performance.
- Dam design approaches generally simplify creep and shrinkage behaviour into an assumed thermal contraction.
- The autogenous shrinkage and creep characteristics of RCC can be highly variable.
- Drying shrinkage effects are negligible within the core of a large dam structure and can be ignored for the purpose of the investigations addressed into the early behaviour of RCC in large dams.
- Creep can be expected to be very high in low strength, low cementitious materials content RCC mixes.
- Creep and autogenous shrinkage will be reduced in concretes with low water contents, high aggregate contents and effective particle-to-particle contact within the aggregate skeletal structure.
- The use of fly ash in RCC is beneficial in respect of reduced shrinkage and creep.
- Whereas a high paste content in CVC usually implies high autogenous shrinkage and creep, “High-paste RCC” would be considered to indicate a relatively low-paste content, and actually indicates a relatively large aggregate content and a low water content, compared to CVC.

On the basis of the preceding review, it is quite clear that the best performance from RCC, in respect of least shrinkage and creep during the hydration cycle, can be anticipated in a high-paste, low water content mix, with well-graded, high quality aggregates and particularly sand with a relatively low compacted void ratio.

With its high aggregate content, low water content, relatively high strength and effective particle-to-particle aggregate skeletal structure, as a concrete, the characteristics of a “high-paste” RCC are probably as ideal as possible for the reduction of autogenous shrinkage and creep.

Evaluating the RCC of the dams investigated as part of this study against these requirements, they would rank as Wolwedans, Knellpoort, Changuinola 1, Çine and Wadi Dayqah; realistically in line with expectations as to apparent level of shrinkage and/or creep.

Early shrinkage and creep in concrete are interdependent effects that occur simultaneously during the process of maturation. The early development of internal shrinkage creates a susceptibility to creep under load. With negligible drying shrinkage in the core of a mass concrete block, the important shrinkage is autogenous shrinkage. While shrinkage and creep are used together in this Thesis, the dominant effect is undoubtedly manifested as creep; a stress relaxation that occurs when the temperature rise associated with the hydration process attempts to cause thermal expansion in immature concrete.

3.11.2. THE WAY FORWARD

On a qualitative basis, the above review has allowed the characteristics of "high-paste" RCC to be demonstrated to be as ideal as possible for a concrete in respect of the reduction of creep and shrinkage. The various information and references quoted, however, confirm that no quantitative analyses have yet been made on a large-scale of the creep and autogenous shrinkage behaviour typical of high-paste RCC in a dam.

The discussions confirm the general problem of sample manufacture and the fact that it is not realistically possible to recreate the full-scale compaction conditions and effect inherent to RCC construction on a laboratory scale.

Having introduced the dams instrumented and discussed the major issues in respect of design and the early behaviour of RCC in dams in this Chapter, the instrumentation data from the dams addressed will be presented in Chapter 4.

3.12. REFERENCES

[1] United States Army Corps of Engineers. *Thermal Studies of Mass Concrete Structures.* Engineering Technical Letter, ETL 1110-2-542. USACE. Washington. May 1997.

[2] United States Army Corps of Engineers. *Roller-Compacted Concrete.* Engineering Manual, EM 1110-2-2006. USACE. Washington. January 2000.

[3] United States Army Corps of Engineers. *Gravity Dam Design.* Engineering Manual, EM 1110-2-2200. USACE. Washington. June 1995.

[4] United States Army Corps of Engineers. *Arch Dam Design.* Engineering Manual, EM 1110-2-2201. USACE. Washington. May 1994.

[5] Boggs HL, Jansen RB & Tarbox GS. *Arch Dam Design and Analysis.* Chapter 17. Advanced Dam Engineering. Van Nostrand Reinhold. New York. 1988.

[6] United States Department of the Interior. Bureau of Reclamation. *Design of Arch Dams.* US Government Printing Office. Denver. 1977.

[7] Noorzaaei J, Ghafouri HR & Aminin R. *Investigation of the Influence of Placement Schedule on the Thermal Stresses of RCC Dams, using Finite Element Analysis.* Proceedings. 4th International Symposium on Roller Compacted Concrete Dams. Madrid, Spain. pp 669-674. 2003.

[8] Zhu, B. *RCC Arch Dams: Temperature Control and design of Joints.* Journal of International Water Power and Dam Construction. Progressive Media. Sidcup, UK. August 2006.

[9] Kaitao X & Yun D. *Study on the Influence of Limestone Powder on Roller Compacted Concrete Performance and Action Mechanism.* Proceedings. 5th International Symposium on Roller Compacted Concrete Dams. Guiyang, China. pp 467-479. 2007.

[10] Cervera, M, Oliver, J & Prato, T. *Simulation of Construction of RCC Dams. I: Temperature & Aging.* ASCE. Journal of Structural Engineering. pp 1053 - 1061. September 2000.

[11] Cervera, M, Oliver, J & Prato, T. *Simulation of Construction of RCC Dams. II: Stress & Damage.* ASCE. Journal of Structural Engineering. pp 1062 - 1069. September 2000.

[12] Chen, Y, Wang, C, Li, S, Wang, R & He, J. *Simulation Analysis of Thermal Stress of RCC Dams using 3-D Finite Element Relocating Mesh Method.* Advances in Engineering Software. Elsevier. Vol. 32 pp 677 - 682. 2001.

[13] Lackner, R & Mang, H.A. *Chemoplastic Materials Model for the Simulation of early-Age Cracking: From the Constitutive Law to Numerical Analyses of Massive Concrete Structures.* Cement & Concrete Composites. Elsevier. Vol. 26 pp 551 - 562. 2004.

[14] Andriolo A. *Materials & RCC Quality Requirements.* Proceedings. 4th International Symposium on Roller Compacted Concrete Dams. Madrid, Spain. pp 61-78. 2003.

[15] Calmon JL, Murcia J, Botassi dos Santos, Gambale E & da Silva CJ. *Numerical Modelling of Thermal Stress in RCC Dams using 2-D Finite Element Method – Case Study.* Proceedings. 4th International Symposium on Roller Compacted Concrete Dams. Madrid, Spain. pp. 569 – 577. 2003.

[16] Husein Malkawi, AI, Aufleger, M, Strobl, TH, Conrad, M, Mutasher, S & Al-Jammal, M. *Computational Analysis of Thermal and Structural*

Stresses for RCC Dams. The International Journal on Hydropower and Dams. Issue Four, pp 86 – 95. 2004.

[17] Penghui L, Hong C, Hongbo L, Yu H & Feng J. *3-D Simulating Analysis for Thermal Control during Construction Period on Dahuashui RCC Arch Dam.* Proceedings. 5th International Symposium on Roller Compacted Concrete Dams. Guiyang, China. 2007. pp 577 – 581.

[18] Conrad M, Hoepffner R & Aufleger M G. *Innovative Monitoring Devices for an Integral Observation of Thermal Stress behaviour of Large RCC Dams.* Proceedings. 5th International Symposium on Roller Compacted Concrete Dams. Guiyang, China. pp 777-784. November 2007.

[19] Conrad M. Aufleger M. Malkawi AIH. *An Advanced Temperature Monitoring System at Mujib and Wala Dam.* - In: Proc. of the Int. Conf. on Roller Compacted Concrete Dam Construction in Middle East 2002, Irbid, Jordan. April 2002.

[20] Aufleger M, Conrad M, Strobl Th, Malkawi AIH & Duan Y. *Distributed fibre optic temperature measurements in RCC dams in Jordan and China.* – Roller Compacted Concrete Dams. Proceedings. 4th Int. Symposium on Roller Compacted Concrete (RCC) Dams, Madrid, pp 401 - 407. November 2003.

[21] Conrad M, Kisliakov D, Aufleger M, Strobl Th & Malkawi AIH. *Simplified Thermo-Mechanical Modelling of a Roller Compacted Concrete (RCC) Dam – Evaluation of the Numerical Model and Influences of some Concrete Parameters.* - Proceedings of the 6th Int. Congress on Thermal Stresses 2005,Vienna. May 2005.

[22] Aufleger M, Conrad M, Goltz M, Perzlmaier S & Porras P. *Innovative Dam Monitoring Tools based on Distributed Temperature Measurement.* – Jordan Journal of Civil Engineering (JJCE), Vol. 3, December 2006. Jordan University of Science and Technology (JUST), Irbid, Jordan, ISSN 1026-3721, 2006.

[23] Yi L, Guoxin Z, Jianwen L, Ping Y, Yihua D & Yongsheng G. *Back Analysis of Temperature Field and Temperature Stress of Jinghong RCC Dam.* Proceedings. 5th International Symposium on Roller Compacted Concrete Dams. Guiyang, China. pp 557-564. November 2007.

[24] Shaw QHW & Greyling RP. *A New Model for the Behaviour of RCC in Dams under Early Thermal Loading.* Proceedings. 5th International Symposium on Roller Compacted Concrete Dams. Guiyang, China. pp 61-68. 2007.

[25] Xia C, Kunhe F & Li Z. *Mineral Admixtures' Impact on RCC Anti-Crack Performance.* Proceedings. 5th International Symposium on Roller Compacted Concrete Dams. Guiyang, China. pp 475-480. 2007.

[26] Zhu B, Xu P & Wang S. *Thermal Stresses and Temperature Control of RCC Gravity Dams.* Proceedings. 3rd International Symposium on Roller Compacted Concrete Dams. Chengdu, China. pp 65-77. 1999.

[27] Schrader, EK. *Roller Compacted Concrete.* Chapter 20. Concrete Construction Engineering Handbook. Second Edition. Edited by Nawy, EG. CRC Press. New Jersey. 2008.

[28] López, J, Castro, G & Schrader, E. *RCC Mix and Thermal Behaviour of Miel I Dam – Design Stage.* – Roller Compacted Concrete Dams. Proceedings. 4th Int. Symposium on Roller Compacted Concrete (RCC) Dams, Madrid, pp 789 - 797. November 2003.

[29] ICOLD. Committee on Concrete for Dams. *Roller Compacted Concrete Dams. State of the Art and Case Histories.* ICOLD Bulletin 126. 2003.

[30] Department of Water Affairs. *External Review Panel Report No 11* - De Hoop Dam. Report No. ERP 11. August 2009.

[31] Neville, AM. *Properties of Concrete.* Chapter 9. Fourth Edition. Pearson Prentice Hall. London. 2002.

[32] Alexander, MG. *Properties of Aggregates in Concrete, Phase I and II.* Research reports prepared for Hippo Quarries. University of Witwatersrand. Johannesburg. 1990 and 1993.

[33] Owens, G. *Fulton's Concrete Technology.* Ninth Edition. Cement & Concrete Institute. Midrand. RSA. 2009.

[34] Bryant, AH. & Vadhanavikkit, C. *Creep Shrinkage - Size and Age at Loading Effect.* ACI Materials Journal. Vol. 84. No. 2. Mar-Apr 1987.

[35] Grieve, GRH. *The Influence of Two South African Fly Ashes on the Engineering Properties of Concrete.* PhD Thesis. University of Witwatersrand. Johannesburg. 1991.

[36] Alexander, MG. *Deformation Properties of Blended Cement Concretes Containing Blastfurnace Slag and Condensed Silica Fume.* Advances in Cement Research. Vol.6. No. 22. Johannesburg. April 1994.

[37] ASTM.*C 512 – 02. Standard Test Method for Creep of Concrete in Compression.* ASTM International, West Conshohocken. USA. August 2002.

[38] Conrad. M, Aufleger, M & Husein Malkawi, AI. *Investigations on the Modulus of Elasticity of Young RCC.* Proceedings. 4th International Symposium on Roller Compacted Concrete Dams. Madrid, Spain. pp 729 - 733. 2003.

[39] Sembenelli, SC & Shengpei, W. *Chinese Experience in the Design and Construction of RCC Arch Dams.* International Journal of Hydropower & Dams. Vol. 5. pp 95 - 100. 1998.

CHAPTER 4

4. INVESTIGATING THE EARLY THERMAL BEHAVIOUR OF ROLLER COMPACTED CONCRETE IN LARGE DAMS

4.1. BACKGROUND

In Chapter 3, the specific behaviour occurring in concrete during the hydration temperature development and dissipation cycle in large dams was investigated through referenced literature. In addition, the associated design methodologies traditionally applied for CVC and RCC dams were presented and discussed. Against this background, data from five prototype RCC dams are presented and evaluated in Chapter 4 in an effort to develop a picture of the actual, measured behaviour of the constituent RCC.

4.2. INTRODUCTION

In this Chapter, the author presents and reviews instrumentation data from Wolwedans and Knellpoort Dams in South Africa, Çine Dam in Turkey and Wadi Dayqah Dam in Oman. In addition, some preliminary data collected for the first RCC placed in the dam wall at Changuinola 1 Dam is presented.

As a means to demonstrate the validity of the thermal analysis for Çine Dam and the consequential patterns of temperature dissipation, a comparison is presented of the predicted and measured temperatures in the dam.

Each of the dams addressed and the associated instrumentation installed is described in Chapter 2. The arrangements of the installed instrumentation are illustrated in Chapter 2 and **Appendix C**.

4.3. WOLWEDANS DAM

4.3.1. INSTRUMENTATION DATA

4.3.1.1. General

The network of monitoring instrumentation installed at Wolwedans Dam comprises Long-Base-Strain-Gauge-Temperature-Meters installed across all induced joints, bearing pressure cells at the dam/foundation contact, a number of water and air temperature meters on the dam surface, piezometers in the foundation, seepage measurement weirs in the galleries, pendulums and inverted pendulums in the dam

wall and the foundation and a total of 86 displacement measurement reference points on the dam wall and in the foundation.

For the purposes of reviewing the behaviour of the RCC, the deformation on the induced joints is considered of greatest importance and for that purpose data from the 209 LBSGTMs installed at 4 different elevations (27 + 60 + 80 + 42) must be studied[1 & 2].

4.3.1.2. Typical LBSGTM Data

Temperature and deformation histories for each of the LBSGTMs for the period from installation until the end of 1996 are provided on a CD included with this Thesis. Typical temperature and deformation histories at LBSGTMs on each of the four instrumentation levels are provided for illustration in **Figures 4.1** to **4.8**.

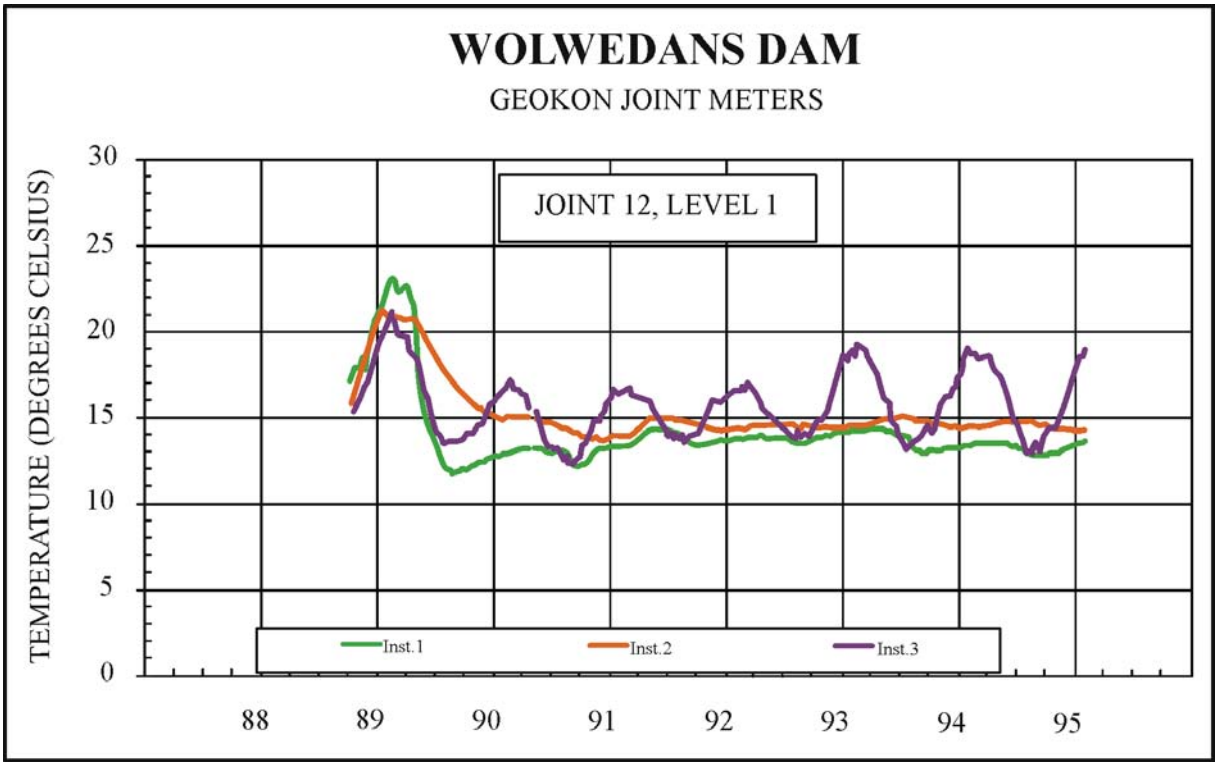

Figure 4.1: Temperatures on LBSGTMs at RL 40.25 m[1 & 2]

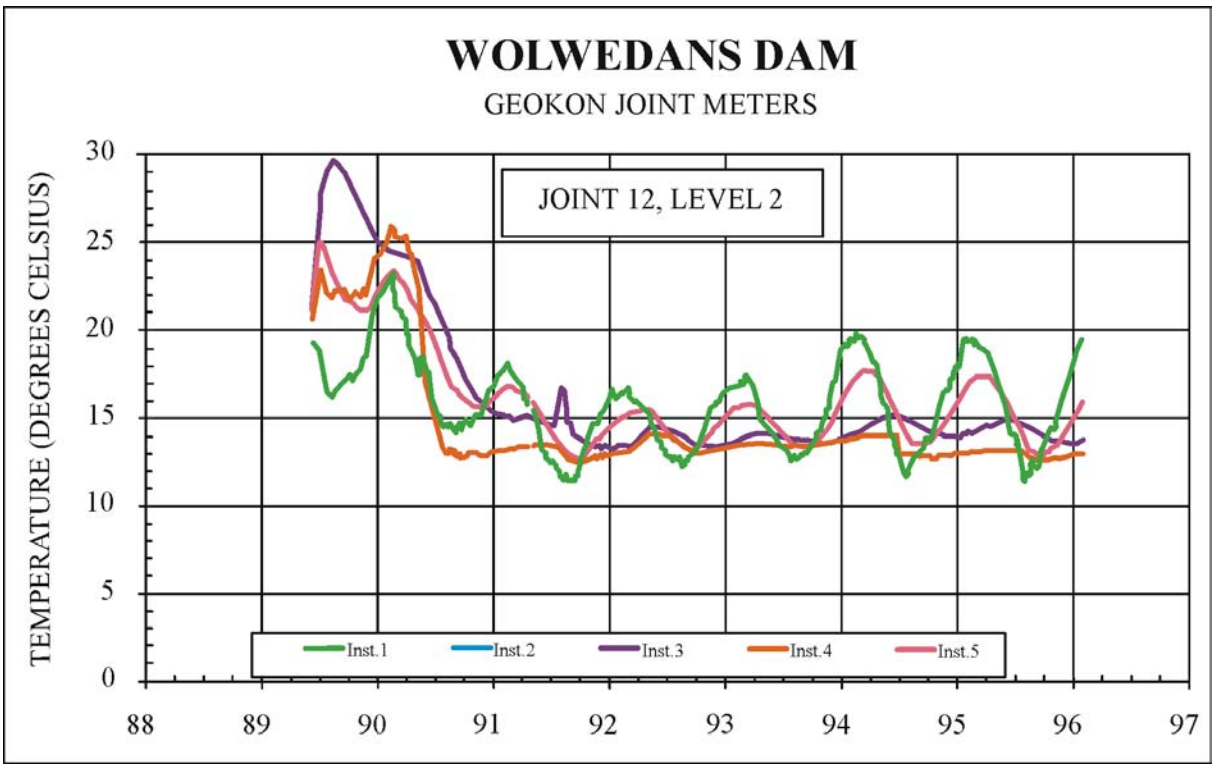

Figure 4.2: Temperatures on LBSGTMs at RL 52.25 m(1 & 2)

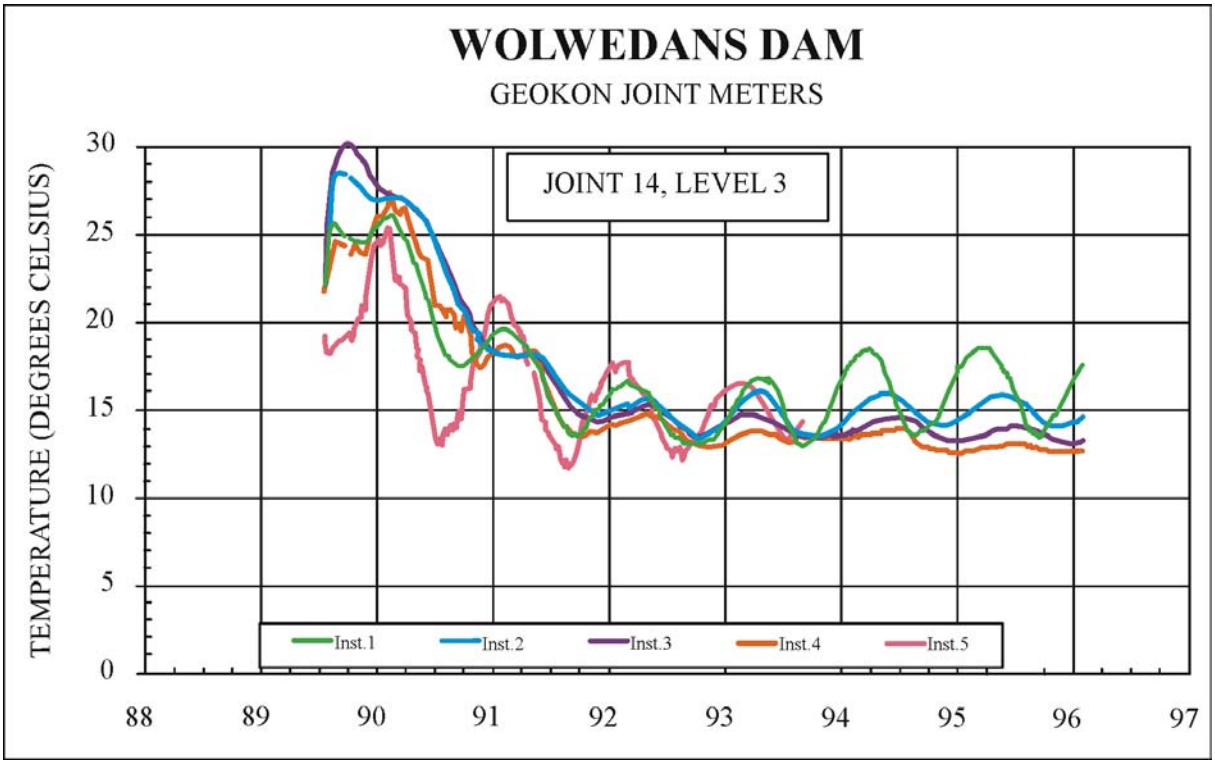

Figure 4.3: Temperatures on LBSGTMs at RL 66.25 m(1 & 2)

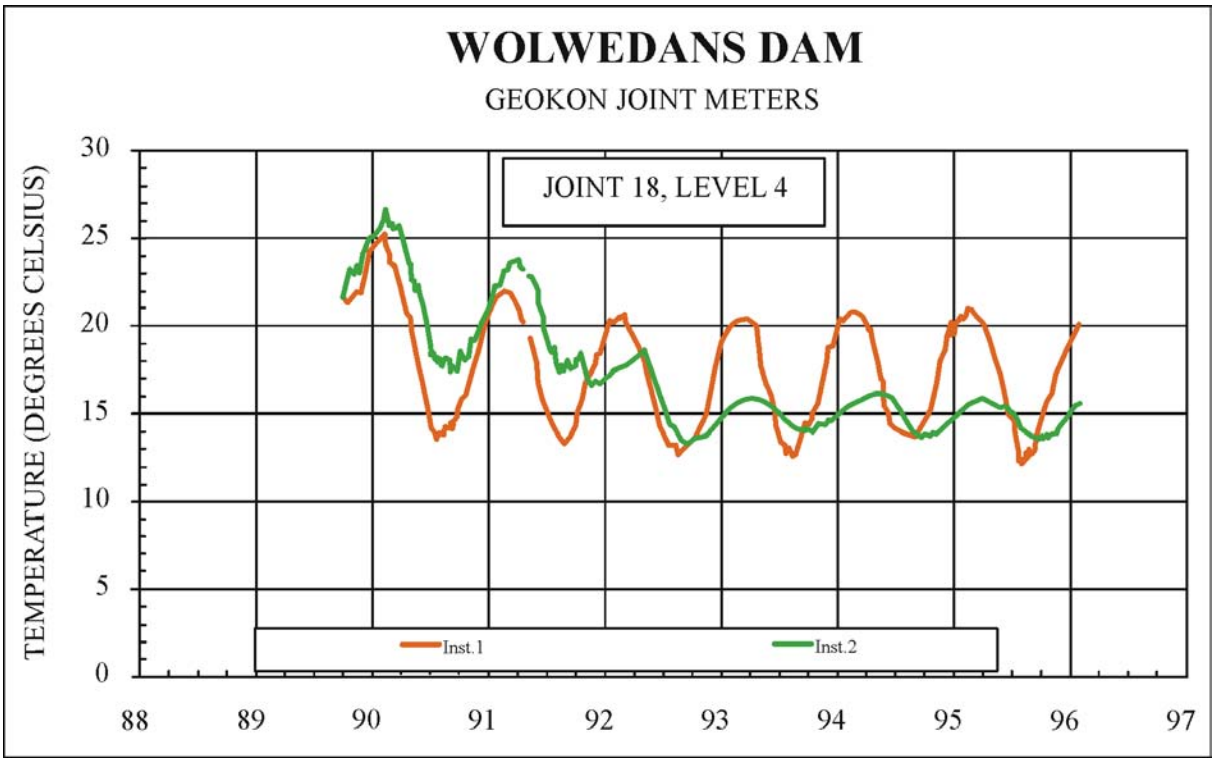

Figure 4.4: Temperatures on LBSGTMs at RL 84.25 m(1 & 2)

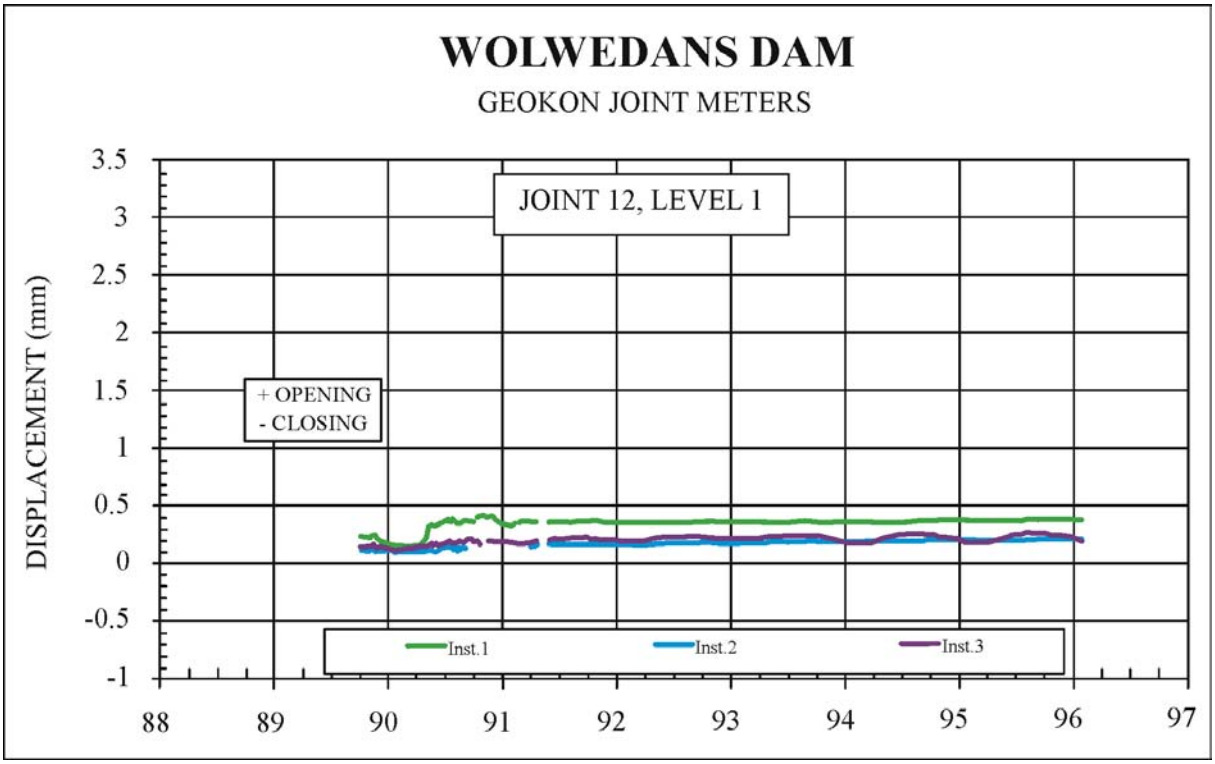

Figure 4.5: Displacement at Joint 12 on LBSGTMs at RL 40.25 m(1 & 2)

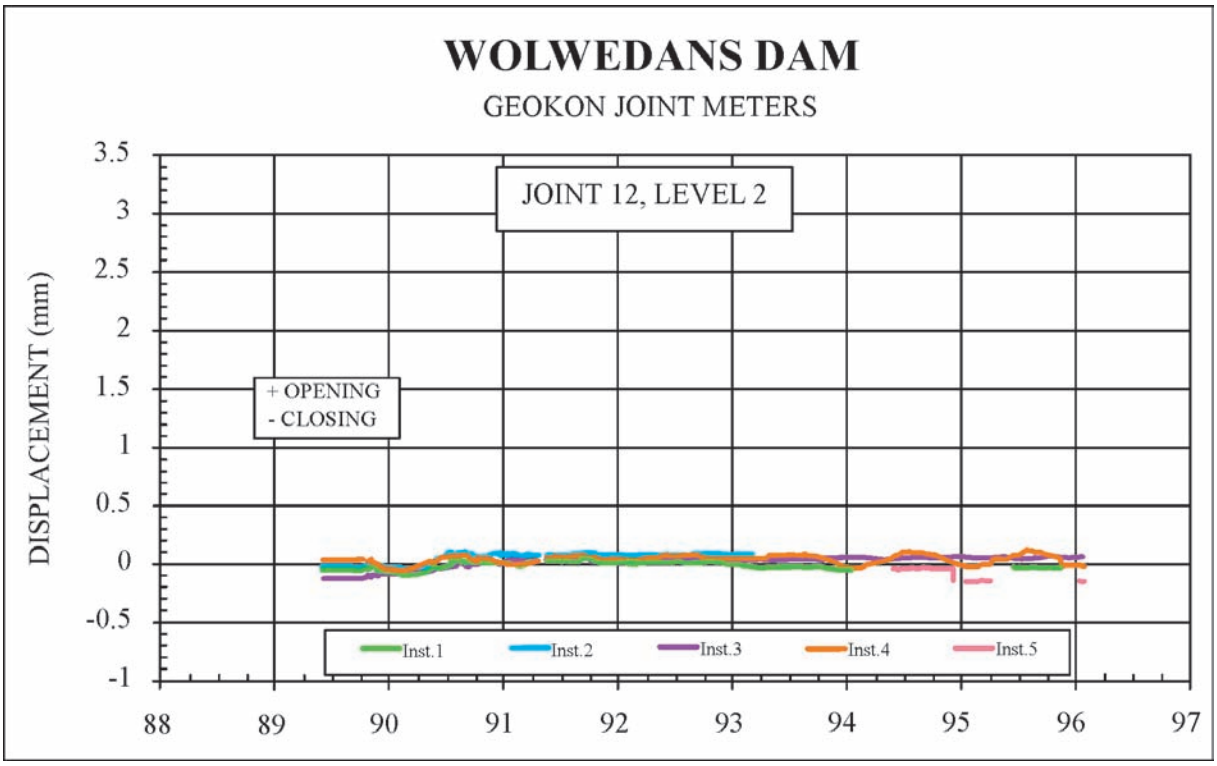

Figure 4.6: Displacement on LBSGTMs at RL 52.25 m(1 & 2)

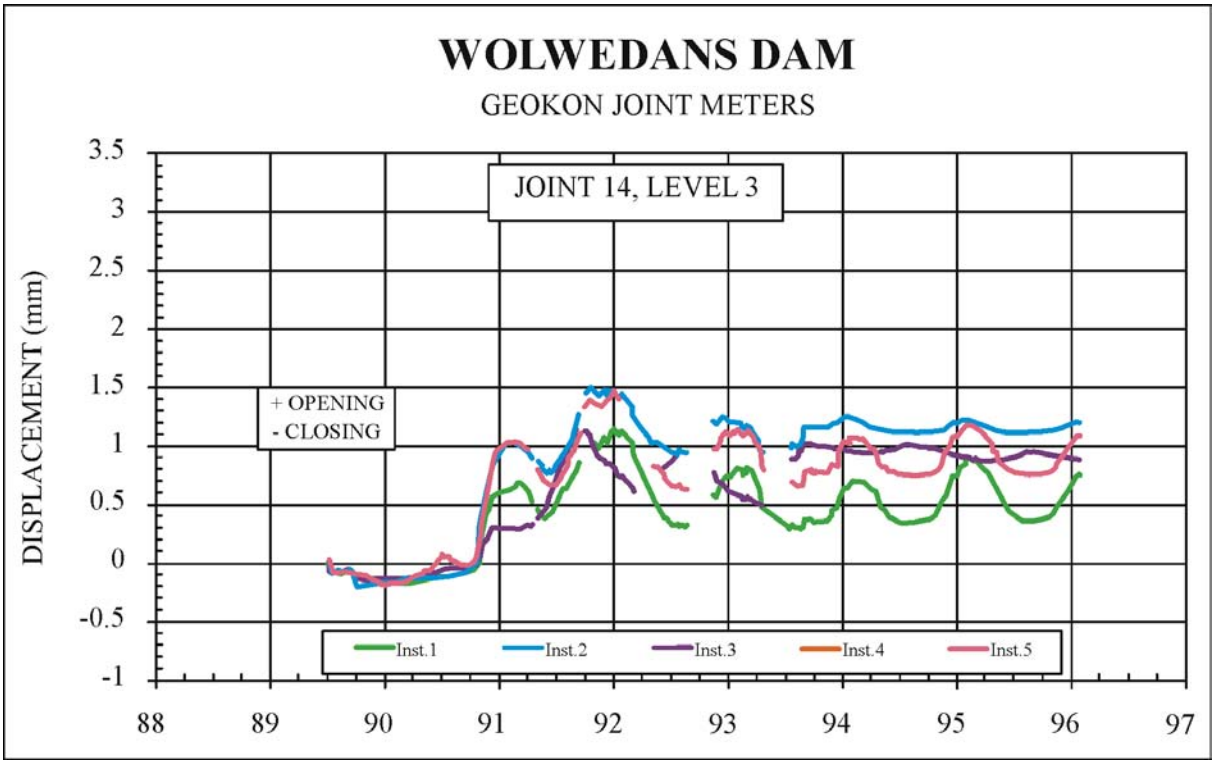

Figure 4.7: Displacement on LBSGTMs at RL 66.25 m(1 & 2)

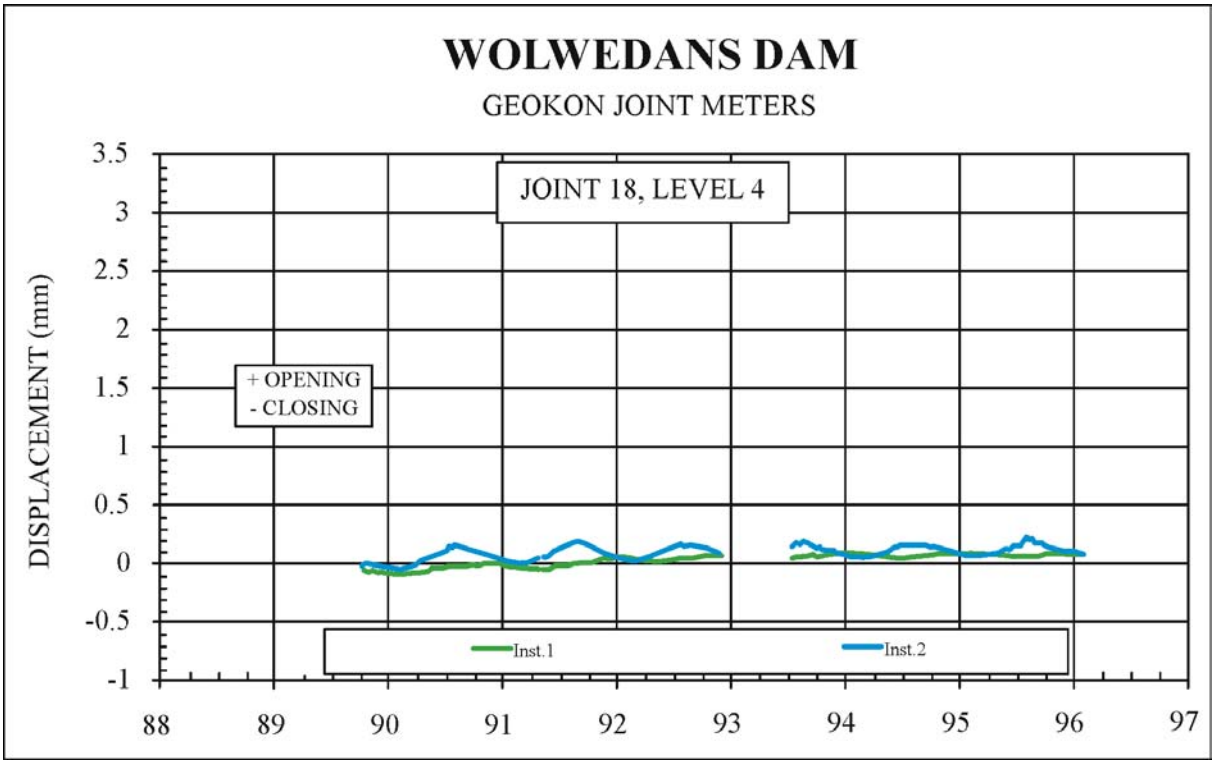

Figure 4.8: Displacement on LBSGTMs at RL 84.25 m(1 & 2)

4.3.1.3. Typical LBSGTM Data Review

The instrumentation levels in Wolwedans dam are numbered from the bottom up and the LBSGTM gauges are numbered from the upstream to the downstream. The various temperature development and dissipation patterns are clearly illustrated, with the core gauges demonstrating the highest rises, as a result of trapped hydration heat, and the smallest long-term seasonal variations and the upstream surface gauges indicating lower seasonal variations than the downstream gauges, as a result of the insulation effect of the reservoir water mass.

Due to the exposure of the first RCC placement to RL 48 m over the period December 1988 to mid May 1989 and the relative proximity of the instruments to the foundation rockmass, it can be seen that the hydration temperature at level RL 40.25 m (Level 1) had essentially fully dissipated by the beginning of 1990. At levels 2 and 3 (RL 52.25 m and RL 66.25 m), it can be seen that the full impact of the hydration heat had only realistically been dissipated during 1992.

It is also significant to note that the only joint to open on the example displacement plots above was Joint No. 14 on Level 3. Bearing in mind that the storage level in the dam had risen to full essentially by late 1992, a situation never consequently existed when the full impact of the loss of hydration heat on the joint opening could be reviewed without the influence of the water load.

Tables 4.1 to **4.4** provide a typical indication of the measured core joint openings during the first winter after the hydration heat had full dissipated (July 1993).

Table 4.1: Core Induced Joint Openings at Level 1 (RL 40.25 m)(1 & 2)

Jt No	11	12	13	14	15	16	17	18	19	Total
Opening (mm)	1.2	0.15	0.45	0.15	0.15	1.6	1.45	0.65	0.1	5.9

In July 1993, the temperature in the core of the dam at RL 40.25 m was approximately 14.5°C, approximately 2°C below the placement temperature, or 8.5°C below the peak hydration temperature. The total joint opening, just 7 m above the foundation, translates into approximately 68 microstrain. Joint 11 is the interface between the RCC and a CVC structure and ignoring this joint would reduce the effective shrinkage across the joints to approximately 50 microstrain. While the levels of residual stress between induced joints and the impact of the foundation restraint cannot be known, the above would suggest some minor creep (approximately 30 microns) occurred in the RCC at this level.

Table 4.2: Core Induced Joint Openings at Level 1 (RL 52.25 m)(1 & 2)

Jt No	9	10	11	12	13	14	15	16	17	18	19	20	Total
Opening (mm)	0.05	0.1	0.9	0	0	1.3	0	0	2.0	0.05	0.75	0	5.15

In July 1993, the temperature in the core of the dam at RL 52.25 m was fractionally below 14°C, approximately 7°C below the placement temperature, or 16°C below the peak hydration temperature. The total joint opening translates into approximately 40 microstrain, suggesting that some closure of the induced joints must have occurred as a result of the water loading, whether, or not any creep of the RCC had occurred.

Table 4.3: Core Induced Joint Openings at Level 1 (RL 66.25 m)(1 & 2)

Jt No	7	8	9	10	11	12	13	14	15	16	17	18	19	20	21	Total
Opening (mm)	0	1.0	0	0	0	0	0	0.95	0	0	1.45	0	0	0	0	3.4

In July 1993, the temperature in the core of the dam at RL 66.25 m was a little below 14°C, approximately 8°C below the placement temperature, or 16°C below the peak hydration temperature. The total joint opening translates into approximately 30 microstrain.

Table 4.4: Upstream Induced Joint Openings at Level 1 (RL 84.25 m)(1 & 2)

Jt No	5	6	7	8	9	10	11	12	13	14	15
Opening (mm)	0	0.15	0	0.2	0	0	0.1	0.08	0.03	0.04	0
Jt No	16	17	18	19	20	21	22	23	24	25	Total
Opening (mm)	0.04	0	0.04	0.1	0.08	0.12	0.11	0.1	2.05	0.08	3.32

* - A LBSGTM was not placed at the centre of the section at RL 84.25 m.

In view of the fact that the gauges at RL 84.25 m were not installed in the centre of the cross section of the dam wall, no real evaluation can be made of the total joint opening, except to state that the variation relate simply to seasonal, surface temperature effects. In this regard, it is particularly pertinent to note that the maximum indicated openings occur during summer on the upstream gauges and during winter on the downstream gauges.

4.3.1.4. LBSGTM Data at RL 66.25 m

In studying the induced joint displacements, the situation at approximately mid-height on the dam (Level No. 3 – RL 66.25 m) is considered to provide the most useful information, as the dam structure at this level is sufficiently broad that temperatures within the core are largely unimpacted by surface effects, while the distance from the foundation is sufficient to minimise the influence of foundation restraint. At this level, which is 33 m above the lowest foundation, the dam wall thickness is approximately 21 m and the core temperature variation over a typical annual cycle is limited to approximately 2°C, while a period of 2 years was required to dissipate the full hydration heat.

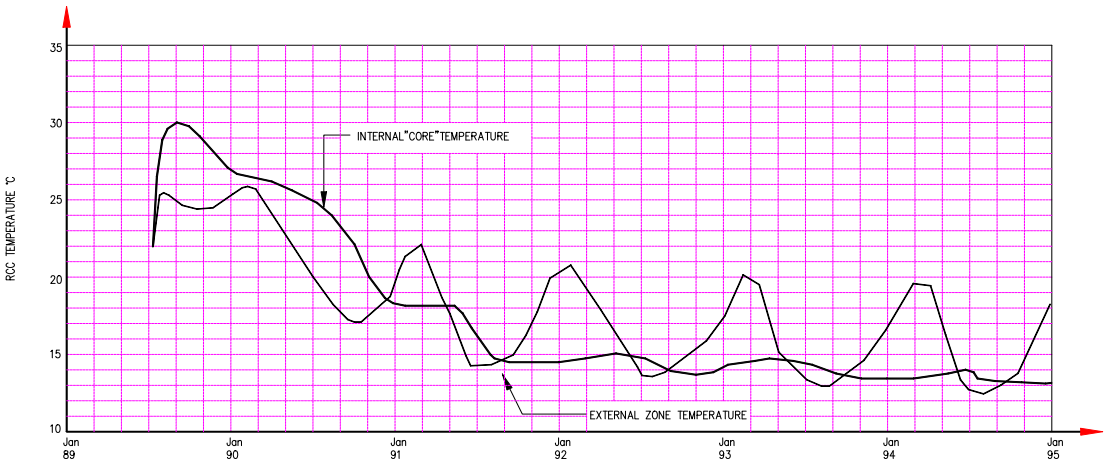

Figure 4.9: Typical RCC Temperature History for Wolwedans Dam[3]

Figure 4.9 illustrates the typical "core" and external RCC temperature history during construction and over the first 5 years after dam completion.

At Instrumentation level No. 3, 16 induced joints were instrumented each with 5 LBSGTMs. With induced joints at 10 m spacings on the upstream face, only three joints indicated any real tension displacement, with the "unopened" joints largely remaining in compression. **Figure 4.10** illustrates the displacement history at a centrally located open joint for a period from placement to five years after dam completion. Whilst this figure indicates a maximum joint tension displacement of approximately 0.8 mm in the internal, or "core" zone, the average maximum winter time joint opening across the full number of joints was approximately 0.28 mm and this was essentially manifested in an average opening of a little under 1.2 mm across three joints (see **Table 4.3**).

Separating the external and internal zones of the dam, the short and long-term thermal insulation at depth within the RCC can clearly be discerned. The hydration heat dissipation and ambient heat absorption within the external zone are equally evident.

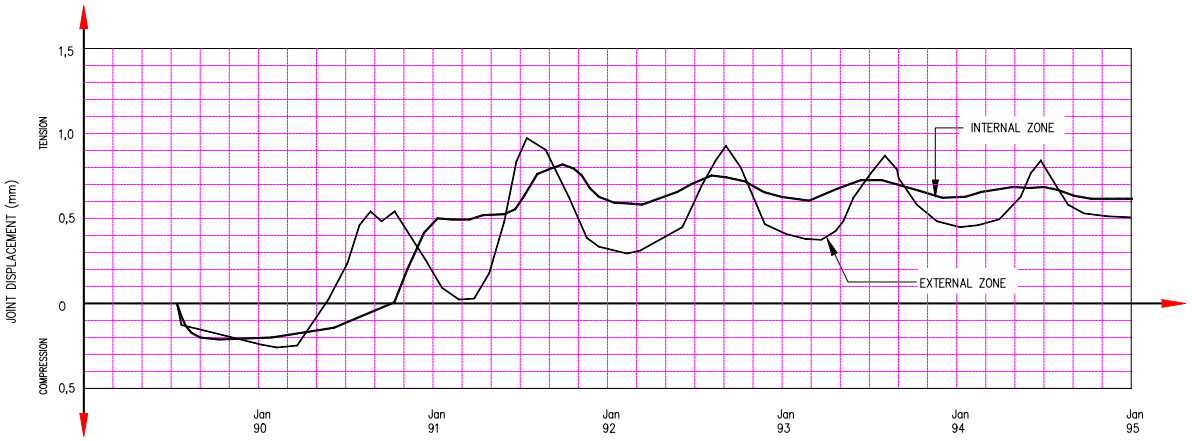

Figure 4.10: Typical Joint Displacement History for Wolwedans Dam[3]

4.3.1.5. Data Review and Analysis for LBSGTMs at RL 66.25 m

The "joint displacements" illustrated on **Figure 4.10** indicate the total displacement experienced between the anchored ends of the 1m long long-base-strain-gauge-temperature-meter. With the induced joint at the centre of these gauges, crack opening width is not measured directly, although when measurable displacements are only registered at (approximately) every third induced joint, the major portion of the indicated displacement in tension obviously represents a crack. It is significant to note that although the tension displacements vary from one induced joint to the next, dependent on which joint actually cracked, the compressions experienced during hydration heat development are substantially constant. Furthermore, the early compression patterns and levels experienced within the internal and external zones are significantly more similar than the tension displacements experienced later. **Figure 4.11** translates the measured internal, or core zone, induced joint displacements (as presented on **Figure 4.10**) into compression and tension strains over the gauge base length of 1m. Over such a gauge base length, a tension strain of 600 microstrain translates into an induced joint opening of 0.6 mm.

It is interesting to note that the compression strain, or joint closure, is apparently capped at approximately 200 microstrain. This could well represent the maximum expansion possible before the geometrical and foundation restraints force all other expansion into direct compressive stress. On the other hand, it could also relate to a susceptibility of the RCC to concentrate initial compression displacements on the induced joints, where installation techniques may result in locally more compressible RCC.

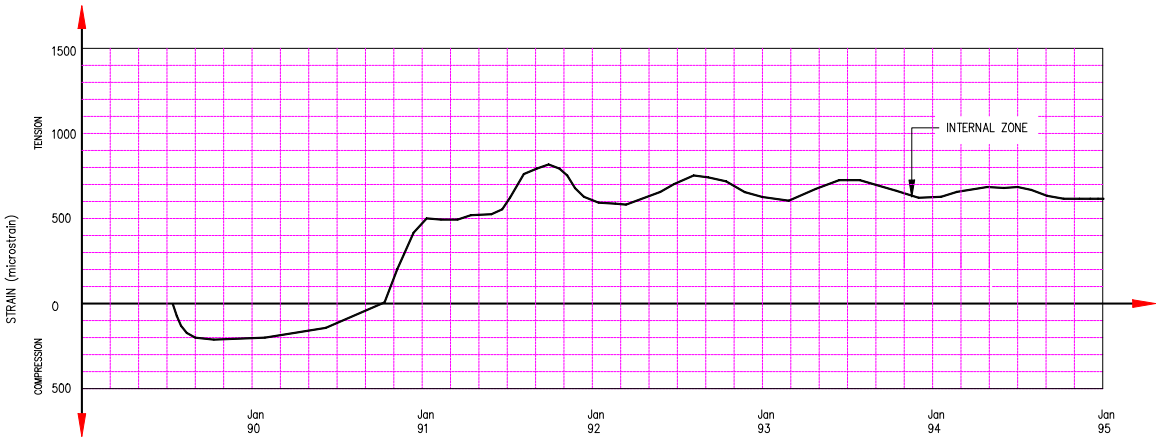

Figure 4.11: Typical Strain History for Induced Joint at which a Crack formed at Wolwedans Dam[3]

Reviewing the strain development at Wolwedans directly against temperature at any particular gauge, it is not possible to determine a direct, or meaningful correlation. Furthermore, significant tension displacements were only observed on three specific joints, effectively equivalent to spacings of approximately 30 m. It is accordingly not realistic to review a single joint in isolation, but it is necessary to observe cumulative displacements and related effects over the total number of joints at each specific instrumentation level.

On the basis of the available instrumentation monitoring data at level No. 3, it can be determined that zero joint displacement is experienced at the point that the dam body cools to a temperature approximately equivalent to the "built-in" placement temperature. In other words, the data suggests that the "zero stress", or natural closure temperature (T3)[4] and the "built-in", or initial placement temperature (T1) are approximately the same. In the absence of any other obvious explanation, this would imply that the hydration temperature rise of approximately 9°C, which developed maximum compression strains of approximately 200 microstrain across the marginally compressible induced joint (see 2.2.5) and possibly significant compressions as a result of strain constraint, seems to have caused no creep in the immature RCC. While this would seem to contradict all expectations of usual concrete behaviour, these indications were the first seeds that grew into the research addressed in this Thesis.

Maximum compression strain within the internal zone of the RCC appears to have been experienced approximately 3 months after placement, with this level of compression strain being maintained for a further 6 months, even though the temperature drops approximately 3°C over this latter period. This particular

phenomenon suggests some creep in the RCC during this period of temperature drop, or inelastic behaviour of the RCC, or physical constraint against expansion for the last 3°C of hydration temperature rise. The last hypothesis is considered the most likely and a 3°C temperature rise would incur a strain of 30 microstrain for a coefficient of thermal expansion of perhaps 10 x 10^{-6}/°C. For a green RCC deformation modulus of perhaps 15 GPa, at 7 days age, such a strain would relate to a 450 kPa compression stress.

For the instrumentation on level No. 3 (RL 66.25 m) at Wolwedans, the "built in" placement temperature (T1) was approximately 22 – 22.5°C, the maximum hydration temperature (T2) approximately 30°C and the lowest final winter temperature (T4) approximately 14°C. At the lowest temperature, the total cumulative openings on the joints, within the centre of the wall, amounted to approximately 3.4 mm, which translates into a direct strain of approximately 30 microstrain (3.4 mm/137 m). Overall associated tension is more difficult to determine, as records exist only for the strain across 1 m long gauges at each of the joints, which are approximately 10 m apart. There is no direct recording of the residual tension levels remaining between joints and across blocks where cracking did not occur. With approximately only every third crack joint actually opening to form a crack, the residual strain within the closed joints, at the coldest winter temperature, varied between 100 microstrain compression and 100 microstrain tension. Whilst this might appear to represent the situation of an average residual strain of 0, it is safer to assume a figure of perhaps 20 microstrain for related analysis. This strain would translate into a residual tension of the order of 300 kPa, for an elastic modulus of 15 GPa.

For a total continuous wall length of 137 m, at the level of the instruments in question, the total shrinkage strain associated with a structural temperature drop of approximately 8.5°C (22.5 – 14) accordingly might be approximately 50 microstrain. Such a strain infers an RCC coefficient of thermal expansion of approximately 6 x 10^{-6} strain per °C, which is lower than the value of 10 to 12 x 10^{-6}/°C, which might more usually be anticipated for a concrete comprising quartzitic aggregates.

The discrepancy in the apparent coefficient of thermal expansion could be a result of underestimated residual tensions within the uncracked RCC, a lower actual effective structural temperature drop, an actual lower coefficient of thermal expansion, creep of the RCC in tension, or a combination these factors. It must also be borne in mind that the dam wall structure was under full water load for most of the period of measurement and the structural closure of the joints under water load should also be considered. Whatever the case may be, the fact is that the deleterious effect of post hydration temperature drop on the structure of the arch wall was significantly less than theoretically predicted.

4.4. KNELLPOORT DAM

4.4.1. INSTRUMENTATION RESULTS

Unlike Wolwedans Dam, Knellpoort[1 & 2] was constructed largely during a particularly cold winter, with built-in temperatures frequently below 15°C. With a similar RCC mix to Wolwedans, compression strain experienced during hydration heat development again peaked at approximately 200 microstrain, or 0.2 mm displacement.

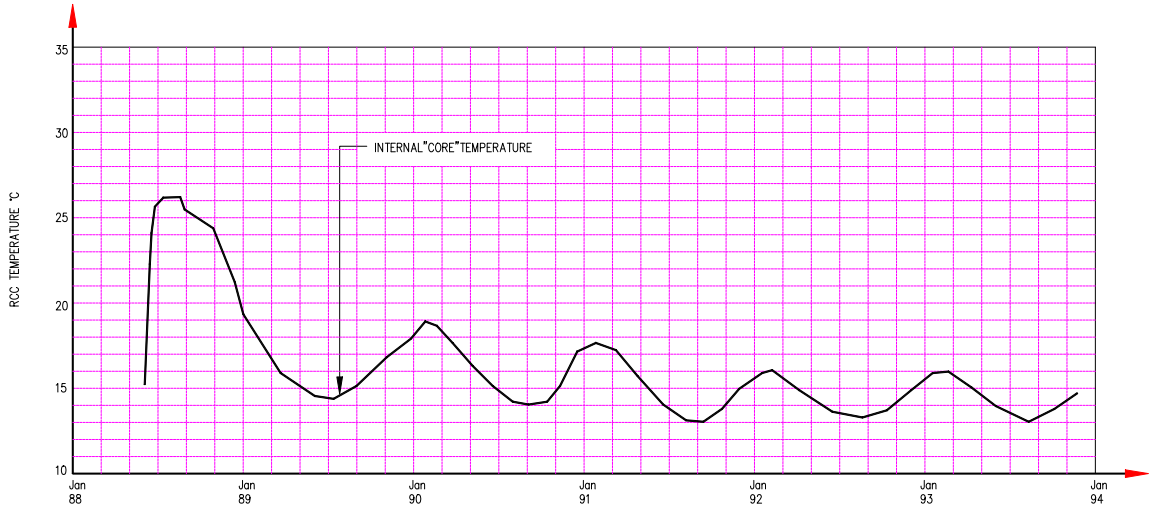

Figure 4.12: Typical RCC Temperature History for Knellpoort Dam[3]

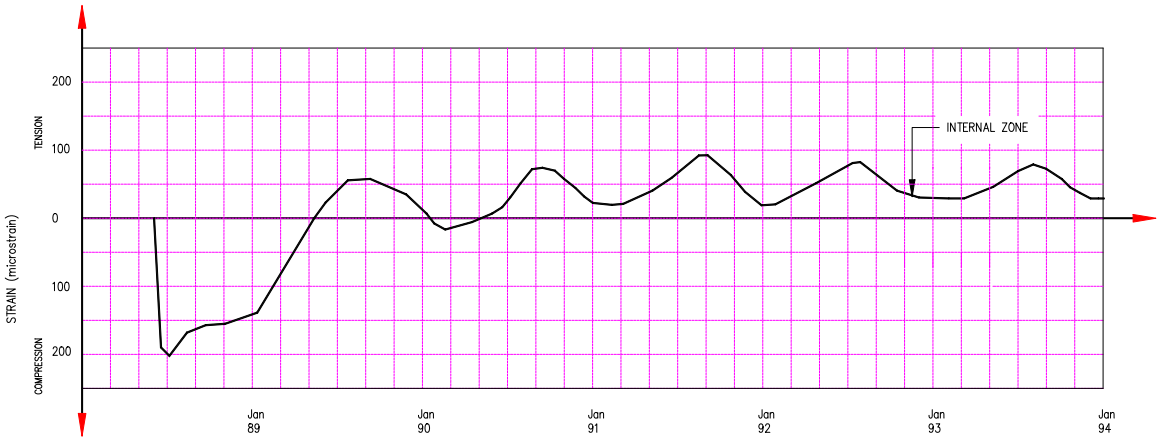

Figure 4.13: Typical RCC Strain History for Knellpoort Dam[3]

4.4.1.1. Data Review and Analysis

In general, the Knellpoort joint displacement and strain results demonstrated a very similar pattern to those for Wolwedans, although a specific difference can be seen in

the low tension strains experienced as a result of the final internal equilibrium temperatures being only fractionally above the placement temperature. Again, within the general variability of the measured data from joint to joint, the placement (T1) and "zero stress temperature" (T3) can be seen to be approximately the same, confirming the lack of creep under the early thermal compressions. Interestingly, the corresponding occurrence of a compression strain peak in conjunction with the temperature peak at Knellpoort suggests that the argument for compression strain being limited by constraint, while compression stress continues to increase, is invalid in this instance. On the other hand, a good elastic correlation of strain and temperature is more clearly evident at Knellpoort. Studying **Figures 4.12** and **4.13**, the proportional relationship between temperature and strain is clearly demonstrated, with an 11°C hydration temperature rise developing a compressive strain of approximately 200 microstrain, while long-term seasonal temperature variations of approximately 3°C give rise to strain variations of approximately 55 microstrain. From these figures, a uniform coefficient of thermal expansion of 1.8 x10^{-5}/°C (55/3 x 10^{-6} = 200/11 x 10^{-6} = 1.8 x 10^{-5}) can be calculated and while this figure is rather high, it is further confirmation of the minimal influence of creep and the apparent elastic behaviour of the RCC body under internal temperature variations. It is considered most likely that the apparent coefficient of thermal expansion is exaggerated as a consequence of the concentration of movements on the induced joints, where a weakness in the body of the RCC is effectively created.

The smaller proportions of Knellpoort (59 000 m^3) compared to Wolwedans (200 000 m^3) imply reduced thermal insulation at the core, with temperatures varying by 3°C seasonally at the instruments indicated for the former dam and only 1.5°C at the latter. The data for Knellpoort was measured at level No. 4, 37m up the 50 m high structure, where cover is limited to approximately 4 m.

4.5. ÇINE DAM

4.5.1. GENERAL

The data evaluation for Çine Dam is subsequently presented in two part; the first part describing the first review of data from Çine Dam in 2007 and the second evaluating data at three levels at the beginning of 2009.

4.5.2. BACKGROUND

Instruments were installed at three elevations; 147.50 mASL in October 2005, 184.25 mASL in November 2007 and 208.50 mASL in November 2008 respectively. A final set of instruments was installed at elevation 232 mASL in November 2009[5].

Plate 4.1: January 2005 – El 147.50 mASL

The Çine instrumentation is comprehensive and focuses on the measurement of strain and temperature, with one set of instruments measuring displacement across each of the induced joints, parallel to the dam axis, and another measuring strain perpendicular to the axis of the dam.

A comprehensive thermal analysis was completed for Çine Dam, with the initial 2005 exercise being supplemented with an evaluation of a possible continuous placement of the top 55 m of the structure in 2008. The placement of the RCC for Çine Dam will be completed during 2010 and the dam has been constructed in a series of 6 winter-season placements, which started in 2004/2005.

With placement initiated in October/November each year, a total of approximately 300 000 m^3 was placed by the following March/April. Thereafter, the structure was left exposed until the following winter placement season. The purpose of the thermal analysis was to model the development and dissipation of the hydration heat and to establish whether the proposed winter-season RCC placement schedule and approach might result in the development of any deleterious stresses at any stage. On the basis of the critical temperature patterns identified, stress analyses were completed in order to isolate and evaluate the consequential maximum tensions developed.

Plate 4.2: April 2007 – El 187 mASL

Plate 4.3: April 2008 – El 208.25 mASL

While the thermal analyses demonstrated that the temperatures within Çine Dam will only reach an equilibrium condition in approximately 50 years after completion of the dam, the winter placement approach further implies that the induced joints are unlikely to open for a long time, if at all. Consequently, it will be many years still before the performance of the dam structure in its cooling cycle can realistically be evaluated and accordingly only the short-term "heated" performance of the dam structure can be investigated at this stage.

4.5.3. INSTRUMENTATION LAYOUTS

The arrangements of the installed instrumentation at Çine Dam are described in Chapter 2. **Figures C5** to **C7** in **Appendix C** provide a basic illustration of how and where the strain gauges and the LBSGTMs were arranged on each of the instrumentation levels for which monitoring data was available by the end of 2008.

4.5.4. INSTRUMENTATION DATA EVALUATION 2007

4.5.4.1. General

Instrumentation was installed in the dam at elevation 147.5 mASL during October 2005 and this is being read and monitored on an ongoing basis[5]. A comprehensive thermal analysis, simulating the anticipated construction sequence, was completed for the dam before RCC placement was initiated and the related actual temperature readings are regularly compared with the predictions of the model.

For the purposes of this work, the strain measurements from the LBSGTMs (termed SGT gauges at Çine Dam), located across the induced joints, and from strain gauges (termed SGA gauges at Çine Dam), orientated in a perpendicular direction to the dam axis, are evaluated. At the level of the installed instruments, the dam section measures almost 115 m in width and accordingly, the internal instruments are well insulated from surface effects.

4.5.4.2. Instrumentation Results

The evaluation presented herein was completed in early February 2007, analysing instrumentation reading records of some 16 months. Both the SGT and SGA gauges measure temperature and demonstrate a hydration temperature rise of the order of 12 to 14°C, with the internal core temperature remaining at around 25°C, while the temperature closer to the surface had dropped during winter 2006 by up to 3°C.

In evaluating the instrumentation readings, it is important to take cogniscance of the installation timing, processes and procedures and the subsequent RCC placement timing. At Çine Dam, RCC is placed annually during winter, between October/November and March/April. The instruments evaluated as part of this work were installed during October 2005 on the surface of a 14 m deep block of RCC placed during the previous winter. The gauges were subsequently covered by the winter 2005/06 RCC placement, which commenced on the 11th of November 2005. A depth of approximately 18 m of RCC was placed during this winter season.

Accordingly, the gauge readings presented document the behaviour of the winter 2005/06 RCC placement.

The general patterns discernable from the strain measuring instrumentation readings to date at Çine Dam are distinct and in accordance with expectations.

The SGA strain gauges demonstrate a total maximum thermal expansion strain of the order of 120 microstrain for a hydration temperature rise of approximately 14°C, which translates into an equivalent RCC coefficient of thermal expansion of 8.4 x 10^{-6}/°C. The magnitudes of both the temperatures and the strains are as expected and predicted.

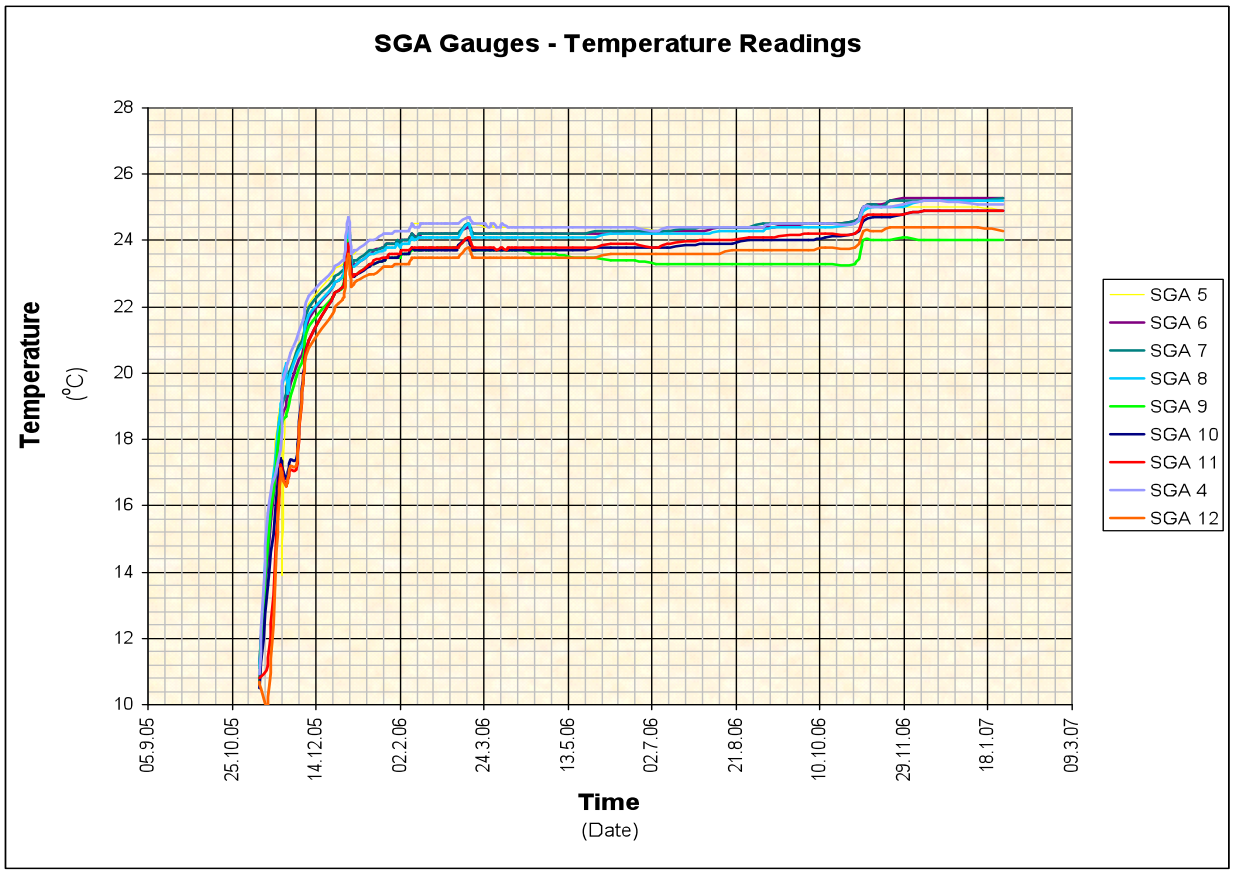

Figure 4.14: Typical RCC Temperature History for Çine Dam(5)

It is considered quite surprising that a direct and apparently linear expansion of the RCC with a temperature rise of 14°C should have been evident less than 20 m above the foundation level, within the core of a dam with a base length exceeding 100 m. It would have rather been expected that internal restraint would have caused most of the associated thermal expansion to have been constrained.

The SGA gauges further demonstrate clearly a strain relaxation (**Figure 4.15**), over the period between 3 and 7 months after the start of RCC placement. While the temperature measured on these gauges remained relatively constant until a further

slight increase was indicated at the start of the winter 2006/07 RCC placement, the total strain relaxation indicated was of the order of 15 microstrain, or 12.5%.

The SGT gauges (**Figure 4.16**) illustrate a relatively rapid increase in temperature over the first two weeks, which slows slightly over the following month and distinctly over the subsequent two and a half months. Approximately 4 months after initiation of the winter 2005/06 RCC placement, the instruments indicate that the maximum temperature has been reached.

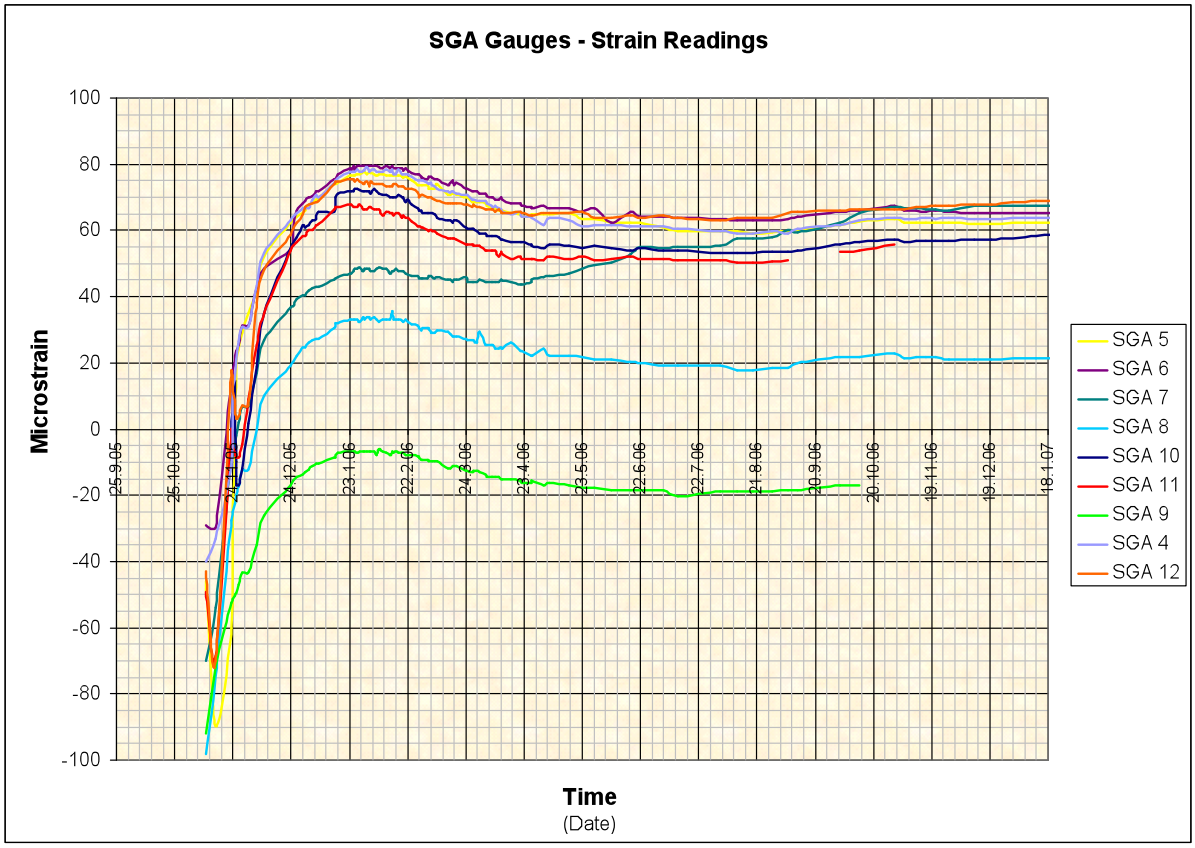

Figure 4.15: Typical Strain History for SGA Instruments[5]

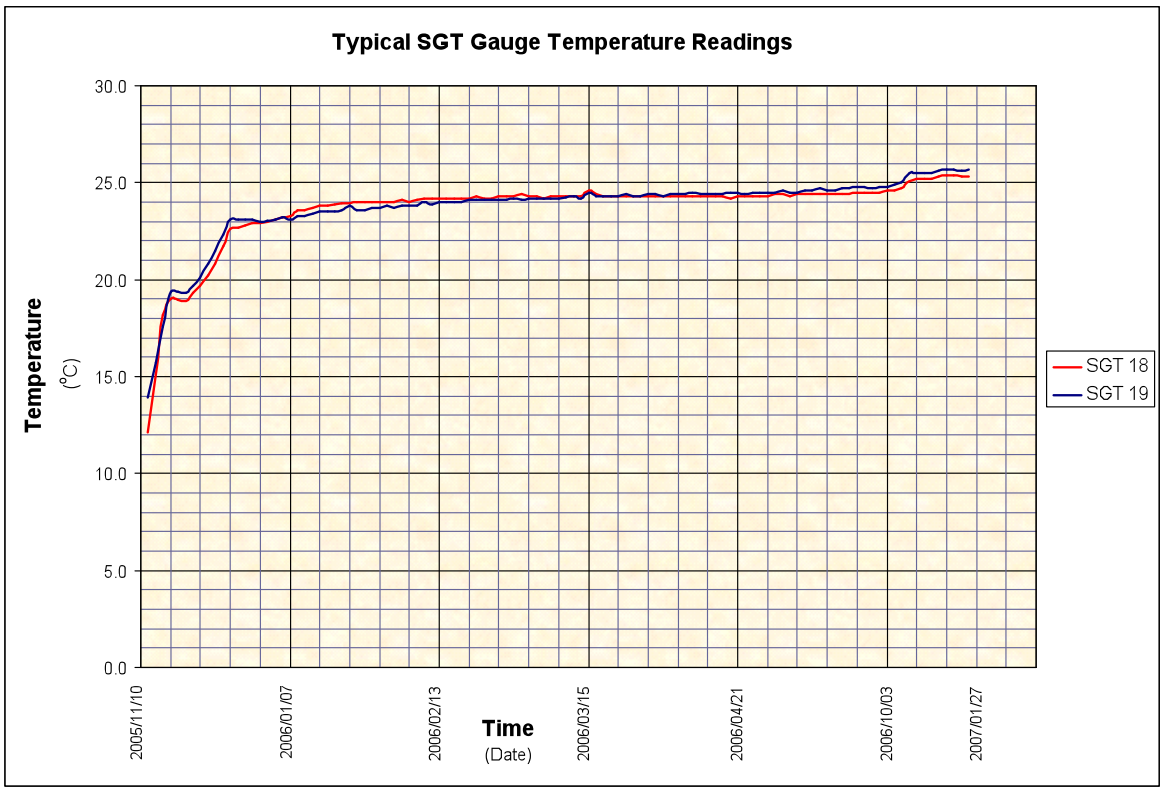

Figure 4.16: Typical Temperature History for SGT Instruments[5]

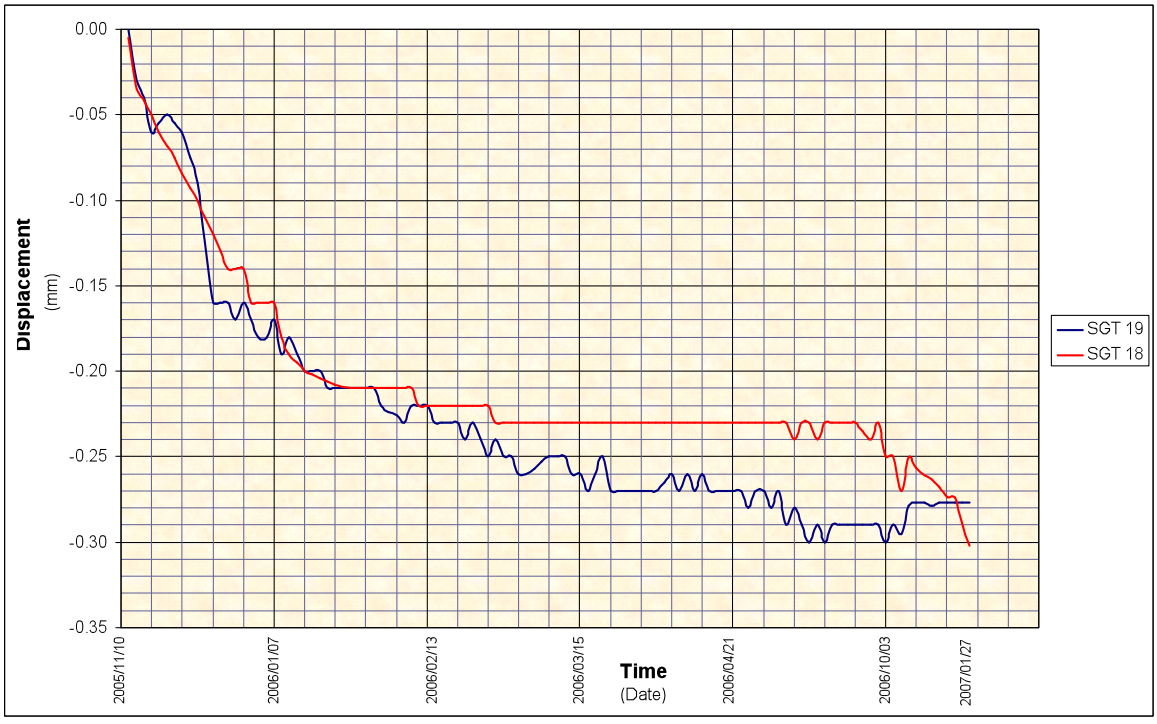

Figure 4.17: Typical Joint Deformation History for SGT Instruments[5]

In relation to strain, the SGT gauges demonstrate compression displacements (**Figure 4.17**) that increase linearly over the first two months after installation followed by an additional 2 months of displacement increasing at a reduced rate. Thereafter, the displacements remain essentially constant. The displacement behaviour of the RCC measured on the gauges can accordingly be seen to follow directly the hydration temperature development. Typical maximum compression displacements vary between 0.11 and 0.50 mm, with an average of approximately 0.28 mm, which translates to 280 microstrain over a gauge length of 1000 mm.

4.5.4.3. Interpretation of Instrumentation Results

Three specific issues come to light and require consideration in respect of the apparent RCC behaviour patterns demonstrated through the Çine Dam instrumentation to date. These can be summarised as follows:

- While the SGA gauges demonstrate expansion strain directly related to the hydration temperature development, they indicate a subsequent relaxation of strain of the order of 15 microstrain over a period of approximately 4 months after the hydration peak temperature is reached and maintained.
- Once the strain relaxation apparent on the SGA gauges has occurred, a constant level of strain is subsequently maintained. Similarly, at maximum strain on the SGT gauges, no change in strain is evident that could signal the occurrence of creep.
- The SGT gauges experience compression strains, which develop with increasing hydration temperature and are maintained without relaxation. The indicated compression displacements suggest some compressibility of the induced joint (see 2.2.5).

It is considered most likely that the strain relaxation indicated on the SGA gauges reflects creep, developed as a consequence of the different behaviour of the RCC materials structure under thermal expansion compared to restrained compression. While this 15 microstrain shrinkage would imply that the RCC, which is generally experiencing compression stresses while its temperature is elevated by hydration heat, will start to experience tension at a temperature of a little less than 2°C above the "built in" temperature, as the hydration heat is gradually dissipated. It should be noted that the lignite fly ash used at Çine Dam is a relatively low grade material, which may play some part in the evident behaviour.

It was initially considered anomalous that compression strains of 250 to 280 microstrain should be indicated on the SGT gauges for a typical hydration temperature rise of 14°C. While lower strains could be anticipated in the direction of the dam axis, as the body of the wall is restrained within the foundation, expansion, as opposed to contraction would be anticipated, corresponding with the expanded materials volume associated with increased temperature.

The evident contraction across the LBSGTMs can, however, be explained by the fact that the meters are located on the induced joint, immediately above a crack director (which are installed in every 4th layer). The method of construction of these induced joints effectively causes them to act, to a minor extent, as compressible expansion joints, as discussed in Chapter 2. While the process of roller compaction results in the development of horizontal restraining stress within the RCC, this stress is broken as the induced joint faces are opened to facilitate the insertion of the de-bonding plate. On completion of the induced joint construction, some capacity to absorb expansion of the adjacent RCC is developed. This is also considered to be the reason for the scatter of the applicable compression strain values evident on the SGT gauges, when compared with the strains indicated on the SGA gauges.

As the temperature in the dam rises during the process of hydration, the resultant restrained expansion will cause compression across the dam wall structure between abutments. With more ability to accommodate contraction across the induced joint than in the remainder of the RCC, a disproportionate part of the thermal expansion of the RCC will be taken up in contraction across the induced joint, while the balance will be experienced as compression in the RCC. Ignoring autogenous shrinkage, a 14°C temperature increase would give rise to a strain of approximately 120 microstrain, as indicated on the SGA gauges. At 1.5 to 2 months age, the long-term RCC deformation modulus might be 10 to 12 GPa, suggesting a restrained compression stress of a little over 1 MPa.

The thermal analyses for Çine Dam indicated that the temperature at the location of the particular instruments addressed in this work will stabilise at around 18.5°C, approximately 50 years after construction completion. In view of the fact that the "built in" temperature for the internal instruments in this installation was between 12 and 14°C, it is accordingly quite possible that tension will never be experienced across the induced joints within this section of the dam wall, as the equilibrium temperature is higher than the natural closure temperature, even allowing for a 2°C increase consequential to shrinkage and creep, or a possible 1°C seasonal variation within the body of the dam wall.

4.5.5. INSTRUMENTATION DATA EVALUATION 2009

4.5.5.1. General

While the top level of instrumentation for Çine Dam had not been installed at the time the present review was undertaken, the value of the instrumentation evaluation undertaken was compromised by the fact that the readout unit started developing inconsistencies during 2007. The consequential problems really serve to demonstrate the critical importance of building redundancy into dam monitoring instrumentation systems. The evaluations in this Chapter were made on the basis of instrumentation measurements from date of installation until the end of 2008.

4.5.5.2. Instrumentation Measurements

Figures 4.18 to **4.33** illustrate the typical temperature and strain/displacement measurements recorded at Elevations 147.50, 185.25 and 208.50 mASL respectively[3, 5 & 7]. The pattern of results indicated at the specific chainages selected was essentially repeated at all of the other induced joints and while the data presented is by no means comprehensive, it is fully representative of the measurements made and the behaviour apparent throughout.

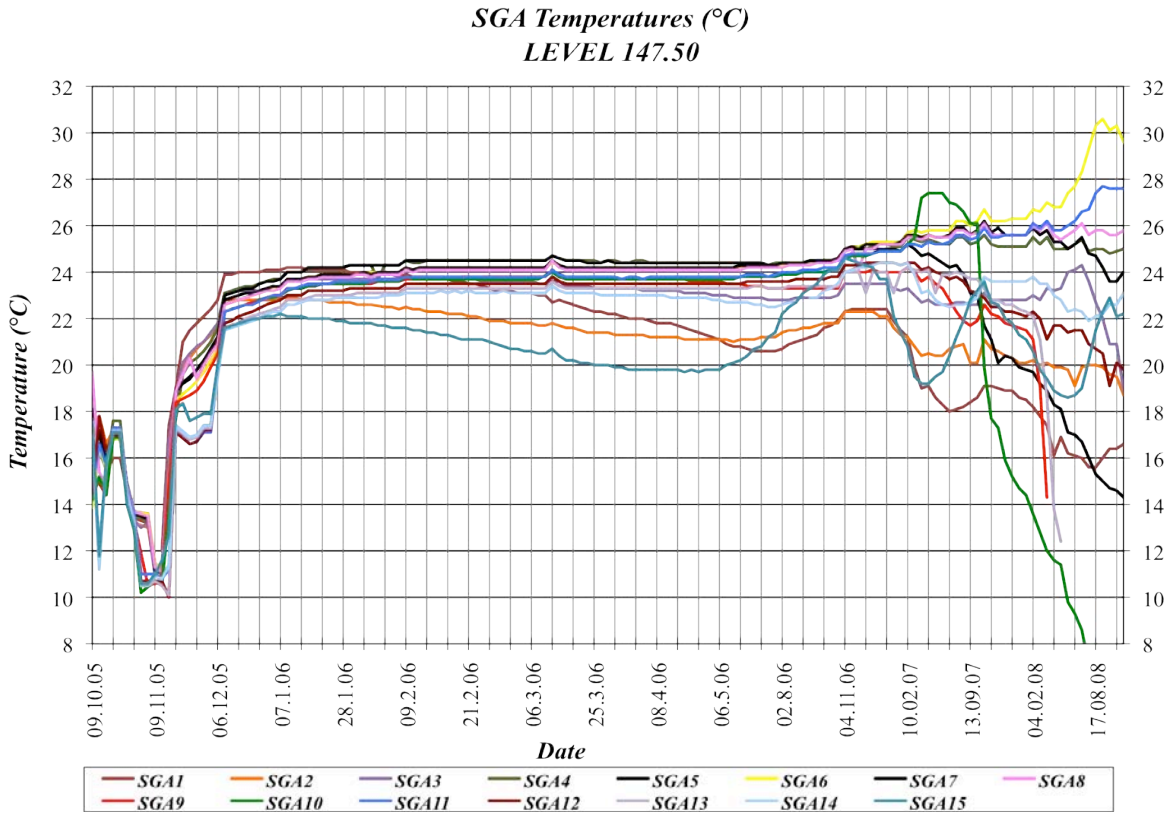

Figure 4.18: Temperature on Strain Gauges (SGA) at El 147.5 m - Ch 127 m[5]

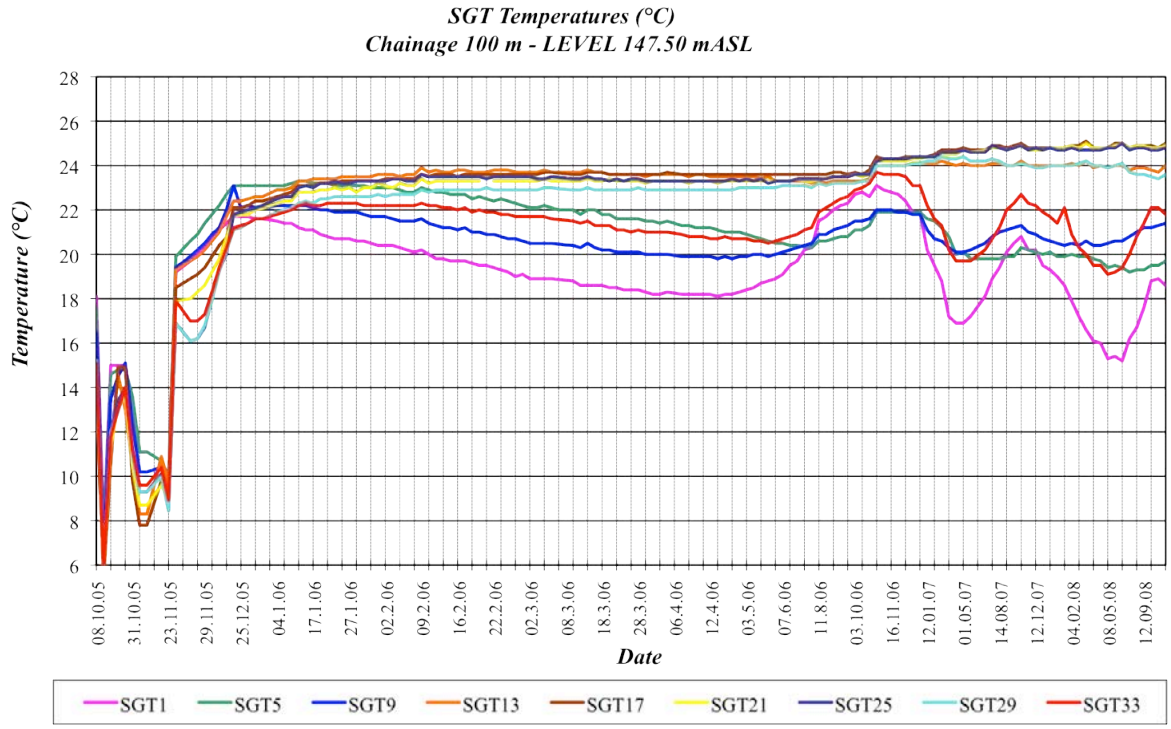

Figure 4.19: Temperature on LBSGTMs (SGT) at El 147.5 m – Ch 100 m[5]

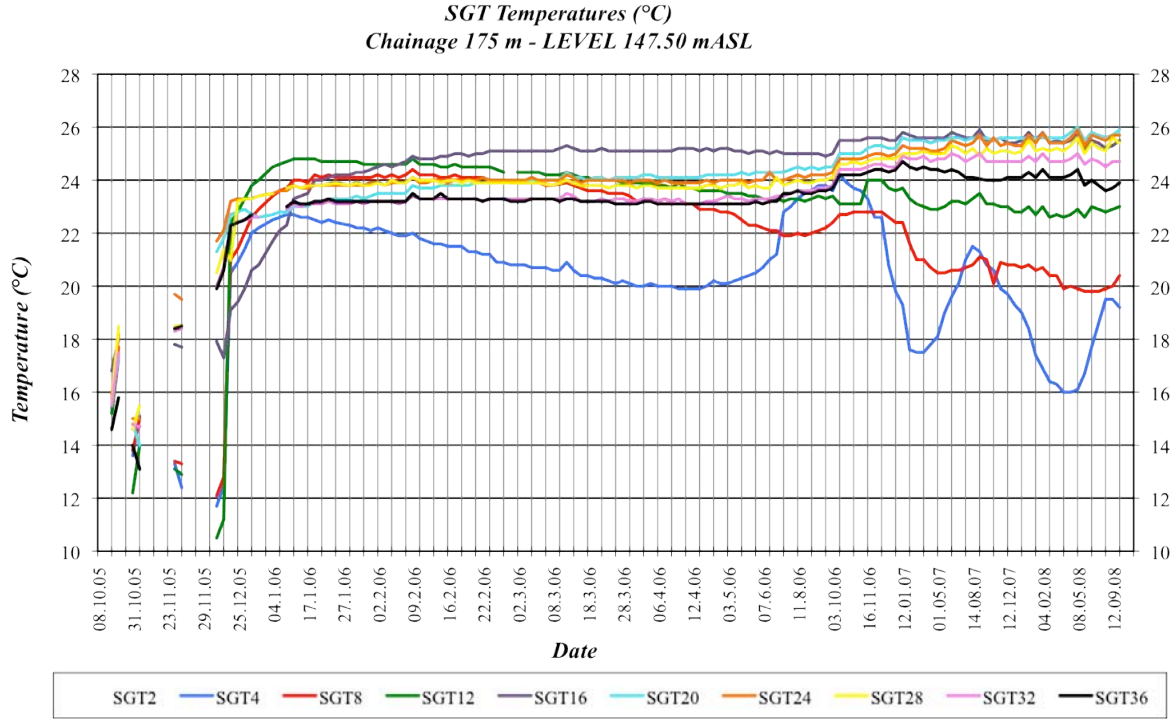

Figure 4.20: Temperature on LBSGTMs (SGT) at El 147.5 m - Ch 175 m[5]

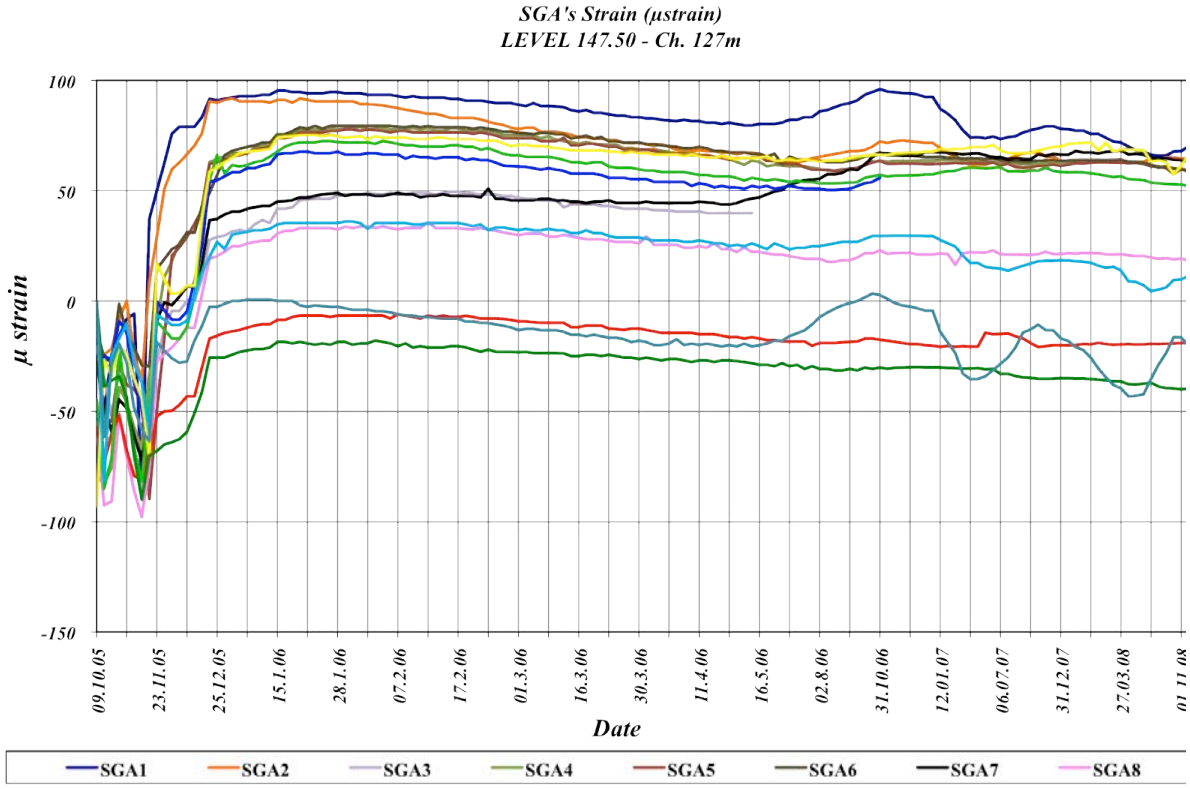

Figure 4.21: Strain on Strain Gauges (SGA) at El 147.5 m - Ch 127 m[5]

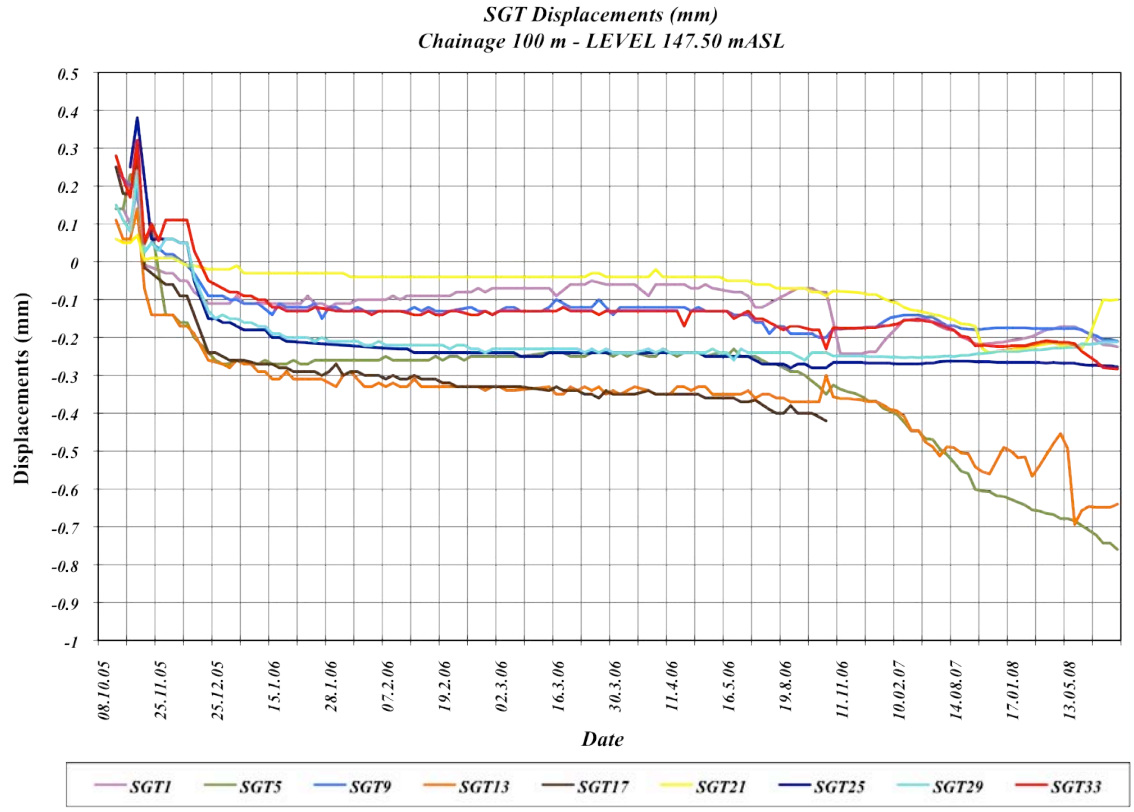

Figure 4.22: Displacements on LBSGTMs (SGT) at El 147.5 m - Ch 100 m[5]

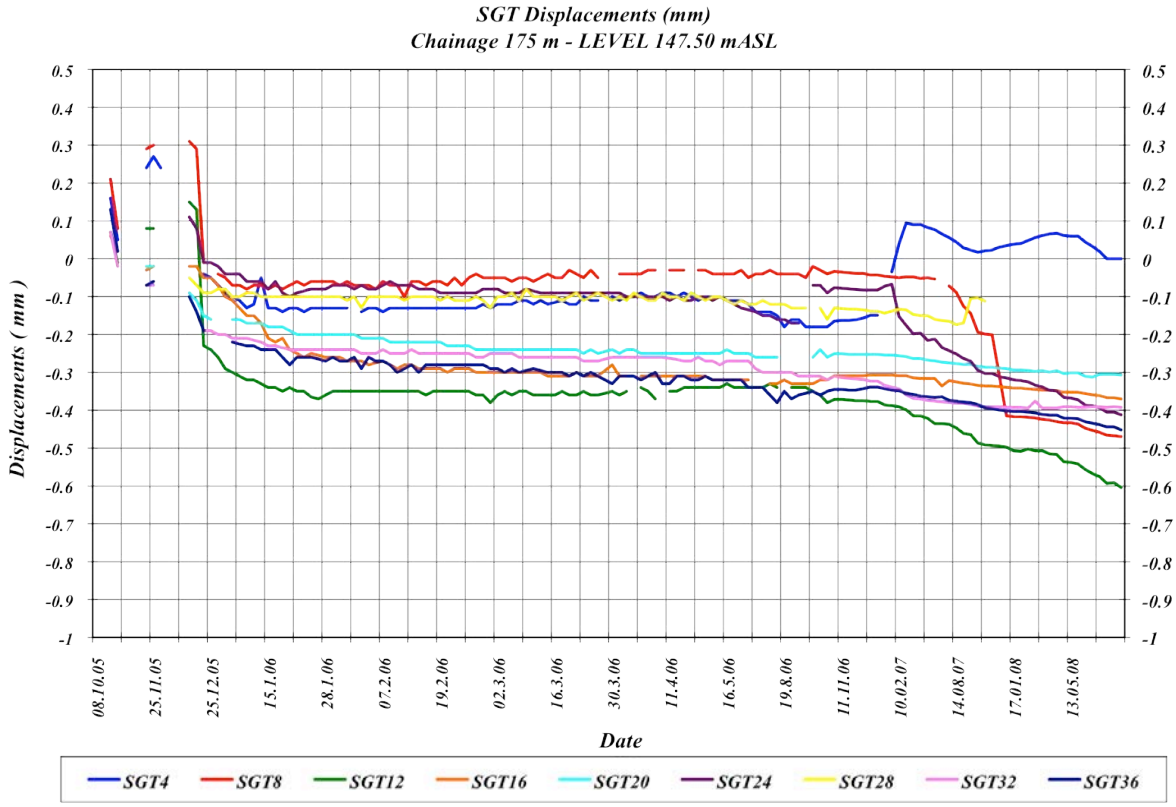

Figure 4.23: Displacements on LBSGTMs (SGT) at El 147.5 m – Ch 175 m[5]

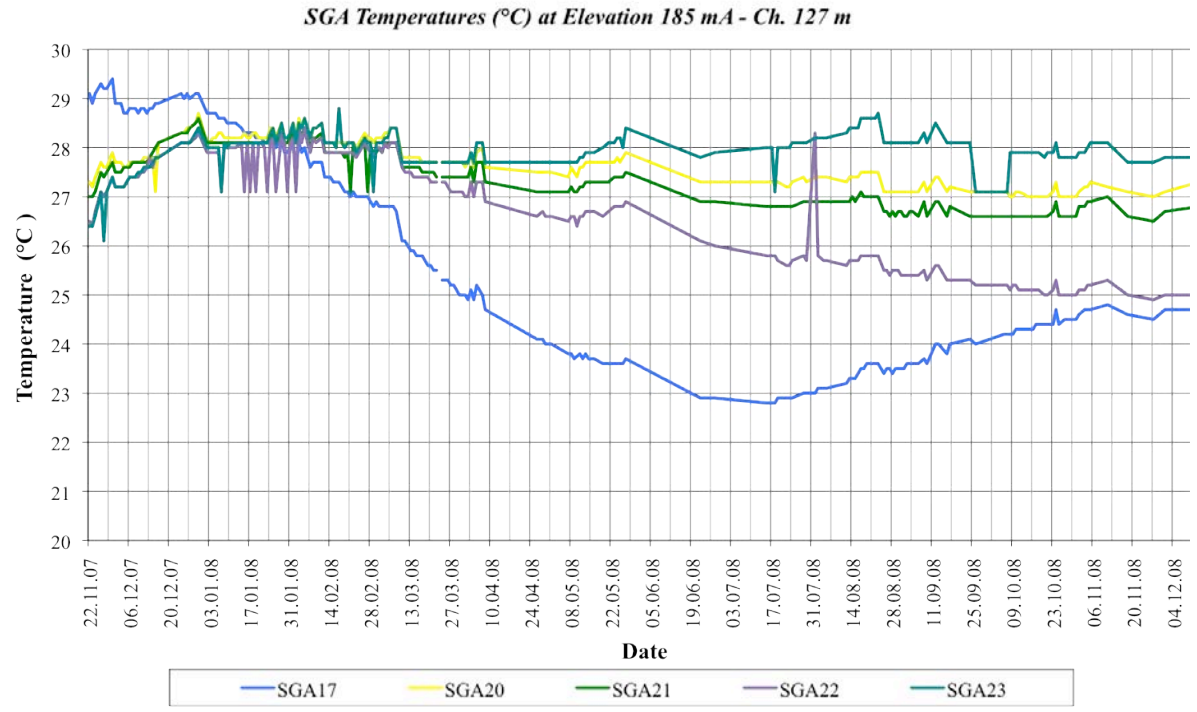

Figure 4.24: Temperature on Strain Gauges (SGA) at El 185 m - Ch 127 m[5]

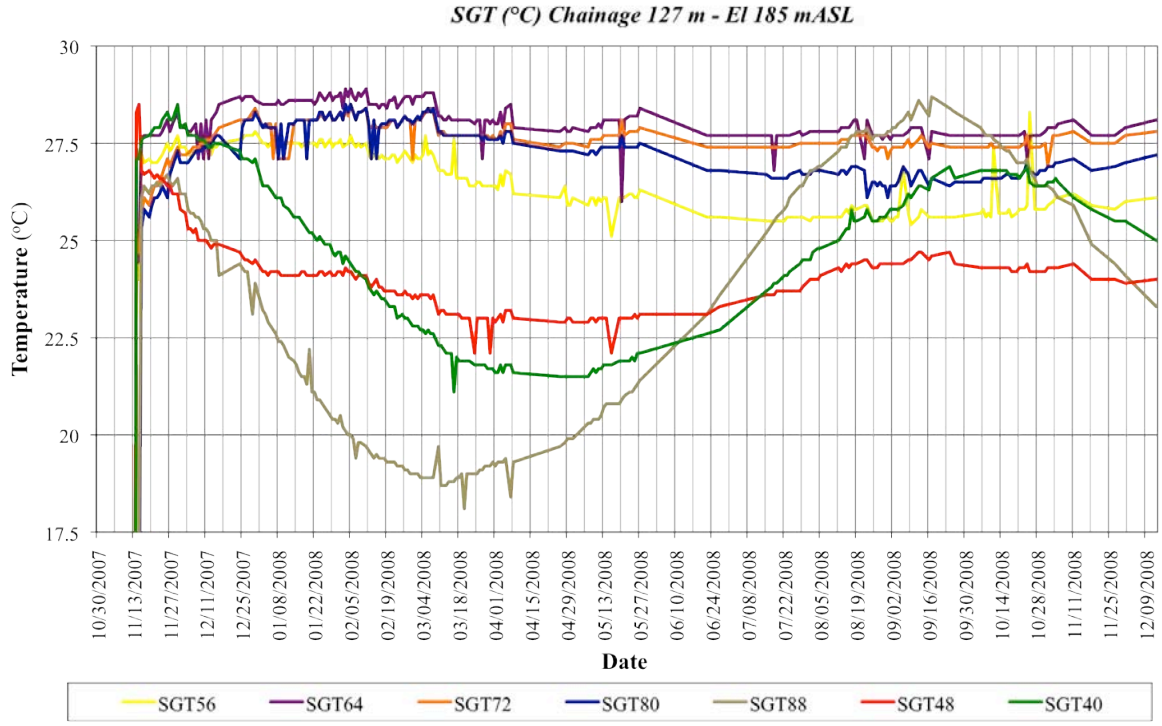

Figure 4.25: Temperatures on LBSGTMs (SGT) at El 185 m – Ch 127 m[5]

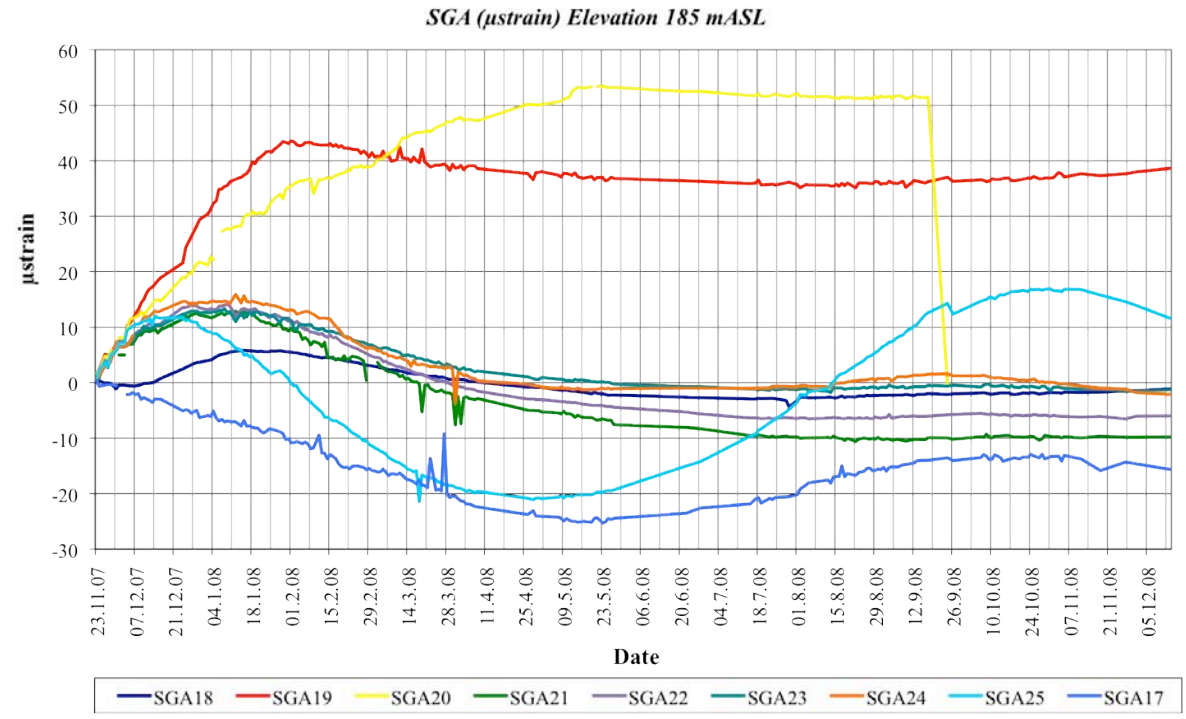

Figure 4.26: Strain on Strain Gauges (SGA) at El 185 m - Ch 127 m[5]

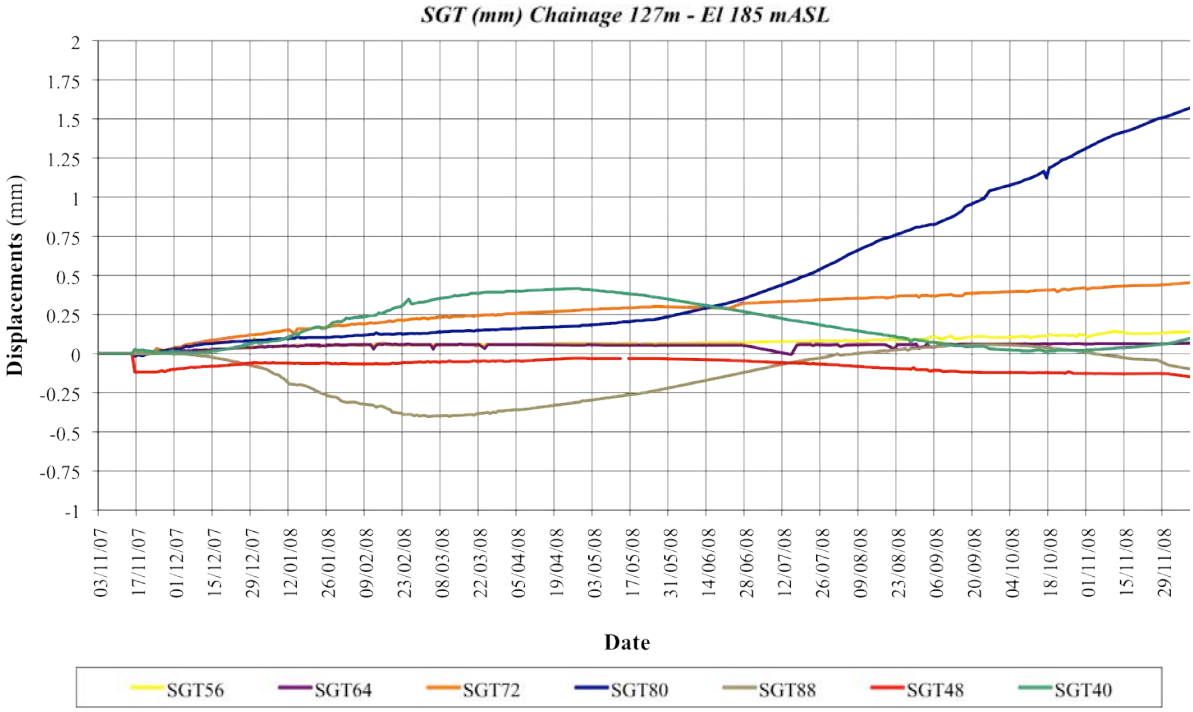

Figure 4.27: Displacements on LBSGTMs (SGT) at El 185 m – Ch 127 m[5]

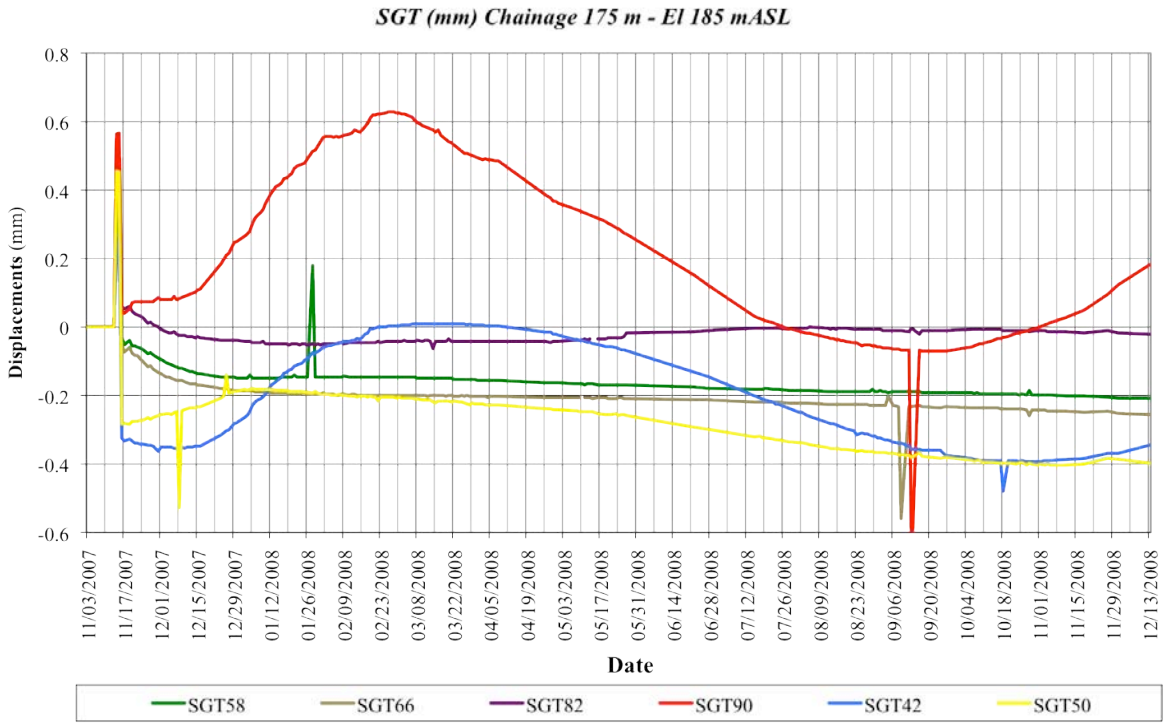

Figure 4.28: Displacements on LBSGTMs (SGT) at El 185 m – Ch 175 m[5]

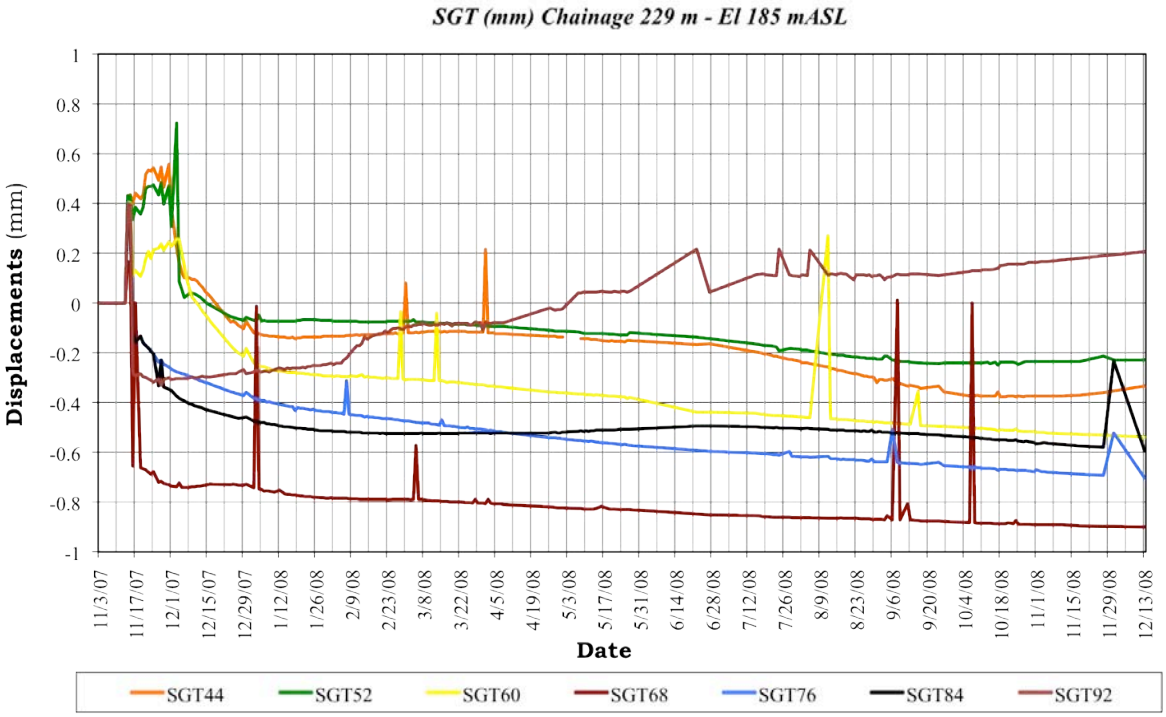

Figure 4.29: Displacements on LBSGTMs (SGT) at El 185 m – Ch 229 m[5]

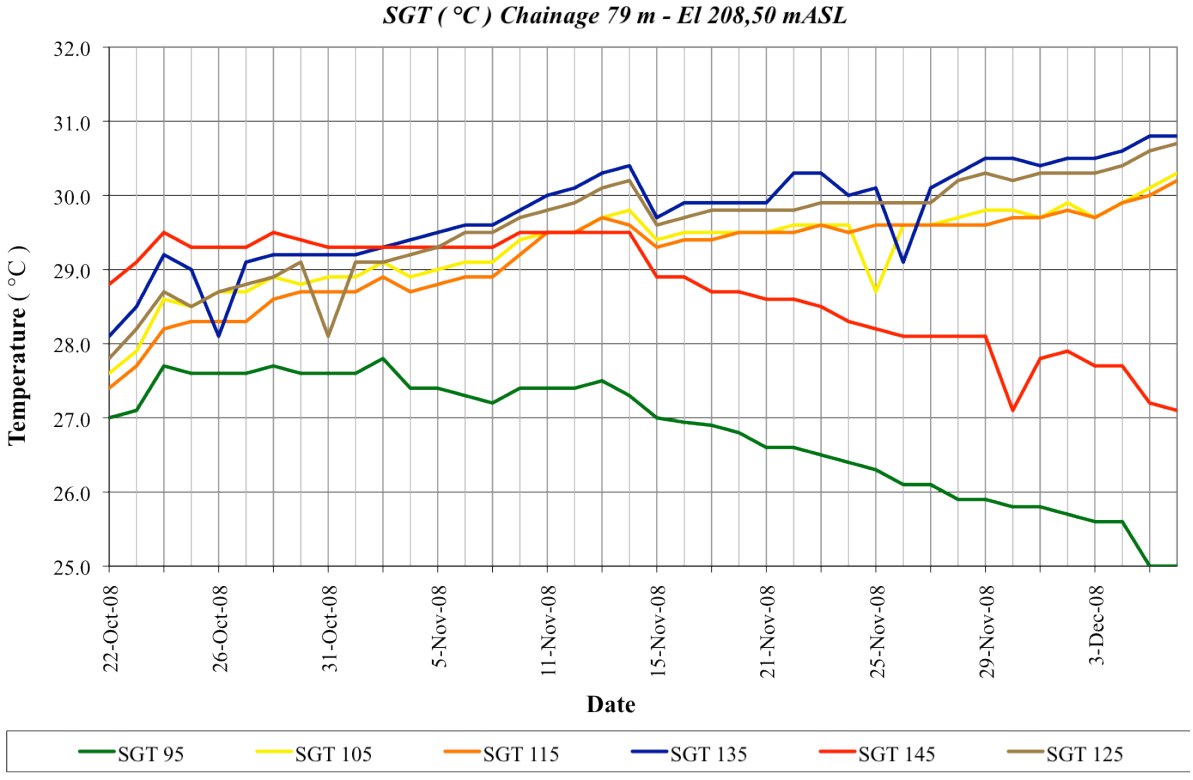

Figure 4.30: Temperatures on LBSGTMs (SGT) at El 208 m – Ch 79 m[5]

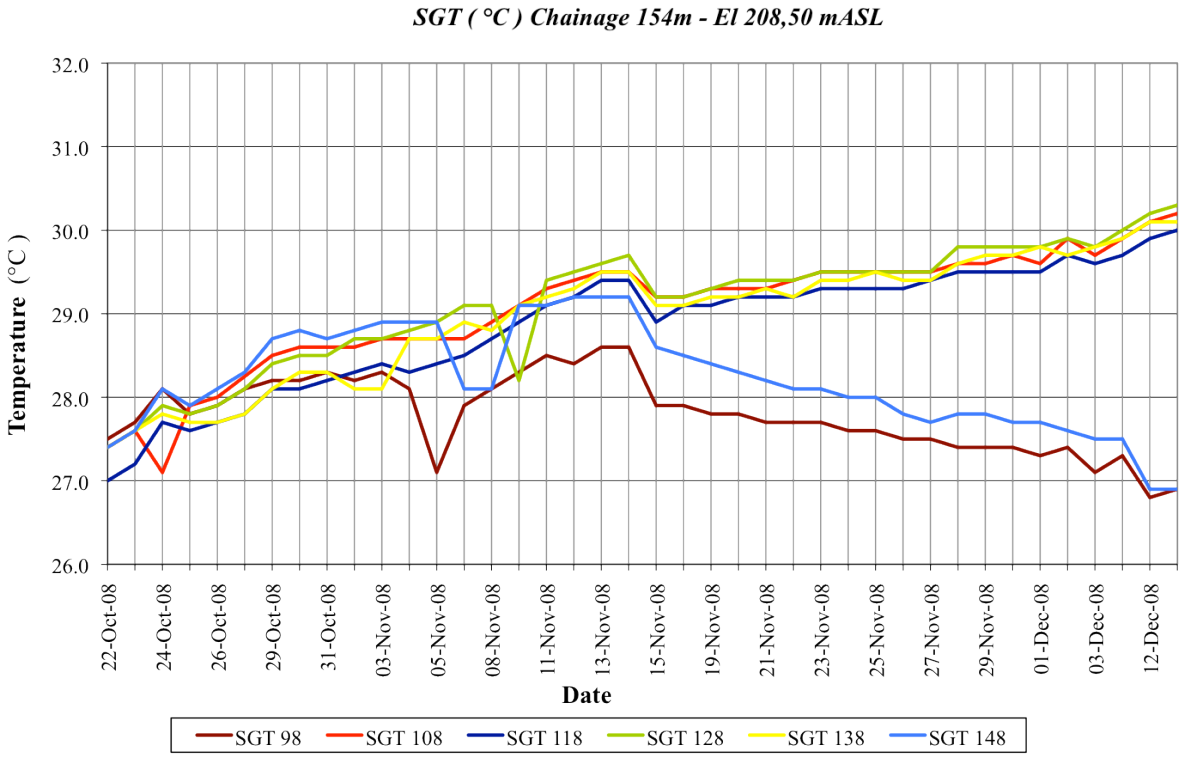

Figure 4.31: Temperatures on LBSGTMs (SGT) at El 208 m – Ch 154 m[5]

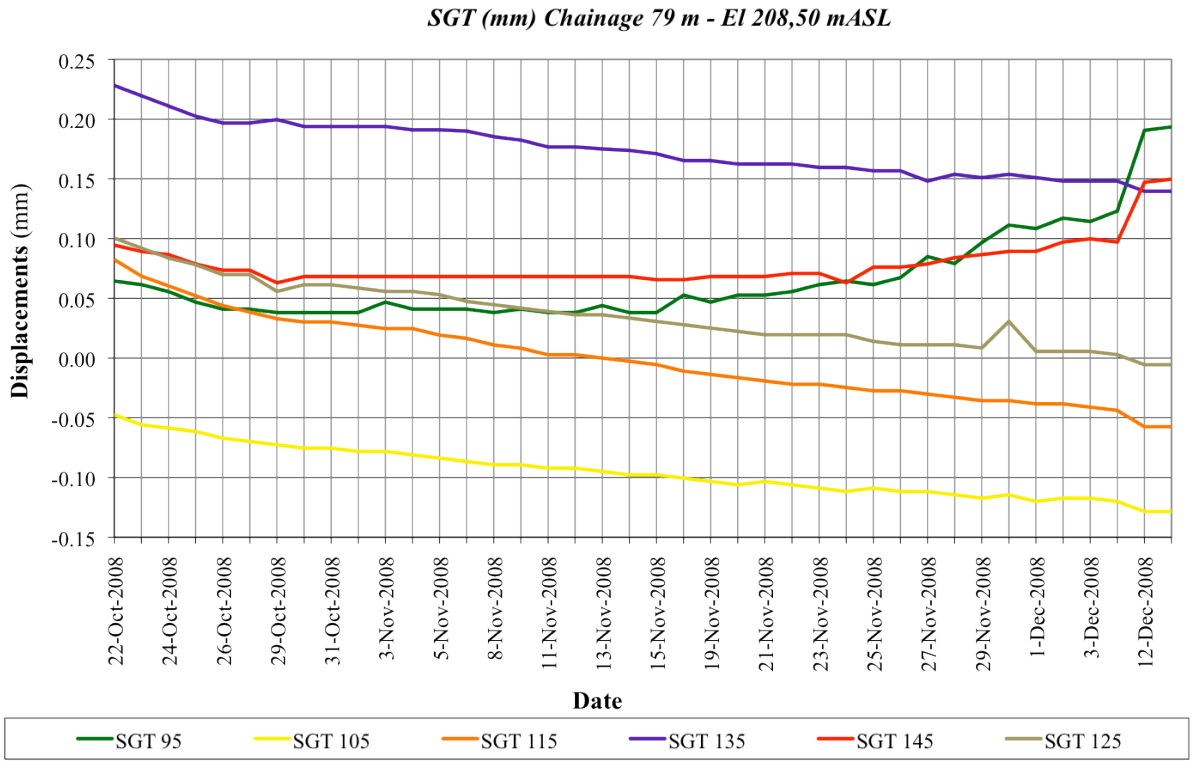

Figure 4.32: Displacements on LBSGTMs (SGT) at El 208 m – Ch 79 m[5]

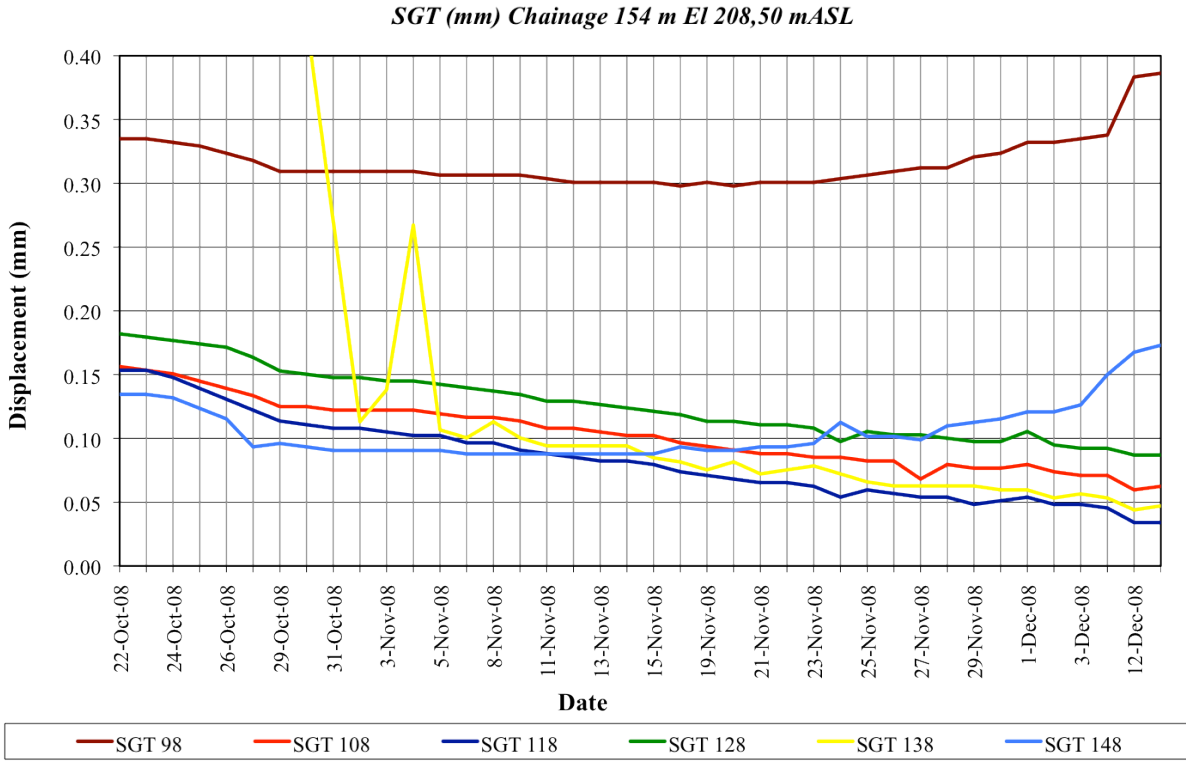

Figure 4.33: Displacements on LBSGTMs (SGT) at El 208 m – Ch 154 m[5]

4.5.6. DISCUSSION OF INSTRUMENTATION DATA FINDINGS

4.5.6.1. General

Before attempting to determine patterns of behaviour within the data available, it is considered important to highlight a number of general comments in relation to the observed data. Firstly, it is clear that a number of errors are present within all data sets and these can be seen in the odd, random and obviously incorrect data point, or "outlier". Secondly, the impact of the faulty instrumentation readout unit can be seen in some strange and, in some cases, contradictory data as early as the beginning of 2007. Thirdly, the occasional inconsistency between the listed location of a specific instrument and the associated temperature measurements suggest that certain of the instrument cables were incorrectly labelled.

As a consequence of the above and the nature of such measurement within a dam structure, the available data is of greatest use in illustrating patterns of behaviour, particularly where consistent patterns are demonstrated. The data available demonstrates clearly that the temperatures within the core zone of the dam structure at the lower elevations have remained fairly constant, at their hydration peak, with no apparent dissipation by the end of 2008. The closer the instrument to the surface, the more dissipation that is evident and correspondingly, the greater the influence of external ambient temperature variations.

Indications from the coffer dam and theoretical calculations suggested that a hydration heat of approximately 12°C should be applicable for Çine Dam and the measurements on the main dam wall have confirmed this figure to be quite realistic. In general, the SGA and SGT temperature measurements indicated a high degree of correlation.

Laboratory testing at the Middle Eastern Technical University (METU)[7] indicated an average instantaneous E modulus of approximately 25 GPa for the Çine Dam RCC. Under a sustained compressive stress of 5.5 MPa, the test cylinders subsequently indicated a creep of approximately 110 microstrain over a period of approximately 60 days. Including the creep, the total strain consequently indicates an E modulus of 16.67 GPa, which corresponds to a sustained E modulus equivalent to 2/3 of the instantaneous value, which is in line with typical expectations[10]. Due to the inelastic properties of concrete, increased deformation under a sustained load, compared to an instantaneous load, is manifested as creep that is gradually reversed on release of the load. For this reason, an effective E modulus under sustained loading equivalent to 2/3 of the instantaneous value is usually assumed. On the basis of the above calculation, it would appear that the creep measured in the METU laboratory accordingly relates only to the reversible phenomenon associated with the response of concrete under sustained loading. The METU testing further confirmed the instrumentation observations that drying shrinkage of the RCC was minimal.

4.5.6.2. Issues Related to Specific Elevations

The instrumentation installed at El 147.50 mASL is the most comprehensive and offers the best and most consistent data. At Elevations 147.50 & 208.25 mASL, the LBSGTMs were not effectively zeroed at installation and accordingly, it is not always straightforward to develop a clear picture of the total displacements caused by thermal effects.

The RCC of the layer in which the instrumentation was installed at El 147.50 mASL indicated a placement/built-in temperature ranging between 10 and 16°C, with an average of the order of 13°C. The maximum temperature reached in the core RCC varied between approximately 24 and 26°C. At El 147.50 mASL, the two gauges on the upstream side of the gallery, the gauge immediately downstream of the gallery and the gauge closest downstream face indicated “surface” temperature behaviour, while the remainder reflected “core” temperature behaviour.

The instruments at El 208.25 mASL had only been installed for around 2 months by the end of 2008, when the data was forwarded for interpretation, and accordingly, the data from these instruments is of little value in respect of the study addressed in this chapter. While the external two gauges at the lower elevations seem to represent “surface” and intermediate temperature behaviour, only the single, outer gauges at El 208.25 mASL reflect “surface” behaviour.

4.5.6.3. SGA Meters

General

Strain gauges orientated perpendicular to the dam axis were only installed on the lower two levels of instrumentation at Çine Dam. In view of the fact that these instruments are not influenced by crack directors, they tend to indicate greater quantitative consistency.

Elevation 147.50 mASL

As a consequence of the apparent problems with the instrumentation readout unit, it is not realistically possible to make any meaningful, or quantitative analysis of the strain variations with rising and falling temperature in the surface zones of the RCC at El 147.50 mASL once this zone reached its long-term equilibrium cycle. However, the behaviour of the RCC in the core zones is very clear, at least until the temperature rise around 1 year after placement. For the first three to four weeks after installation, the strain gauges appear to have experienced some minor contraction. Thereafter, the RCC expands. Examining, the temperatures confirms that the initial contraction occurred before the instruments were covered with RCC. While this resulted in divergent zero values across the gauges, it is clearly evident that total strain increases of between 62 and 155 microstrain occurred as a consequence of the hydration heat development.

As this strain was a thermal swelling, it can be observed that the peak values were recorded at 1/3 and 2/3 points across the dam section. The maximum strain increased from the upstream surface to the 1/3 point, decreased slightly to the middle of the section, increased to the 2/3 point and decreased to the downstream surface, as illustrated in **Figure 4.34**.

The average strain across the section, as measured on the SGA gauges, was approximately 105 microstrain. This can be compared with a figure of approximately 85 microstrain, which would have been anticipated for a temperature increase of 12°C and a coefficient of thermal expansion of 7.1 x 10^{-6}/°C. The fact that the measured expansion exceeds that predicted probably relates to a lack of accuracy in the tested thermal expansion coefficient, but more importantly it confirms that the early expansion occurred in a very elastic manner, with no apparent losses to creep, despite the immature nature of the RCC at the time. The strain values measured suggests that the RCC might have an initial coefficient of thermal expansion of approximately 8.75 x 10^{-6}/°C. A second possible origin of the unexpectedly high expansion is that this occurs due to constraint in the perpendicular direction. However, it did not prove possible to verify this hypothesis through analysis.

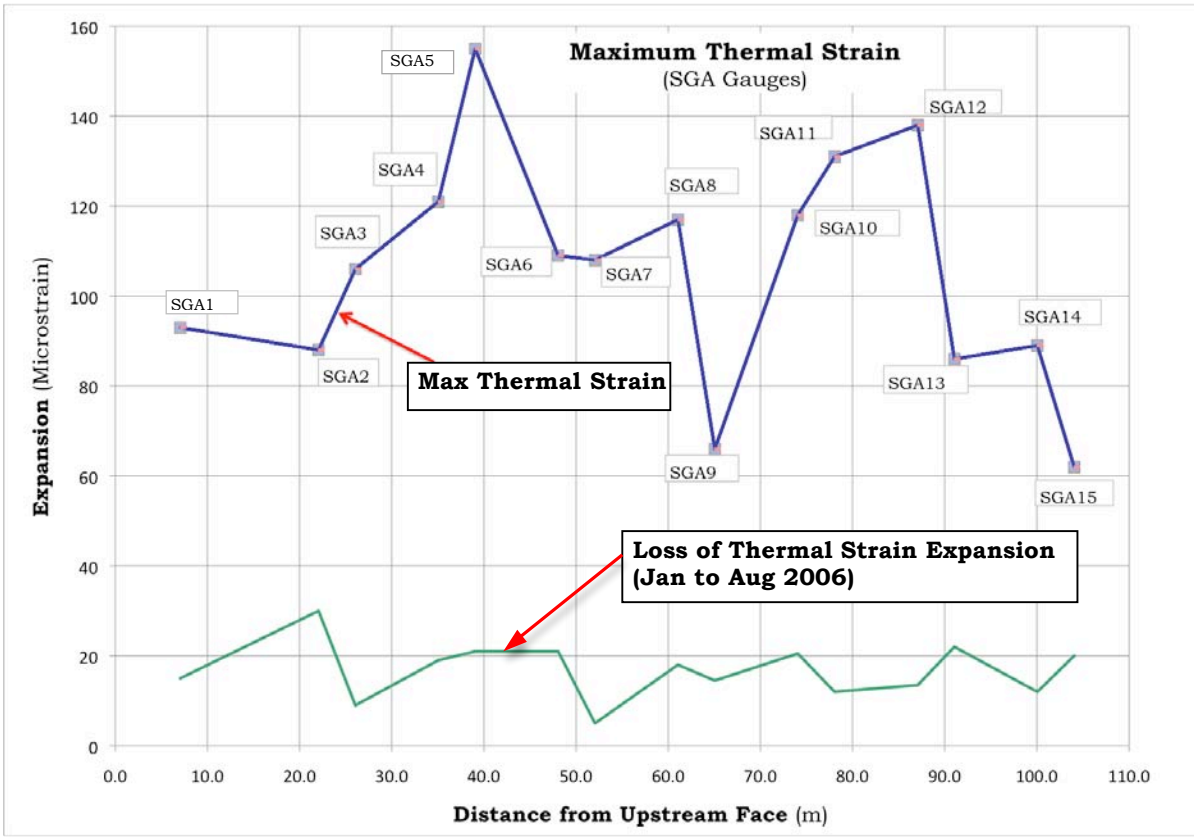

Figure 4.34: Strain Distribution Across Cross Section Measured on SGA Gauges

During the subsequent 7 to 8 months, a gradual relaxation in the expansion strain is evident on all gauges apart from SGA 7, which is located at the centre of the section. The average strain relaxation experienced over this period within the zone where the temperature remains constant is approximately 16 microstrain (or 15%). When the section starts to experience an increase in temperature again, towards the end of 2006, an average expansion of approximately 7 microstrain is experienced for an average temperature increase marginally exceeding 1°C. To all intents and purposes, it appears that no further strain relaxation is experienced after mid 2008. For the same coefficient of thermal expansion that was demonstrated during hydration heating, an expansion of slightly in excess of 9 microstrain would be anticipated, so it remains possible that approximately 2 microstrain (or 25%) has been lost to creep. On the other hand, the latter expansion corresponds accurately with the coefficient of thermal expansion measured in laboratory testing[7] (7.1 x 10^{-6}/°C), without any losses to creep. By the same token, the initial hydration expansion, less the loss for apparent creep, approximately corresponds to a net expansion at a coefficient of thermal expansion of 7.4 x 10^{-6}/°C (89 microstrain/12°C), which is again approximately equivalent to the average laboratory figure.

In summary, the data for the SGA strain gauge instrumentation installed at El 147.50 mASL appear to be demonstrating that a total creep/drying shrinkage of less than 20 microstrain (or approximately 15% of the total expansion developed as a result of hydration heat) occurred at Çine Dam over a period of 2 to 3 years, where unrestrained expansion was allowed to occur, perpendicular to the axis of the dam. The 200 microstrain autogenous and creep shrinkage traditionally assumed definitely did not occur at Çine Dam and, even if the measured strain relaxation was a consequence of autogenous shrinkage and/or creep, the reality is less than $1/10^{th}$ of the figure traditionally assumed. The fact that thermal expansion was evident in a situation where internal restraint would be expected to be dominant, however, was considered quite surprising and a strong indication of the different behaviour of high-paste RCC compared to CVC.

Elevation 185.00 mASL

At El 185.00 mASL, some anomalies exist in respect of data from some of the SGA gauges. For example, the temperature data from SGA24 makes no sense and yet the strain readings for the same instrument are quite believable. While the origin of these problems is unclear, additional care must be applied in all consequential interpretations.

The RCC placement above El 185 mASL started on 15/16 November 2007, but strain measurement on the SGA gauges was only initiated approximately 1 week later, when a substantial amount of the hydration heat would have already developed. Gauges SGA17, 21, 22, 23, 24 & 25, however, provided data that is significantly useful. All gauges were zeroed for strain approximately 7 days after RCC placement and accordingly it is apparent that the expansion due to the first period of hydration heat development was not measured, or is not recorded in the available data. While this implies that it is not possible to compare the actual and the anticipated coefficient of thermal expansion, the instruments that indicated temperatures remaining at the peak hydration level until the end of 2008 demonstrated an expansion strain development of around 10 microstrain, which was dissipated over the following four to five months. Thereafter, no further creep/shrinkage was apparent. In gauge SGA23, where a net temperature drop of around 1.3°C was experienced, the expansion strain was dissipated earlier and a further 10 microstrain in tension was developed, as would be expected for a linear shrinkage at a coefficient of thermal expansion of approximately 7×10^{-6}/°C. Gauge SGA22 indicated an additional shrinkage of approximately 5 microstrain, despite an apparent temperature drop of 3°C, although such a temperature drop is viewed with suspicion at a gauge within the core zone of the dam cross-section.

While the temperature reading function of gauge SGA25 (close to downstream surface) seems to have failed very early on, the strain readings indicate a seasonal strain variation of just under 40 microstrain, which makes some sense compared to

an anticipated temperature variation range of the order of 6°C. Gauge SGA17 (close to upstream surface) indicates a seasonal strain variation of approximately 13 microstrain after an apparent creep/shrinkage of approximately 12 microstrain. This corresponds to a temperature variation range of 1.9°C, indicating a linear-elastic response for a coefficient of thermal expansion of approximately 7 x 10^{-6}/°C.

4.5.6.4. SGT Meters

Elevation 147.50 mASL

At El 147.50 mASL, the joint closure measured across the LBSGTMs apparently generally peaked at 0.40 mm at maximum hydration temperature. Over an instrument length of 1 m, this represents a strain of 400 microstrain. For a hydration temperature rise of 11°C, this would translate directly into a thermal expansion coefficient of approximately 36 x 10^{-6}/°C, which is obviously rather improbable. Furthermore, while the effects of the increase in temperature during 2008 are evident, the problem with the instrumentation readout unit cloud any real quantitative analysis. However, the fact that a 1°C temperature rise might result in compression across the induced joints of the typical order of 0.02 to 0.04 mm again suggests relatively linear-elastic behaviour.

Should the RCC of Çine Dam have behaved in the traditionally assumed manner, shrinkage/creep of approximately 200 microstrain should have exceeded the temperature expansion of approximately 78 microstrain (11°C x 7.1 x 10^{-6}/°C) by 122 microstrain. The net shrinkage should have caused a tensile stress of approximately 1.8 MPa, which should have consequently exceeded the tensile strength of the weakened induced joints, which are spaced at 27 m centres, and translated into an opening of approximately 3.3 mm in width. Instead, a joint closure of approximately 0.4 mm has been maintained since the peak temperature was reached, which increased with increasing temperature.

The behaviour recorded suggests, again, that the RCC of Çine Dam cannot be behaving in a manner at all like that traditionally assumed. While no evidence of shrinkage, or creep can be determined on the SGT meter readings, should any in fact be evident, it can only be of an order of magnitude different to that which might traditionally be assumed.

Elevation 185.00 mASL

At El 185 mASL, the temperature data is apparently consistent in demonstrating a hydration temperature rise of the order of 12°C. Interpretation of the displacements on the SGT gauges, however, is less straightforward, with some anomalous and contradictory readings.

The SGT gauges at Chainage 127 m indicate some strange behaviour. SGTs 72 and 80 suggest that a significant crack is developing towards the downstream of the

section, but SGT 88 (closest to the downstream face) indicates exactly the opposite. SGT 40 (closest to the upstream face) indicates a crack of 0.4 mm width that opens with dropping temperature, while SGT 88 indicates a joint closure of the same order, while experiencing a greater temperature drop. It is accordingly considered that a sufficient level of confidence cannot be placed in this data and that any attempt at interpretation would consequently not be of any value.

While inconsistent zero readings complicate the interpretation of the data from the SGT gauges at Chainage 175 m, the "core" instruments indicate compression strain that follows the temperature pattern and is apparently maintained without creep. The upstream surface gauge SGT42 indicates a change in strain of 400 microstrain for a temperature change of approximately 6°C, superficially suggesting a coefficient of thermal expansion of 67 x 10^{-6}/°C, while the adjacent gauge, SGT50, indicates a strain change of 200 microstrain for a temperature variation of approximately 3°C, superficially suggesting a coefficient of thermal expansion of the same order. The gauge closest to the downstream face suggests that a crack of 0.6 mm opened when the temperature dropped by approximately 8°C, while the crack closes and indicates a compression strain of approximately 55 microstrain for a temperature increase of 12°C above minimum, or approximately 4°C above maximum hydration temperature.

At Chainage 229 m, the SGT gauges indicate substantially more consistent behaviour and behaviour more similar to the gauges at El 147.50 mASL. Again, it is difficult to isolate a realistic zero value for the displacements due to an apparent break in RCC placement at this specific chainage. However, in the core zone the slow increase of temperature throughout 2008 is reflected in continuously increasing compression strain. For a temperature increase of perhaps 0.5°C over this period, the strain at gauges 60, 68 & 76 increases by approximately 100 microstrain. The reason for this last behaviour is not completely clear, but it is perhaps indicative of some creep compression across the induced joint.

Elevation 208.50 mASL

At El 208.5 mASL, neither temperature, or strain/displacement seem to have been measured from first placement of the RCC layer above and accordingly a fully comprehensive analysis of the data at this elevation is again not possible. Evaluating the concrete placement data, it would appear that the built-in (placement) temperature for the SGT gauges was approximately 22°C. Seven weeks after placement, the temperature in the core zone was steadily rising, at approximately 30 – 31°C. Referring to temperature measurements at the lower levels suggests that the indicated temperatures should rise a further 1 to 2°C before reaching their peak. The only conclusions that can be drawn from the SGT instrumentation at El 208.5 mASL is that for fairly linear rise in "core" temperatures at just under 1°C in a month, SGT compression strain increased at a

rate of approximately 30 microstrain/month. Conversely, in the "surface" zones indicated tension movements in a fairly linear manner, suggesting coefficients of thermal expansion of between 18 and 50 x 10^{-6}/°C. All expansions and contractions as a consequence of temperature changes, when measured across the induced joints, were greater than would have been anticipated within a simple block of RCC and while no indication of any shrinkage, or creep was evident, the apparent effective action of the induced joints as an expansion joint compromises any ability to make any real quantitative evaluations.

4.5.7. EVALUATION FINDINGS

4.5.7.1. Reliability & Consistency

Although quantitative interpretation of instrumentation installed in a dam is notoriously problematic, where considered reliable, the data analysed in this case at Çine Dam demonstrates a consistent pattern of behaviour. This consistency and its corroboration of the behaviour patterns observed at Wolwedans and Knellpoort Dams, further serve to confirm a high level of reliability in respect of interpretation. The fact that the METU testing on Çine RCC cores[7] did not demonstrate creep, beyond that which differentiates the behaviour of concrete under an instantaneous and a sustained load, and indicated minimal drying shrinkage, further increases the perceived reliability of the interpretations of the instrumentation data.

4.5.7.2. Value of Results

While the behaviour observed on the instrumentation at Çine Dam confirms in principle the findings at Wolwedans and Knellpoort Dams, the Çine records are particularly useful in providing strain measurement perpendicular to the dam axis and the related linear thermal expansion under conditions of significant internal restraint is considered one of the most important observations in respect of the Çine RCC behaviour.

The fact that unrestrained expansion occurred in the RCC under a temperature rise is quite surprising. In a block of over 100 m in length and less than 20 m in height, it would have been assumed that most of the thermal expansion due to the hydration temperature rise would have been constrained by foundation and internal restraint. As will be discussed in Chapter 6, it is hypothesised that it is the cause of this very effect that is the origin of the difference in the early behaviour of high-paste RCC, compared to CVC.

All other measurement at Çine Dam recorded displacement across induced joints, parallel to the dam axis, measuring the dam behaviour in compression, as a consequence of restrained thermal expansion.

Unfortunately, insufficient time has passed to determine the final behaviour of the Çine RCC across the induced joints at their final equilibrium temperature, after all the hydration heat has dissipated. As a consequence of the applicable thickness of the section, it will in fact be several decades before cooling to the equilibrium temperature cycle will be achieved at the base of the dam and due to winter-season RCC placement, cracking will almost certainly not occur on all of the induced joints in this location.

4.5.8. CONCLUSIONS

4.5.8.1. General

Despite problems with the instrumentation readout unit, some incorrect cable labelling and some apparently conflicting data, the instrumentation confirms the early thermal RCC behaviour at Çine Dam to comply with the indications from Wolwedans and Knellpoort Dams and correspondingly to suggest lower shrinkage/creep that would be traditionally assumed.

Undoubtedly some creep relaxation was experienced when unrestrained thermal expansion of RCC occurred at Çine Dam. However, this was more than an order of magnitude less than would be expected according to the traditionally accepted materials models. Furthermore, the net expansion recorded after creep relaxation corresponds with the coefficient of thermal expansion indicated for the Çine Dam RCC in laboratory testing.

Accordingly, it is apparent that the behaviour recorded at Çine Dam so far confirms the findings indicated for Wolwedans and Knellpoort Dams.

4.5.8.2. Summary

The data recorded at Çine Dam provides a different, and yet confirmatory, slant on the apparent early behaviour of RCC. While the Çine Dam RCC was similar to that used at Wolwedans and Knellpoort, it was also quite different in using a low-grade fly ash and a lower total cementitious materials content.

4.5.9. ÇINE DAM THERMAL ANALYSIS

4.5.9.1. Background

In reviewing the instrumentation data recorded at Çine Dam, it is considered of value to demonstrate briefly the indications developed through a Thermal analysis for the dam and the consequential accuracy with which the measured temperature development and dissipation were predicted. A more comprehensive Thermal analysis is presented for Changuinola 1 Dam in Chapter 5, where the methodology

and modelling are described in some detail, and the thermal analysis for Çine Dam addressed in this Chapter is presented simply to demonstrate the correlation of modelling results with actual measurement.

4.5.9.2. Introduction

The Çine Dam thermal modelling was undertaken in mid 2005[8 & 9], after the first season of RCC placement had seen the dam constructed from its lowest foundation level of EL 128.5 mASL to EL 147.5 mASL. Thereafter, it was initially assumed that the construction would proceed at a slightly more rapid rate than that finally realised.

Compared to reality, the temperatures built into the model for Çine Dam were on the higher side, taking a conservative view to ensure that the related consequences of thermal gradients were not under-estimated. However, as a consequence, the measured maximum temperatures were generally lower than those modelled, particularly at EL 147.50 mASL.

4.5.9.3. Çine Dam RCC Materials Properties

For the Thermal Analysis of Çine Dam, various important thermal properties for the RCC were determined by laboratory testing at the Middle Eastern Technical University (METU)[7]. The following average values for the important indicated properties were determined:

Coefficient of Thermal Expansion	7.10 x 10^{-6} strain/°C
Elastic Modulus under 5.5 MPa	24.7 GPa
Creep under 5.5 MPa for 1500 hours	110 microstrain
Drying Shrinkage	< 25 microstrain

4.5.9.4. Comparative Analysis Results

The Çine Dam thermal modelling indicated that a period of approximately 50 years would elapse before the effects of the trapped heat of hydration would be fully dissipated. The most immediate effects, however, that could be seen to occur within the first few years of placement was a complete absence of temperature drop within the core of the structure and a movement of heat downwards that caused a rise in temperature at EL 147.5 mASL, for example, of around 1°C by October 2008. While both these effects were observed in the measurements on the prototype, the temperature increase was essentially from 24°C to 25°C on the prototype, compared to 26°C to 27°C on the model, as illustrated on **Figures 4.35** and **4.36**.

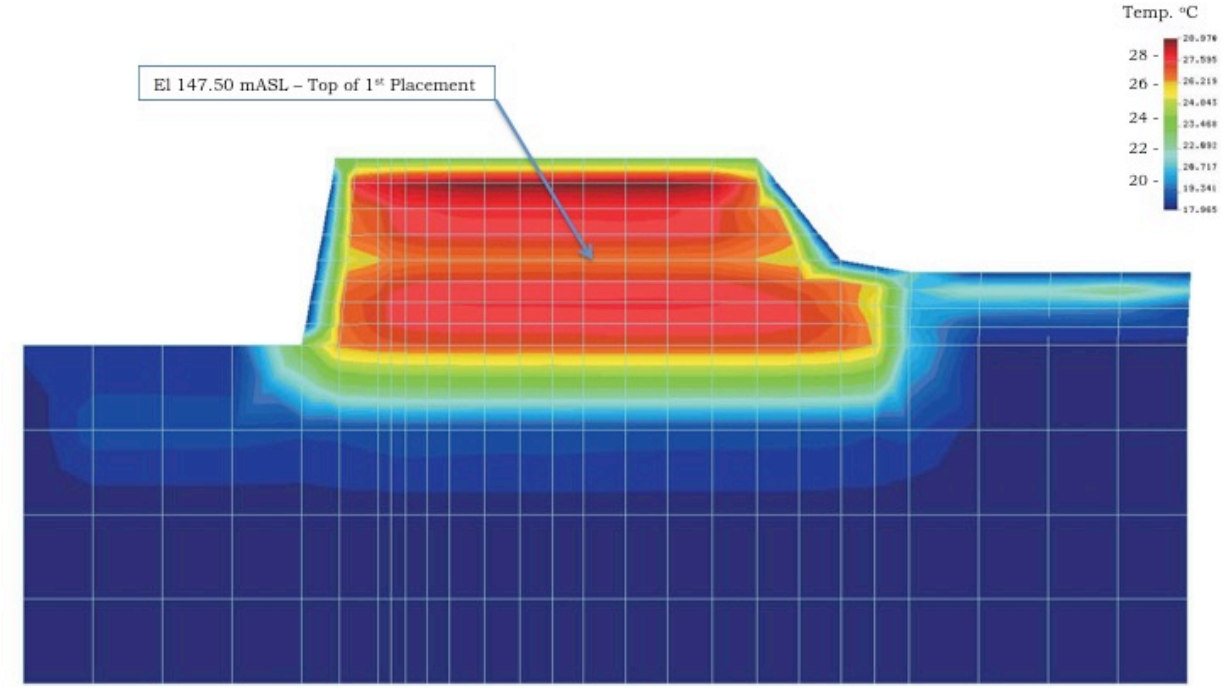

Figure 4.35: Çine Dam Thermal Analysis Temperature Plot – October 2006(9)

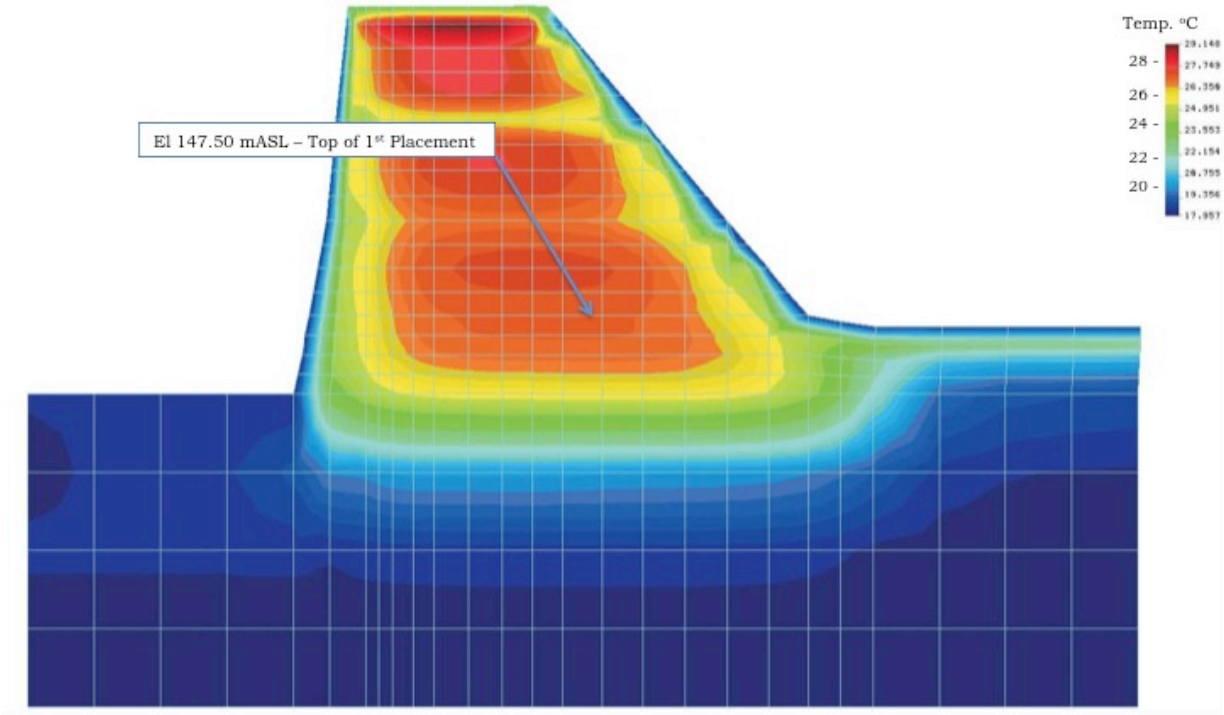

Figure 4.36: Çine Dam Thermal Analysis Temperature Plot – October 2008(9)

At Elevation 185.25 mASL, the modelling predicted a temperature of approximately 26.5°C in October 2008, while the actual measurements reflected temperatures ranging from 25.5 to 27.5°C.

4.6. WADI DAYQAH DAM

4.6.1. GENERAL

The general arrangements of Wadi Dayqah Dam and the layout of the instrumentation installed are described in Chapter 2. In this Chapter, the early thermal behaviour of the RCC structure is evaluated through an analysis of the temperature and induced joint strain/displacement data from placement to March 2009.

4.6.2. INSTRUMENTATION

Due to a relatively restrictive budget and the simplicity of the dam structure, the thermal monitoring instrumentation for Wadi Dayqah Dam was relatively simple, comprising air temperature, water temperature and arrays of concrete temperature meters (termed RTD gauges) at five elevations (El 109.80, 125.00, 140.00 & 155.00 mASL) on two cross sections[11]. In addition, Long-Base-Strain-Gauge-Temperature-Meters (LBSGTMs – sometimes abbreviated to LBSG) were installed across all of the induced joints, approximately in the centre of the cross section at two elevations. The LBSGTMs at elevation EL 135 mASL were installed in mid August 2008 and those at elevation EL 150 mASL were installed in mid October 2008[12].

Figure 4.37 illustrates the basic layout of the important thermal behaviour monitoring instrumentation. The LBSGTMs at EL 135 mASL are located in the centre of the section, at approximately 15 m from the up- and downstream faces, while the LBSGTMs at EL 150 mASL are located at approximately 12 m from either face.

Plate 4.4: Early RCC Placement

4.6.3. IMPORTANT CONSIDERATIONS

In the case of Wadi Dayqah Dam and the interpretation of the installed instrumentation, a number of specific factors of influence must be given careful consideration, as follows:

- The RCC was generally cooled to approximately 24 to 26°C for placement[13], a temperature well below that of the ambient environment;
- The LBSGTMs were installed in the top of a layer, which was approximately at ambient/ maximum hydration temperature, having been exposed to intense solar radiation for 5 to 6 days when the new RCC was placed above;
- Joint inducers were placed in every second layer of RCC, giving rise to a particularly low effective tensile strength across the induced joints;

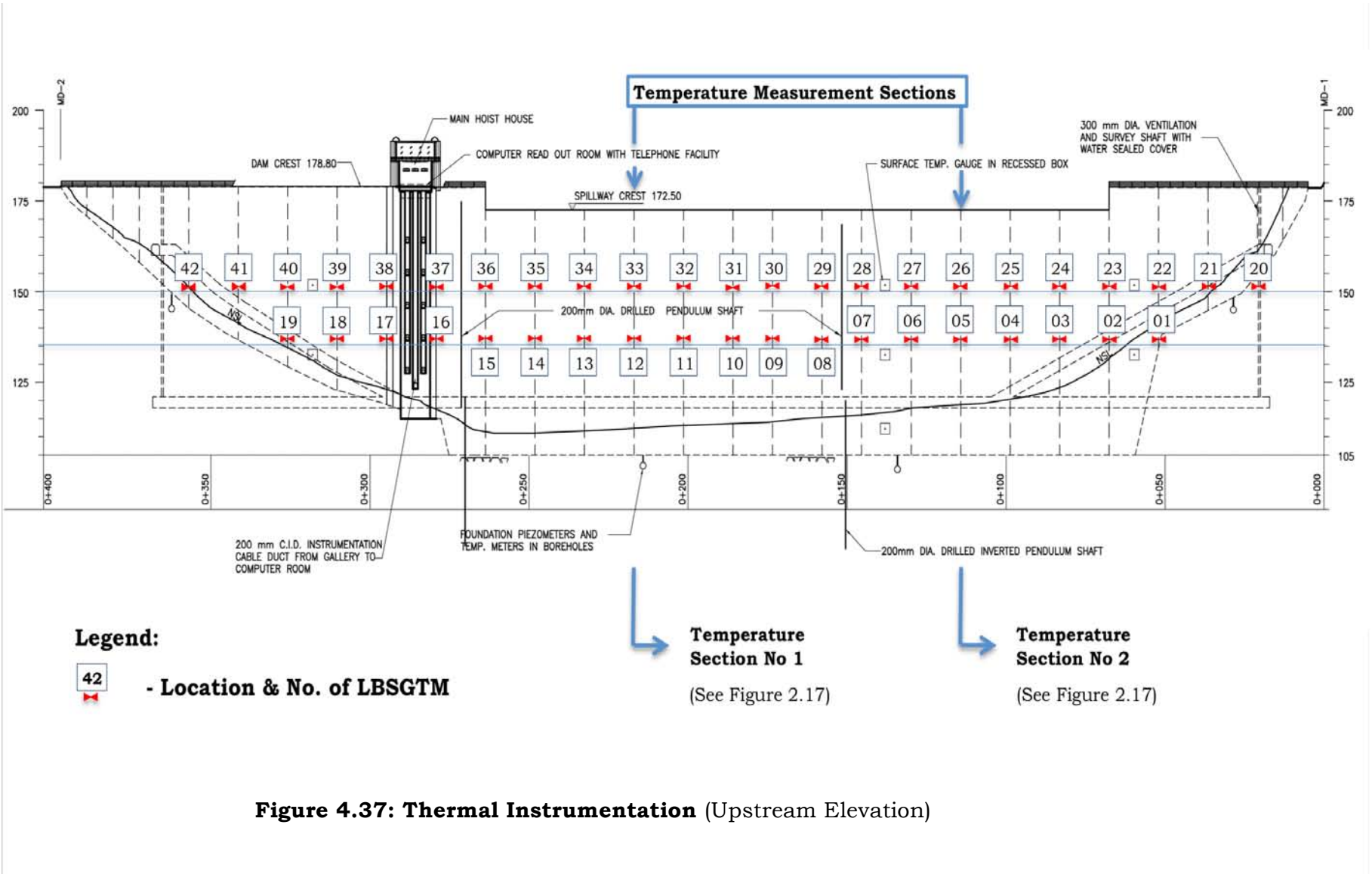

Figure 4.37: Thermal Instrumentation (Upstream Elevation)

- The RCC mix had a low cementitious materials content;
- The RCC mix contained a ground limestone filler material;
- The RCC mix contained crushed natural limestone as part of the sand fraction;
- The RCC mix contained a large proportion of fines;
- The RCC contained a sand/aggregate ratio of 0.44; and
- The aggregates comprised a partially crushed colluvial gravel, which was probably not of the highest quality.

Over the main period of placement between August and October 2008, the daytime ambient temperatures on site typically ranged between 30 and 40°C. From mid October, the ambient temperatures started dropping, indicating a minimum in mid to late January.

As a consequence of the above, several apparently strange behaviour patterns were observed.

When the RCC into which a LBSGTM was installed was particularly warm, the "zero" temperature of the gauge was substantially higher than that of the artificially cooled RCC placed immediately above. By the same token, the RCC immediately around the gauge had experienced expansion stress in the process of its temperature gain from placement. As a consequence, a complex and localised temperature/stress environment was developed. While the gauge was inserted into

Plate 4.5: Wadi Dayqah Dam – May 2009

RCC that had already been heated by the environment and hydration heat, the cooler temperature of the RCC placed above caused the temperature of the gauge and its surrounding concrete to cool rapidly by a few degrees. Thereafter, the hydration heat development in the RCC above started raising the temperature of the concrete around the gauge. As the increasing temperature created expansion/swelling stresses in the newly placed RCC above, the RCC below would have experienced shear stresses, as it effectively acted as a partial restraint against expansion for the RCC above.

This process gave rise to a very different pattern of early behaviour compared to a situation where a gauge was embedded in RCC at a similar temperature to that of the new RCC placed above. In the latter case, the rapid hydration temperature rise caused the gauge, located above a joint inducer, to contract. On the graphs of LBSGTM data for Wadi Dayqah, the above phenomena caused patterns at the different gauges that apparently contradicted each other significantly, with one set of gauges indicating rapid expansion that gradually slowed and another indicating rapid contraction that gradually slowed and in some cases subsequently reversed to expansion.

4.6.4. RCC MIX, MATERIALS & PROPERTIES

As described in Chapter 2, two RCC mixes were specified for Wadi Dayqah Dam; a 15 and a 12 MPa mix. The former mix was specified for the upstream impermeable zone and the toe zone of higher stress. The latter mix was specified for the bulk, core zones in which all of the LBSGTMs were installed.

The Wadi Dayqah Dam RCC mix was unusual in that it was a “high-paste” RCC that contained only 112 kg/m^3 of cement combined with 48 kg/m^3 of ground limestone filler, in the case of the Zone 2, 12 MPa mix. Furthermore, the crushed sand was blended with 34% crushed limestone. The resultant RCC mix contained over 13% fines and over 26% of the RCC material was finer than 1.2 mm. The mix further indicated a rather high sand content, with a sand/aggregate ratio of 0.44. Treating the ground limestone as a non-cementitious filler, the Zone 1 and 2 RCCs indicated w/c ratios of 1.02 and 1.11, respectively.

On the basis of an extensive programme of core extraction and testing, the in-situ properties listed in **Table 4.5** were determined for the two RCC mixes[13].

Table 4.5: Average RCC Properties measured on Cores (90 days age)[13]

Parameter		**RCC**	
		15 MPa (Zone 1)	**12 MPa** (Zone 2)
Compressive Strength (MPa)	90 days	15.3	14.2
	365 days	20.3	17.0
Tensile Strength (MPa) - 90 days		1.10	0.81
Permeability (m/s)		3.1×10^{-11}	4×10^{-8}
Direct Shear Strength (MPa)		1.80	1.16
Modulus of Elasticity (GPa) – 365 days		23.5	20.8
Poisson's ratio		0.15	0.1
In-situ Measured Density (kg/m^3)		2420	2428
Vebe Time (seconds)		14 - 15	12 - 13

4.6.5. TEMPERATURE DATA

4.6.5.1. Heat of Hydration

Theoretical calculations for the adiabatic heat of hydration, based on the anticipated cement and aggregate characteristics, indicated an anticipated temperature rise of 13.5°C for the Zone 1 RCC and 12.5°C for the Zone 2 RCC, respectively. The temperature data recorded within the dam would suggest that these figures over-estimate the actual situation by up to 2°C, suggesting that the Omani cement used was probably a relatively low heat material.

4.6.5.2. Measured Temperatures

The RCC temperatures were measured using resistance thermal detectors (RTDs) at four separate elevations on two different cross-sections on the dam wall, as illustrated on **Figure 4.37**. **Figures 4.38** to **4.43** illustrate the temperatures recorded to March 2009 on each of these levels, at both cross-sections.

In **Figure 4.38**, a significant delay between the installation of the temperature meters at Sections 1 and 2 can clearly be seen. Furthermore, the placement temperature was evidently substantially higher at the latter section.

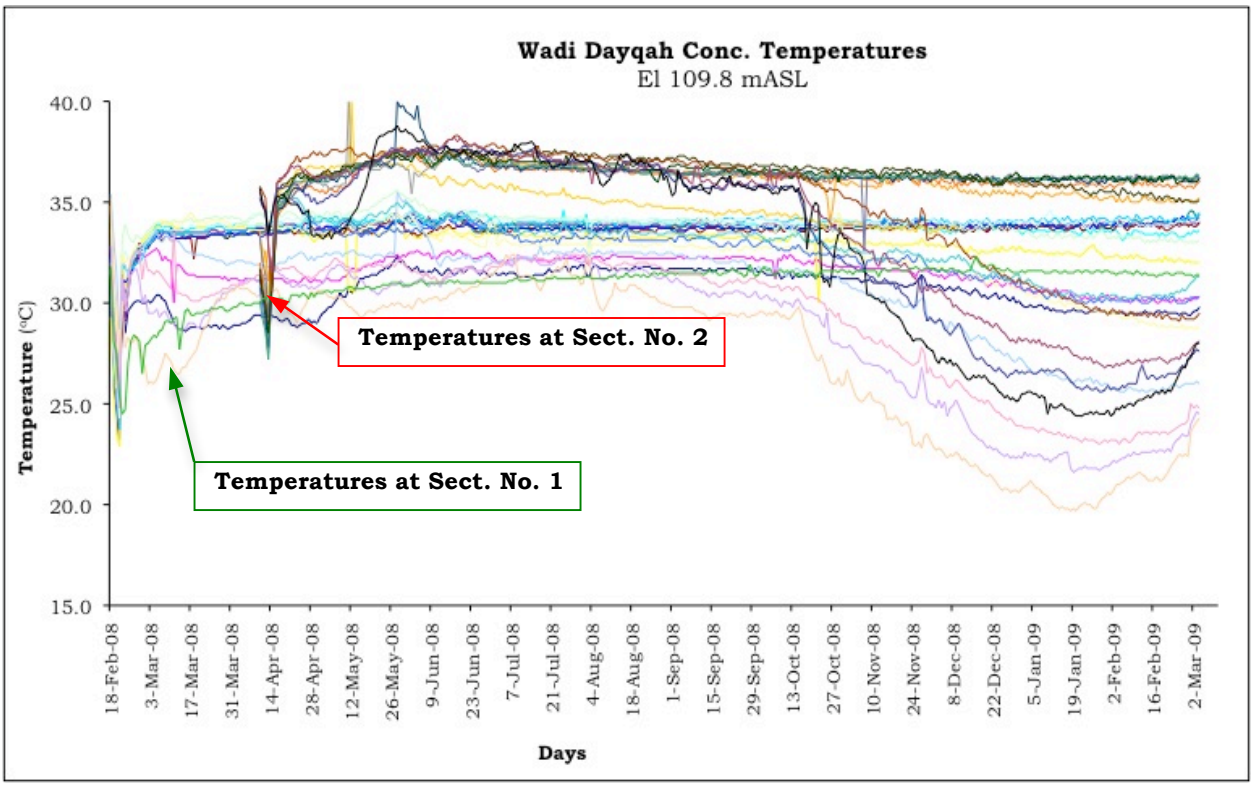

Figure 4.38: Temperatures Measured on RTD Gauges at EL 109.8 mASL(12)

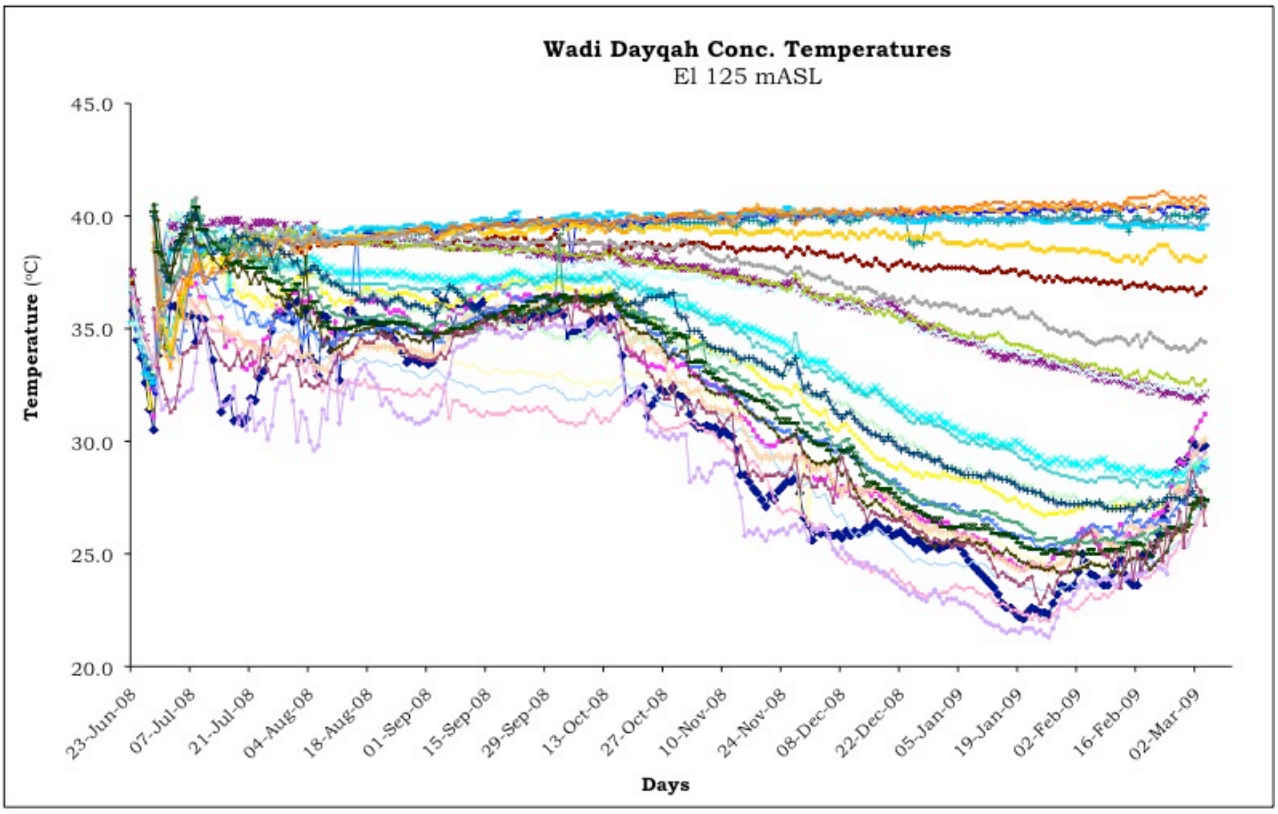

Figure 4.39: Temperatures Measured on RTD Gauges at EL 125 mASL(12)

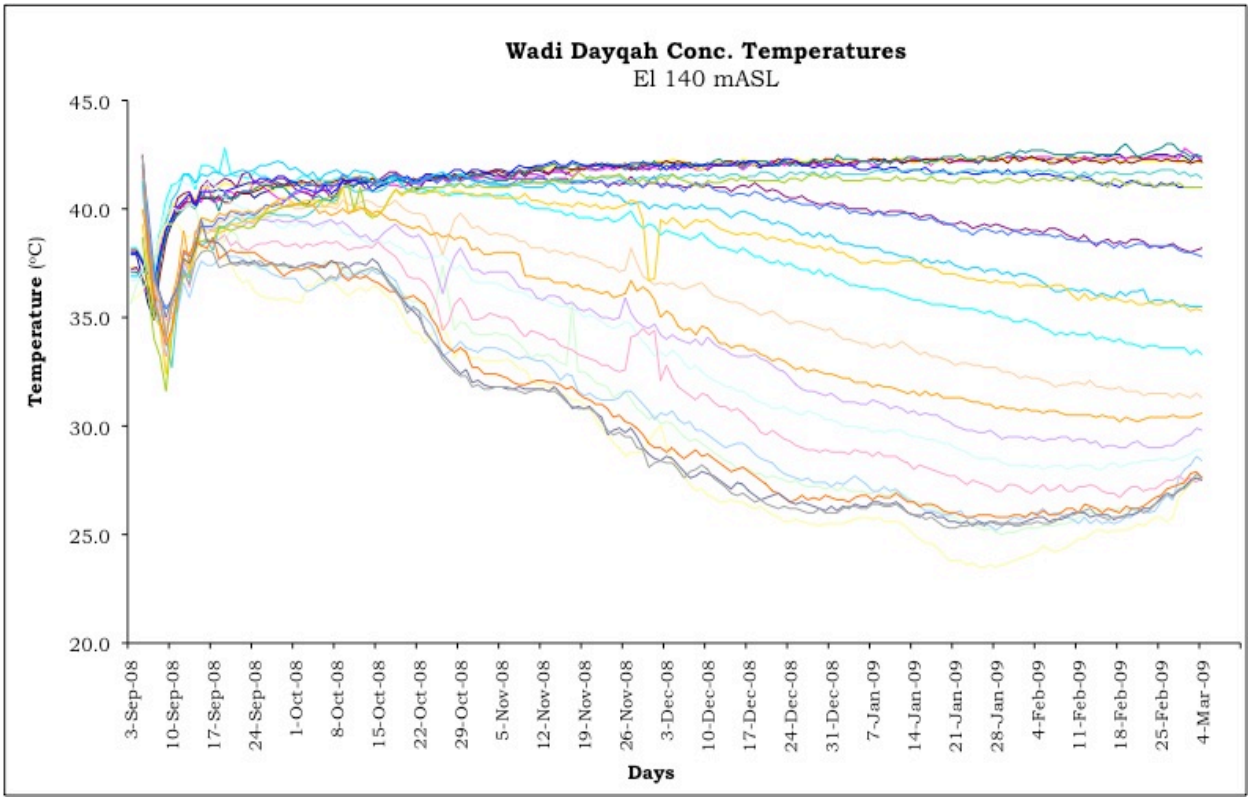

Figure 4.40: Temperatures Measured on RTD Gauges at EL 140 mASL(12)

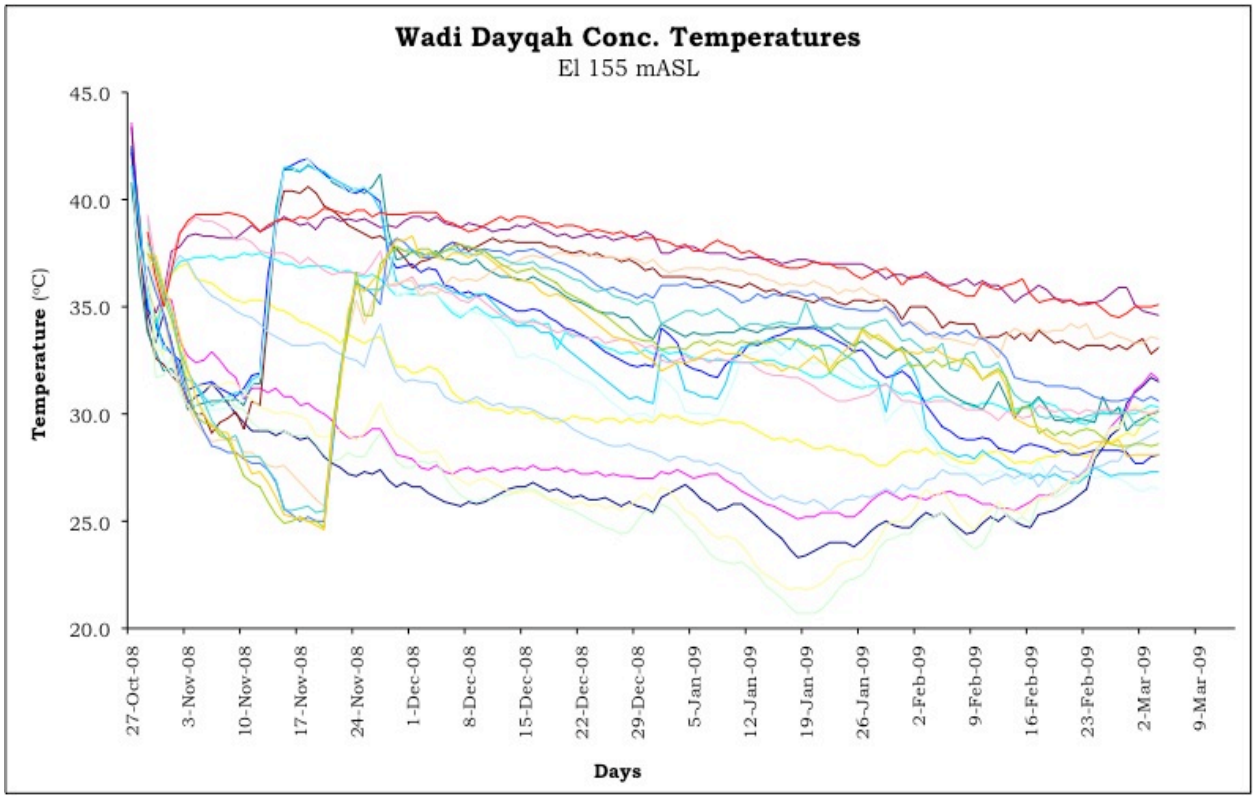

Figure 4.41: Temperatures Measured on RTD Gauges at EL 155 mASL(12)

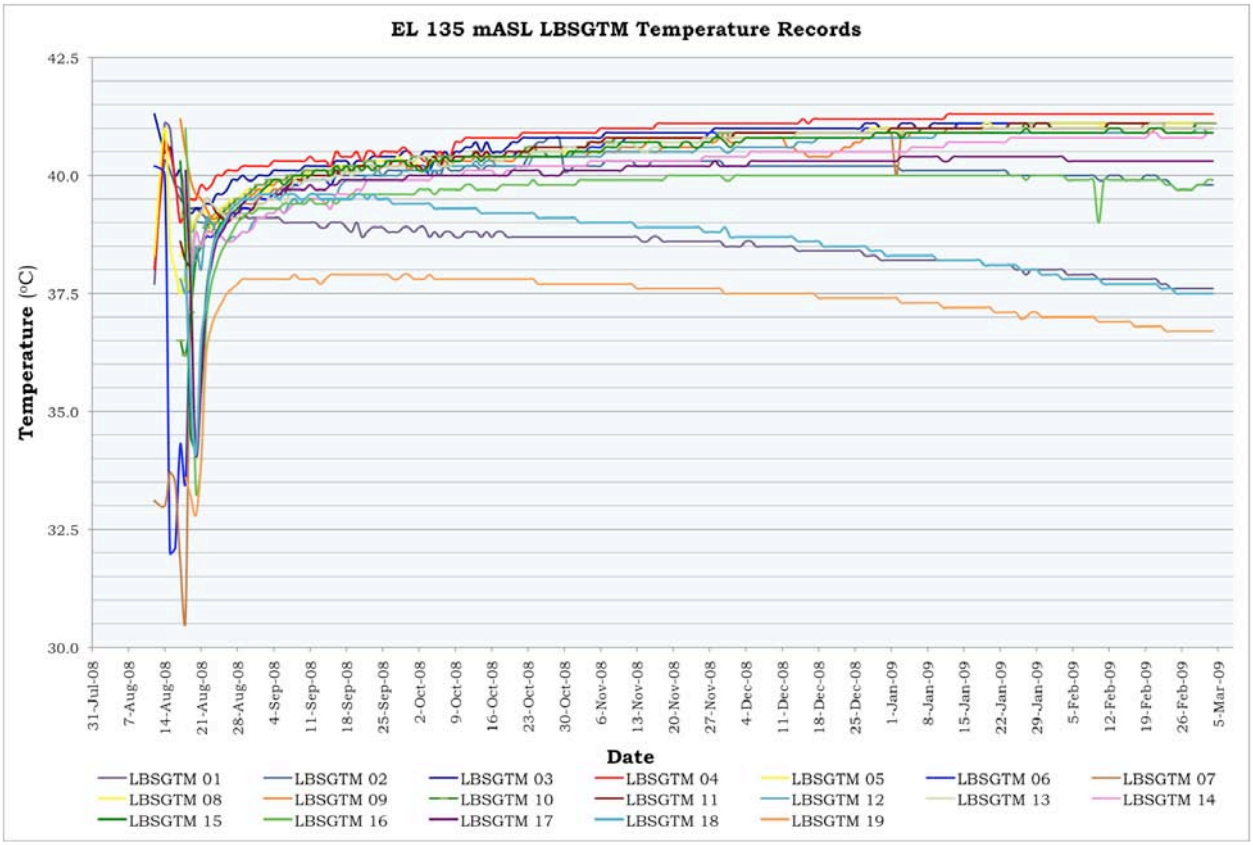

Figure 4.45: Temperatures on LBSGTM Gauges at EL 135 mASL(12)

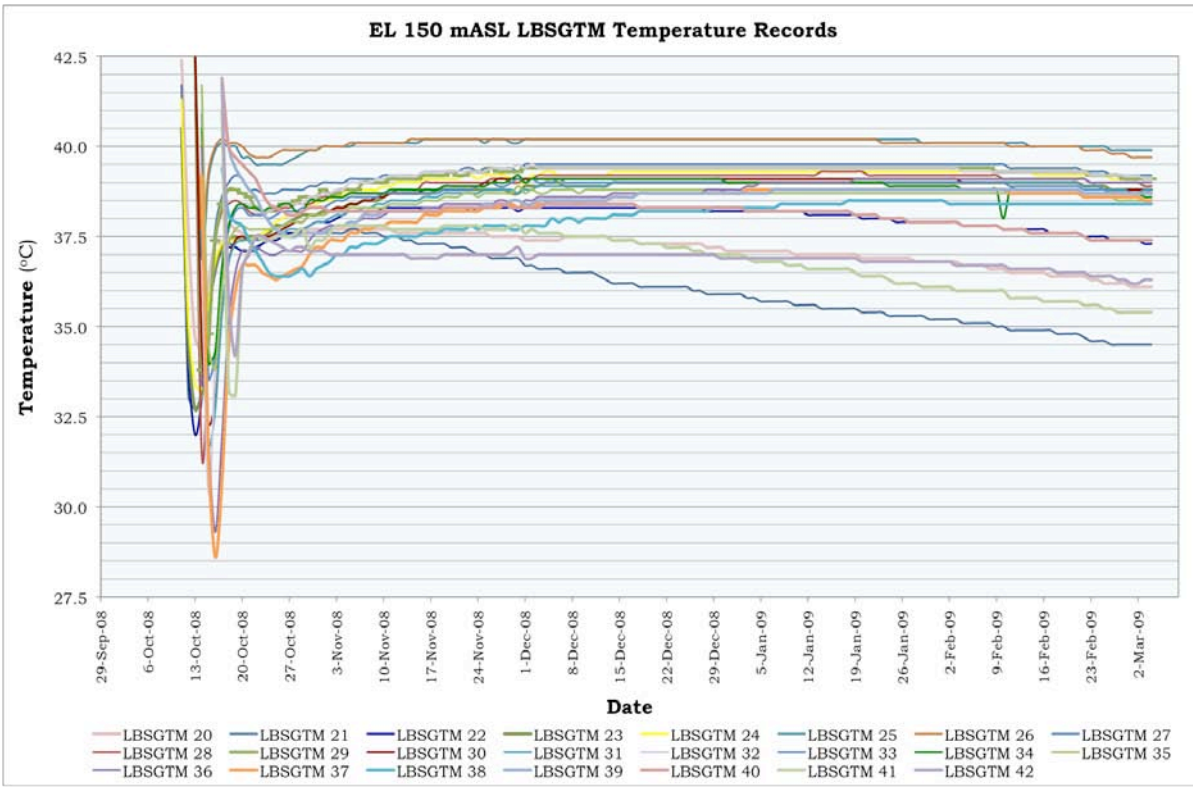

Figure 4.43: Temperatures on LBSGTM Gauges at EL 150 mASL(12)

4.6.5.3. Discussion of Temperature Patterns

The observed temperature patterns are generally consistent with expectations. Where the section is relatively wide, temperatures are either maintained at their hydration peak, or were still climbing slowly in March 2009. Where the section is thinner, closer to the faces and close to the foundation, the temperatures had started to drop from peak. Close to the dam faces, the hydration heat had already been dissipated and the temperature was observed to follow the external ambient patterns.

At El 109.8 mASL, the temperature gauges (RTDs) placed in the core zone of the dam on the first instrumentation section, where the foundation level is deeper, can be seen to be indicating a continuing rise in temperature. On the second section, where the temperature gauges (RTDs) are located only a few metres above the foundation, the opposite trend can be perceived, with the temperatures gradually dropping as a result of the proximity of the cooler foundation rockmass. At El 125 mASL and El 140 mASL, on the other hand, the temperature of all core zone RTDs can be seen again to be slowly rising. At El 155 mASL, not only is the section substantially narrower, but all of the RTDs are essentially in the surface zone and, unsurprisingly, it can be seen that the temperatures are quickly influenced by the cooler external ambient conditions.

On the LBSGTMs, the temperature patterns are similarly in accordance with expectations, with the core temperatures at the lower elevation continuing to rise slowly, except where close to a cooler foundation. At El 150 mASL, the thinner section can be seen in the fact that the temperatures appear to have peaked and were starting to drop by March 2009. Again, on either abutment, the influence of the proximity to the foundation could clearly be determined, with the temperatures generally becoming more depressed with time, the closer to the cooler rockmass.

Two specific peculiarities, however, could be determined from the recorded temperature data. Firstly, the placement of significantly cooled RCC could be determined in the initial drop in temperature measured on all of the installed instruments. Secondly, the apparent hydration temperature rise, after this initial drop, never exceeded 10°C and was quite often significantly less.

4.6.6. LBSGTM Deformation Readings

4.6.6.1. General

Deformations were recorded on LBSGTMs across each of the joints at two elevations, as described earlier. All of these instruments proved to be reliable, although oscillations of the readings of as much as 0.1 mm were frequently observed. Whereas the deformation patterns generally evident were quite different from those observed on other dams addressed in this study, Wadi Dayqah is the

only dam investigated for which the RCC was significantly artificially cooled well below ambient temperature for placement, while it is also the only lean RCC considered in this investigation.

4.6.6.2. LBSGTM Behaviour at El 135 mASL

The deformations measured on the LBGTMs at El 135 mASL from installation to March 2009 are illustrated on **Figure 4.44**. The same deformations are presented again, but separated into the gauges close to the abutment on **Figure 4.45** and those remote from the abutment on **Figure 4.46**.

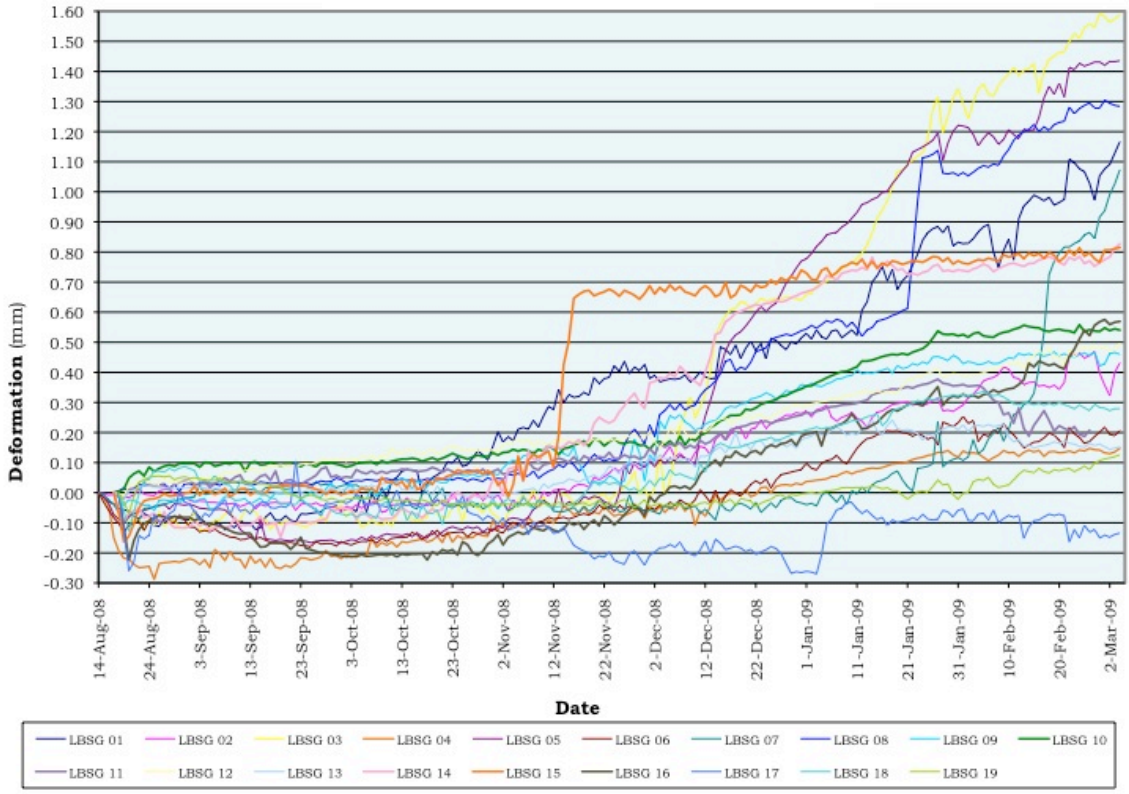

Figure 4.44: LBSGTM Deformation Measurement at EL 135 mASL(12)

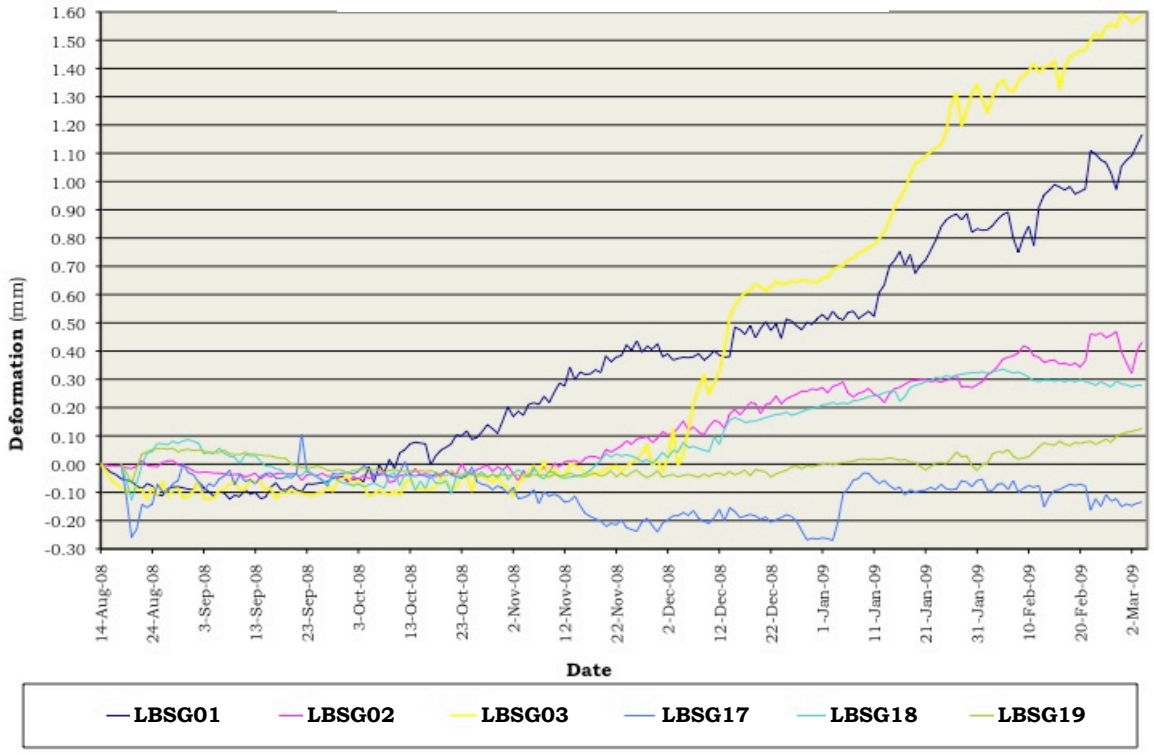

Figure 4.45: LBSGTM Deformations at EL 135 mASL Closer to Abutments(12)

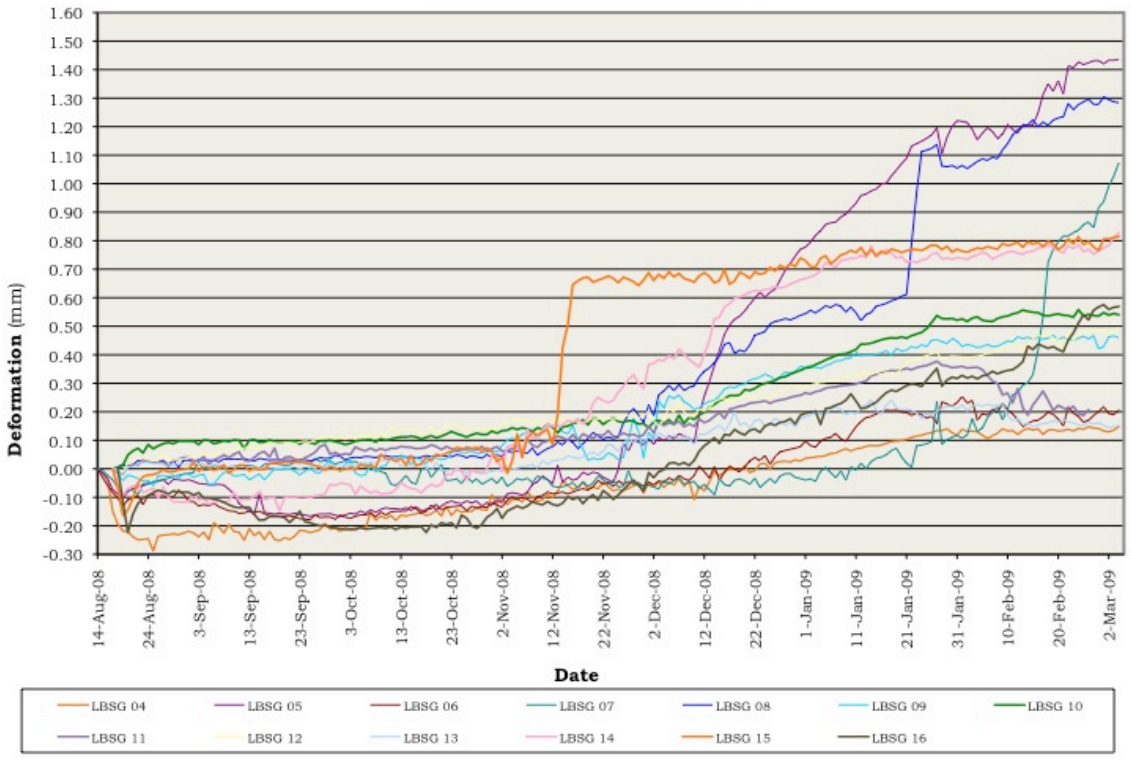

Figure 4.46: LBSGTM Deformations at EL 135 mASL Remote from Abutments(12)

At El 135 mASL, the temperature of the core LBSGTMs (LBSG gauges) was generally still rising very slowly by March 2009. The exceptions were the gauges at either end, closest to the abutments, where temperatures had fallen by as much as 2°C.

The most significant issue in respect of the LBSGTMs installed at El 135 mASL is the fact that it is not possible to determine distinctive and predictable patterns that are repeated. The gauges on the abutments at the right side of the dam (LBSG 01, 02 & 03 on Figure 4.45) indicated significant expansion/cracking, still increasing in March 2009, while the gauges on the left abutments indicated little, or no expansion at all (LBSG 17, 18 & 19 on Figure 4.45).

Certain of the LBSGTMs indicated very obvious cracking, while others demonstrated the steady development of strain. Of the 19 gauges installed at El 135 mASL, 16 indicated a very distinct levelling-off of the expansion strain by March 2009, while the remaining 3 (1 centrally located & 2 on the abutments) indicated continued expansion. Over December 2008 and January 2009 the majority of the gauges indicated fairly linear expansion at approximately the same rate.

The measured total maximum expansion across all the gauges sums to 11.5 mm.

4.6.6.3. LBSGTM Behaviour at El 150 mASL

The deformations measured on the LBGTMs at El 150 mASL from installation to March 2009 are illustrated on **Figure 4.47**. The same deformations are presented on the following two figures, with the gauges close to the abutment on **Figure 4.48** and those remote from the abutment on **Figure 4.49**.

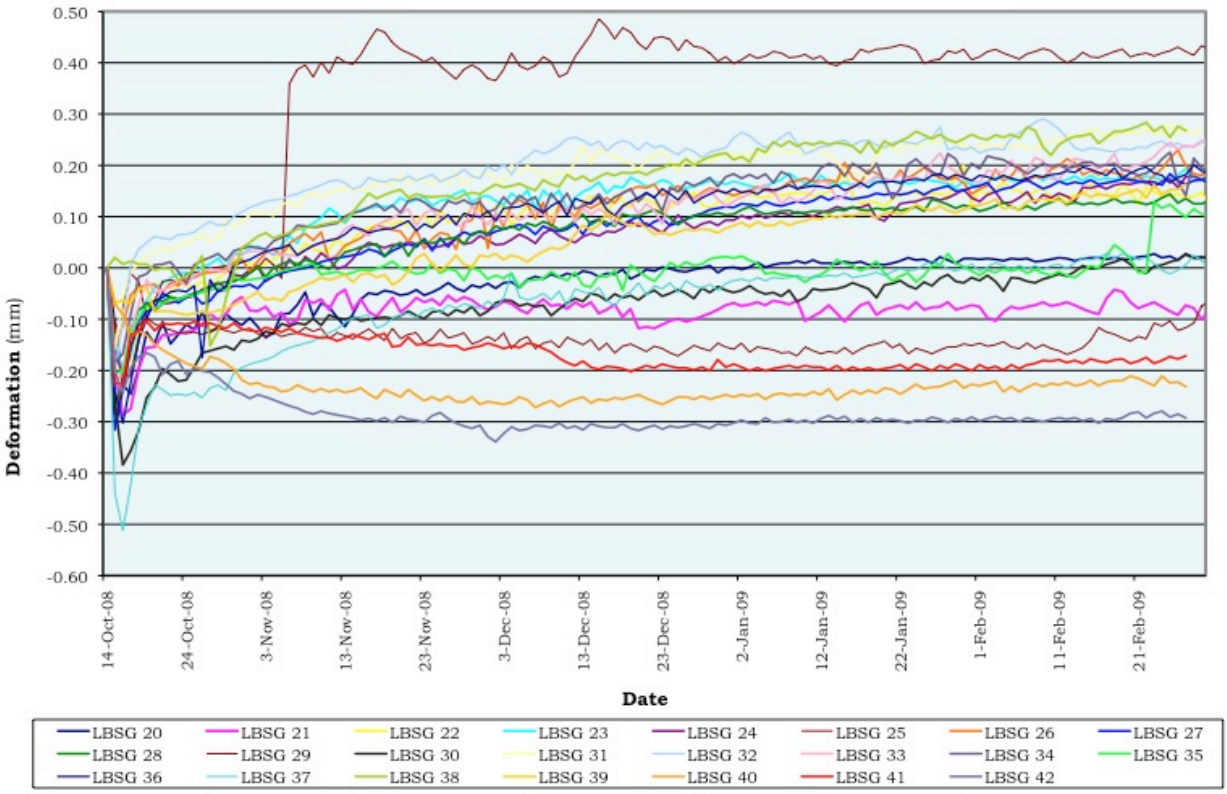

Figure 4.47: LBSGTM Deformations Measurement at EL 150 mASL(12)

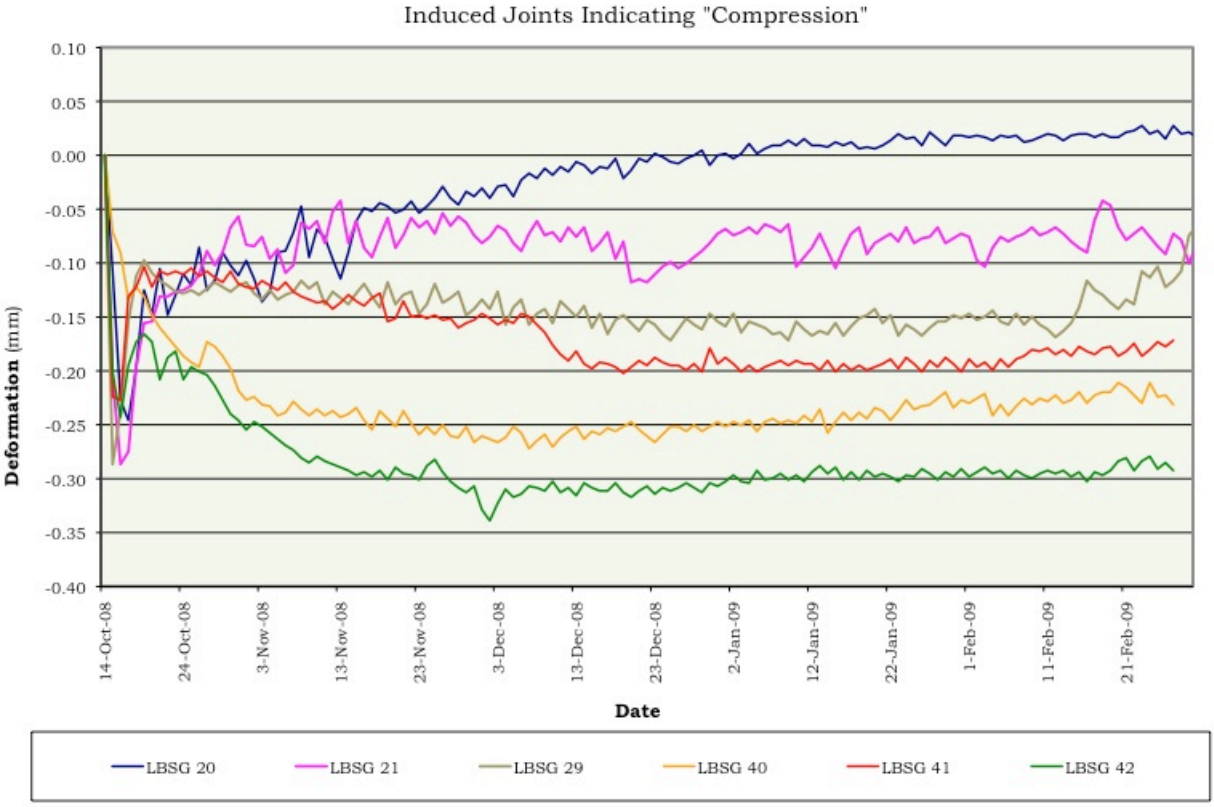

Figure 4.48: LBSGTM Deformations at EL 150 mASL Closer to Abutments(12)

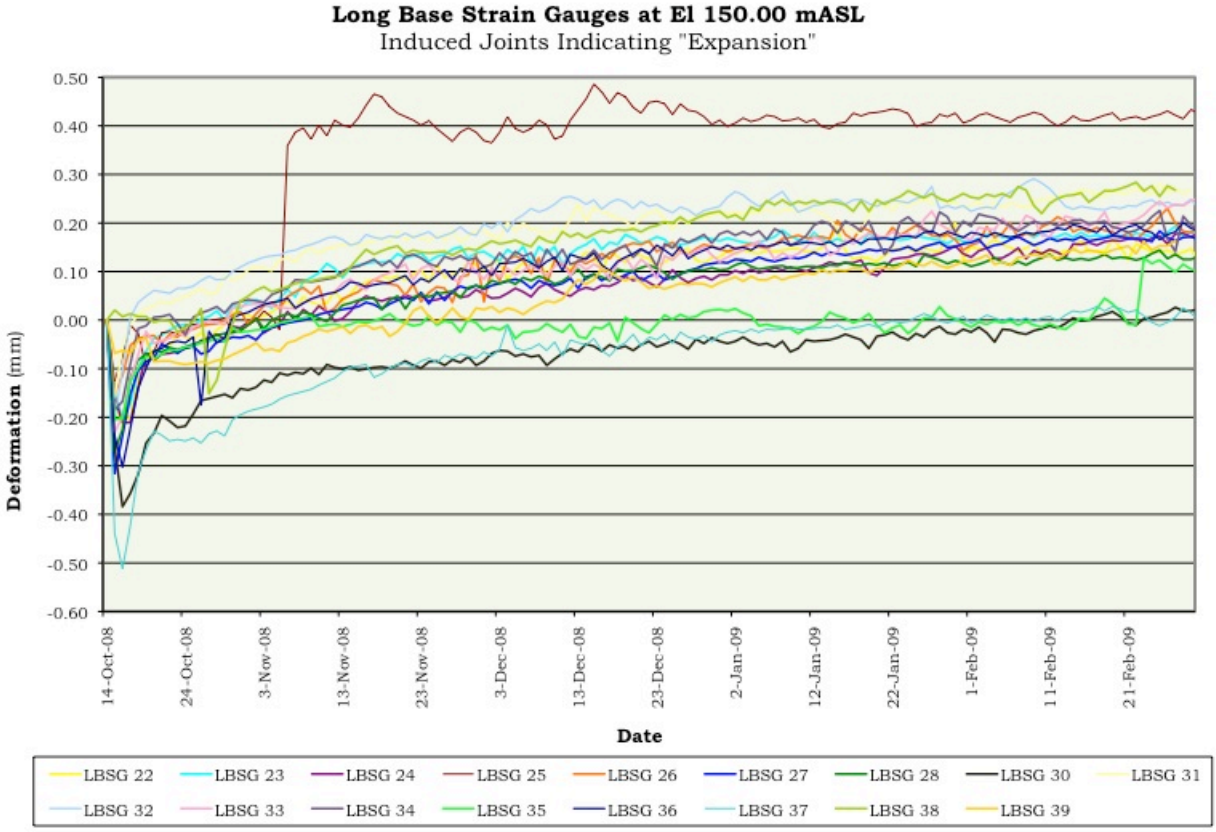

Figure 4.49: LBSGTM Deformations at EL 150 mASL Remote from Abutments(12)

The LBGTMs at El 150 mASL indicate a pattern of compression where close to the abutments and expansion away from the abutment rockmass. Similarly to the gauges at El 135 mASL, a pattern of greater compression/joint closure is evident on the gauges on the left abutment (LBSG 40, 41 & 42 on Figure 4.48), while a greater tendency towards expansion/joint opening can be discerned on the right abutment (LBSG 20 & 21 on Figure 4.48). While this situation might seem difficult to understand, it is important to take note that although the majority of the gauges, and the top of the previous RCC layer, were exposed to severe solar radiation for a period of 5 to 6 days before the cooler RCC was placed on top, four gauges at El 150 mASL were in fact installed immediately before new RCC placement. **Figure 4.50** illustrates the deformation histories for these gauges.

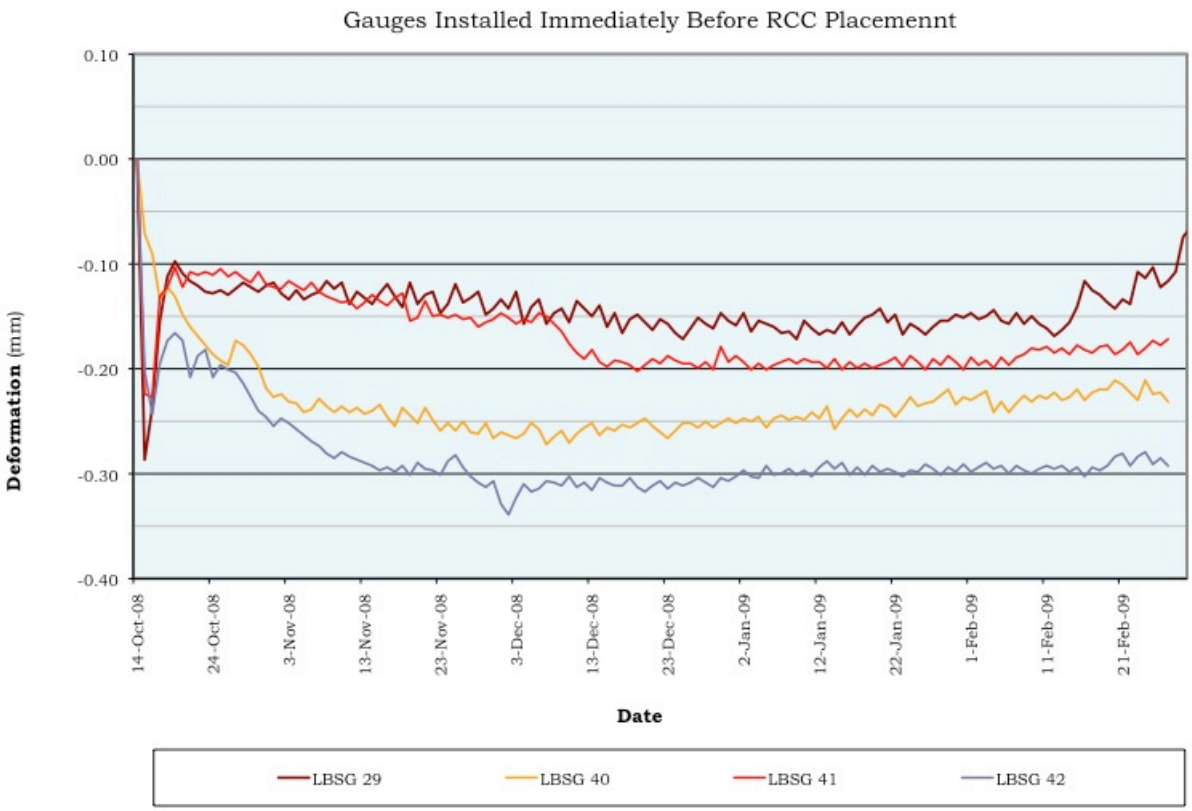

Figure 4.50: Deformations on LBSGTMs Installed Shortly Before New RCC(12)

A particular point of interest lies in the fact that the above gauges all remained in compression and behaved in a manner much more similar to that of the gauges installed at other dams where significant RCC cooling was not applied.

The deformations of all gauges at El 150 mASL have apparently arrived at a point of greater stability/finality than have the gauges at El 135 mASL, despite the older age of the concrete in the latter location. While the gauges on the abutments indicate no real joint opening in this area, the total maximum displacements/joint openings across the other induced joints sum to approximately 3.25 mm.

4.6.7. DISCUSSION OF FINDINGS

4.6.7.1. General

While some of the LBSGTM gauges indicated the development of cracks exceeding 1 mm, no signs of the same effects have become evident on the surface of the dam. If these readings were a real reflection of the general development of RCC shrinkage, this would have been expected to have been manifested in significant cracks at the induced joints on the dam surface. It is of course possible that such surface cracking will become apparent during the next cool period in December/January.

The low tensile strength across the joints was demonstrated in most instances by a gradual opening deformation being registered on the LBSGTM gauges. On only four gauges at El 135 mASL and one at El 150 mASL was the rapid development of a "crack" clearly evident.

The "expansion" measured on the majority of the LBSGTMs can only relate to the shrinkage of RCC blocks (between induced joints) away from each other. If the gauges were measuring general shrinkage strain in the RCC, they would contract, as opposed to expand, while if the gauges were subject to a swelling associated with temperature rise, thy would either contract across the more compressible induced joint, or remain unchanged, with the expansion strain being converted to restrained compressive stress. With an induced joint spacing of just 15 m, this implies that a relatively high level of confidence can be ascribed to the fact that all of the RCC shrinkage is measured on the installed gauges.

It is very significant to note that significant opening of a crack (> 0.5 mm) was indicated at El 135 mASL on induced joint Nos 4, 6, 8, 10, 11, 12, 13, 15, 17, 18 and 19 and at El 150 mASL only really on induced joint No 7. It is, however, equally significant to note that the gauges that were not installed into an environment of divergent temperatures behaved quite differently and in a similar manner to the instruments at the other dams that form part of this study.

4.6.7.2. Discussion

In the core zone of the RCC at El 150 mASL, it is apparent that the temperature is still being fairly constantly maintained at the peak hydration temperature. The exceptions to this observation are the areas at each end of the dam, where the cooler adjacent foundation has started to bring the temperatures down by as much as 3°C. On the LBSGTMs close to the foundations, this temperature reduction is starting to give rise to slight reduction in compressive strain.

As mentioned under 4.6.3 above, a specific behaviour pattern was observed wherever the temperature of the RCC into which the LBSGTMs were installed was substantially below that on the artificially cooled RCC placed immediately above. This situation was further exacerbated in most instances by the fact that the subsequent temperatures experienced in these gauges never exceeded the original "zero" temperature of the gauge. In relation to this apparent pattern, it is considered important to understand that it is very much the behaviour of the RCC in the layer beneath that is being monitored in this instance, as opposed to the fresh RCC that is placed above.

On the gauges where foundation restraint and temperature influence were not significant, it is clear that the gauges returned to their "zero" expansion at a lower temperature than that at which "zeroed". The reason for this observation cannot be determined with certainty. Should creep have occurred in the cooled RCC, the "zero" expansion should only have been reached at a temperature above, rather

than below, the "zero" temperature. It is accordingly considered that this effect arises as a result of micro adjustments in the green concrete, as a consequence of the fact that the cooling happened very rapidly, over a period of between 1 and 3 days, while the re-warming took place over a period of around a month.

It is also considered important to note that the apparent process of slow expansion that continued after the maximum hydration temperature was reached does not demonstrate any abrupt change when the state of zero deformation is reached. If the gauge and its surrounding concrete was rapidly cooled and consequently shrank, it would be expected that it would expand easily with increasing temperature until its original volume state was reached, after which the expansion forces would be resisted by the compressive strength of the concrete and expansion would abruptly diminish. The fact that the expansion appears to be gradually and very slowly diminishing is consequently considered to be a sign either of the fact that the induced joint is opening, or it is a consequence of the fact that the temperature experienced never reaches the "zero" temperature of the gauge and the surrounding RCC at the time the new RCC was placed above.

In all instances where the "zero" temperatures of the gauges were not significantly above the temperature of the new RCC, or when an obvious cracking occurs on the induced joint, no ongoing expansion is evident and the behaviour is as expected. However, it is important to take cognizance of the fact that the gauges in question were also located close to the foundation, where the restraint against movement will be greatest.

4.6.7.3. Quantitative Evaluation

General

Should RCC have behaved like conventional concrete, it would have demonstrated a combined shrinkage and creep of around 200 microstrain over a period of probably around 6 months. With no cracking at the induced joints, this would have been manifested on the LBSGTMs as an expansion of approximately 0.14 mm. If all of the movements were concentrated at the induced joints, the gauges would have indicated a net expansion of 3 mm across each of the induced joints.

LBSGTMs at EL 135 mASL

The measured total maximum expansion across all the gauges sums to 11.5 mm, implying an average opening of approximately 0.6 mm per induced joint, which translates into an average shrinking strain of approximately 43 microstrain. Three of the gauges indicated some ongoing crack development in March 2009; two very minor, one quite significant. If we assume a further 0.5 mm for the former and 0.2 mm each for the latter two, total shrinkage strain would still be less than 50 microstrain.

LBSGTMs at El 150 mASL

It is further important to note that the apparent expansion indicated on the LBSGTM gauges at El 150 mASL cannot be representative of the behaviour of the RCC between the induced joints. If this was the case, it would imply that the dam is expanding between its abutments by 165 microstrain and that the dam has increased in length by approximately 50 mm. Should it be possible to make any interpretation of the indicated expansions, it would be necessary to assume a worst-case scenario of the dam shrinking, due to autogenous/drying shrinkage and/or creep, and the induced joints accordingly opening to accommodate this process. This is considered to be a conservative assumption at best and unrealistic at worst as a consequence of two factors; namely, the fact that this behaviour is not evident at all on the gauges where the substantial temperature differences were not noted and secondly because, it appears that some slippage has occurred between the gauge and the green adjacent concrete during the process of rapid cooling when the cold new RCC was placed on top.

Reviewing this, possibly unrealistic, worst-case scenario would indicate a cumulative joint opening of approximately 3 mm across the central 19 blocks of the dam wall, which translates into a shrinkage strain of approximately 11 microstrain. If this shrinkage strain is a reality, it would probably represent a creep, as the temperature was maintained at its peak within the core of the dam over the applicable period. It is, however, possible that some form of drying shrinkage is occurring as the aggregates release the significant quantity of moisture absorbed during mixing of the RCC.

Summary

Although a similar shrinkage is apparently demonstrated at both LBSGTM installation levels, the extent of shrinkage is quite different. While it might be to be expected that the shrinkage would be greater at the gauges installed earliest, in the evaluation the shrinkage appeared to have in fact fully stabilised at the gauges at El 150 mASL, despite the fact that the temperatures were starting to drop by March 2009, but not completely at the gauges at El 135 mASL. This suggests that the cause of the shrinkage must, at least partly, be caused by some variation in materials characteristics.

4.6.7.4. Behaviour Hypothesis

Taking cognizance of the above discussion, it is considered that the behaviour of the LBSGTMs installed in Wadi Dayqah Dam relates primarily to two significant factors; firstly, the complex temperature/strain field that was set up between the placed and new RCC as a result of the significant RCC cooling applicable and secondly, some autogenous/drying shrinkage of the RCC.

It is considered most likely that the instrument readings, for the gauges away from foundation restraint, are reflecting the following behaviour scenario:

- The LBSGTMs were installed in placed RCC, where the temperature had already risen to its hydration peak. Zero strain was accordingly linked to the peak hydration temperature, while the RCC whose behaviour the gauge was intended to measure experienced zero stress at a substantially lower temperature;
- The temperature of the gauge and the surrounding RCC was dropped by between 5 and 12°C by the influence of the cooler RCC above. The gauge and the RCC across the joint shrank by between 200 and 400 microstrain, with particularly intense shrinkage occurring at the gauge due to its location immediately above a crack inducer.
- As the temperature of the RCC above rose, the RCC below acted as a partial restraint against the thermal expansion of the RCC above and it accordingly experienced expansion forces that would again have been exaggerated at the gauge by the tensile weakness in the induced joint below.
- Once the RCC above and below had reached their peak hydration temperatures, no further movement on the LBSGTMs would have been observed until the temperatures started dropping, unless some shrinkage/compression creep occurred. In view of the measured expansion while the peak temperatures were sustained, it is evident that a certain amount of creep/shrinkage in the Wadi Dayqah RCC has occurred.

4.6.7.5. Summary

Because the LBSGTMs were installed in RCC at it maximum hydration temperature, the measured shrinkage/creep could be observed. Should the gauges have been installed in the RCC at its placement temperature, constrained compression of the gauges would have masked the shrinkage until the temperature had dropped well below the peak hydration temperature. Considering the temperature flows and the consequential restraining and expanding forces, it is not considered possible that any real conclusions can be drawn in respect of the early shrinkage/creep behaviour of the RCC at Wadi Dayqah. It is considered, however, on the basis of these effects that assuming that all of the measured expansion strain can be ascribed to shrinkage/creep of the RCC under thermal expansion would be rather conservative.

It must also be borne in mind that the Wadi Dayqah RCC was a lean mix material with relatively low strength, a high w/c ratio and a high sand/aggregate ratio. Furthermore, the mix contained a very high percentage of non-cementitious fines. Considering the fineness of the aggregate/materials used, the high w/c ratio that might have resulted in excess water (not being used in hydration) being lost to

drying shrinkage, the high aggregate moisture absorption and the use of a partially crushed gravel aggregate, for which the paste/aggregate bond may not have been particularly strong, the Wadi Dayqah Dam RCC is likely to have been more susceptible to shrinkage and creep than other, higher strength RCCs investigated as part of this study. In an exposed environment, a conventional structural concrete using fine limestone filler might indicate an autogenous and drying shrinkage of around 450 x 10^{-6}[14]. Accordingly, while the origin of the measured deformations cannot be ascertained with any certainty, even in the worst-case scenario of all of the measured deformations being attributable to autogenous/drying shrinkage/creep, the maximum measured shrinkage is almost certainly substantially less than would be the case for a conventional concrete using a limestone filler in the core of a dam.

The De Mist Kraal weir in South Africa was constructed with a low cement content RCC mix[15], but high quality aggregates and this structure exhibited no detectable cracking of any significance. It is accordingly considered that the observed behaviour of the Wadi Dayqah Dam RCC is significantly more likely to relate to the aggregate quality and the high fines content than the low cement content.

4.6.7.6. Reliability & Consistency

The temperature readings at Wadi Dayqah Dam are consistent and comply with expectations. Consequently, a high degree of reliability can be ascribed to this data and a high level of confidence can be placed in the temperature distributions and the ongoing cooling process. The deformation readings from the LBSGTMs on the other hand present the opposite scenario. The pattern of behaviour is not generally consistent with that evident at any other dam for which the author has data and the indicated behaviour is quite different at each of the two elevations at which the gauges were installed.

Together with the possibility of poor aggregate performance, the complexity of the temperature flows and the respective constraining forces and the consequential data uncertainties realistically imply that any meaningful quantitative analysis of the gauge measurements is not possible.

4.6.7.7. Value of Results

The data from Wadi Dayqah Dam is of significant value, as it suggests that RCC is not immune to shrinkage/creep, confirming the findings of others in respect of lean RCC. While only qualitative analysis is realistically possible, it remains of value to observe that even in the case of an RCC mix that is relatively susceptible to shrinkage, the total creep/shrinkage strain remains very significantly less than that assumed in terms of traditional RCC materials models.

4.6.8. CONCLUSIONS

4.6.8.1. General

On the basis of an analysis of the temperature and deformation data measured for Wadi Dayqah Dam, it can be stated that some shrinkage in the RCC was evident, although it cannot be known with any certainty how much was due to autogenous shrinkage, drying shrinkage or creep. As a consequence of the continued development of shrinkage once the RCC was experiencing tension, it is considered most likely that its primary origin lies in autogenous or drying shrinkage, as opposed to creep under stress. However, the total early shrinkage was less than 50 microstrain and substantially less than would be assumed on the basis of a traditional RCC materials model. The Wadi Dayqah Dam RCC contained a high proportion of fine aggregates, a high content of non-cementitious fines and a high w/cement ratio. The aggregate quality, shape and surface texture may also not have been ideal, while the high moisture absorption of the aggregates may indicate a tendency for drying shrinkage. It is considered that these factors are the primary reason for the expansion observed on the gauges.

The findings for Wadi Dayqah Dam further demonstrate that some additional care must be taken in determining appropriate aggregates for RCC in the case of dam designs that are susceptible to materials shrinkage. Verification of appropriate materials should accordingly be demonstrated by installing temperature and strain gauges into the Full Scale Trials, or earlier in a relatively large mass of RCC.

On the basis of the findings of this Chapter, it is also suggested that very careful attention be given to the method of installation of strain gauges and LBSGTMs, particularly in the case of significantly cooled RCC. In such instances, it would be useful to position strain gauges away from the induced joint in both the receiving RCC layer and the newly placed RCC.

4.6.8.2. Implications for a New Understanding of the Early Behaviour of RCC

The implications of the findings of the Wadi Dayqah Dam instrumentation data, in respect of understanding the early behaviour of RCC, can be summarised as follows:

- The fact that shrinkage can be determined through very obviously different behaviour patterns at Wadi Dayqah serves to further validate the lack of evidence of shrinkage at the other dams investigated as part of this study.
- Aggregate quality and behaviour and the RCC mix composition must be given careful attention, as these can impact the drying shrinkage behaviour of RCC.
- Even with relatively poor materials, a high sand content and a high content of non-cementitious fines, the applicable shrinkage remains less than that assumed for a traditional RCC materials behaviour model.

- It is considered good practice to verify the early shrinkage behaviour of the proposed RCC by installing temperature and strain gauges in the RCC of the Full Scale Trial.
- The shrinkage evident in the lean RCC of Wadi Dayqah Dam is in accordance with the findings of other testing on lean mix RCC described in literature. This is not seen as detracting from the indicated behaviour for the high-paste RCC of the other dams addressed herein, but rather to further emphasise the distinction in early behaviour between high-paste RCC and lean RCC.
- In the case of an RCC arch dam for which materials shrinkage might be problematic, additional laboratory and practical testing of the RCC will be required.

4.6.8.3. Summary

The instrumentation data from Wadi Dayqah Dam provide a picture of early RCC behaviour for a quite different concrete mix, compared to Wolwedans, Knellpoort and Çine Dams. While the findings of the data evaluation highlight the caution necessary when considering the early behaviour of RCC, it further validates all other indications that the traditional model for RCC behaviour is not valid.

4.7. CHANGUINOLA 1 DAM

4.7.1. GENERAL

The general arrangements of Changuinola 1 Dam and the layout of the instrumentation installed are described in Chapter 2.

The instrumentation to be installed in Changuinola 1 is comprehensive. At the time of completing this Thesis, only the first level of instruments had been installed and only a little over 1 month of data was available, providing little information of significance at this stage. A strain gauge was, however, installed in the first RCC placed to the right side of the diversion culvert during December 2009 and this has provided data of some interest, which will be addressed in this Chapter. Furthermore, a comprehensive thermal analysis was completed for Changuinola 1, as described briefly in Chapter 5, and the associated modelling was useful in being able to simulate and confirm RCC behaviour.

4.7.2. INSTRUMENTATION

The strain gauge was installed directly into a trench cut into the RCC during the course of placement and the instrument was orientated in an upstream-downstream direction, perpendicular to the axis of the dam. The gauge is located approximately 2 m above the foundation and placement proceeded to a depth of approximately 6 m above the gauge without significant interruption. After a delay of

approximately 9 weeks, placement resumed and a further 11 m of RCC was placed above the gauge.

4.7.3. MATERIALS PROPERTIES

Laboratory testing indicated the following materials properties for the Changuinola 1 Dam RCC.

Thermal Diffusivity	1.6 m/°C
Coefficient of Thermal Expansion	8.8 x 10^{-6}/°C
Density	2475 kg/m^3
Compressive Strength at	
7 days	11.7 MPa
28 days	16.07 MPa
90 days	26.7 MPa
365 days	36.2 MPa

4.7.4. INSTRUMENT DATA

Figures 4.51 and **4.52** below indicate the temperature and strain history recorded between placement and July 2010.

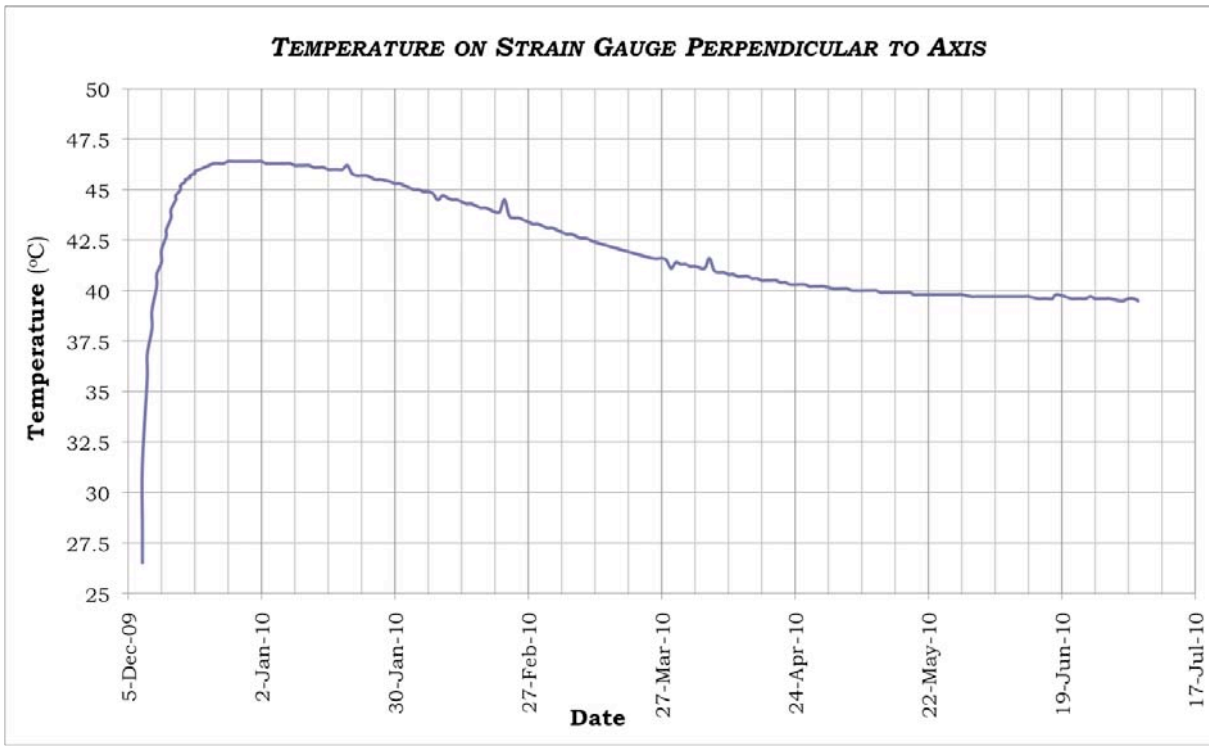

Figure 4.51: Temperature on Strain Gauge(16)

The measured temperature rise of approximately 20°C is essentially equivalent to the expected adiabatic hydration temperature rise, which is indicative of the significant level of thermal insulation provided to the gauge. The gradual (6°C) temperature drop between early January and March was halted when the impact of the RCC placed above took effect.

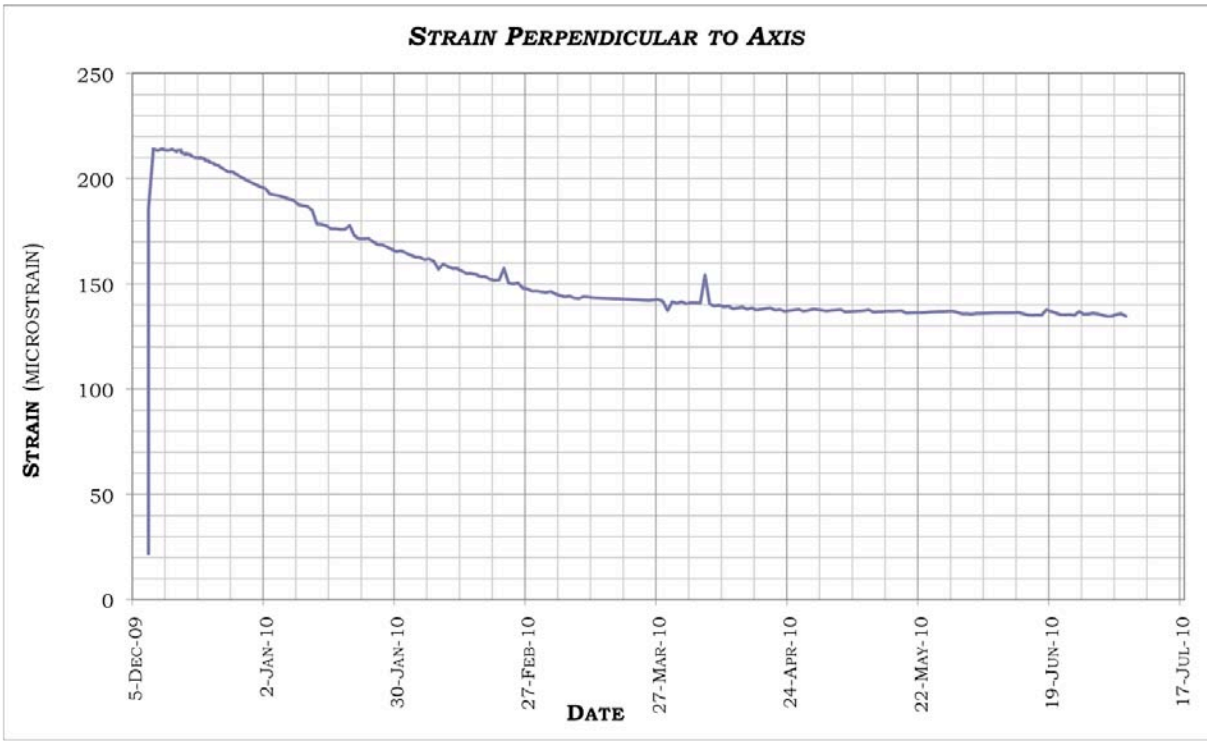

Figure 4.52: Strain Measured Perpendicular to Dam Axis(16)

A maximum expansion of 194 microstrain was developed, suggesting an effective coefficient of thermal expansion of 9.75 x 10^{-6}/°C. After the indicated 6°C temperature drop, the net expansion measured 113 microstrain for a temperature increase of 13°C, suggesting an effective thermal expansion of 8.7 x 10^{-6}/°C, which is essentially the equivalent value indicated through laboratory testing.

4.7.5. DISCUSSION

It is considered particularly interesting to note that the behaviour observed on the first strain gauge installed in Changuinola 1 Dam, orientated perpendicular to the dam axis, demonstrated the same behaviour as the gauges similarly installed in Çine Dam. The data suggests an initial over-expansion of some 12% with a subsequent relaxation to finally indicate a net RCC expansion equivalent to the temperature increase x the coefficient of thermal expansion. This confirms the indications from Çine Dam that high-paste RCC expands essentially linear-elastically under a temperature rise and that the internal restraint that would cause

part, or all of this expansion to be transformed into constrained compression and subsequently creep in CVC would not seem to be evident in high-paste RCC.

It is also significant that, whereas the strain gauges at Çine Dam were installed into the surface of a cold joint in the RCC placement, the gauge at Changuinola Dam was installed in RCC during ongoing placement. This is considered of particular importance, as it substantially eliminates any possible ambiguity that the expansion recorded at Çine might have related to the behaviour of the RCC in the cooled surface of a cold joint.

4.8. DISCUSSION AND CONCLUSIONS

4.8.1. CONCLUSIONS

Instrumentation specifically designed to measure temperature, strain and induced joint opening in RCC at Wolwedans, Knellpoort and Çine dams has repeatedly demonstrated a relatively linear relationship between temperature and strain, suggesting that the "zero stress", or T3 temperature is substantially closer to the "built in", or T1 placement temperature, than the maximum hydration, or T2 temperature, as commonly accepted for conventional mass concrete in dams. With no measurable shrinkage/creep experienced during thermal expansion and minor relaxation creep/shrinkage under thermal expansion representing the only apparent non-linearity in early RCC behaviour, the long-term structural temperature drop applicable in the case of large RCC dams is in fact significantly less than would otherwise be considered.

With thermal considerations being fundamental for RCC dams, the data presented in this Chapter has demonstrated that high-paste RCC does not exhibit shrinkage and particularly creep during the hydration heating and dissipation cycle to the same extent as CVC.

It is also considered important to take cognisance of the fact that all four of the RCC mixes for which the RCC behaviour was better than anticipated were high-paste RCC containing high proportions of fly ash.

While the evident early behaviour at Wadi Dayqah Dam was the exception, in demonstrating some definite non-linearity in temperature-strain behaviour, this confirms the finding from laboratory testing described in literature, which indicates similar, or greater creep in lean RCC, to CVC in dams. It is accordingly apparent that the key to the improved early RCC behaviour lies in the high-paste mix and the associated compaction.

4.8.2. DISCUSSION

The findings of the instrumentation data studies presented herein are of key importance for the design and analysis of significant high-paste RCC dams and of particular criticality in relation to the design and construction of RCC arch dams. For example, in the case of Çine Dam, it is unlikely that any structural temperature drop will ever be experienced within the lower body of the structure, even though a

conventional evaluation would suggest an applicable temperature drop of between 5 and 8°C. Furthermore, the practical implications for large RCC arch/gravity dams are significant. While conventional analysis might suggest that it would be possible to complete at least a first grouting of the induced joints on a large, naturally cooled RCC arch/gravity dam after perhaps 2 to 3 years, in reality the necessary delay might be substantially longer, an eventuality that would be difficult to manage.

Measurement of elastic thermal expansion, or a relatively linear temperature-strain relationship in the RCC in a direction perpendicular to the axis at Changuinola 1 Dam is considered particularly important, as this verifies the similar observations made at Çine Dam. Furthermore, in a constrained mass, with significant internal and foundation restraint, such expansion would not be expected and this is considered particularly important, as it probably represents the key to the difference in the behaviour of a high-paste RCC, compared to CVC.

It is important to bear in mind that, apart from Changuinola 1, the total hydration temperature rise applicable in the cases considered in this study is relatively low, particularly in relation to conventional vibrated mass concrete. For a higher hydration temperature rise, greater related expansion strain and higher associated stress levels can be anticipated and these may give rise to the introduction of more significant levels of creep.

4.8.3. ONGOING INVESTIGATIONS

The study presented in this Chapter forms the foundation of the programme of research and investigation subsequently addressed.

In this Chapter, the fact that high-paste RCC behaves differently to CVC, or to the manner traditionally assumed for design, is demonstrated. However, many questions remain and these cannot be answered without quantitative analysis. Consequently, the performance of Wolwedans Dam is explored in greater detail in Chapter 5, while early indications of the RCC behaviour at Changuinola 1 Dam are also discussed.

4.9. REFERENCES

[1] Oosthuizen C. *Behaviour of Roller Compacted Concrete in Arch/Gravity Dams.* Proceedings. International Workshop on Dam Safety Evaluation. Grindelwald, Switzerland. April 1993.

[2] Oosthuizen C. *Performance of Roller Compacted Concrete in Arch/Gravity Dams.* Proceedings. 2nd International Symposium on Roller Compacted Concrete Dams. Santander, Spain. pp 1053-1067. 1995.

[3] Shaw QHW. *An Investigation into the Thermal Behaviour of RCC in Large Dams.* Proceedings. 5th International Symposium on Roller Compacted Concrete Dams. Guiyang, China. pp 271-282. 2007.

[4] United States Army Corps of Engineers. *Thermal Studies of Mass Concrete Structures.* Engineering Technical Letter, ETL 1110-2-542. Washington. May 1997.

[5] Özkar Construction Internal Report. *Instrumentation Readings. Quality Control Unit.* Özkar Construction, Ankara, Turkey. October 2005 – February 2008.

[6] Geoconsult. Gibb. ARQ. *Çine RCC Dam. Phase 2 Design Report.* Vol. 4 of 4. Drawings. Özkar Construction. Ankara, Turkey. January 2000.

[7] Turanli L. *Determination of Thermal Diffusivity and Creep for Concrete Core Specimens Taken from Çine Dam.* Middle Eastern Technical University. Report Code No. 2001-03-03-2-0033. Ankara, Turkey. September 2001.

[8] Shaw QHW. ARQ (PTY) Ltd. *Çine Dam. Design Thermal Analysis Report.* Özkar Construction Internal Report No. 1596-8539. Ankara, Turkey. September 2005.

[9] Greyling R & Shaw QHW. ARQ (PTY) Ltd. *Çine Dam. Supplementary Thermal Analysis Report.* Özkar Construction Internal Report No. 1596-10288. Ankara, Turkey. June 2008.

[10] United States Army Corps of Engineers. *Arch Dam Design.* Engineering Manual, EM 1110-2-2201. USACE. Washington. May 1994.

[11] Wadi Dayqah Dam JV. *Wadi Dayqah Dam. Drawings for Construction.* Sultanate of Oman. M.R.M.E.W.R. Muscat, Oman. August 2006.

[12] Richards, M. *Instrumentation Readings, Data and Information. Wadi Dayqah Dam Joint Venture.* Quriyat, Oman. March & August 2009.

[13] Vinci & CCC Construction JV. Wadi Dayqah Dam. *Quality Control Records*. Quriyat, Oman. February 2008.

[14] Neville, AM. *Properties of Concrete.* Chapter 9. Fourth Edition. Pearson Prentice Hall. London. 2002.

[15] Hollingworth F, Druyts FHWM & Maartens WW. *Some South African Experiences in the Design and Construction of Rollcrete Dams.* Proceedings. 17th ICOLD Congress. Q62. R3. San Francisco. pp 33-51. 1988.

[16] CCWJV. *Instrumentation Readings, Data and Information. Changuinola 1 Dam.* Changuinola, Panama. January to July 2010.

CHAPTER 5

5. SIMULATING PROTOTYPE MATERIALS BEHAVIOUR THROUGH FINITE ELEMENT MODELLING FOR WOLWEDANS DAM

5.1. BACKGROUND

In Chapter 4, instrumentation data for five prototype RCC dams was evaluated and a picture emerged that suggested that high-paste RCC in large dams demonstrates significantly less early shrinkage/creep during the hydration heating and cooling cycle than does conventional mass concrete (CVC) and than is assumed in traditional dam design.

Building on the largely qualitative evaluations in Chapter 4, Finite Element modelling is used in Chapter 5 to explore quantitatively the RCC materials behaviour that gives rise to the measured performance that differs from expectations.

On the basis of the earlier data evaluations, a number of questions persist as to the most realistic interpretation of certain of the apparent behaviour. This is particularly true in respect of residual stress and strain conditions in RCC between the open induced joints and the need was accordingly perceived to develop structural models to replicate the apparent RCC behaviour through analysis, isolating the actual characteristics by comparing measurements on a prototype with analytical predictions.

5.2. INTRODUCTION & DEFINITION OF OBJECTIVES

5.2.1. GENERAL

Chapter 5 presents four analyses; three addressing the early and operational performance of Wolwedans Dam and one addressing the early materials behaviour during construction at Changuinola 1 Dam

5.2.2. ANALYSIS 1: MODELLING INDUCED JOINT OPENINGS FOR WOLWEDANS DAM

In the review of the instrumentation data presented in Chapter 4, it became clear that a meaningful analysis of the low induced joint openings was not possible without an evaluation of the residual stress in between the open induced joints and an understanding of the impact on joint opening of the applicable hydrostatic water load.

The first analysis presented in this Chapter accordingly investigates the low measured induced joint openings at mid-dam height at Wolwedans through Finite Element modelling of the structure under load. Applying a parametric approach to focus in on the actual measured openings, an initial indication is developed of the behaviour of the constituent RCC, specifically in terms of the extent of shrinkage/creep that occurred during the hydration heating and cooling cycle.

The associated stress patterns on the induced joints and in the blocks in between are also reviewed.

5.2.3. ANALYSIS 2: SIMULATING TEMPERATURE DISTRIBUTIONS FOR WOLWEDANS DAM

In order to enable more accurate modelling, a study was required to establish the actual distribution of the temperature variations applicable across the surface and core zones of the Wolwedans Dam structure. For this purpose, measured temperatures and joint opening profiles from the instrumentation records were examined in detail.

5.2.4. ANALYSIS 3: MODELLING WOLWEDANS DAM PROTOTYPE BEHAVIOUR

A reduction in volume of the RCC in Wolwedans Dam due to shrinkage and creep during the hydration heating and cooling cycle will significantly influence the structural behaviour of the dam wall. By evaluating the measured crest displacements and joint openings against a number of shrinkage/creep scenarios, a good indication of the actual extent of the related effect is developed.

5.2.5. ANALYSIS 4: THERMAL ANALYSIS FOR CHANGUINOLA 1 DAM

The Thermal analysis for Changuinola 1 Dam was able to effectively predict surface gradient cracking that developed during June 2010 and the related modelling allowed some significant insights into the manner in which the RCC behaved during the early stages of the hydration heating and cooling cycle.

In order to illustrate the related findings, a brief description of the Thermal study for Changuinola 1 Dam is included in this Chapter.

5.3. ANALYSIS 1: MODELLING INDUCED JOINT OPENINGS

5.3.1. ANALYSIS APPROACH & PROTOTYPE BEHAVIOUR TO BE MODELLED

5.3.1.1. General

As discussed in Chapter 4, comparing the early temperature-time history at Wolwedans Dam[1, 2, 3, 4 & 5] with the concurrent induced joint displacements indicated that the joints started opening essentially once the internal RCC temperature dropped below the original placement temperature, suggesting that no shrinkage, or creep, or anything other than linear-elastic behaviour, had occurred in the green RCC during the process of concrete hydration[2]. This behaviour is reflected on **Figures 5.1** and **5.2**, which illustrate typical temperature and joint opening histories for the first five years of the life of the dam, for the internal zone of the structure.

Focusing on the third level of instrumentation, installed across 16 joints at approximately mid dam height (RL 66.250 m), the primary purpose of the investigations presented in this Chapter was to gain an understanding of the low measured induced joint openings by modelling the RCC behaviour within the body of the dam structure. By replicating similar joint openings on the model as measured on the prototype, under the same load conditions, it was considered possible to develop a picture of the thermal and structural behaviour of the dam wall and, by implication, to evaluate the performance of RCC as a material under these conditions.

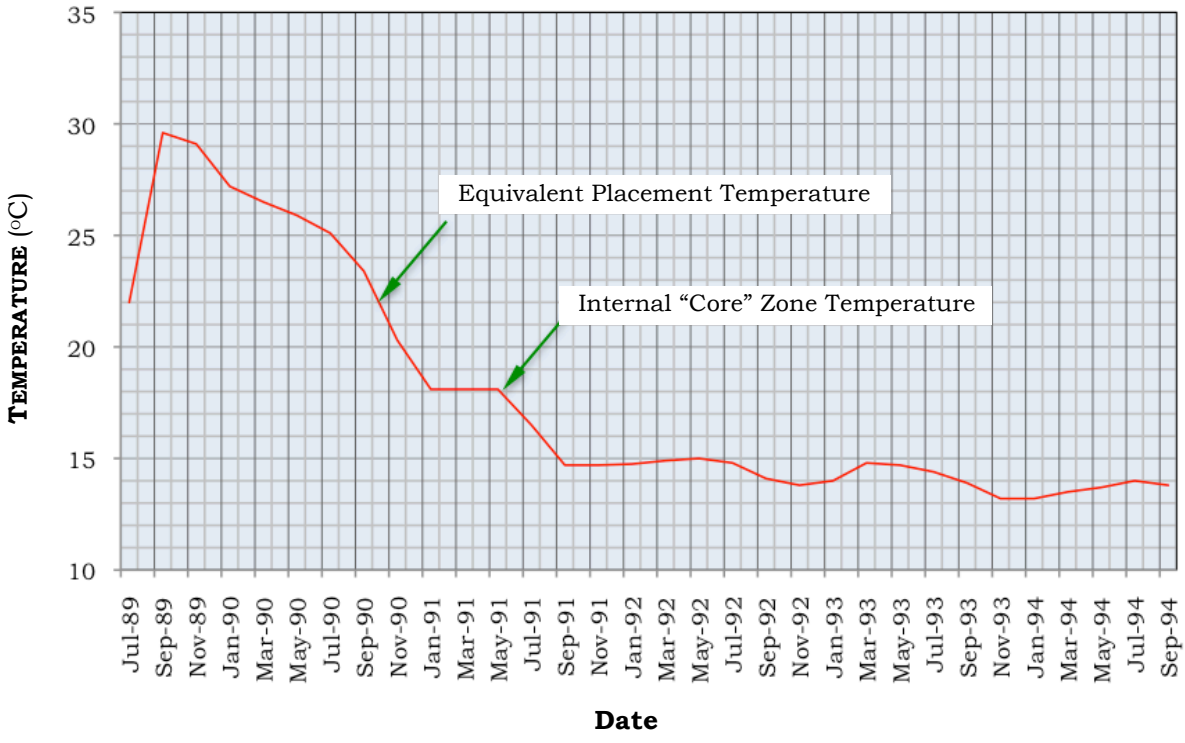

Figure 5.1: Temperature-Time History for Wolwedans Dam[2]

At elevation RL 66.250 m, the central blocks of the dam are sufficiently high to be largely free of the influence of any foundation restraint, but the RCC section is still adequately thick to ensure that the centre is well insulated from surface temperature variations. The dam wall is divided into seventeen blocks by sixteen induced joints at this level, with the joints numbered from 7 to 22 from the left to the right bank (**Figure 5.3** & **Figure 2.13**). Only three of the induced joints at Wolwedans actually opened to any real extent[2], specifically Joint Nos. 8, 14 and 17, and while the instrumentation records under scrutiny in this study cover a period of approximately 5 years, it is important to take cogniscance of the fact that full hydrostatic loading was essentially continually present from 2 years after construction completion.

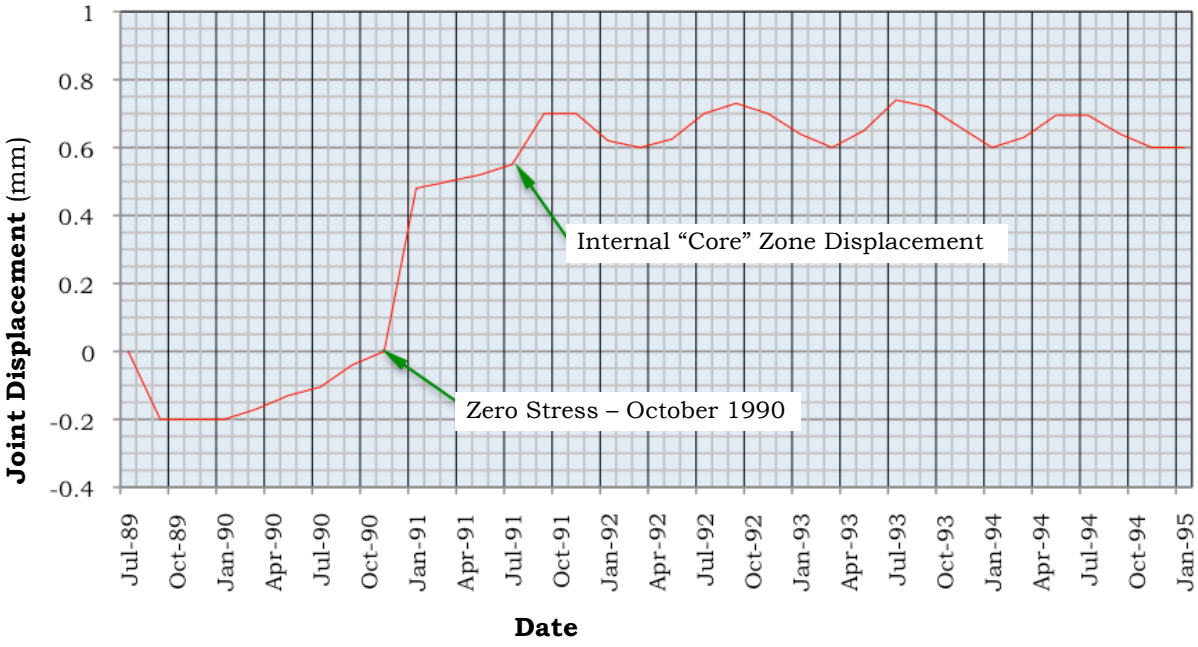

Figure 5.2: Joint Displacement – Time History for Wolwedans Dam[2]

5.3.1.2. Apparent Measured Behaviour

All of the induced joints at Wolwedans were comprehensively instrumented[4], with four levels of instruments and a minimum of 2 long-base-strain-gauge-temperature-meters (LBSGTMs) across each joint at each level. Despite all joints being weakened through de-bonding 25% of the RCC contact area, only three of the 16 joints at elevation RL 66.25 m demonstrated any real opening. In view of the fact that the dam structure took a period of approximately 3 years to cool to an equilibrium temperature cycle, the impoundment was essentially full by the time the first cold internal winter temperatures were experienced. Accordingly, no instrumentation data at a representative low temperature is available for an empty dam and the displacement information on the joints correspondingly represents the structural performance under temperature drop and hydrostatic loading.

At either end of the structure at elevation RL 66.25 m, the dam wall is obviously in contact with the foundation and accordingly experiences restraint. While the total length on the centerline of the wall at this elevation measures approximately 150 m, the distance between the outermost joints is 137 m and it is considered that this distance effectively represents the length of the wall over which shrinkage as a consequence of temperature drop can occur.

By winter 1993, the hydration heat had essentially dissipated from the core of the dam structure and the minimum temperature within the dam wall at elevation RL 66.25 m was measured as approximately 14°C. Comparing this figure with an RCC placement temperature that averaged approximately 22 – 22.5°C accordingly implied a maximum apparent core temperature drop of approximately 8 to 8.5°C, which can be compared with a total summed associated simultaneous measured joint opening, on the centreline of the dam wall, of 3.4 mm. While this full joint opening was concentrated at just 3 induced joints (Nos. 8, 14 and 17), surface joint opening was also experienced at a further four induced joints (Nos. 11, 12, 18 and 21), where maximum displacements of approximately 0.5 mm were observed. Surface temperature and joint opening variations are subsequently explored under section 5.4.

The above figures relate to the winter of 1993, before the induced joints were grouted. They are, however, similarly applicable for August 1995, after grouting, when an equivalent temperature drop and comparable joint openings were measured at RL 66.25 m.

Over a total length of approximately 137 m, the summed contraction on the joints can be translated into a direct tensile strain of 25 microstrain. For an 8°C temperature drop, such a strain would suggest an associated thermal expansivity of approximately 3×10^{-6}/°C, which is significantly less than half of the figure that would be anticipated for a concrete comprising quartzitic aggregates.

As mentioned in Chapter 4, it is considered that the apparent discrepancy in thermal expansivity/induced joint opening could relate to underestimated residual tensions within the uncracked RCC, a lower actual effective structural temperature drop, an actual lower thermal expansivity, creep of the RCC in tension, or a combination these factors. The imposition of the hydrostatic water load will obviously also significantly influence the displacements across the joints that have opened as a consequence of thermal shrinkage. In view of the repetition of the same joint openings at RL 66.25 m two years later, it can be concluded that joint grouting was not the cause of the smaller than expected joint openings. The primary purpose of the analyses addressed in this Chapter was accordingly to simulate the displacements measured on the prototype structure and consequently to identify the origin of this apparent discrepancy, thereby gaining an understanding of the associated behaviour of RCC under early thermal loads.

5.3.2. 3-DIMENSIONAL ANALYSIS OF WOLWEDANS DAM

5.3.2.1. Wolwedans Dam

Wolwedans Dam was used as the central focus for the analyses completed as a consequence of the availability of comprehensive instrumentation records[1, 3, 4, 5, 6 & 7], full geometrical details and its familiarity to the author. Wolwedans is a single curvature arch/gravity dam with a maximum height of 70 m, an extrados arch circular radius of 135 m and a crest length of 270 m. The dam and its instrumentation are described in more detail in Chapter 2. A total number of 27 induced joints were comprehensively instrumented at Wolwedans Dam, for the primary purpose of establishing the degree to which each joint opened and the associated need for grouting to re-establish the structural continuity of the arch as a consequence of post-hydration thermal shrinkage.

The dam was completed and began impounding water early in 1990[1], filling to capacity and spilling for the first time in October 1992. A programme of joint grouting was carried out during late winter 1993.

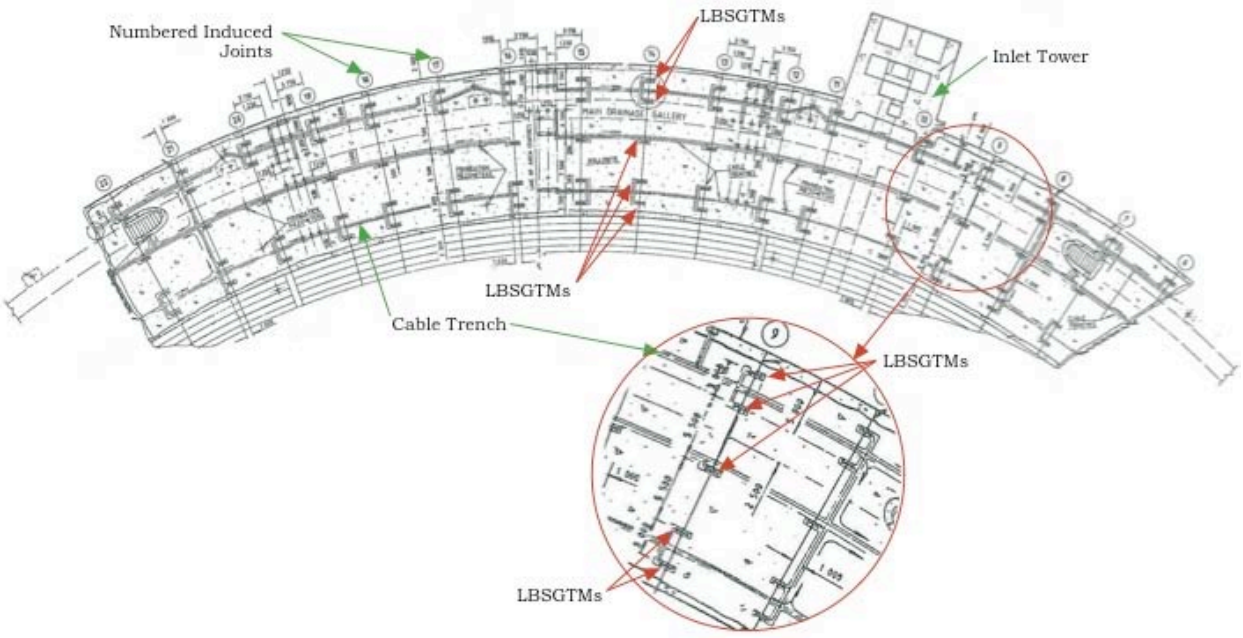

Figure 5.3: Wolwedans Dam – Illustration of Instrumentation at RL 66.25 m[1]
(For more detail see **Figure C3**)

5.3.2.2. FE Analysis Model

For the purposes of the early investigative analyses addressed in this Chapter, a comprehensive, 3 dimensional Finite Element model was established using the COSMOS[8] general structural analysis software. The model simulates the dam and the foundation, with each radial dam block between induced joints being developed as separate parts and joined with Gap elements. Ten-noded solid tetrahedral elements

were used in a high-density mesh. For analyses in which induced joints were not allowed to open, replicating the fact that these joints had not opened on the prototype, the Gap elements were simply omitted. Representations of the FE model are presented for illustration on **Figures 5.4** and **5.5** overleaf.

In accordance with accepted practice for a rockmass with a similar deformation modulus to that of the dam concrete[9], the modelled foundation block extended approximately 1.5 x dam height (H) below, upstream and downstream of the dam and 1 x H on either flank. At the extremes, the foundation block was fully restrained.

Although it is not strictly representative of the actual situation applicable on the prototype structure, temperature drops were applied for the preliminary analyses as a single drop from a reference temperature (zero stress temperature) to all areas of the dam wall, but not the foundation. In reality, the internal and external zones of the dam wall will be subject to different effective structural temperature drops, while heat will move into the cooler foundation from the warm dam, and the foundation will provide additional insulation to the adjacent concrete during seasonal cycles.

An evaluation of the actual distribution of temperature drops is presented as a later part of this Chapter. For the purpose of the early investigations addressed here, however, a simplified approach was considered appropriate.

5.3.2.3. Materials Properties

While a number of the RCC materials properties for Wolwedans Dam are known[1], it was necessary to make a number of assumptions for the analyses undertaken. The following properties were available from site and construction records[1]:

Average RCC Density:	2400 kg/m^3
Average 1 year RCC compressive strength:	35 MPa

The following materials property assumptions were made for the analyses completed:

RCC Elastic Modulus:	15 - 25GPa
RCC Poisson's Ratio:	0.20
Rockmass/Foundation Elastic Modulus:	8 - 15GPa
Rockmass/Foundation Poisson's Ratio:	0.30

In view of the fact that no measured data is available for the thermal expansivity of the RCC at Wolwedans, but on the basis of knowledge of the quartzitic constituent aggregates, it was assumed that an applicable value would lie between 9 and 11 x 10^{-6}/°C[10]. Within typically realistic ranges for concrete and rock[11], the Poisson's ratio has very little influence on the behaviour of interest and accordingly, typical values were assumed, with no variations.

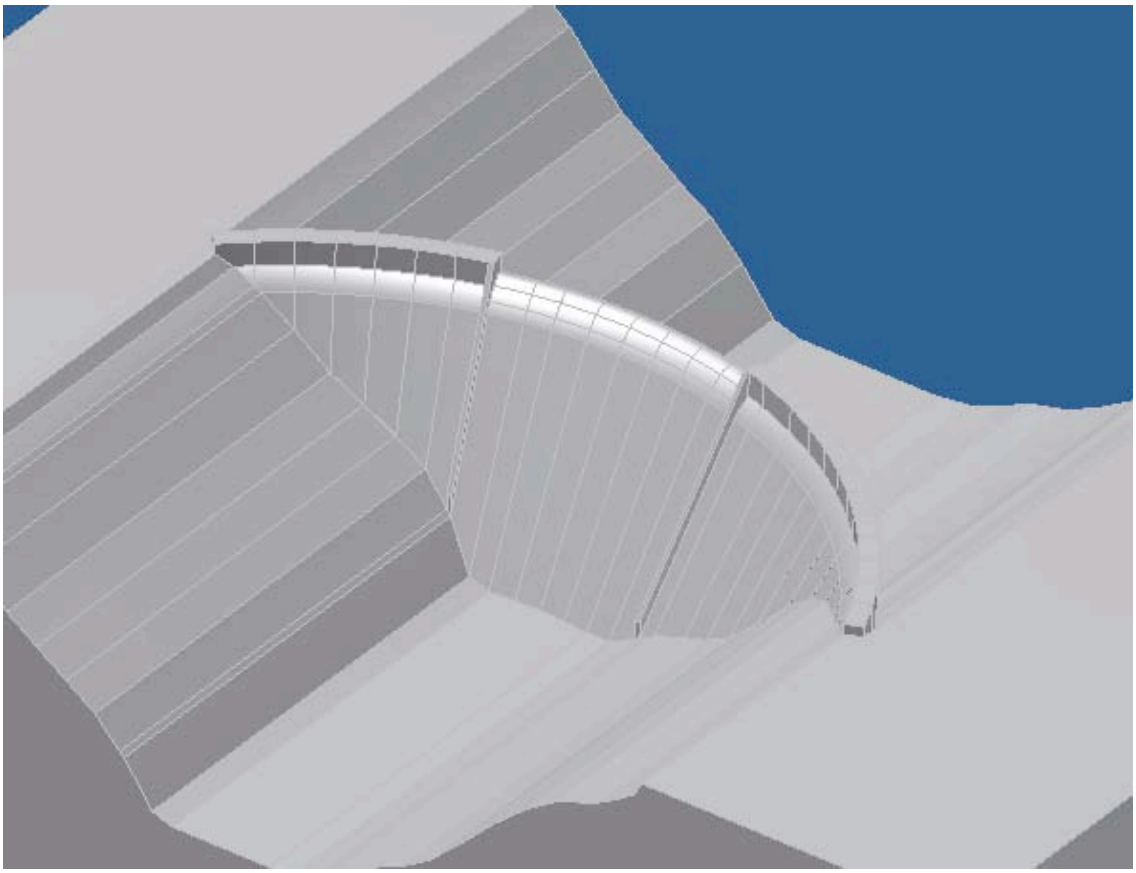

Figure 5.4: Wolwedans Dam FE Model – Illustrating "Part" Structures

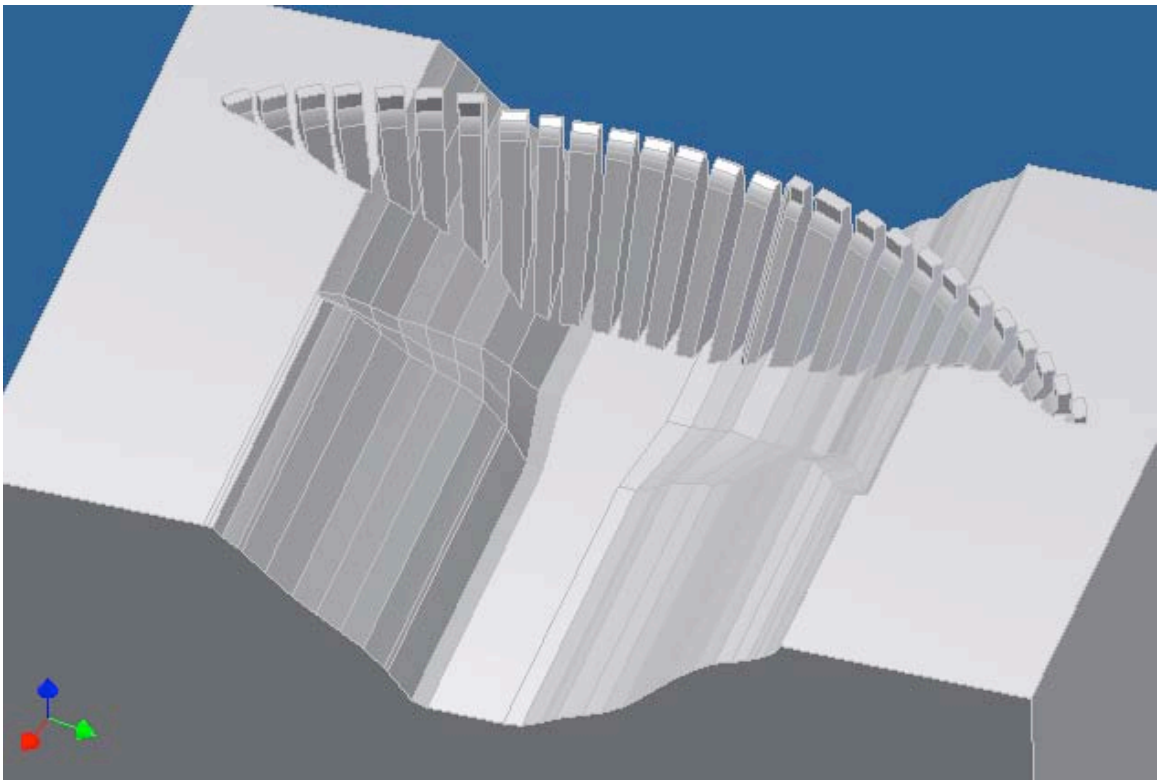

Figure 5.5: FE Model –Split & Lifted to Illustrate Location of "Gap" Elements

5.3.2.4. Analysis Development

A series of analyses was completed in the process of developing a first representation of the actual prototype behaviour characteristics. Initially, a uniform 8°C temperature drop was applied across the full dam, with no hydrostatic, gravity or uplift loading. A thermal expansivity of 10 x 10^{-6}/°C was assumed, together with a long-term deformation modulus of 15 GPa and the early analyses were linear-elastic, allowing all induced joints to open. The sustained E modulus applied is reduced from the instantaneous, tested value to take cognisance of the inelastic behaviour of concrete that is manifested as a reversible creep under sustained loading.

Subsequently, the input and materials parameters were varied, while only joint Nos 8, 14 and 17 were allowed to open, in accordance with the prototype. The following step involved the addition of hydrostatic, uplift and gravity loadings to simulate as realistically as possible the actual conditions under which the prototype joint measurements were taken.

For each analysis, the opening of each induced joint was evaluated at elevation RL 66.25 m, on a local co-ordinate system, on the centreline of the dam, as illustrated on **Figure 5.6**. In addition, the level of residual stress in a direction parallel to the dam axis was reviewed in the centre of the blocks between open induced joints and in the flank zones of the structure, where no joint openings were observed.

Early analyses demonstrated potential variations of the E modulus of the rockmass/foundation to have only a minor influence on the magnitude of the induced joint openings. In view of the fact that it would never be possible to develop any degree of certainty in respect of the foundation rockmass properties, a more conservative stiffer foundation was assumed for all subsequent analyses, with an E modulus of 15 GPa.

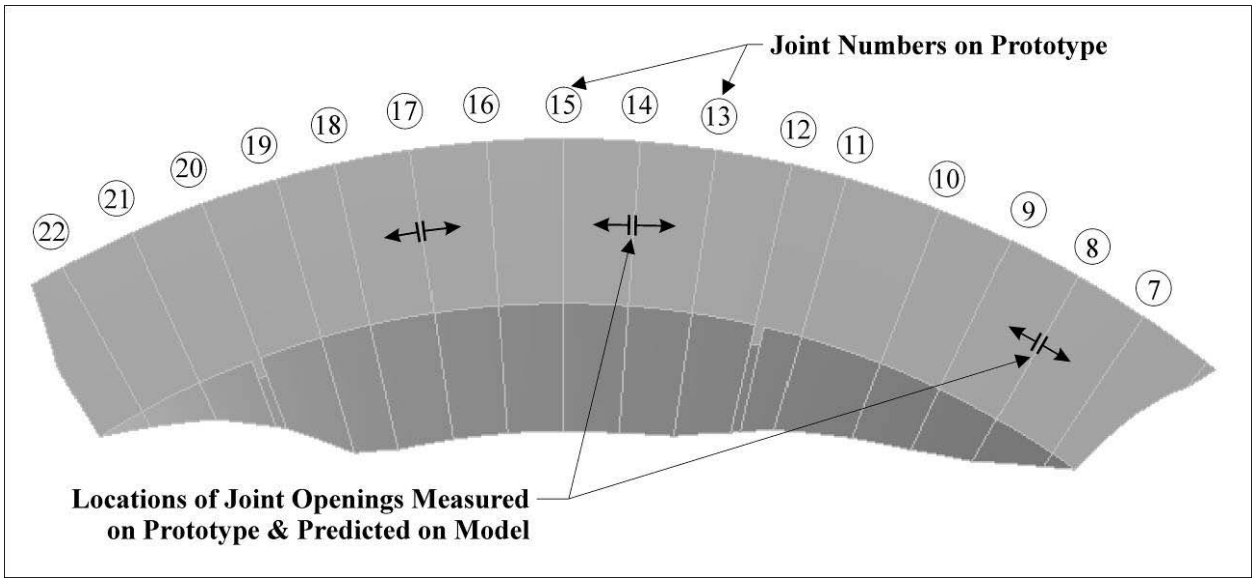

Figure 5.6: Horizontal Section through FE Model Illustrating Location of Joint Opening Reference Points

5.3.2.5. Analysis Findings

Initial Indications

The early analyses quickly demonstrated that the site topography, the steep abutments and the arch geometry exert significant influence on the displacements across the open induced joints. However, for the analyses without gravity, or hydrostatic water loading and all joints allowed to open, a very direct correlation between joint opening and predicted thermal shrinkage was evident, suggesting very low levels of residual stress within the RCC blocks, whether every induced joint, or only every third joint, was allowed to open.

For an 8°C temperature drop and a thermal expansivity of 10 x 10^{-6}/°C, the summed total of all horizontal joint openings, with all joints allowed to open, was indicated as 10.8 mm, while the indicated residual stresses between induced joints was negligible.

For a similar analysis, with only joint Nos. 8, 14 and 17 allowed to open, the summed horizontal joint openings was indicated as 10.5 mm, while residual stresses between induced joints were typically less than 50 kPa on the blocks between induced joints and less than 100 kPa on the blocks at either end of the dam structure. Converting the average residual stress between open joints on the basis of a deformation modulus of 15 GPa confirms that a total strain shrinkage of approximately 0.3 mm is retained in residual stress.

For an applicable dam wall length of 137 m, an 8°C temperature drop and a thermal expansivity of 10 x 10^{-6}/°C should produce a total joint opening of 11.0 mm, if no residual tension remains, confirming the accuracy and representivity of the analyses completed.

Adding, gravity, hydrostatic and uplift loading in the case of this last analysis, with joint Nos. 8, 14 and 17 allowed to open, the summed horizontal joint openings reduced to approximately 3.5 mm.

Modelling to Reproduce the Prototype Measurements

In modelling a dam structure using Finite Elements, a specific problem relates to the imposition of gravity as a load case. When gravity is imposed as a load on the completed dam, but not the foundation, the dam structure will want to pull downwards into the valley bottom. This tends to develop shear forces between the shoulders/abutments of the dam structure and its foundation on the FE model (see **Figure 5.7**). When specific discontinuities are present, or when the abutments flatten with height, a hanging effect is created and tensions are developed in the dam structure model, which would not be so pronounced in reality, where gravitational forces are progressively developed during the construction process. Reviewing the structural modelling for Wolwedans Dam, such an effect is evident at Joint No. 8, particularly when this joint is allowed to open. Ignoring the hydrostatic loads, a joint opening of 3.57 mm is anticipated by the model, 2.85 mm associated with a temperature drop of 8°C and 0.72 mm associated with the imposition of gravitational

forces. Such an effect is not present at Joint Nos. 14 and 17, where the impacts of foundation anomalies and gravity-related shears are reduced due to height above foundation and location close to the centre of the dam. In order to make a more realistic comparison of the model joint openings with those measured on the prototype, the unrealistic modelling effects caused by the imposition of gravity as a load were taken into account by subtracting 0.72 mm from the opening on Joint No. 8 at RL 66.25 m for all subsequent analyses.

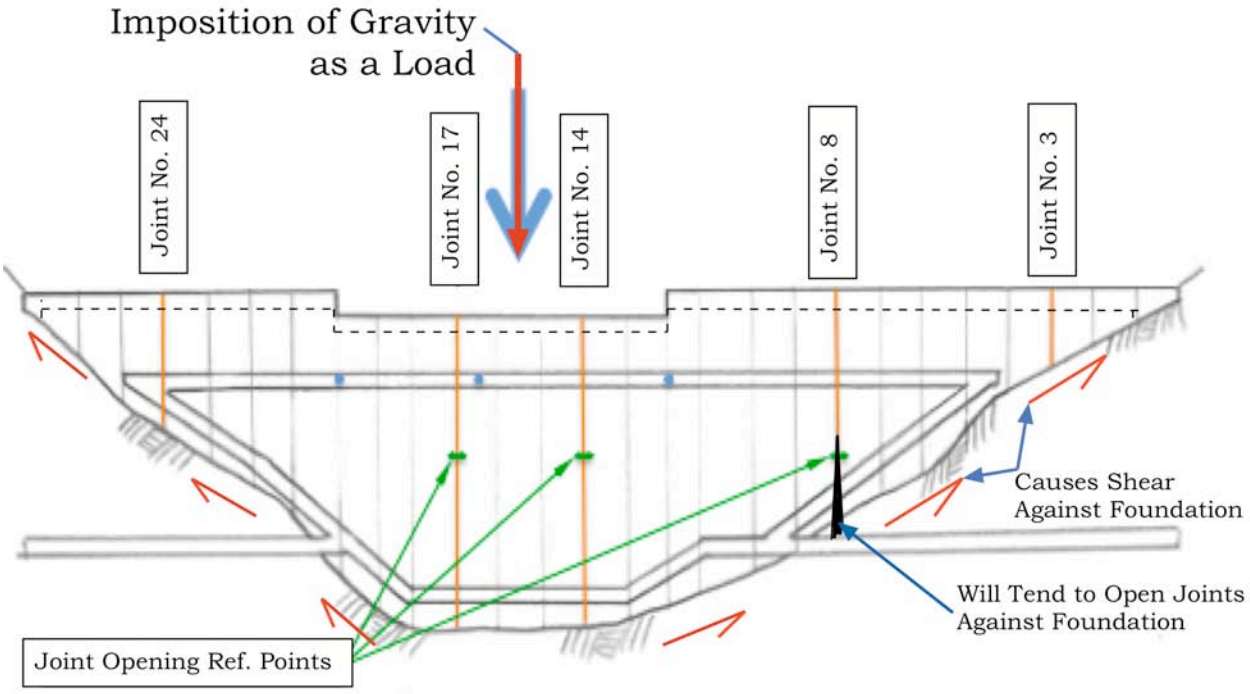

Figure 5.7: Illustration of Impact of Imposing Gravity as a Load

To simulate the prototype structure loading, gravity, hydrostatic and uplift loads were added to the FE analyses and only joint Nos. 8, 14 and 17 were allowed to open, as only these had opened on the prototype. In order to isolate the observed prototype behaviour, a number of the model input parameters and properties were varied as follows (with the remainder fixed as indicated under 5.3.3):

Property/Input Parameter	Unit	Values Considered
Temperature drop	˚C	8, 8.2, 8.5 & 8.7
Thermal expansivity	Microstrain / ˚C	9, 10, 10.5 & 11
RCC Elastic Modulus	GPa	15, 20 & 25
Uplift	-	As per design & 50% design

The hydrostatic load was input with the impounded water surface at FSL, while uplift was modelled as two load cases; firstly as full hydrostatic at the upstream face, reducing by 2/3 on the line of the gallery and to zero at the toe (as per the dam design - no tailwater applicable) and secondly as 50% of the same load (50% of dam design load). While the former uplift loading represents a typical design assumption, the latter is probably more realistic for a competent, grouted and drained foundation.

The joint openings on the centreline of each of the joints allowed to open was subsequently summed and compared with the total joint displacements measured on the prototype.

5.3.2.6. Modelling Results

Table 5.1 provides a summary of the study results.

Table 5.1: Joint Openings at RL 66.25 m for Various Scenarios

Scenario						Joint Openings			
Scenario	**Uplift**	**E Modulus Dam**	**E Modulus Foundation**	**Thermal Expansion Coefficient**	**Temperature Drop**	Jt. 8	Jt. 14	Jt. 17	Combined
No.	% Design	(GPa)	(GPa)	(x 10^{-6}/°C)	(°C)	(mm)	(mm)	(mm)	(mm)
1	50	15	15	10	8	1.40	0.52	0.85	2.77
2	50	20	15	10	8	1.56	0.77	1.17	3.50
3	50	25	15	10	8	1.72	0.88	1.37	3.97
4	50	15	15	11	8	1.75	0.76	1.12	3.63
5	50	20	15	11	8	1.97	0.93	1.47	4.37
6	50	25	15	11	8	2.09	1.06	1.71	4.86
7	50	15	15	9	8	1.01	0.38	0.61	2.00
8	50	20	15	9	8	1.22	0.56	0.87	2.65
9	50	25	15	9	8	1.36	0.65	1.07	3.08
10	50	15	15	10	9	1.84	0.81	1.20	3.85
11	50	20	15	10	9	2.04	1.01	1.55	4.60
12	50	25	15	10	9	2.16	1.13	1.79	5.08
13	100	15	15	10	8	1.36	0.55	0.81	2.71
14	100	20	15	10	8	1.56	0.74	1.10	3.41
15	100	25	15	10	8	1.70	0.83	1.33	3.86
16	100	20	15	10	9	2.03	0.96	1.50	4.49
17	100	25	15	10	9	2.15	1.09	1.73	4.97

5.3.2.7. Discussion

When initially running the above analyses, it was assumed that it would be necessary to review the joint openings against a preliminary "no creep" case and subsequently to increase the Temperature drop to account for shrinkage/creep. This, however, did not prove realistically possible, as the variation of the result data, around credible RCC input parameters, did not seem to allow for such an eventuality. The only scenario to approach the measured joint openings that might have possibly allowed any creep would indicate 50% design uplift, a coefficient of thermal expansion of 10 x 10^{-6}/°C, a temperature drop of 9°C and an E modulus of 15 GPa for the dam. However, the indicated joint openings were slightly larger than those measured, while any creep that might have occurred would relate to the difference in temperature drop between 9 and 8°C, which is realistically within the margin of error of the analysis. The analyses, however, indicated higher crest displacements than actually measured for this scenario.

In reviewing the results in **Table 5.1**, it is important to include a number of significant considerations. The assumptions for uplift in dam design (see **Appendix B**) are conservative and in the case of Wolwedans, the abutments are drained by tunnels and the foundation pore pressure measurements have never indicated any significant pressures[7]. Accordingly, 50% design uplift load is considered the more realistic loading situation. For a concrete manufactured using a quartzitic aggregate in South Africa, a high coefficient of thermal expansion would usually be expected[10] and accordingly, it is considered that any associated value below 10 x 10^{-6}/°C would not indicate a high credibility.

Consequently, in terms of reproducing the prototype behaviour, the most credible scenarios modelled would be either No. 2, or No. 4. While the individual displacements predicted for each of the joints are anyway more accurate in the case of Scenario 2, the analyses indicated excessive crest displacements for Scenario 4.

As can be seen from **Table 5.1**, the typical, summed joint openings for the properties and loads considered varied between 2 and 5 mm. Changing the uplift load by 50% indicated an impact of less than 3%, with increased uplift causing increased joint closure, while higher temperature drops and coefficients of thermal expansion unsurprisingly resulted in increased joint openings. Closure of the induced joints under load was demonstrated to reduce with increasing RCC E modulus.

While it is not considered that the preliminary modelling undertaken could identify a single solution, or behaviour mode, with any certainty, on the basis of indicating the closest individual and combined joint openings to those measured on the prototype structure, Scenario 2 is considered most representative of the reality. Accordingly, the most representative behaviour of Wolwedans Dam in July 1993 was represented by an 8°C temperature drop, an RCC coefficient of thermal expansion of 10 x 10^{-6}/°C, an RCC elastic modulus of 20 GPa, a foundation elastic modulus of 15 GPa and 50% uplift load. In view of the fact that an actual temperature drop from placement of approximately 8°C was measured, this scenario would suggest that no significant

shrinkage or creep had in fact occurred at Wolwedans Dam during the hydration heating and cooling cycle.

In the case of Scenario 2, the maximum residual tensile stress between the internal joints was indicated to lie between 23 and 26 kPa, while the maximum residual tensile stress between the abutments and the external induced joints was indicated as between 220 and 290 kPa.

Table 5.2 compares the actual and predicted openings on the centre of each of the "open" induced joints for Scenario 2.

Table 5.2: Predicted and Measured Displacement on Induced Joints for Full Dam, 8°C Temp. Drop, 10 x 10^{-6}/°C Thermal Expansivity, 20 GPa RCC Modulus, 50% Design Uplift & 15 GPa Foundation Modulus.

Joint No.	Displacement on Centre of Joint (mm)	
	Measured on Prototype	Predicted on FE Model
8	1.0	1.56*
14	0.95	0.77
17	1.45	1.17
Total	**3.4**	**3.50**

* - Joint displacement with unrealistic gravity-modelling related displacement deducted (2.28 – 0.72), as discussed under 5.3.3.3.

5.3.2.8. Residual Stress Levels

The low levels of the residual stress indicated between the induced joints through the analyses completed clearly demonstrate the cause of only three induced joints opening to any depth at Wolwedans Dam. Even with the weakening created by de-bonding surfaces on the joints, tensile stresses of less than 300 kPa are not likely to induce cracking. With residual stress levels as low as 22 kPa between the open joints, it is clear that a joint spacing at Wolwedans Dam of approximately 30 m would have been quite adequate. Despite surface and internal de-bonding being provided on 16 joints at RL 66.25 m, joint opening even at the surface was only measured on 7 joints.

5.3.3. DISCUSSION & CONCLUSIONS

5.3.3.1. Validity of Modelling

Despite the simplicity of the modelling completed, the lack of accuracy in respect of the distribution of the temperature drop loading applied and the linear materials properties assumed, a meaningful simulation of the prototype dam behaviour was developed. Admittedly, the analyses focused only on joint openings on the centreline of the dam wall and at an elevation where foundation restraint does not play a significant role, but the reproduction of the prototype behaviour with temperature

drops that can be substantiated through measurement and materials properties in line with expectations confirms the validity of the apparent findings.

The structural function of an arch/gravity dam under hydrostatic and temperature drop load is such that displacements throughout the dam wall will be dependent on the placement temperature conditions within the upper section of the dam wall, where structural contact occurs first. This is illustrated on **Figure 5.8**, which demonstrates that sufficient arch action is incurred within the top 20 m of the dam structure to carry the applied water load. If the effective placement temperature within this specific zone were to be different, the structural action of load transfer within the wall would change significantly. In view of the fact that the applicable temperature drop within the top section of the dam structure, where seasonal temperature variations will be greater, is likely to be different to the lower section, careful thermal analysis will be required to ensure a realistic temperature drop assessment in this zone.

In the case of an analysis of this nature, it is not considered possible to predict strains and displacements with complete accuracy, as other, unmeasured factors could influence the performance of the prototype; such as variations in foundation stiffness, differential surface heating caused by solar radiation, variable placement temperatures at different heights and locations on the dam wall, etc. In the case of Wolwedans Dam, additional influences will include the fact that the first three blocks of the dam wall were constructed using a conventional formed joint at Joint No. 3 and the fact that the dam was constructed in two separate seasons, allowing substantial cooling of the lowest 15 m of the dam, which caused cracks to open at Joint Nos. 11, 14, 16 and 17, before placement was re-started for the remaining 55 m of the dam.

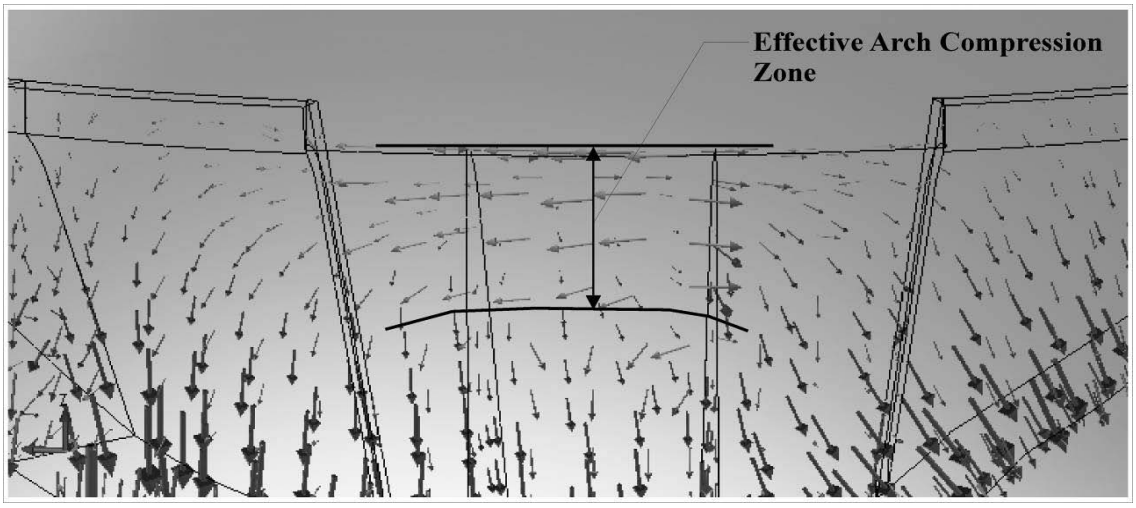

Figure 5.8: Arch Stress Distribution for FSL + 8ºC Temperature Drop

Furthermore, the effective temperature drop experienced across the full structure was undoubtedly not constant. However, considering all of these potential difficulties in simulating the actual conditions, the modelled joint openings are in fact surprisingly consistent with the measurements from the prototype.

While the applied RCC deformation modulus of 20 GPa is relatively high, testing on RCC cores revealed an average modulus at 24 months age of approximately 32 GPa, indicating that the modulus applied for analysis concurs well with an anticipated sustained deformation modulus equivalent to 60 to 70% of the instantaneous value[11].

The next step in the development of the investigation of the early thermal behaviour of RCC will accordingly encompass detailed thermal analysis to establish a more realistic temperature drop distribution and to enable a comparison of the profile of the induced joint openings across the width and height of the dam wall.

5.3.3.2. Summary of Findings

The preliminary analyses presented indicate that the apparent discrepancy between the predicted and apparent openings on the induced joints at Wolwedans Dam can be directly ascribed to the application of the hydrostatic, uplift and gravity loads.

Furthermore, the analyses clearly demonstrate that a simple, linear elastic RCC materials model can be applied to relatively accurately replicate the apparent thermal and structural behaviour of a prototype RCC structure.

The analyses consequently confirm the indications that the applicable long term-temperature drop load is significantly closer to the difference between the placement temperature and the final cold winter cycle temperature within the dam wall than the difference between the maximum hydration temperature and the cold winter cycle temperature, as more generally applied as part of accepted practice for CVC[12] and RCC dams. The modelling completed accordingly endorses the observations made through instrumentation on the Wolwedans, Knellpoort and Çine Dams.

5.3.3.3. Value of Findings

The findings of these preliminary analyses provide a definitive indication that the early behaviour of RCC in dams under thermal loading is different to that of CVC and although more detailed and substantiated investigation is still necessary, the outcome of the work presented in this Chapter provides a platform and a validation for developing more detailed studies. Furthermore, it is considered that the cross correlation of confirmatory evidence from three prototype structures, and the simplicity with which the prototype behaviour was replicated through modelling, together already serve to provide confidence in the analysis results.

5.4. ANALYSIS 2: SIMULATING TEMPERATURE DISTRIBUTIONS FOR WOLWEDANS DAM

5.4.1. BACKGROUND

The initial structural modelling presented earlier in this Chapter assumed a uniform temperature drop across the full section of the dam structure, for the purposes of simplicity. In reality, the surface zones will not experience as high peak temperatures during the hydration cycle, but will be exposed to significantly greater variations of seasonal temperatures during the operational life of the dam. The impact and influence of temperature gradients and differential cooling that will have consequently occurred across the section of Wolwedans Dam is investigated in this Chapter.

At 70 m in height and comprising approximately 200 000 m^3 of concrete, Wolwedans Dam is relatively small compared to many present-day RCC dams. However, the configuration of the structure is such that the core RCC is well thermally insulated in the lower parts of the wall, while the bulk of the upper part of the structure will be subject to surface zone temperature variations. In view of the fact that the dam arches and that the majority of this arching occurs in the upper part of the structure, it is considered important to gain an understanding of the different seasonal thermal cycles and the associated performance in all areas of the structure, and across the full section width. Only with such an understanding will it be possible to develop a realistic picture of the manner in which temperature affects the overall structural function.

5.4.2. INTRODUCTION

The comprehensive instrumentation and the fact that the dam has remained relatively consistently full since first filled in 1992[1 & 4], approximately 2 years after completion, implies that Wolwedans represents a particularly good source of information on which to basis the thermal/structural behaviour of RCC can be evaluated. The bulk of the hydration heat had dissipated from the body of Wolwedans only by late 1991, by which time the dam was impounded to 80% of full height, and accordingly, no data exists as to the extent of the induced joint openings without the influence of water loading.

In this analysis, the apparent thermal and shrinkage behaviour across and at different elevations on an RCC dam wall is investigated and the associated impact on the overall behaviour of the arch dam structure is reviewed. While the temperature cycles experienced across the section width will vary, dependent on the respective levels of thermal insulation, the influence of reduced insulation in the thinner, upper sections of the structure compared to the deeper, lower sections, is evaluated.

5.4.3. WOLWEDANS INSTRUMENTATION RECORDS

5.4.3.1. Instrumentation

The instrumentation installed and monitored at Wolwedans Dam is described in some detail in Chapter 2 of this study. For the purpose of the analysis addressed in this Chapter, temperature and displacement measurement at the long-base-strain-gauge-temperature-meters on each of the 4 levels of installed instrumentation were evaluated.

Plate 5.1: Wolwedans Dam Instrumentation Installation at RL 66.25 m

5.4.3.2. Data and Records

The temperature records for Wolwedans Dam indicate that the hydration heat had substantially been dissipated from the core of the dam wall in late 1991/early 1992[1, 3 & 4]. After that time, the temperature at the core of the structure has tended to follow a pattern of varying by approximately + 1°C in summer and – 1°C in winter around an average temperature of approximately 13.5°C.

In the surface zones of the structure, measured temperature variations are substantially larger, with summer maxima generally in the region of 20 – 21°C on the downstream side of the dam dropping to winter minima of approximately 11 to 13°C. Equivalent figures on the upstream side (under water) are 15 to 17°C and 12.5 to 13.5°C respectively.

In the core zones of the dam wall, the placement temperatures and the peak hydration temperatures averaged approximately 20 to 21°C and 30 to 33°C respectively, while the hydration heat was observed to be dissipated fairly immediately in the surface zones (within 2 m of the surface). Measurement in an intermediate zone, 5 m from the dam surface, indicated maximum hydration temperature rises of 3 to 4°C and subsequent

long-term variations of around 2.5°C around an average of approximately 15°C (i.e. higher than the core zone).

Table 5.3 summarises the zonal temperature variations recorded.

Table 5.3: Typical Zonal Extreme Temperatures

Zone	Seasonal Temperatures (°C)				Temperature Variations (°C)	
	Placement (T1)	Max Hydration (T2)	Max Summer	Min Winter (T4)	T2-T4	T1-T4
Core	20 - 21	30 - 33	14.5	12.5	17.5 - 20	7.5 – 8.5
External - upstream	20 – 21	21/24-26*	15 - 17	12.5 – 13.5	11.5 – 13.5	7.5 – 9.5
External - downstream	20 – 21	21/23-25*	20 - 21	11 - 13	10 - 14	7 - 10
Intermediate	20 - 21	23 – 25	16.25	13.75	9 - 11	7.5 – 8.5

* - maximum hydration temperature/maximum temperature.

It is important to note that although the hydration heat was rapidly dissipated from the surface zones and that the consequential maximum hydration temperature was low in these areas, the temperature was subsequently raised by the adjacent warmer internal RCC mass. By the same token, the temperature experienced in the external zones during the subsequent winter had dropped substantially, creating a significant differential between the external and the core zones (4 – 7°C).

The indicative differential temperatures are illustrated on **Figure 5.9** overleaf.

5.4.3.3. Joint Opening Profiles

Corresponding to the above "temperature zones", **Table 5.4** below lists the typical variations of the joint openings measured at Wolwedans at RL 66.25 m. See **Figure 5.6** for the locations of the listed joints.

As can be seen from **Table 5.4**, in the case of the open joints, the surface zone on the downstream face opens by between 0.2 and 0.5 mm more than at the core during winter despite experiencing similar minimum temperatures. During summer time, the joint openings on the same joints are similar in the core and the downstream surface zone, despite a temperature difference of around 6°C.

Annual temperature variations at the core of the dam structure of 2°C can be compared with downstream external zone variations of 7 to 10°C.

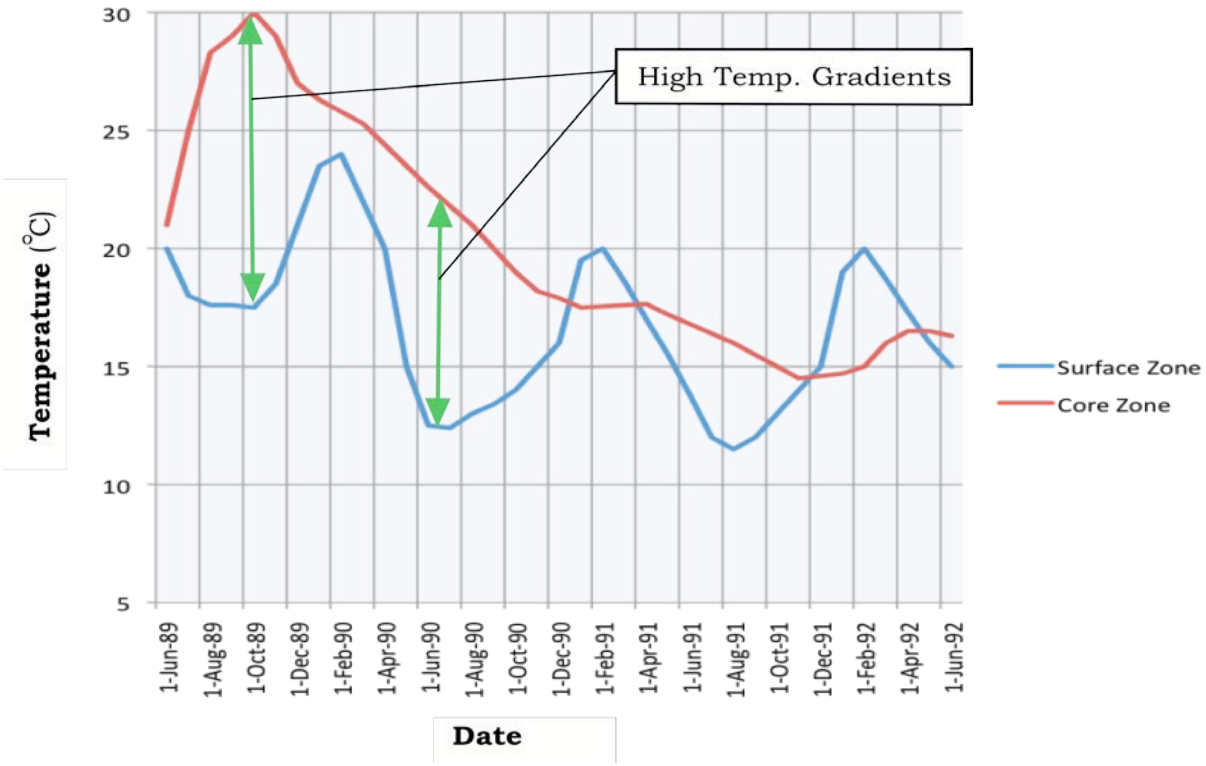

Figure 5.9: Typical Surface/External & Core Zone Temperature Histories(1)

Table 5.4: Maximum and Minimum Seasonal Joint Openings

Joint Nos.	**Surface Zone** (mm)				**Intermediate Zone** (mm)		**Core Zone** (mm)	
	Upstream		**Downstream**					
	Summer	Winter	Summer	Winter	Summer	Winter	Summer	Winter
7, 9, 10, 13, 15, 16, 19 & 22	0	0	-0.05	0.05	0	0	0	0
20	-0.15	-0.1	-0.1	0.05	0	0	0	0
11, 12	0.25	0.35	0.15	0.6	0	0	0	0
8	0.95	1.25	0.8	1.25	0.5	0.6	0.9	1.0
14	-	-	0.8	1.2	0.35	0.8	0.85	1.0
17	0.9	1.6	1.0	1.5	1.2	1.6	0.9	1.0
18	0.15	0.2	0	0.3	0.15	0.2	0	0
21	0.35	0.4	0.35	0.4	0.35	0.4	0	0.15

+ve indicates joint opening -ve indicates joint closing

The induced joints that remain closed indicate only a minor compression across the downstream surface zone in summer, which translates into a minor tension in winter.

In the upstream external zone, the observed joint openings do not indicate any real seasonal variation on the joints without any separation at the core. In the case of the open joints, the increased winter opening appears essentially equivalent to that apparent on the downstream, despite a reduced seasonal temperature variations of only approximately 3°C.

Reviewing the T1 – T4 temperature drop, similar values of approximately 8°C are indicated for both the core and intermediate zones, while a value of the order of 8.5 to 9°C is applicable for the external zones.

When reviewing the joint opening differences between the core and surface zones on the open joints and on the closed joints, it is important to consider the structural movement that will occur on these joints. When cold, the arch will tend to displace downstream, causing a closure between adjacent blocks at the upstream face and an opening at the downstream face. This was clearly evident on the structural analyses completed for Analysis 1 (parameters as per **Table 5.2**), where Joint 14, for example, indicated an opening of 0.1 mm at the upstream face, 0.77 mm on the centreline and 1.6 mm at the downstream face at RL 66.25 m.

5.4.3.4. RCC Temperature & Joint Behaviour at Elevation RL 84.25 m

In the top level of instrumentation at Wolwedans Dam (see **Figure 5.10**), the two LBSGTMs installed are within 2 m of the up- and downstream surfaces respectively (on either side of the gallery) and while the seasonal temperature variations experienced are typically 8°C on the downstream side and 2.5°C on the upstream side, the joints have never essentially opened, presumably as a consequence of the constant water load. Only at the extreme end of the right flank, at Joint 24, is any real displacement indicated. The fact that no arch action remains within the structure at this point confirms the fact that arch action is causing the complete closure of all of the other induced joints across the arch at this level.

In this upper area of the dam structure, the RCC placement temperature averaged approximately 22°C, the maximum hydration temperatures averaged 25 - 26°C and minimum winter temperatures experienced are approximately 13°C. With so little cover on these instruments from both the external faces of the dam and the gallery, they are effective entirely located in external zones.

With constant water load, the non-opening of the joints at RL 84.25 m implies that arch action is strongly and uniformly present in at least the top 15 m (below FSL) of the dam. This actually suggests stronger arching action than predicted by the finite element analysis modelling for design, which indicated that arching would be confined essentially to the spillway section and would be dissipated within 10 m below FSL.

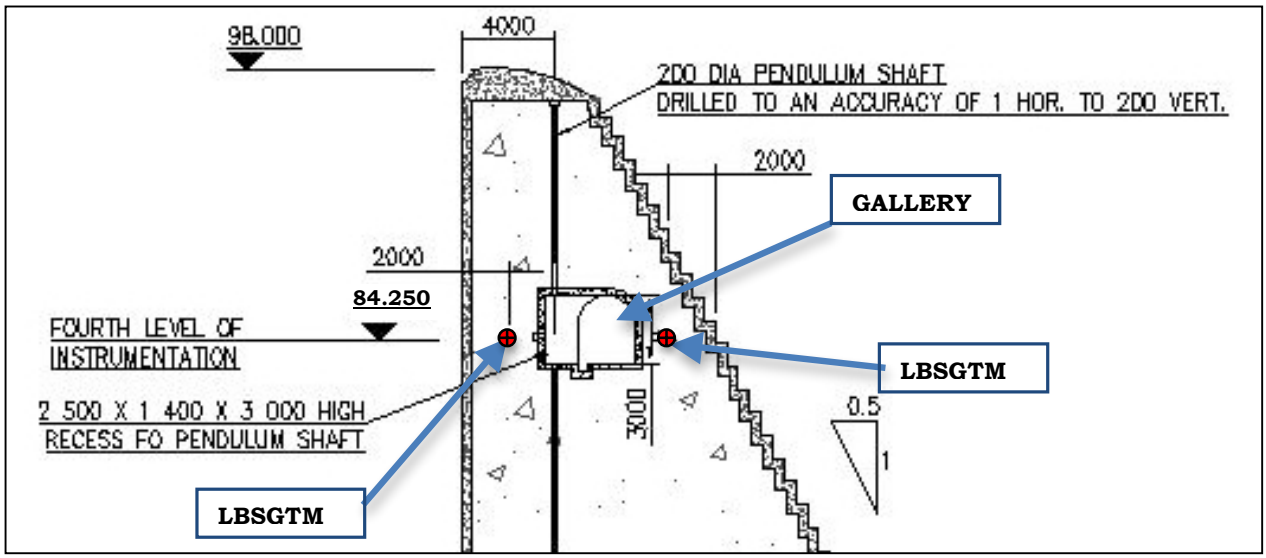

Figure 5.10: Typical Section of 4th Level (Top) Instrumentation at Wolwedans[1]

5.4.3.5. Core RCC Joint Openings

As previously mentioned, Wolwedans Dam first filled to capacity in early 1992, while at the bulk of the hydration heat had substantially been dissipated by late 1991/early 1992. From August 1991 to February 1992, the water level rose from 65% to 88% of full height. Subsequently, the water level rose slowly, but steadily for the remainder of 1992. Structural analysis revealed that arch action starts to develop in the dam wall at Wolwedans when the water level exceeds approximately 90% of the maximum service water level. This water level was reached during April 1992.

Examining the joint opening data, it is apparent that peak values were experienced during late 1991 and early 1992 and these were probably around 30% higher than the subsequent winter maxima. Summing the total maximum central joint openings at instrumentation level No. 3 (RL 66.25 m) during late 1991 indicates a total joint opening of approximately 4.7 mm, for a corresponding core temperature of approximately 14°C. Assuming a thermal expansivity of 10 x 10^{-6}/°C, a total joint opening of 4.7 mm would translate into an effective temperature drop across the 130 m long wall at this elevation of 3.6°C. Assuming that 25% of the shrinkage remained in the form of tensile stress would still only suggest an effective structural temperature drop of 4.5°C.

Comparing this situation with an analysis based on commonly accepted principles, it is possible to put the apparent performance of the RCC into perspective. For a shrinkage/creep volume reduction of 200 microstrain, a temperature drop of the order of 6°C to 14°C and a thermal expansivity of 10 x 10^{-6}/°C, total shrinkage of the order of 260 microstrain might be anticipated for the core RCC at Wolwedans. For a wall length of 130 m at RL 66.25 m and joint spacings at the centre of approximately

9.2 m, a total shrinkage of approximately 34 mm would equate to average joint openings of the order of 2.4 mm. Taken over the three joints that opened on the prototype, the full shrinkage across each joint would average more than 11 mm. The fact that the theoretical and measured joint openings are an order of magnitude different clearly demonstrates that the shrinkage and creep traditionally assumed for RCC in a dam did not materialise at Wolwedans Dam.

Either the shrinkage and the creep experienced under restrained expansion are substantially less than generally expected, or a very high level of creep must have been experienced in the RCC under tension. The latter hypothesis is considered extremely unlikely, as the compression strain is evident on all instrumented joints at Wolwedans and this compression tended to reduce to zero around mid 1990, which coincides with the time that the core temperature was equal to the placement temperature. If significant compression and tension creep had occurred, the compression strain would have reduced to zero substantially before the RCC cooled to the placement temperature and significant tensile strains would have been evident on joints that did not open, or more joints would have opened.

5.4.4. MODELLING OF OBSERVED DIFFERENTIALS

The instrumentation measurements demonstrate that the openings on the open joints are fairly even across all zones during summer, but that the external zones open on average approximately 0.3 mm more than the rest of the section during winter.

In an attempt to establish the implications of these apparent measurements, a simple thermal model of a single wedged 10 m block was set up and a temperature drop of 8°C was applied to the core and intermediate zones and 8, 9 and 12°C temperature drops were applied to the surface 3 m zones on the up- and downstream sides, with a thermal expansivity coefficient of 9 x 10^{-6}/°C, in a series of analyses. The block essentially represents a single block of the Wolwedans dam wall between induced joints at the elevation of the third set of instrumentation (RL 66.25 m).

For these analyses, the deformation along the length of one of the lateral block surfaces was evaluated.

The results of this analysis, as presented in **Figure 5.11**, indicated a lateral shrinkage of approximately 0.32 mm for the 8°C temperature drop, which was locally increased to 0.37 mm with an external surface temperature drop of 9°C and 0.50 mm with an external surface temperature drop of 12°C. The 12°C temperature drop accordingly indicated an increased external zone joint opening of approximately 0.36 mm (2 x (0.50 - 0.32)), suggesting that the external zone effectively experiences a larger effective temperature drop than the core zone of between 3 and 4°C. For a thermal expansivity of 10 x 10^{-6}/°C, the effective temperature drop differential would probably be 3°C.

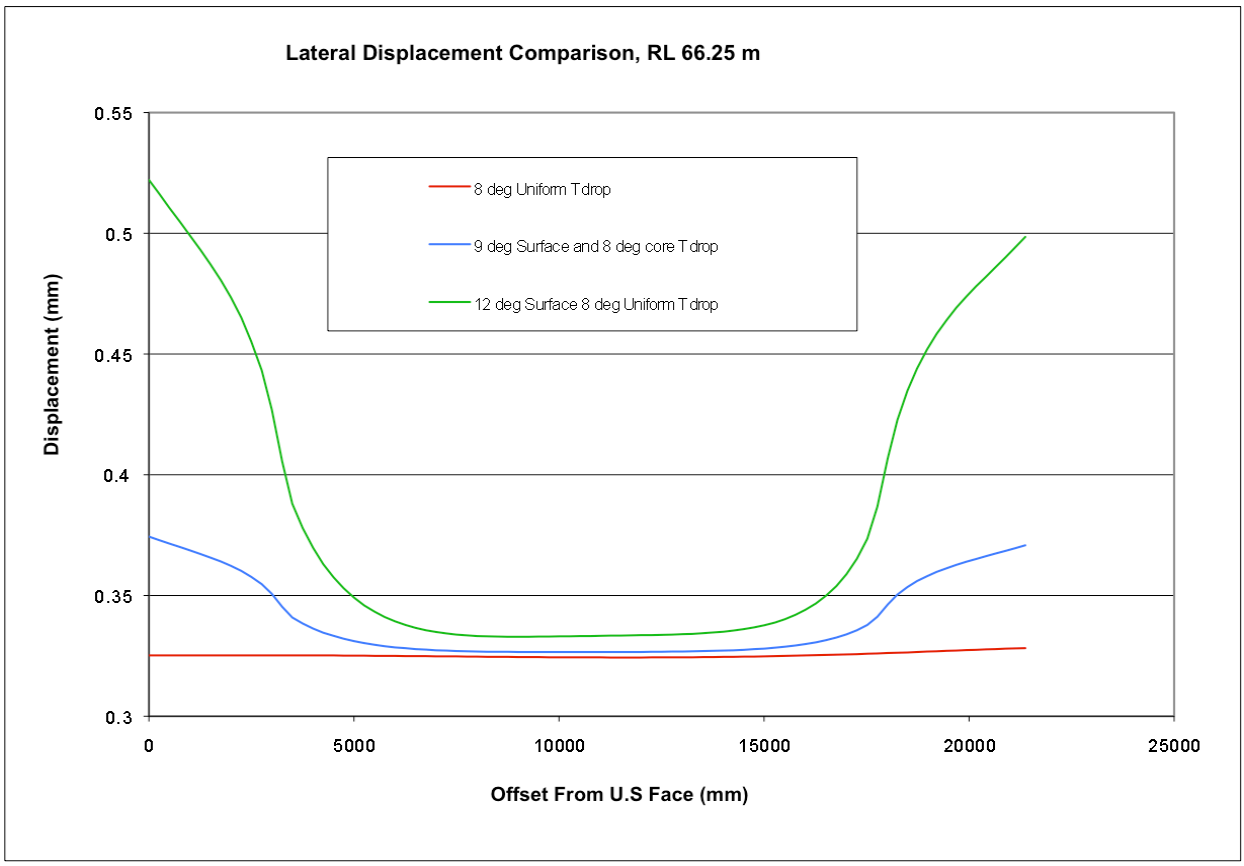

Figure 5.11: Displacement Profile for Differing Differential Temperatures

For a thermal expansivity of 10 x 10^{-6}/°C and a conservative long term elastic modulus of 20 GPa, a restrained 3°C temperature drop would give rise to a tension of 600 kPa, which would not be sufficient to exceed the RCC's horizontal tensile strength and explains why the closed joints would not experience the differential opening apparent on the open joints. However, the same logic suggests that the external zones of the dam would have been subject to a total effective temperature drop in winter of approximately 11°C. For a modulus of elasticity of 15 GPa, which is probably conservative, as much of the associated tensile stress would have occurred while the concrete was relatively young, a consequential maximum tension of 1.65 MPa would be developed. Considering the fact that the RCC of Wolwedans indicated an average core crushing strength of the order of 35 MPa, a horizontal tensile strength exceeding the apparent thermally induced tension could be anticipated, confirming the reason why surface zone cracking was not more generally apparent. On the other hand, it is considered unlikely that the effective differential temperature drop could exceed approximately 3°C, or there would have been more evidence of surface zone joint opening.

5.4.5. DISCUSSION OF WOLWEDANS DAM BEHAVIOUR

The instrumentation data for Wolwedans demonstrate that no real gain in temperature was experienced in the surface zones during the hydration cycle, although the heat in the adjacent core zone caused the temperature finally to be raised by between 2 and 6°C above the placement temperature. In the insulated core zone, a total temperature increase of the order of 10 to 12°C was experienced, while a heat gain of 3 to 4°C was experienced in the intermediate zone. Over the long term, the total temperature drop from the peak during hydration to the minimum during a cold winter can be seen to be of the order of 12°C and 20°C in the surface and core zones respectively.

The typical T1 – T4 temperature drop in the core zone and intermediate zones apparently increased by only approximately 1°C (8°C to 9°C) in the external zones, although distinct temperature gradients were developed between the zones during the first winter after placement.

At the open joints, the relative opening that occurs between summer and winter can be seen to increase from the core, to the intermediate, to the surface zone. The modelling undertaken suggests that the differential joint openings originate as a result of the fact that the total effective surface temperature drop experienced in the external zone is approximately 3°C higher than that experienced in the core zone.

This apparent behaviour suggests that some creep and/or micro-cracking must have occurred in the surface zones as a result of the temperature gradients experienced whilst the core zone was significantly heated with hydration energy and the surface was cooled during the winters of 1989 and 1990.

5.4.6. SUMMARY

The above review and analysis suggest that the application of a simple, linear temperature drop across the full arch section, as applied in the analyses described earlier in this Chapter, is not completely realistic and that thermal gradient effects gave rise to an effective maximum winter surface temperature drop of some 3°C more than was experienced within the core zone at Wolwedans.

For the purposes of the subsequent structural analyses of Wolwedans Dam, it is accordingly considered that it should be more accurate to apply a thermal loading more in line with that presented in **Figure 5.12**, although a verification of the validity of this pattern will only realistically be possible through 3-dimensional structural finite element modelling, as addressed subsequently in this Chapter.

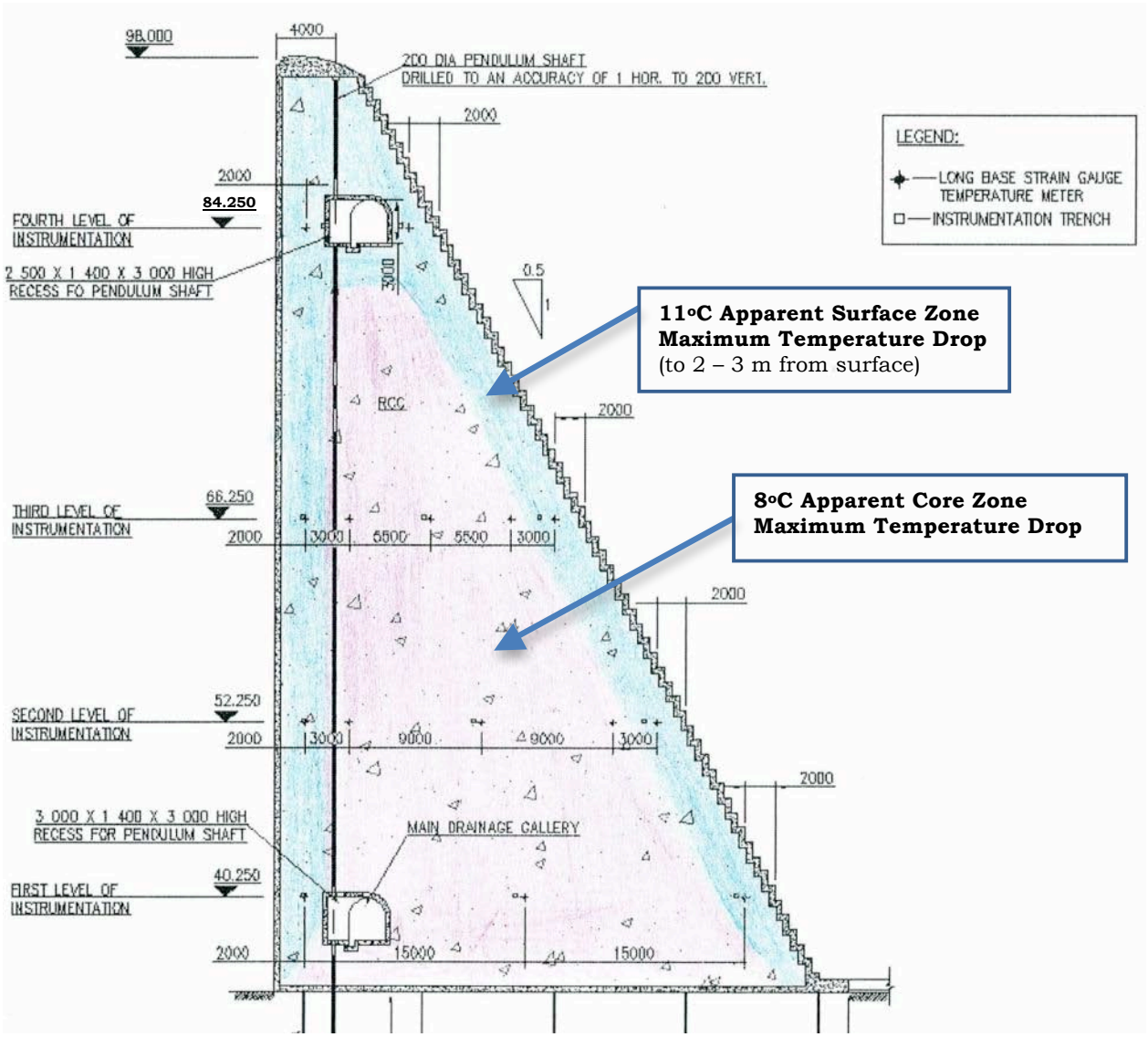

Figure 5.12: Apparent Effective Temperature Drop Distribution(1)

On the basis of the evaluation completed in this Chapter, it is considered that a greater knowledge of the influence of the differential cooling and associated temperature drop loads has been developed. Obviously, this phenomenon will indicate a variable level of influence, depending on the proportions of the structure in question. In view of the fact that most RCC arches will be relatively thin towards the crest, where the significant arching occurs, however, it is important to consider this effect when analysing all RCC dams with 3-dimensional stress transfer.

The understanding of the influence of differential temperature drops across the dam section developed through the above review is considered of benefit in respect of the detailed structural analysis of Wolwedans Dam, subsequently addressed.

5.5. ANALYSIS 3: MODELLING WOLWEDANS PROTOTYPE BEHAVIOUR

5.5.1. BACKGROUND

With the analyses described earlier in this Chapter providing a deeper understanding of the early thermal behaviour of the constituent RCC material and a greater confidence in the applicable pattern of temperature drop distributions within the dam body, it was considered appropriate to evaluate the behaviour of the dam structure as a whole, comparing modelled performance with measurements from the prototype.

In the case of an arch dam, the maximum crest displacements will vary significantly, dependent on the temperature drop applicable. Accordingly, comparing modelled and measured crest displacements for a range of effective temperature drops would allow the actual apparent temperature drop applicable on the prototype to be isolated with a high level of confidence. From an alternative perspective, applying a range of equivalent RCC shrinkage/creep volume reduction values, the materials behaviour that most closely reproduces the measured crest displacement and joint opening performance can be identified.

5.5.2. INTRODUCTION & OBJECTIVES

As presented earlier in this Chapter, the comparisons made on a specific level of installed instrumentation confirmed that RCC does not behave in the manner conventionally assumed. On the basis of maximum crest displacements, the analyses now addressed compare the overall structural performance measured on the prototype dam structure with that predicted by a Finite Element model for a range of shrinkage/creep scenarios.

In the text of this Chapter, only a summary of the findings of the described analysis is presented and the full investigation results are addressed in greater detail in **Appendix B**.

5.5.3. THE IMPACT OF TEMPERATURE DROP LOAD, OR SHRINKAGE ON ARCH ACTION

Before addressing in detail the Wolwedans Dam structural analysis, it is worthwhile to provide the reader with a background as to the significance of the modelling applied and accordingly the value of the results developed. For this purpose, it is particularly important to understand the influence of temperature drop loads and shrinkage on the function of an arch dam.

Temperature drop loads fundamentally impact the structural function of an arch dam as a consequence of the associated thermal shrinkage. While the associated impacts are described in detail in **Appendix A**, which is a partial extract from the author's Masters degree Thesis. 2001[13], a summary is provided in the subsequent text.

When subjected to depressed temperatures, the concrete of a dam structure obviously shrinks while the foundation rockmass remains unaffected. The net impact is a structure that is effectively marginally too small for its foundation and consequently tensions are experienced. Water load is transferred laterally in compression in an arch

dam into the abutments. When thermal shrinkage has resulted in tensile stresses in a similar direction, these must be overcome before arch compression can be re-established. When the water load is imposed on this structure under tension, increased arch and cantilever displacements must occur to close the tensile shrinkage and take up the load. With proximity to the foundation increasing structural stiffness within the dam wall, the displacement increases with distance from the foundation. Accordingly, the displacements on the arches and cantilevers are greatest in the centre and at the top of the structure, as indicated in **Figures 5.13** to **5.15**.

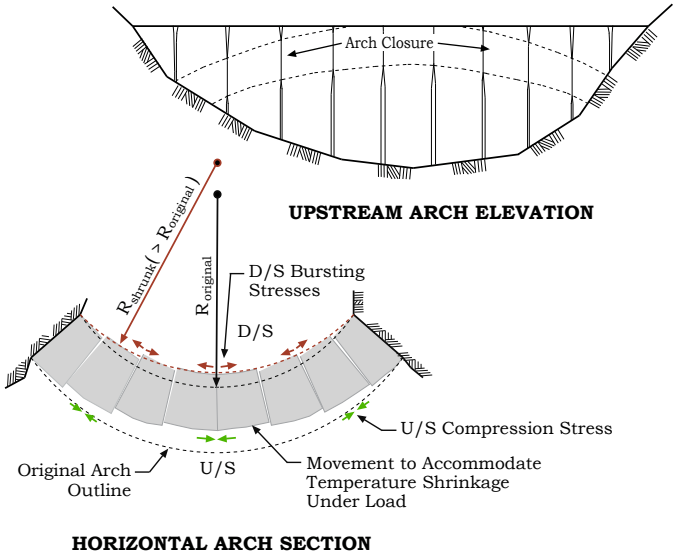

Figure 5.13: "Shrunk" Arch under Water Load

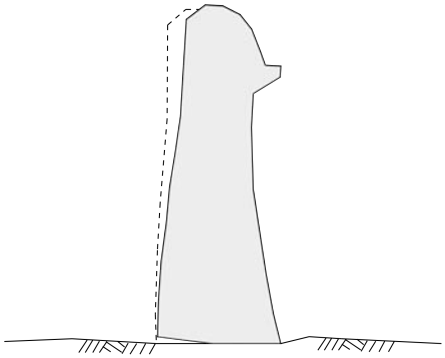

Figure 5.14: Deflection of Cantilevers

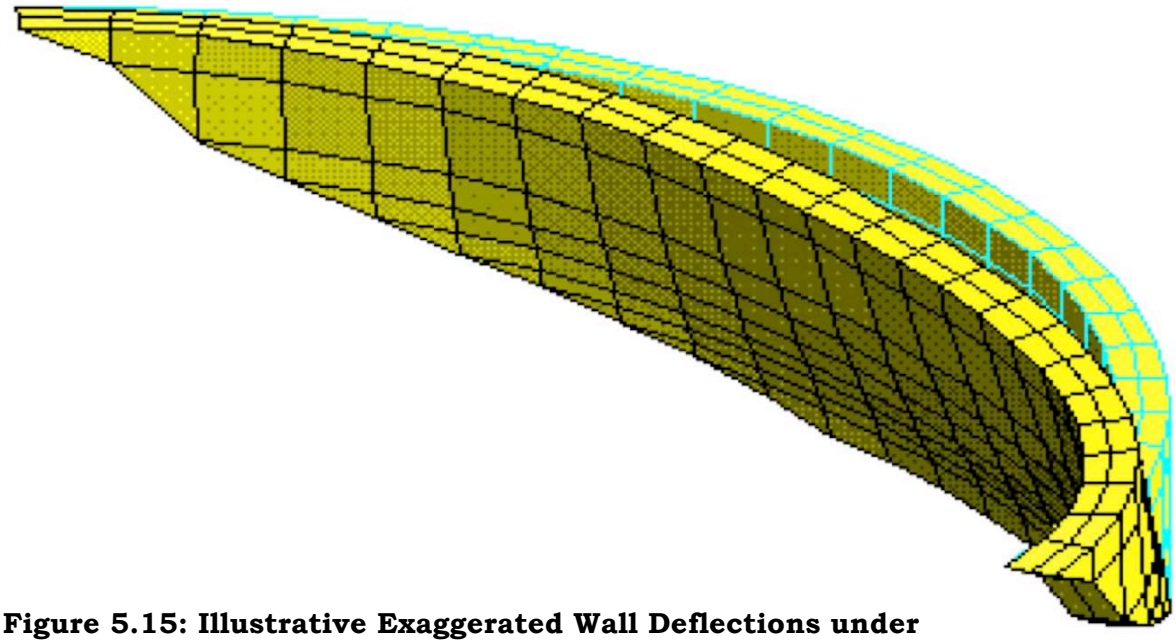

Figure 5.15: Illustrative Exaggerated Wall Deflections under Temperature Drop & Water Load

The above effect can substantially compromise the efficiency of arch action and this is addressed in **Appendix A**. Whether the result of creep, autogenous shrinkage, thermal shrinkage or a combination thereof, when an arch dam is subject to such shrinkage, the consequence is larger downstream displacements, increasing with distance from the foundation.

The importance of the above in respect of the analysis of Wolwedans Dam lies in the fact that increased shrinkage of the RCC will unavoidably be demonstrated in increased crest displacements on the arch structure. This is an impact that is unambiguous and cannot be disguised. The more "shrinkage" that occurred during the hydration heating and cooling cycle in the constituent RCC at Wolwedans Dam (due creep and autogenous shrinkage), the greater the measured crest displacements.

5.5.4. WOLWEDANS DAM INSTRUMENTATION RECORDS

5.5.4.1. Instrumentation

The instrumentation installed and monitored at Wolwedans Dam is described in some detail in Chapter 2 of this study. For the purpose of the analyses addressed in this Chapter, only the structural wall displacements and the joint openings at RL 66.25 m were considered alongside measured temperatures, with displacements being measured by geodetic survey and joint opening and temperature using long-base-strain-gauge-temperature meters. As a consequence of the spillway at Wolwedans being located in the centre of the dam wall, it is not possible to measure the maximum, central crest displacement, but only displacements on the non-overspill crests (NOCs). While the maximum crest displacements measured were accordingly at either end of the NOC adjacent to the spillway, displacement measurements from the upper gallery (at RL 85 m) covering the spillway section were available. Accordingly, it was considered that the behaviour of the prototype dam structure could be effectively defined through the displacements/deformations measured at the ends of the NOCs immediately adjacent to the spillway, three points within the upper gallery and the joint openings measured at RL 66.5 m on Joint Nos. 8, 14 and 17. The measurement positions on the dam structure are illustrated on **Figure 5.16**.

5.5.4.2. Geodetic Survey Instruments

Crest and other displacements are measured at Wolwedans Dam twice a year[7], in late January, or early February and in August, on the basis of taking measurements when the dam structure experiences its maximum and minimum temperatures. Measured data for the period January 1990 to August 2008 was provided to the author by the Spatial & Land Information Directorate of the Department of Water Affairs & Forestry (see **Appendix B**). To correspond with the temperature and joint opening data available to the author, specific attention was paid to the displacement data for the period 1990 to 1996, with the coldest temperatures within the dam structure during that time being measured in August 1995. At this time, the temperature within the core of the dam structure measured approximately 13 - 14°C.

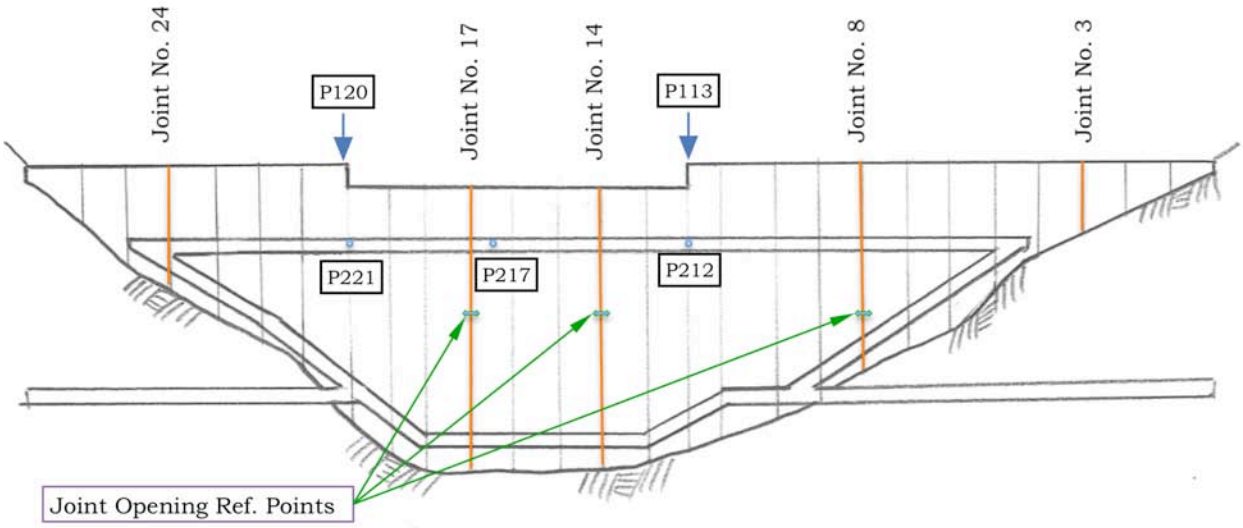

Figure 5.16: An Illustration of the Measurement Reference Points on Wolwedans Dam (viewed from Downstream)

Compared to 1995, the winter temperatures of 1993 were almost as cold, but at that time, the induced joints had not been grouted. This implies that the displacement measurements for 1993 can be more easily interpreted, without having to hypothesise any potential impacts consequential to joint grouting.

5.5.4.3. Induced Joint Grouting

Grouting of the induced joints at Wolwedans Dam is addressed in a DWAF report[14] and summarised in a technical paper presented at the Santander RCC symposium in 1995[15]. The induced joints at Wolwedans Dam were grouted in two phases between June and November 1993. The first phase encompassed grouting of the structure from the base to mid-height and was completed during the winter months of June to August. The impounded water level was reduced over this period, reaching a minimum of 8 m below FSL. The second phase of grouting, from mid-height to crest level, was undertaken during the Spring and early summer months of September to November, during which time the impoundment was at full capacity.

Studying the deformation data records over the period that grouting was undertaken at Wolwedans Dam, a number of significant observations can be made, as follows:

- On July 3rd 1993, early during the grouting exercise, a total downstream horizontal crest displacement (compared to January 1990) of 14.4 mm was measured at the end of the left flank NOC, at which time the impoundment was almost full.

- Lowering the impoundment water level by 8 m during the first phase grouting operations gave rise to an upstream movement of the crest of the order of 2.5 mm and an equivalent upstream movement at the upper gallery level of

approximately 0.5 mm. No similar effect could be discerned in the form of induced joint opening, or closing at any of the instrumentation levels.

- A net upstream movement of the dam crest of approximately 2.5 mm was recorded in February 1994, compared to February 1993, despite a 2 m higher impounded water level. This suggests that the grouting caused an upstream movement of the crest towards the centre of the dam of approximately 3 mm.
- Of the 58 instrumentation sections, across four levels, the impact of the joint grouting is only really discernable at three (as indicated on **Figures 5.17**, **5.18** and **5.19**) in the form of reduced seasonal joint movement.
- At the time of grouting, the only induced joint to have opened above RL 84.25 m was Joint No 24 (at the far end of the right flank).
- The only joint at which a distinct and definitive impact of the grouting was apparent was Joint No. 24, which demonstrated significantly reduced movement after grouting (see **Figure 5.19**).

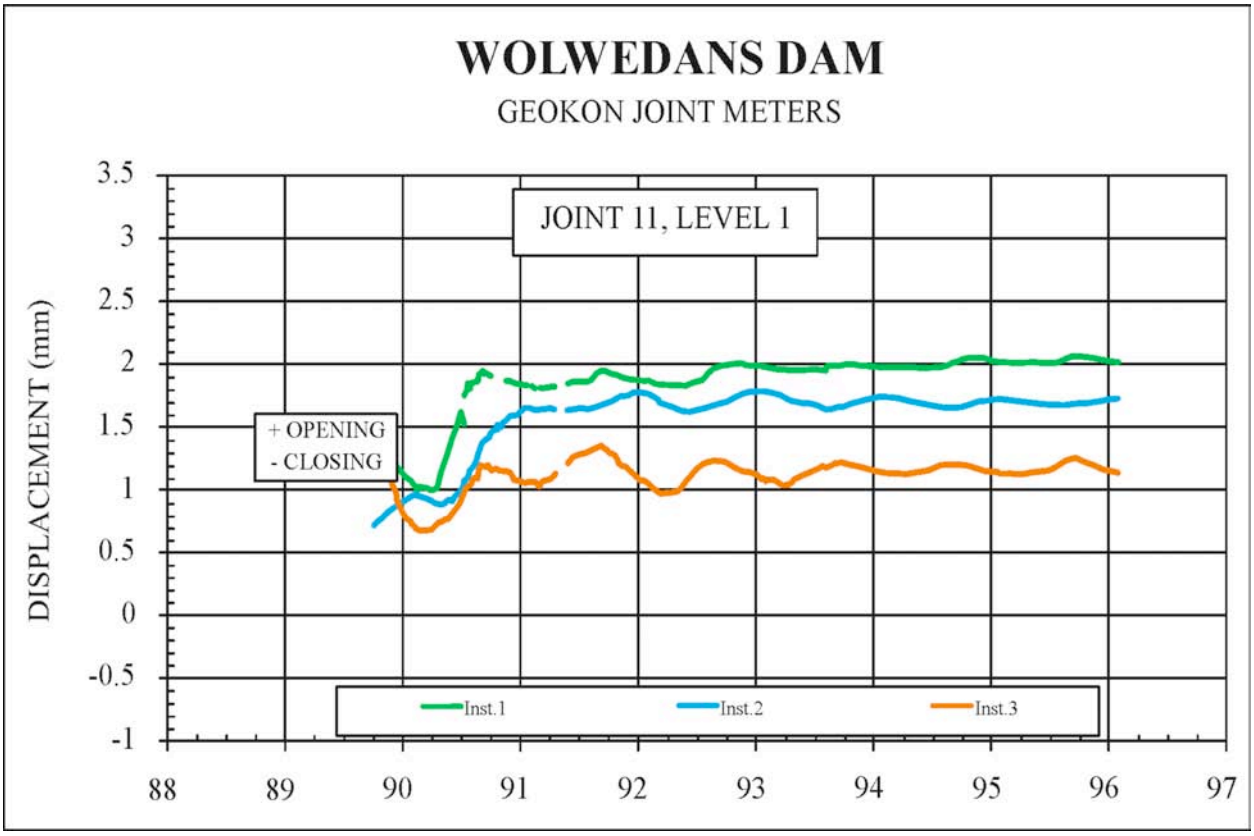

Figure 5.17: Displacement History for Joint No 11 at RL 40.25 m[7]

It is considered particularly significant that the behaviour of joint Nos 11 and 24 appeared to be impacted most obviously by grouting, as these were also the joints that indicated the most significant opening. Grout penetration of the induced cracks was obviously most successful on these joints.

It is also particularly interesting to note that the behaviour of the dam structure after grouting has changed substantially more in the warmth of summer than in the cold of winter and this is easily explained.

In the case of a CVC arch dam, the hydration heat is artificially dissipated and the concrete temperature is usually further depressed while the dam is empty and before any hydrostatic loading is imposed. In this process, the monolithic blocks in which the dam is constructed shrink away from each other, with the resultant gap between blocks increasing with distance from the foundation restraint. The gap between blocks is subsequently filled with grout and the continuity of the structure between the abutments is re-established at the temperature at which grouting is undertaken (see **Appendix A**). By grouting at, or close to, the coldest operational temperature, the dam structure would never subsequently suffer from any significant temperature drop loading, but only increased temperatures that will increase arch stresses.

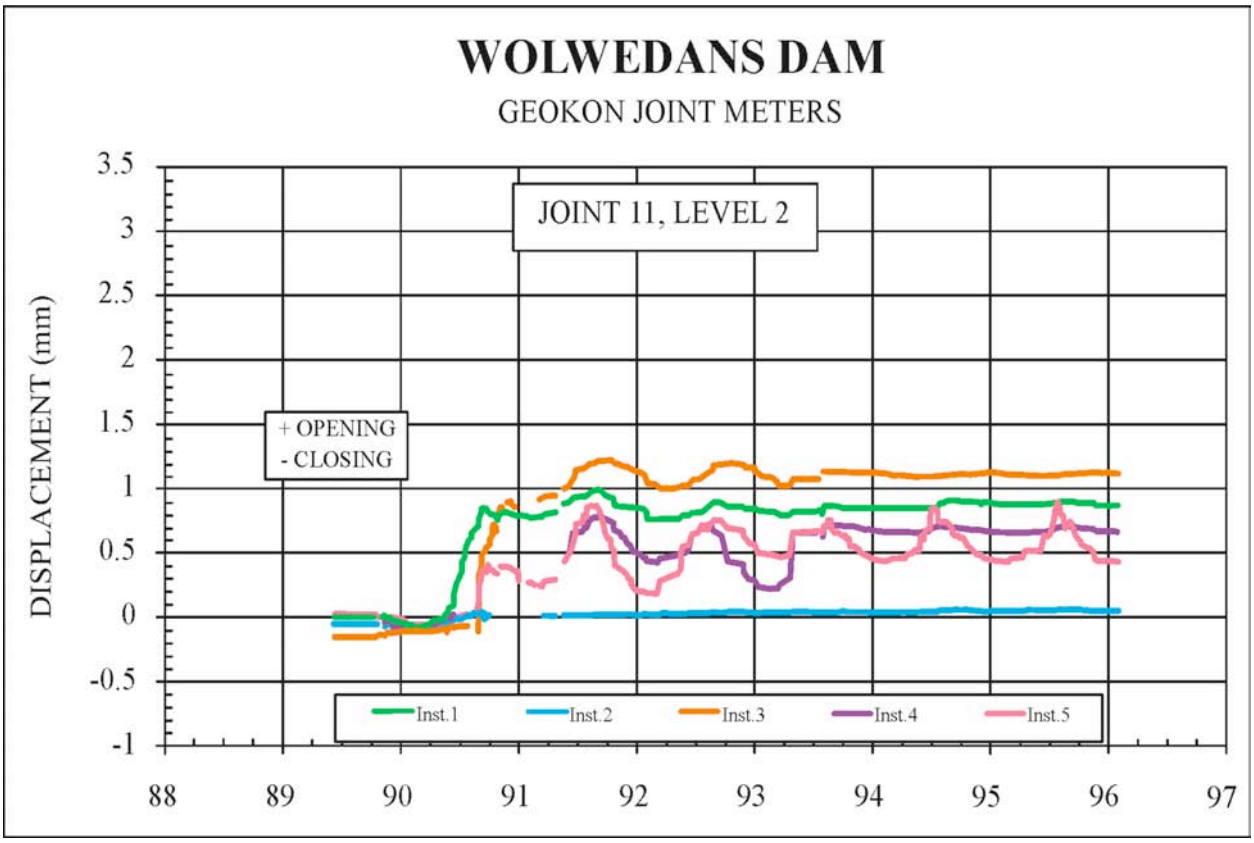

Figure 5.18: Displacement History for Joint No 11 at RL 52.25 m[7]

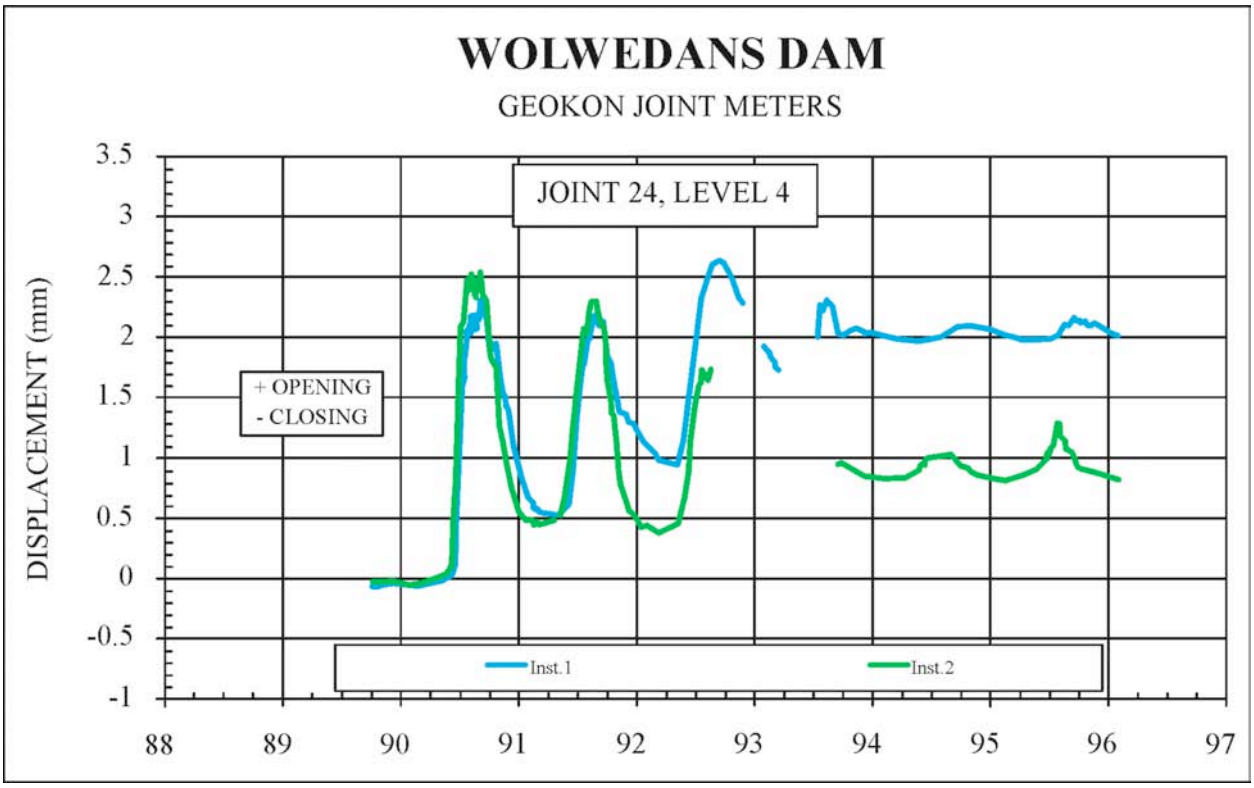

Figure 5.19: Displacement History for Joint No 24 at RL 84.25 m[7]

In the case of Wolwedans Dam, however, the dam structure had been carrying the full hydrostatic load for a while by the time that the full temperature drop load had developed. Observing only a single induced joint open at elevation RL 84.25 m is indicative of the fact that the hydrostatic loading had caused sustained arch compression stresses at this level of the dam (and above) since first impoundment. A crack was observed at Joint No. 24 as this area of the dam falls outside the section that carries arch stresses. At the time of grouting, the dam was accordingly shrunk by temperature drop, with arching limited to the upper zones of the structure and the induced joints tending to be open in the lower parts of the structure, as the shrunk cantilevers are too stiff to adequately deform and transfer stress laterally.

During grouting, it is obviously the open joints that are most effectively filled with grout. Where the structure has no open joints and transfers compression arch stresses, very little grout penetration of the joints would have been achieved. Consequently, the dam structure was effectively simply grouted up in its deformed shape. The areas most successfully grouted are those of least importance in respect of the impact of a temperature drop load and those areas least successfully grouted are conversely the most important.

The above situation is borne out by the fact that the dam structure displaces further upstream under the influence of the warmth of the summer months than previously, but no less far downstream during winter cooling. With the induced joints wherever previously open now filled with grout in a cold winter, any subsequent temperature

increases will cause expansion, resulting in the structure tending to bulge in an upstream direction.

5.5.4.4. Interpretation of Crest Displacement Measurements

The base survey data for the geodetic displacements at Wolwedans was recorded in January 1990, soon after the dam was completed, but before impoundment. The data was then translated to a zero reference in August 1992, when the dam first filled. Before examining the crest displacements measured, it is important to attempt to establish the absolute zero reference displacements. At the time of the first geodetic survey, the dam wall had essentially just been completed and the temperature within the structure was elevated. This would cause the empty dam to lift and displace upstream. Furthermore, under gravity load alone, the empty structure will tend to lean towards the upstream, with the highest bearing stress under the heel, and an upstream crest displacement would result. As cooling of the hydration heat subsequently occurred, the dam was filling and accordingly it was not possible to gain a clear picture of the crest movement that related specifically to temperature alone.

The picture related to the crest displacement behaviour is further clouded by two other factors; the fact that the upstream displacements apparently increased when the dam was full to around 2/3 height during the summer of 1991 and the fact that the placement and equilibrium temperatures in the dam structure undoubtedly increased towards the right flank. Both of these issues probably relate directly to the same climatic effects. The upstream face of Wolwedans Dam faces almost directly north and the top 30 m of the upstream face was probably warmed by particularly intense solar radiation during the summer of early 1991 before the dam filled. Similarly, the right flank of the dam and the right abutment rockmass would be exposed to direct sunlight early and through the warmest part of the day, whereas the left flank would only start receiving solar radiation later in the day, when the intensity has significantly diminished. The impact of the latter effect is tangible and the instrumentation at RL 84.25 m demonstrates typical seasonal temperature variations in the concrete between 12.5 to 21°C on the left flank that can be compared directly with equivalent variations of 14 to 23.5°C on the right flank (see **Figure 5.20** and **5.21**).

However, despite an apparent increased upstream movement of the crest in 1991 compared to 1990 of between 1.5 and 2 mm, instrumentation at RL 84.25 m clearly indicated a net drop in temperature of 3 to 4°C, which could further be seen in a general downward movement of the crest by approximately 3 mm. Furthermore, although the dam has been consistently full since late 1992, similar upstream displacements as those evident when the dam was empty and warmed by hydration have apparently been experienced occasionally since, specifically on the right flank. Instrumentation at level RL 84.25 m indicates that the temperature of the upper section of the dam typically varies on an annual cycle from approximately 13 to 22°C, which corresponds with a measured displacement variation range of between 10 and 13 mm on the dam non-overspill crest and 4 to 6 mm at the central monitoring points within the upper gallery.

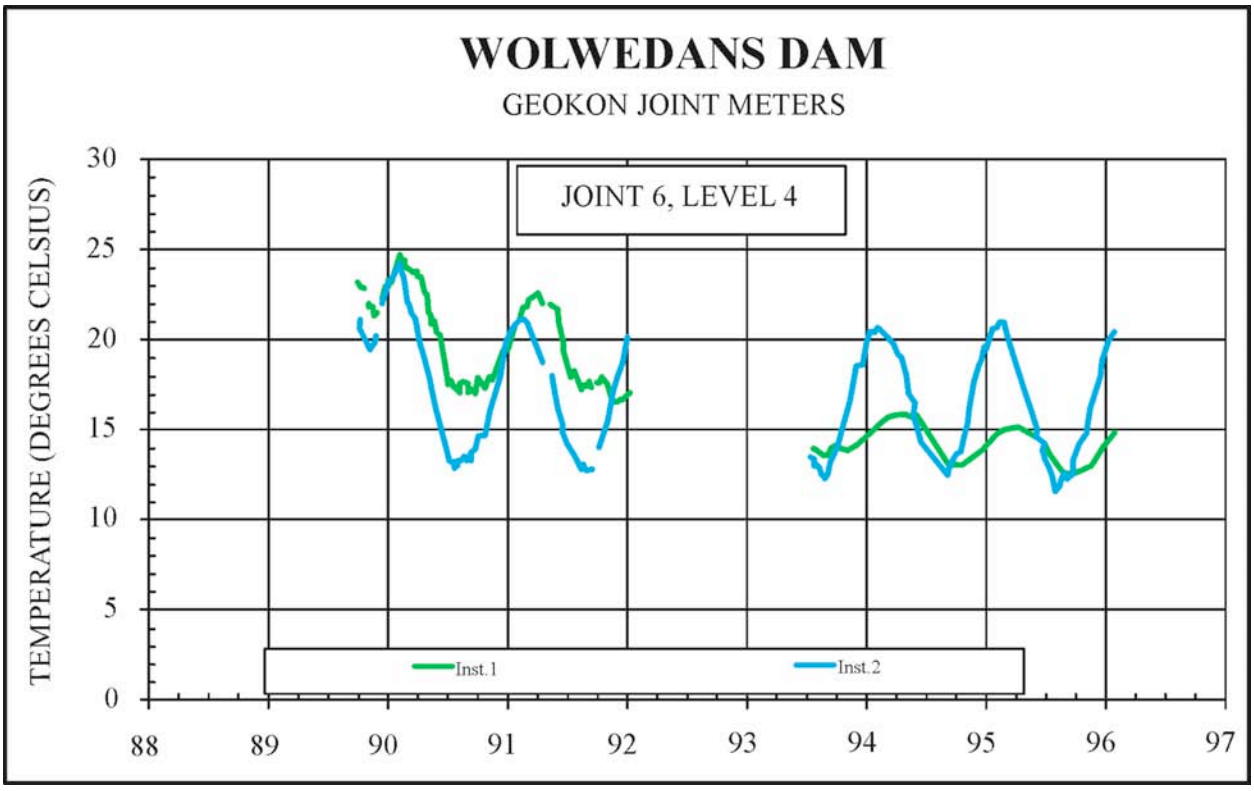

Figure 5.20: Typical Temperature History at RL 84.25 m on Left Flank[7]

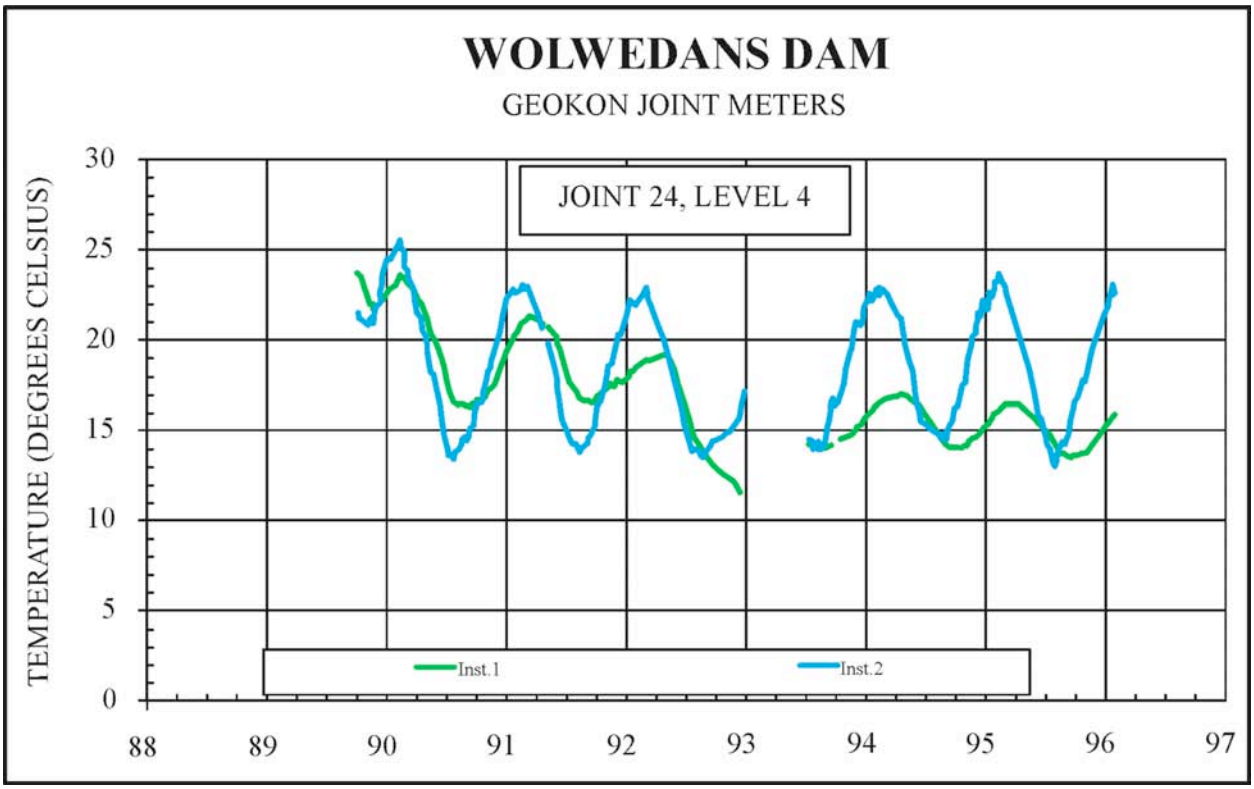

Figure 5.21: Typical Temperature History at RL 84.25 m on Right Flank[7]

It should be noted that throughout the parts of the Wolwedans Dam structure for which data exists, even the warmest temperatures experienced during the typical seasonal cycle are lower than the equivalent placement temperatures.

Reviewing the temperature data in January 1990, it would seem that the temperature of the section of the dam below RL 48 m (which was placed during 1988) was actually depressed by around 3°C below the average placement temperature, while the temperature of the RCC placed during 1989 (RL 48 – 103 m) was raised by between 2 and 3°C above the average placement temperature. Inputting this information into the finite element model, with gravity loading but without water load, indicated that the dam crest at the NOC on either side of the spillway would displace upstream by between 3.5 and 5 mm compared to its "zero temperature" state. Under water loading, this upstream displacement would be translated into a net downstream displacement. Considering the fact that the net temperature changes from placement should subsequently almost always be temperature drops, it is very surprising to observe an apparent, large upstream movement, as evident on the right flank.

Reviewing the seasonal temperature histories at elevation RL 84.25 m, the insulating effect of the impounded water is clearly demonstrated through a significantly greater temperature variation range on the downstream side, compared to the upstream. Within the NOC, however, no water insulation will be present and, with greater exposure to solar radiation, the upstream and top sides will experience higher temperatures during summer than the downstream side. With just a 5 m wide section and greater exposure to climatic effects (on 3 surfaces), it is considered certain that the temperature variations experienced within the NOC will consequently exceed those at the upper gallery level and it is very likely that the Non Overspill Crest of the dam correspondingly experiences temperatures above placement during the warmest summer months, particularly on the right flank. The fact that the only joint to open (No 24) on the right flank was successfully grouted will further increase the tendency of the right flank crest to indicate upstream movement during periods of particularly warm temperatures.

This issue is also addressed in **Appendix B** and the pattern of movement of the right flank of the dam is reviewed in more detail and in tandem with the seasonal rockmass movements. It is concluded that the most likely cause of the apparent additional upstream crest movements of between 3 and 7 mm on the right flank of the dam is higher summer season increases in temperature, both within the affected upper section of the dam structure and in the abutment rockmass on the right flank. However, it is recognised that ascertaining real certainty in respect of these observed phenomena was not possible within the scope of the work addressed in this study and consequently, less credibility and importance was placed in the accurate replication of displacements on the right flank of the dam.

In respect of the overall displacements measured on the prototype dam structure, the impact of the induced joint grouting exercise is difficult to determine with certainty. While the data would tend to suggest that a net upstream summer movement of the

upper part of the dam was incurred through the grouting, the total downstream displacements in winter seem unaffected. This observed behaviour is consistent with a hypothesis that the open sections of the induced joints of the cooled dam structure were filled with grout, while no grouting was really achieved in the areas under structural compression at the time of the grouting exercise, where the joints were closed. In terms of long-term behaviour, this implies that the grouting exercise did not drop the "zero stress" temperature as intended and that the same temperature drop load as before grouting will be applicable.

On the basis of the various uncertainties, it is considered that the most reliable data sets, in respect of structural displacements, are the displacements measured from January 1990 to July 1993 and the seasonal displacement variations.

5.5.4.5. Crest Displacement Measurements

Measurement points P113 and P120 are located at the beacons on the NOC immediately to the left and right sides of the spillway at Wolwedans Dam, respectively. The total horizontal, downstream crest displacement measured at these beacons in July 1993 was recorded as 14.5 and 11.7 mm respectively, compared to a base reference of January 1990. Equivalent seasonal displacement variations at these two points are approximately 10.9 and 12.8 mm respectively. While the data from the reference point P113 appears consistent with expectations, the seasonal variations and the total displacements indicated for point P120 are substantially higher than anticipated.

Plate 5.2: Wolwedans Dam – Illustrating Crest Beacons P113 & P120

5.5.4.6. Discussion on Measured Displacements

The spillway of Wolwedans Dam is located closer to the right flank than to the left, effectively as a result of the steepness of the right abutment (see **Figure 5.22**). However, while the dam height is also less at the point of the start of the NOC on the

right flank, compared to the left, the inlet tower is situated close the start of the NOC on the left flank. In order to establish the stiffening effect of the inlet tower, a series of analyses with and without the tower were run. While these indicated that the tower resulted in reduced displacements across the full arch, the impact was marginal, with displacements only reduced by slightly more than 1% at the end of the left flank NOC. However, where the surveyed displacements on the crest to the right side of the spillway were generally 15 to 20% lower than the equivalent values recorded on the left flank, the FE model un-surprisingly predicted that displacement on the right flank at P120 should be approximately 60% of that on the left flank at P113.

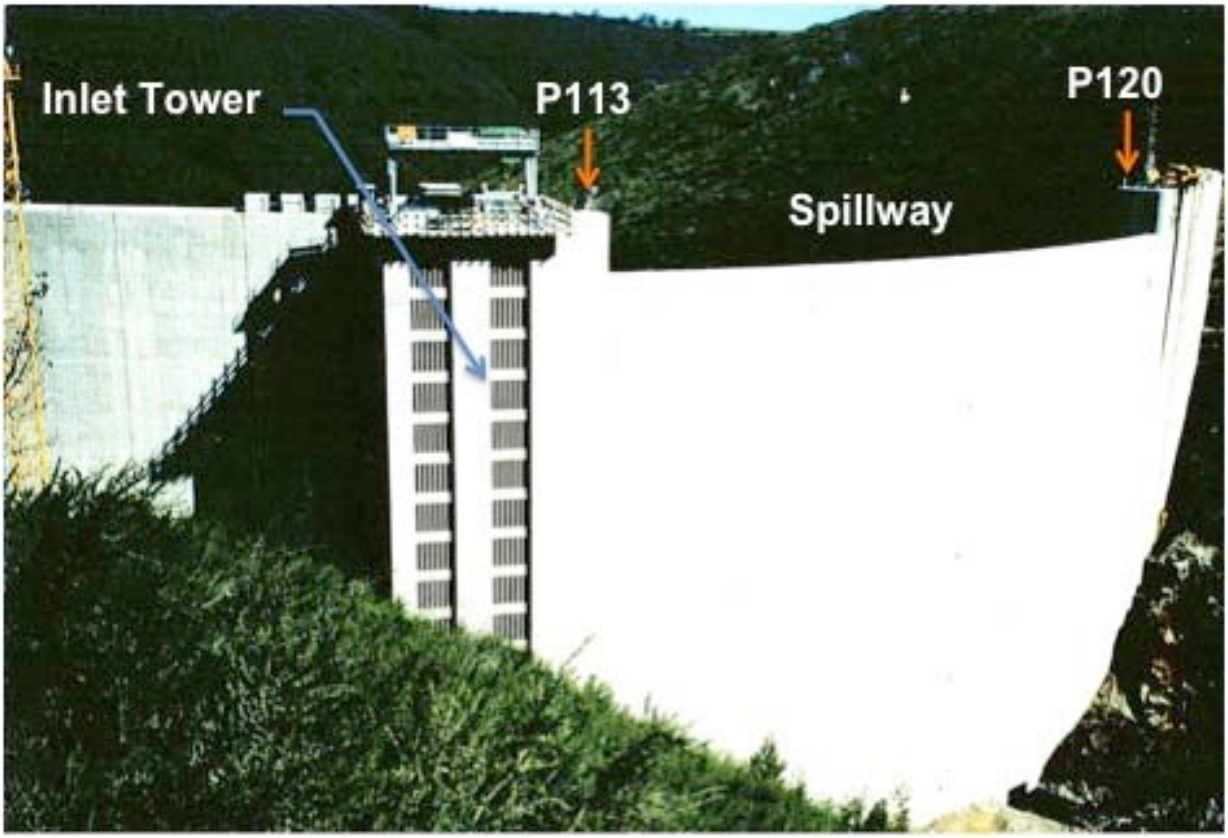

Plate 5.3: Upstream View of Dam Illustrating Beacons, Tower & Spillway

It is not possible to discern any specific related patterns in the survey data over the past 20 years that might explain this anomaly and the displacements appear equally elastic on both flanks.

The issue of the unexpectedly high upstream crest displacements on the right flank is discussed in more detail in **Appendix B** and it would appear that temperature rises in the right flank rockmass may also contribute to the observed movements. No similar movement can be discerned in the induced joints at the upper gallery level, which all remain closed at all times.

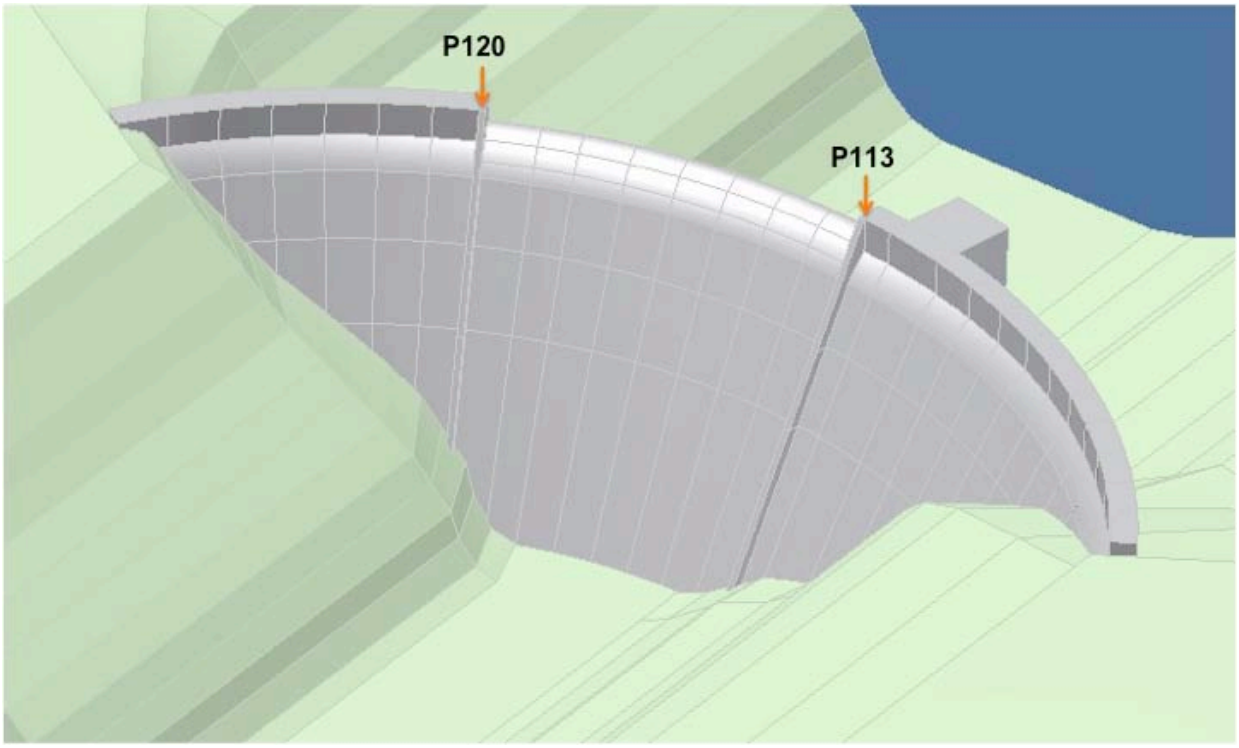

Figure 5.22: FE Model Illustrating Crest Displacement Monitoring Points

5.5.4.7. Displacement Measurements in the Upper Gallery

Due to the fact that the displacement measurement within the upper gallery at Wolwedans Dam was only initiated in August 1992, it is not possible to establish a "zero" reference for this data with real confidence. The measured data within the gallery, however, can be seen to be very consistent, with displacement increasing in line with expectations with distance from the abutments, although unexpectedly high displacement variations on the right flank are again evident. The manner in which the measured data was adjusted to a "zero" reference is discussed in **Appendix B** and the approach applied implies that the prototype reference displacements almost certainly conservatively overestimate the reality.

5.5.5. PROTOTYPE REFERENCE BEHAVIOUR

On the basis of the above, the data listed in **Table 5.5** for July 1993 was defined as the target reference behaviour for the prototype Wolwedans Dam under a nominal core 8°C temperature drop from placement temperature.

Table 5.5: Measured Displacement Data at Reference Points 1993 (mm)[7]

Reference Point	**113**	**120**	**212**	**217**	**221**
Reference Horizontal Downstream Displacement	14.5	11.7*	7.65	10.1	7.5*
Seasonal Variations 1993	8.0	10.5*	3.2	4.5	3.5

Induced Joint No.	**8**	**14**	**17**	Total
Central Opening at RL 66.25 m July 1993 (mm)	1.0	0.95	1.45	3.40

The data indicated with an asterisk (*) is located on the right flank and viewed with reduced confidence.

5.5.6. DAM STRUCTURE DISPLACEMENT MODELLING

5.5.6.1. Background & Objectives

The objective of the analyses addressed in this Chapter is to compare the overall structural performance of the Wolwedans arch/gravity dam wall, as measured on the prototype through crest displacement and joint opening, with a range of RCC shrinkage/creep materials models through simulation using Finite Element analysis.

For the early behaviour assumed for RCC, or the "Traditional RCC Materials Model" it would be usual to assume a "typical" total effective volume reduction of approximately 200 microstrain due to shrinkage and creep during the hydration heating and cooling cycle, as discussed in Chapter 3. If a further temperature drop of the order of 8°C to the long-term minimum core body temperature is assumed, at a thermal expansivity of 10 x 10^{-6}/°C, the total post-placement volume reduction, or shrinkage would consequently equate to 280 microstrain.

In reviewing the analyses undertaken, it must be recognised that the modelling presented can never be anything more than an approximation of the reality. As discussed in Chapter 3, due to the complex elastic and inelastic behaviour of concrete, the influences of seasonal and site-specific placement temperature variations, varying degrees of internal restraint caused by the size of the structure in question, differential stiffness values across the foundation rockmass, etc, an evaluation of the early behaviour of RCC within a dam can be regarded as an estimation at best. However, the traditional theory and the conventional approach to dam design assumes a volume reduction of the order of 200 microstrain as a consequence of creep (and autogenous shrinkage) during the hydration heating and cooling cycle and this will have an impact on the structural behaviour of the dam that should be very obvious.

The objective of the analysis undertaken was accordingly not to precisely identify the actual behaviour mode of the dam and its constituent materials, but to establish the nature of the performance that would have been expected on the basis of the

traditional design approach and assumed materials characteristics for RCC and to compare the actual performance with a number of possible RCC behaviour scenarios.

It is, however, considered particularly important to take note that the structural modelling is attempting to reproduce crest displacements and induced joint openings. Having opened due to a temperature drop and possibly creep during the hydration heating and cooling cycle, the induced joints close under the water load as the separated cantilevers (between open induced joints) displace forward and make contact at the crest to develop arch action. The higher the E modulus applied for the RCC, the less the cantilevers deflect, the lower the total crest displacement and the wider the induced joints remain open. Consequently, while it is possible to assume some creep in conjunction with a higher E modulus for the RCC in order to reproduce the measured crest displacements, the higher E value will result in reduced closure of the induced joints, while the joint openings will also have been increased by the creep. The consequence would be the prediction of substantially greater induced joint openings than measured in reality. Accordingly, matching the measured induced joint openings and the crest displacements will require a reasonably realistic simulation of the actual RCC behaviour.

5.5.6.2. Earlier Analyses

The Wolwedans Dam arch/gravity RCC dam structure was modelled as part of the first dam safety evaluation, completed in 1997, 5 years after full impoundment was first achieved. This work is summarized in the Department of Water Affairs and Forestry report "3-D Structural Analysis of Wolwedans Dam"[16]. This study, which was relatively simplistic in nature, demonstrated that a maximum, central crest displacement of approximately 4 mm under (FSL) normal hydrostatic loading was increased to approximately 12 mm when a uniform 6°C temperature drop was applied to the complete structure.

This analysis was undertaken using three different FE analysis programs; ABAQUS, ANSYS and NISA. For the same material properties, element meshes and load cases, the maximum horizontal crest displacements indicated by each of the three programs varied by approximately 12%, while the maximum toe stresses presented varied by over 50% and the maximum heel tensions by over 25%, providing an indication of the divergence in analysis result presentation typically evident for different FE analysis systems and models, particularly at discontinuities. While the actual FE analytical processes cannot differ between the various different software versions, the divergence in output is found in the manner and precise location within each element that the stresses are indicated.

An analysis with the same geometry, materials properties and loadings was repeated as part of this investigation using COSMOS[8] and the maximum indicated in-stream crest displacement was 4.6 mm, which was approximately 5% higher than the highest value for the other three programs. While the analysis completed as part of this study used a denser mesh with tetrahedral elements, the results serve to confirm the

COSMOS user manual's assertion that the program is conservative and will generally present displacements and stresses that are on the higher side, when compared with a typical range of FE analysis systems. While this again relates to the particular approach taken by COSMOS to the presentation of output from the model elements, it is stated here simply to recognise an additional factor of conservatism in the analysis results presented.

5.5.6.3. Modelling the Wolwedans Dam RCC Arch/Gravity Structure

Analysis Methodology

To maintain the approach applied for the earlier analyses, only linear-elastic FE modelling was undertaken. While this is not considered completely realistic, as the increased cantilever displacements are highly likely to give rise to plastic deformation as tensions develop at the heel, it is a conservative, tending to result in underestimated crest displacements on the model.

While the materials behaviour to be modelled relates to shrinkage caused by creep during the hydration process, as well possibly as early autogenous shrinkage, these can best be simulated as elastic shrinkage caused entirely by a temperature drop. Accordingly, the 280 microstrain shrinkage that the conventional approach (traditional RCC materials model) would suggest occurs in mass RCC would be simulated on the FE model by applying a temperature drop of 28°C at a coefficient of expansion of 10 x 10^{-6}/°C.

For each of the behaviour scenarios analysed, the in-plane displacements on the crest on either side of the spillway and at the strategic locations in the upper gallery were noted, together with the central joint opening predicted on open Induced Joint Nos. 8, 14 and 17 at elevation RL 66.25 m.

Materials Properties & Loadings

It is acknowledged that it would never be possible to precisely establish the actual mechanical properties of the dam RCC and its foundation rockmass and that it would be possible to produce an almost limitless quantity of analysis results, depending on the combination of E values, coefficients of thermal expansion, uplift load and effective temperature drop applied. However, reproducing induced joint openings and crest displacements that both reasonably accurately correspond to the measured values does narrow the possible materials property and loading variations.

For the purposes of the analysis presented herein, the measured materials properties for the RCC of Wolwedans Dam[1] and those properties and characteristics demonstrated through modelling in the first set of analyses presented in this Chapter to be most valid were applied for the analyses addressed. These and the loadings that were considered as constant are summarised in **Table 5.6**. At the time that the critical displacement values were measured in July 1993, the impounded water level was

recorded as just 300 mm below FSL and accordingly, hydrostatic loading equivalent to water storage at the Full Supply Level was applied for all comparative analyses.

In order to demonstrate the validity, or the apparent representivity, of the selected materials properties a sensitivity analysis was also completed, applying a higher E modulus value (25 GPa) for the RCC in conjunction with some creep (30 and 50 microstrain).

Table 5.6: Materials Properties & Constant Loads Applied for All Analyses

Property	**Value Applied**	**Loading**	**Value Applied**
RCC Density	2400 kg/m^3	Hydrostatic	FSL (RL 98 m)
RCC Compressive strength	35 MPa	Uplift*	50% Design
RCC Elastic Modulus (sustained)	20 Gpa	Silt	None
RCC Thermal Expansivity	10 x 10^{-6}/^{o}C	*Note:* *"Massless" foundation applied & Jt. 8 opening reduced by 0.72 mm on all analyses to compensate for gravitational modelling effects (see 5.3.2.5).*	
RCC Poisson's Ratio	0.2		
Foundation Elastic Modulus	15 GPa		
Foundation Poisson's Ratio	0.2		
Foundation Thermal Expansivity	10 x 10^{-6}/^{o}C		

* - The issue of the applied uplift pressure is discussed in **Appendix B**.

Finite Element Model

The same structural FE model described earlier in this Chapter was applied for the analyses undertaken, with a foundation rockmass extending 1.5 x the dam height upstream, downstream and beneath the dam and 1 x the dam height on either flank. The boundaries of the foundation model were fully constrained against movement.

As discussed earier, the common practice of adopting a massless foundation[9] for FE analysis requires that gravity is imposed as a load on the dam structure, but not on the foundation. This gives rise to a distortion of certain displacements, particularly close to the foundation where unrealistic shears are indicated on the model. An analysis indicated that the central opening on Joint No. 8 at RL 66.25 m was increased by 0.72 mm by this modelling effect. The openings on Joint Nos. 14 and 17 were not affected. Consequently, for comparison with measurements on the actual dam, 0.72 mm was deducted from the central opening indicated for Joint No. 8 on all analyses.

Materials Models / Loading Cases

With the above listed properties as constant, a net core temperature drop from placement of 8°C, as indicated on the installed instrumentation for winter 1993, was applied together with a number, or range of possible RCC creep/shrinkage behaviour scenarios, as indicated in **Table 5.7**. In accordance with the findings of the previous

analysis, a model that assumed an 8°C core temperature drop in conjunction with an 11°C external, or surface zone drop, as indicated in **Figure 5.12** (Scenario 2), was also investigated. Scenarios 1 and 2 accordingly represent the same situation of no autogenous/drying shrinkage and no creep of the RCC during the hydration and cooling cycle, with Scenario 2 simply representing a refinement based on the apparent differences in core and surface temperature drops that were found to be evident through a detailed examination of the recorded instrumentation data.

Table 5.7: Analysis Scenarios

Scenario	**Temperature Drop** (°C)		**Volume Reduction /Shrinkage** (microstrain)	**Effective Total Temperature Drop** (°C)
	Core	**Surface**		
1	8	8	0	8
2	8	11	0	8 / 11
3	8	8	70	15
4	8	8	160	25
5	8	8	300	38

Analysis Results

The following presents a summary of the displacement results obtained through the analyses completed. For the purposes of clarity of presentation, only the key results and findings are illustrated in this Chapter. A more comprehensive set of output and results, however, is included in **Appendix B** and that presentation describes in greater detail the impacts of the temperature drop, or shrinkage, on the structural function of the dam wall, with displacement plots and stress plots for each of the listed Scenarios.

The total horizontal displacements at the reference points and central joint openings at elevation RL 66.25 m predicted by the FE model for each of the Scenarios developed are listed in **Table 5.8**.

Table 5.8: Predicted Horizontal Displacements & Openings

Scenario	Effective Total Temp. Drop (°C)	Displacements (mm)						Central Joint Openings (mm)			
		P113	P120	P212	P217	P221	Total	Jt. 8	Jt.14	Jt.17	Total
1	8	12.7	8.4	8.8	10.1	6.1	46.1	1.17	0.77	1.56	3.50
2	8 / 11	14.3	8.6	9.4	12.4	6.8	51.5	1.20	0.46	1.88	3.54
3	15	18.1	10.0	11.7	14.4	7.7	61.9	4.60	2.67	4.54	11.81
4	25	26.1	13.2	15.1	17.3	10.9	82.6	10.16	5.58	8.51	24.25
5	38	35.3	16.5	20.3	21.3	13.6	107.0	10.83	9.75	13.60	34.18

Result Discussion

The above results can be compared with the equivalent figures measured on the prototype structure in July 1993, as listed in **Table 5.9** (and Table 5.5).

Table 5.9: Measured Displacements & Openings(2, 3, 4, 5 & Appendix B)

Measured Data	Displacements (mm)						Central Joint Openings (mm)			
	P113	P120	P212	P217	P221	Total	Jt. 8	Jt. 14	Jt. 17	Total
	14.5	11.7*	7.65	10.1	7.5*	51.5	1.00	0.95	1.45	3.40

The levels of confidence in the data indicated "*" are not considered as high.

Ignoring the displacement at P120, it is significant to note that the measured displacements and joint openings are generally less than any of those predicted applying the modelling scenarios considered. However, within a realistic level of accuracy, it is considered that the models applied under Scenarios 1 and 2 realistically represent the actual behaviour. Certainly, it can be stated that the crest displacements predicted for the "traditional" RCC materials model presented under Scenario 4 are almost double those measured on the prototype, while the predicted joint openings are sevenfold those actually measured.

Even a net 70 microstrain volume reduction (Scenario 3) as a result of shrinkage and stress relaxation creep would have given rise to a total joint opening of approximately 3.5 times that measured in reality.

It should be borne in mind that the analyses presented assume a fully linear concrete Deformation Modulus. Even though the value used is relatively high for a long-term modulus, in reality a non-linear stress-strain relationship will exist and the modulus that would in fact apply at the low levels of stress within the majority of the dam structure would result in reduced crest displacements. Experience with many structural dam analyses suggests that this impact might reduce the total crest displacements by 10 to 20% where no, or only minor heel tensions are evident. Conversely, experience of analysis using the COSMOS system would suggest that the crest displacements are likely to be over-estimated, by 5 to 15% compared to those predicted using other FE systems. In addition, where heel tensions are high, as is the case for Scenarios 3 to 5, it is quite possible that the elastic analyses under-state the actual displacements that would be developed. Accordingly, while it is clear that an absolute reproduction of the measured crest displacements will not be possible using a FE model, the crest displacements predicted using an elastic analysis with the COSMOS[8] FE system are probably as realistically comparable with those of the prototype structure as can be expected to be achieved.

Evaluating the crest displacements against those measured within the upper drainage gallery, a greater level of accuracy is considered to exist in respect of the predicted displacements for the latter location. Taking into account the larger than expected crest movements on the right flank, it is suggested that the full crest of the dam is probably subject to greater temperatures during summer than measured at the upper gallery level. This has almost certainly resulted in an inaccurate, but conservative, estimation of the “zero” displacement location for the crest monitoring points, which has consequently exaggerated the total downstream displacement considered to be the result of hydrostatic loading and temperature drop.

Considering the above factors and the findings of the temperature drop distribution analysis, it is postulated that Scenario 2 is probably most realistically representative of the actual RCC behaviour at Wolwedans Dam.

Sensitivity Analysis

In order to test the sensitivity of the above results, additional analyses were completed to review possible scenarios of increased RCC E modulus in conjunction with some creep/shrinkage. **Table 5.10** lists the associated characteristics, the loads evaluated, the predicted summed induced joint openings at RL 66.25 m and the downstream displacements at reference points P113 and P217, respectively.

Table 5.10: Sensitivity Analysis Results

Characteristics							Displacements		
Scenario	**Uplift**	**E Modulus Dam**	**E Modulus Foundation**	**Thermal Expansion Coefficient**	**Temperature Drop**	**Creep/ Shrikage**	Combined Induced Joint Opening	P113	P217
No.	% Design	(GPa)	(GPa)	(x 10^{-6}/°C)	(°C)	(Micro-strain)	(mm)	(mm)	(mm)
6	50	15	15	10	8	10	3.85	14.70	11.60
7	50	15	15	11	8	0	3.63	14.60	11.50
8	50	25	15	10	8	10	4.97	12.1	10.11
9	50	25	15	10	8	20	6.24	12.71	10.68
10	50	25	15	10	8	30	7.42	13.51	11.38

The analysis results presented in **Table 5.10** demonstrate that applying some creep/shrinkage for a lower RCC E modulus, it is possible to reproduce joint openings of the order measured on the prototype, but at the expense of higher crest and upper gallery-level displacements. Conversely, the measured crest and upper-gallery displacements can be reproduced with a higher RCC modulus and some creep, but only with higher induced joint openings. The analyses accordingly demonstrated that both the measured induced joint openings and the crest displacements could only realistically be reproduced with a no creep and 20 GPa RCC E modulus scenario.

Summary & Conclusions

The above analysis clearly demonstrates that Scenarios 1 and 2 most closely replicate the actual field measurements. Even the apparent surface creep effects caused by the temperature gradients across the section, as discussed earlier in this Chapter and as presented in Scenario 2, might seem to represent a conservative assumption.

The use of elastic materials properties for analysis may have resulted in marginally conservative displacement results, but the reference displacements are also conservative and the evident correlation accuracy between the crest displacements and the joint openings adds further confidence to the results presented and the validity of the assumed RCC materials behaviour. As demonstrated, a higher E modulus for the dam RCC in conjunction with some creep might be able to reproduce similar crest displacements to the prototype, but at the expense of significantly greater induced joint openings than were actually evident.

While the accuracy with which the application of a "no creep and no shrinkage" RCC materials model can reproduce the prototype behaviour is impressive, much more significant is the unquestionable invalidity of the traditional RCC materials model, as represented by Scenario 4. The significant increase in the crest displacements and

joint openings that result with even an additional 7 degrees of temperature drop (or 70 microstrain shrinkage) strongly suggest a “no creep and no shrinkage” situation for the RCC at Wolwedans Dam.

The anomalous behaviour in respect of the displacements read at P120, when compared to P113, and the generally excessive displacements apparent on the upper right flank of the dam demonstrates the complexity of analysis of the effects under scrutiny and confirms that it is simply not realistic, nor possible, to expect a completely accurate correlation between a FE model and a prototype dam.

The results of the analyses presented are not considered valid justification as a basis to conclude that the precise behaviour of the constituent RCC of Wolwedans Dam has been identified and that no creep and no shrinkage was accordingly evident. Such a conclusion was indeed never the objective of this study. There are too many variations of input parameters, too many variables in respect of non-linear materials behaviour and the foundation deformation characteristics to draw any precise conclusions.

Although an alternative scenario is not obvious, it cannot be concluded with certainty that extensive fine-tuning of the dam and foundation E moduli, the coefficient of thermal expansion, etc, etc, might not identify a solution that would include some creep in the RCC. However, it can be stated with absolute certainty that if such a scenario exists, the associated level of creep could not exceed a few tens of microstrain and certainly would be a great deal less than is applied in the conventional design approach for RCC dams.

The analysis presented can accordingly be considered to answer definitively one specific research question. Applying the typical CVC creep/shrinkage assumptions traditionally assumed in dam design is not valid in the case of high quality, high-paste RCC.

5.6. ANALYSIS 4: THERMAL ANALYSIS FOR CHANGUINOLA 1 DAM

5.6.1. BACKGROUND

At the time of writing, approximately one third of the volume of RCC required for the construction of the 105 m high Changuinola 1 Dam in Panama had been placed. While some of the main instrumentation had been installed, the available records were too short to be of any value. A strain gauge installed perpendicular to the dam axis in the first RCC placement, however, has provided some very interesting data over a period of seven months, confirming a very similar pattern of behaviour to the similarly installed instruments at Çine Dam.

Furthermore, a detailed Thermal study for the dam[17] has been completed and this analysis proved very effective in modelling the early RCC behaviour, accurately predicting the development of two surface gradient cracks. It is accordingly considered that worthwhile information from the Changuinola 1 Dam is available for inclusion in the investigations presented and accordingly, the indications of RCC behaviour that can be derived through correlating measurements, observations and analysis at this early stage are presented in this Chapter.

5.6.2. INTRODUCTION

A summarised description of the methodology applied for the Changuinola 1 Dam Thermal Analysis is provided in this Chapter and the findings of the study are compared with the behaviour observed to date. The Thermal Analysis included a sensitivity study, with the objective of developing a greater understanding of the behaviour of the placed RCC under the measured hydration temperature rise and this is subsequently addressed.

The general arrangements, the RCC mix and the instrumentation for Changuinola 1 Dam are presented in Chapter 2, while the data from the first strain gauge are presented and briefly discussed in Chapter 4.

The RCC placed at Chaguinola 1 Dam is a high-workability mix, with a modified Vebe time of 6 to 8 seconds. The high workability allows compaction with an immersion vibrator, without the addition of supplementary grout, although this technique is only used where the finish will not be exposed during operation and beneath the reinforced concrete of the chute spillway.

Plate 5.4: RCC Placement at Changuinola 1

5.6.3. CONSTRUCTION APPROACH

Before addressing the actual analysis undertaken, it is considered of value to describe the construction approach applied for Changuinola 1 Dam, as this was seen to be of specific influence on the levels of thermal stresses developed in the structure.

From approximately 40 m height, Changuinola 1 Dam will be constructed in a conventional manner, placing RCC continuously between abutments. Up to that level, however, in order to accommodate seasonal river flow and to maximise the RCC placement period, placement was split into two components. While excavation and foundation preparation was underway in the main river course, RCC placement was initiated around the river diversion culvert, comprising two 9 x 9 m culverts, on the right flank. On completion of consolidation grouting and the placement of dental concrete on the foundation in the original river course, the location of the RCC delivery system was re-routed and RCC placement was initiated on the left flank, as illustrated on **Plate 5.5**.

Plate 5.5: RCC Placement at Changuinola 1

This approach implied that the RCC surface on the right flank at elevation 111.375 mASL was left exposed for a period of approximately 10 weeks and a crack was observed approximately midway across the block, running parallel to the dam axis, at the end of the first week of June 2010.

5.6.4. MATERIALS COMPOSITION & PROPERTIES

5.6.4.1. General

The Changuinola 1 RCC contains 70 kg/m^3 of Portland cement, blended with 145 kg/m^3 of fly ash and testing on the full-scale trials revealed an adiabatic hydration temperature of the order of 21°C, which is high for an RCC and suggests that the cement used evolves a relatively high hydration heat energy.

Laboratory testing indicated the following RCC materials characteristics:

Table 5.11: Changuinola 1 RCC Laboratory Testing Results[18]

Property	Unit	Value
Coefficient of Thermal Expansion	Strain/°K	8.8 x 10^{-6}
Thermal Diffusivity	m^2/hr	0.002415
Compressive Strength (365 days)	MPa	36.2
Tensile Strength (56 days)	MPa	1.8
Density	KN/m^3	24.6
Poissons Ratio	-	0.2

The following properties were calculated on the basis of an empirical knowledge of the constituent materials:

Table 5.12: Changuinola 1 RCC – Calculated/Estimated Properties

Property	Unit	Value
Specific Heat Capacity	J/Kg.°K	980.9
Thermal Conductivity*	W/m.°K	1.65

* - For concrete, values of Thermal Conductivity usually lie between 2 and 4 W/m.°K and the value indicated for Changuinola 1 is accordingly unusually low. While this may well be a laboratory error, the associated implications are that the dissipation time for the hydration heat will be artificially extended.

5.6.4.2. Elastic Modulus

An age-dependent value for the RCC Elastic Modulus was applied for the Thermal Analysis, calculated on the basis of the tested compressive strength development. On the basis of the average compressive strength indicated on **Figure 5.23** the equivalent instantaneous E modulus value was calculated in accordance with the equation:

$$E_c = 57\,000 \sqrt{f'c}\ (\text{PSI})$$ [19 & 20]

where $f'c$ is the RCC cylinder strength = 0.78 f_{cu}

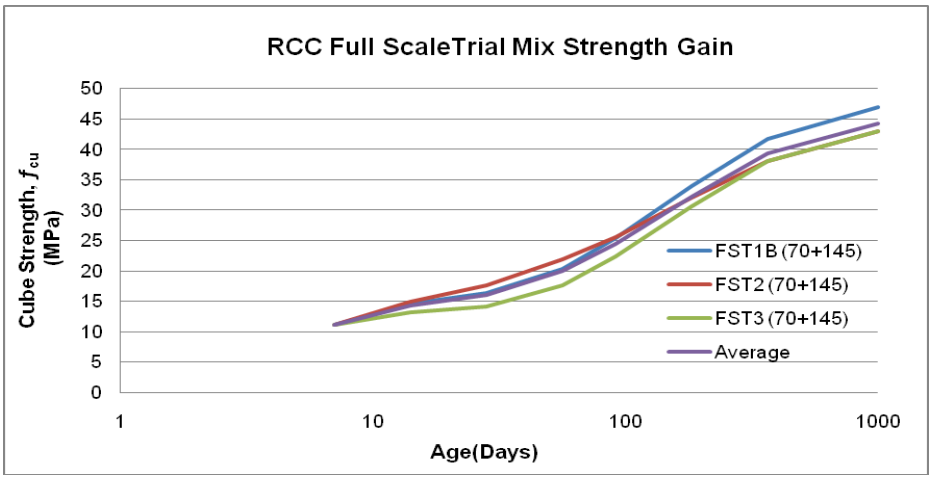

Figure 5.23: RCC Strength-Age Relationship[17]

The consequential values of instantaneous E modulus were reduced by 1/3 to represent sustained values and the derived age relationship for the E value applied for the Thermal Analysis is presented in **Figure 5.24**.

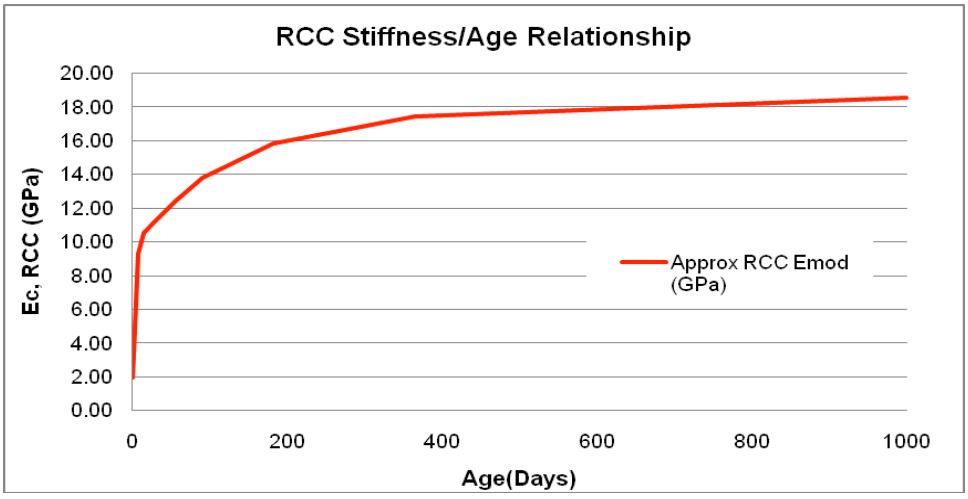

Figure 5.24: RCC E Modulus-Age Relationship[17]

For RCC ages beyond 2 years, a constant value of 18 GPa was assumed for the sustained E modulus.

5.6.4.3. Tensile Strength & Cracking

Computing tensile stresses on the basis of the time-dependent E modulus value, the tensile strength of the parent RCC was assumed to be equivalent to the 56 day value of 1.8 MPa indicated from testing on the full scale trials.

To evaluate the potential development of tensile cracking, the recommendations of the USACE's EP 1110-2-12 *Seismic Design Provisions for Roller Compacted Concrete Dams.* 1995[18] were applied as follows:

for $f_t < 0.6\ f_t'$, i.e. $f_t < 1.08$ MPa, No cracking is expected;

for $0.6\ f_{t'} < f_t < 1.25\ f_{t'}$, i.e. 1.08 MPa $< f_t <$ 2.25 MPa, Surface cracking is anticipated;

for $1.25\ f_{t'} < f_t < 1.33\ f_{t'}$, i.e. 2.25 MPa $< f_t <$ 2.4 MPa, Macro cracking is expected;

where $f_{t'}$ = Indicated tensile stress & f_t = Peak Tensile Strength (1.8 MPa).

The temeparture gradients and associated stresses for the analysis addressed were reviewed at 31st May, 30th June and 31st July, when the RCC at elevation 111.375 mASL on the right flank block had reached ages of 42, 72 and 103 days, respectively.

According to the testing from the full-scale trials, the 56 day age compressive strength of the RCC at Changuinola will be approximately 21 – 22 MPa, implying that the tensile strength is approximately 8.5% of the compressive strength.

Extrapolating from the RCC strength testing records for the full scale trials would suggest compressive strengths for the RCC at 42, 72 and 103 days age of approximately 19.2, 24.8 and 27.6 MPa, respectively.

Applying a similar tensile/compressive strength ratio as indicated for the 56 day test results would suggest tensile strengths at 42 days age of 1.6 MPa, 72 days age of 2.1 MPa and 103 days age of 2.35 MPa, respectively. On the basis of the anticipated crack development criteria above, it would accordingly be anticipated that cracking would become visible on the surface at elevation 111.375 mASL for tensile stresses exceeding approximately 2 MPa by 31st May, 2.6 MPa by 30th June and/or 2.9 MPa by 31st July, respectively.

5.6.5. THERMAL ANALYSIS

5.6.5.1. Analysis Objectives

The objectives of the Thermal Analysis for Changuinola 1 Dam can be defined as follows:

- To confirm the appropriateness of the maximum allowable RCC placement temperature of 29°C.
- To investigate the impact of the phase construction approach.
- To confirm the appropriateness of the proposed 20 m induced joint spacing.

To achieve the above objectives, the analysis was structured on the following basis:

1. Develop the anticipated temperature histories during construction.
2. Develop the long-term temperature histories until the trapped hydration heat is fully dissipated and thereby predict long-term stable seasonal temperature distributions.
3. Analyse the initial temperature histories for associated stress and consequential surface gradient cracking.
4. Analyse long-term temperature histories for associated stress (with and without creep) and consequential mass gradient cracking.
5. Predict contraction joint openings.

It is not intended to address the full analysis in the study presented herein, but rather to focus on the related findings and implications of the Thermal Analysis in respect to the early behaviour of the constituent RCC.

5.6.5.2. Analysis Approach

General

A comprehensive transient thermal analysis was completed for Changuinola 1 Dam, modelling the actual construction sequence applied for the first one third of the RCC placed and the intended programme for the balance. On the spillway section, the analysis also included the construction of the reinforced concrete chute, placed on top of the RCC, but lagging RCC placement by a period of not less than 2 weeks.

The transient thermal analysis was used to determine the evolution of the temperature distributions across two critical sections at a number of intervals from 1 week to 40 years, while the same distributions were subsequently analysed for associated strain and stress distributions and these were evaluated for the potential development of cracks.

Modelling

The Finite Element Mesh for the analysis was constructed in 300 mm layers, as applied in reality on the dam, with 300 x 300 mm elements. Weekly construction progress was modelled using a daily time step, with the evolution of the full hydration heat assumed over 7 days. The hydration temperature development, as per **Figure 5.25**, was converted into an associated daily heat energy value (W/m^2) and this was applied to each element within the mesh individually. In this manner, the hydration heat evolution was allowed to develop concurrently with convection and radiation dissipation at the exposed surfaces, simulating the actual situation in which core temperature rises due to hydration are significantly greater than surface values.

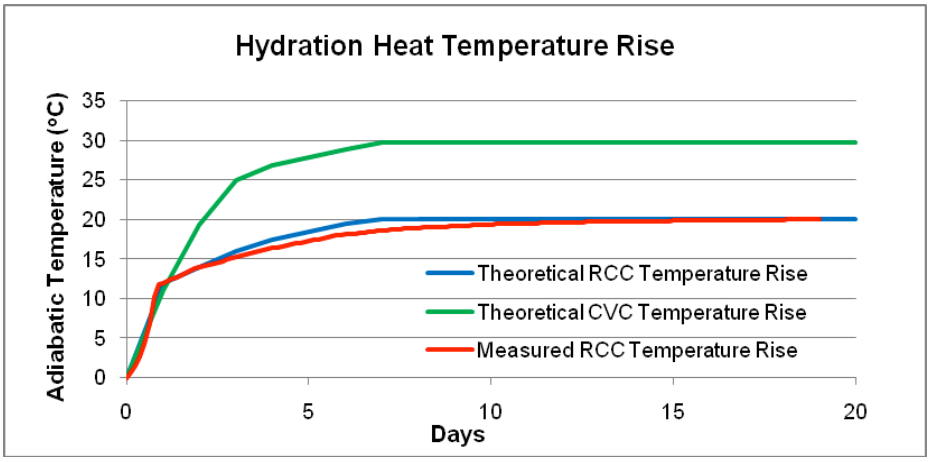

Figure 5.25: Concrete Hydration Temperature Development[16]

For the Thermal Analysis, the COSMOS[8] GeoStar and DesignStar Finite Element software was used, applying 2-dimensional shell element for the sectional analyses and 3-dimensional tetrahedral solid elements for the long-term evaluation of the induced joint spacings and predictions of associated openings.

Simulating RCC placement temperatures on the basis of average monthly temperatures increased by 2°C to allow for mixing and handling heat inputs, the surfaces of the structure, as placed in weekly intervals, were exposed to the external climatic conditions using surface convection on the basis of a nominally assumed wind speed. In addition, assumed values of solar radiation were applied and an estimated heat transfer coefficient was applied for the gallery surfaces, together with estimated gallery air temperature variations. After March 2011, an increased heat transfer coefficient was applied to the upstream face, in conjunction with appropriate seasonal water temperature variations with depth to simulate the presence of the dam reservoir.

The modes of heat development and dissipation applied for analysis during construction and long-term operation are illustrated in a simplified format in **Figures 5.26** and **5.27**.

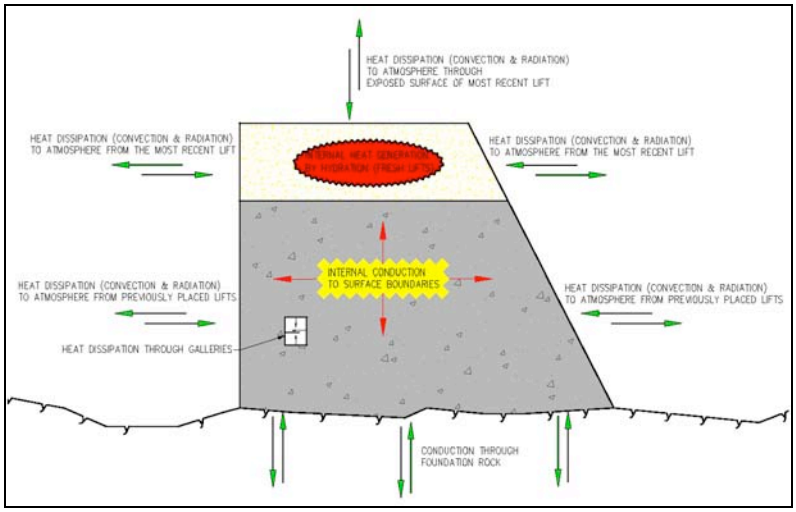

Figure 5.26: Thermal Model Heat Inputs & Losses During Construction[16]

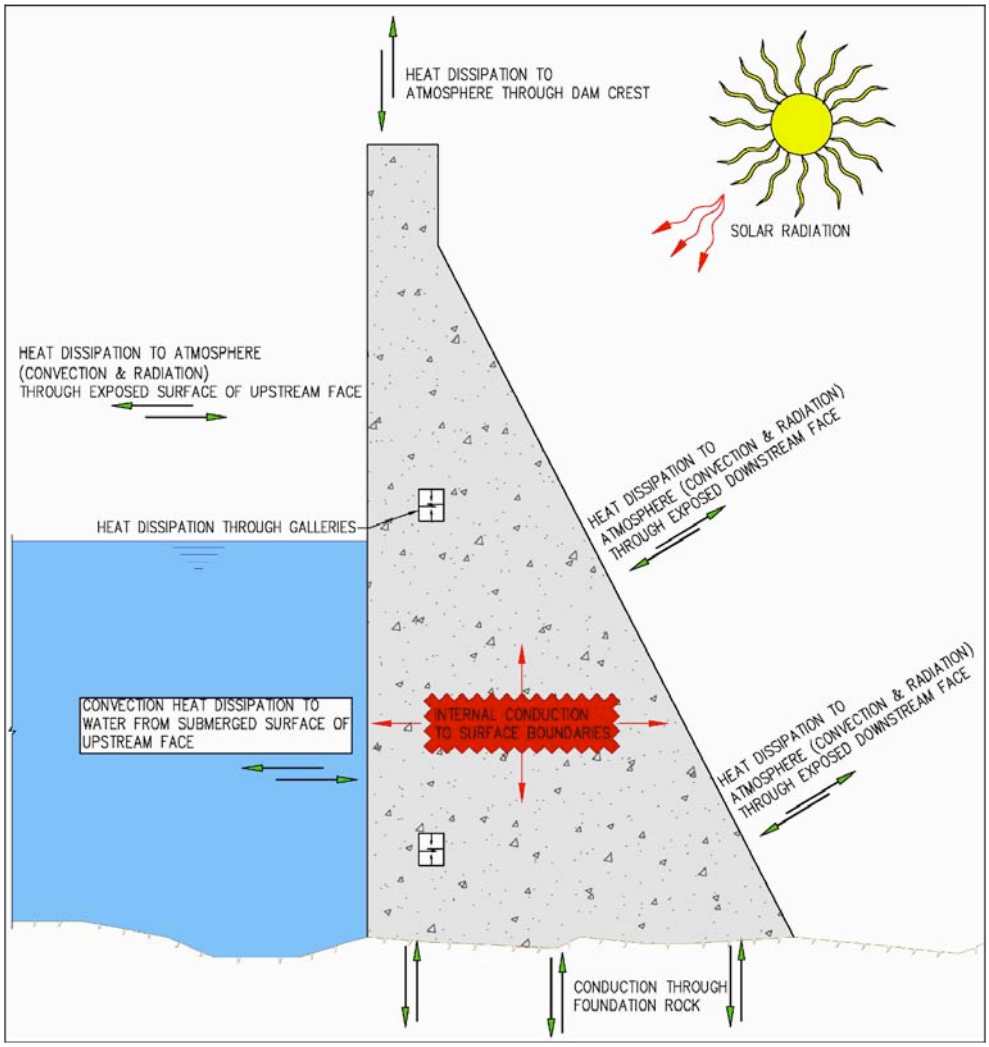

Figure 5.27: Long-Term Thermal Model Heat Inputs & Losses(16)

Relevant Analyses

For the purposes of this Thesis, only the analysis that can be compared with measured behaviour and observations to date is addressed and this accordingly deals with the first placement to elevation 111.375 m on the right flank (as illustrated on **Plate 5.5**).

The analysis addressed accordingly deals with the placement of RCC in the right side block from foundation level to elevations 111.375 mASL, which was undertaken between the beginning of December 2009 and 20th April 2010, with a break between 1st January and 2nd March while the RCC placement in this area was stopped at elevation 90.975 mASL. After exposure for a period of approximately 7 weeks, a crack was noticed in the surface at elevation 111.375 mASL and the primary objective of the analysis addressed is to provide an interpretation of this observation, considering the measured behaviour of this RCC, as indicated on the installed strain gauge.

For this evaluation, two scenarios of RCC behaviour were considered:

- **Scenario 1** assumes no creep in the core RCC.
- **Scenario 2** assumes creep of the order of 25 microns in the core RCC.

As mentioned elsewhere in this Thesis, the occurrence of creep as a consequence of internal restraint within the core of mass concrete is often considered as advantageous from the point of view of reducing the occurrence of surface cracking due to excessive thermal gradients. Correspondingly, an assumption of no creep in this situation would be considered conservative in enabling a review of the maximum possible surface tensile stresses that could develop as a result of temperature gradients.

Scenario 2 includes the effect of approximately 25 microns of creep by reducing the maximum core RCC temperature by 3°C, effectively limiting the total core thermal expansion as a result by 8.8 x 10^{-6} x 3°C = 26.4 microstrain.

5.6.5.3. Analysis Results

General

While extracts from the preliminary thermal analysis dealing with the joint spacing design and the arch design for Changuinola 1 Dam are presented in Chapter 7, only the results of the detailed thermal analysis relating to the surface gradient cracking evaluation of the first placement to elevation 111.375 m on the right flank are addressed in this Chapter.

Presentation of Results

The results of the surface gradient analysis undertaken are presented in **Figure 5.28** to **5.33** in the form of temperature and horizontal (upstream-downstream) stress distribution plots for the two creep scenarios at 31st May, 30th June and 31st July.

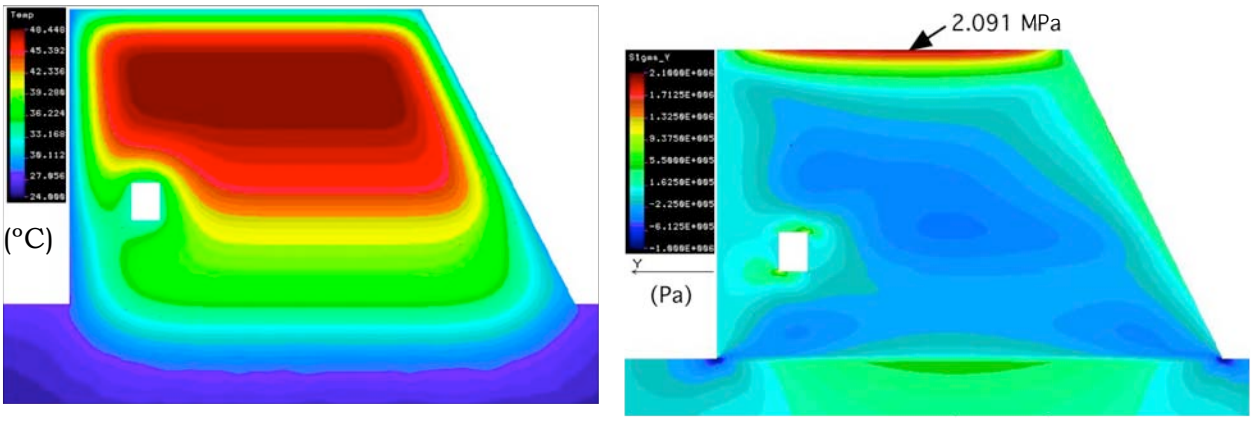

Figure 5.28: Temperature & Horizontal Stress Distributions 31 May 2010 – Scenario 1(17)

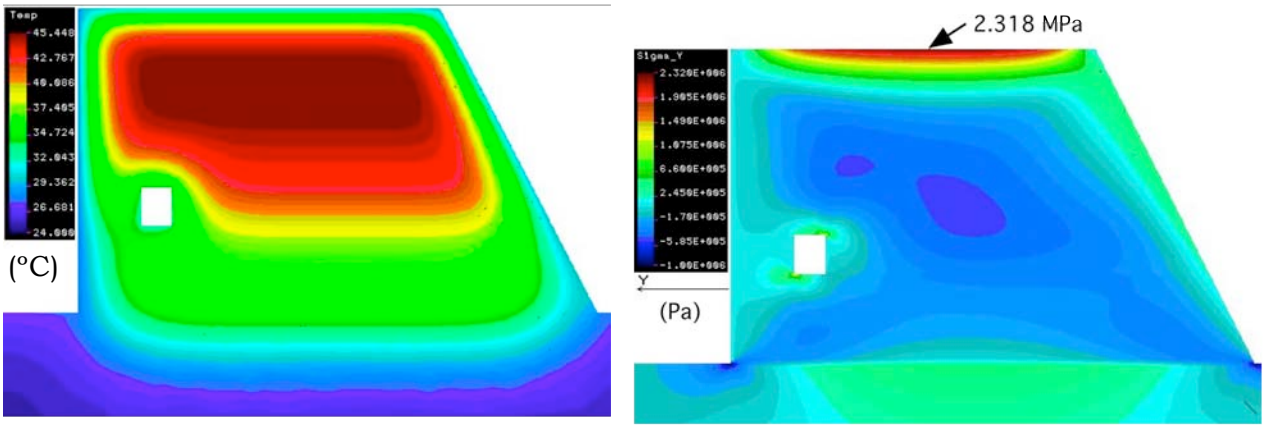

Figure 5.29: Temperature & Horizontal Stress Distributions 30 June 2010 – Scenario 1(17)

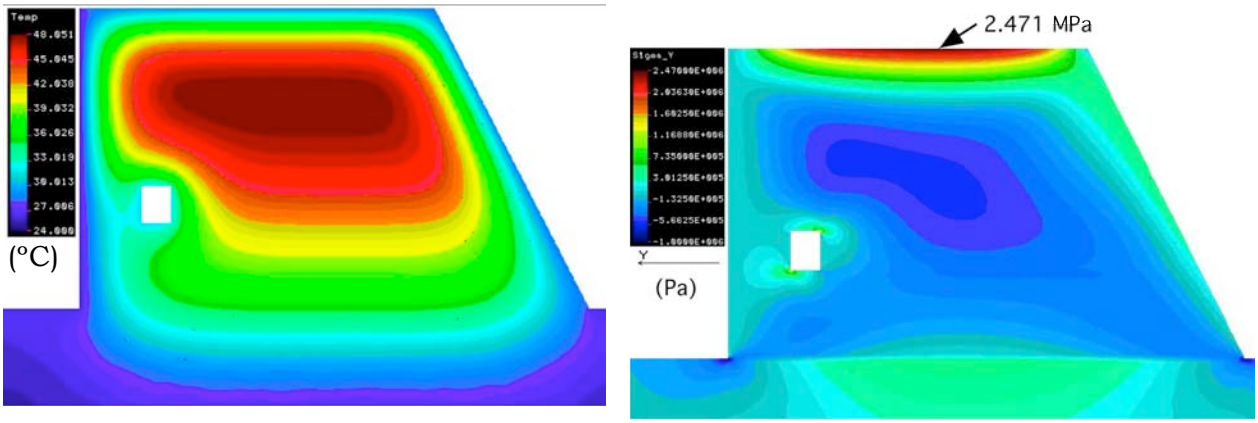

Figure 5.30: Temperature & Horizontal Stress Distributions 31 July 2010 – Scenario 1(17)

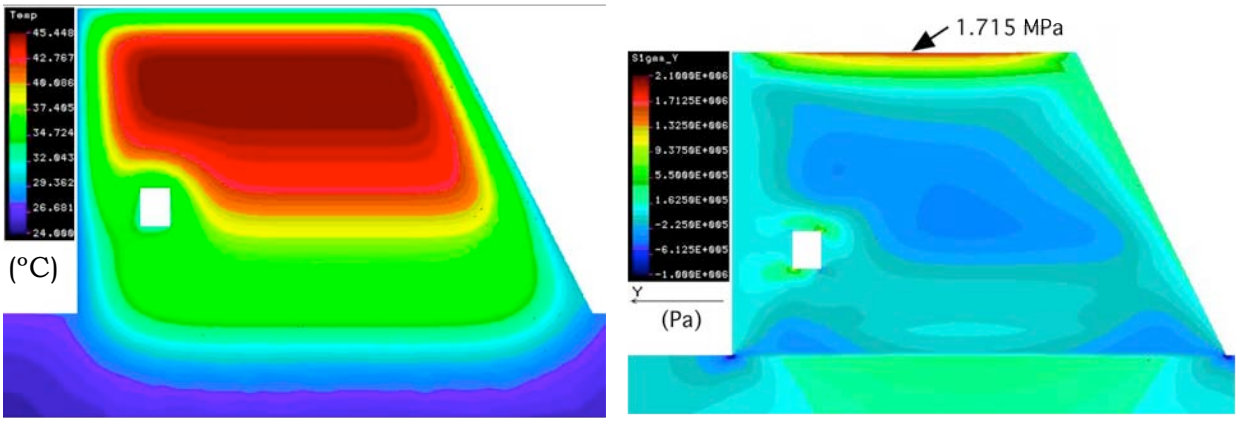

Figure 5.31: Temperature & Horizontal Stress Distributions 31 May 2010 – Scenario 2(17)

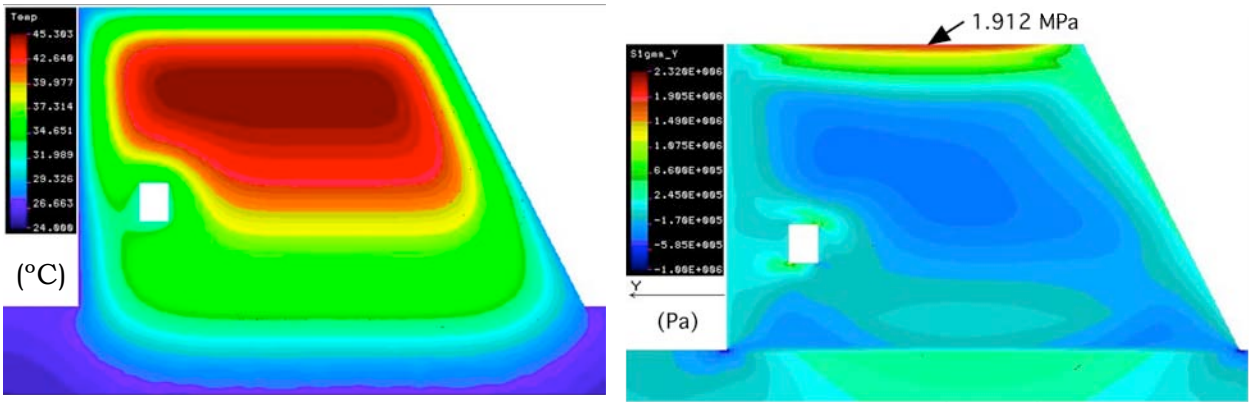

Figure 5.32: Temperature & Horizontal Stress Distributions 30 June 2010 – Scenario 2(17)

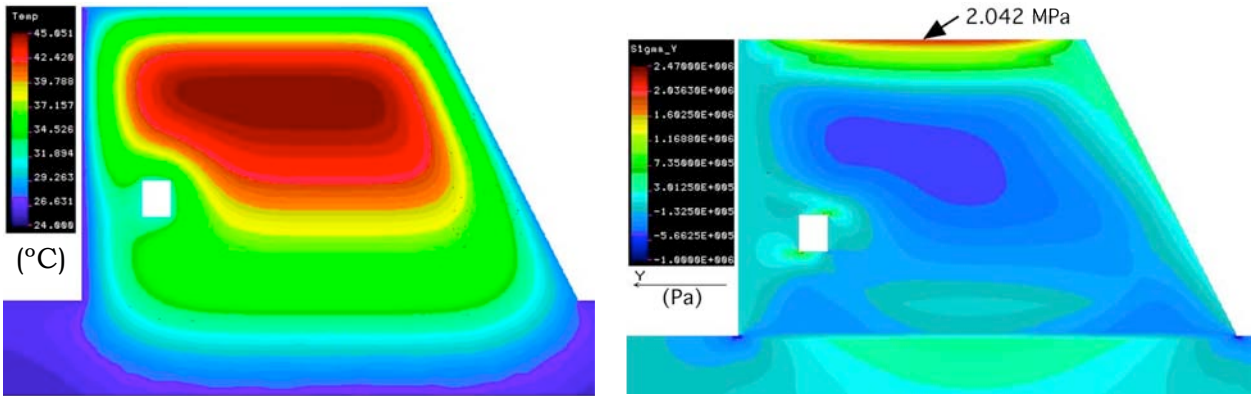

Figure 5.33: Temperature & Horizontal Stress Distributions 31 July 2010 – Scenario 2(17)

A summary of the critical maximum surface stresses indicated in the analysis is provide in **Table 5.13**.

Table 5.13: Summary of Tensile Stress Results

Scenario	**Maximum Surface Tensile Stress** (MPa)		
	31 May	30 June	31 July
Scenario 1	2.09	2.32	2.47
Scenario 2	1.72	1.91	2.04

Evaluating the above stresses in relation to the criteria established under 5.6.4.3, cracking could be anticipated under Scenario 1 by the end of May, while no cracking would be anticipated by the end of July for Scenario 2.

5.6.5.4. Conclusions

While the data from the strain gauge installed in the first RCC placement at Changuinola 1 Dam indicated unrestrained thermal expansion within the core, with no apparent reduction in expansion, or creep occurring as a consequence of internal restraint, the same effect is confirmed through the stress interpretation of the thermal analysis. The “no creep” Scenario 1 seems to closely replicate the observations made on the dam, while the introduction of just 25 microstrain of creep would appear to have been adequate to have prevented the evident crack from developing.

5.7. DISCUSSION

The analyses presented in this Chapter are considered to have produced some very interesting results. Certainly, it may not be realistic to conclude that high-paste RCC does not suffer from any shrinkage and creep, but this is a result of the typical level of accuracy with which the behaviour of a prototype dam can be analysed and the apparent unlikeliness of such a conclusion, rather than as a consequence of an inadequate strength of results. All of the analyses completed suggest the same pattern of behaviour for high quality, high-paste RCC in exhibiting negligible creep and/or shrinkage during the hydration heating and cooling cycle.

5.8. CONCLUSIONS

Although it may not be possible to simulate all of the actual displacements and joint openings measured with complete accuracy, the very significant difference between the displacements and joint openings measured compared with those that would have been anticipated if any significant creep and drying shrinkage had occurred leaves no ambiguity in the conclusions that must be drawn.

The analyses presented in this Chapter serve to confirm that the level of creep and shrinkage conventionally assumed for RCC, as discussed in Chapter 3, did not occur at Wolwedans Dam. This is consequently considered to answer one of the specific research questions posed and to correspondingly confirm that adopting the same design approach as has been traditionally applied for CVC in respect of the concrete volume reduction experienced during the hydration heating and cooling cycle is not necessarily valid for high-paste RCC.

5.9. A NEW UNDERSTANDING OF THE EARLY BEHAVIOUR OF RCC IN LARGE DAMS

5.9.1. DISCUSSING THE IMPACT OF A NEW UNDERSTANDING OF EARLY RCC BEHAVIOUR

On the basis of the analyses completed, it is would seem that a new design approach for joint spacings in RCC dams can, and should, be developed. The findings presented can readily be applied to establish the levels of residual stress within the body of an RCC dam wall for specific, selected induced joint spacings, thereby allowing the design of appropriate joint spacings.

The findings presented in this Chapter are considered of particular importance in relation to the design of RCC arch dams. While the findings suggest that lower temperature drop loadings than originally considered are in fact applicable, this can

present greater problems in respect to the grouting of induced joints on an RCC arch. If little, or no creep occurs during hydration heat development and dissipation, post-cooling of RCC performs no function other than limiting differential temperatures and potentially lowering the RCC temperature to facilitate joint grouting. Such an eventuality, however, also implies that a greater lowering of temperature is necessary before joint opening is initiated and any grouting becomes possible.

The analyses addressed are furthermore of particular relevance in respect of the susceptibility of large RCC dam structures to cracking parallel to the axis. In view of the fact that such cracking will occur as a consequence of long term temperature drop loads within the well insulated internal core zones of a dam wall, it is considered that the principle findings have an immediate and direct application in respect of this condition.

5.9.2. FURTHER DEVELOPING THE UNDERSTANDING OF EARLY RCC BEHAVIOUR

On the basis of the investigations and analyses completed, it is considered appropriate to attempt to develop an understanding of the reasons that RCC is apparently less susceptible to early shrinkage and creep than is the case for CVC. In Chapter 6, these issues are discussed and a new understanding of the early behaviour of RCC is proposed.

5.10. REFERENCES

[1] Shaw QHW, Geringer JJ & Hollingworth F. *Mossel Bay (Wolwedans Dam) Government Water Scheme. Wolwedans Dam Completion Report*. DWAF Report No. K200/02/DE01. April 1993.

[2] Shaw QHW. *An Investigation into the Thermal Behaviour of RCC in Large Dams.* Proceedings. 5th International Symposium on Roller Compacted Concrete Dams. Guiyang, China. 2007

[3] Oosthuizen C. *Behaviour of Roller Compacted Concrete in Arch/Gravity Dams.* Proceedings. International Workshop on Dam Safety Evaluation. Grindelwald, Switzerland. April 1993.

[4] Oosthuizen C. *The Use of Field Instrumentation as an Aid to Determine the Behaviour of Roller Compacted Concrete in an Arch/Gravity Dam.* Proceedings. 3rd International Symposium on Field Instruments in Geomechanics. Oslo, Norway. September 1991.

[5] Oosthuizen C. *Performance of Roller Compacted Concrete in Arch/Gravity Dams.* Proceedings. 2nd International Symposium on Roller Compacted Concrete Dams. Santander, Spain. 1995.

[6] Hattingh LC, Heinz WF & Oosthuizen C. *Joint Grouting of a RCC Arch/Gravity Dam: Practical Aspects.* Proceedings. 2nd International Symposium on Roller Compacted Concrete Dams. Santander, Spain. pp 1037–1051. 1995.

[7] Precise Engineering Surveys. Department of Water Affairs. *Instrumentation Data for Wolwedans Dam. 1990 to 2008.* August 2008.

[8] Structural Research and Analysis Corporation (SRAC). *COSMOSM Finite Element Analysis Program.* General-purpose, modular FE Analysis system. SRAC, a division of SolidWorks Corporation, Dassault Systemes S.A., Paris, France.

[9] United States Army Corps of Engineers. *Time History Dynamic Analysis of Concrete Hydraulic Structures.* Engineering Manual, EM 1110-2-6051. USACE. Washington. December 2003.

[10] Owens, G. *Fulton's Concrete Technology.* Chapter 8. Ninth Edition. Cement & Concrete Institute. Midrand. RSA. 2009.

[11] United States Army Corps of Engineers. *Arch Dam Design.* Engineering Manual, EM 1110-2-2201. USACE. Washington. May 2004.

[12] United States Army Corps of Engineers. *Thermal Studies of Mass Concrete Structures.* Engineering Technical Letter, ETL 1110-2-542. USACE. Washington. May 1997.

[13] Shaw QHW. *The Role of Temperature in Relation to the Structural Behaviour of Continuously Constructed Roller Compacted Concrete and Rubble Masonry Concrete Arch Dams.* MSc Thesis, University of Brighton. UK. 2001.

[14] Hattingh LC. *Completion Report for the Crack Joint Grouting. Wolwednas Dam.* Mossel Bay Government water Scheme. Internal Department of Water Affairs & Forestry. Report No. K200-02-DD05. November 1994.

[15] Hattingh LC, Heinz WF & Oosthuizen C. *Joint Grouting of a RCC Arch/Gravity Dam: Practical Aspects.* 2nd International Symposium on Roller Compacted Concrete Dams. Santander, Spain. pp 1037-1051. 1995.

[16] Cai Q, Kotsiovos M & Durieux JH. *3-D Structural Analysis of Wolwedans Dam.* Internal Report No. K200/02/DK03. Sub-Directorate Structural Studies. Directorate Design Services. Department of Water Affairs & Forestry. Pretoria. February 1997.

[17] Greyling, RG & Shaw QHW. *Changuinola 1 Dam. Thermal Analysis Report.* Report No. 4178/11436-R1. MD&A. July 2010.

[18] Dunstan, MRH. *Changuinola 1 Dam. Review of the In-situ Properties of Full-Scale Trial 1B.* Report No. Chan1/461/090923. MD&A. September 2009.

[19] Neville, AM. *Properties of Concrete.* Chapter 9. Fourth Edition. Pearson Prentice Hall. London. 2002.

[20] United States Army Corps of Engineers. *Seismic Design Provisions for Roller Compacted Concrete Dams.* Engineering Pamphlet, EP 1110-2-12. USACE. Washington. September 1995.

CHAPTER 6

6. DEVELOPING A NEW UNDERSTANDING OF THE EARLY BEHAVIOUR OF RCC IN LARGE DAMS

6.1. INTRODUCTION

On the basis of the reviews, evaluations and analyses presented in earlier chapters, it is clear that the traditional assumptions in respect of the early behaviour of high-paste RCC in large dams are not generally valid. In this Chapter, the origins of the apparent reduced shrinkage and creep experienced in high-paste RCC, compared to CVC, are explored, reasoned and motivated.

Plate 6.1: Wadi Dayqah Dam, Quriyat, Oman – August 2009

6.2. THE FINDINGS OF THE INVESTIGATIONS AND ANALYSES

6.2.1. DEFINITIVE FINDINGS

The structural modelling completed as part of the investigations addressed herein suggested that the RCC of Wolwedans Dam could not have been impacted by any significant shrinkage or creep during the hydration heating and cooling cycle. There can be no doubt that should the level of shrinkage and creep conventionally assumed for dam design have in fact occurred, very different structural behaviour to that recorded on the installed instrumentation would have been evident.

The measured un-restrained thermal expansion of the RCC in the core zones of both Çine Dam and Changuinola 1 Dam is considered extremely significant and strongly indicative of the mechanisms that cause RCC to be more creep-resilient than CVC. In mass concrete (CVC) in the core of a dam structure, it would typically be assumed that internal restraint would cause most of the theoretical thermal expansion due to the hydration temperature rise to be lost to creep in the immature concrete. The fact that the thermal analysis of an observed crack in the RCC at Changuinola 1 Dam demonstrated that no significant creep could have occurred is considered to further increase the confidence levels in the observed linear thermal expansion.

While the instrumentation data indicated that some creep or shrinkage undoubtedly did occur in the RCC at Wadi Dayqah Dam, this was a lean mix RCC containing a high quantity of non-cementitious fines and lower quality coarse aggregates. Considering the analyses presented, the instrumentation data evaluated and information available from earlier publications, it would seem that the reduced shrinkage/creep behaviour very specifically relates to higher strength, high quality, high-paste RCC.

On the basis of the above, it can be stated with confidence that it is no longer necessary to assume in dam design that a high-paste RCC acts in the same manner as CVC in respect of the development of shrinkage and creep during the hydration cycle.

6.2.2. REMAINING QUESTIONS & DISCUSSION

Realistically, it will never be possible to model the behaviour of a large prototype dam structure with complete accuracy. Too many indeterminate factors can influence the final behaviour and consequently, although the analysis results for Wolwedans Dam suggest no creep, or shrinkage occurred during the hydration heating and cooling cycle, an appropriate conclusion would be that the impacts of creep and/or shrinkage were negligible.

As concrete, by its nature, is inherently susceptible to autogenous shrinkage and creep, such a conclusion can be considered surprising and it is necessary to advance a meaningful hypothesis on which basis the mechanism that causes the related behaviour of RCC to be so different from that of CVC can be meaningfully proposed. In addition, it must be remembered that Wolwedans Dam is an arch structure and the measured displacements relate specifically to the structural behaviour of the arch and

particularly the upper part of the structure. Consequently, it would be of value to investigate the actual stress condition is this upper section of the arch whilst the dam temperature was elevated by the hydration heat.

6.3. SIMPLIFIED ANALYSIS OF WOLWEDANS BEHAVIOUR UNDER HYDRATION TEMPERATURE RISE

6.3.1. GENERAL

As mentioned in Chapter 5, most of the structural arch action in Wolwedans Dam is carried within the upper 20 m in the centre of the dam. Consequently, it is in this particular area that the specific early behaviour of the RCC is most relevant and accordingly, it is considered of value to review the associated stresses and strains that would be developed there due to the hydration temperature rise.

6.3.2. MODELLING

To construct a true, three-dimensional model of the actual conditions experienced within the dam structure immediately after construction completion would be extremely complicated and it would never be possible to assure a high degree of accuracy. In the case of an RCC dam, as any particular part of the dam structure is being placed, the temperature of the part beneath that is one week old is approaching its peak hydration temperature. Consequently, RCC at any point is generally placed on top of other RCC that has been effectively swollen by thermal expansion, assuming that restrained expansion stresses are not dissipated in creep. While this will develop consequential internal stress mechanisms of indeterminate impact, it also implies that any related modelling cannot realistically be anything more than indicative.

6.3.3. ANALYSIS

With the above in mind, the hydration temperature rises measured within the Wolwedans Dam[1] wall were applied in a simplified and simplistic manner to a Finite Element model. Acknowledging that the model will tend to overstate the reality as the temperature rises are applied to the final structure instantaneously, the resultant stresses and displacements can only be evaluated on a qualitative basis.

Figure 6.1 indicates the distribution of the temperature rises that was applied in conjunction with a coefficient of thermal expansion of 10 x 10^{-6}/°C and an E modulus of 20 GPa.

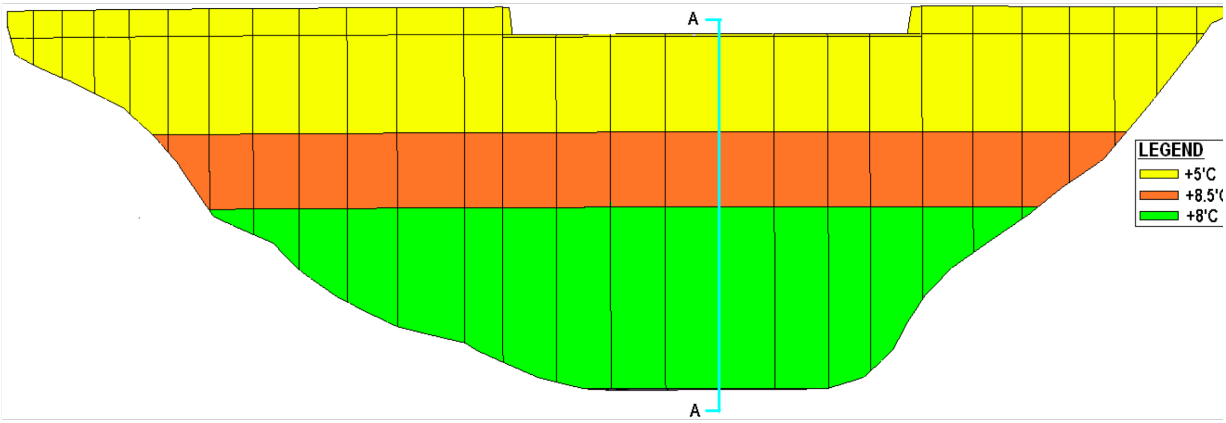

Figure 6.1: Simplified Hydration Temperature Rise Inputs

6.3.4. ANALYSIS RESULTS

Figures 6.2 to **6.5** present the resultant displacements and the arch (lateral - abutment to abutment) stresses on the crown cantilever (Section A-A) for the above temperature rises, with and without the inclusion of gravity. Compression stresses are indicated as -ve.

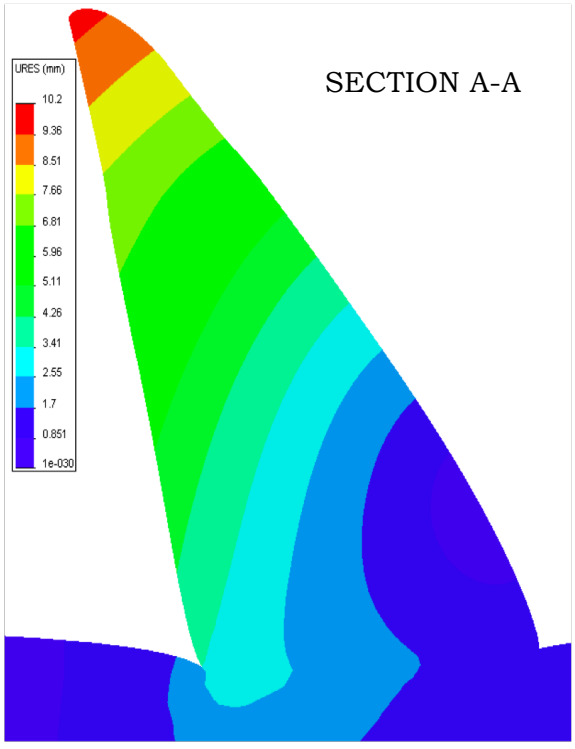

Figure 6.2: Deformation – Temperature Rise + Gravity

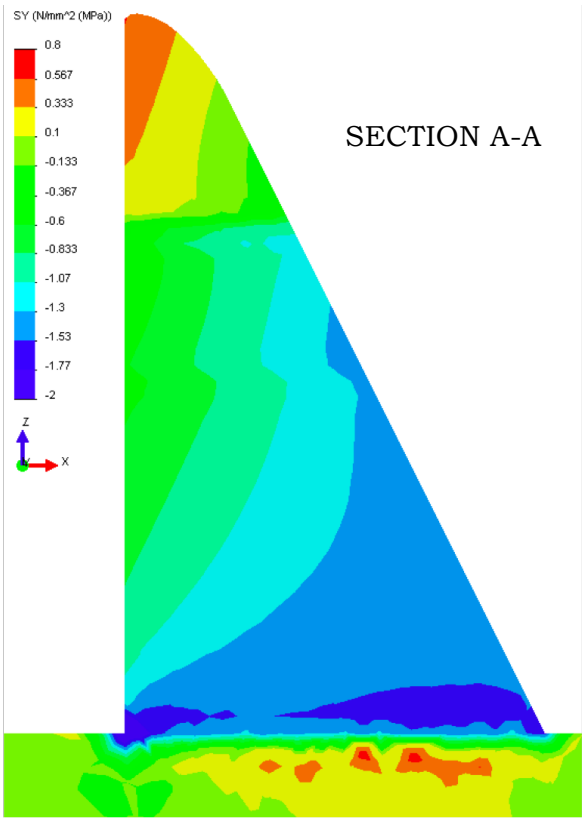

Figure 6.3: Arch Stress – Temp. Rise + Gravity

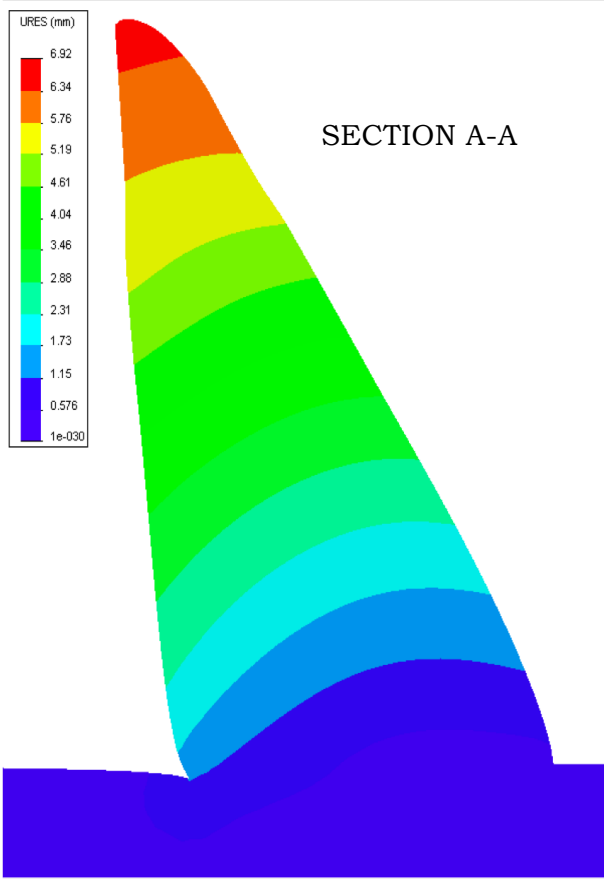

Figure 6.4: Deformation – Temperature Rise (No Gravity)

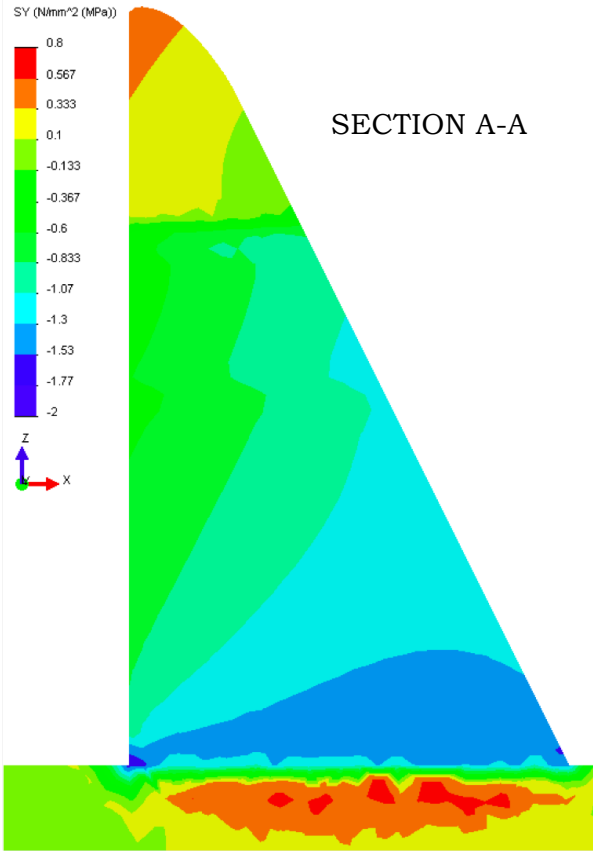

Figure 6.5: Arch Stress – Temp. Rise (No Gravity)

6.3.5. RESULT INTERPRETATION

The analysis results indicate that thermal expansion causes the crest of the dam structure to displace upstream. With gravity load, the upstream displacement increases. Reviewing the arch (lateral) stresses, it can be seen that the thermal expansion and upstream gravity movement cause tensile stresses to develop in the top 20 m of the dam structure in the centre, increasing towards the upstream face. At mid-height, the level of the instrumentation at which the joint openings were referenced for the analyses in Chapter 5, lateral compressions vary from approximately 350 kPa at the upstream face to approximately 1 MPa at the downstream face.

For a contained thermal expansion associated with a temperature rise of approximately 8°C, a coefficient of thermal expansion of 10×10^{-6}/°C and an E modulus of 20 GPa, a direct lateral compression of 1.6 MPa could be anticipated. On the stress plots, such high lateral compressions are only indicated close to the base of the dam.

It can accordingly be seen that the evident upstream movement of the crest effectively increases the radius of curvature of the arch with height, causing increasing tension in the direction of the arch (laterally) to be experienced with increasing height and distance from the downstream face. This would imply that the RCC in the crest of the

dam structure would have been able to expand in an unconstrained manner when subject to the hydration temperature rise.

6.3.6. RESULT IMPLICATIONS

The indicated behaviour will have effectively given rise to low, or no lateral containment stresses in the RCC placed in the upper section of the dam structure at Wolwedans. With strain gauges in this type of RCC indicating no measurable creep due to internal restraint under thermal expansion, even on very large RCC sections, it is accordingly not surprising that none would then have been incurred in the relatively thin section of the crest at Wolwedans Dam. With no lateral containment stress, it would seem very likely that completely unrestrained thermal expansion consequently occurred and without stress, no stress-relaxation creep can occur.

At mid-height, some compression/containment stresses are evident, although on average probably less than half the value that might have been anticipated for full containment. In view of the fact that no quantifiable creep/shrinkage could be determined through the evaluation of the joint openings at this level, it would appear that the indicated stress levels remain too low to incur any significant creep.

6.3.7. DISCUSSION & CONCLUSIONS

While the analysis completed is simplistic in nature, the impacts of the arch geometry, gravity forces and thermal expansion in effectively opening up the crest of the arch at Wolwedans is clear. While this effect could go some way in explaining the lack of measurable creep in the RCC in the important structural areas of Wolwedans Dam, particularly when considering the evident ability of high-paste RCC to expand relatively freely under a temperature rise, the RCC similarly does not seem to have suffered creep under compressive stress levels of up to 1 MPa.

Due to the simplifications made in the model and analysis presented, it is considered that the beneficial, stress reduction effect demonstrated is overestimated, although not by a particularly significant margin. The arch geometry, gravity and the overall swelling caused by thermal expansion will, however, undoubtedly have contributed to a reduction in the containment stresses in the direction of the arch curvature in Wolwedans Dam, as it will in any RCC arch dam, and this can only be seen as beneficial in reducing the risks and/or magnitude of creep in RCC during the hydration heating cycle.

It is further considered that the indicated effect is likely to be more pronounced in RCC than CVC due to the former's increased resilience to creep under thermal expansion, as demonstrated at Çine and Changuinola. In CVC, creep under internal restraint during the hydration temperature rise will limit the extent of the thermal expansion that serves to reduce constraining stress in the arch towards the crest.

6.4. RCC BEHAVIOUR MECHANISMS

6.4.1. LITERATURE & INVESTIGATIONS

Discussing the typical influences listed in published literature, it is clear that the materials composition and the compaction process applied for high-paste RCC gives rise to perhaps the most ideal conditions possible in a concrete for minimising shrinkage and creep. Furthermore, the fact that the reduced creep behaviour of an RCC with aggregate particle-to-particle contact has been previously recognised[2] confirms the fact that roller compaction can develop such a structure in an RCC mix.

The evident unrestrained expansion measured under a temperature rise at both Çine and Changuinola 1 dams provides evidence that the early behaviour of high-paste RCC would seem to be determined much more significantly by its aggregate skeletal structure and aggregate-to-aggregate particle contact than its paste content, as is the case for CVC.

6.4.2. AGGREGATE SKELETAL STRUCTURE

It is considered that the method of compaction is a factor in decreasing the susceptibility of RCC to shrinkage and creep. The skeletal structure of the aggregates in concrete acts to restrain the shrinkage of the paste during hydration and the compaction energy exerted on RCC undoubtedly ensures that this skeletal structure is better developed, with significant inter-aggregate particle contact.

In an over-pasted RCC, with a low modified Vebe time, the roller compaction squeezes the aggregates together, lubricated by the paste. With the kneading action and energy of the roller, the aggregate particles re-orientate and displace paste until full inter-particle contact is created and the minimum void ratio of the particular blend of aggregates used is achieved, with all voids filled with paste and the excess paste displaced onto the top surface.

Plates 6.1, **6.2** and **6.3** compare typical mass concrete cores from dams with a core from a typical modern high-paste RCC.

The higher coarse aggregate content in the RCC is very evident, as is the better particle shaping and the continuity of the aggregate grading. The significantly better developed aggregate skeletal structure in the RCC compared to the CVC can also be readily discerned.

Plate 6.1: Typical Low Grade Dam Mass Concrete (1950s)

Plate 6.2: Typical Modern Dam Mass Concrete

Plate 6.3: Typical Modern High-Paste RCC

Essentially, in a concrete with a structure made up of aggregate-to-aggregate contact, compacted together tightly, autogenous shrinkage of the in-filling paste will be of substantially less impact than for a concrete in which loose aggregates are effectively suspended in a medium of paste. In the former case, while the paste shrinkage will be reduced by the restraining action of the surrounding skeletal structure, the skeletal aggregate structure itself will further resist the consequential tendency for the concrete to shrink due to the fact that it is already at its minimum void ratio. Accordingly, while the paste can shrink within the spaces between the aggregates, these spaces cannot reduce in size without movement, or collapse of the skeletal

structure. In the case of aggregate suspended in a medium of paste, paste shrinkage and any subsequent moisture loss will result in significantly more direct shrinkage of the concrete.

Where paste shrinkage does not result in a fully equivalent shrinkage of the concrete, some internal micro-cracking must be incurred. This, in turn implies that voids have been developed within the concrete, which will increase its susceptibility to creep under compressive loading. Similarly, any subsequent loss of moisture will give rise to voids and an increased susceptibility to creep under compression. A well-developed and fully compacted aggregate skeletal structure will again serve to reduce the susceptibility to creep under low levels of compressive stress, as the majority of micro-cracking will occur inside the in-filled voids of the aggregate skeletal structure and a greater amount of strength will accordingly be maintained within the structure itself.

A comparison can be made between RCC and Rubble Masonry Concrete, which seemingly never exhibits cracking in dams. This material is formed by the insertion of large rock plums into a medium of mortar. Again the rock structure seems to predominate, with all shrinkage occurring in the form of micro-cracking within the mortar. During paste and mortar shrinkage, the overall volume of the matrix is maintained by the structure of the interlocking large rock particles.

The above discussion and the associated differences between RCC and CVC are illustrated in **Figures 6.6** and **6.7**.

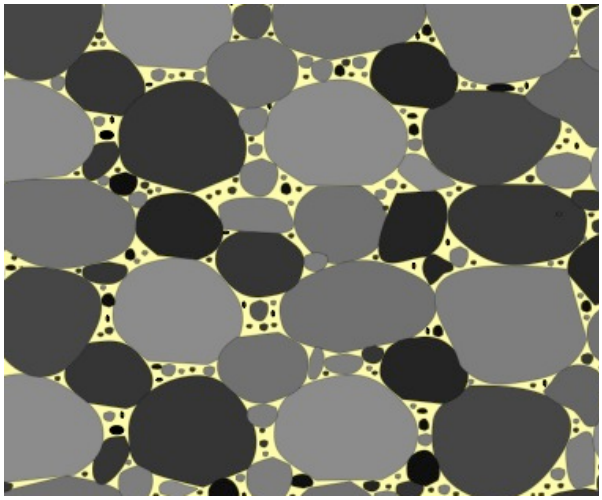

Figure 6.6: RCC Aggregate Skeletal Structure

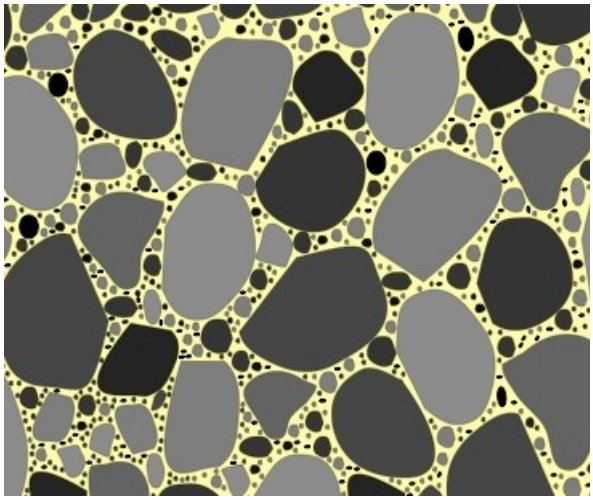

Figure 6.7: CVC Aggregate Skeletal Structure

With the process of compaction of a modern, mobile, high pozzolan content RCC involving expelling of the air and paste from the internal structure until the aggregates achieve their minimum void ratio, the resultant concrete is a structure of aggregates, with the voids filled with paste. In the case of CVC, the paste must provide a more liquid medium through which to move the aggregates and to lubricate their motion

with substantially less energy. An immersion vibrator-compacted concrete is consequently more a structure of paste containing aggregate particles.

In a constrained condition the aggregate skeletal structure in high-paste RCC will be maintained in its closed, tightly compacted state, implying a certain ability to carry load even without any paste strength and a significant resistance to a reduction in volume, which would be maintained despite internal shrinkage of the paste. When expanded by temperature in an un-constrained state, the tightly bound and inter-locked aggregate skeletal structure may even result in exaggerated expansion. Should this occur, a certain amount of aggregate point-to-point contact would be developed. With time, some crushing/collapsing of these aggregate points may well occur, resulting in a gradual relaxation (creep) of the expansion.

It is considered likely that fly ash in an RCC mix adds significant benefits, through increasing the mobility of the paste and slowing the rate of moisture loss by reducing permeability. Despite the fact that modern, high pozzolan content RCC takes on a spongy appearance once all the air is removed and full compaction is achieved, experience has repeatedly demonstrated that this RCC remains exceptionally resilient to shrinkage and creep. In view of the fact that fly ash has been demonstrated to reduce creep in concrete[3], it is considered likely that the autogenous shrinkage of cementitious paste is reduced when fly ash is used in relatively large proportions.

6.4.3. SUMMARY

On the basis of the preceding review, it is quite clear that the best performance from RCC, in respect of least shrinkage and creep during the hydration cycle, can be anticipated in a high-paste, low water content mix, with well-graded, high quality aggregates and particularly sand with a relatively low compacted void ratio.

6.5. A NEW UNDERSTANDING OF THE EARLY BEHAVIOUR OF RCC IN DAMS

6.5.1. DISCUSSION

The investigations and analyses completed as part of the studies addressed in earlier chapters have demonstrated that a high-paste, high strength RCC mix in an arch structure need not exhibit any significant levels of shrinkage, or creep during the hydration cycle. Lower strength and lean RCCs and mixes with less than ideal materials, however, remain likely to exhibit shrinkage and creep and a correspondingly increased susceptibility to creep under stress. Particularly low strength RCC mixes and those designed for a high deformability can actually demonstrate very high levels of creep under load[4].

It is, however, high quality, high-paste RCC that is of greatest interest as part of this Thesis, the type of RCC that would be used for the construction of a significant arch dam. In this regard, it is significant to note that the typical mix proportions, the improved aggregate specifications, the mobility of the mix under compaction, the aggregate skeletal structure developed and the continuity of construction associated with high-workability RCC create possibly the ideal circumstances for the minimisation of creep during the hydration cycle. Constructing a dam structure on a curve and thereby reducing the constraining stresses in the crest is also considered beneficial in reducing the likelihood of creep. The thinner and more flexible the arch, the lower the associated constraining stresses.

The strain gauge (SGA gauges) data recorded at Çine Dam and Changuinola 1 Dam are considered of particular importance. The apparent linear thermal expansion evident in a location that would be assumed to be subject to significant internal restraint is considered to provide evidence of a behaviour that is dominated by aggregate-to-aggregate particle contact. The fact that such linear expansion occurs in RCC at such an early age provides further evidence of an inherent early resistance to creep and the likelihood of increased creep resistance in the mature concrete.

As a result of the fact that early shrinkage and creep in concrete are interdependent effects that occur simultaneously during the process of maturation, a realistic separation of the two is not practically possible. Furthermore, the early development of internal shrinkage obviously creates a susceptibility to creep under load. With drying shrinkage in the core of a mass concrete block generally agreed as being negligible[5], unless related to a specific problem in the aggregates, the important shrinkage is autogenous shrinkage. While the terms shrinkage and creep are used together in this Thesis, the dominant effect is undoubtedly manifested as creep; a stress relaxation that occurs when the temperature rise associated with the hydration process attempts to cause thermal expansion in immature concrete.

6.5.2. DEFINITION OF RCC SHRINKAGE AND CREEP BEHAVIOUR

On the basis of the findings of these studies, it is clear that high-paste RCC indicates less shrinkage and creep than an equivalent CVC during the hydration and cooling cycle. Certainly, the conventionally accepted combined shrinkage and creep values varying between 125 and 200 microstrain are not evident in such an RCC.

For a high-paste, high pozzolan content RCC mix, with well-graded, high quality aggregates in an arch dam, it is undoubtedly possible to produce an RCC with negligible shrinkage and creep.

In view of the fact that the shrinkage/creep characteristics of any RCC will always be dependent on the nature, gradings and the effective compaction of its constituent materials, it is considered essential to treat each set of circumstances on a case-specific basis. If a low shrinkage/creep RCC is important to the dam design, as would

be in the case of an arch, specific efforts should be invested in materials testing and the construction and instrumentation of a full scale RCC trial. In such circumstances, all aggregate sizes should undergo absorption and shrinkage testing.

For the preliminary design of a gravity dam constructed with a high quality, high-paste RCC, it is considered appropriate to assume a total shrinkage and creep of approximately 50 microstrain.

In the case of an RCC arch, or arch/gravity dam, it would generally be appropriate to design the RCC mix for minimum shrinkage and creep, which would require high quality aggregates and a mix comprising approximately 200 kg/m^3 cementitious materials, of which approximately 70% would be a high quality fly ash. In such a situation, however, it is considered appropriately conservative at this stage to assume a total shrinkage/creep of the order of 20 microstrain for preliminary design, but verification testing would be required before a definitive reliance could finally be placed on such performance.

In the design analyses for an RCC arch/arch gravity dam, it is considered important to include some form of an evaluation of the anticipated construction behaviour and the associated stresses in the critical parts of the structure.

As the findings of the investigations described herein gain broad exposure and become generally accepted, more dams will be appropriately instrumented, more information will be reported and a significantly greater database of RCC shrinkage and creep behaviour will be developed. With the confidence that a broader base of information will provide, it may eventually be possible to design RCC for negligible shrinkage and creep with complete certainty. However, until that time, it considered appropriate that some degree of conservatism be retained.

Significant attention should be given to the composition and structure of RCC mixes and the findings of this study are not considered to be applicable in the case of lower quality aggregates, with a tendency for drying shrinkage.

6.5.3. NECESSARY TESTING

The SGA strain gauges at Çine Dam and the first strain gauge installed in Changuinola 1 Dam demonstrated that it is in fact possible to predict over a relatively short period, the typical creep behaviour under thermal expansion that might be anticipated for a particular RCC mix. It is consequently recommended for all significant RCC dams, where the early thermal behaviour is of importance, that strain gauges be installed in the full scale RCC trial embankments, such that a record of temperature and strain can be developed and any plastic behaviour can be observed and measured. This monitoring should be preceded by aggregate and mortar laboratory testing to ensure that the characteristics of the constituent materials are well known by the time a full-scale trial is constructed.

6.5.4. SUMMARY

As a consequence of a substantially better developed aggregate skeletal structure, high-paste RCC indicates less shrinkage and creep during the hydration heating and cooling cycle than an equivalent CVC. With a high-paste mix and good quality materials and within the context of a reasonably flexible arch dam in a relatively temperate climatic environment, it is further possible to substantially eliminate the effects of shrinkage and creep in RCC. With lower quality materials, low paste mixes and mixes with high moisture contents, shrinkage and creep should be anticipated. Generic rules in respect of creep and shrinkage that were developed for CVC, however, should not be assumed to be applicable for RCC.

6.6. RCC MIX REQUIREMENTS FOR IMPROVED EARLY BEHAVIOUR

6.6.1. INTRODUCTION

It is clear from the various references, investigations and discussion that there is a specific composition and type of RCC that indicates increased resilience to creep and shrinkage. All of the examples quoted where the associated behaviour has demonstrated negligible shrinkage and creep have been what is defined as “high-paste” RCC and all of the testing in published literature that relates to high creep relates to a “lean” RCC. With “high-paste” RCC defined as a mix with a cementitious materials content exceeding 150 kg/m^3 and “lean” RCC defined as a mix with less than 100 kg/m^3 cementitious materials, two additional factors common to the RCCs that have demonstrated low creep/shrinkage performance are high fly ash contents and total cementitious materials contents approaching, or exceeding 200 kg/m^3.

With particular reference to the author’s experience and knowledge of RCC mixes, the key attributes that will indicate a greater resilience to creep are discussed in the subsequent text.

6.6.2. KEY ISSUES

The key issues in respect of increasing the resilience of an RCC mix to creep can be summarised as follows:

- Developing a strong aggregate skeletal structure with aggregate-to-aggregate contact.
- Providing sufficient paste to ensure that the process of compaction is well lubricated and that a strong aggregate skeletal structure can be formed, with all surplus paste squeezed up to the placement surface.
- Only high quality aggregates are used.
- The content of non-cementitious fines does not become excessive (< 100 kg/m^3).
- Included non-cementitious fines are non-plastic.

- Autogenous shrinkage of the paste is minimised.

It is becoming common practice in high-workability RCC to apply specifications for the aggregates that are stricter than generally applied for CVC and this is seen as particularly beneficial in respect of ensuring a well developed skeletal structure. While continuous aggregate gradings have generally been applied for RCC, maximum aggregate particle flakiness and elongation, for all sizes, is typically now specified as 25% (tested in accordance with BS812 Part 105), as opposed to an earlier typical maximum of 35%. Furthermore, a maximum compacted bulk density (CBD) void ratio of 32% is applied for the fine aggregate fraction, although it is quite common to aim for 27 to 28%.

6.6.3. RCC COMPOSITION

High-paste RCC is designed on a volumetric basis and it is generally considered that the best performance under compaction is achieved when the nominal paste/mortar ratio exceeds the void content of the sand by approximately 12%. In this manner, effective lubrication to the compaction process is provided. For a sand CBD void content of 30%, a paste/mortar ratio of 42% would accordingly be applied for best performance.

As indicated in Chapter 2 for each of the dams investigated, the paste content in high-paste RCC is usually approximately 200 litres/m^3 (excluding aggregate fines), with aggregates comprising 800 litres/m^3. Modern mixes indicate a maximum aggregate size of approximately 40 mm, to limit segregation, and the fine aggregate content usually represents between 35 and 40% of the total aggregate content. Water contents will obviously depend on the nature of the aggregates, but the main purpose of the tighter aggregate specifications is to limit the water content required to achieve a workability equivalent to a modified Vebe (19.1 kg surplus mass) time of around 8 seconds. Typically, high-paste RCC water contents are between 100 and 125 litres/m^3.

While the dam structure design and the construction programme will play a role in determining the containment stresses incurred in the key structural zones during the period that the structure is heated by hydration, the total hydration heat evolved will also play a role in determining the levels of containment stress developed. Although the high-paste RCC described may exhibit a particularly significant resilience to creep, the likelihood and degree of creep that might be experienced will increase with the intensity of the containment stresses and accordingly, a low heat cement would be advantageous, in tandem with a mix design approach seeking to minimise the heat of hydration.

It is considered that the ideal RCC, in respect of developing resilience to creep, would indicate the following composition:

Constituents	Portland Cement	Fly Ash	Water	Coarse Aggregate	Fine Aggregate	Retarder
By Mass (kg/m³)	62	143	115	1400	800	3.4
By Volume (litres/m³)	20	62	115	500	300	3
Net Paste (l/m³)	Fines (l/m³)	Aggregate (l/m³)	Paste/ Mortar	Sand/ Aggregate		
200	30	800	0.40	0.375		

6.6.4. TESTING REQUIREMENTS & RCC MIX DEVELOPMENT

While it is considered of absolute importance to test the characteristics of RCC mixes on a project-specific basis, the technical feasibility of an RCC arch dam may depend on the availability of high quality cementitious and aggregate materials. It is not uncommon to import cementitious materials for large RCC dams, the cement and fly ash used for Changuinola 1 Dam in Panama for example are imported in bulk by ship from Tampa Bay, Florida in the USA. During the dam type selection study for a particular project, an economic comparison should be made of the various possible dam types and this will include reference to available materials and the costs of sourcing high quality materials for an arch dam would be compared with other dam type options with lesser concrete performance requirements.

However, with the number of variables that impact concrete mix design, it is not considered appropriate at this stage to be able to propose a “negligible-creep” RCC without appropriate site-specific materials testing, which should include the construction and instrumentation of a large-scale RCC placement trial.

With a new understanding of the early behaviour of high-paste RCC in large dams, it was considered necessary to evaluate and to illustrate the impact of the new model on the design of large dams. Chapter 7 is consequently dedicated to exploring, through example, the influence of the new RCC materials understanding on future dam design.

6.7. REFERENCES

[1] Precise Engineering Surveys. Department of Water Affairs. *Instrumentation Data for Wolwedans Dam. 1990 to 2008*. August 2008.

[2] Schrader, EK. *Roller Compacted Concrete.* Chapter 20. Concrete Construction Engineering Handbook. Second Edition. Edited by Nawy, EG. CRC Press. New Jersey. 2008.

[3] Grieve, GRH. *The Influence of Two South African Fly Ashes on the Engineering Properties of Concrete.* PhD Thesis. University of Witwatersrand. Johannesburg. 1991.

[4] López, J, Castro, G & Schrader, E. *RCC Mix and Thermal Behaviour of Miel I Dam – Design Stage.* – Roller Compacted Concrete Dams. Proceedings. 4th Int. Symposium on Roller Compacted Concrete (RCC) Dams, Madrid, pp 789 - 797. November 2003.

[5] United States Army Corps of Engineers. *Roller-Compacted Concrete.* Engineering Manual, EM 1110-2-2006. USACE. Washington. January 2000.

CHAPTER 7

7. THE INFLUENCE OF THE BENEFICIAL BEHAVIOUR OF HIGH-PASTE RCC ON DAM DESIGN

7.1. INTRODUCTION

Earlier chapters clearly demonstrated that the early behaviour of RCC during the hydration cycle differs significantly from that of CVC and Chapter 6 consequently proposed a new understanding of the early behaviour of high-paste RCC in large dams. However, it is considered of particular importance to go on to demonstrate the impact of applying this new understanding on the design of RCC dams. In this Chapter, the author consequently discusses the implications and applications of the findings of his research in respect of a number of key aspects of the design of a large RCC arch/gravity dam.

For the purpose of comparing the conventional theory in respect of induced joint spacing and openings with a more modern approach and of comparing the related implications of traditionally assumed RCC behaviour with that developed on the basis of this Thesis, the example of the joint spacing evaluation for the Changuinola 1 Dam in Panama is summarised in the ensuing Chapter.

The influence of the new understanding of the behaviour of high-paste RCC is most critical in respect of the design and performance of arch dams and the related impacts are demonstrated through comparative analysis and discussion for the Changionola 1 Dam.

Changuinola I Dam is a 105 m high RCC arch/gravity structure, the first in the world outside China and South Africa. The dam is currently under construction on the Changuinola River in Bocas del Toro province on the Gulf coast of northern Panama. The dam site is located at approximately 9° north of the equator and in a particularly temperate climatic region where monthly average temperatures range between 23.5 and 27.2°C.

7.2. JOINT SPACING DESIGN

7.2.1. THE CONVENTIONAL APPROACH TO DETERMINING CRACK JOINT SPACING

7.2.1.1. Background

The approach to determining appropriate induced joint spacing in RCC dams has essentially evolved directly from the methods traditionally applied for conventional concrete dams. This approach functions on the principle that the spacing of the joints

should be sufficient to ensure that the tensile strain capacity of the concrete is not exceeded in between.

Transverse induced joints are included in RCC dams as a means to manage mass gradient thermal effects. As discussed in Chapter 3, the induced joints must accommodate the thermal shrinkage that will occur as the concrete temperature drops from its "zero stress" temperature (T3) to its final long term equilibrium state seasonal minimum, reached only once all of the hydration heat has finally been dissipated (T4). Considering the fact that it can take some decades for the hydration heat to be fully dissipated from the core of a large RCC dam, the maximum opening of transverse induced joints can take some time to be realized. By the same token and dependent to a certain extent on climatic conditions, the seasonal temperature experienced within the core of a large dam will not vary by more than a degree, or two and accordingly, the temperature T4 is relatively easily determined. As discussed in Chapter 3, while the temperature T3 is somewhat more difficult to define, the same value as T2, or the maximum hydration temperature, is usually accepted as the "zero stress", or T3 temperature.

7.2.1.2. The Function of Joint Openings

In view of the fact that the purpose of the transverse induced joints is to manage a long-term effect and one that will usually take a number of years to be fully realised, it is appropriate to use mature RCC strength properties for the calculation of joint openings, etc. The relevant RCC properties for thermal shrinkage cracking are the thermal expansivity and the tensile strain capacity.

In respect of the transverse induced joints, it is the horizontal tensile stress capacity that is of importance. Unlike the vertical tensile strength of RCC, the horizontal tensile strength is not compromised through placement in horizontal layers and a value of approximately 10% of the compressive strength is consequently probably typical for tensile strength. For RCC with compressive strengths of between 15 and 30 MPa and corresponding long-term elastic moduli of between 10 and 20 GPa[1], a tensile strain capacity of approximately 150 microstrain might be evident[2]. To make an allowance for a factor of safety, it might be more appropriate to assume a tensile strain capacity for RCC of approximately 100 microstrain.

Whether the transverse induced joints either function to create a substantial tensile weakness in the RCC, or to completely de-bond the RCC on a specified cross section, it can be assumed that the tensile stresses developed as a consequence of the long term thermal shrinkage will cause crack development and opening to be initiated at these joints. The design principle for the joint spacing is consequently to ensure that the tensile strain capacity of the RCC is not ever exceeded between the induced joints. Accordingly, should the total long-term thermal shrinkage in a particular dam measure 300 microstrain, it would be assumed that the RCC tensile strain capacity would be exceeded by 150 microstrain and the induced joints would be assumed to open to accommodate that shrinkage.

With a shrinkage strain to be accommodated, the joint opening is a function of the joint spacing applied. Theoretically, an infinite number of opening and spacing combinations exist. However, dependent to some extent on the total temperature drop to be accommodated, a practical minimum joint spacing would probably be 10 m and a maximum, 30 to 50 m. In reality, the foundation restraint condition must be given adequate consideration in deciding on joint spacings and discontinuities, singularities, roughness and general geometrical constraints will usually induce stress concentrations that might result in intermediate cracking for joint spacings exceeding 30 to 50 m. On a particularly uneven foundation, a 30 m induced joint spacing could even be excessive. Subjectively, it would also seem unadvisable to design for maximum induced joint openings of more than perhaps 3 to 5 mm.

A further factor to be considered is the dam height at the location in question. An induced joint spacing/height ratio exceeding 2/3 would rarely be considered advisable.

Some thermal shrinkage of the concrete immediately against the foundation will occur in all dams and while this will largely be accommodated through plastic deformation and micro cracking in the concrete and the foundation rockmass, it is not realistically possible to quantify the influence of this effect. For this reason, it is always particularly advisable to limit concrete placement temperatures immediately against the foundation, or other structural restraints.

7.2.1.3. Quantifying Joint Openings

Theoretically, unrestrained concrete subject to a temperature drop will simply shrink linearly. When restrained against such shrinkage, the concrete will obviously experience tensile stress in proportion to the extent of the restraint.

To establish the induced joint spacings/openings, it is first necessary to establish the total restrained thermal shrinkage strain as follows[2]:

$$\epsilon = (C_{th}).({}_dT).(K_R).(K_f)$$

where

ϵ	=	Strain in concrete caused by temperature change
C_{th}	=	Coefficient of thermal expansion (microstrain/°C)
${}_dT$	=	Temperature change in concrete causing strain (°C)
K_R	=	Structure restraint factor
K_f	=	Foundation restraint factor

The structure restraint is a function of the length/height ratio (L/H), while the foundation restraint factor is a function on the nature and rigidity of the foundation.

The following empirical relationship for K_R was developed by the American Concrete Institute[3]:

$$K_R = \left[\frac{\frac{L}{H} - 1}{\frac{L}{H} + 10}\right]^{\frac{h}{H}}$$

where

L = Length of block

H = Height of block

h = Height above foundation of point of interest.

While K_R might be negligible at the top of an 80 m high block in a dam, it will be very significant at the base of the same block and it is often consequently appropriate to apply a value of 1.

On a rigid rockmass, as generally appropriate for a concrete-type dam, the foundation restraint would probably be only marginally less than 1, perhaps 0.95.

For the following typical conditions:

C_{th} = 10×10^{-6} /°C.

$_dT$ = 30°C

K_R = 1

K_f = 0.95

a thermal shrinkage strain of 285 microstrain would be developed.

Assuming that 100 microstrain remains in the tensile capacity of the RCC, a shrinkage of 185 microstrain shrinkage must be accommodated at the induced joints. For an induced joint spacing of 30 m, this translates into a maximum joint opening of 5.55 mm, or 3.7 mm for a spacing of 20 m.

7.2.1.4. Comparing Traditionally Predicted Joint Openings with those Anticipated by the New RCC Materials Model

Taking the case of Changuinola 1 Dam, a maximum placement temperature of 29°C is to be applied and a heat of hydration of 22°C has been predicted by heat-box testing. Subsequently the thermal analysis predicted a maximum core temperature of approximately 51°C, during construction, and a final long-term minimum core temperature of approximately 25°C. Situated only 9° north of the equator, the dam will experience a particularly temperate climate and accordingly, the long-term temperature drop from peak hydration will be limited to approximately 25°C.

In accordance with the traditional approach and RCC behaviour model, the induced joints would be designed for a temperature drop of a full 25°C. With a coefficient of thermal expansion of 8.8×10^{-6}/°C, a structural restraint factor of 1 and a foundation restraint factor of 0.95, the total shrinkage strain to be developed would accordingly

be 209 microstrain. Allowing for a residual RCC tensile strain of 100 microstrain, the maximum joint opening at a spacing of 20 m would be 2.18 mm.

Applying a more realistic RCC behaviour on the basis of the findings of this Thesis, and allowing for creep equivalent to increasing the "zero stress" temperature by 2°C, then the total maximum applicable temperature drop would be between 1 and 5°C. The total shrinkage associated with such a temperature drop would develop a tensile strain of approximately 25 microstrain, which is significantly less than the RCC tensile strain capacity.

In accordance with the traditional approach, this would imply that the RCC would not crack. However, in reality, with joint inducing substantially reducing the tensile strength of the structure, the indicated thermal shrinkage would probably cause core joint openings of approximately 1 mm on every second, or third induced joint.

7.2.1.5. Discussion

The traditional approach to the evaluation of induced joint spacings and openings has proved to function well in practical application because it is in reality rather conservative. However, it is in fact unrealistic in allowing such high levels of residual tensile stress in the RCC between induced joints. The Finite Element analyses completed for Wolwedans Dam and presented in Chapter 5 clearly demonstrate that the residual tensile stresses between induced joints in a large dam are surprisingly low, even when only every third joint opens.

Considering this fact, it is apparent that a linear shrinkage, equivalent to $C_{th.d}T$ should be applicable at a location remote from any restraint. Taking the example under 7.2.3 above, the total joint opening at the crest of a high dam, with joint spacings of 30 m, would exceed 6.5 mm.

The USACE EM 1110-2-2006 guideline on *Roller Compacted Concrete*. 2000[4] addresses the subject of transverse induced joint openings on RCC dams, reflecting the fact that typical maximum joint openings vary between 1 and 3 mm. The same publication indicates that transverse induced joints have generally been spaced at separations of between 15 and 40 m, although some instances of over 90 m exist.

Again, the conventionally accepted practices and design procedures for RCC in dams and the realities of measured performance can be seen to be disparate.

7.2.2. CHANGUINOLA 1 DAM JOINT SPACING DESIGN

7.2.2.1. Introduction & Approach

For the purpose of establishing the maximum joint spacing in tandem with a maximum RCC placement temperature for the Changuinola 1 RCC arch/gravity dam, a detailed thermal analysis was undertaken[5] and this is described briefly in Chapter 5. The first phase of analysis incorporated a 2-dimensional sectional profile that was essentially built up on the basis of the proposed construction programme. Through this model, it was possible to evaluate the critical temperature gradients and

the resultant stresses that are likely to develop through the dam section in the process of hydration heat development and subsequent cooling. In addition, the long-term equilibrium temperature state for the dam could be established. While the former was used to investigate whether cooling of placed RCC would be required at any stage to prevent the development of surface gradient cracking, the latter was of most specific relevance in respect of the spacing of the transverse induced joints.

With the temperature distributions at placement and at maximum hydration, it was possible to establish the effective long-term temperature drops that would be anticipated for the conventional RCC materials behaviour model and for the proposed new materials model.

7.2.2.2. Thermal Analysis

The thermal analysis simulated construction on a weekly basis, applying a daily time step and inputting heat energy in 300 x 300 mm elements to realise the maximum hydration temperature rise after 7 days, while allowing surface convection over the same period. The RCC placement temperature at any particular point in time was input as the average monthly ambient + 2°C. Measurement on the first full scale trial for the dam suggested that heat of approximately 3°C was added to the RCC through all of the various handling processes, etc. Not all of the temperature control measures to be applied for the dam were in use during the trial and accordingly, it was considered that a temperature increase of 2°C for the handling processes, etc, would be a more appropriate figure. On the basis of this scenario, a maximum placement, or built-in RCC temperature of 29.2°C was found to be applicable for the warmest period of the year, while a maximum temperature of 48.5°C was indicated within the core of the dam structure shortly after completion in August 2011. It should be noted that this maximum temperature has already dropped slightly from the peak of approximately 51°C experienced during construction between September and November 2010.

Building up the dam model using the COSMOS[6] Finite Element software (see **Figure 7.1**), the structure was subsequently subjected to external seasonal air and water temperature variations over a period of 4 decades. In this process, it was established that an equilibrium state of seasonal temperature variations was reached, with all hydration heat dissipated, approximately 30 years after construction completion. The subsequent minimum seasonal temperature distribution within the dam structure was consequently established as the final (T4) state against which the long-term temperature drop was measured. The process of cooling from the maximum heat state, on completion of construction, to the final cool equilibrium state is illustrated on **Figure 7.2**.

For the above model, a foundation depth equal to twice the dam height was applied and the initial temperature of the rockmass was established by subjecting the FE model to the external monthly average ambient temperature until a final condition of equilibrium was reached.

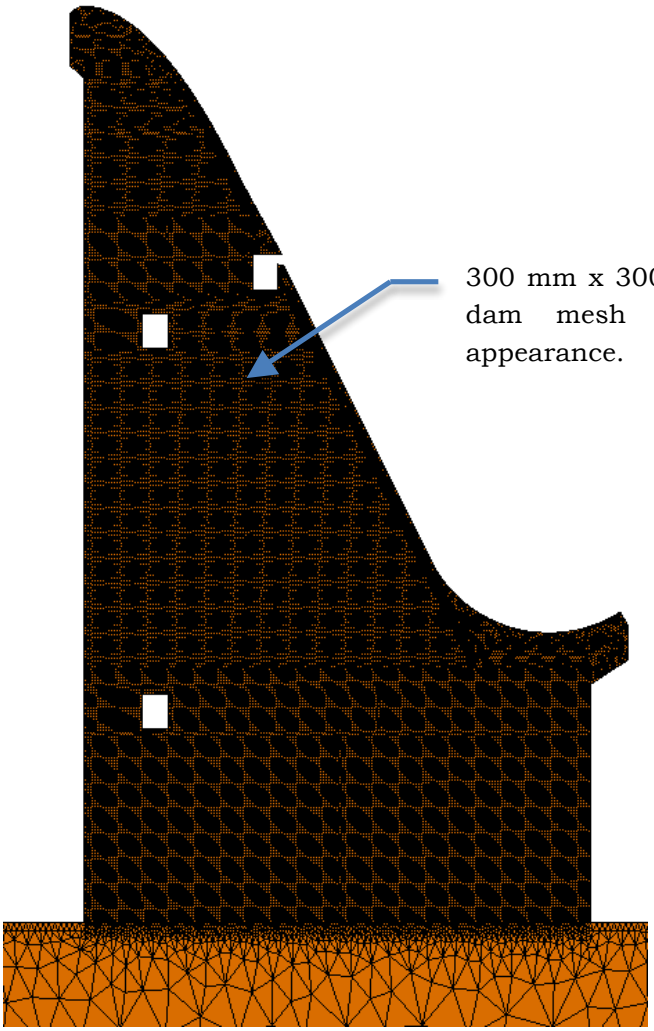

2 Dimensional FE Mesh

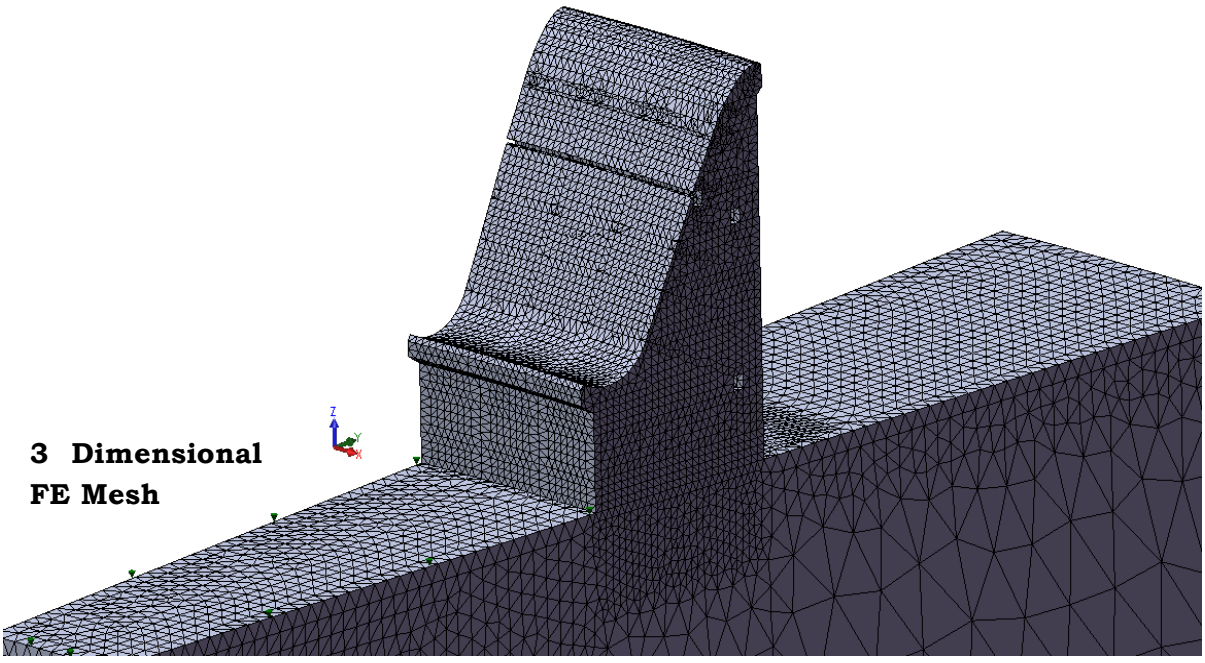

3 Dimensional FE Mesh

Figure 7.1: 2 & 3-D Finite Element Meshes used for Thermal Analyses[5]

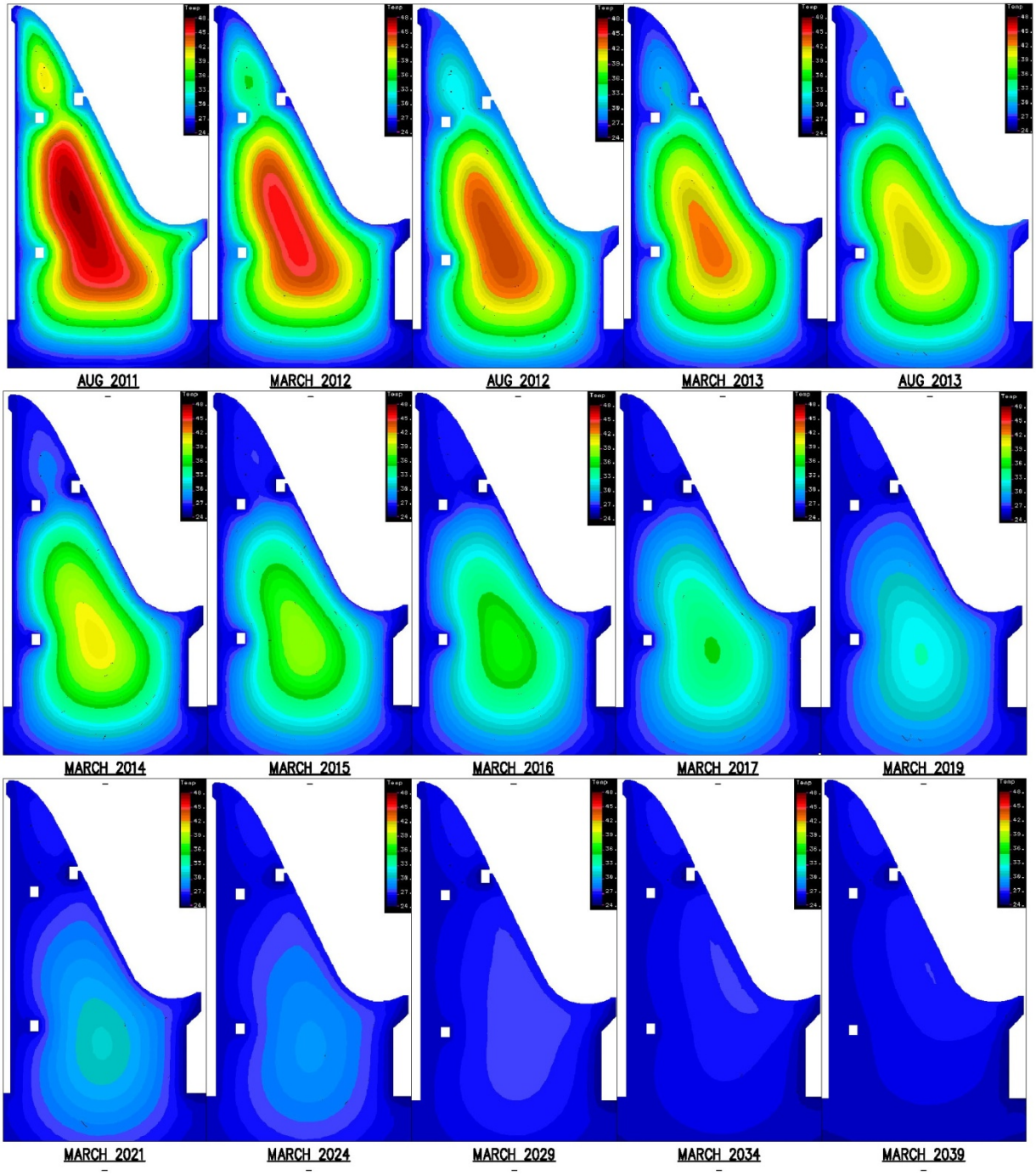

Figure 7.2: Process of Dam Body Cooling to Long-term Equilibrium State

7.2.2.3. Joint Spacing Evaluation

To evaluate an appropriate maximum transverse induced joint spacing to be applied for Changinola 1 Dam, a 100 m long FE model (see **Figure 7.1**) was established with gap elements spaced at 5 m centres. By binding, or releasing these elements, it was possible to investigate joint spacings at various multiples of 5 m. The model was taken at the tallest section of dam structure, on the spillway, and a flat foundation geometry

was assumed to ensure that the temperature-related influences could be evaluated in isolation.

Applying a distribution of temperature drops down to the final cool equilibrium state, two conditions for the "zero stress" (T3) temperature were applied; the first taking the maximum hydration temperature distribution, in accordance with a conventional RCC materials model, and the second conservatively assuming an effective creep equivalent to 2°C, in accordance with the RCC materials behaviour established in this Thesis (termed "New" RCC model for brevity), and setting the "zero stress" temperature at 2°C above the effective placement temperature. While it has been demonstrated that an RCC with no significant shrinkage, or creep is possible, and while the Changuinola 1 RCC is extremely high quality, the thermal analysis was completed before the final full scale trial, for which strain measurement will be undertaken and accordingly, it was considered appropriate to retain a degree of conservatism.

Figures 7.3, **7.4** and **7.5** illustrate the final T4 distribution and the T3 states at maximum hydration (T3 = T2) and at placement + 2°C (T3 = T1 + 2°C) respectively.

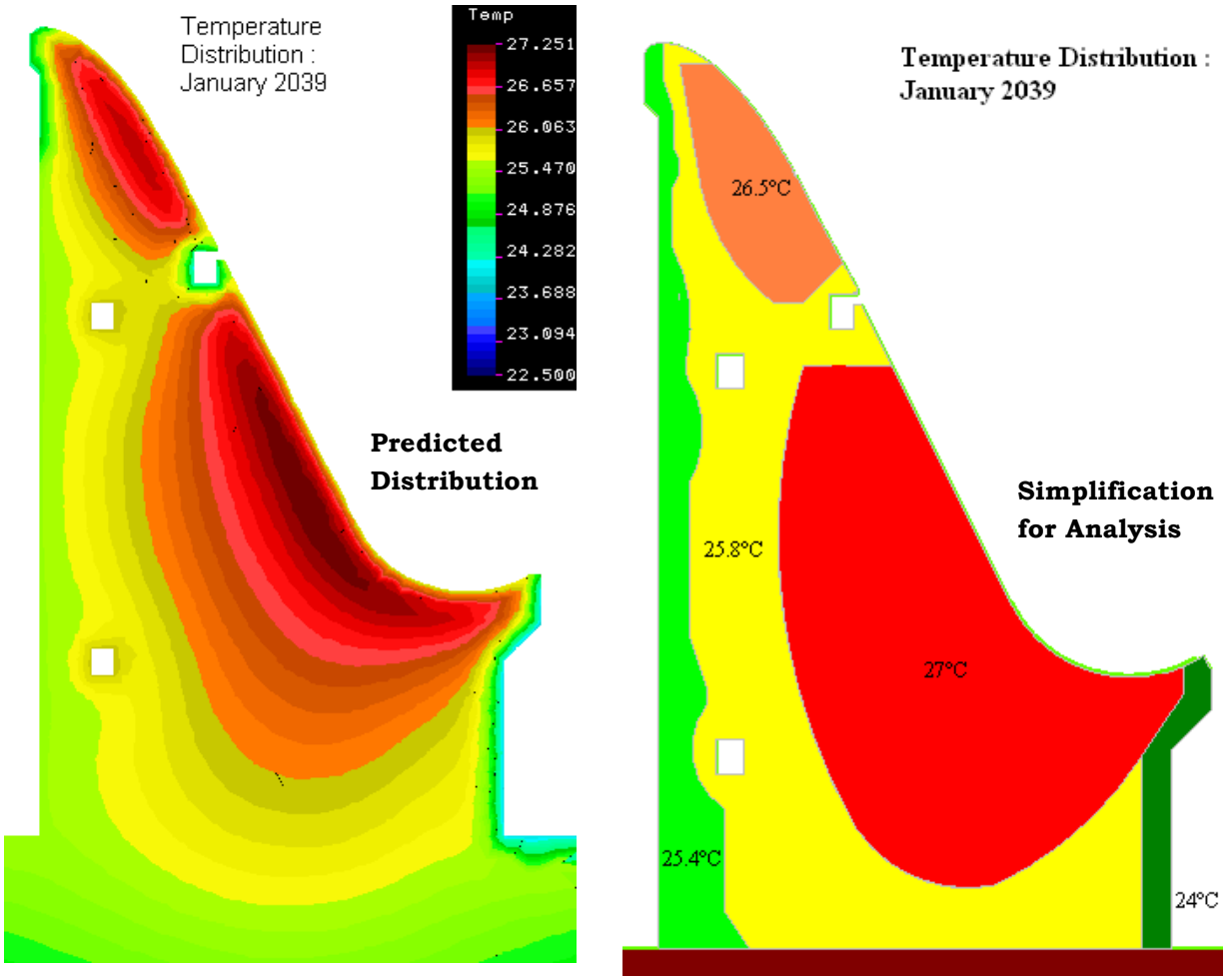

Figure 7.3: T4 Temperatures Predicted at Jan 2039 & Associated Simplified Distribution for Analysis(°C)

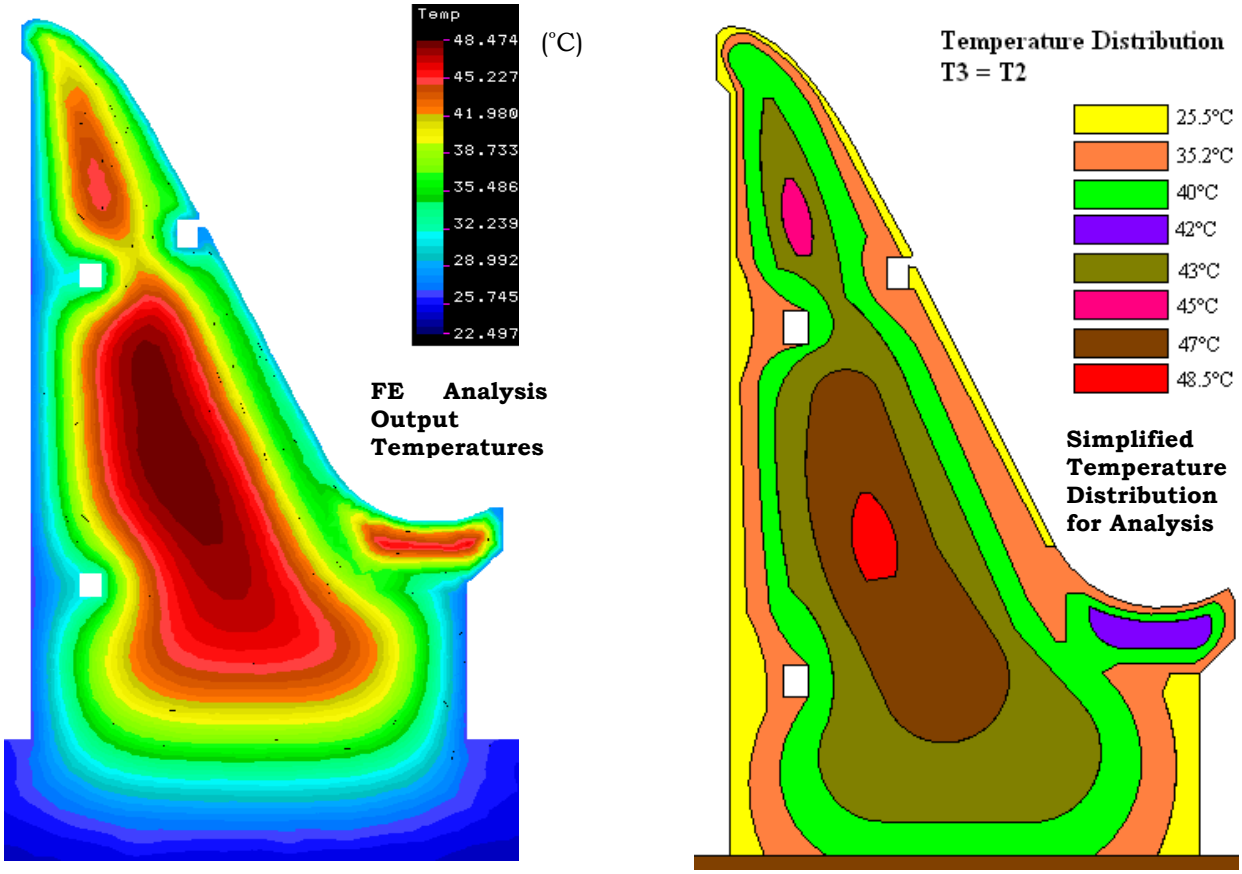

Figure 7.4: T3 Temps for Traditional RCC Model – Actual & Simplified (°C)

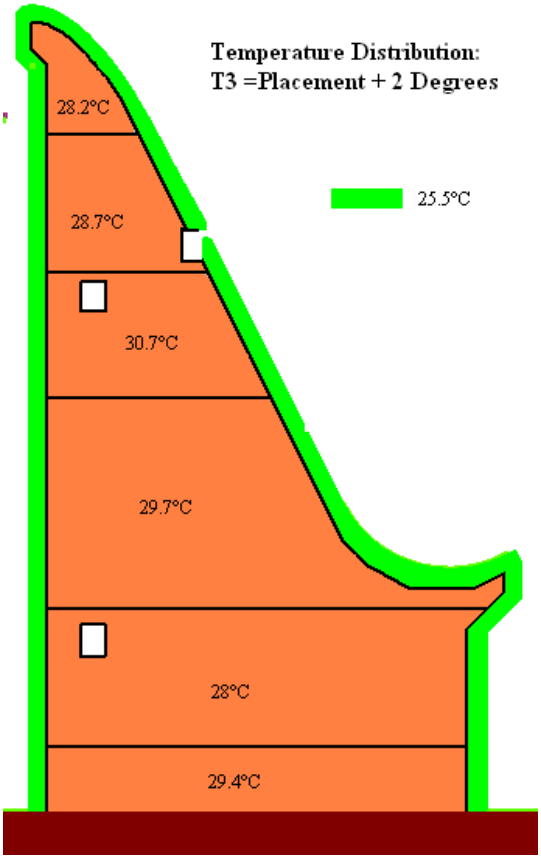

Figure 7.5:
T3 Temperatures for "New" RCC Model (°C)

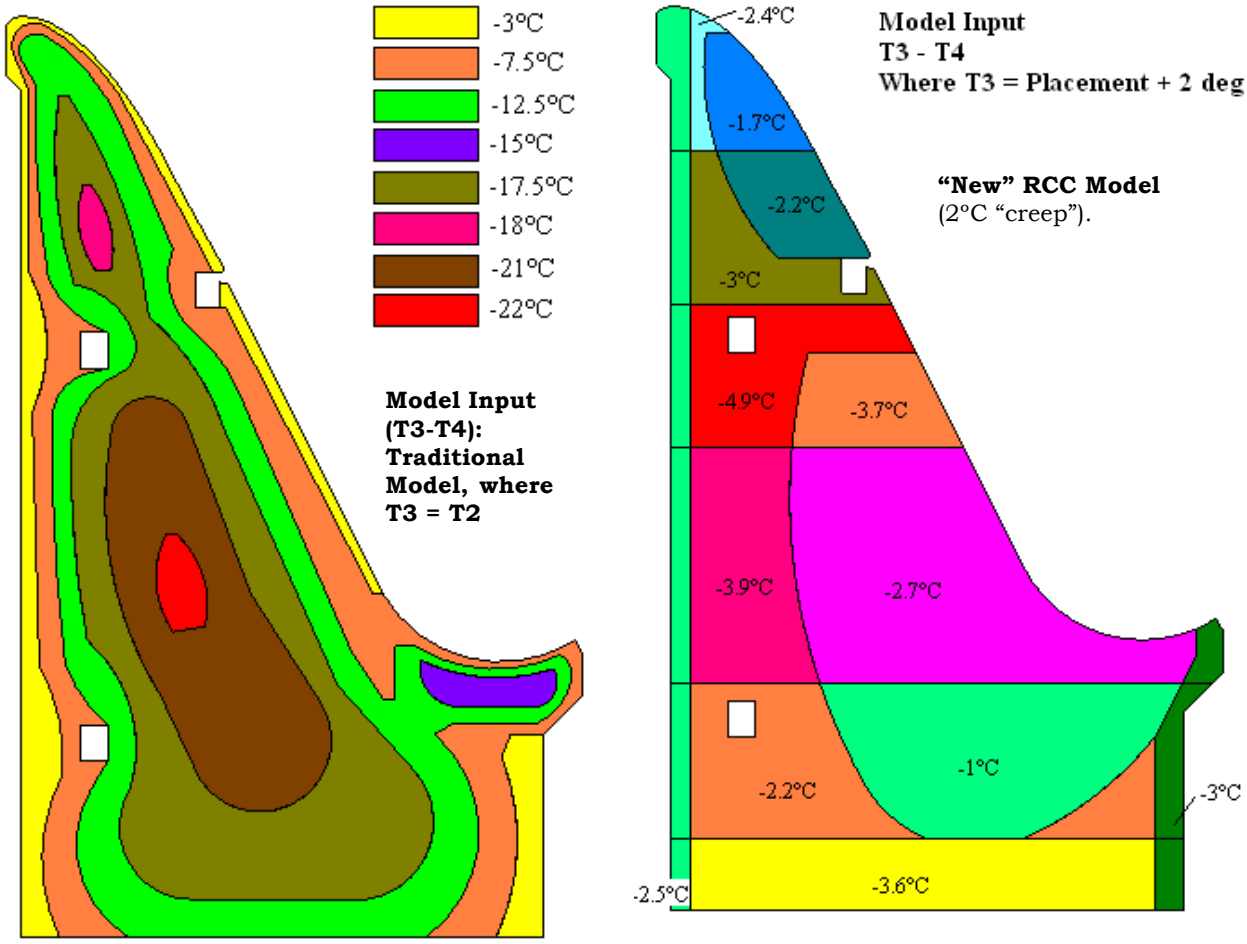

Figure 7.6: Temp. Drop Loads Applied for Traditional & "New" RCC Models (°C)

Figure 7.6 illustrates the effective structural temperature drop loads applied for analysis to represent the Conventional and the "New" RCC materials models respectively.

7.2.2.4. Presentation of Results

It is considered important to take note of the fact that the Finite Element analysis takes into account the initial cooling effect of the foundation on the heated dam structure. Using the temperature distributions developed through the thermal analysis as input data for the temperature drop analysis, the consequential cooling of RCC placed close to the foundation implies a relatively gentle temperature gradient between the base of the dam structure and the foundation rockmass. The simplified conventional theory effectively assumes an abrupt interface between the concrete, in which a temperature drop is applied, and the foundation, in which no temperature drop is applied.

The results from the joint spacing analyses are presented here for the selected maximum spacing of 20 m. **Figures 7.7** and **7.8** present the predicted maximum induced joint openings and the mid-block maximum residual tensile stresses for the

conventional RCC materials model, respectively, while **Figures 7.9** and **7.10** present the same for the "New" RCC materials model.

Table 7.1 provides a summary of the critical observations in respect of the two models/modes of behaviour:

Table 7.1: Finite Element Joint Spacing Model Critical Output

RCC Materials Model/Behaviour Mode	**Critical Behaviour**		
	Max Opening (mm)	**Max Residual Tensile Stress** (MPa)	**Max Residual Tensile Strain**
Traditional	3.85	1.0	50 microstrain
"New"	0.76	0.4	20 microstrain

The above FE analysis results can be compared with conventional joint theory predicted openings of 2.18 mm and 0 for the traditional and the "New" RCC materials model, respectively, assuming 20 m joint spacings and 100 microstrain residual tensions.

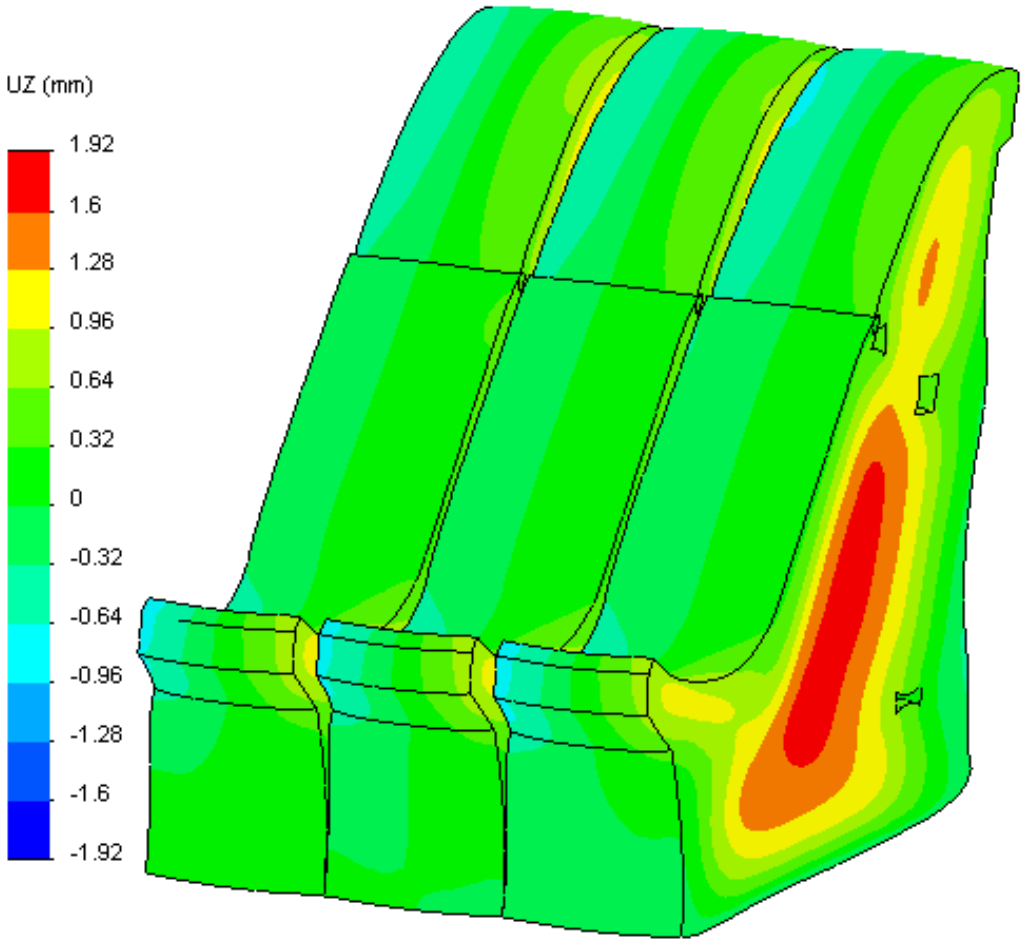

Figure 7.7: Maximum Induced Joint Openings for Traditional RCC Model

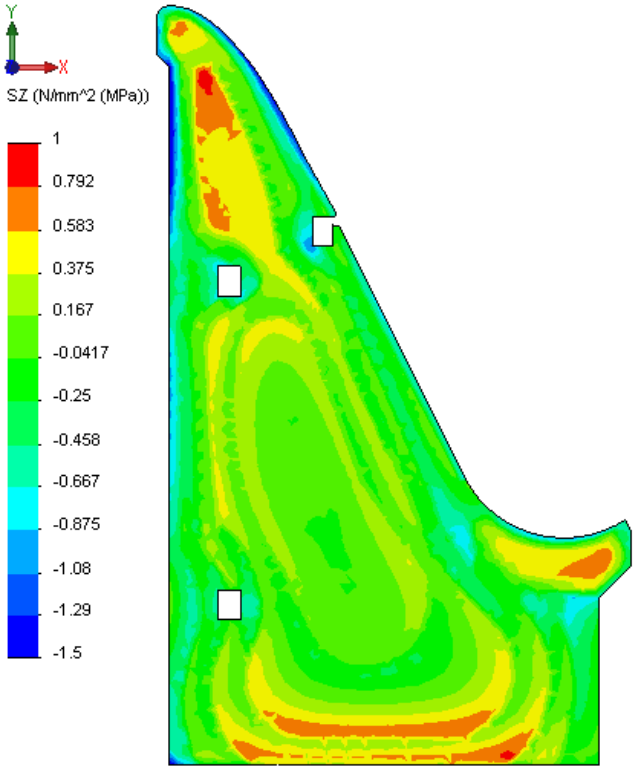

(+ve = Tension, -ve = Compression)

Figure 7.8: Central Block Residual Stress for Traditional RCC Model

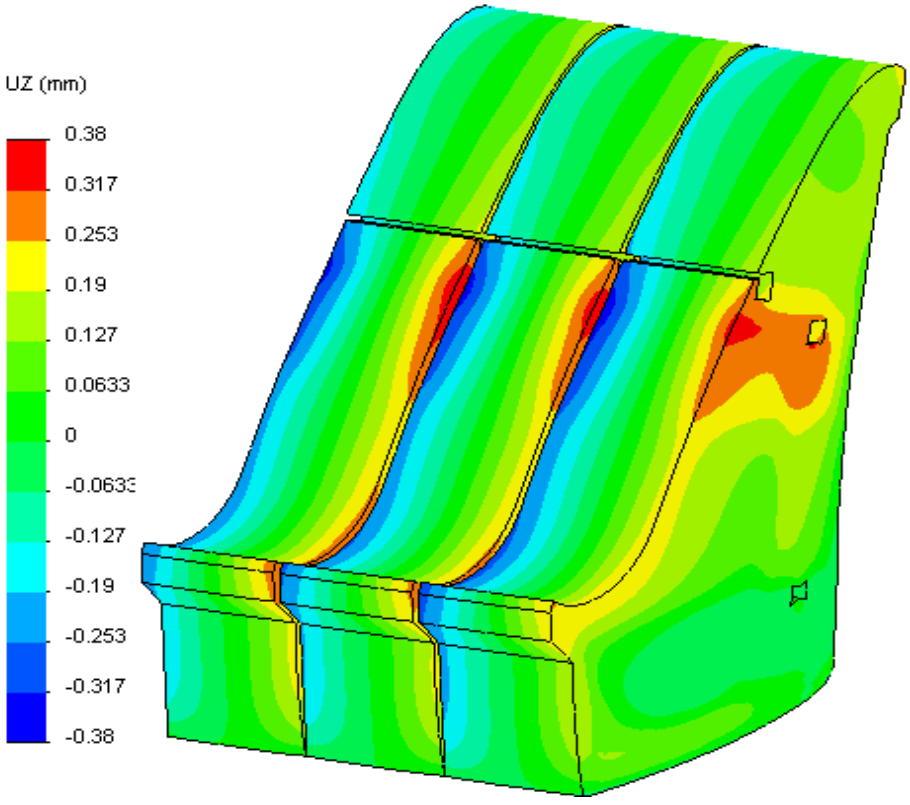

Figure 7.9: Maximum Induced Joint Openings for "New" RCC Model

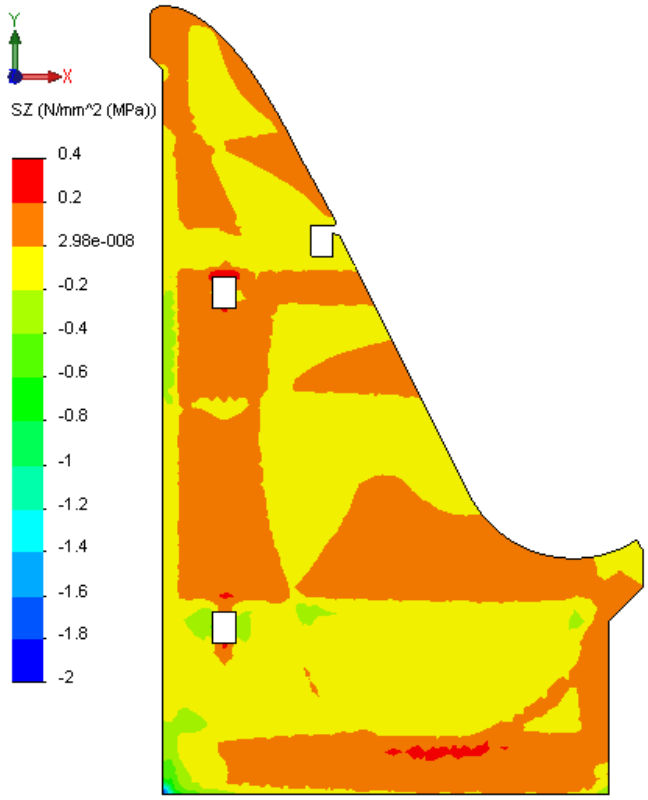

(+ve = Tension, -ve = Compression)

Figure 7.10: Central Block Residual Stress for "New" RCC Model

7.2.2.5. Discussion of Results

The FE analyses summarised above confirmed that the anticipated residual tensile stresses between induced joints spaced at 20 m are in fact minimal, peaking at only 50 microstrain even for a temperature drop of the order of 20°C. As a consequence, however, the induced joint open in an unrestrained manner and the maximum joint openings predicted for the traditional RCC model/behaviour mode are approximately double those estimated in accordance with the conventional, simplified theory.

In the case of the "New" RCC materials model/behaviour mode, even the residual tensile stress indicated immediately against the foundation was low and well within the tensile strength capacity of the RCC. The very fact that the joint opening is of the same order as would have been anticipated for a simple linear shrinkage, however, confirms the indications of the stress plot that residual stress within the block at crest elevation is negligible.

It is in this last fact that the most important comparison can be made with the conventional theory. As previously demonstrated on the Wolwedans Dam model and confirmed on the prototype structure, only a few open joints across the length of a relatively large structure are sufficient to dissipate the great majority of the tensile stress associated with the long-term temperature drop. Consequently, the full shrinkage associated with the temperature drop should be evident on the induced joints at the crest of the dam. In the particularly temperate climate of the

Changuinola 1 Dam site, maximum induced joint openings of no more than 1 mm would be anticipated. If an induced joint opening of 4 mm were realistically to be anticipated at a dam such as Changuinola 1, as predicted for the traditional RCC materials model/behaviour mode, very significantly greater induced joint openings would have been measured on other major RCC dams in more extreme climates, contradicting the 1 to 3 mm stated as typical in the USACE's EM 1110-2-2006. *Roller Compacted Concrete.* 2000[4] guideline on the subject.

The fact that the conventional theory significantly over-estimates the magnitude of the effective temperature drop that causes thermal shrinkage is substantially mitigated by its incorrect assumption of the level of the residual tensile stresses within an RCC block between induced joints.

7.2.2.6. Induced Joint Spacing for Changuinola 1 Dam

The joint spacing analysis summarised above allowed the following conclusions to be drawn for Changuinola 1 Dam;

1. No matter what the material model adopted, an induced joint spacing of 20 m was sufficient to ensure that residual tensions do not exceed the concrete tensile strain capacity;
2. No artificial RCC cooling will be required for an induced joint spacing of 20 m, as long as the temperature control measures put in place are sufficient to ensure that the placement temperatures do not generally exceed 2°C above the average ambient, with an associated maximum allowable placement temperature of 29°C; and
3. Considering the obvious conservatism of the conventional RCC materials model in respect of the high-paste RCC used at Changuinola 1, a significant factor of safety can be considered to exist in the proposed induced joint design.

The above findings might suggest that a placement temperature of well above 29°C could be allowed, or that a transverse induced joint spacing of well in excess of 20 m could be applied. In the case of Changuinola 1, however, other factors in respect of the arch/gravity dam design needed to be given consideration. Bearing in mind the construction schedule and the need for rapid impoundment, a significant advantage was perceived in being able to eliminate grouting of the arch/gravity structure before impoundment and therefore minimising the applicable maximum temperature drop load.

7.2.3. CONCLUSIONS

The above analyses and comparisons clearly demonstrate the over-simplification of the conventional theory for induced joint spacing and opening. Furthermore, the assumptions in respect of residual tension and consequently the methods for calculating joint openings have been demonstrated to be flawed. To date, conventional theory has worked because it substantially over-estimates the magnitude of the long-term temperature drop that is applicable in the case of RCC. Applying the "New"

materials model for early RCC behaviour, in line with the findings of this Thesis, the conventional joint spacing model must be modified. This model is anyway a rather crude tool that should only realistically be used for first estimation, as simple FE modelling can readily provide substantially more credible analysis.

The FE analyses clearly demonstrate that residual tensile stresses are fully dissipated within approximately 10 m above the constraint of the foundation for a joint spacing of 20 m. This is particularly important, as it implies that the full thermal shrinkage will be manifested in the opening of the induced joints at the crest of the dam. When reviewing the induced joint openings typical on RCC dams on the basis of this knowledge, it is quite clear that the magnitude of opening that the traditional RCC model would predict simply does not occur in reality. While experience demonstrates induced joint openings typically in the range of 1 to 3 mm, even such openings are never evident at every induced joint, unless the spacing is very significant. Although this observation may be subjective, it is yet another confirmation that the traditional materials model does not correctly predict the actual behaviour of RCC and that certainly high-paste RCC in fact behaves quite differently to CVC in respect of shrinkage and creep during the hydration heat development and cooling cycle.

7.3. THE IMPACT OF TEMPERATURE DROP LOADS ON ARCH DAMS

7.3.1. INTRODUCTION

The application of the findings of this Thesis will be of greatest importance in respect of RCC arch dams. While the new understanding of the early behaviour of high-paste RCC will give rise to new opportunities for dam design, its application will also require that a number of aspects, from aggregate testing to the construction programme, be given greater attention at the design stage.

7.3.2. TEMPERATURE DROP LOADS

The impact of temperature drop loads on arch dams is discussed in **Appendix A** and summarised in Chapter 5. For further information, reference should be made to the author's MSc thesis entitled "The Role of Temperature in Relation to the Structural Behaviour of Continuously Constructed RCC and RMC Dams"[7], or his 2003 paper "The Development of RCC Arch Dams"[8].

In summary, a temperature drop load on an arch dam essentially implies that the structure shrinks to a smaller size than the space that it was constructed to fill. With shrinkage increasing with distance from the restraining foundation, the central crest of the dam is most significantly impacted. If the structure is constructed with transverse joints, or induced joints, these will open and the structure will effectively stand as a series of separated vertical, cantilever monoliths. When water load is applied to this structure, the cantilevers are inadequately stiff to carry the full load and they consequently deflect downstream. With deflection increasing with distance

from the restraint of the foundation, they make contact with each other, first at the crest and then progressively lower as greater load is applied. In this process, the cantilevers shed load laterally at the top, the crest area becomes an arch and additional structural stiffness is provided to the top of the cantilevers, as arch action assists in resisting additional downstream displacement.

In this process, the longer central cantilevers deflect more than the shorter cantilevers on the flanks and the centre of the arch effectively moves downstream relative to the flanks. As resistance to downstream deflection is provided to the top of the cantilevers in the form of arching, the central section of the cantilevers begins to experience vertical bending (or beam) stresses as they span between the supports of the foundation at the bottom and the arch at the top. The consequence is that the central portion of the arch structure begins to experience vertical (and subsequently horizontal) tensions on the downstream face, in a sort of bursting action (see **Appendix A**).

Imposing a temperature drop onto an arch dam reduces the extent of the structure that contributes to transferring stress through arch action, concentrates stresses towards the crest and initiates distress on the longer cantilevers. Accordingly, it can be seen that a temperature drop substantially compromises the efficiency of an arch structure, consequently compromising its final load carrying capacity.

7.3.3. The Traditional Approach to Arch Dam Design for temperature Drop loads

As a consequence of the above impact of temperature drop loading on the efficiency and the load carrying capacity of an arch structure, it is general practice to restore the original "un-shrunk" geometry of an arch dam by filling contraction joints with cementitious grout at an appropriately low temperature.

CVC arch dams are constructed as a series of independent vertical monoliths, each usually the full thickness of the dam wall, but limited in width to approximately 15 m. Assuming the "zero stress" temperature approximately, or marginally conservatively, equal to the maximum hydration temperature (T2), a significant temperature drop load is applicable down to the final long-term equilibrium state winter minimum. For a hydration heat of perhaps 25°C and a difference between placement and the final minimum internal winter temperature of perhaps an additional 10°C, the total applicable temperature drop would be 35°C. For such a temperature drop, the contraction joints between 15 m wide monoliths would open by over 5 mm, creating a void that can readily be filled with grout.

The hydration heat within the dam, however, can take years to dissipate naturally and it is not a practical option to wait for this to occur before impounding water, or before grouting the contraction joints. Consequently, it is common practice to install pipe loops in the mass concrete through which chilled water is circulated in order to accelerate the withdrawal of the hydration heat. While the cooling process is sometimes applied to cool to the final winter equilibrium minimum, an alternative

approach is to pump the grout into the joints under pressure, effectively further opening the joints using grout pressure. Provision must of course be made for the quite considerable autogenous shrinkage of a cement/water grout. The grouting systems are usually designed to allow re-grouting at some time in the future, should this ever be considered necessary. Depending on the temperature at which the grouting is undertaken and the pressure applied, the dam structure may still be designed to accommodate a minor temperature drop below its grouted temperature.

7.3.4. RCC ARCH DAM DESIGN AND TEMPERATURE DROP LOADS

7.3.4.1. General

Constructing RCC dams in continuous horizontal layers does not allow the inclusion of formed joints, with shear keys and grouting systems, as applied for CVC. Furthermore, placement in 300 mm layers using large, vibratory rollers makes the inclusion of pipe cooling loops rather impractical, although this has apparently been successfully accomplished in China[9]. In view of the fact that one of the primary benefits of RCC dam construction is speed, it further makes no practical sense to wait for natural cooling to occur before grouting and impounding the reservoir. Consequently, the design of an arch, or an arch/gravity dam in RCC must include careful consideration of the processes and methods applied to ensure structural integrity at all times.

If impounding is commenced at an RCC arch immediately on completion of the RCC placement, the structure will still retain a good proportion of its hydration heat, with the structural integrity only starting to become compromised as the heat is dissipated into the water, the atmosphere and the foundation. However, to wait to grout until the heat has dissipated naturally, with a filled dam, would effectively require the structure anyway to be structurally safe for the full applicable long-term temperature drop, without grouting of the induced joints.

7.3.4.2. Discussion on the Accommodation of Temperature Drop Loads in RCC Arch Dams

Depending on the nature of the arch dam design, a number of alternative approaches can be considered for the accommodation of temperature drop loads; the case of a thin RCC arch in a narrow valley being quite different to that for a heavy arch/gravity structure in a wide valley. The situation in an extreme climate will also be quite different to the situation in a climatically temperate region. In general, however, the approach will either be one of designing the arch for temperature drop loads without grouting, or one of cooling the concrete, locally or generally, to allow early grouting of the induced joints. Whatever the approach, a grouting system will usually be included on the induced joints to ensure that grouting can be undertaken, should the need ever be considered to arise.

While artificial cooling to withdraw all of the hydration heat is only realistically practical where the dam section is thin, it is probably only realistically necessary in such instances, where the structural reliance on arching is high and the arch action is continued quite low in the dam wall structure. In the case of an arch/gravity structure, three dimensional stress transfer will only really ever occur within the upper portion of the wall, where some flexibility of the stiff cantilevers exists, and arch function will never be required in the lower sections of the structure, where more heat retention will be experienced.

7.3.4.3. Comparing Predicted Arch Behaviour for a Traditional RCC Model with that Anticipated for the "New" RCC Materials Model

Taking into account the above, the findings presented in Chapter 6 and the practical realities of timing the induced joint grouting and the reservoir impoundment, a completely different situation can be perceived whether the traditional, or the "New" RCC materials behaviour model is applied. In the case of Changuinola 1 Dam, a long-term structural temperature drop of approximately 22°C must be taken into account in the dam design when applying the traditional model, while this figure becomes approximately 3°C when applying the "New" RCC model/behaviour mode.

In the case of the former temperature drop, the structural impact would be too great to allow any question of loading before full joint grouting within the critical zones of the dam crest had been completed. In the case of the latter temperature drop, the structural integrity of the arch structure would undoubtedly be assured without any joint grouting.

7.3.5. The Influence of the "New" RCC Materials Model/Behaviour Mode on RCC Gravity Dam Design

7.3.5.1. Background

In the case of RCC gravity dams, the only critical issue in respect of long-term temperature drop loads is the potential for the development of cracking parallel to the dam axis. This problem has long been acknowledged as an important factor to be considered in the design and construction of large mass concrete dams and there are many examples where such cracks have developed in mass concrete. In the warmer areas of South Africa, thermal cracking has occurred at several CVC dams, such as Gariep and Inanda Dams, while these problems are currently being experienced at De Hoop Dam for concrete placed during the winter months.

Generally, this problem is addressed in CVC through pre-cooling of the concrete by incorporating ice in the mix, or by post-cooling, both with the objective of limiting the maximum temperature experienced within the concrete mass compared to the external ambient. On the basis of limiting the T2 temperature (hydration peak), the T3 temperature (zero stress) temperature is reduced, as the two temperatures are generally considered as the same for CVC.

7.3.5.2. The Situation for RCC Dams

Applying a CVC materials behaviour model for RCC, this problem is generally approached in a similar manner to the derivation of appropriate transverse joint spacing. It is also, however, one of the primary reasons for which a comprehensive thermal study is considered necessary for all major RCC dams. Limiting horizontal tensile stresses in an upstream – downstream direction in a large RCC dam will usually represent the determining factor in establishing the maximum allowable RCC placement temperature and accordingly, the level of the expensive pre-cooling measures that need to be applied.

In the cases of the two largest RCC gravity dams constructed to date, the issue in respect of potential cracking parallel to the dam axis has been handled differently. In the case of La Miel Dam (190 m) in Columbia[10], an induced joint was constructed from the base to 1/3 height in the middle of the dam wall, running parallel to the dam axis. While provision has been made to grout this joint, it has not yet indicated any signs of opening, as the dam was completed in 2002 and it will be many decades before all of the hydration heat has been dissipated from the core.

At Longtan Dam (195 m – phase 1) in China[11 & 12], post-cooling pipes were installed to draw out the hydration heat and to limit the maximum temperatures experienced.

7.3.5.3. Applying the "New" RCC Materials Model for Gravity Dams

Applying the proposed "New" RCC early material behaviour model, a very different situation is created in respect to the long-term temperature drop loads for large RCC gravity dams.

For a 150 m high gravity dam, a typically appropriate RCC mix might indicate an adiabatic hydration heat of approximately 15°C. In a relatively temperate climate, the critical placement temperature might be 25°C, while the long-term equilibrium core temperature might be in the vicinity of 18°C. Applying a traditional CVC model, a zero stress temperature (T3) of 40°C (maximum hydration) would be considered to apply, resulting in a final long-term temperature drop of 22°C. For a thermal expansivity of 10 x 10^{-6}/°C and an elastic modulus of 15 GPa, the above would give rise to a final shrinkage of 220 microstrain and a maximum theoretical restrained tension against the foundation of 3.3 MPa. Such a tension would substantially exceed the actual RCC horizontal tensile strength, which is likely to be less than 1.5 MPa.

Applying the proposed new RCC materials behaviour model and conservatively allowing for 2°C of shrinkage/creep, the total long-term temperature drop applicable would be 9°C (25 + 2 – 18). On the basis of the same material parameters, this would give rise to a maximum shrinkage of 90 microstrain and an associated maximum tensile stress of 1.35 MPa, which is consequently substantially less likely to cause any cracking.

Taking the case of Çine Dam (see Chapter 4), the 136.5 m high structure, which is located in a relatively temperate climate, was constructed over 6 winter seasons. With an adiabatic heat of hydration of approximately 12°C, maintaining placement temperatures at around 10 to 12°C ensured that the core temperatures within the

structure never really exceeded 24°C. For a long-term core equilibrium temperature of approximately 18.5°C, the applicable maximum temperature drop to be experienced will consequently be just 5.5°C. For a thermal expansivity of 7.1 x 10^{-6}/°C, even assuming a CVC materials behaviour model would only give rise to a final shrinkage of less than 40 microstrain.

However, according to the "New" RCC materials behaviour model and even assuming a shrinkage/creep equivalent to 2°C, the RCC of the core of Çine Dam will never experience any long-term thermal shrinkage.

The implications of the proposed new RCC materials behaviour model in respect of large gravity dams are obvious; temperature issues represent a lesser constraint on dam height than had been previously considered, while significant savings in pre-cooling of RCC will be possible. Furthermore, as a consequence of the apparent elastic behaviour of RCC during the hydration cycle and the apparent absence of creep, post-cooling in gravity dams has no real purpose, but to limit the short-term thermal gradients across the dam structure.

While a high gravity dam is likely to use a high strength RCC, designing a high quality mix for negligible shrinkage and creep will incur additional cost. The savings associated with the reduction, or elimination of mix cooling would, however, substantially outweigh any such costs.

7.3.6. CHANGUINOLA 1 DAM PRELIMINARY STRUCTURAL ARCH DESIGN

7.3.6.1. Introduction

The Changuinola 1 arch/gravity RCC dam presents a particularly useful example through which to illustrate the influence and impacts of the new RCC behaviour materials model on the design of an arch dam. While the applicable climatic conditions are extremely mild, the 100 m high structure is a relatively heavy arch/gravity dam currently under construction in a wide valley.

7.3.6.2. Dam Description

Changuinola 1 Dam is a 105 m high structure with a crest length of 510m, comprising 890 000 m^3 of RCC. The central section and the right flank of the dam are on an arch with an upstream face radius of 525 m, while the left flank has a straight alignment. The spillway section has a downstream face slope of 0.5H:1V and is flanked on either sides by transition zones and gravity walls thereafter, as illustrated on **Figure 7.11**.

The dam is located on the Carribean coast of Panama at 9° North of the equator, where the climate is extremely temperate, with average monthly temperatures varying between 23.5 and 27.2°C year round. The area is also relatively seismically active and the dam is consequently subject to comparatively high earthquake loadings.

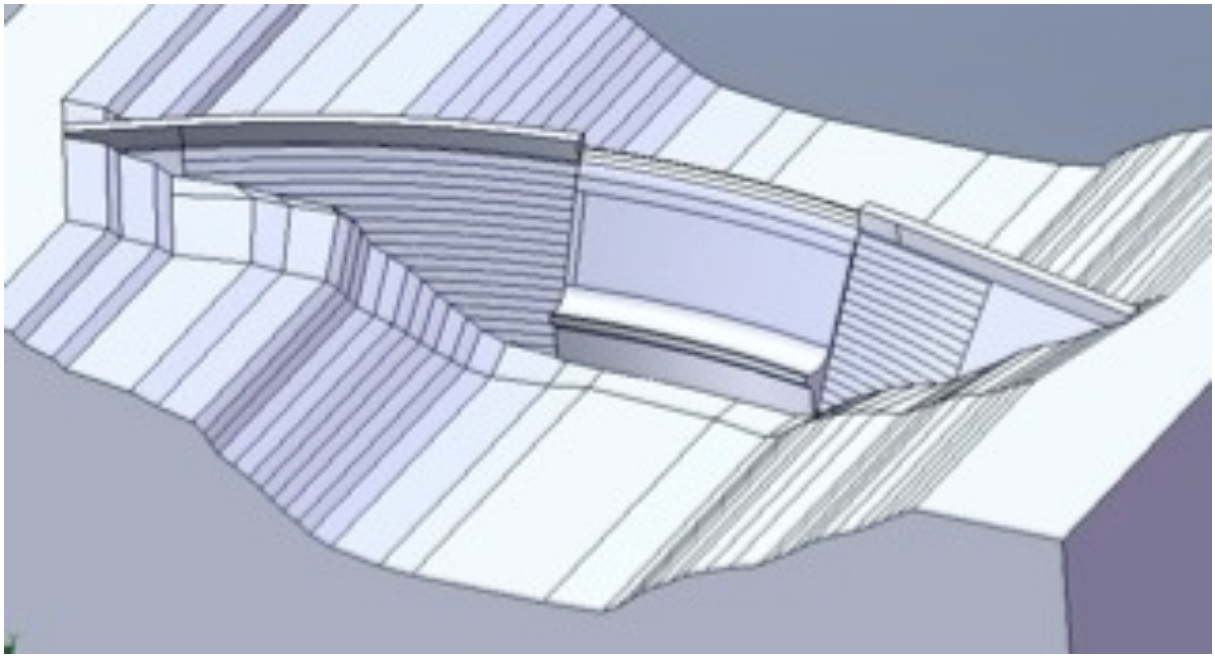

Figure 7.11: Layout of Changuinola 1 Dam

7.3.6.3. Thermal Analyses

For the purposes of illustrating the impact of the new RCC materials model on the design of an RCC arch dam, only the relevant design issues in respect of Changuinola 1 Dam are discussed.

For Changuinola 1 Dam a comprehensive thermal analysis was undertaken on the basis of measured materials properties, recorded climatic data from the site and the proposed construction programme[5]. A basic outline of the thermal analysis is provided in Chapter 5 of this Thesis. On completion of the dam construction, the model applied external conditions equivalent to the annual climate cycle and an assumed water temperature cycle for a period of a few decades, until it was evident that an annual equilibrium temperature cycle was reached. Comparing these temperatures with the placement and the maximum hydration temperatures, the applicable maximum, long-term temperature drop for a traditional RCC model (as per CVC) and the "New" model could be developed.

For the purposes of ensuring a realistic approach, an effective 2°C creep was applied for the "New" RCC model.

Figures 7.12 and **7.13** illustrate the effective structural long-term temperature drop that would consequently be applicable for the traditional and the "New" RCC materials behaviour model, respectively.

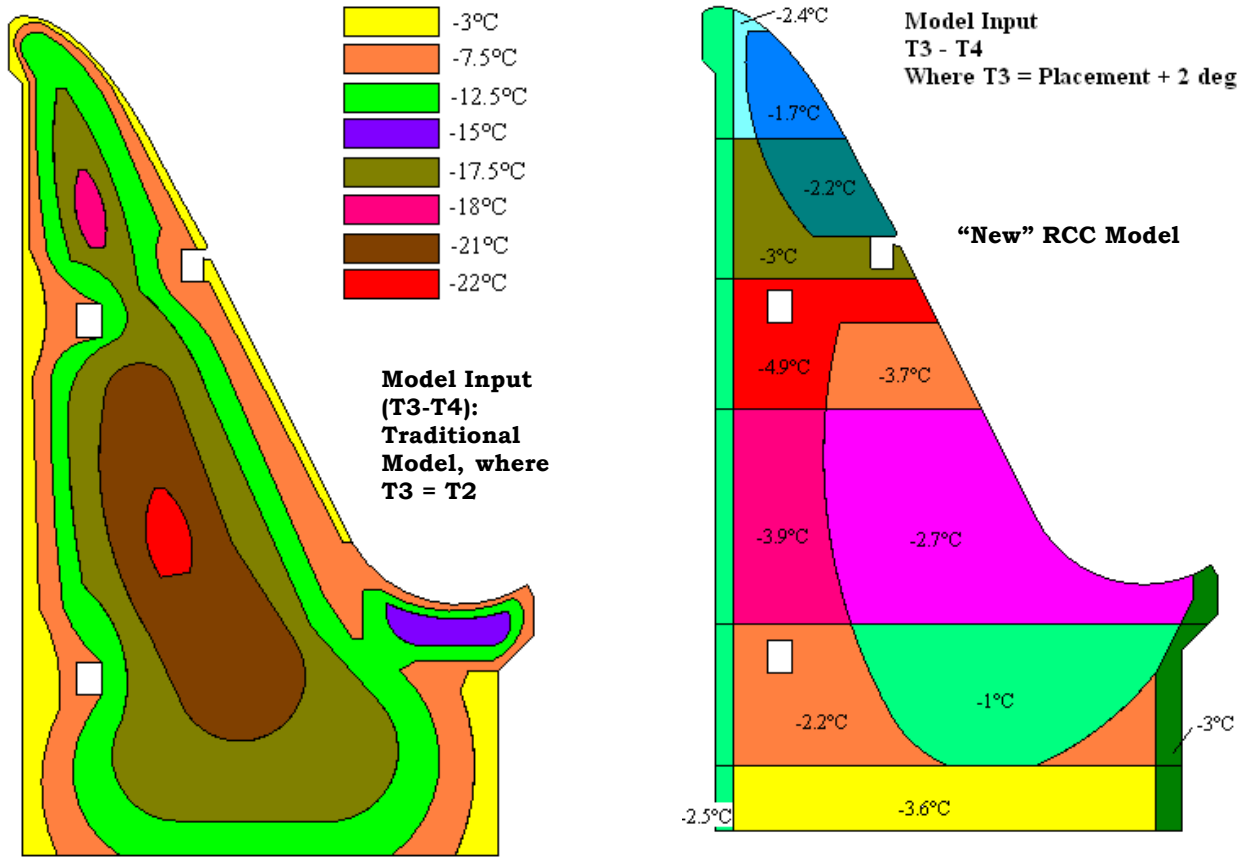

Figure 7.12 & 7.13: T3-T4 for Traditional and "New" RCC Materials Models (°C)

In addition, a study of potential cooling options was undertaken. Focusing on the section of the dam structure at and above the upper gallery, various options for the inclusion of cooling pipes were investigated. Realistically, only this upper section of the dam structure will carry any arch action under load and as long as this portion of the structure is effectively managed, ongoing cooling in the lower core of the structure can continue with no impact on the load carrying capacity of the dam.

A final arrangement was selected, whereby 4 No. 300 mm steel pipes were included in the dam model at 4 to 5 m vertical intervals between the upper gallery and the dam crest. Two cooling scenarios were subsequently analysed; one circulating chilled water at an average temperature of 6°C and the other circulating river water at approximately 25°C.

Figure 7.14 illustrates the temperatures of the concrete within the upper section of the dam structure on completion in April 2011, while **Figure 7.15** illustrates the same section after water at a temperature of 25°C has been circulated through the four cooling pipes for a period of 1 year and **Figure 7.16** illustrates the same situation after 4 months of circulation of water chilled to 6°C.

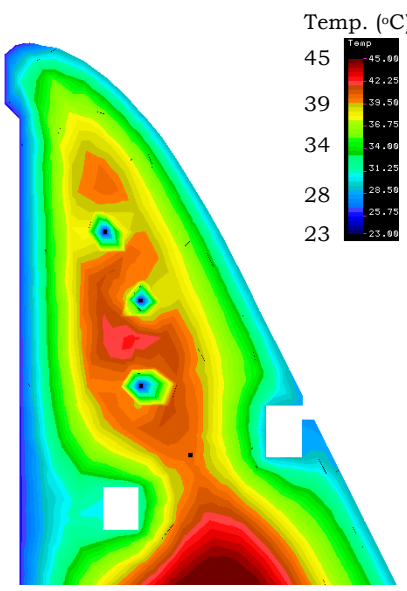

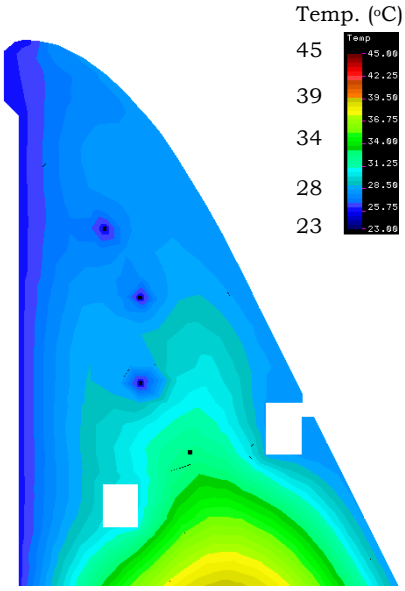

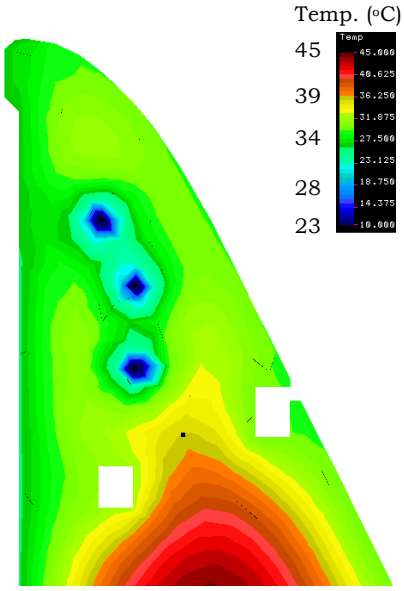

Figure 7.14
Temp. after Construction (°C)

Figure 7.15
12 months of 25°C Water

Figure 7.16
4 months of 6°C Water

7.3.6.4. Structural Design for Long-Term Temperature Drop

Traditional RCC Materials Model

According to the traditional RCC materials behaviour model, an 18°C structural temperature drop would be experienced within the core of the important upper section of the Changuinola 1 Dam structure. Over a crest length of approximately 500 m, this would imply a total shrinkage of the order of 90 mm. This is a very significant figure and, without completing a structural analysis, it can be stated with confidence that such a temperature drop would undoubtedly unacceptably compromise the structural integrity of the dam. Consequently, adopting a traditional RCC materials behaviour model implies that at least the crest of the dam structure must be cooled significantly and grouted before impoundment loading is commenced.

Circulating water chilled to between 4 and 6°C through the 300 mm steel pipes previously discussed, such cooling could be achieved within 4 months of the dam completion. A period of a full 12 months would be required if water were to be circulated at approximately 25°C.

Considering a penalty of US$ 90 000 per day for delayed commissioning of the hydropower project of which Changuinola 1 Dam is a part, there can be no question of delaying impoundment to grout the dam structure. While it would probably be possible to accommodate the 4 month 6°C cooling period within the envisaged construction programme, the impact of the significant temperature gradients between the upper section and the lower core section of the dam wall would still have to be investigated in great detail.

Proposed New RCC Materials Model

In the case of the proposed "New" RCC materials behaviour model, the thermal analyses indicated that a structural temperature drop of just 1.7 to 3°C would be applicable for the upper section of the dam, even allowing for an additional 2°C creep effect.

In order to ensure a significant level of conservatism, the proposed dam structure was analysed for long-term structural temperature drops of up to 6°C using the COSMOS[7] Finite Element structural analysis software. **Figure 7.17** illustrates the dam analysis model used, including a large massless foundation block, while **Figures 7.18** to **7.25** illustrate the critical stresses and displacements for the dam under full supply loading conditions (non-linear analysis), with and without a 6°C temperature drop applied across the full structure.

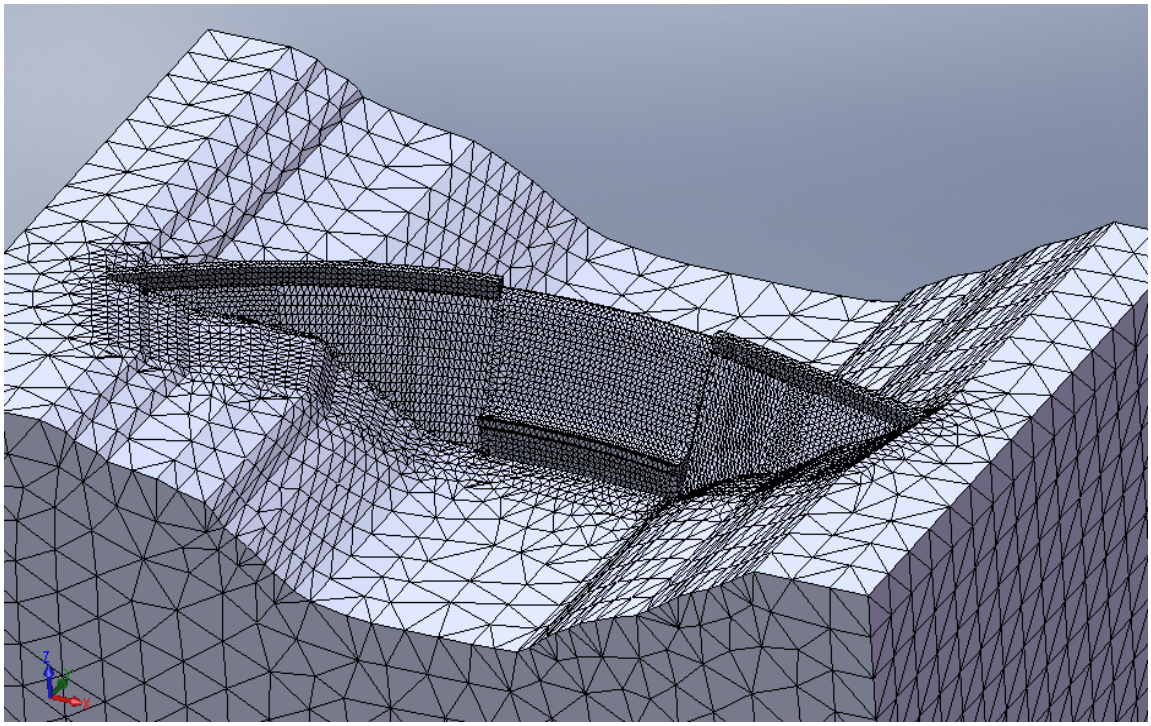

Figure 7.17: FE Analysis Model Mesh

For the above FE model, the extremes of the foundation block were constrained against movement in all directions. The 6°C temperature drop was uniformly applied to the dam wall, but not to the foundation. While this will give rise to exaggerated stresses immediately against the foundation, it is the stress state higher up the dam structure that is of specific interest in terms of this exercise.

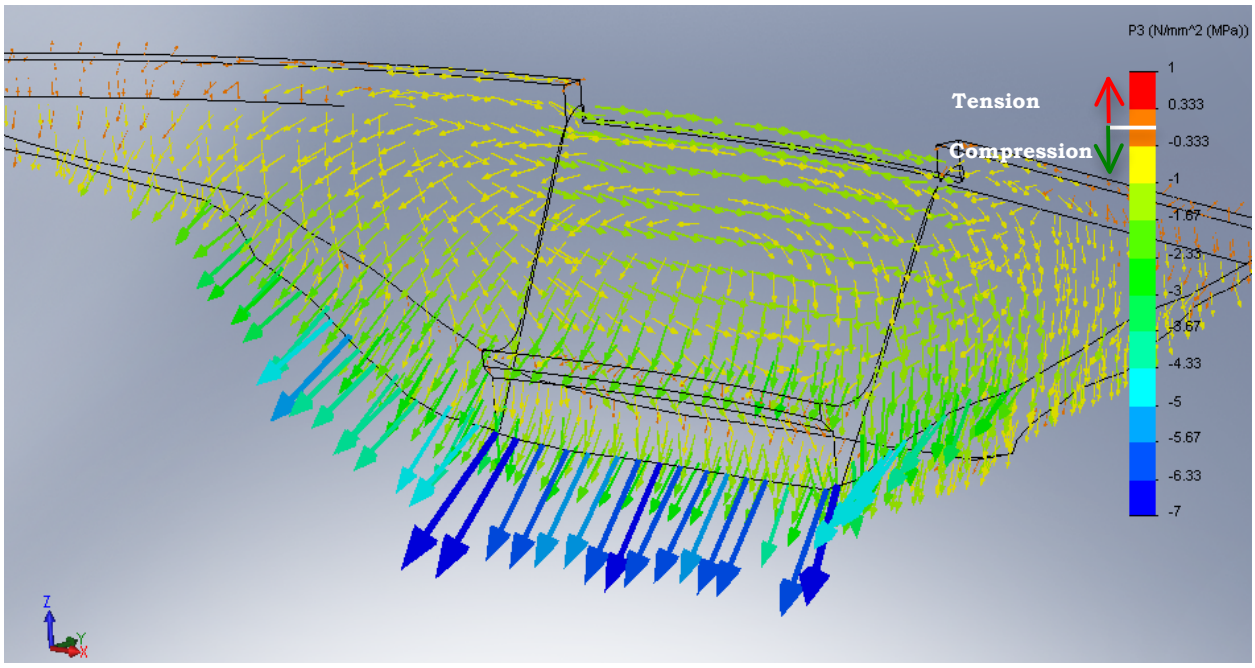

Figure 7.18: Maximum Principal (Surface) Stress Plot for FSL Load Case

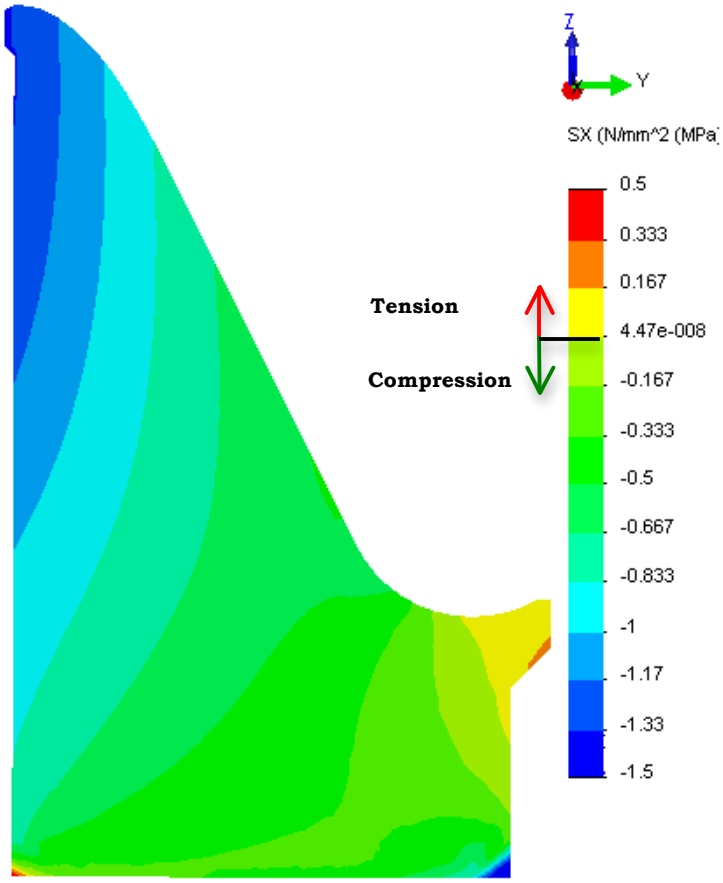

Figure 7.19: Horizontal Stresses (due to Arch Action) on Crown Cantilever for FSL Load Case (No Temperature Drop)

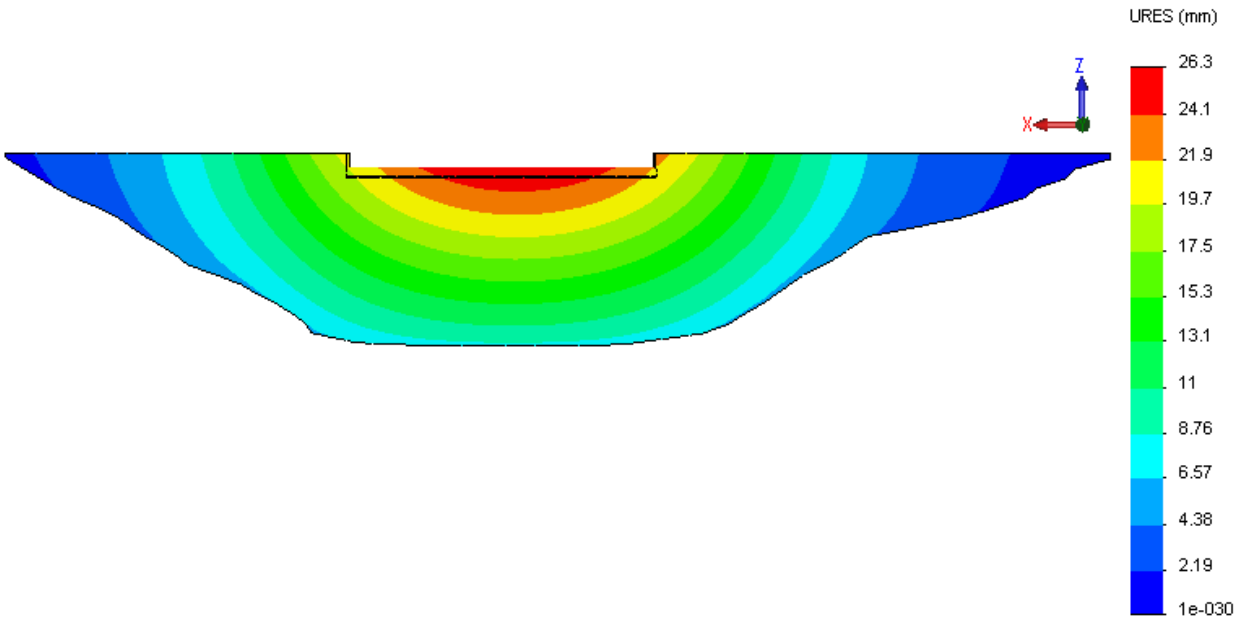

Figure 7.20: Maximum D/S Displacements for FSL Load Case (viewed from U/S)

As illustrated, ignoring temperature drop loading, the zone of arching covers almost the entire dam section, with arch stresses peaking at the upstream crest and progressively reducing with height and in a downstream direction. The maximum compressive arch stresses are 1.5 MPa.

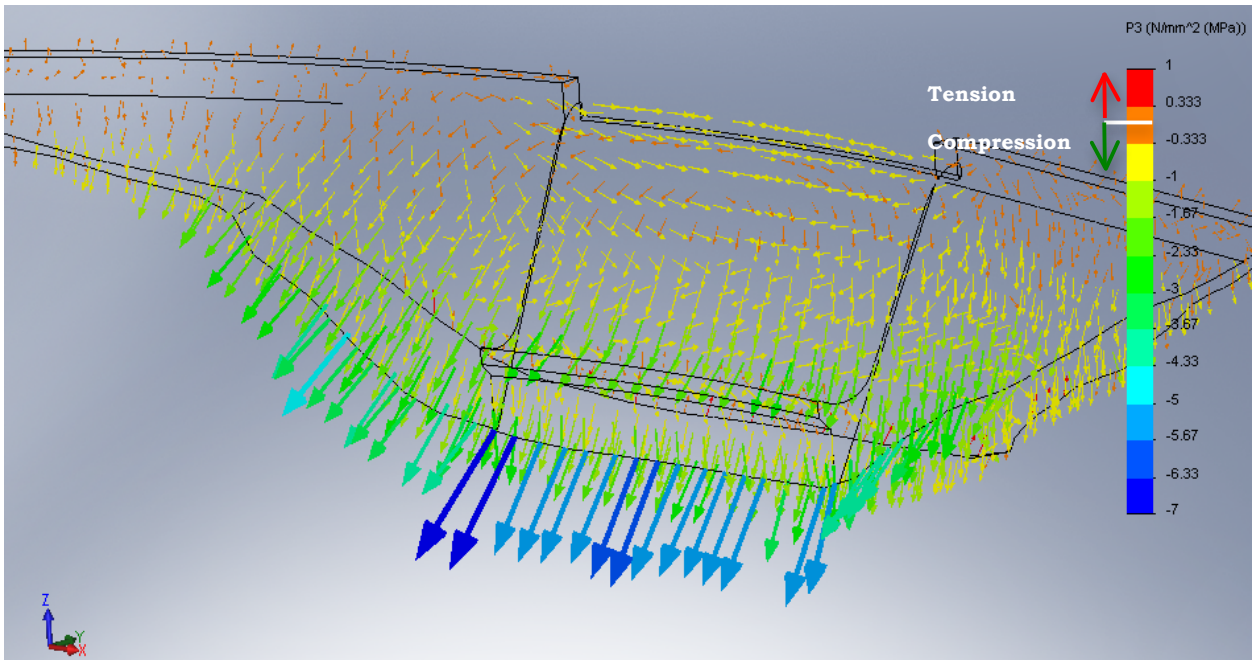

Figure 7.21: Maximum Principal (Surface) Stress Plot for FSL + 6°C Temperature Drop Load Case

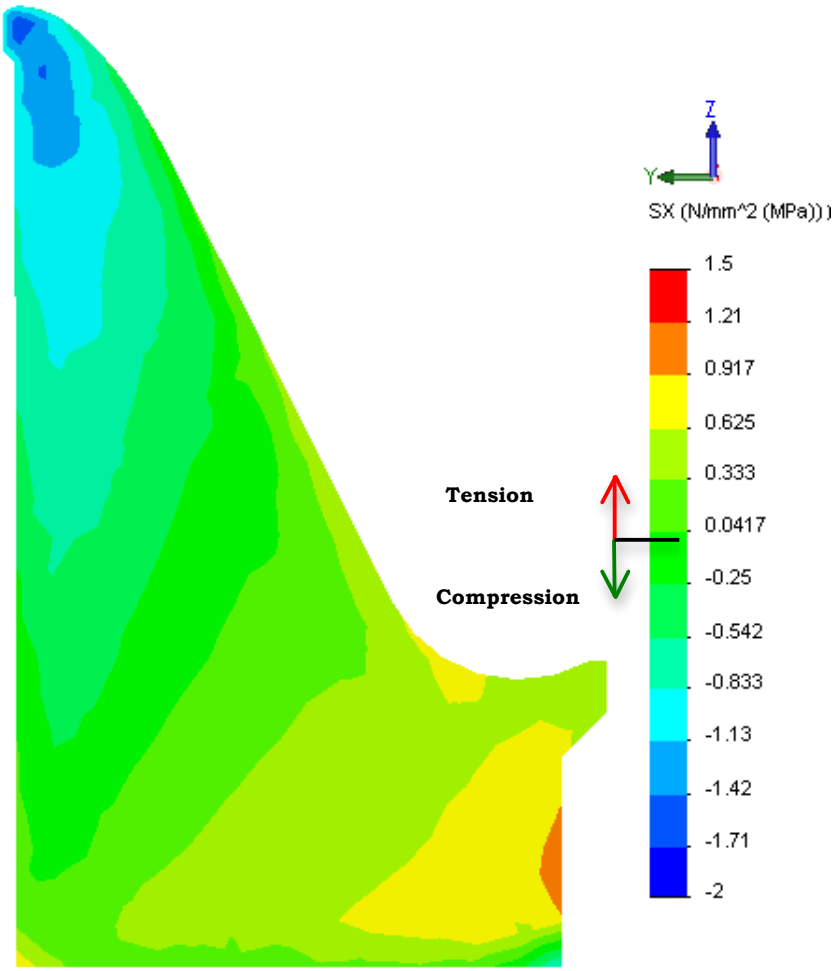

Figure 7.22: Horizontal Stresses (due to Arch Action) on Crown Cantilever for FSL + 6°C Temperature Drop Load Case

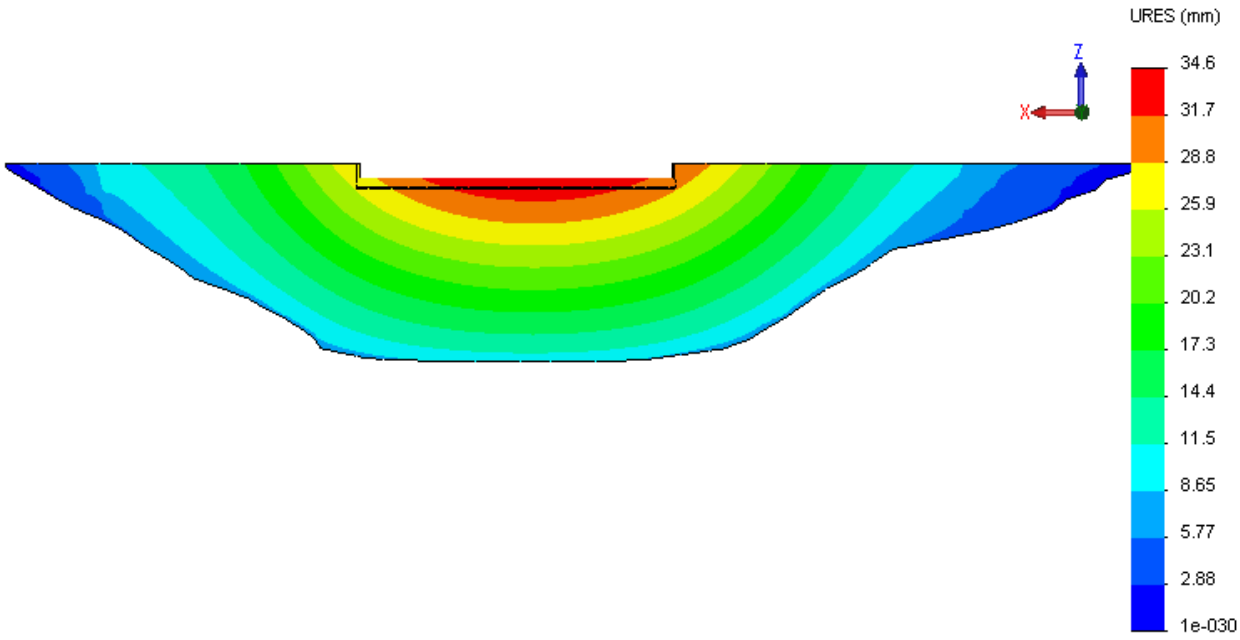

Figure 7.23: Maximum D/S Displacements for FSL + 6°C Temp. Drop Load Case
(Viewed from Upstream)

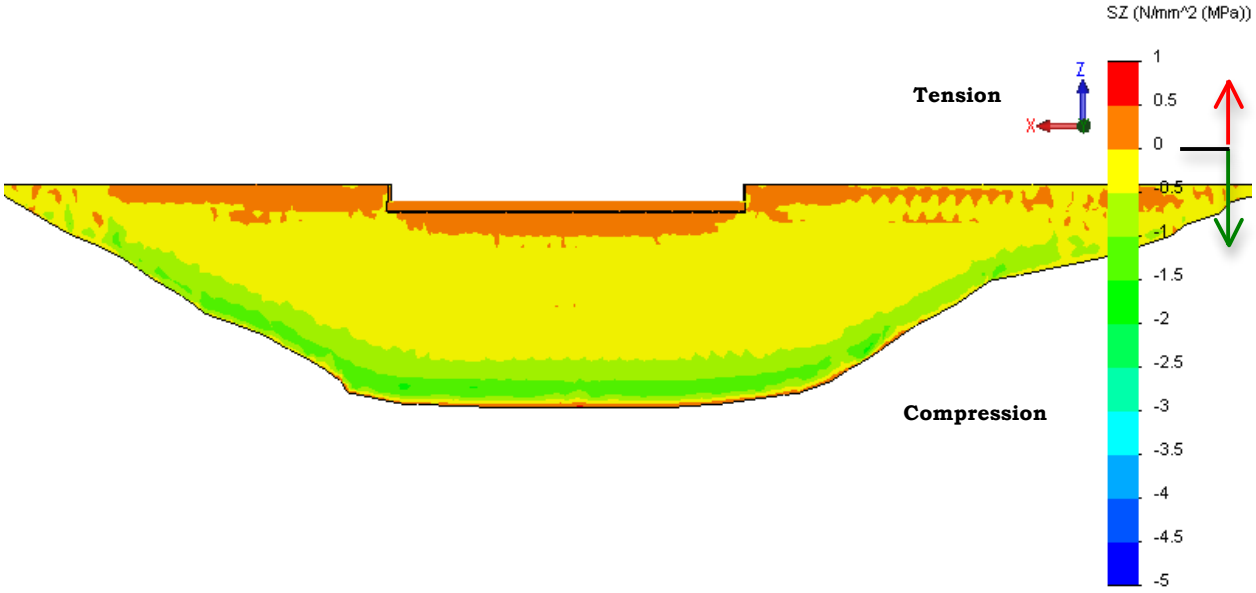

Figure 7.24: Upstream Face Vertical Stress for FSL + 6°C Temp. Drop Load Case

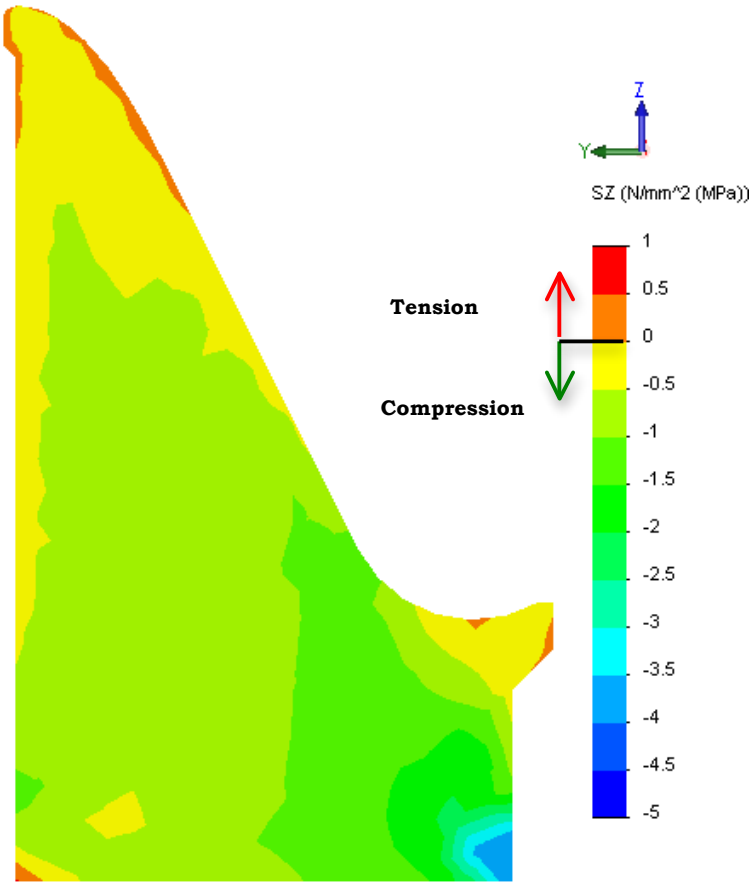

Figure 7.25: Vertical Stress on Crown Cantilever for FSL + 6°C Temp. Drop Load Case

The analysis completed applied a uniform deformation modulus with a limiting vertical RCC tensile strength of 500 KPa, which is conservative, as the RCC has been designed for a characteristic vertical tensile strength of 1.07 MPa. The materials property curve applied assumed that the RCC indicated a deformation modulus of 15 GPa for compression stresses and tensile stresses below 500 KPa. For tensions exceeding 500 KPa, the deformation modulus was reduced to zero.

Applying the 6°C temperature drop load, the arch stresses become more horizontal through the central section of the structure, but dip down more steeply through the gravity flanks. The maximum arch stresses increase to approximately 2 MPa, while the maximum downstream crest displacement increases from 26 to approximately 35 mm. The displacement plot also illustrates the evenness of the arch deflections, indicating that the structure retains an effective and efficient action, despite the imposition of the temperature drop.

The section presented in **Figure 7.22** illustrates unsurprisingly that arch stresses peak at the dam crest and decrease with height, while it can further be seen that a very substantial part of the dam structure still experiences arch compression stresses. Comparing the crown-cantilever arch stresses with and without the temperature drop, however, the introduction of horizontal tensile stresses on the downstream face as a consequence of the temperature drop is clearly evident.

Although the analyses demonstrate that the structural function of the Changuinola 1 arch/gravity structure would be compromised by the imposed 6°C temperature drop, reducing the total load carrying capacity, the relatively conservative geometry of the dam ensures that all critical stresses remain well within the capacity of the RCC, confirming the fact that the structure can satisfactorily withstand a temperature drop of this level, without joint grouting.

While a 500 KPa limiting vertical tensile strength was applied for the structural analyses, it can be seen that the residual tensions were confined to a very localized area at the heel of the structure, with the remainder of the base of the dam on the central section exhibiting compressive bearing stresses.

7.3.6.5. Discussion of Results

The above design example illustrates very simply the critical beneficial impact that the new RCC materials behaviour model will have on the future design of RCC arch dams.

Applying the traditional model would imply that extensive joint grouting would be required before loading of the dam could be permitted. In view of the fact that this grouting could only realistically be undertaken after adequate cooling of at least the upper section of the dam structure had been successfully achieved, a very significant impact on the dam design and the construction programme could be anticipated. On the other hand, structural analysis using the new RCC model, even when conservatively applied, suggests that the dam structure would perform quite adequately without joint grouting, removing any constraint on impoundment. To maintain even greater levels of conservatism and to recognise that new developments

take time to gain general acceptance, Changuinola 1 Dam will be constructed with a groutable induced joint system installed in all of the structurally critical sections of the dam structure. The option of artificially cooling the concrete of the upper dam structure with water circulated through large steel pipes will also be retained until the properties of the RCC have been adequately confirmed.

It should further be noted that testing is currently underway at Changuinola 1 Dam to verify the fact that no significant creep will be encountered in the high quality RCC to be placed there and to verify the effectiveness of the joint inducing and grouting systems to be installed.

It should further be noted that the structural/thermal analyses have indicated significant upstream movement of the dam crest under gravity and temperature loading and accordingly, low containment stresses in the critical central upper arch will very likely prevent any creep being incurred during the hydration temperature rise.

7.3.7. CONCLUSIONS

7.3.7.1. Summary of Findings

In this Chapter, the author has illustrated the very significant impact of the new materials model for RCC on the design of large new gravity and arch dam structures. Furthermore, the findings of the investigations addressed herein go a substantial distance in removing a significant impediment in the design of large RCC dams. If RCC does not suffer from many of the problems inherent to CVC, there is no reason to be compromised by those problems in the design of RCC dams.

7.3.7.2. The Impact of the New Understanding of RCC Materials Behaviour

Adopting the proposed new understanding of the early behaviour of RCC, or the “New” materials behaviour model for RCC, consideration can be given to the construction of RCC arch-type dams in temperate climates without groutable joints, while the need and approach to pre- and post-cooling of RCC will require a re-think.

7.3.7.3. Application of the New Understanding of RCC Materials Behaviour

Considering the fact that the proposed new understanding of the early behaviour of RCC has yet to be broadly tested and explored, it should be conservatively applied at this stage. However, it is considered that testing of RCC on a full-scale trial should be routinely undertaken in an effort to more clearly understand the nature of the specific RCC to be used at each and every dam. Furthermore, the inclusion of appropriate temperature and strain measurement instrumentation in all RCC dams is encouraged as a means to develop a broader database and to better understand how, when and why RCC behaves differently to CVC. On the basis of this information, associated confidence levels will be increased and it will consequently be appropriate to apply the new materials understanding for RCC less conservatively.

Testing at Changuinola 1 Dam has verified the functionality of the joint inducing and grouting system to be installed. During early testing with grouting of the joint system to be included in the main dam structure, it proved possible to sustain a grout pressure of 2 MPa and to consequently break open and comprehensively grout a crack.

In the event that it is decided to grout the installed system at Changuinola 1, the 2 MPa grout pressures that can be achieved would be able to effectively mitigate the impacts of a 13°C temperature drop. This would also potentially allow the grouting of induced joints while the dam structure is under load, implying that grouting might not need to delay the impoundment date.

Testing is also ongoing on the main dam at Changuinola 1 in effort to confirm whether any shrinkage, or creep in the RCC might be experienced during the hydration cycle. Should this testing yield meaningful results, it is considered that the groutable joint system will be installed as a safety back-up, with the intention only to grout the joints should some unexpected behaviour be observed.

7.4. REFERENCES

[1] United States Army Corps of Engineers. *Arch Dam Design.* Engineering Manual, EM 1110-2-2201. USACE. Washington. May 2004.

[2] United States Army Corps of Engineers. *Thermal Studies of Mass Concrete Structures.* Engineering Technical Letter, ETL 1110-2-542. Washington. May 1997.

[3] American Concrete Institute. ACI 207.2R-07. *Effects of Restraint, Volume Change, and Reinforcement of Cracking of Massive Concrete. Part 1.* September 2007.

[4] United States Army Corps of Engineers. *Roller Compacted Concrete.* Engineering Manual, EM 1110-2-2006. Washington. January 2000.

[5] Greyling, RG & Shaw QHW. *Changuinola 1 Dam. Thermal Analysis Report.* Report No. 4178/11436-R1. MD&A. July 2010.

[6] Structural Research and Analysis Corporation (SRAC). *COSMOSM Finite Element Analysis Program.* General-purpose, modular FE Analysis system. SRAC, a division of SolidWorks Corporation, Dassault Systemes S.A., Paris, France.

[7] Shaw, QHW. *The Role of Temperature in Relation to the Structural Behaviour of Continuously Constructed RCC and RMC Dams.* MSc Thesis. University of Brighton, UK. 2001

[8] Shaw, QHW. *The Development of RCC Arch Dams.* Proceedings. 4th International Symposium on Roller Compacted Concrete Dams. Madrid, Spain. pp 363-371. November 2003.

[9] Zhu, B. *RCC Arch Dams: Temperature Control and Design of Joints.* Journal of International Water Power and Dam Construction. Wilmington Media. Sidcup, UK. August 2006.

[10] Leguizamo, P.M. *La Miel I Dam – Design of the Geotechnical and Structural Instrumentation Program for the World's Highest RCC Dam.* Roller Compacted Concrete Dams. Proceedings. 4th International Symposium on RCC Dams. Madrid, Spain. pp 633 – 640. November 2003

[11] Dazhi, W & Xu, W. *Temperature Control for RCC Dam at Longtan Hydropower Station.* New Progress on RCC Dams. Proceedings. 5th International Symposium on RCC Dams. Guiyang, China. pp 213 – 222. November 2007.

[12] Bo, D & Gangwei, C. *Studies of the Construction Technology under High Temperature Condition and its Application in Longtan Dam.* New Progress on RCC Dams. Proceedings. 5th International Symposium on RCC Dams. Guiyang, China. pp 213 – 222. November 2007.

CHAPTER 8

8. STUDY CONCLUSIONS

8.1. INTRODUCTION

In this Chapter, the author summarises the investigations and studies undertaken, presents the conclusions that can be drawn and discusses the important implications and applications of his research in respect of the future design of large RCC dams.

8.2. BACKGROUND

8.2.1. RCC DAMS: OBSERVATION & DESIGN

The author of this work has over 25 years experience in the design and construction of major RCC dams and over this period, his observations have repeatedly suggested a quite different behaviour and performance for high-paste RCC in dams compared to that universally assumed and applied in design. The behaviour of concrete during the exothermic process of hydration and the subsequent heat dissipation has always required careful management in the construction of large dams. With a continuous, horizontal construction and an approach of inducing, rather than forming, transverse joints, these issues are of equal if not greater concern in the case of RCC.

Yet, designers and design literature still fail to take cogniscance of the differences between CVC and RCC. There are undoubtedly a number of reasons for this fact; the difficulties associated with testing the early properties of RCC, the variability of RCC types and approaches applied to date and most importantly, the fact that assuming early CVC behaviour properties for RCC is generally conservative, at least in the case of gravity dams. However, as RCC arches and arch/gravity dams gain increasing acceptance, the unqualified application of CVC models, or models that incorrectly predict the behaviour of RCC, carries a certain number of risks.

Structurally, RCC is substantially more susceptible to shrinkage and creep in an arch dam than is CVC, due to the fact that an RCC dam is not constructed in vertical monoliths, with groutable joints in between, and as a result of the fact that cooling pipe loops cannot be as easily installed. It is consequently imperative to be able to quantify the respective impacts of temperature drop loads on RCC in arch dams and accordingly to understand when and by how much induced joints are likely to open.

8.2.2. LITERATURE & REFERENCES

Much has been published over the years on the design and construction of RCC dams. Amongst this work, a constant thread can be observed in the fact that whenever the

early thermal behaviour of RCC is analysed, the shrinkage and creep behaviour characteristics of CVC are applied. While the author would have seen significant advantage in being able to reference similar and related work on RCC, a large part of the motivation for the investigations undertaken was the apparent absence of earlier studies that have investigated the differences between early CVC and particularly high-paste RCC behaviour on prototype structures.

It is considered extremely pertinent to note that the literature searches undertaken during the course of the studies addressed herein repeatedly encountered cases that simply assumed and applied CVC materials models for RCC.

Certainly, some work has been undertaken to investigate the early drying shrinkage and creep behaviour of RCC, but this has been laboratory-based and most specifically related to lean mix (low strength) RCC. Consequently, very little of the published literature and investigation findings has much relevance to high-paste RCC.

While many thermal and structural analyses of RCC dams have been presented in technical literature, not a single one has been encountered that compares the actual behaviour of RCC on a prototype dam structure with that predicted through analysis.

8.2.3. RCC MATERIALS TESTING

One of the most significant reasons that RCC materials models have to date not realistically represented RCC behaviour in application is considered to be the methods applied for laboratory testing.

When the behaviour of high-paste RCC in a dam structure is so dependent on the aggregate skeletal structure developed through the method of construction, it is essential that this same structure be recreated in samples tested. Realistically, this cannot be achieved in a laboratory. The process of kneading and orientating the aggregate structure that happens on a large scale beneath a vibratory roller simply cannot be recreated with the tools available on a laboratory scale, or within the context of a 150 mm mould, or cylinder. Drilled cores will better reflect reality. However, even the scale of a 150 mm diameter core is probably too small. Furthermore, it is notoriously difficult to extract a core from immature RCC, implying that the current methods available for early creep and shrinkage testing of RCC simply cannot produce results with adequate levels of confidence. Testing RCC mortar, or samples compacted with the coarse aggregates screened off, in a small cube, or cylinder can never realistically be expected to reflect the properties of the in situ material.

Due to the compaction method applied, it is also more than likely that the aggregate skeletal structure would indicate greater strength in RCC in a horizontal, rather than a vertical direction. In view of the fact that the majority of strength and elasticity testing on RCC samples is likely to be orientated in a vertical direction, the validity of the results is compromised in respect of the critical horizontal behaviour characteristics that are of most relevance to temperature effects in arch dams.

8.2.4. FOCUS OF WORK ADDRESSED IN THIS STUDY & RESEARCH OBJECTIVES

The primary focus of the work addressed in this study was to demonstrate that high-paste RCC in large dams does not necessarily behave in the same manner as CVC under the early hydration heating and cooling cycle. On the basis of observation and instrumentation data records at five prototype RCC dams, as presented in Chapter 2, indications of RCC behaviour are derived. For the first time in the development of the technology, this study subsequently develops a new understanding of the behaviour of high-paste RCC in a large dam through a comparison of the three-dimensional structural behaviour of a prototype structure with that predicted using a comprehensive Finite Element model.

Through the research and investigations completed, the key research question is answered and it is consequently demonstrated that the traditional approach to dam design for shrinkage and creep during the hydration cycle is not applicable in the case of high-paste RCC dams.

8.3. THE EVIDENCE OF RCC MATERIALS BEHAVIOUR IN LARGE DAMS

8.3.1. GENERAL

The first stage of investigation of the apparent early behaviour of RCC involved a direct interpretation, as far as this was possible, of measurements recorded through the instrumentation installed at Wolwedans and Knellpoort Dams in South Africa, Çine Dam in Turkey, Wadi Dayqah Dam in Oman and Changuinola 1 Dam in Panama, as presented in Chapter 4.

8.3.2. WOLWEDANS & KNELLPOORT DAMS

The instrumentation data recorded at both the Wolwedans and Knellpoort dams suggests a relatively linear relationship between temperature and strain across the induced joints (see **Figures 8.1** and **8.2**).

Making a general interpretation of the measurements made, it is apparent that the core RCC experiences compression at temperatures above placement and tension at temperatures below that at placement.

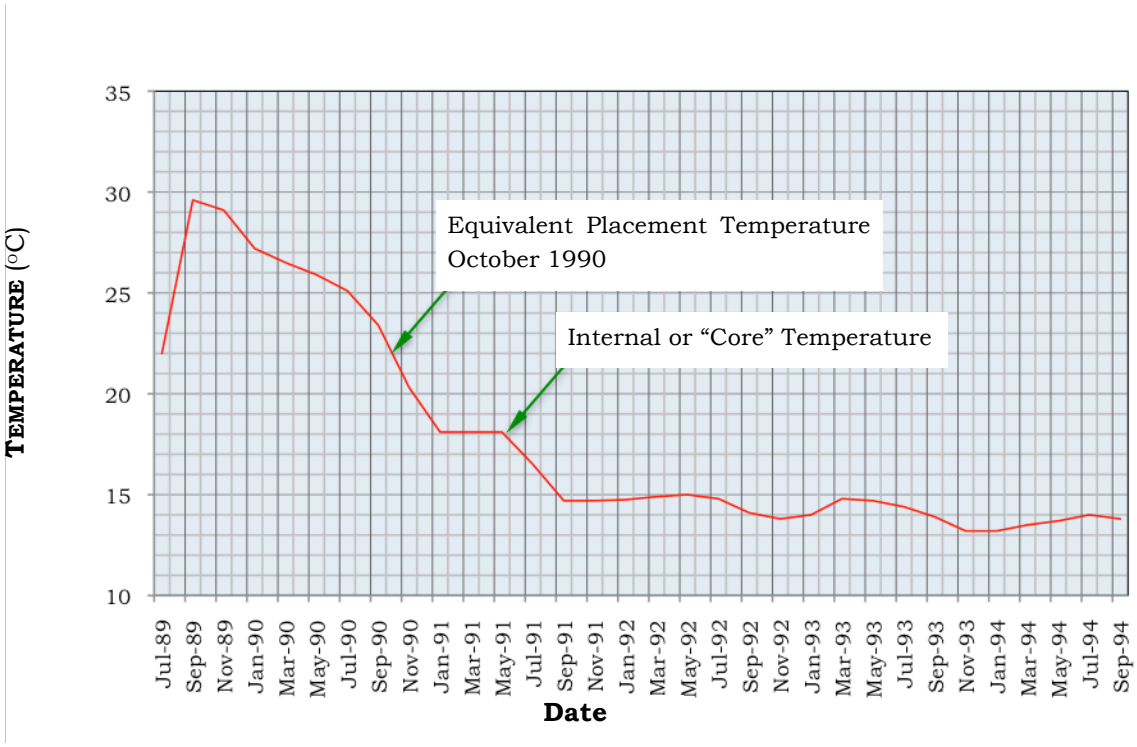

Figure 8.1: Typical "Core" Temperature – Time Curve for Wolwedans

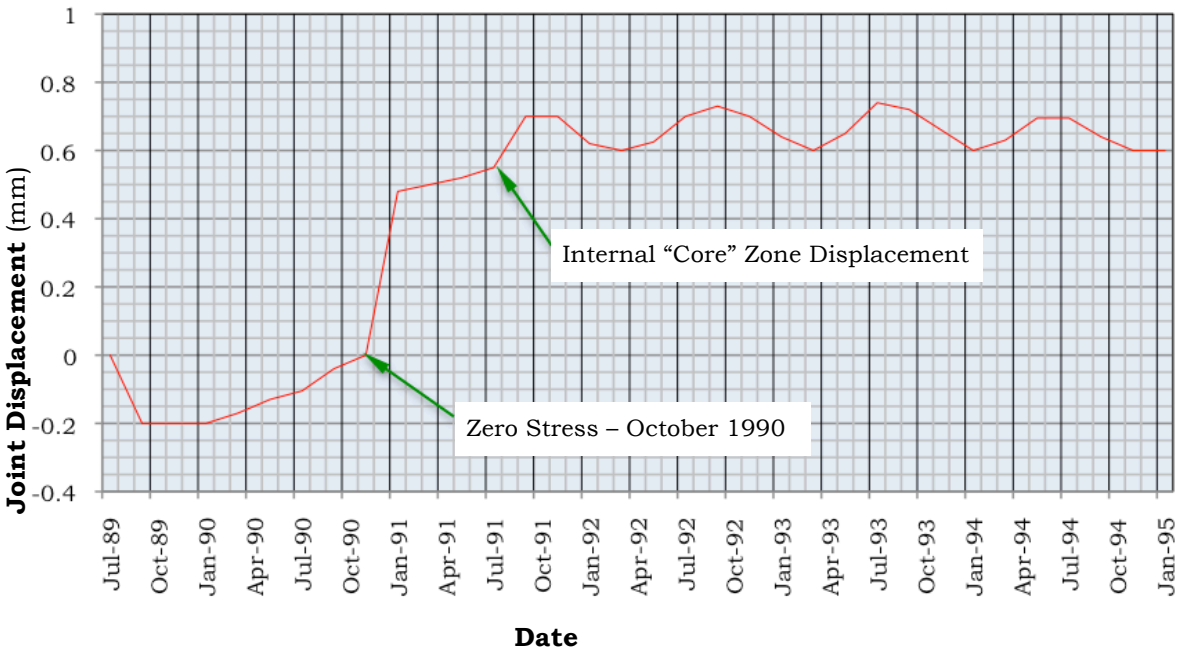

Figure 8.2: Typical "Core" Joint Opening – Time Curve for Wolwedans

In the case of Wolwedans Dam, only five of the 27 induced joints opened and of these, only three central joints were of significance, with the outer two realistically beyond the extent of the arch action. At the three open joints, the measured openings were

substantially less than a linear application of the apparent temperature drop from placement would suggest.

By the time that the hydration heat had effectively been dissipated from the dam structure at Wolwedans, the reservoir had essentially filled and accordingly, a certain amount of structural displacement had occurred. Consequently, the reason for the induced joint openings being less than anticipated could not be determined, whether it was the result of residual tensions between the induced joints, or structural deflection, or some other reason.

8.3.3. ÇINE DAM

The instrumentation data for Çine Dam illustrates a clear pattern. While the temperature within the core of the dam has remained elevated, with no significant dissipation yet evident, the Long-Base-Strain-Gauge-Temperature-Meters (LBSGTMs – also termed SGT gauges) have indicated no strain relaxation. The fact that a linear increase in closure strain was demonstrated on the induced joints when an increase in temperature was caused, between 1 and 2 years after placement, by the downward flow of heat within the structure, however, further provides strong evidence that no significant creep, or shrinkage in the RCC could have occurred, as illustrated in **Figures 8.3** and **8.4**.

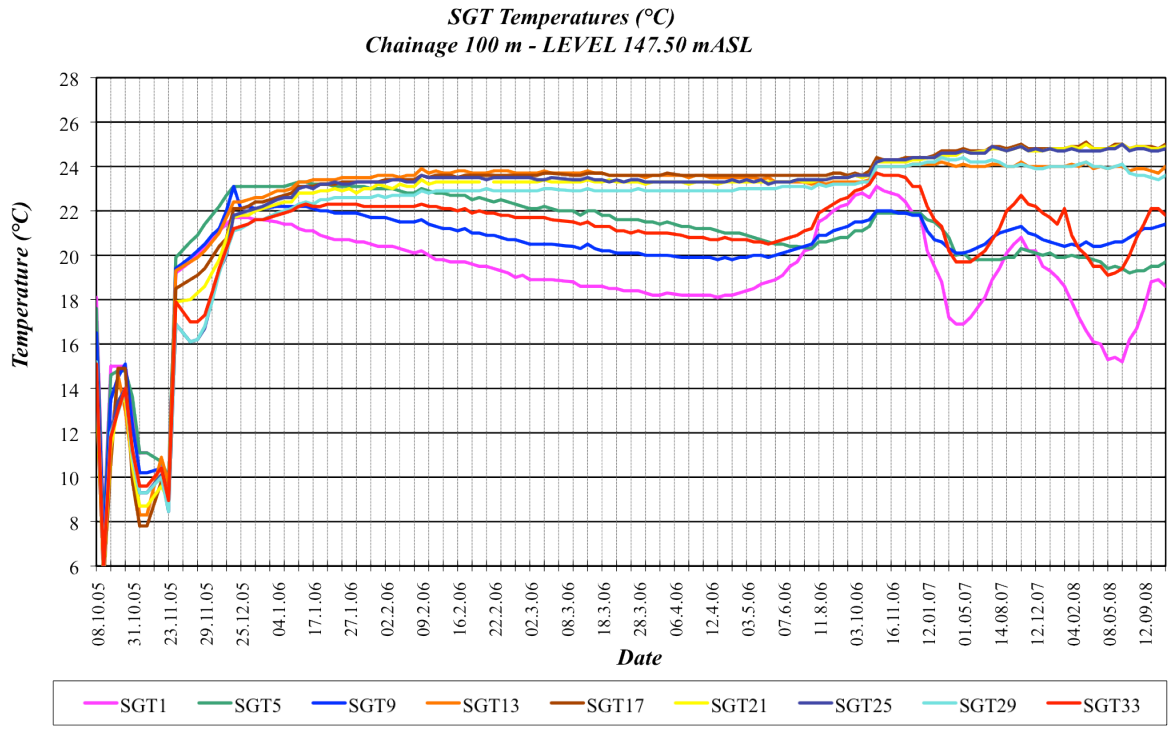

Figure 8.3: Typical "Core" & Surface Temperatures for Çine Dam

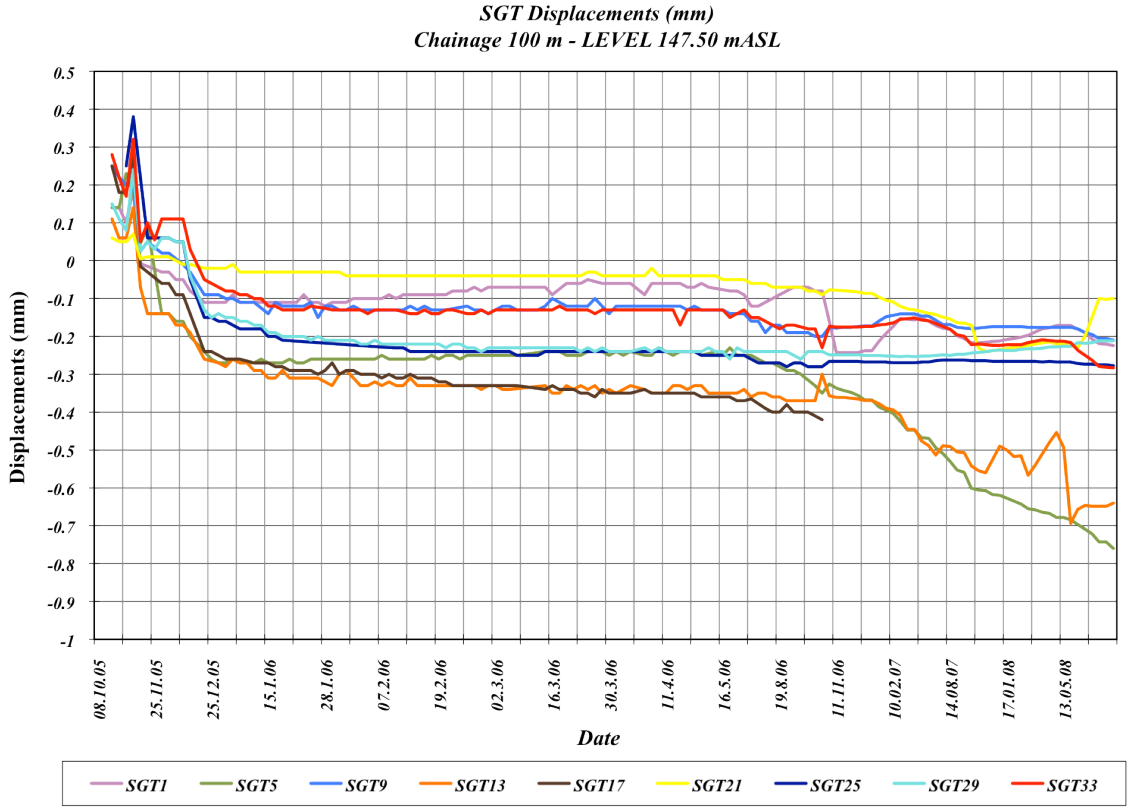

Figure 8.4: Typical "Core" Joint Displacements for Çine Dam

Measuring temperature and strain in the RCC at Çine Dam in an upstream-downstream direction (SGA gauges), in which the RCC is subject to less restraint, a total maximum thermal expansion strain of the order of 120 microstrain was recorded, as illustrated in **Figure 8.5**. For a hydration temperature rise of approximately 14°C, this strain translates into an equivalent RCC thermal expansivity of 8.4 x 10^{-6}/°C.

Over the period between 3 and 7 months after RCC placement, a strain relaxation of approximately 12.5% was measured, as illustrated in **Figure 8.6**, despite the fact that the temperature remained essentially constant.

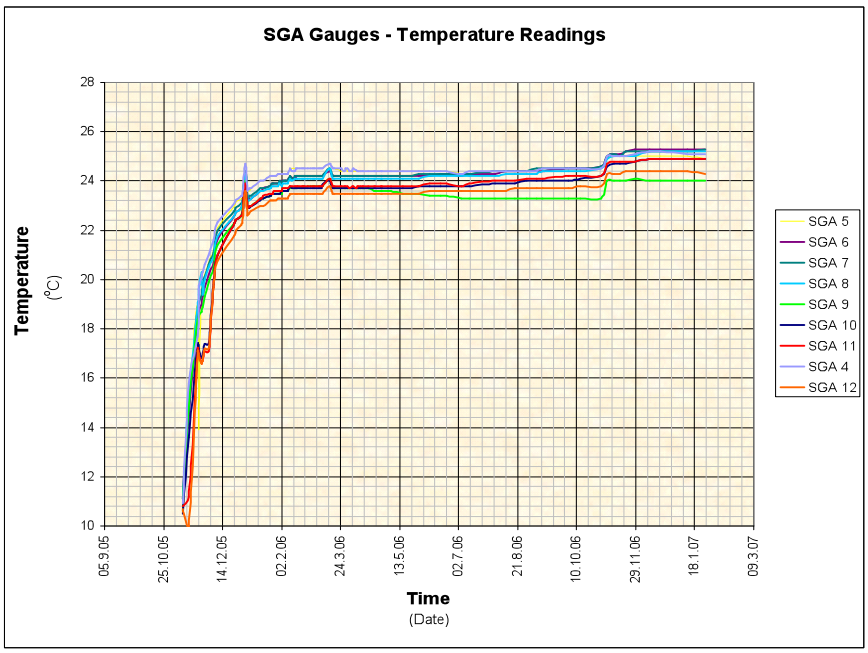

Figure 8.5: Temperature on U/S – D/S Strain Gauges

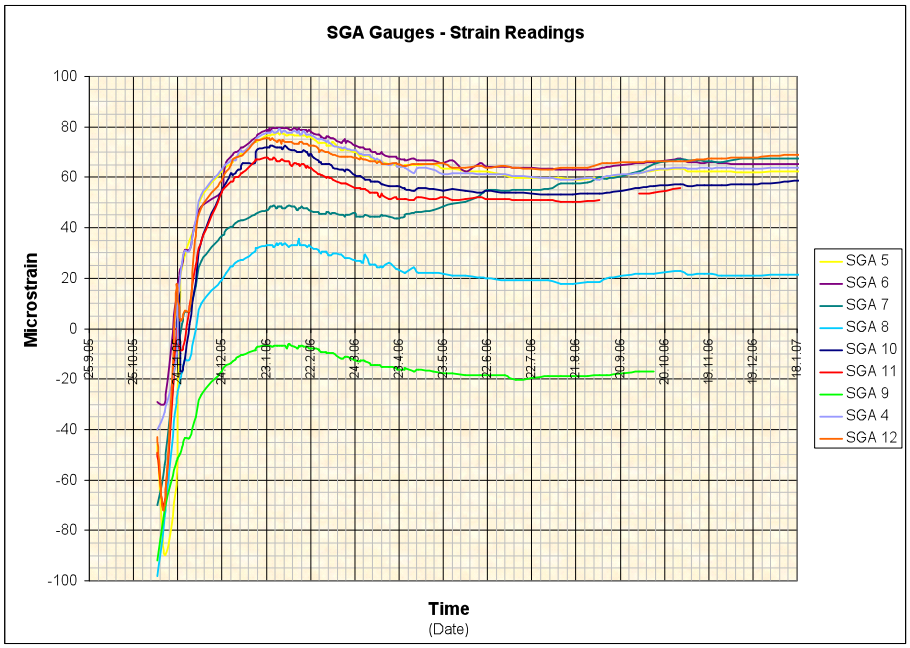

Figure 8.6: Strain Measured in Upstream-Downstream Direction

After the evident expansion strain relaxation of approximately 15 microstrain, the net effective expansivity corresponded more closely to the 7.1 x 10^{-6}/^{o}C measured for the Çine RCC in the laboratory.

8.3.4. WADI DAYQAH DAM

The RCC of Wadi Dayqah Dam was a lean mix, low strength material that did not perform, or behave as well as the RCCs of Wolwedans, Knellpoort, or Çine. While the precise performance of the RCC will never be known with any certainty and some significantly different behaviour was evident at the two separate levels instrumented, some shrinkage/creep could be determined in the instrument data.

In the case of Wadi Dayqah Dam, with core temperatures sustained at their hydration peak (see **Figures 8.7**), compressions gradually relaxed and tensions developed across the majority of the induced joints (see **Figure 8.8**). It is considered that the observed behaviour can be attributed to two factors; the fact that the gauges were installed into RCC that had reached its peak hydration temperature and was then cooled by the superposition of artificially chilled RCC, which subsequently expanded when warmed by the concrete hydration process and secondly, that some drying shrinkage and creep were probably experienced in the lean RCC, which contained a very high content of non-cementitious fines and aggregates with a very high moisture absorption.

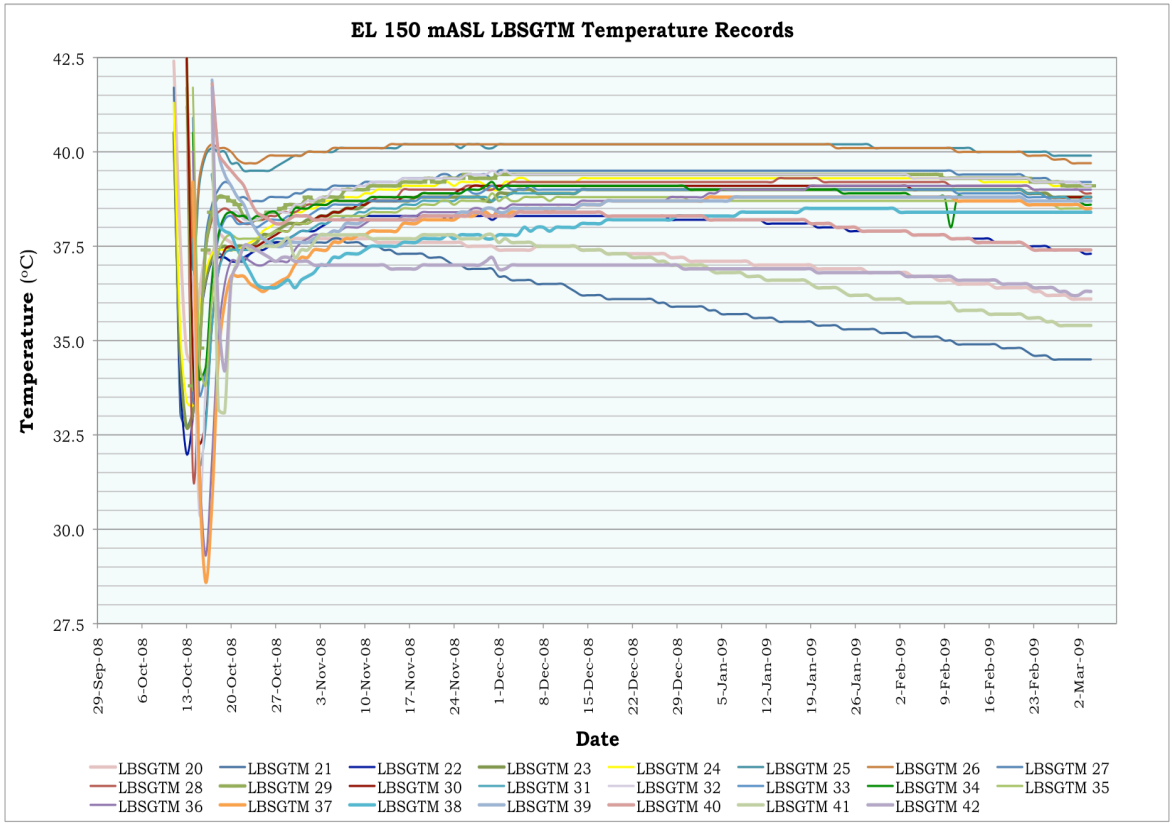

Figure 8.7: Typical Temperature History for Wadi Dayqah Dam

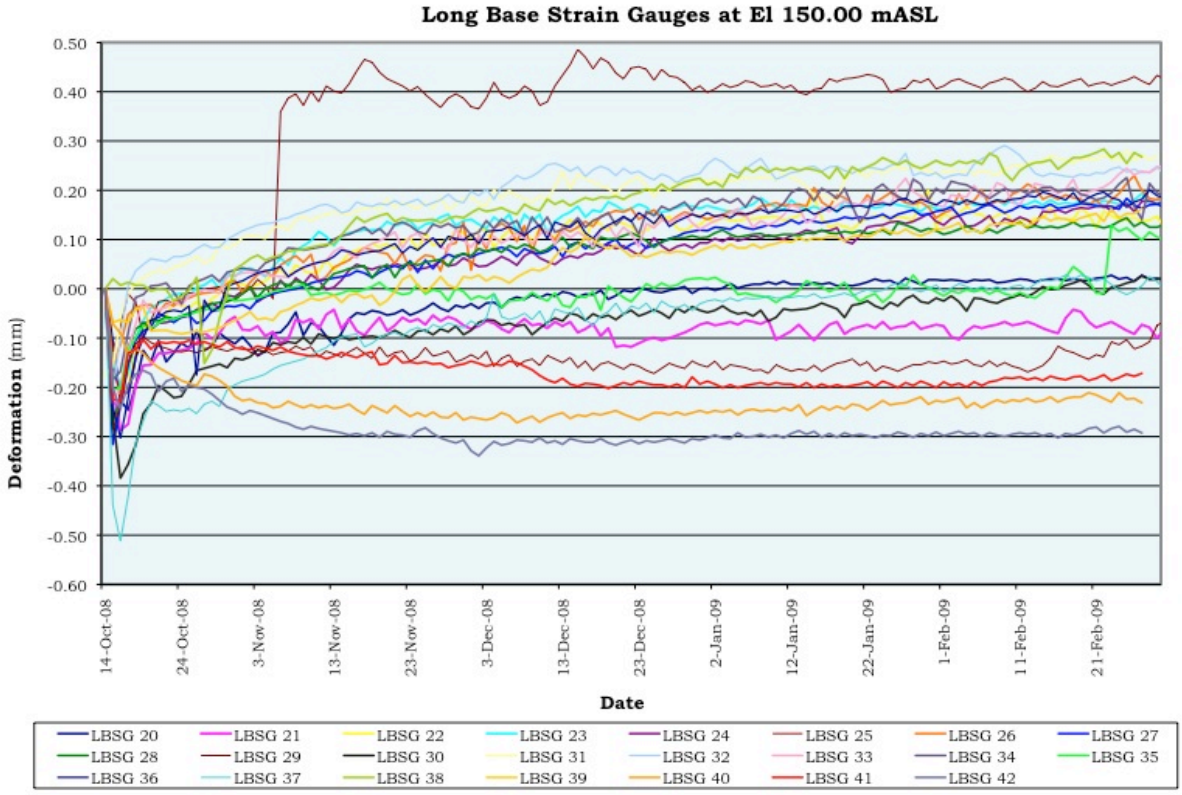

Figure 8.8: Typical Induced Joint Displacement for Wadi Dayqah Dam

A further paradox was observed in a complete disparity in the strain measured in the two separate levels of instrumentation installed. The strain measured in the second level of instrumentation, just 15 m above the first, was less than 30% of that measured on the instrumentation in the level below.

The Wadi Dayqah Dam RCC contained a high proportion of fine aggregates, a high content of non-cementitious fines and a high w/c ratio. The aggregate quality, shape and surface texture may also not have been ideal. Accordingly, all of the factors that are likely to increase shrinkage and creep in concrete were evident in the RCC at Wadi Dayqah Dam and despite this fact, the shrinkage measured was significantly less than that typically expected in CVC. As a consequence of the continued development of shrinkage after the RCC was experiencing tension, it is considered most likely that its primary origin lies in autogenous and drying shrinkage, as opposed to creep under stress.

8.3.5. CHANGUINOLA 1 DAM

At the time of writing, approximately one third of the RCC had been placed at Changuinola 1 Dam in Panama and while the first level of instrumentation had been installed, the data record was insufficient to provide any opportunity for useful analysis. A single strain gauge, however, was installed perpendicular to the dam axis directly into the high-workability, high-paste RCC during the initial placement and over six months of measurement was available for review. The associated record indicated almost identical behaviour to that from similar gauges at Çine Dam, with an initial linear thermal expansion reducing by approximately 12% over the first few months to reflect a consequent expansion proportional to the laboratory-measured coefficient of thermal expansion. Furthermore, cracks were observed in the RCC placement surface, when left exposed for several weeks, suggesting excessive thermal gradients and linear expansion under the hydration temperature rise.

8.3.6. SUMMARY

In summary, the above evaluations provided evidence suggesting that the RCC at Wolwedans, Knellpoort and Çine Dams suffered no perceptible autogenous, or drying shrinkage and no creep shrinkage under restrained thermal expansion. While the instrumentation at Çine Dam indicated that some expansion strain relaxation occurred when the RCC thermal expansion was partly unrestrained, the fact that linear thermal expansion was evident in such a massive section of concrete (> 100 m in length), where significant internal restraint would normally be expected to constrain such expansion, was considered surprising. Recording almost identical behaviour in the RCC of Changuinola 1 Dam was considered to provide a significant validation of the apparent resilience of immature high-paste RCC to creep under thermal expansion.

While a quantitative interpretation of the findings at Wadi Dayqah Dam was somewhat more complicated, it is considered that some drying shrinkage must have occurred, quite possibly related to the use of lower quality aggregates. It is, however, considered

particularly significant that this behaviour was only determined in the single example of lean RCC reviewed in this study. Although this implies that some additional care must be taken in determining appropriate aggregates for RCC in the case of dam designs that are susceptible to materials shrinkage, it also serves to confirm that similar behaviour would have been observed at Wolwedans, Knellpoort, Çine and Changuinola 1 should any significant drying/autogenous shrinkage, or creep have occurred in the RCC at these dams.

8.4. MODELLING THE BEHAVIOUR OF RCC IN LARGE DAMS

8.4.1. GENERAL

While the observations made on the basis of the data gathered at the five dams clearly demonstrate that the extent of any shrinkage and creep that might have developed in the RCC during the early hydration heating and cooling cycle is undoubtedly very substantially less than would typically be the case for CVC, it appeared that these effects were in fact negligible, or even completely absent in the cases of Wolwedans and Knellpoort dams. This assertion, however, could not be proved quantitatively through simply reviewing the available data, as the influence of too many potential secondary factors could not be ascertained with any certainty.

As it is currently only realistically possible to measure strain in RCC, the associated stresses could not be determined and, while it was obvious that the induced joint openings were substantially less than the traditional theory would have anticipated, it could not be determined whether significant residual stress was evident between the joints, or whether some joint closure had occurred as a consequence of the 3-dimensional structural deflections in the case of the arch dams.

In view of the comprehensiveness of the instrumentation and monitoring, the availability of data, its three dimensional structural function and the fact that the dam has remained relatively consistently full from 2 years after completion, Wolwedans Dam represented the ideal case for the development of a finite element model and a consequential determination of the behaviour of its constituent materials. Through modelling Wolwedans Dam under hydrostatic and temperature drop loads, it was considered that the behaviour measured on the prototype structure could be reproduced by isolating the actual degree of shrinkage/creep of the RCC that had occurred during the hydration heating and cooling cycle.

The subsequent analyses undertaken, and presented in Chapter 5 and Appendix B, represent the key focus of the investigations for this doctoral research programme. The validity of small-scale laboratory testing of such complex phenomena as shrinkage and creep in RCC will always be questionable, as discussed under section 8.2.3. However, the behaviour of RCC measured on the scale of a prototype dam cannot be denied. Comparing the measured performance with a structural model allows the development

of a real understanding of how the material is behaving within the dam. While good comparisons can be made in 2-dimensional structures, comparing modelled and actual performance for a 3-dimensional structure provides a platform on which basis many ambiguities can be removed and consequently meaningful conclusions can be drawn.

The specific value of this work is found in the use of measured performance on a prototype dam to demonstrate with a high level of confidence the actual early shrinkage/creep behaviour of high-paste RCC.

8.4.2. STRUCTURAL MODELLING APPROACH

The target reference performance for modelling was taken as the induced joint openings at approximately mid dam height, central crest displacements and displacements at reference points in the upper gallery, as measured on the prototype structure (as illustrated on **Figure 8.11**) during a winter after the heat of hydration had been fully dissipated. While grouting of the induced joints did not impact the behaviour of the structure to any real extent, it was considered that a higher level of confidence would be possible for simulation of the structural behaviour pre-grouting. Using the known materials characteristics of the RCC and the As-built structural geometry, a range of possible shrinkage/creep behaviour characteristics were modelled in an effort to reproduce the measured displacement behaviour of the prototype Wolwedans Dam structure.

With a temperature drop from placement of approximately 8°C at elevation RL 66.25 m by July 1993, total shrinkages from 80 to 380 microstrain were modelled through the imposition of temperature drops of between 8 and 38°C in conjunction with a thermal expansivity for the RCC of 10 x 10^{-6}/°C.

A sensitivity analysis was also completed in an effort to establish whether it might be possible to reproduce the measured crest displacements and joint openings with some creep and higher, or lower E modulus values for the dam RCC.

8.4.3. PROTOTYPE REFERENCE BEHAVIOUR

Only 3 of the 16 induced joints at mid-height opened at Wolwedans and only these joints were allowed to open on the FE model analysed, as illustrated on **Figure 8.9**.

For displacement reference, survey data recorded twice annually at the beacons located on the non-overspill crest at either side of the spillway (P113 & P120) were used, as illustrated on **Figures 8.10** & **8.11**. The winter displacements recorded in early July 1993, when a temperature drop of approximately 8°C was recorded within the core zones of the dam, were compared with deflections read from the FE model.

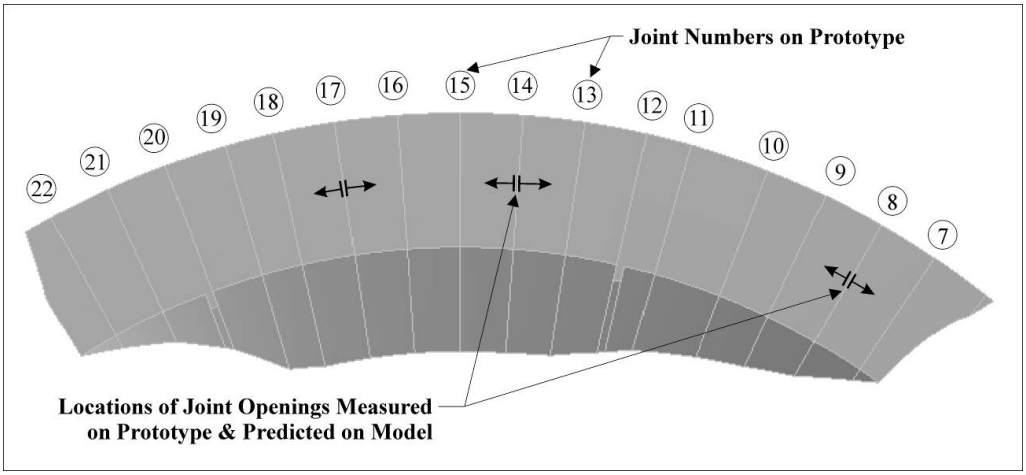

Figure 8.9: Horizontal Section Illustrating Induced Joints at Mid-Height

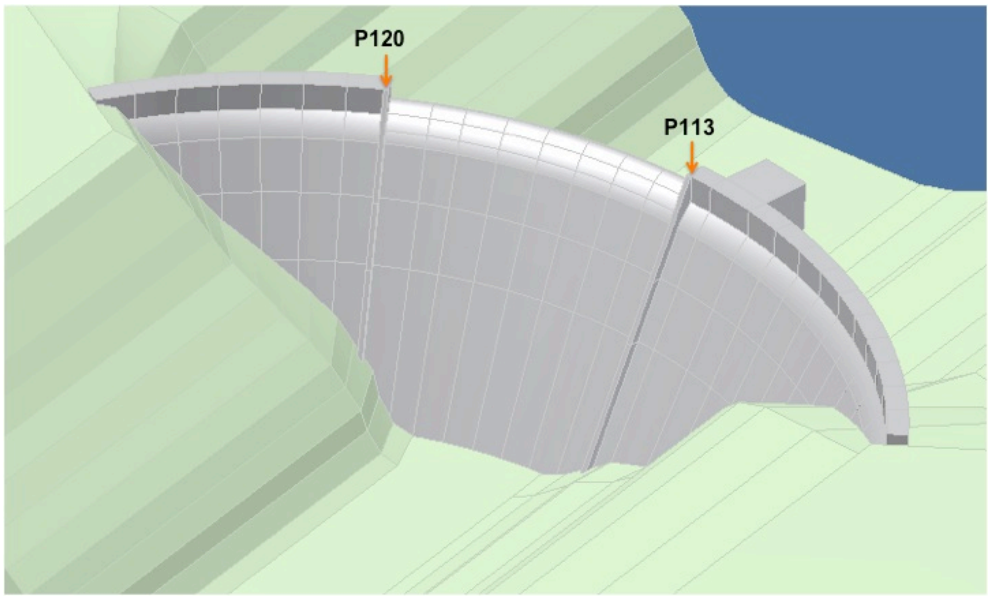

Figure 8.10: FE Model – Illustrating Crest Displacement Monitoring Points

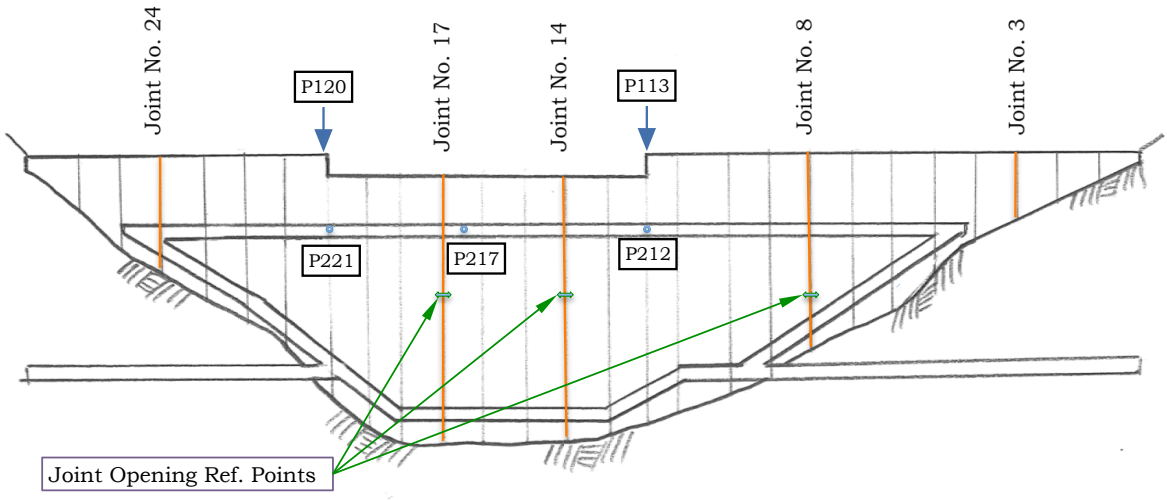

Figure 8.11: Primary Prototype Structure Behaviour Reference Points

8.4.4. MODELLING RESULTS

As expected, the model demonstrated the joint openings and crest displacements to increase with temperature drop. The stress distribution patterns were also significantly impacted by the applied temperature drops, with increased cantilever action being indicated through the elastic analyses and higher, but more localised arch compression stresses. For an effective temperature drop exceeding 15°C, the indicated level of heel tensions is such that cracking would undoubtedly occur, which in turn would give rise to increased structural displacements. It is consequently considered that the displacements predicted through elastic analysis under-estimate the real situation for the higher temperature drop simulations.

Reviewing the indicated stress patterns, the analyses further demonstrated that some concerns in respect of the structural behaviour would exist should the effective temperature drop be 25°C, or higher. Interestingly, the model also confirmed that the residual stress level between the open joints remained insignificant (< 0.02 MPa).

Table 8.1 presents a summary of the important predicted displacements and joint openings, compared to those measured at the beginning of July 1993, before the induced joints were grouted.

Table 8.1: Predicted & Measured Horizontal Displacements & Openings

Scenario	**Effective Total Temp. Drop** (°C)	**Displacements** (mm)					**Central Joint Openings** (mm)			
		P113	P120	P212	P217	P221	Jt. 8	Jt.14	Jt.17	Total
1	8	12.7	8.4	8.8	10.1	6.1	1.17	0.77	1.56	3.50
2	8 / 11**	14.3	8.6	9.4	12.4	6.8	1.20	0.46	1.88	3.54
3	15	18.1	10.0	11.7	14.4	7.7	4.60	2.67	4.54	11.81
4	25	26.1	13.2	15.1	17.3	10.9	10.16	5.58	8.51	24.25
5	38	35.3	16.5	20.3	21.3	13.6	10.83	9.75	13.60	34.18
Measured July 1993		14.5	11.7*	7.65	10.1	7.5*	1.0	0.95	1.45	3.40

The figure marked with "*" are those in which a lower level of confidence is considered to exist.

** - Scenario 2 assumed an internal zone temperature drop of 8°C and an external zone temperature drop of 11°C, in line with the findings of Chapter 5.

The sensitivity analysis established that the equivalent measured crest displacements could be reproduced on a model with a higher E modulus and some RCC creep, but such a scenario caused the induced joint openings to be substantially larger than measured on the prototype. Similarly, it was possible to reproduce the measured induced joint openings with a lower RCC E modulus and some creep, but for such a scenario, the crest displacements exceeded those measured.

8.4.5. RESULT DISCUSSION AND SUMMARY

Ignoring reference points P120 and P221, it can be seen that a simple, uniform temperature drop of 8°C most closely replicated the displacements and joint openings measured on the prototype dam. Only the higher displacement measured at point P113 would remain unexplained, although it is considered that this reference point is also subject to exaggerated upstream crest movements caused by high summer temperatures within the NOC section of the dam.

On the basis of the analyses completed as part of Chapter 5, the Wolwedans Dam structure is more likely to behave in accordance with Scenario 2 than Scenario 1 and considering the levels of confidence that can realistically be expected for FE modelling of a concrete dam on a variable foundation rockmass, it is suggested that Scenario 2 should be assumed as the most realistic replication of the actual dam behaviour.

With RCC placement temperatures generally varying between 21 and 22°C and with temperatures across the dam section in July 1993 generally between 13 and 14°C, the dam structure can be seen to have experienced a "core" temperature drop from placement of approximately 8°C. Scenarios 1 and 2 accordingly represent situations that would require that the RCC of Wolwedans Dam demonstrated elastic behaviour characteristics right from placement.

8.4.6. THERMAL MODELLING OF CHANGUINOLA 1 DAM

Through a detailed thermal analysis, described in Chapter 5, the development of an observed crack in the surface of the RCC placement at Changuinola 1, after several week's exposure, was modelled. Assuming a worse case scenario of no creep in the RCC, the modelling predicted the development of the crack with a high level of accuracy. Adding creep of the order of 25 microstrain was demonstrated to be adequate to substantially eliminate the likelihood of cracking within the first 3 months after placement, indicating strongly that the RCC had therefore in fact exhibited little, or no creep during thermal expansion.

8.4.7. CONCLUSIONS

The structural modelling completed as part of the investigations addressed herein clearly demonstrated that the RCC of Wolwedans Dam could not have suffered from any significant shrinkage or creep during the hydration cycle. A similar behaviour was indicated through thermal modelling for the Changuinola 1 Dam. In view of the complexities in defining the elastic and inelastic behaviour of concrete subject to

temperature changes and the inherent variability of a foundation rockmass, modelling the performance of a prototype dam structure can only be considered an estimation and accordingly, it cannot be stated with certainty that no shrinkage, or creep occurred in the RCC at Wolwedans Dam. However, it can be stated with certainty that the shrinkage and creep that would be typically assumed for CVC, or RCC did not occur and consequently the traditionally assumed design approach can be seen to be inappropriate.

8.5. THE COMPARATIVE COMPOSITION & PROPERTIES OF CVC & RCC

8.5.1. GENERAL

Through a literature study, the phenomena of shrinkage and creep in concrete were addressed in detail in Chapter 3.

Shrinkage and creep in concrete are very similar, inter-related effects and the susceptibility of concrete to both of these phenomena relates to the nature of its composition and the manner in which the composite material is formed and develops strength. As the cementitious materials in concrete hydrate, they form a gel, which has a smaller volume than its constituents. As the cement paste shrinks in this process, the bond between the paste and the aggregates and the skeletal structure between the different sized and shaped aggregate particles serve to resist a general shrinkage of the concrete. The net result is a structure with internal residual shrinkage stresses and micro-cracks.

The better developed the aggregate skeletal structure within concrete, the less the paste shrinkage impacts the overall internal composite structure of the concrete. Essentially, in a concrete with a structure made up of aggregate-to-aggregate contact, the in-filled paste will experience substantially less autogenous shrinkage and be less susceptible to creep than a concrete comprising aggregates suspended in a medium of paste. From a geotechnical point of view, when constrained and before the paste itself has developed strength, the former concrete type will also indicate a substantially greater rigidity than the former.

8.5.2. HIGH-PASTE RCC IN LARGE ARCH DAMS

On the basis of a review of the factors that make concrete susceptible to autogenous and drying shrinkage and creep, it becomes apparent that high-paste RCC is perhaps the ideal concrete format in respect of minimising the impacts of shrinkage and creep.

The method of construction and the consequential development of aggregate-to-aggregate contact and a strong aggregate skeletal structure are further considered to represent a significant factor in the creep-resilient nature of high-paste RCC. As discussed in Chapter 6 and illustrated on **Plates 8.1** and **8.2**, the better shaped,

continuously graded aggregate, the high aggregate content and the method of compaction together contribute to causing the behaviour of immature high-paste RCC to be influenced more strongly by the aggregate skeletal structure, while the behaviour of immature CVC will be more strongly influenced by the paste.

Plate 8.1: Typical CVC Core

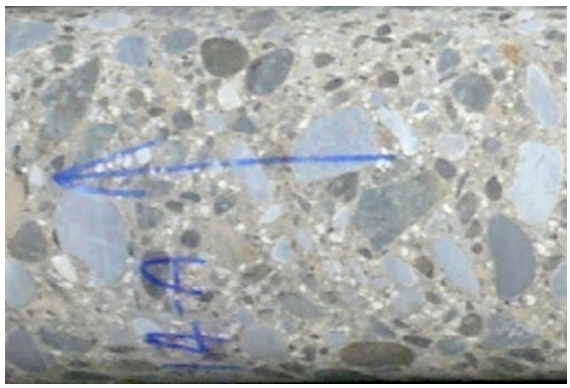

Plate 8.2: Typical RCC Core

Furthermore, as described in Chapter 6, a simplified analysis of Wolwedans Dam under the heating action of hydration, without hydrostatic load, indicated that upstream movement of the central crest due to both thermal expansion and gravity caused the containing stresses within the critical upper section of the structure to be eliminated. Bearing in mind the evident ability of high-paste RCC to expand linearly with a temperature rise even under considerable internal restraint, the identified effect would have undoubtedly given rise to unrestrained expansion of the RCC in the crest at Wolwedans under the hydration temperature rise. In the absence of containing stress, stress relaxation creep is no longer a factor and accordingly, this finding provides further motivation to justify the apparent absence of creep in the critical structural elements of Wolwedans Dam. This effect will generally be apparent in the crest of any dam with a curvature and particularly in relatively flexible arch structures.

8.6. A NEW UNDERSTANDING OF THE EARLY BEHAVIOUR OF RCC IN LARGE DAMS

8.6.1. MOTIVATION

As discussed in Chapter 6, the investigations and analyses completed have demonstrated that a high-paste, high strength RCC mix in an arch structure need not exhibit any significant shrinkage, or creep during the hydration cycle. Lower strength, lean RCCs will indicate some creep, while mixes with less than ideal materials remain susceptible to drying shrinkage and the findings presented relate very specifically to high quality, high-paste RCC.

The strain gauge (SGA gauges) data recorded at Çine Dam and Changuinola 1 Dam are considered of particular importance. The apparent linear thermal expansion evident in a location that would be assumed to be subject to significant internal restraint is considered to provide evidence of a behaviour that is dominated by aggregate-to-aggregate particle contact. The fact that such linear expansion occurs in RCC at such an early age provides further evidence of an inherent early resistance to creep and the likelihood of increased creep resistance in the mature concrete.

As a result of the fact that early shrinkage and creep in concrete are interdependent effects that occur simultaneously during the process of maturation, a realistic separation of the two is not practically possible. Furthermore, the early development of internal shrinkage obviously creates a susceptibility to creep under load. With drying shrinkage in the core of a mass concrete block generally agreed as being negligible, unless related to a specific problem in the aggregates, the important shrinkage is autogenous shrinkage. While the terms shrinkage and creep are used together in this Thesis, the dominant effect is undoubtedly manifested as creep; a stress relaxation that occurs when the temperature rise associated with the hydration process attempts to cause thermal expansion in immature concrete.

8.6.2. Definition of Appropriate RCC Shrinkage and Creep Behaviour

The study has clearly demonstrated that the 125 to 200 microstrain combined shrinkage and creep that is conventionally accepted for an equivalent CVC in a dam during the hydration cycle does not occur to anywhere close to the same extent in high-paste RCC.

For a high-paste, high pozzolan content RCC mix, with well-graded, high quality aggregates in an arch dam, it is undoubtedly possible to produce an RCC with negligible shrinkage and creep.

As a result of an inherent dependence on the nature, grading and the effective compaction of the constituent materials, it is considered essential to treat each set of circumstances for an RCC mix on a case-specific basis and appropriate materials testing should be exhaustive when reliance on a low shrinkage/creep RCC is important to the dam design.

For the preliminary design of a gravity dam constructed with a high quality, high-paste RCC, it is considered appropriate to assume a total shrinkage and creep of approximately 50 microstrain.

The RCC mix for an arch dam will usually be designed for minimum shrinkage and creep and should contain high quality aggregates combined with approximately 200 kg/m^3 cementitious materials, of which approximately 70% would be a high quality fly ash. Even in such circumstances, the assumption of a total shrinkage/creep of the order of 20 microstrain should be applied for preliminary

design, but verification testing would be required before a definitive reliance could finally be placed on such performance.

In the design analyses for an RCC arch/arch gravity dam, it is considered important to include an evaluation of the anticipated behaviour during construction and the consequential impacts of temperatures elevated by hydration heat.

As the opportunities in respect of the evident better early behaviour of high-paste RCC are investigated, more dams will be appropriately instrumented, more information will be reported and a significantly greater database of RCC shrinkage and creep behaviour will be developed. As such information becomes available, the definition of the associated behaviour of high-paste RCC for dam design will progressively evolve.

8.6.3. KEY ISSUE IN RESPECT OF RCC CREEP RESILIENCE/IMPROVED EARLY BEHAVIOUR

The study demonstrates that there is undoubtedly a specific composition and type of RCC that indicates increased resilience to creep and shrinkage. All examples of negligible shrinkage and creep behaviour relate to "high-paste" RCC and all of the references to high creep relate to a "lean" RCC. A further two factors are common to the low creep/shrinkage RCCs and these are a high fly ash content and total cementitious materials contents approaching, or exceeding 200 kg/m^3.

Evaluation of the factors of influence would suggest that the development of a strong aggregate skeletal structure with aggregate-to-aggregate contact is also particularly important and this is best achieved with a high-workability RCC, with high quality, well-graded and well-shaped aggregates, as discussed in Chapter 6.

A high-paste RCC will typically comprise approximately 200 litres/m^3 of paste (excluding aggregate fines) and 800 litres/m^3 of aggregates and the RCC must be designed volumetrically, with all voids in the aggregates slightly over-filled with lubricating paste that is squeezed up to the surface as the RCC is compacted and a strong aggregate-to-aggregate contact is developed.

The ideal RCC mix composition for maximising resilience to creep might be as follows:

Constituents	Portland Cement	Fly Ash	Water	Coarse Aggregate	Fine Aggregate	Retarder
By Mass (kg/m^3)	62	143	115	1400	800	3.4
By Volume (litres/m^3)	20	62	115	500	300	3
Net Paste (l/m^3)	Fines (l/m^3)	Aggregate (l/m^3)	Paste/ Mortar	Sand/ Aggregate		
200	30	800	0.40	0.375		

In order to minimise the likely impact of creep, it is also considered appropriate to design the dam structure for minimum possible containment stress during the period that peak hydration temperatures are experienced and to design the RCC mix for the lowest possible heat of hydration.

Notwithstanding the above, it is considered necessary to embark on an extensive and case-specific testing and development programme when intending to design an RCC for minimal shrinkage and creep and this should include the construction and instrumentation of a full scale trial.

8.7. THE APPLICATION OF THE NEW RCC MATERIALS MODEL

8.7.1. THE IMPACT ON DAM DESIGN

In order to develop a meaningful understanding of the implications of the new understanding of the early behaviour of high-paste RCC in large dams, it was considered beneficial to illustrate the consequences of its application, as discussed in Chapter 7.

The most important issues in respect of temperature and the early behaviour of RCC in a dam relate to tension stresses developed as a result of the long-term loss of temperature, as the hydration heat is dissipated. In the case of an RCC gravity dam, these tensions are managed in a direction parallel to the dam axis by including induced transverse contraction joints, which are generally sealed on the upstream face with embedded waterstops. In the case of large gravity dams, however, these tensions can also develop cracking parallel to the dam axis and many examples of such cracking have been observed over the years in South Africa in mass concrete dams.

8.7.2. THE IMPACT ON INDUCED JOINT SPACINGS AND OPENINGS

Taking Changuinola 1 Dam in Panama as an example, an analysis clearly illustrated the traditionally accepted method for establishing induced joint spacing and openings to be substantially flawed, whatever RCC behaviour model is assumed. The analysis further demonstrated the unrealistic level of conservatism inherent to applying a traditional RCC materials behaviour model in respect of anticipated induced joint openings.

8.7.3. THE IMPACT ON RCC ARCH DAM DESIGN

In the case of an arch dam, a temperature drop load substantially compromises the entire structural function by shrinking the structure to a smaller size than the space that it was constructed to fill, as discussed in **Appendix A**. A mass concrete arch dam is constructed in monolithic blocks that are simply allowed to shrink away from each other, with the gap in between being filled with grout under pressure at a suitably low temperature. Usually, looped pipes are built into the concrete and chilled water is

circulated soon after casting in order to draw out the hydration heat and reduce the concrete temperature sufficiently to allow grouting.

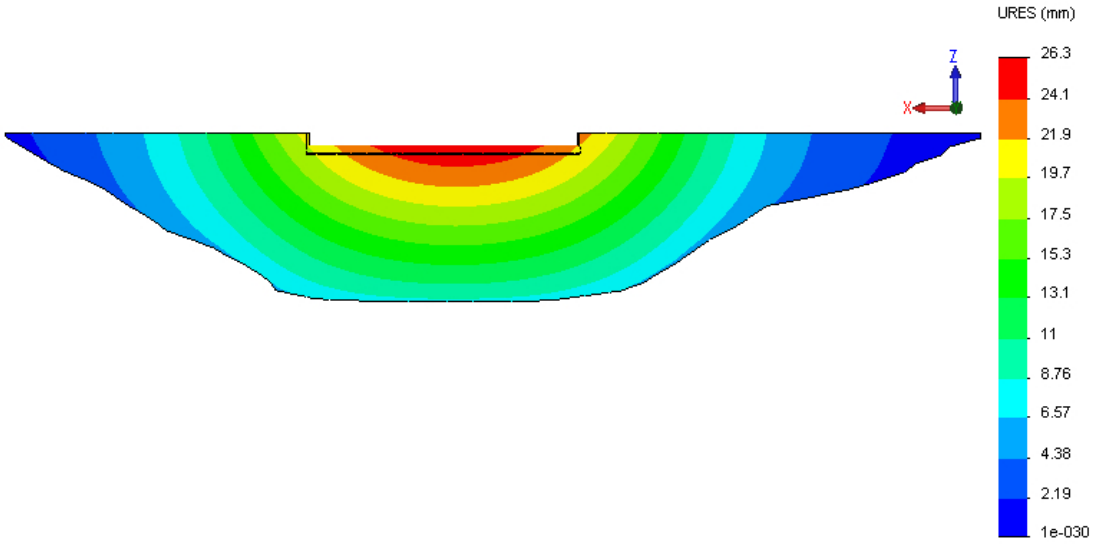

Figure 8.11: Total Horizontal Downstream Displacement for Changuinola 1 Dam with Hydrostatic Load and no Temperature Drop

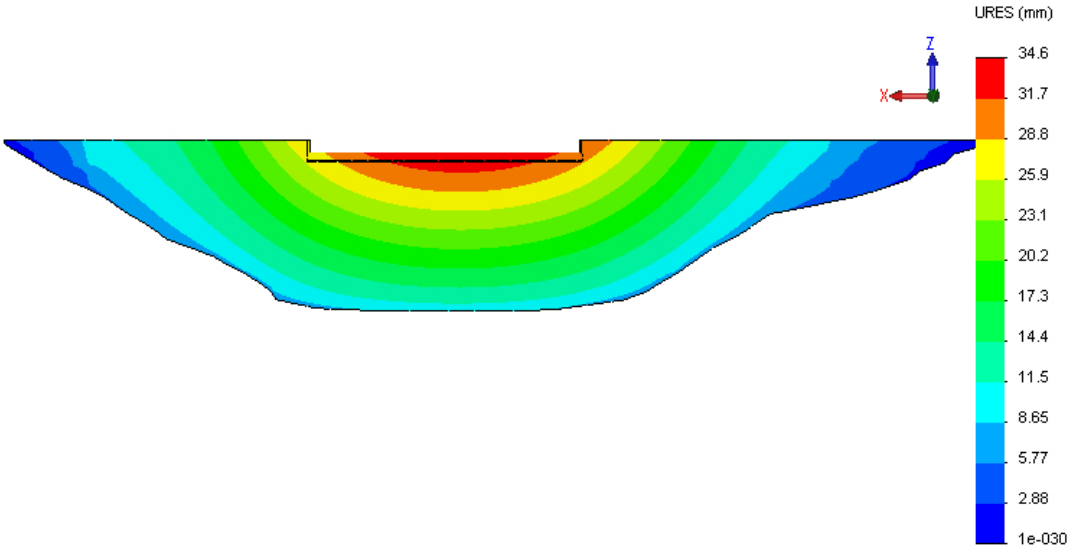

Figure 8.12: Total Horizontal Downstream Displacement for Changuinola 1 Dam with Hydrostatic Load and 6°C Temperature Drop

In view of the fact that RCC is constructed in horizontal layers, transverse joints are induced, as opposed to being formed, and the installation of looped cooling pipes is rather impractical. Consequently, grouting systems must be installed in the induced joints, while grouting must either be undertaken after the natural cooling process has run its course, or earlier under appropriate pressures, or not at all. With significant pressure commonly to impound as early as possible, very rarely does the opportunity exist to wait to grout the induced contraction joints and it is correspondingly

extremely important to understand exactly how the RCC has behaved through the hydration cycle.

The design example of Changuinola 1 Dam in Panama demonstrated that, applying the new understanding of the early behaviour of RCC in a temperate climate, it would be possible to avoid joint grouting in an RCC arch/gravity dam. With the traditional materials model adopted for RCC, this would certainly never be the case. Although the impact of a 6°C temperature drop on the dam structure can be clearly observed in the increased maximum crest displacements illustrated by comparing **Figures 8.11** and **8.12**, critical stresses remain comfortably within acceptable limits.

While the impact of the new understanding of the early behaviour of RCC was demonstrated to be critical in respect or arch-type dams, the situation in respect of gravity dams is simply one of demonstrating the unnecessary conservatism applicable when the traditional RCC materials model is applied. In both cases, however, substantial advantage is perceived in understanding the actual mode of behaviour of RCC as a material. Applying assumptions in dam design, the real situation and the real factors of safety will never be known.

8.7.4. THE NEED FOR TESTING

While the investigations and analyses undertaken demonstrated without doubt that RCC in large dams behaves quite differently to CVC during the course of the hydration cycle, the need for as much verification testing of the shrinkage characteristics of each specific RCC mix was recognised.

Depending on the importance of shrinkage and creep in respect of the design of a particular dam, the following testing recommendations were considered appropriate:

- For all significant RCC dams, temperature and strain gauges should be installed and monitored in the RCC of the Full Scale Trial.
- In the case of an RCC arch dam for which materials shrinkage might be problematic, additional laboratory and practical testing of the RCC will be required.

8.8. CONCLUSIONS

8.8.1. DEFINITIVE FINDINGS

The investigations and analyses presented herein illustrate probably the first publicly documented case whereby the early behaviour of RCC in large dams is validated against a prototype structure, which relies on 3-dimensional arch action for stability.

The findings conclusively prove that the RCC of Wolwedans Dam did not suffer the level of shrinkage and creep that would traditionally have been assumed for RCC, or CVC dam design. Within the level of accuracy realistically possible when modelling a

prototype dam structure, it would in fact appear that no perceptible volume reduction, associated with shrinkage and creep during the hydration heat development and dissipation cycle, occurred in the critical structural components at Wolwedans Dam.

While the measured data for Wadi Dayqah Dam demonstrated that drying shrinkage can be experienced in RCC when high w/c ratios, high percentages of non-cementitious fines and poorer quality aggregates are used, the related findings confirm the identified lower creep/shrinkage behaviour as applicable only to high-paste RCC.

8.8.2. APPROPRIATE CAUTION IN APPLYING NEW CONCEPTS

While the findings of this investigation are considered definitive, the fact that the new understanding of early RCC behaviour has yet to be broadly tested and explored implies that it should be conservatively applied in the short term. As a result of the study findings, however, it is considered that all full-scale RCC construction trials should include temperature and strain measurement instrumentation specifically designed and configured to develop an understanding of the shrinkage and creep characteristics of the specific RCC to be used. This data should be supported with adequate laboratory testing specifically of the shrinkage characteristics of all of the aggregates to be used.

8.8.3. THE NEED FOR CONTINUED OBSERVATION

The conclusions presented are based on instrumentation data from prototype dam structures. The comprehensive data recorded at Wolwedans Dam was sufficient to allow a definitive replication of the actual dam behaviour through Finite Element modelling. Until now, it has only been possible to point towards apparent differences between the early behaviour of RCC and CVC, on the basis of observation, and to try to evaluate this through laboratory testing of inadequately sized and unrealistically manufactured samples.

The limited instrumentation installed in Wadi Dayqah Dam implies that the precise early behaviour of the RCC will probably never be known and accordingly, an important opportunity to increase knowledge of RCC has been lost. The value of the instrumentation installed at Wolwedans, Knellpoort and Çine Dams cannot be overstated and with the knowledge gained, the instrumentation installed in future RCC dams can be improved and more accurately targeted towards the particular measurement of specific phenomena.

The value of the findings of these investigations have been demonstrated, but it is important to continue to gather data on which basis greater levels of confidence can be developed in the new understanding of high-paste RCC behaviour, which will in turn allow greater consequential benefit in terms of economic and safe dam designs. Accordingly, it is strongly advocated that all future RCC dams be appropriately and intelligently instrumented.

8.9. RECOMMENDATIONS FOR CONSEQUENTIAL RESEARCH & DEVELOPMENT

It is considered of specific importance that the investigations addressed in this Thesis represent the first published work to evaluate the behaviour of RCC through a comparison of modelled and measured prototype performance. Admittedly, such an analysis is only specifically applicable in the case of an RCC arch dam and there are not yet a significant number of dams of this type that have been constructed around the world. It is also considered of specific importance that most laboratory testing for creep and shrinkage to date has related to lean mix RCC.

In order to ensure maximum benefit is gained from the findings presented in this study, ongoing verification on future RCC dam projects will require laboratory testing, structural modelling and detailed site instrumentation. Only through the repetition of the modelling and prototype comparisons presented herein, can levels of confidence in the early behaviour of all types of RCC be effectively increased.

APPENDICES

APPENDIX D

LIST OF REFERENCES

APPENDIX D

D. LIST OF REFERENCES

Reference	Related Subject	Applicable Chapters
Alexander MG. *Deformation Properties of Blended Cement Concretes Containing Blastfurnace Slag and Condensed Silica Fume.* Advances in Cement Research. Vol. 6. No. 22. Johannesburg. April 1994.	Concrete Research	3 & 6
Alexander MG. *Properties of Aggregates in Concrete, Phase I and II.* Research reports prepared for Hippo Quarries. University of Witwatersrand. Johannesburg. 1990 and 1993.	Concrete Research	3 & 6
Alexander MG & Beushausen H. *Deformation and Volume Change of Hardened Concrete.* Chapter 8. Fultons Concrete Technology. Ninth Edition. Cement & Concrete Institute, Midrand, South Africa. 2009.	Concrete Research	6
Alexander MG & Davis DE. *The Influence of Aggregates on the Compressive Strength and Elastic Modulus of Concrete.* The Civil Engineer in South Africa. Vol. 34, No. 5. Pp 161 -170. May 1992.	Concrete Research	6
American Concrete Institute. ACI 207.2R-07. *Effects of Restraint, Volume Change, and Reinforcement of Cracking of Massive Concrete. Part 1.* September 2007.	Concrete Practice Guideline	7
Andriolo A. *Materials & RCC Quality Requirements.* Proceedings. 4th International Symposium on Roller Compacted Concrete Dams. Madrid, Spain. pp 61-78. 2003.	RCC Materials	3
ASTM.*C 512 – 02. Standard Test Method for Creep of Concrete in Compression.* ASTM International, West Conshohocken. USA. August 2002.	Concrete Standard	3
Aufleger M, Conrad M, Strobl Th, Malkawi AIH & Duan Y. *Distributed Fibre Optic Temperature Measurements in RCC Dams in Jordan and China.* 4th International Symposium on Roller Compacted Concrete Dams. Madrid, Spain. pp 401-407. November 2003.	Instrument-ation	3

Reference	Related Subject	Applicable Chapters
Aufleger M, Conrad M, Goltz M, Perzlmaier S & Porras P. *Innovative Dam Monitoring Tools based on Distributed Temperature Measurement.* – Jordan Journal of Civil Engineering (JJCE), Vol. 3,. Jordan University of Science and Technology (JUST), Irbid, Jordan, ISSN 1026-3721, December 2006.	Instrument-ation	3
Bo D & Gangwei C. *Studies of the Construction Technology under High Temperature Condition and its Application in Longtan Dam.* New Progress on RCC Dams. Proceedings. 5th International Symposium on RCC Dams. Guiyang, China. pp 213 – 222. November 2007.	RCC Construction	7
Boggs HL, Jansen RB & Tarbox GS. *Arch Dam Design and Analysis.* Chapter 17. Advanced Dam Engineering. Van Nostrand Reinhold. New York. 1988.	Arch Dams	3
Bryant AH. & Vadhanavikkit C. *Creep Shrinkage - Size and Age at Loading Effect.* ACI Materials Journal. Vol. 84. No. 2. March to April 1987.	Concrete Guideline	3
Cai Q, Kotsiovos M & Durieux JH. *3-D Structural Analysis of Wolwedans Dam.* Internal Report No. K200/02/DK03. Sub-Directorate Structural Studies. Directorate Design Services. Department of Water Affairs & Forestry. Pretoria. February 1997.	Dam FE Analysis	5
Calmon JL, Murcia J, Botassi dos Santos, Gambale E & da Silva CJ. *Numerical Modelling of Thermal Stress in RCC Dams using 2-D Finite Element Method – Case Study.* Proceedings. 4th International Symposium on Roller Compacted Concrete Dams. Madrid, Spain. pp. 569 – 577. 2003.	Thermal Analysis	3
CCWJV. *Instrumentation Readings, Data & Information. Changuinola 1 Dam.* Panama. January to July 2010.	Instrumentati on Data	4
Cervera, M, Oliver, J & Prato, T. *Simulation of Construction of RCC Dams. I: Temperature & Aging.* ASCE. Journal of Structural Engineering. pp 1053 - 1061. September 2000.	Thermal Analysis	3

Reference	Related Subject	Applicable Chapters
Cervera M, Oliver J & Prato T. *Simulation of Construction of RCC Dams. II: Stress & Damage.* ASCE. Journal of Structural Engineering. pp 1062 - 1069. September 2000.	Thermal Analysis	3
Chen Y, Wang C, Li S, Wang R & He J. *Simulation Analysis of Thermal Stress of RCC Dams using 3-D Finite Element Relocating Mesh Method.* Advances in Engineering Software. Elsevier. Vol. 32 pp 677 - 682. 2001.	Thermal Analysis	3
Conrad M. Aufleger M. & Malkawi AIH. *An Advanced Temperature Monitoring System at Mujib and Wala Dam.* - In: Proc. of the Int. Conf. on Roller Compacted Concrete Dam Construction in Middle East 2002, Irbid, Jordan. April 2002.	Instrument-ation	3
Conrad. M, Aufleger, M & Husein Malkawi, AI. *Investigations on the Modulus of Elasticity of Young RCC.* Proceedings. 4th International Symposium on Roller Compacted Concrete Dams. Madrid, Spain. pp 729 - 733. November 2003.	RCC Behaviour	3
Conrad M, Hoepffner R & Aufleger M G. *Innovative Monitoring Devices for an Integral Observation of Thermal Stress behaviour of Large RCC Dams.*Proceedings.5th International Symposium on Roller Compacted Concrete Dams. Guiyang, China. pp 777-784. November 2007.	Instrument-ation	3
Conrad M, Kisliakov D, Aufleger M, Strobl Th & Malkawi AIH. *Simplified Thermo-Mechanical Modelling of a Roller Compacted Concrete (RCC) Dam – Evaluation of the Numerical Model and Influences of some Concrete Parameters.* - Proceedings of the 6th Int. Congress on Thermal Stresses 2005, Vienna. May 2005.	Thermal Analysis/ RCC Behaviour	
Dazhi W & Xu W. *Temperature Control for RCC Dam at Longtan Hydropower Station.* New Progress on RCC Dams. Proceedings. 5th International Symposium on RCC Dams. pp 213 – 222. Guiyang, China. November 2007.	RCC Construction	7
Department of Water Affairs. *External Review Panel Report No. 11 – De Hoop Dam.* Report No. ERP 11. DWA. August 2009.	Construction Report	3

Reference	Related Subject	Applicable Chapters
Dunstan MRH. *Changuinola 1 Dam. Review of the In-situe Properties of Full-Scale Trial 1B.* Report No. Chan1/461/090923. MD&A. September 2009.	Construction Report	5
Geoconsult. Gibb. ARQ. *Çine RCC Dam. Phase 2 Design Report.* Vol.4 of 4. Drawings. Özkar Construction. Ankara, Turkey. January 2000.	Dam Design Drawings	2
Greyling R & Shaw QHW. ARQ (PTY) Ltd. *Çine Dam. Supplementary Thermal Analysis Report.* Özkar Construction Internal Report No. 1596-10288. Ankara, Turkey. June 2008.	Thermal Analysis	4
Greyling RG & Shaw QHW. *Changuinola 1 Dam. Thermal Analysis Report.* Report No. 4178/11436-R1. MD&A. July 2010.	Thermal Analysis	7
Grieve GRH. *The Influence of Two South African Fly Ashes on the Engineering Properties of Concrete.* PhD Thesis. University of Witwatersrand. Johannesburg. 1991.	Concrete Research	3 & 6
Hattingh LC. *Completion Report for the Crack Joint Grouting. Wolwedans Dam.* Mossel Bay Government water Scheme. Internal Department of Water Affairs & Forestry. Report No. K200-02-DD05. November 1994.	Construction	5
Hattingh LC, Heinz WF & Oosthuizen C. *Joint Grouting of a RCC Arch/Gravity Dam: Practical Aspects.* Proceedings. 2nd International Symposium on Roller Compacted Concrete Dams. Santander, Spain. pp 1037-1051. 1995.	Construction Records	5
Hollingworth F, Druyts FHWM & Maartens WW. *Some South African Experiences in the Design and Construction of Rollcrete Dams.* Proceedings. 17th ICOLD Congress. Q62. R3. San Francisco. pp 33-51. 1988.	RCC Experience	4
Husein Malkawi AI, Aufleger M, Strobl TH, Conrad M, Mutasher, S & Al-Jammal M. *Computational Analysis of Thermal and Structural Stresses for RCC Dams.* The International Journal on Hydropower and Dams. Issue Four, pp 86 – 95. 204.	Thermal Analysis	3

Reference	Related Subject	Applicable Chapters
ICOLD. Committee on Concrete for Dams. *Roller Compacted Concrete Dams. State of the Art and Case Histories.* ICOLD Bulletin 126. 2003.	RCC Guideline	2 & 3
Kaitao X & Yun D. *Study on the Influence of Limestone Powder on Roller Compacted Concrete Performance and Action Mechanism.* Proceedings. 5th International Symposium on Roller Compacted Concrete Dams. Guiyang, China. pp 467-479. 2007.	RCC Mix Testing	3
Lackner R & Mang H.A. *Chemoplastic Materials Model for the Simulation of early-Age Cracking: From the Constitutive Law to Numerical Analyses of Massive Concrete Structures.* Cement & Concrete Composites. Elsevier. Vol. 26 pp 551 - 562. 2004.	Theoretical RCC Materials Model	3
Leguizamo PM. *La Miel I Dam – Design of the Geotechnical and Structural Instrumentation Program for the World's Highest RCC Dam.* Roller Compacted Concrete Dams. Proceedings. 4thInternational Symposium on RCC Dams. pp 633 – 640. Madrid, Spain. November 2003	Instrumentation	7
López J, Castro g & Schrader E. *RCC Mix and Thermal Behaviour of Miel 1 Dam – Design Stage.* Proceedings. 4th International Symposium on Roller Compacted Concrete Dams. Madrid, Spain. pp 789-797. November 2003.	RCC Testing	3 & 6
McCrae, JB & Simmonds, T. *Long-Term Stability of Vibrating Wire Instruments: One Manufacturer's Perspective.* Proceedings of 3rd International Symposium on Field Measurements in Geotechnics. Field Measurement in Geomechanics. Oslo. September 1991.	Dam Instrumentation	2
Neville, AM. *Properties of Concrete.* Chapter 9. Fourth Edition. Pearson Prentice Hall. London. 2002.	Concrete Technology Textbook	3, 4 & 5
Noorzaaei J, Ghafouri HR & Aminin R. *Investigation of the Influence of Placement Schedule on the Thermal Stresses of RCC Dams, using Finite Element Analysis.* Proceedings. 4th International Symposium on Roller Compacted Concrete Dams. Madrid, Spain. pp 669-674. November 2003.	Thermal Analysis	3

Reference	Related Subject	Applicable Chapters
Oosthuizen C. *Behaviour of Roller Compacted Concrete in Arch/Gravity Dams.* Proceedings. International Workshop on Dam Safety Evaluation. Grindelwald, Switzerland. April 1993.	RCC Dam Behaviour	1, 4 & 5
Oosthuizen C. *Performance of Roller Compacted Concrete in Arch/Gravity Dams.* Proceedings. 2nd International Symposium on Roller Compacted concrete Dams. Santander, Spain. pp 1053-1067. 1995.	RCC Dam Behaviour	1, 4 & 5
Oosthuizen C. *The Use of Field Instrumentation as an Aid to Determine the Behaviour of Roller Compacted Concrete in an Arch/Gravity Dam.* Proceedings. 3rd International Symposium on Field Instruments in Geomechanics. Oslo, Norway. September 1991.	Instrument-ation	5
Owens G. *Fulton's Concrete Technology.* Chapter 8. Ninth Edition. Cement & Concrete Institute. Midrand. RSA. 2009.		1, 2, 3, 5
Özkar Construction Internal Report. *Instrumentation Readings. Quality Control Unit.* Ankara, Turkey. October 2005 – February 2008.	Instrumentation Data	4
Özkar Construction Internal Report. *Work Reports. Quality Control Unit.* Ankara, Turkey. July 2005 – February 2008.	Quality Control Report	2
Penghui L, Hong C, Hongbo L, Yu H & Feng J. *3-D Simulating Analysis for Thermal Control during Construction Period on Dahuashui RCC Arch Dam.* Proceedings.5th International Symposium on Roller Compacted Concrete Dams. Guiyang, China. pp 577 – 581. 2007.	Thermal Analysis	3
Precise Engineering Surveys. Department of Water Affairs. *Instrumentation Data for Wolwedans Dam5 1990 to 2008.* August 2008.	Instrument-ation Data	5 & 6
Richards M. *Instrumentation Readings, Data and Information. Wadi Dayqah Dam Joint Venture.* Quriyat, Oman. March & August 2009.	Instrument-ation Data	4

Reference	Related Subject	Applicable Chapters
Sembenelli SC & Shengpei W. *Chinese Experience in the Design and Construction of RCC Arch Dams.* International Journal of Hydropower & Dams. Vol. 5. pp 95 - 100. 1998.	RCC Arch Dams	3
Schrader, EK. *Roller Compacted Concrete.* Chapter 20. Concrete Construction Engineering Handbook. Second edition. Edited by Nawy, EG. CRC Press. New Jersey. 2008.	RCC Textbook	2, 3 & 6
Shaw QHW. *The Role of Temperature in Relation to the Structural Behaviour of Continuously Constructed Roller Compacted Concrete and Rubble Masonry Concrete Arch Dams.* MSc Thesis, University of Brighton, UK. 2001.	Dam Behaviour Investigation	5 & 7
Shaw QHW. *An Investigation into the Thermal Behaviour of RCC in Large Dams.* Proceedings. 5th International Symposium on Roller Compacted Concrete Dams. Guiyang, China. pp 271-282. 2007	RCC Behaviour Evaluation	4 & 5
Shaw QHW. ARQ (PTY) Ltd. *Çine Dam. Design Thermal Analysis Report.* Özkar Construction Internal Report No. 1596-8539. Ankara, Turkey. September 2005.	Thermal Analysis	4
Shaw, QHW. *The Development of RCC Arch Dams.* Proceedings. 4th Symposium on Roller Compacted Concrete Dams. Madrid, Spain. pp 363-371. November 2003.	RCC Arch Dams	7
Shaw QHW, Geringer JJ & Hollingworth F. Department of Water Affairs Internal Report. *Mossel Bay (Wolwedans Dam) Government Water Scheme. Wolwedans Dam Completion Report.* DWAF Report No. K200/02/DE01. Pretoria. April 1993.	Construction Report	2 & 5
Shaw QHW & Maartens, WW. Department of Water Affairs Internal Report. *Construction & Grouting of the Wolwedans Dam Test Section.* Un-numbered DWAF Report. Mossel Bay. October 1988.	Construction Report	2
Shaw QHW & Greyling RP. *A New Model for the Behaviour of RCC in Dams under Early Thermal Loading.* Proceedings. 5th International Symposium on Roller Compacted Concrete Dams. Guiyang, China. pp 61-68. 2007.	RCC Behaviour Evaluation	3

Reference	Related Subject	Applicable Chapters
Shaw, QHW. *DWS 740. Standard Specification. Roller Compacted Concrete for Dams.* Department of Water Affairs & Forestry. Second Edition. August 2005.	RCC Specification	2
Shengpei W. *The Technology Development of RCC Dam Construction in China.* Proceedings. 5th International Symposium on Roller Compacted Concrete Dams. Guiyang, China. pp 41-52. 2007.	RCC Technology	1
SANCOLD. *Large Dams and Water Systems in South Africa.* SANCOLD. CTP-Book Printers. Cape Town, South Africa. 1994.	Reference Book	2
Structural Research and Analysis Corporation (SRAC). *COSMOSM Finite Element Analysis Program.* General-purpose, modular FE Analysis system. SRAC, a division of SolidWorks Corporation, Dessault Systemes, S.A., Paris, France.	Computer Software	5 & 7
The Department of Water Affairs & ESCOM. *Hendrik Verwoerd Dam – SA Water Giant.* Information Brochure. New Graphis, Johannesburg. 1972.	Descriptive Project Booklet	1
The Department of Water Affairs & Forestry Internal Report. *Knellpoort Dam Completion Report.* Information Report No. D203/39/DD04. DWAF, Pretoria. 1991.	Construction Report	2
Turanli L. *Determination of Thermal Diffusivity and Creep for Concrete Core Specimens Taken from Çine Dam.* Middle Eastern Technical University. Report Code No. 2001-03-03-2-0033. Ankara, Turkey. September 2001.	Laboratory Testing Report	4
United States Army Corps of Engineers. *Arch Dam Design.* Engineering Manual, EM 1110-2-2201. USACE. Washington. May 2004.	Dam Design Guideline	1, 3, 4, 5 & 6
United States Army Corps of Engineers. *Gravity Dam Design.* Engineering Manual, EM 1110-2-2200. Washington. June 1995.	Dam Design Guideline	3
United States Army Corps of Engineers. *Roller Compacted Concrete.* Engineering Manual, EM 1110-2-2006. USACE. Washington. January 2000.	Dam Design Guideline	3, 6 & 7

Reference	Related Subject	Applicable Chapters
United States Army Corps of Engineers. *Thermal Studies of Mass Concrete Structures.* Engineering Technical Letter, ETL 1110-2-542. USACE. Washington. May 1997.	Dam Design Guideline	1, 3, 4, 5 & 6
United States Army Corps of Engineers. *Time History Analysis of Concrete Hydraulic Structures.* Engineering Manual, EM 1110-2-6051. USACE. Washington. December 2003.	Dam Design Guideline	5
United States Army Corps of Engineers. *Seismic Provisions for Roller Compacted Concrete Dams.* Engineering Pamphlet, EP 1110-2-12. USACE. Washington. September 1995.	Dam Design Guideline	5
United States Department of the Interior. Bureau of Reclamation. *Design of Arch Dams.* US Government Printing Office. Denver. 1977.	Dam Design Guideline	3
Vinci & CCC Construction JV. Wadi Dayqah Dam. *Quality Control Records*. Quriyat, Oman. February 2008.	Recorded Data	2 & 4
Wadi Dayqah Dam JV. *Wadi Dayqah Dam. Drawings for Construction.* Sultanate of Oman. M.R.M.E.W.R. Muscat, Oman. August 2006.	Dam Design Drawings	2 & 4
Xia C, Kunhe F & Li Z. *Mineral Admixtures' Impact on RCC Anti-Crack Performance.* Proceedings. 5th International Symposium on Roller Compacted Concrete Dams. Guiyang, China. pp 475-480. 2007.	RCC Materials	3
Yi L, Guoxin Z, Jianwen L, Ping Y, Yihua D &Yongsheng G.*Back Analysis of Temperature Field and Temperature Stress of Jinghong RCC Dam.*Proceedings.5th International Symposium on Roller Compacted Concrete Dams. Guiyang, China. pp 557-564. November 2007.	Thermal Analysis	3
Zhu, B. *RCC Arch Dams: Temperature Control and design of Joints.* Journal of International Water Power and Dam Construction. Progressive Media. Sidcup, UK. August 2006.	Technical Paper on Arch Dams	3 & 7

Reference	Related Subject	Applicable Chapters
Zhu B, Xu P & Wang S. *Thermal Stresses and Temperature Control of RCC Gravity Dams*.Proceedings.3rd International Symposium on Roller Compacted Concrete Dams. Chengdu, China. pp 65-77. 1999.	Thermal Analysis	3

APPENDIX A

THE EFFECT OF TEMPERATURE DROP LOAD ON STRUCTURAL ARCH ACTION

THE EFFECT OF TEMPERATURE DROP LOADS ON STRUCTURAL ARCH ACTION

Background

Conventional mass concrete dams are constructed as a series of vertical, monolithic blocks (see **Figure A1**). These blocks are proportioned to accommodate concrete autogenous and drying shrinkage and shrinkage creep that occurs during the hydration cycle. Limiting the dimensions of each block, restraint against shrinkage is reduced and residual tensile stresses are maintained below the concrete tensile strength, to eliminate the possibility of cracking. In the case of a gravity dam, which functions to transfer the water load directly into the foundation in 2 dimensions, the monoliths are connected with waterstops, but are otherwise simply allowed to shrink away from each other.

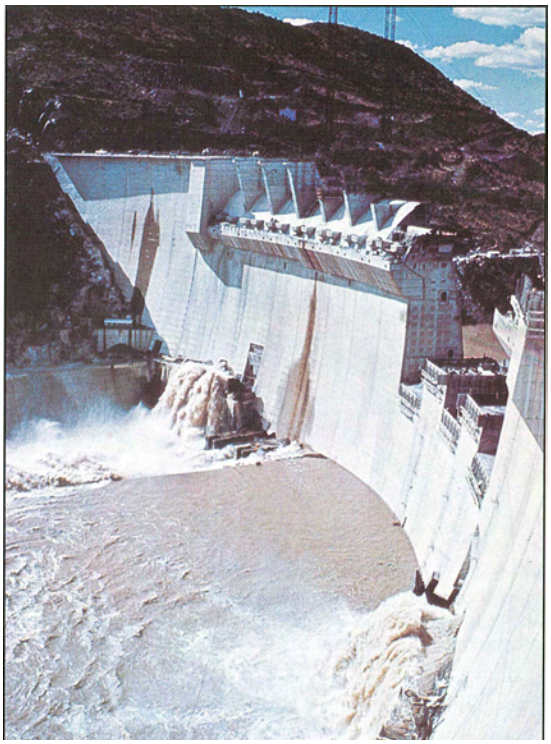

Figure A.1: CVC Arch Dam Construction in Monoliths

In the case of an arch dam, which transfers the water load in 3 dimensions into the foundation, it is necessary to re-establish structural continuity between the monolithic blocks. Once all shrinkage and creep has occurred, the hydration heat has been dissipated and the concrete is at a low temperature, continuity is consequently re-established by filling the gap between the monoliths with grout under pressure. In order to allow the joint grouting to be undertaken and subsequently the structure to be loaded, it is often necessary to draw out the hydration heat using chilled water circulated through looped pipes, which are cast into the concrete. In addition, ice is quite often added into the concrete during mixing in an effort to suppress the maximum temperature experienced during hydration. Constructing in vertical monoliths, with lift heights commonly of the order of 2.5 m, also allows some of the hydration heat to be dissipated before the subsequent lift is superimposed.

In the case of Roller Compacted Concrete (RCC) construction, the dam is essentially placed horizontally and contraction joints are induced rather than formed, while the process of bulldozer-spreading and roller compaction does not lend itself readily to the incorporation of cooling pipe loops. Furthermore, the rapid nature of the placement implies that the majority of the heat generated in the process of hydration is trapped within the body of the dam.

In Rubble Masonry Concrete (RMC) construction, the dam is also essentially placed horizontally, but in this case, no contraction joints are included. As the structures

are generally small, the sections are thin, the cement content is low and construction is slow, instrumentation has demonstrated that the entire hydration heat escapes quickly and the temperature of the RMC material is not really raised in the process ofthe hydration cycle. While the temperature drop load on an RMC arch is accordingly limited to the difference between the placement temperature and the final coldest winter temperature, the thin sections imply that very little insulation is provided to the core of the dam and consequently, this load can quite easily exceed 10°C. With no contraction joints and consequently no facilities to redress temperature shrinkage, the dam structure itself must be designed to accommodate the full temperature drop without developing deleterious stress levels.

Introduction

This brief document presents an explanation of the impacts of temperature drop loads on the structural function of arch dams. In view of the fact that they never have formed, or induced joints, RMC dams will be used to demonstrate the associated effects and impacts of a typical range of temperature drops.

Arch Dams and Temperature Drop Loads

Due to the fact that RMC arch dams are constructed without contraction, or expansion joints, all thermal effects, expansion as a result of hot temperatures and contraction as a result of cold, must be accommodated within the body of the structure itself. In relatively thin structures, such as arch and arch buttress dams on the scale applicable to RMC, the entire wall will be largely subject to surface temperature effects, significant insulation from external temperatures typically only occurring at depths in excess of 3 - 4 m from surface. Similar thermal phenomena and consequential effects have been studied in some depth for other concrete dam types and specifically for RCC dams. RCC arch dams suffer similar effects, particularly in respect of the fact that both RCC and RMC dams are constructed as continuous bodies, usually in horizontal placement layers from one flank to the other, and not monolithic vertical blocks as is the case for conventional concrete. Although placement rates and hydration heat related problems are significantly different in each case, parallels may be drawn and much experience gained in thermal and related structural analysis of concrete and RMC arches may be applied to RCC arches.

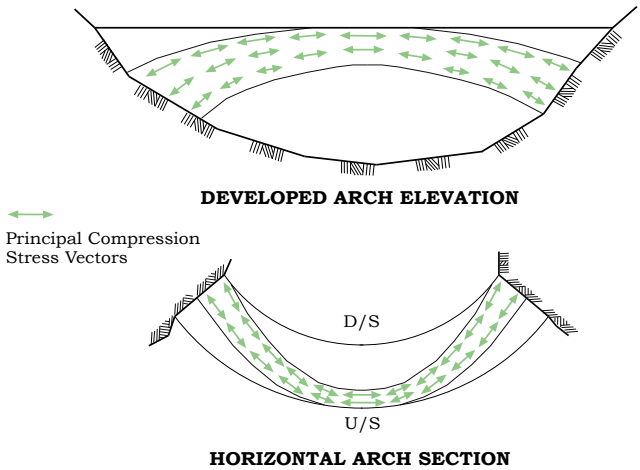

Figure A.2: Typical Stress Flow in Arch

All variants of the concrete arch dam are inherently susceptible to temperature related effects, although very efficient arches, such as those in tight V shaped

valleys where arch stresses are high, are less sensitive than those in wider, open valleys, where cantilever stresses are more pronounced. Whilst an arch dam is an inherently safe structure which can generally be pushed way beyond design loadings before failure, nevertheless it is considered important that efficient function is preserved and that the mode of structural function is well understood by the designer.

In the case of an arch dam in a wide valley (width/height, or canyon factor > 3.5), the water load develops arch stresses that are transferred internally through the top of the dam in the centre down into the lower portion of the abutment on each flank (see **Figure A.2**). Very little lateral compression is developed in the lower portion of the central section of the wall. When subjected to low temperatures, the wall structure effectively shrinks, although its foundation remains unaffected, causing tension across the structure, from one abutment to the other. To accommodate the water load, the structure must take up these tensions through movement, which occurs by a general deflection of the crest downstream and an associated tipping forward of the dam wall, which causes increased tensions at the upstream heel and increased compressions at the downstream toe. In addition, the area of effective arch compression, through the upper portion of the dam in the centre (between abutments), decreases and associated levels of compression over this smaller area correspondingly increase. In broad and general terms, less of the structure functions to transfer water load into the foundations, stress within the effective areas increases and the structure becomes effectively less efficient in function, with a significant portion of its volume no longer carrying structural load.

This effect can be described by imagining the dam wall as a series of monolithic blocks as pictured in **Figures A.3 to A.6**. Temperature shrinkage of the wall would cause each of these blocks to reduce in size and shrink away from each other as illustrated in **Figure A.4**, the most significant opening between blocks occurring farther away from the restraining points (abutments).

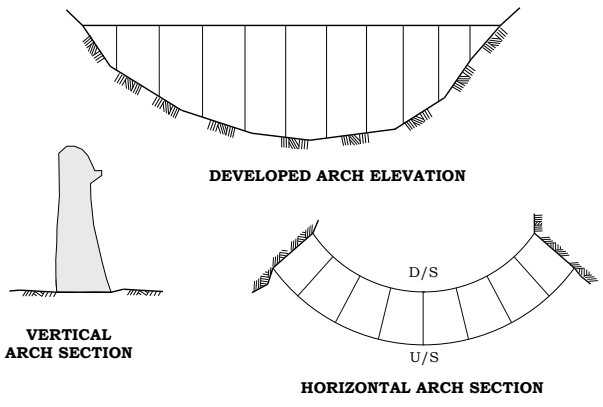

Figure A.3: Arch as Series of Blocks

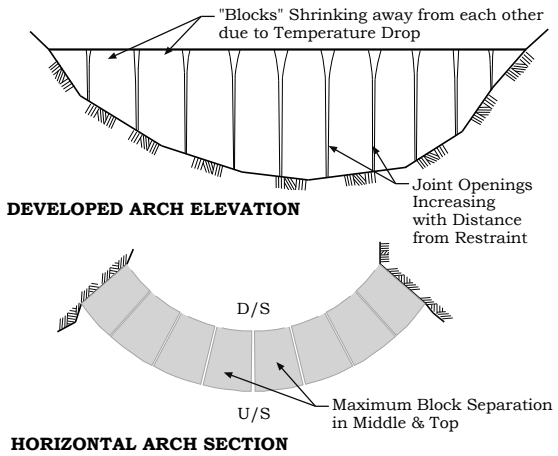

Figure A.4: Typical Temperature Loss Shrinkage

To accommodate the water load and associated arching stresses, the blocks deflect as cantilevers in a downstream direction until closure between blocks occurs at the crest. As a result of restraint of the wall against the abutment on either flank and the higher flexibility of the taller cantilevers, the central portion of the crest moves farthest, with each successive block to the sides moving less. The consequence of this effect is a final arch with a larger effective radius (see **Figure A.5**). The alignment of the sides of each block remains oriented on the original radius and accordingly the wedge shaped blocks are effectively too narrow at their downstream faces to form complete and even contact with each other on the larger, deflected radius. This in turn implies that the blocks will make contact with each other initially only over the upstream side of their respective surfaces and the arch will accordingly display a "bursting" effect. In this process horizontal compressive stresses in the central upstream portion of the arch increase, as do horizontal tensions in the downstream portion and tensions in the heel and compressions in the toe at the abutments. Looking at the wall in terms of a series of cantilevers, this effect is seen as a tipping forward of the upper portion as shown in **Figure A.6**.

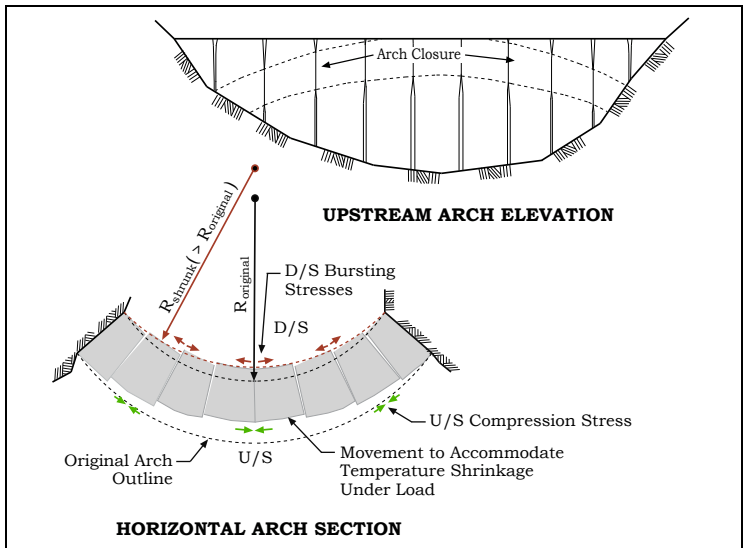

Figure A.5: Shrunk Blocks under Water Load

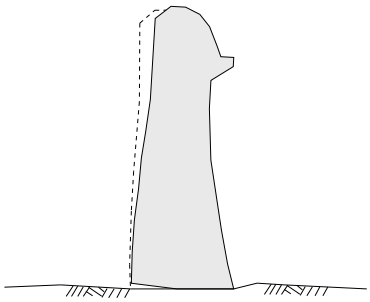

Figure A.6: Deflection of Cantilever

In the described process a great deal of the efficiency of the arch is lost, with only the portions of the structure illustrated in **Figure A.4** actually being effective. If a zero tensile stress is assumed for the RMC all areas of tension will be subject to cracking and compressive stresses in the remainder of the wall will correspondingly increase to redistribute structural load.

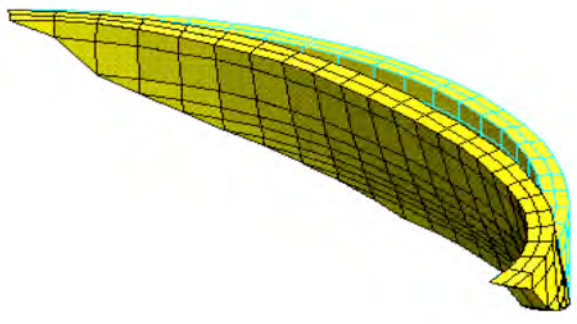

Figure A.7: Exaggerated Wall Deflections for Temp. Drop & Water Loads

In the case of a conventional concrete arch dam, these temperature effects are mitigated by construction in monolithic blocks, with subsequent grouting at low temperature to re-establish structural continuity between the blocks, on the original arch radius. In the case of an RMC dam, it is not possible to re-establish structural continuity by grouting and the design must accommodate these effects; in virtually every case, the most severe loading case for an RMC arch being hydrostatic, gravity, uplift and temperature drop loads.

Quantification of Typical Temperature Drop Impacts

In order to quantify the above temperature drop effects in the case of a typical RMC arch dam and to provide some illustration of the impact on stress patterns, a simple elastic Finite Element analysis was completed. The arch model was configured to a maximum height of 20 m using the COSMOS/M FE analysis system, with a constant extrados (upstream face) radius of 60 m, a wide valley canyon factor (crest chord length/height) of 5, a constant wall thickness of 3 m and a crest arch aperture angle of 120°. Whilst this geometry is fairly typical of a larger scale wide valley arch constructed in RMC, it also represents a very effective arch shape, in terms of structural function. Furthermore, an idealised, symmetrical arch was applied, as opposed to a real example, in order to ensure that secondary effects, or stress peculiarities resulting from topographical discontinuities, or irregularities did not cloud the structural and temperature evaluation.

A typical South African climate might see effective RMC placement temperatures averaging 22°C, final minimum winter water temperatures of 10°C and a minimum average daily winter air temperature of 8°C. Assuming some insulation and temperature time lag, and remembering the thin sections typical of RMC arches, an effective temperature drop of the RMC from placement to minimum winter temperature might exceed 10°C. For the Finite Element analysis, the stress patterns in a full dam were compared for the cases of an 8°C uniform body temperature drop and no temperature drop.

The following series of figures is presented as a means to illustrate the comparative critical stress levels and patterns, when temperature drop loads are ignored and when they are taken into account.

Figures A.8 and **A.9** illustrate clearly the impact of the 8°C temperature drop on the downstream face stresses, with the strong pattern of horizontal arching disappearing to be replaced by bursting tensions and a more vertical transfer of stresses into the foundation at the base of both flanks. The concentrated stress levels can further be seen to increase dramatically.

Figures A.10 and **A.11** illustrate the manner in which the temperature drop causes the even, horizontal arch stresses in the upstream face to become concentrated toward the top of the structure, as the shrunk cantilevers displace toward the downstream under load and make contact with each other at the crest. The concentration of stresses over a small contact area correspondingly causes the maximum values to increase. The general tipping forward of the cantilevers causes the heel tensions (and toe compressions) to rise very dramatically. In effect, the temperature drop causes the arch structure to become a series of propped cantilevers, with a propping action being provided by arching developed at the crest, as contact between adjacent cantilevers prevents further downstream

movement. This further accounts for the vertical tensions on the tallest portions of the downstream face, as bending between the foundation and the "propped crest" induces a beam action.

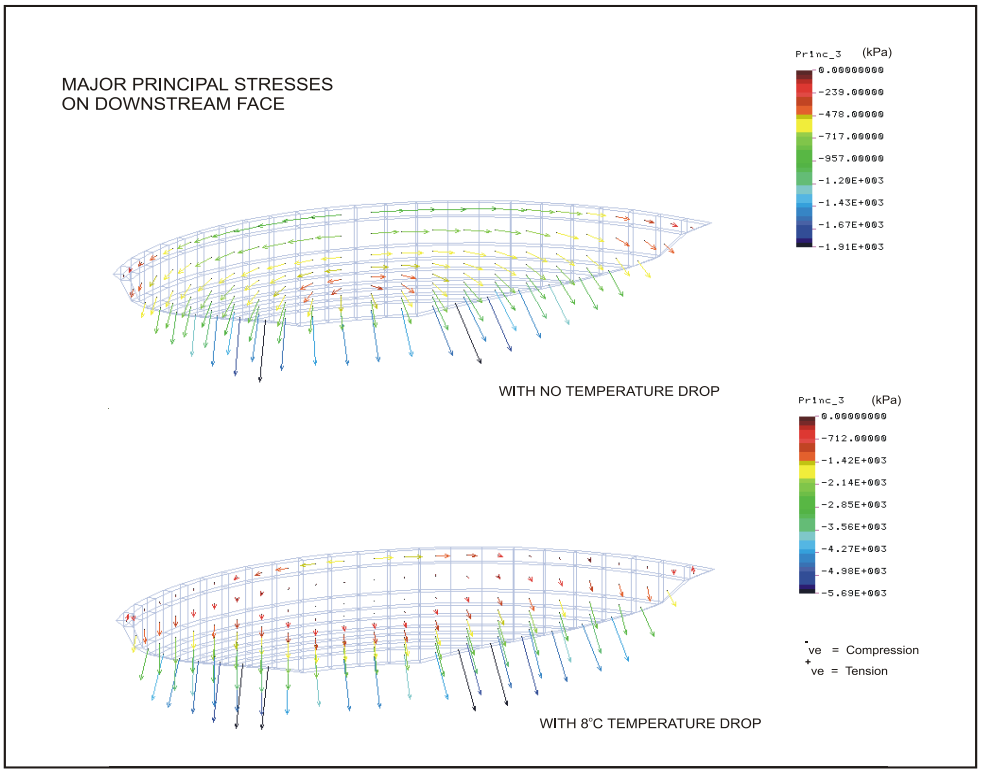

FIGURE A.8: MAJOR PRINCIPAL STRESSES ON DOWNSTREAM FACE

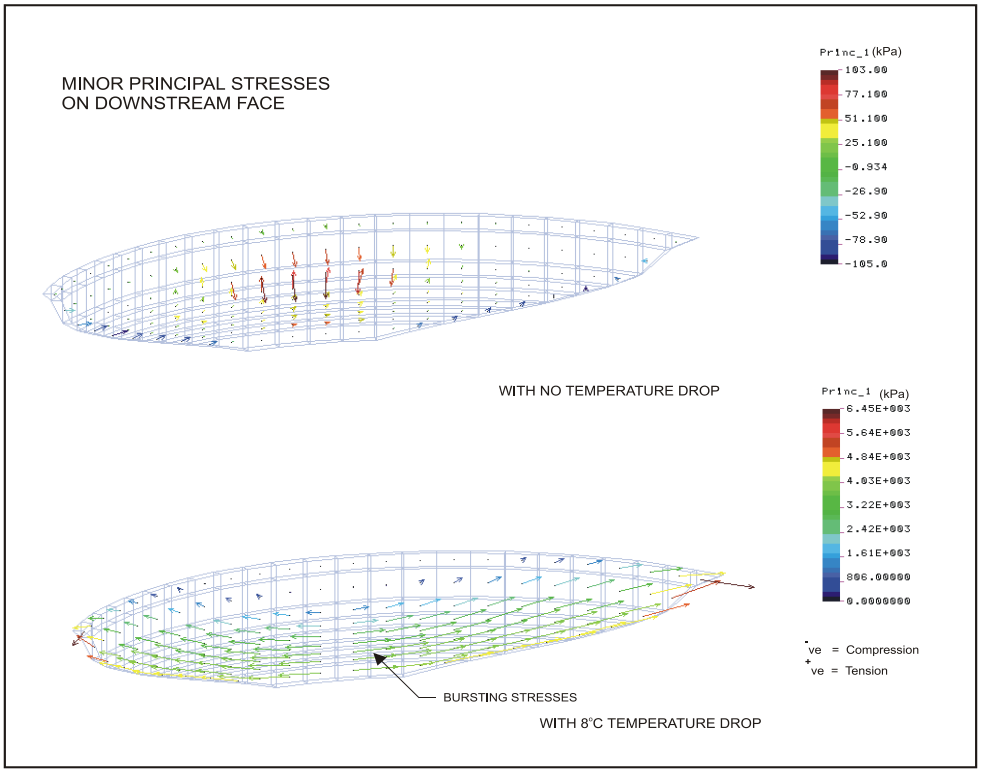

FIGURE A.9: MINOR PRINCIPAL STRESSES ON DOWNSTREAM FACE

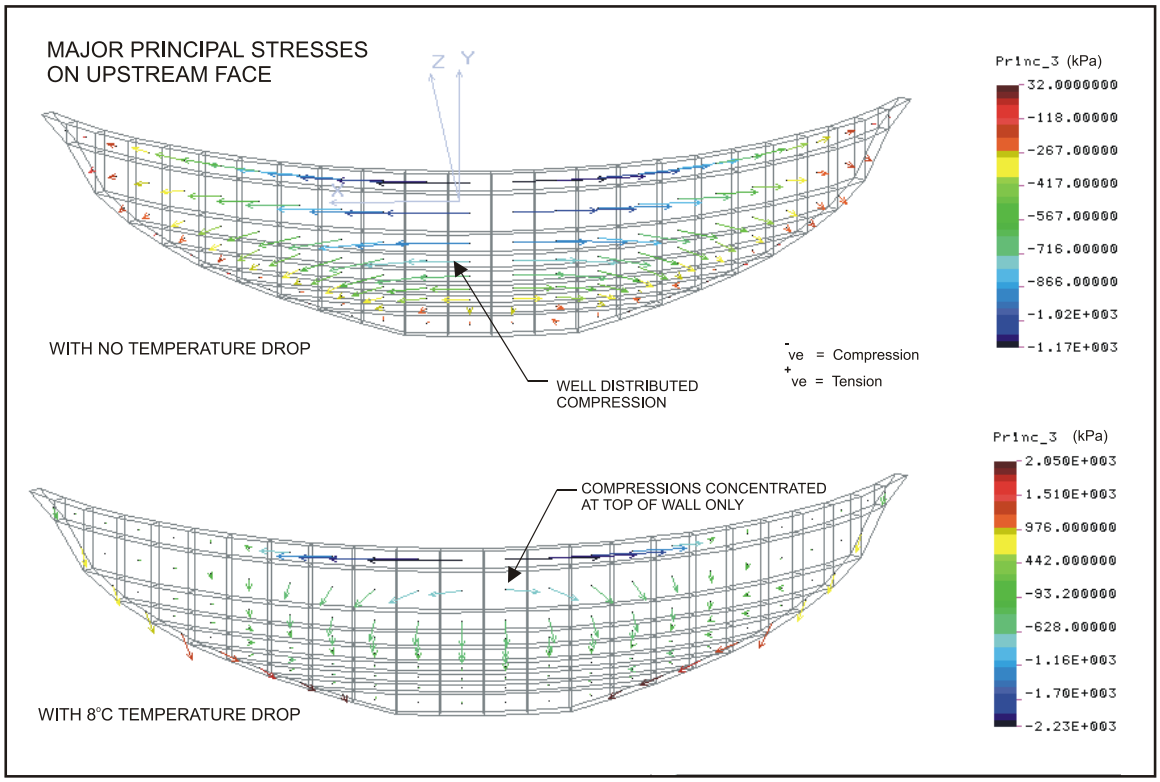

FIGURE A.10: MAJOR PRINCIPAL STRESSES ON UPSTREAM FACE

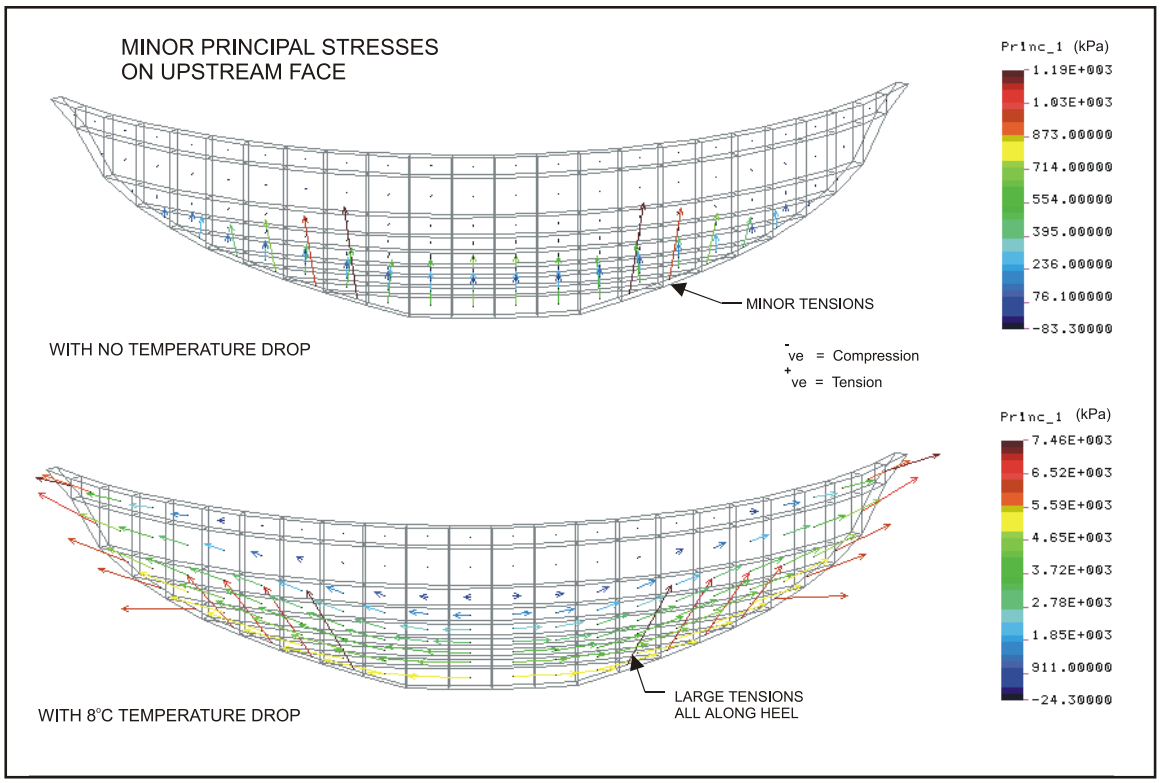

FIGURE A.11: MINOR PRINCIPAL STRESSES ON UPSTREAM FACE

Figure A.12 reflects the manner in which very significantly greater shear stresses are developed in the structure as a consequence of temperature drop. It should of course be borne in mind that the shear stresses indicated relate primarily to the restraint of the shrunk dam structure by the fixed foundation. In reality this effect will be mitigated slightly by the fact that the virtually constant temperature of the foundations will tend to ensure that temperature variations in the immediate areas of the dam are less significant than elsewhere.

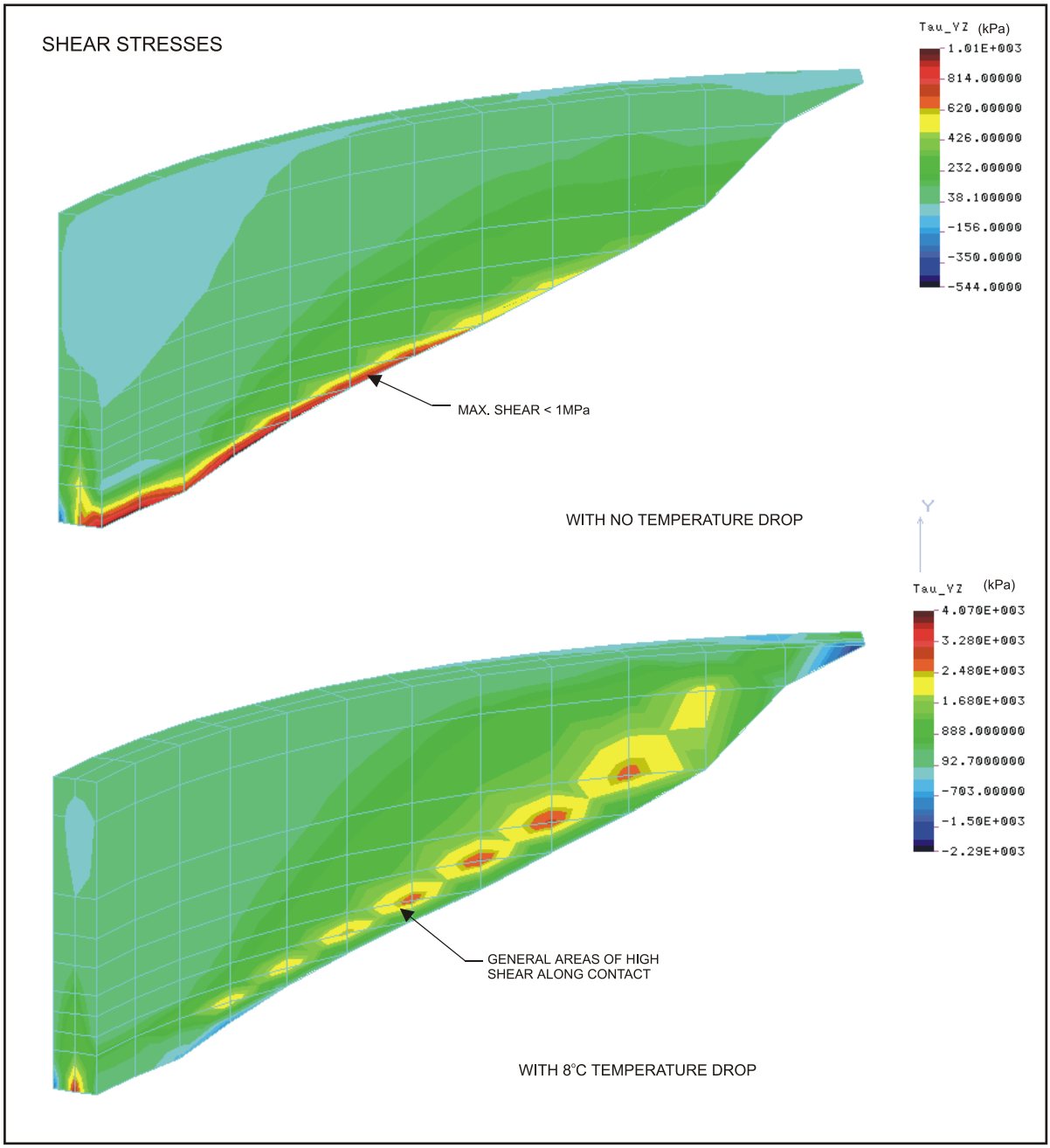

FIGURE A.12: SHEAR STRESSES

QUANTITATIVE ANALYSIS OF CRITICAL STRESS VARIATIONS FOR VARIOUS TEMPERATURE DROP LOADS AND MATERIALS PROPERTIES

Background

The foregoing discussion and analyses clearly reflect the very significant impact of a range of typical temperature drop loadings on an RMC arch dam, in terms of stress patterns. The following set of analyses was completed in order to quantify the impacts in terms of critical maximum stress levels in relation to variations in temperature drop and RMC constituent materials properties.

Analysis Description

For the purpose of this temperature sensitivity analysis, the same idealised, symmetrical, wide valley arch dam as developed for the previously described analysis was applied; with a maximum height of 20 m, a developed crest length of 120 m, an arch extrados radius of 60 m, a constant wall thickness of 3 m and a crest arch aperture angle of 120°.

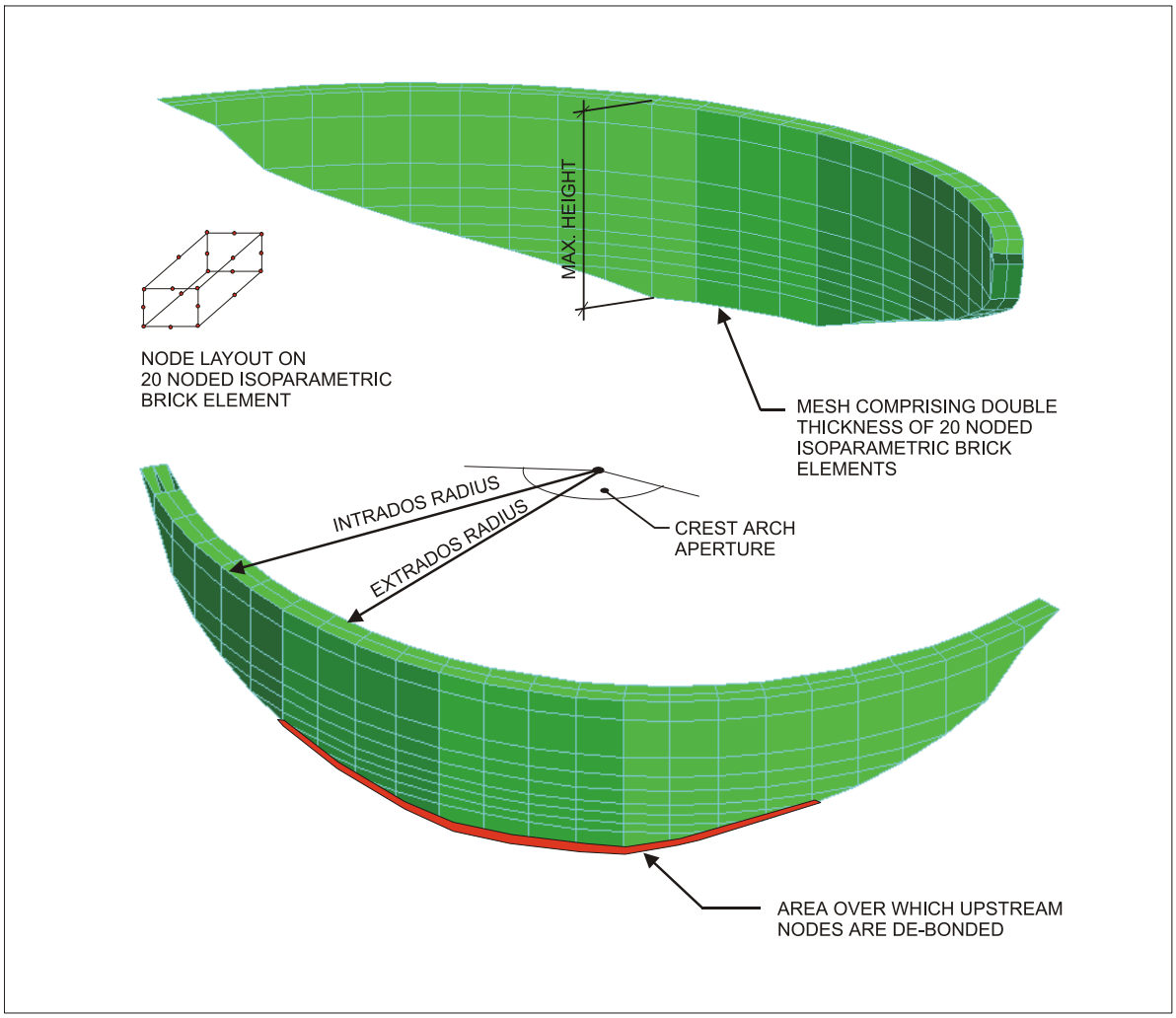

FIGURE A.13: ARCH MODEL DEFINITIONS AND DESCRIPTION

Analysis Methodology

All analyses were undertaken using a material density of 25 kN/m^3 and full supply hydrostatic loading, ignoring uplift and silt. Against these constants, the relative effects of various uniform temperature drops and variation of effective elastic modulus and thermal expansivity were reviewed. Whilst the actual effects of uplift are not likely to be significant, with a wall thickness of just 3 m, in particular circumstances, it could be unwise to ignore silt accumulation in a real design. However, in the case of the analyses addressed herein, the structural loading only really represents a reference against which respective temperature effects are evaluated in a qualitative manner and stresses are not derived for review against specific target, or limiting values. Indicated stresses are accordingly under-estimated. The COSMOS/M Finite Element Analysis system was applied for these analyses, using only the elastic module for simplicity.

Analysis Model

To reduce overall process time on the 33 analyses comprising this sensitivity study, the dam wall alone was analysed, without a foundation. Nodes on the foundation were constrained against translation, which creates conditions equivalent to a fully rigid foundation. While the wide-valley arch shape of the wall will allow this simplification without developing stress anomalies, the over-rigid foundation will result in an underestimation of total arch deflection and any downstream face bursting stresses (S1 - D/S) and an exaggeration of toe compressions (S3 – D/S).

Analysis Loadings and Material Properties

For the thermal sensitivity analyses, a range of three temperature drops was adopted; 6^o, 8^o and 10^{o}C. These figures represent realistic total structural temperature drops in a structure of relatively thin section (< 4m), in relatively moderate climatic conditions. Whilst the 6^{o}C temperature drop is considered low for all but thicker section structures in a very temperate climate, even 10^{o}C might be considered too low for a dam built during the summer months in an area that experiences low winter temperatures. A range of elastic moduli and thermal expansivities for RMC were adopted, in line with the appropriate values for concrete composed of various typical aggregate types. For example, RMC elastic moduli of 15, 20 and 40 GPa were applied. While 40 GPa might be considered rather high as an effective elastic modulus for RMC, it was included in an effort to evaluate the influence of a particularly high modulus that might result as a consequence of the direct contact of large size, high quality rock particles. Thermal expansivities of 5, 7 and 12 x 10^{-6} per ^{o}C were evaluated, which values reflect a typical range of equivalent figures for concretes composed of aggregates of granites and gneisses to quartzites and cherts respectively.

De-bonding Interface Nodes in Tension

The initial analyses revealed relatively high levels of tension at the upstream heel of the dam under normal loading conditions, ignoring temperature drop effects. To relieve some of these stresses and to bring the general tension to a more acceptable level, the upstream row of nodes at the heel in the centre of the wall was freed from restraint and allowed to move. Whilst this lowered general upstream tensions to typically acceptable levels under normal loading conditions, the imposition of temperature drop and a worsening in material properties took tensions on certain of the inner nodes to extremely high levels. Such tension would undoubtedly cause cracking and a significant rise in related toe compression levels. However, the model was not changed for such loading situations, as its purpose is one of comparison rather than isolating final stress levels.

Analysis Results

Stress and displacement plots were developed for each loading case and material property combination and contour versions of two such plots are illustrated here in **Figures A.15** to **A.18**. Colour vector plots are the preferred medium for result analysis for arch dams, as this output format allows the most effective evaluation of stress movement through the structure and the typical stress patterns applicable in the case of the arch dam studied can be observed on **Figures A.8** to **A.12**. The major stresses and displacements read off these plots are listed in **Table A.1**. The stress values listed are nodal values and these can be rather exaggerated in elastic FE analysis, particularly at a discontinuity.

In **Table A.1** the principal stresses indicated may be defined as follows:

- S3 (D/S) - Downstream Face Cantilever Toe Compressive Stress;
- S1 (U/S) - Upstream Face Cantilever Heel Tension;
- S3 (U/S) - Upstream Face Arch Compressions; and
- S1 (D/S) - Downstream Face Arch bursting Tensions.

The location of the critical stresses listed in the table are indicated on **Figure A.14**.

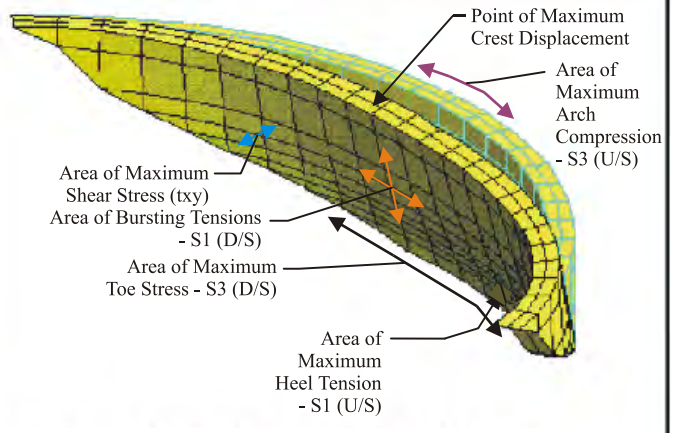

FIGURE A.14: AREAS OF MAXIMUM STRESS IN WIDE VALLEY ARCH DAM

Table A.1: Summary of Stress Analysis Results

Total Temp. Drop (°C)	Thermal Expans-ivity (Strain/°C)	Elastic Modulus (GPa)	Max D/S Displac'nt (mm)	Stress (MPa)				
				S3 (D/S)	S1 (U/S)	S3 (U/S)	S1 (D/S)	txy
10	5 x 10^{-6}	15	10.3	7.25	- 4.75	1.65	- 0.76	1.30
		20	8.8	7.87	- 5.41	1.75	- 1.01	1.39
		40	6.5	10.40	- 8.09	2.51	- 2.01	2.00
	7 x 10^{-6}	15	12.0	7.99	- 4.75	1.77	- 1.06	1.41
		20	10.5	8.87	- 5.41	1.93	- 1.41	1.56
		40	8.2	12.40	- 8.09	3.28	- 2.82	2.60
	12 x 10^{-6}	15	16.2	9.88	- 7.55	2.32	- 1.81	1.85
		20	14.7	11.4	- 9.16	2.90	- 2.41	2.30
		40	12.4	15.8	- 16.2	3.23	- 4.83	4.12
8	5 x 10^{-6}	15	9.5	6.88	- 4.35	1.59	- 0.605	1.24
		20	8.0	7.37	- 4.88	1.67	- 0.805	1.32
		40	5.7	9.37	- 7.01	2.33	- 1.607	1.71
	7 x 10^{-6}	15	10.8	7.47	- 5.00	1.69	- 0.84	1.33
		20	9.3	8.17	- 5.73	1.87	- 1.13	1.44
		40	7.0	11.00	- 8.73	2.74	- 2.25	2.18
	12 x 10^{-6}	15	13.9	8.82	- 6.40	1.91	- 1.39	1.59
		20	12.4	9.98	- 7.66	2.35	- 1.85	1.94
		40	10.1	14.70	- 12.60	4.29	- 3.70	3.37
6	5 x 10^{-6}	15	8.6	6.51	- 3.96	1.23	- 0.46	1.18
		20	7.1	6.88	- 4.35	1.31	- 0.61	1.24
		40	4.8	8.37	- 5.94	1.83	- 1.20	1.47
	7 x 10^{-6}	15	9.7	6.95	- 4.43	1.60	- 0.64	1.25
		20	8.1	7.47	- 4.99	1.69	- 0.85	1.33
		40	5.8	9.58	- 7.23	2.2	- 1.69	1.77
	12 x 10^{-6}	15	12.2	8.07	- 5.62	1.78	- 1.09	1.42
		20	10.7	8.97	- 6.58	1.97	- 1.45	1.59
		40	8.4	12.6	- 10.50	3.36	- 2.90	2.66
0		15	6.2	5.43	- 0.5	1.36	-	1.06
		20	4.6	5.43	- 0.5	1.36	-	1.06
		40	2.3	5.43	- 0.5	1.36	-	1.06

$^{+}$ve compression $^{-}$ve tension

Stress levels shaded in red are considered excessive/unacceptable for RMC.

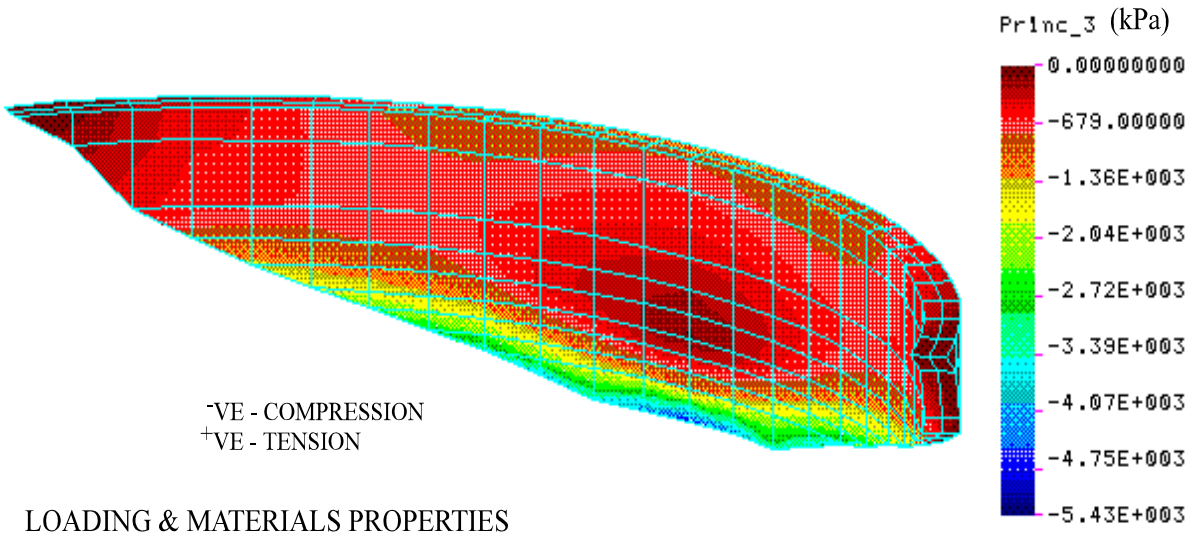

LOADING & MATERIALS PROPERTIES

FSL + Gravity + No Temperature Drop
Elastic Modulus = 40GPa
Thermal Expansivity = 12 x 10^{-6}

FIGURE A.15: CONTOUR STRESS PLOT – S3 DOWNSTREAM FACE

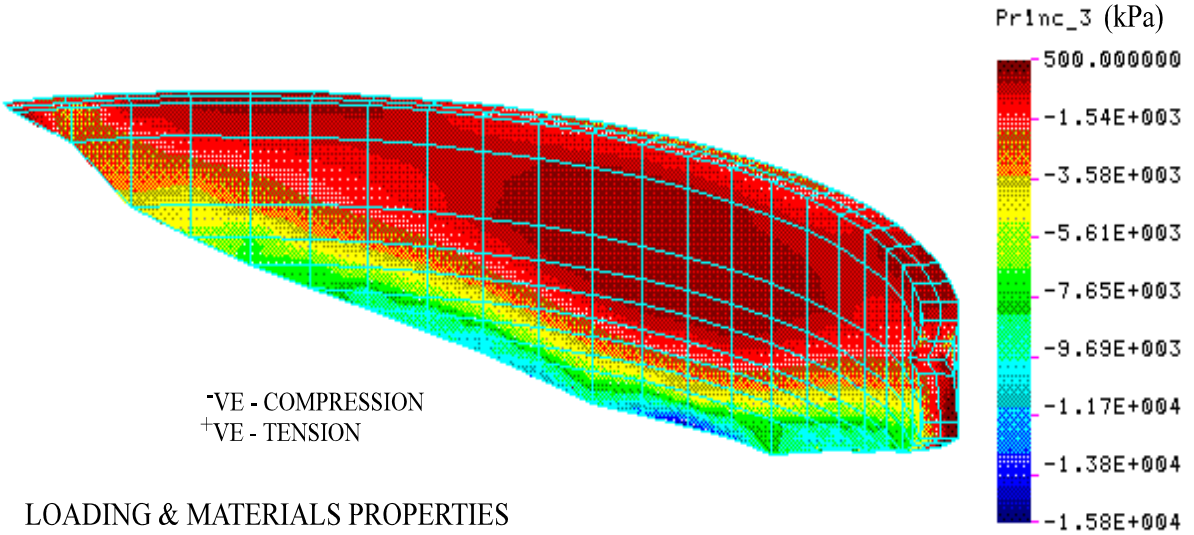

LOADING & MATERIALS PROPERTIES

FSL + Gravity + 10^{o}C Temperature Drop
Elastic Modulus = 40GPa
Thermal Expansivity = 12 x 10^{-6}

FIGURE A.16: CONTOUR STRESS PLOT – S3 DOWNSTREAM FACE

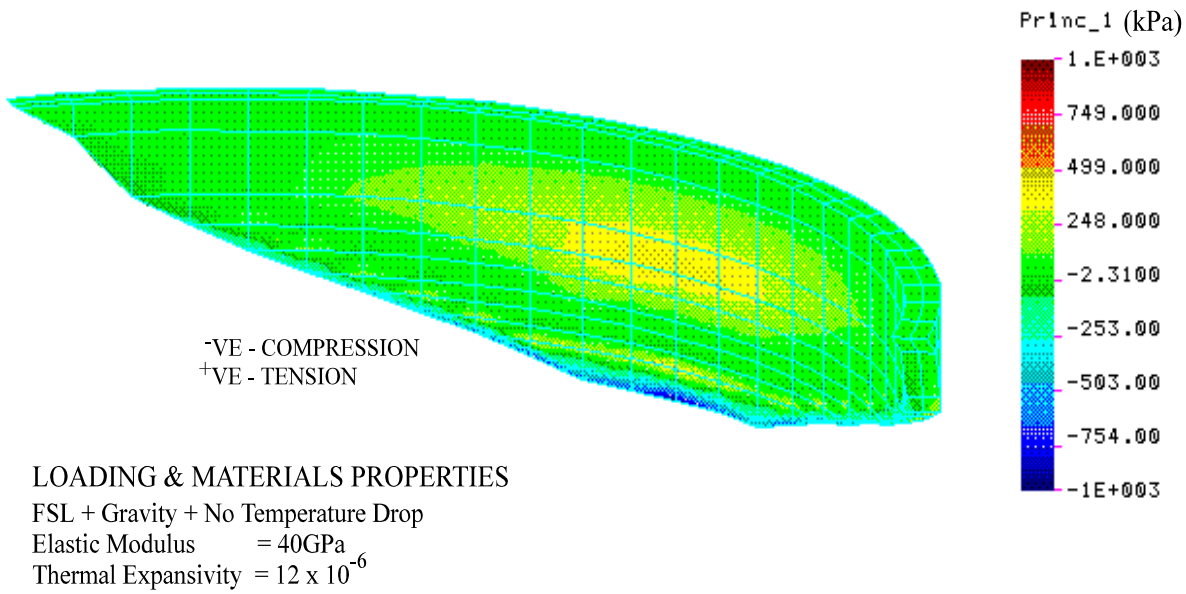

LOADING & MATERIALS PROPERTIES
FSL + Gravity + No Temperature Drop
Elastic Modulus = 40GPa
Thermal Expansivity = 12 x 10^{-6}

FIGURE A.17: CONTOUR STRESS PLOT – S1 DOWNSTREAM FACE

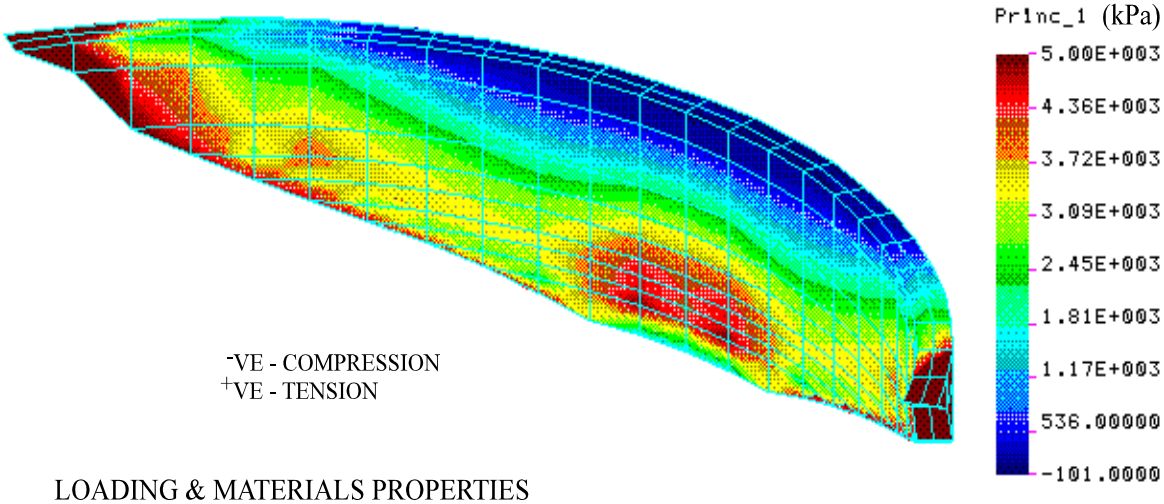

LOADING & MATERIALS PROPERTIES
FSL + Gravity + 10^{o}C Temperature Drop
Elastic Modulus = 40GPa
Thermal Expansivity = 12 x 10^{-6}

FIGURE A.18: CONTOUR STRESS PLOT – S1 DOWNSTREAM FACE

Result Summary

Table A.2 provides a basic summary of the findings presented above.

Table A.2: Impact of Material Properties and Temperature on Arch Stresses

Environment & Materials	**Max. Compression** (MPa)	**Max. Shear** (MPa)	**Max. Displacement** (mm)	**Max. Tension** (MPa)
Good Materials Ignoring Temp.	5.4	1.1	6.2	0.5
Good Materials + mild Temp effects	6.5	1.2	8.6	3.9
Unfavourable Materials + cold climate	15.8	4.1	12.4	16.2

Discussion

The shaded blocks in **Table A.1** indicate stress levels that might be considered unacceptable for RMC of typical strength. It is worth, however, bearing in mind that these high stresses are largely located against the foundation and the FE analysis method applied, using wedge elements in these areas and using node fixity to represent a completely rigid foundation, will tend to over-estimate toe compression stresses.

For certain of the material property-temperature drop combinations, stresses are undoubtedly high enough to result in failure, even allowing for stress re-distribution that would be evident through non-linear analysis. Ignoring the actual values of the stresses indicated, the results produced reflect the clear influence of temperature effects and RMC material properties on stress intensities.

When a temperature drop load is applied, significant advantage is obviously gained when the available construction materials produce an RMC of low thermal expansivity. It is, however, interesting to note that stress levels are typically increased by a similar factor by a doubling of the RMC Elastic Modulus, as a doubling of the RMC Thermal Expansivity. The same dam wall, under the same water load, will exhibit stresses over 3 times higher when constructed in a more extreme climate with harder materials of higher thermal expansivity than when constructed in a temperate climate with softer materials of lower thermal expansivity. Furthermore, toe compressive stresses can treble when a significant temperature drop is applied to a rigid structure of high thermal expansivity.

It is significant to note that the majority of RMC arch structures in southern Africa are exposed to a relatively mild climate.

Analysis Conclusions

The following primary conclusions may be drawn from the fore-going analyses:

1. Thermal effects are as critical in the design of RMC arch dams as the hydrostatic loads;

2. Thermal effects are highly dependent on RMC material properties, specifically thermal expansivity and elastic modulus;

3. Even in ideal climatic conditions, temperature drop related stresses are significant in relation to hydrostatic structural stresses, irrespective of RMC material properties;

4. A low thermal expansivity in RMC is of significant advantage in lowering temperature related structural stresses;

5. RMC with a low modulus of elasticity displays greater deformation, but lower critical stress levels, as the more malleable structure deforms and re-develops arching more effectively than a stiffer structure, in which stress is passed through smaller contact areas;

6. Where RMC of relatively high thermal expansivity and high elastic modulus is constructed in an extreme climate, temperature effects are critical and stresses may very easily reach dangerous levels. In such an environment, construction temperature control measures will be necessary; and

7. The slender structures typically applied for RMC arch dams give rise to their particular susceptibility to temperature drop loadings.

The above conclusions are valid, in principle, for all arch dams and the importance of addressing temperature drop loads in all arch design is consequently quite obvious. While the analyses presented are less critical and relevant in the case of a CVC arch dam, where structural continuity can easily be re-established by grouting the open joints between the blocks, they are specifically relevant in the case of RCC arch dams, where the grouting of induced joints and the timing of that grouting become fundamental considerations.

REFERENCES

[1] Rankine, RGD, Krige, GJ, Teshome, D, Grobler, LJ. *Structural aspects of labour-intensively constructed, uncut stone masonry arch bridges.* SAICE Journal. Volume 37, Number 3. 1995.

[2] Shaw, QHW. *The Development of Concrete Technologies in Dam Engineering and Beyond.* Proceedings. Concrete Society National Convention. Sun City. September 1994.

[3] Shaw, QHW. *Rubble Masonry Concrete Dam Design and Construction. Part 1: New Generation RMC Dams in RSA, as illustrated through the Bakubung, Welgevonden and Genadendal Dams*. SAICE Journal. April 1998.

[4] Shaw, QHW. *Rubble Masonry Concrete Dam Design and Construction. Part 2: Proposed Design Standards and Related Influences*. SAICE Journal. April 1998.

[5] US Army Corps of Engineers. *Thermal Studies of Mass Concrete Structures*. Engineering Technical Letter. ETL 1110-2-542. May 1997.

[6] US Army Corps of Engineers. *Arch Dam Design*. Engineering and Design Manual. EM 1110-2-2201. May 1994.

Quentin Shaw

APPENDIX B

WOLWEDANS DAM STRUCTURAL ANALYSES

APPENDIX B

B. WOLWEDANS DAM STRUCTURAL ANALYSES

B.1. INTRODUCTION

Chapter 5 summarises the analysis on which basis it was possible to evaluate and quantify the early behaviour of the RCC of Wolwedans Dam under the hydration heating and subsequent heat dissipation cycle. In order to effectively illustrate the important finding that the RCC of Wolwedans clearly did not experience the shrinkage and creep that has been generally assumed to occur in RCC, as it does in CVC, only a summary of the analyses completed was presented in that Chapter.

In this Appendix, a more detailed presentation of the Wolwedans analysis is presented, illustrating clearly and specifically the impact of shrinkage and temperature drop on the structural function of the dam.

Wolwedans Dam is a 70 m high RCC structure, with a crest length of 270 m and an upstream face radius of 135 m. A 12.5 m deep by 13 m wide reinforced concrete inlet tower is attached to the upstream face immediately to the left flank side of the spillway and the full dam comprises approximately 200 000 m^3 of concrete. The dam was constructed with a high quality RCC, which typically indicated 180 day strengths exceeding 30 MPa. The surface was constructed in a conventional mass “skin” concrete and it was later found that the interface between the RCC and the skin concrete was porous and low strength. Although the RCC was high strength and of good quality, the dam was constructed in the early days of the RCC construction technology and the bond between layers was not always good and segregation of the RCC was occasionally evident.

The induced joints at Wolwedans Dam were grouted in two phases between June and November 1993[1]. The first phase encompassed grouting of the structure from the base to mid-height (RL 66.25 m) and this was completed during the winter months of June to August, during which time the impoundment water level was dropped by a maximum of 8 m. The second phase of grouting from RL 66.25 m to the RL 103 m crest level was undertaken between September and November 1993, when the impounded water level and seasonal temperatures were rising.

The dam is comprehensively instrumented and a full geodetic survey of the dam structure is undertaken twice a year, generally in early February and early August[2]. A continuous monitoring programme of the installed instrumentation is maintained and most of the instrumentation remains fully functional. The structure can be considered to have functioned very successfully to date.

B.2. FINITE ELEMENT MODEL

B.2.1. GENERAL

For the purposes of the investigative analyses completed, a comprehensive, 3 dimensional Finite Element model was established using the COSMOS[3] general structural analysis software for Wolwedans Dam. The model simulated the dam and the foundation, with each radial dam block between induced joints being developed as separate parts and joined with Gap elements. Ten-noded solid tetrahedral elements were used in a high-density mesh (see **Figures B1** & **B2**). For the analyses completed, only induced joint Nos 8, 14 and 17 were assumed to be open, replicating the actual situation at the dam. In addition, a Gap element was included at Joint No 3, where a formed joint was included in the dam. Otherwise, Gap elements were not included at the location of the closed induced joints. In COSMOS, Gap elements associate nodes through a friction factor when compressive contact exists. Under tension, the nodes are allowed to separate and form a gap.

To recreate the actual situation of the dam structure as closely as possible, the inlet tower was attached to the upstream face. The 13 m wide x 12.6 m deep tower contains wet wells, dry wells, shafts and a staircase and was modelled as a solid structure of the same external proportions. The equivalent stiffness of the prototype was modelled by reducing the applied E modulus such that the product of the E modulus and the second moment of area (EI value) of the model was equal to that of the actual tower.

The foundation block modelled with the dam structure extended 1.5 x the dam height upstream, downstream and beneath the dam and 1 x the dam height on either flank (see **Figure B1**). The external boundaries of the foundation model were constrained against movement in all directions.

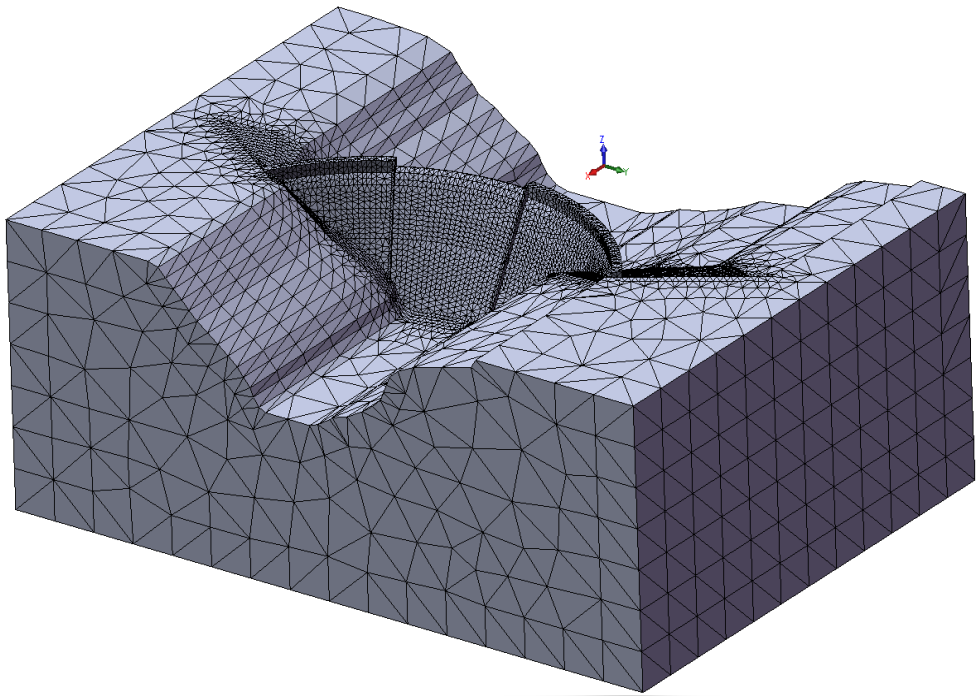

Figure B1: Wolwedans Dam & Foundation FE Analysis Mesh

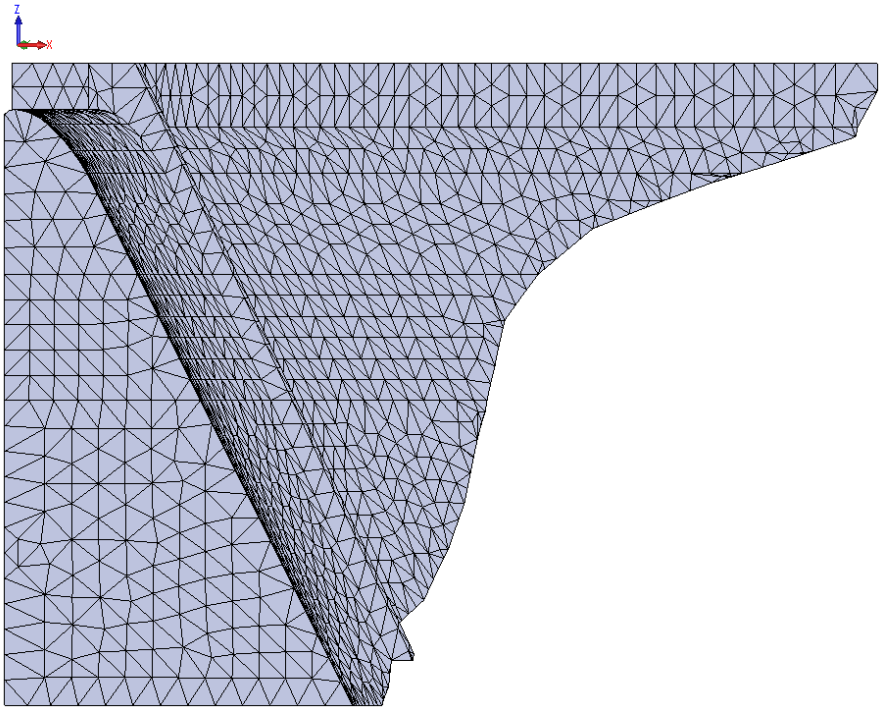

Figure B2: Wolwedans Dam FE Mesh

The basic layout of the dam is illustrated in **Figure B3**.

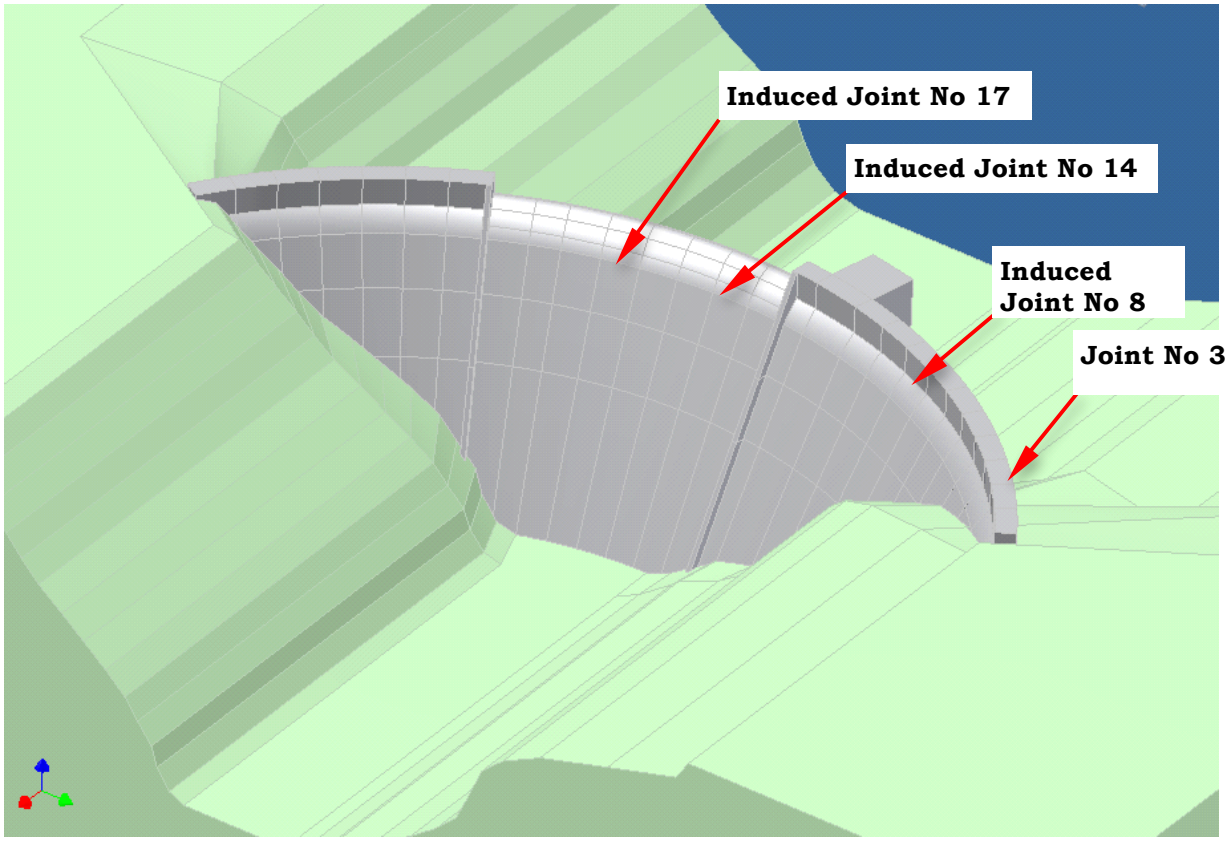

Figure B3: Illustration of Wolwedans Dam & Foundation

B.2.2. MATERIALS PROPERTIES & LOADING CONDITIONS

For the purposes of the analysis presented herein, the materials properties that were demonstrated in Chapter 5 to be most valid were applied. These and the loadings that were considered as constant are summarised in **Table B.1**.

Table B.1 (5.6): Materials Properties & Constant Loads Applied for All Analyses

Property	**Value Applied**	**Loading**	**Value Applied**
RCC Density	2400 kg/m^3	Hydrostatic	FSL (RL 98 m)
RCC Compressive strength	35 MPa	Uplift	50% Design
RCC Elastic Modulus	20 GPa	Silt	None
RCC Thermal Expansivity	10 x 10^{-6}/^{o}C	*Note:*	
RCC Poisson's Ratio	0.2	*"Massless" foundation applied & Jt. 8 opening reduced by 0.72 mm on all analyses to compensate for gravitational modelling effects (see 5.3.2.5).*	
Foundation Elastic Modulus	15 GPa		
Foundation Poisson's Ratio	0.17		
Foundation Thermal Expansivity	10 x 10^{-6}/^{o}C		

Uplift Loading

In accordance with the USACE. EM 1110-2-2200. *Gravity Dam Design.* 1995[4], standard practice in dam design assumes a distribution of uplift loading beneath the base of the structure as illustrated on the graphic below. Where a drainage curtain is included beneath the structure, it is assumed that the drainage relieves the pressure by 2/3 of the head difference between the upstream heel and the downstream toe.

accordingly $hd = 1/3\ (hm - hv) + hv$

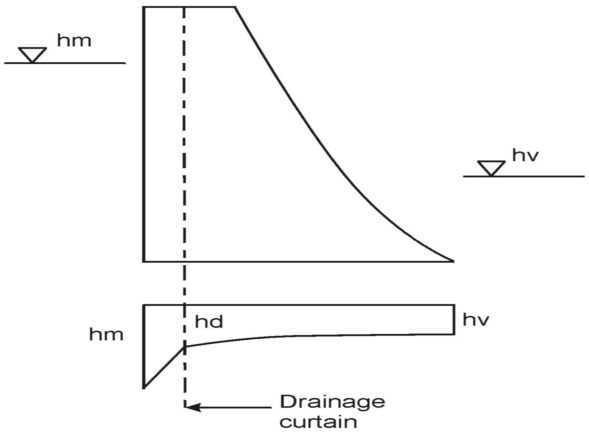

Figure B4: Standard Design Assumptions for Uplift Pressures[4]

The above approach represents an assumption that is generally applied in the case of a foundation rockmass that is grouted and drained. In the case of a competent

rockmass, the assumed loading is quite probably conservative and for the purposes of the analyses undertaken in this study, total forces equivalent to 50% of those applied in accordance with this design approach were applied in order to more realistically simulate probable service conditions.

B.3. INVESTIGATION METHODOLOGIES

B.3.1. GENERAL

The analyses undertaken as part of this investigation compare the impacts of various degrees of materials shrinkage on the structural behaviour/performance of the dam model with that measured on the prototype structure under the same loading conditions. The comparison is made in the form of displacements on two points on the dam crest and three points in the upper gallery of the dam and against the degree of opening at the centreline of the three open joints at approximately mid-height on the dam. These points were chosen as they were considered to represent points of definitive performance. While the situation in respect to the core RCC performance at mid-height of the dam is such that the behaviour is not clouded by foundation restraint, or surface cooling effects, as would have been the case at the top, or bottom instrumentation levels, the overall performance of the arch will always be clearly demonstrated through structural displacements. The more shrinkage that is experienced in an arch dam, the greater the crest must displace downstream in order to fully take up the imposed water load through arching (see **Appendix A**).

Simulating the equivalent loading state of the dam structure as at July 1993, a number of shrinkage strains were applied to the dam structure in the form of temperature drops. Noting the critical displacements and joint openings for each "shrinkage scenario" and comparing these with the values measured on the prototype, it would be possible to identify the degree of shrinkage that occurred in reality.

B.3.2. INDUCED JOINT GROUTING

B.3.2.1. General

The induced joints of Wolwedans Dam were grouted between June and November 1993, starting at the bottom and working upwards. While the impounded water level was dropped by a maximum of 8 m during the course of early grouting, it was maintained at that level for less than 1 month before being filled again by seasonal runoff. Accordingly, the dam structure was essentially under load during the course of grouting.

Examining the joint and crest displacement records, it is apparent that increased upstream movement of the crest occurred post-grouting, while reduced seasonal movement was also subsequently observed on the two joints that had opened most significantly (Nos 11 & 24). Otherwise, the grouting appears to have had very little impact on the structural behaviour of the dam. It is considered that this is a consequence of the fact that the dam structure was under load and significantly displaced, due to the temperature drop experienced at the time of grouting.

However, the records for all four levels of instrumentation demonstrate that the hydration heat had been fully dissipated from the dam by winter 1993 and, as the reservoir was full immediately before grouting, instrumentation data for the beginning of July 1993 reflects a full, but un-grouted dam with a nominal temperature drop load (at RL 66.25 m) of 8°C from placement.

B.3.3. MEASURED CREST DISPLACEMENTS

B.3.3.1. General

Copies of the key displacement data for Wolwedans Dam are attached at the end of this Appendix. From the beginning of 1993 and for the first decade of operation, the impoundment of Wolwedans Dam was fairly consistently full and, over this time, the geodetic survey data indicates that the central crest displacement generally moved seasonally by a maximum of approximately 11 mm in a horizontal, upstream-downstream direction. At the upper gallery level, the central displacements generally vary seasonally by between 5 and 7 mm.

Figure B5 illustrates the critical crest and upper gallery displacement measurement reference points, while **Table B2** compares the typical measured and predicted seasonal displacement variations under operational conditions.

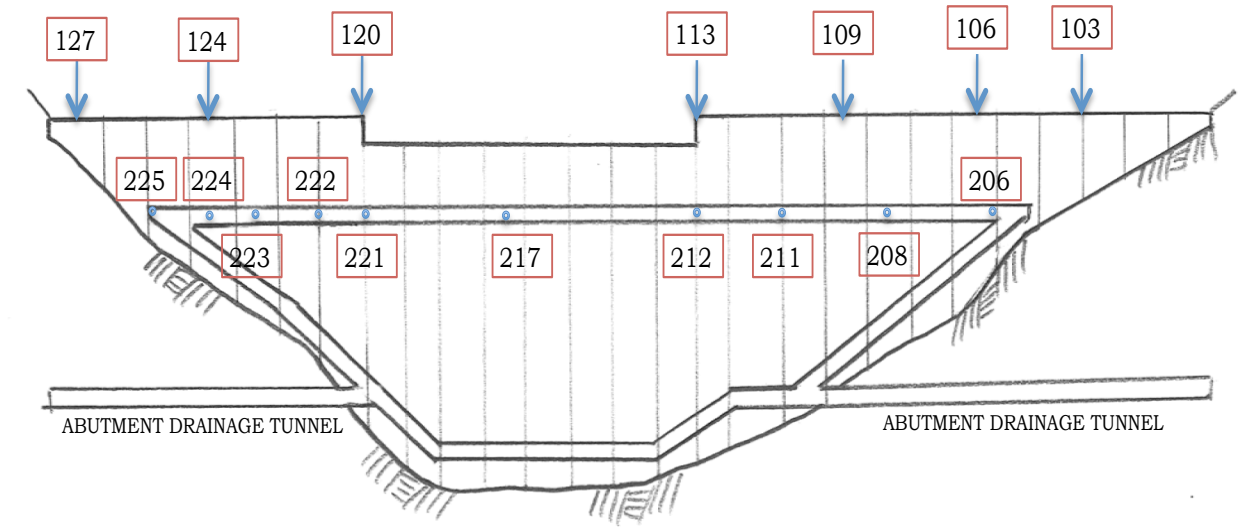

Figure B5: Illustration of Important Displacement Reference Points

Table B2: Predicted & Measured Seasonal Horizontal Movement Variations (mm)

Reference Point - Dam Crest	**103**	**106**	**109**	**113**	**120**	**124**	**127**
Measured (Average - Dam Full 1993 to 2008)	2.6	6.4	8.5	10.5	12.1*	6.3*	1.7
Predicted (for 8/11°C T Drop)	3.1	3.0	10.1	10.8	5.6	4.6	2.3

Table B2 *continued*

Reference Point - Top Gallery	**206**	**208**	**211**	**212**	**217**	**221**	**222**	**223**	**224**	**225**
Measured (Average - Dam Full 1993 to 2008)	1.2	2.8	3.8	4.3	5.9	4.5	3.5	2.4	2.3	1.8
Predicted (for 8/11°C T Drop)	1.4	1.7	5.9	6.0	8.2	3.8	3.5	3.1	2.6	1.6

The above table clearly illustrates that the displacement behaviour of the structure in the region of the crest and the upper gallery was consistent with expectations, except on the central right flank crest.

As can be seen from the measured readings highlighted in **Table B2** with an asterisk (*), two of the three displacements measured on the right flank crest exceeded expectations. With a lower dam height at the NOC on the right side of the spillway, compared to the left, and a steeper right abutment, a substantially stiffer right flank of the dam would be anticipated and this would be expected to be confirmed in lower crest displacements on the right flank compared to the left, as predicted by the FE model.

Reviewing all of the available data that could have some influence on the apparent displacements on the right flank, it is clear that the climatic conditions and the orientation of the site cause the right side of the valley at Wolwedans to be warmer than the left. At the top instrumentation level (RL 83.25 m), seasonal temperature variations of 12.5 to 21°C on the left flank can be compared directly with equivalent variations of 14 to 23.5°C on the right flank. With both sides of the NOC exposed to the atmosphere and the upstream side and the crest exposed to solar radiation for extended periods, it is more than likely that the crest above the water level on the right flank experiences temperatures that exceed the original RCC placement temperature.

Examining the displacement measurements recorded for the abutment drainage tunnels on both flanks at RL 48 m (indicated in **Figure B5**), it is apparent that seasonal movements of between 1 and 2 mm are recorded throughout the foundation rockmass. In view of the magnitude of the displacements recorded in relation to the accuracy of measurement, it is not considered possible, however, to meaningfully analyse these movements. Nonetheless, the consistency and repetition of direction of movement implies that the seasonal patterns observed cannot be denied.

Considering the higher temperatures measured in the dam on the right flank, the evidence of seasonal movement in the foundation rockmass and the elastic nature of the movements observed, it is considered that the exaggerated right flank displacements must be the result of seasonal temperature effects. With displacements measured within the upper gallery in line with corresponding measured temperature variations, it is considered most likely that the exaggerated crest displacements on the

right flank crest are the result of greater temperature variations in this region. Unfortunately, the installed instrumentation does not measure concrete temperatures above the upper gallery level and consequently no related data is available for the dam crest, the top of which is some 20 m above the gallery floor level. Consequently, the same seasonal temperature variations as measured within the upper gallery were applied for the crest on the analyses undertaken.

A further factor to be considered is the grouting of Joint No 24. With this joint grouted at a depressed temperature, and no other open joints on the right flank, a subsequent elevation of the temperature in the right flank crest would be translated directly into increased upstream movement. The tendency for the upper section of the dam to displace further upstream than anticipated is also evident on the induced joints at the highest instrumentation level (RL 84.25 m), where the downstream joint openings are greatest during winter and the upstream openings are greatest during summer, as indicated on **Figure B6**.

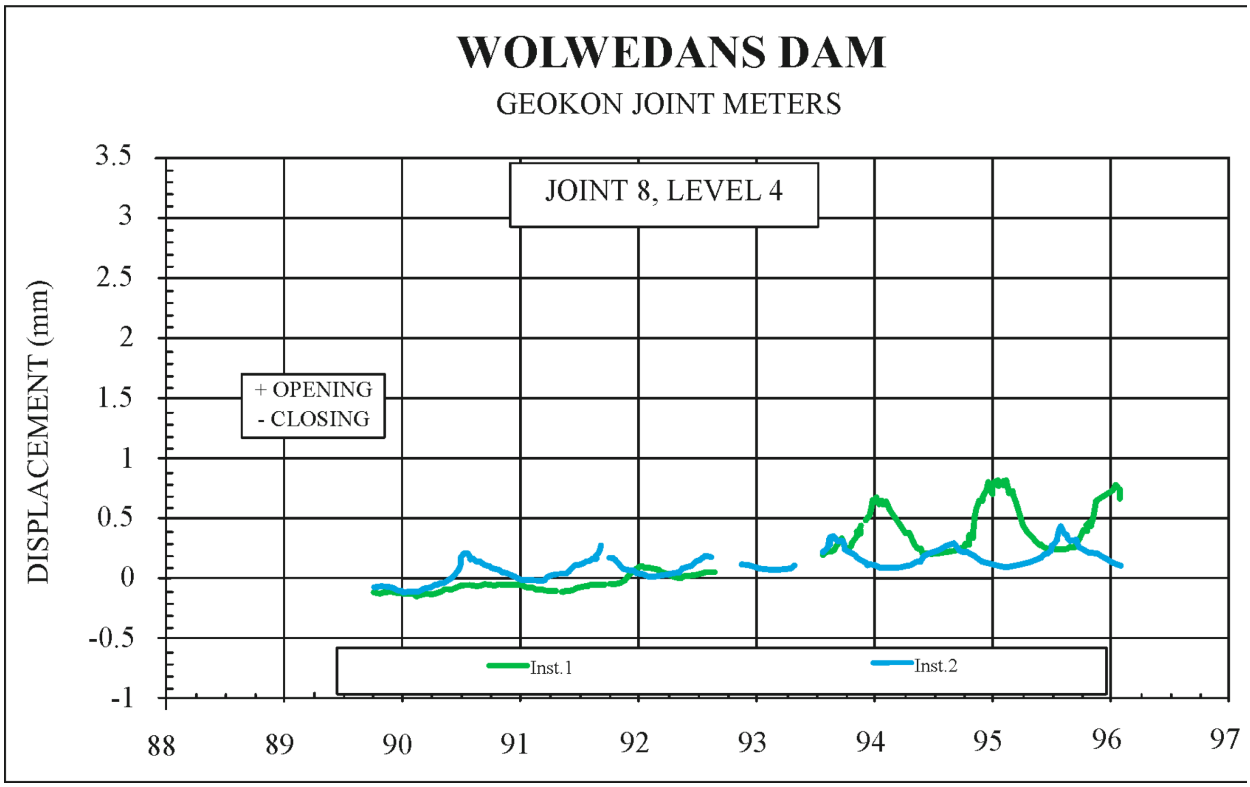

Figure B6: Displacement History at Induced Joint No. 8 RL 84.25 m

In view of the fact that the joints, even close to the surface, will tend to close during periods of warmer temperatures, the obvious explanation of the general pattern of the upper part of the joints opening during summer is an expansion movement of the upper part of the dam in an upstream direction.

Accordingly, it is considered very likely that the higher than expected seasonal crest movements observed on the right flank at Wolwedans Dam are the result of summer temperature increases within the right side NOC crest of the structure that exceed the

placement temperature and, to a lesser extent, summer temperature increases within the surface of the right abutment rockmass.

In view of the fact that the above hypothesis cannot be verified quantitatively, it is considered that a lower level of confidence exists for the comparison of modelled and measured displacements on the right flank crest of the dam. Considering the fact that this enigmatic behaviour takes the form of an increased upstream movement that recurs regularly during summer, however, would suggest that the "zero" stress temperature in the RCC is exceeded and this further serves to provide more confirmatory evidence that significant shrinkage of the RCC cannot have occurred.

While this upstream movement is most pronounced on the right flank, it undoubtedly also affects the left flank and this implies that the reference downstream displacements applied for the modelling analysis are almost certainly over-estimated. This will add further to the conservatism applied in the analysis.

B.3.3.2. Establishing Displacement Reference Values

A definitive interpretation of the structural displacement performance of Wolwedans Dam is frustrated by difficulties in establishing a realistic zero reference. The displacement performance of the dam was "zeroed" on 7th August 1992, when the water level had risen to 95% full for the first time. At that time, the hydration temperature had essentially been dissipated from the dam structure and the winter of 1992 does seem to have been particularly cold. Subsequently the dam structure has demonstrated additional downstream (+ve) displacement in colder winters and upstream displacement (-ve) in summer.

With the first displacement survey during the summer of early 1990, the recently completed and hydration-heated empty dam structure should have indicated its maximum upstream crest displacements at that time. Paradoxically, however, the upstream displacements at the reference points on either end of the NOC, immediately on either side of the spillway (113 and 120 – see **Figure B5**), peaked a year later (in early summer 1991), when the impounded water level had risen to approximately mid-height and internal temperatures were cooler than the previous year, due to dissipation of some of the hydration heat.

Structural modelling of the empty dam indicated that its heated state at the beginning of 1990 should have caused the crest to move upstream by 5 mm at point 113 and 3.5 mm at point 120. The same modelling suggested that this displacement would be translated into a 3.4 mm downstream crest movement at 113 and 3.2 mm at 120 when the dam impoundment filled and the hydration temperature had dissipated. In other words, the net downstream displacement from January 1990 to January 1993 should have been 8.4 mm for 113 and 6.7 for 120.

In relation to the predicted upstream movement as at January 1990, only 0.5 mm was associated with the temperature rise, with the balance associated with the imposition of gravity load. In fact the NOC crest displacement in early February 1993, as measured at reference points 113 and 120, indicated horizontal downstream

displacements of approximately 7.2 mm and 3.1 mm, respectively, while the crest level dropped by over 5 mm, confirming the impact of the measured drop in temperature.

The records demonstrate that the core sections of the dam experience a temperature of 6 to 7°C below placement temperature even during summer, while the upstream surface zones are generally at a maximum of 2 to 3°C below placement and the downstream surface zones reach a maximum temperature approximately equivalent to the placement temperature during summer. Considering the fact that the dam has remained under load and is generally at a temperature below placement, in theory, the structure should never displace upstream under operation to the extent experienced in January 1990. Taking note of the fact that only external, crest displacement measurement was made prior to August 1992, the only explanation is that perceptibly higher temperatures are experienced during summer in the crest of the dam, where no data is available, than elsewhere within the structure.

As a consequence of the above, defining a realistic zero reference point for the measured crest displacements was not possible and accordingly, it was decided that the information to be extracted from the model in respect to crest displacements should be the maximum movements experienced to July 1993 and the typical seasonal displacement variations. In view of the fact that part of the total seasonal crest displacement variations very likely relates to higher temperatures than measured elsewhere being experienced in the crest in summer, this approach implies a significant degree of conservatism in the analyses undertaken.

Displacement measurement in the upper gallery at Wolwedans Dam was only initiated in August 1992 and consequently it is not possible to ascertain a “zero” reference for the actual displacements. According to the FE analysis, ignoring temperature drop, the structural, downstream displacement associated with the hydrostatic load at reference points 212, 217 and 221 would be 3.35, 4.2 and 3.0 mm, respectively. Adding these displacements to the apparent measured maximum seasonal values (when the dam is consistently full) will indicate total maximum measured horizontal displacements.

Comparing the 1993 seasonal displacement variations in the upper gallery with the average maximum displacement variations measured during subsequent years during periods when the dam was full, it is apparent that the 1993 values are lower. Most of this difference is found in the form of increased upstream movement and this is undoubtedly a result of the open sections of the induced joints being filled with grout during the late winter of 1993. While this will have had little impact on the dam structure’s response to a temperature drop, it will have changed the response to an increase in temperature, tending to cause increased upstream displacement, particularly towards the crest of the dam.

Although not the major part, some of the additional displacement evident at the upper gallery reference points during the winter seasons following 1993 was downstream movement. It was consequently considered appropriate, if rather conservative, to

adopt the maximum seasonal displacement variation data in order to establish the reference behaviour for the dam, as opposed to the 1993 figures.

B.3.3.3. Measured Displacement Reference Data

On the basis of the above, reference behaviour for the prototype dam structure to a base date of July 1993 was developed as a target to be replicated through modelling. **Table B3** presents the measured displacement data for July 1993 that was used for comparison with predictions from the FE modelling.

Table B3: Measured Displacement Data at Important Reference Points 1993 (mm)

Reference Point	**113**	**120**	**212**	**217**	**221**
Horizontal / Downstream	14.5	11.7*	7.65	10.1	7.5
Seasonal Variations	8.0	10.5*	4.3	5.9	4.5

B.3.4. MATERIALS MODELS / LOADING CASES

With the properties listed in **Table B1** as constant, a net core temperature drop from placement of 8°C, as indicated on the installed instrumentation for winter 1993, was applied together with a number, or range of possible RCC thermal behaviour scenarios, as indicated in **Table B.4**. In accordance with the findings of Chapter 5, a model that assumed an 8°C core temperature drop in conjunction with an 11°C external, or surface zone drop, as indicated in **Figure 5.12**, was also investigated (Scenario 2).

Table B.4 (5.7): Analysis Scenarios

Scenario	**Temperature Drop** (°C)		**Volume Reduction / Shrinkage** (microstrain)	**Effective Total Temperature Drop** (°C)
	Core	**Surface**		
1	8	8	0	8
2	8	11	0	8 / 11
3	8	8	70	15
4	8	8	170	25
5	8	8	300	38

B.4. ANALYSIS RESULTS

B.4.1. Presentation of Results

The following figures present the behaviour of the dam under each of the “Shrinkage” Scenarios, as well as for a no shrinkage, or temperature drop “Scenario 0”.

B.4.2. Scenario 0: No Temperature Drop + FSL Hydrostatic + 50% Design Uplift

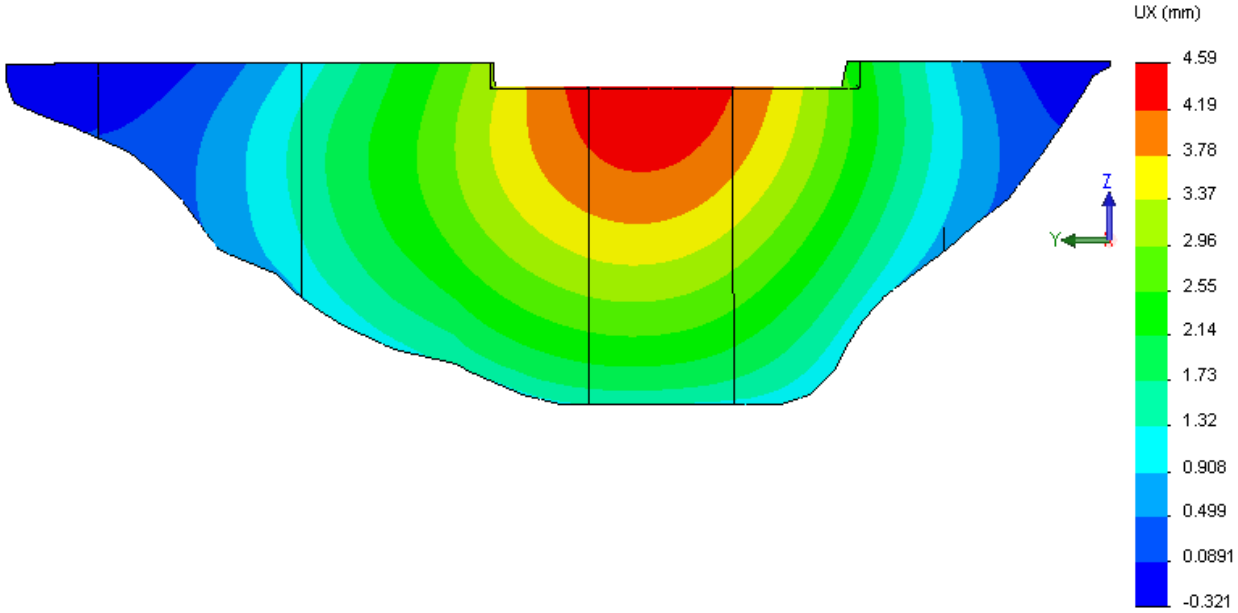

Figure B7: Sc 0 - Downstream Displacements (viewed from upstream)

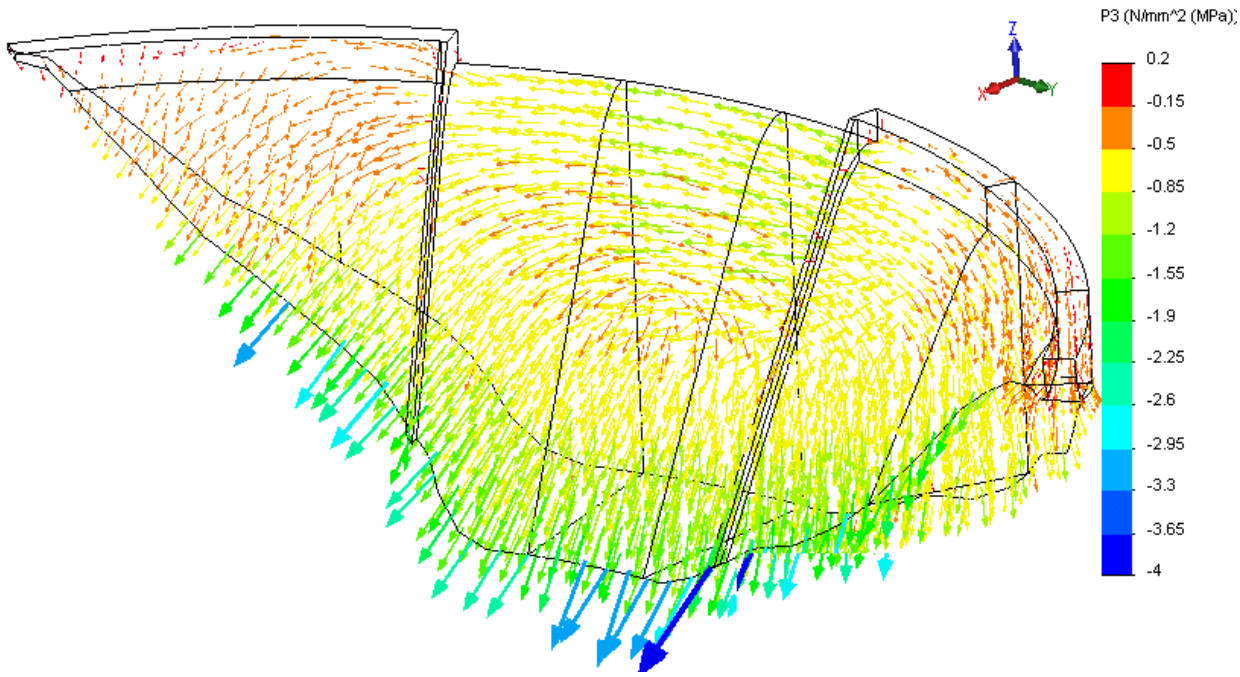

Figure B8: Sc 0 - Principal Stresses

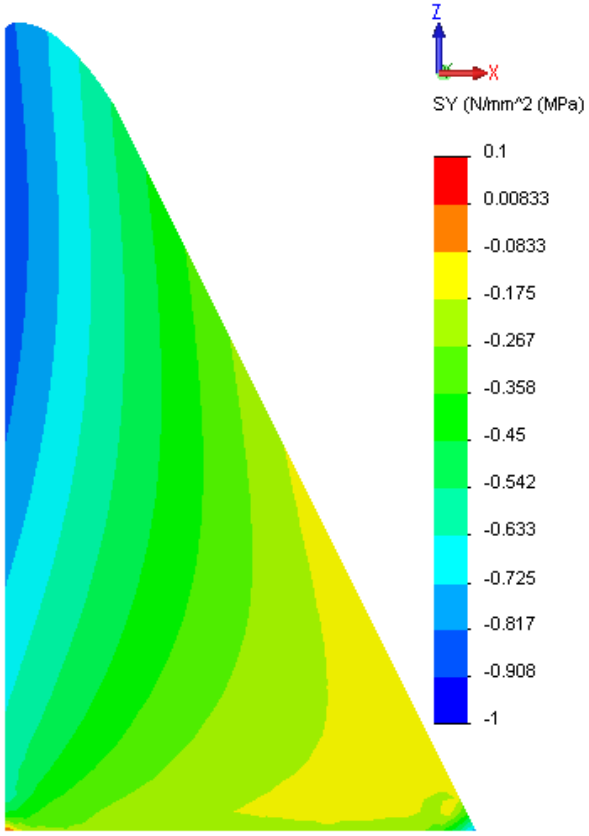

Figure B9: Sc 0 - Crown Cantilever Arch Stresses

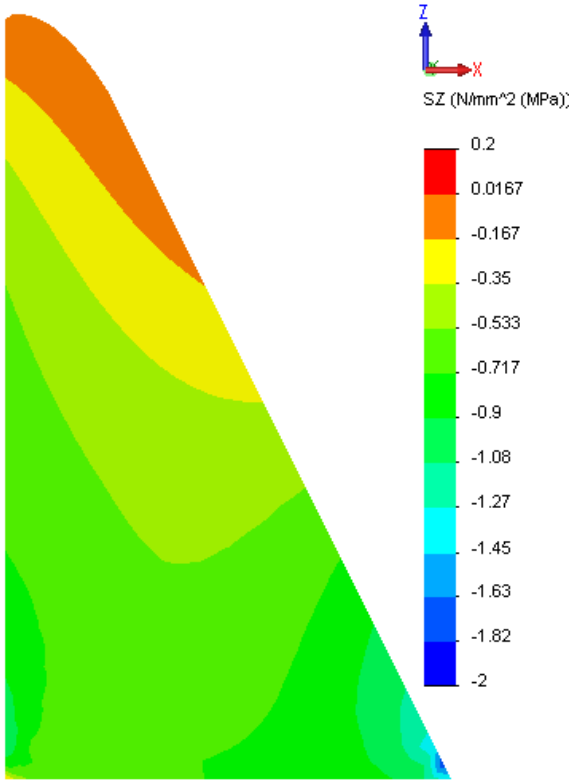

Figure B10: Sc 0 - Crown Cantilever Vertical Stresses

B.4.3. Scenario 1: 8°C Temperature Drop

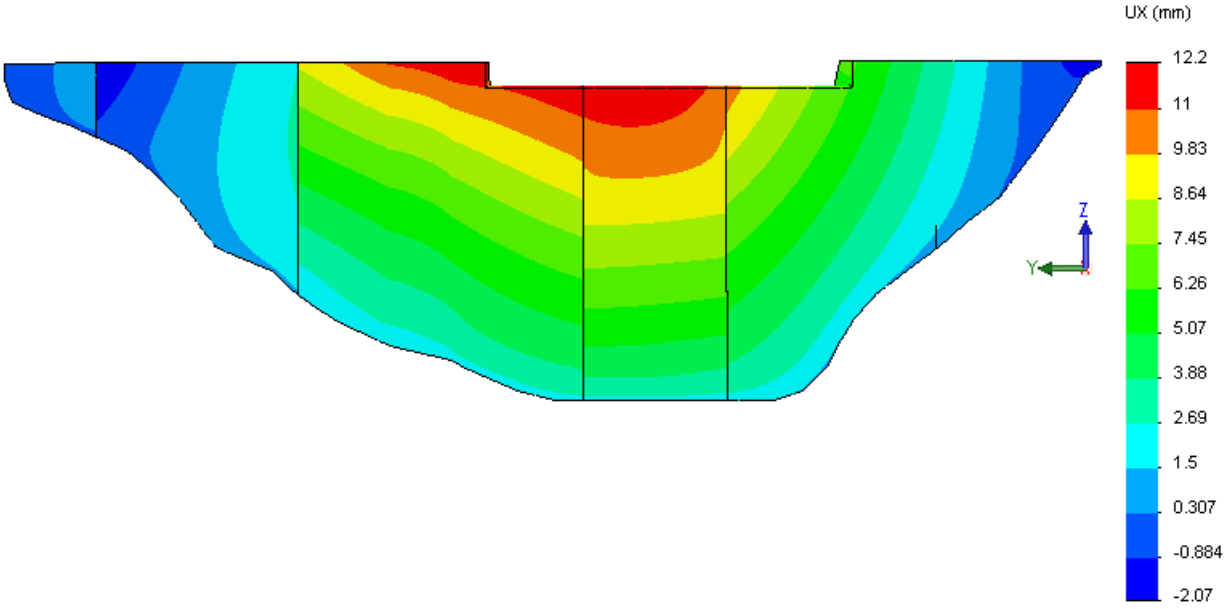

Figure B11: Sc 1 - Downstream Displacements (viewed from upstream)

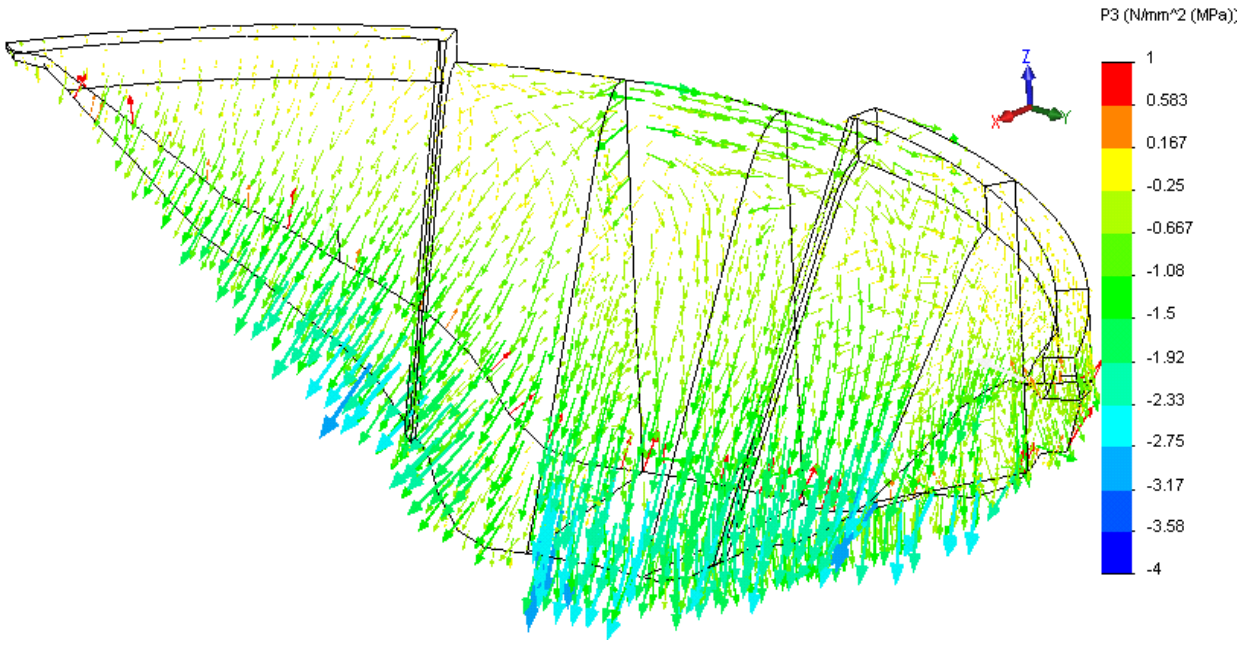

Figure B12: Sc 1 - Principal Stresses

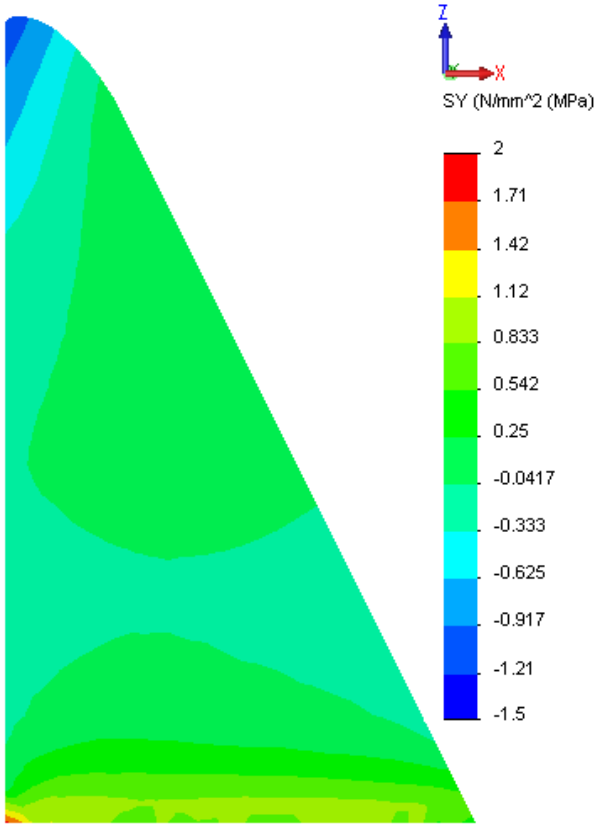

Figure B13: Sc 1 - Crown Cantilever Arch Stresses

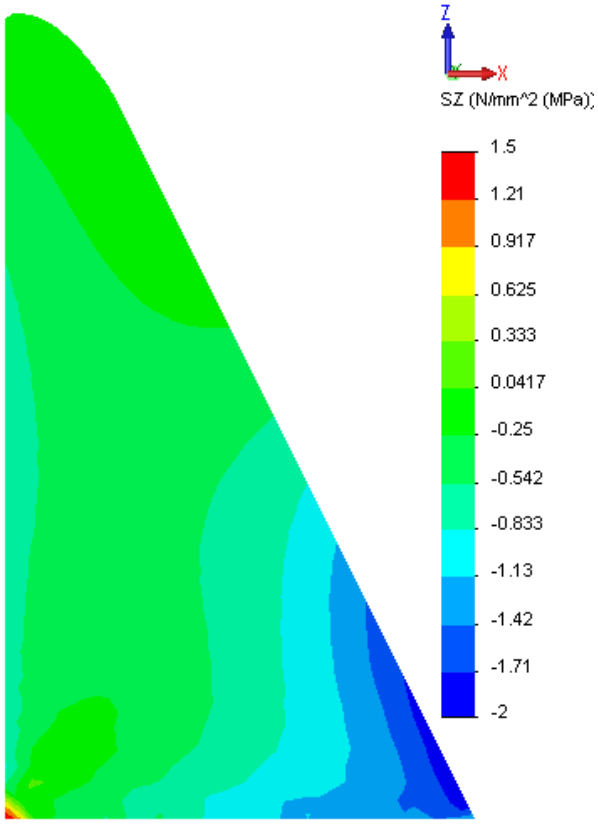

Figure B14: Sc 1 - Crown Cantilever Vertical Stresses

B.4.4. Scenario 2: 8°C Core & 11°C Surface Temperature Drop

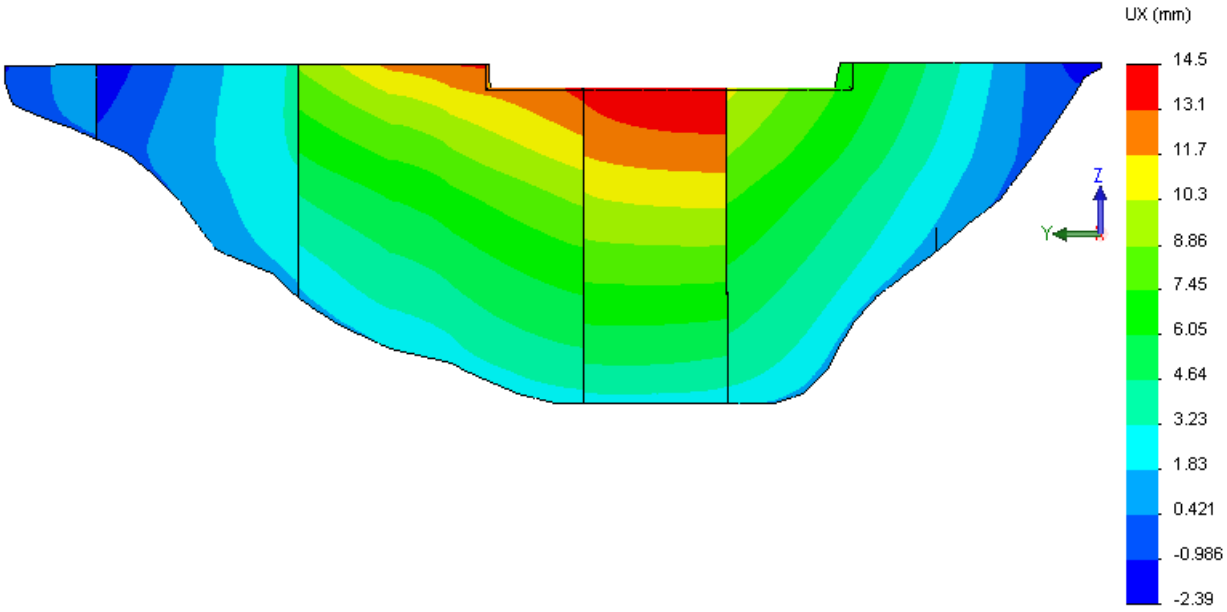

Figure B15: Sc 2 - Downstream Displacements (viewed from upstream)

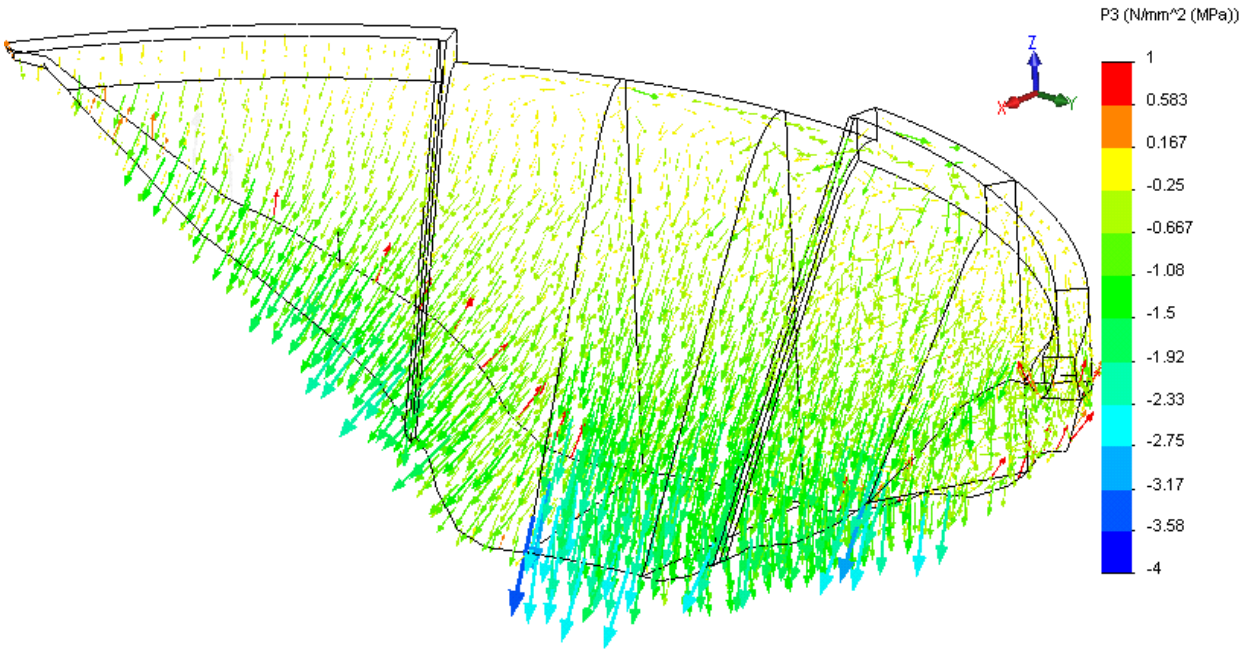

Figure B16: Sc 2 - Principal Stresses

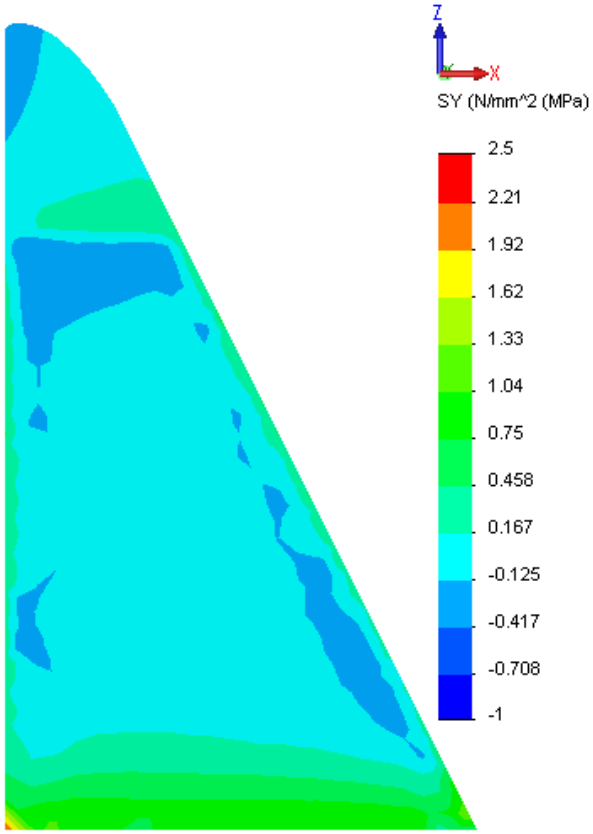

Figure B17: Sc 2 - Crown Cantilever Arch Stresses

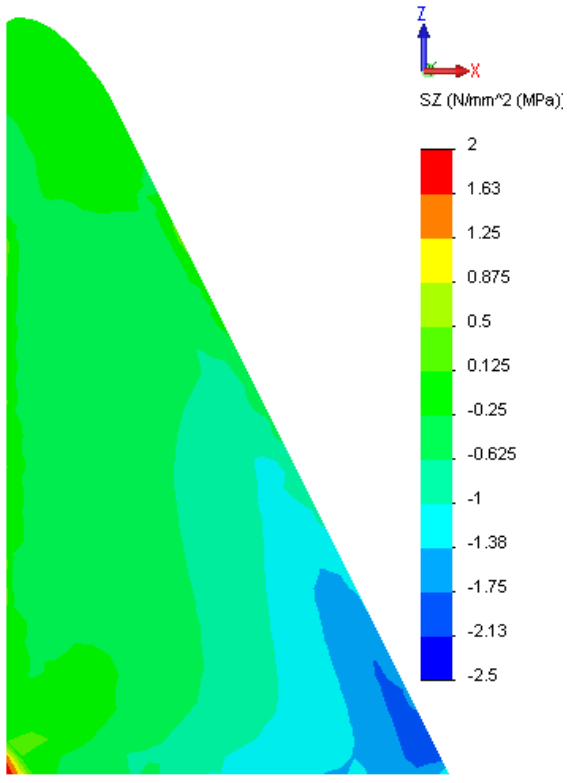

Figure B18: Sc 2 - Crown Cantilever Vertical Stresses

B.4.5. Scenario 3: 15°C Temperature Drop

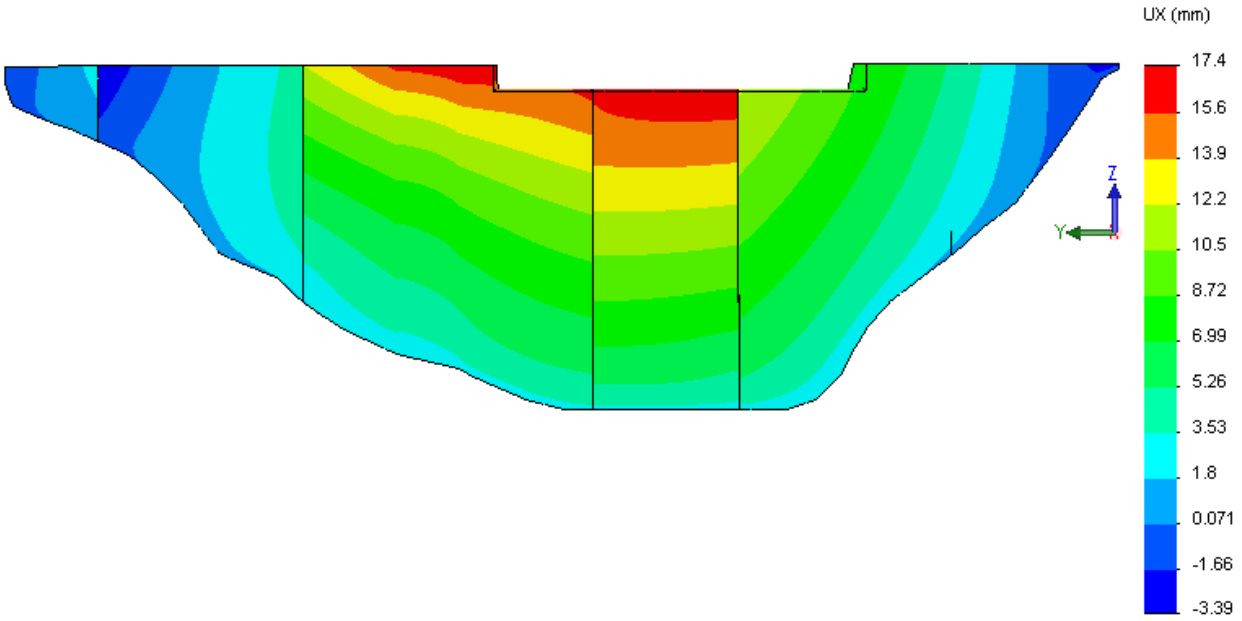

Figure B19: Sc 3 - Downstream Displacements (viewed from upstream)

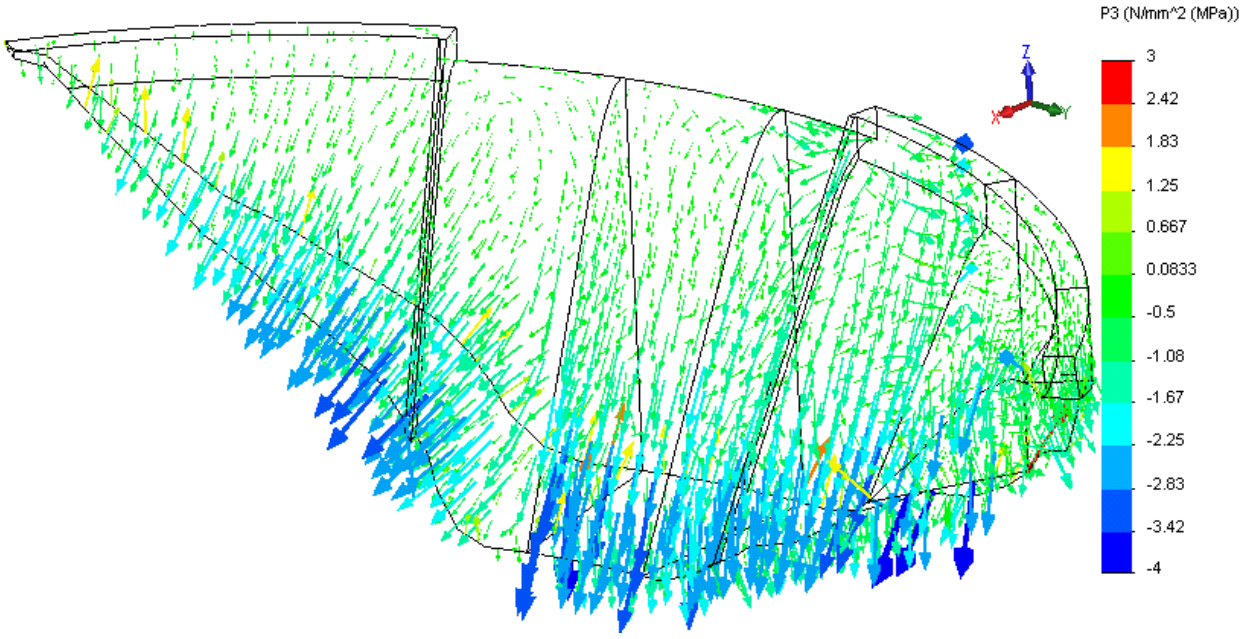

Figure B20: Sc 3 - Principal Stresses

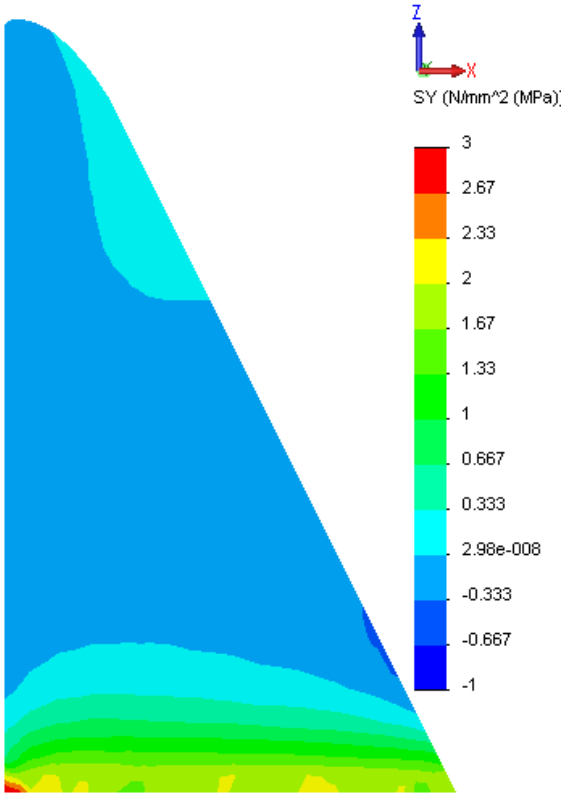

Figure B21: Sc 3 - Crown Cantilever Arch Stresses

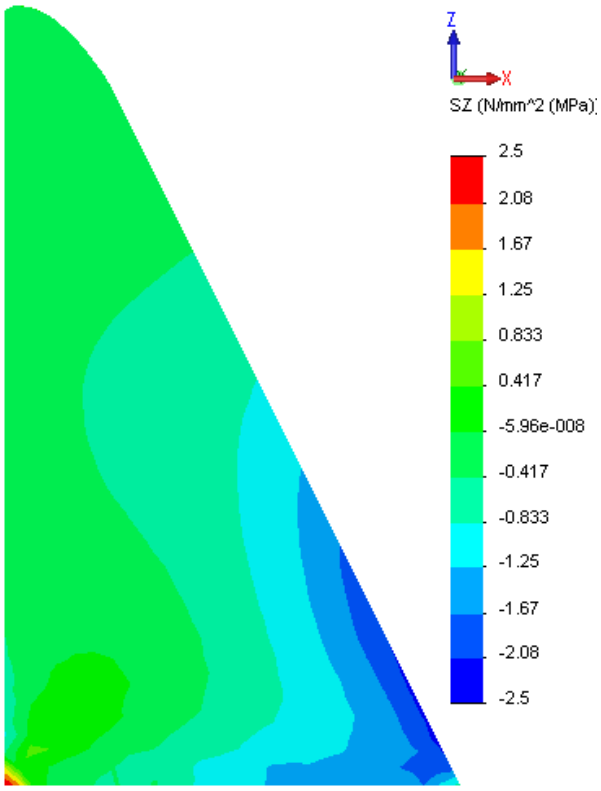

Figure B22: Sc 3 - Crown Cantilever Vertical Stresses

B.4.6. Scenario 4: 25°C Temperature Drop

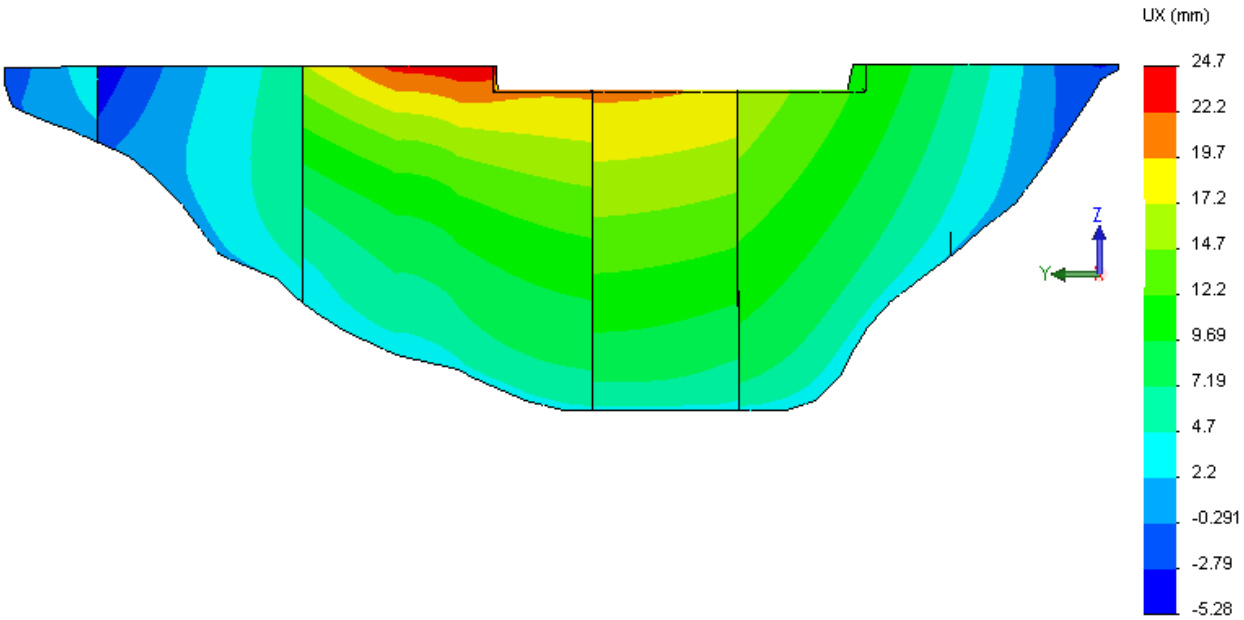

Figure B23: Sc 4 - Downstream Displacements (viewed from upstream)

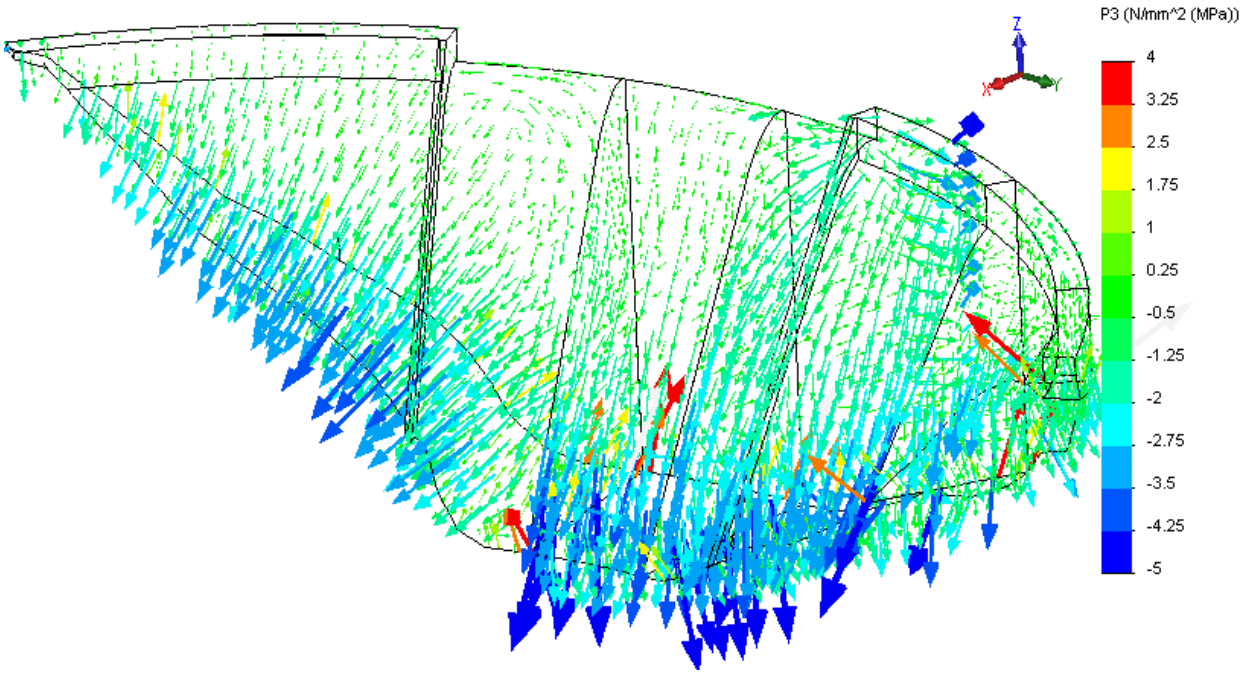

Figure B24: Sc 4 - Principal Stresses

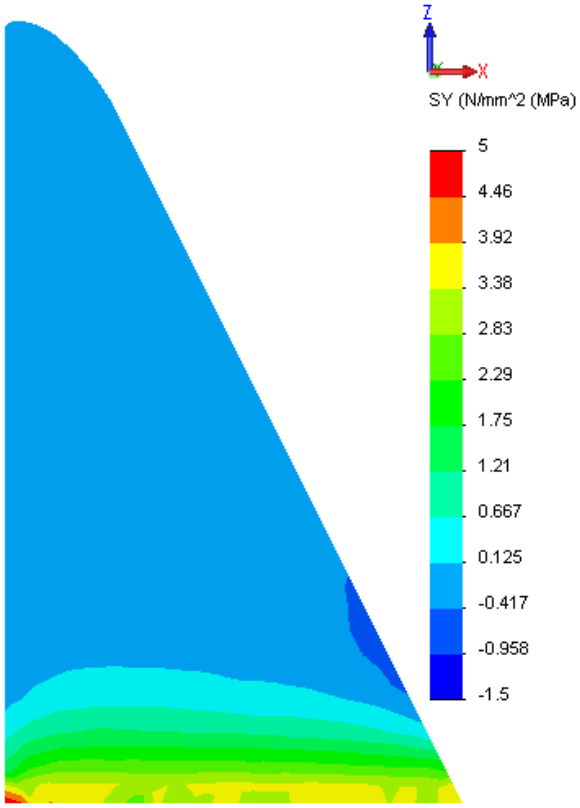

Figure B25: Sc 4 - Crown Cantilever Arch Stresses

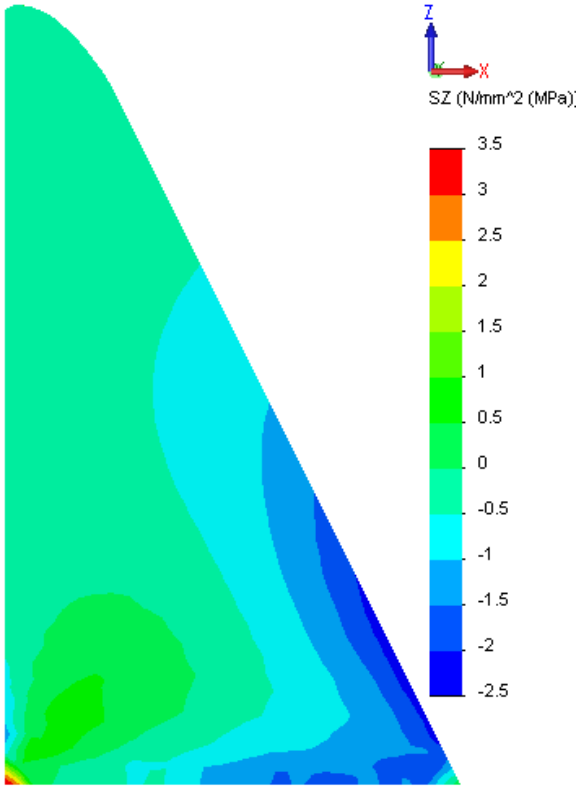

Figure B26: Sc 4 - Crown Cantilever Vertical Stresses

B.4.7. Scenario 5: 38°C Temperature Drop

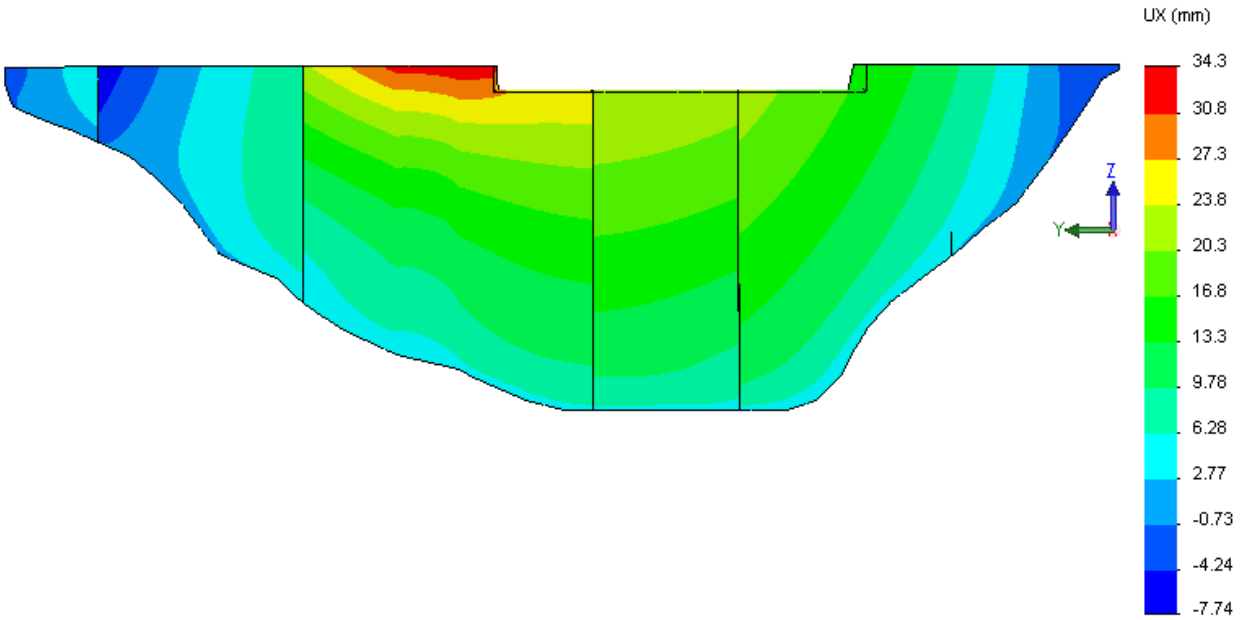

Figure B27: Sc 5 - Downstream Displacements (viewed from upstream)

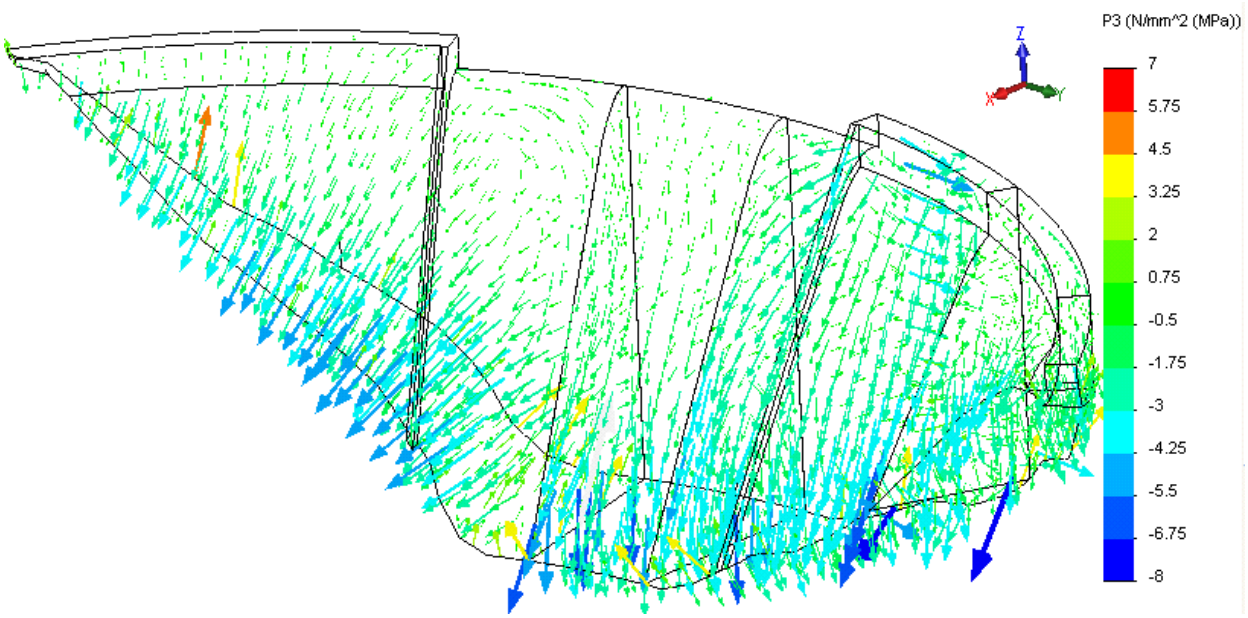

Figure B28: Sc 5 - Principal Stresses

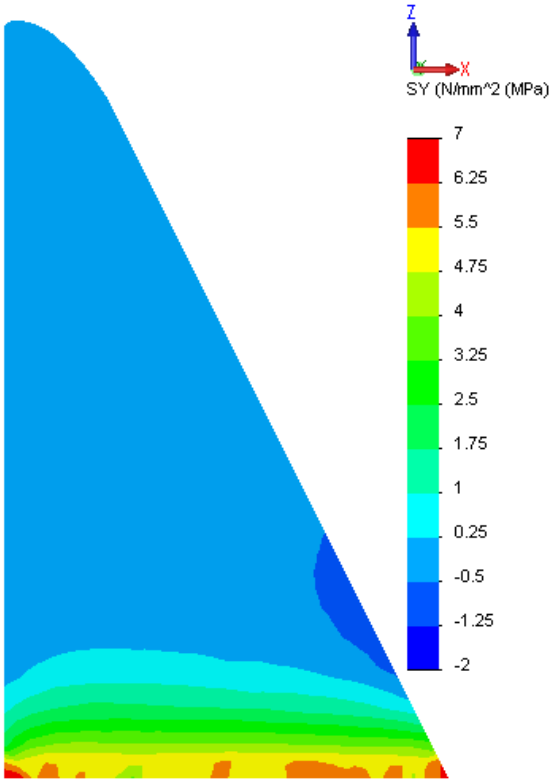

Figure B29: Sc 5 - Crown Cantilever Arch Stresses

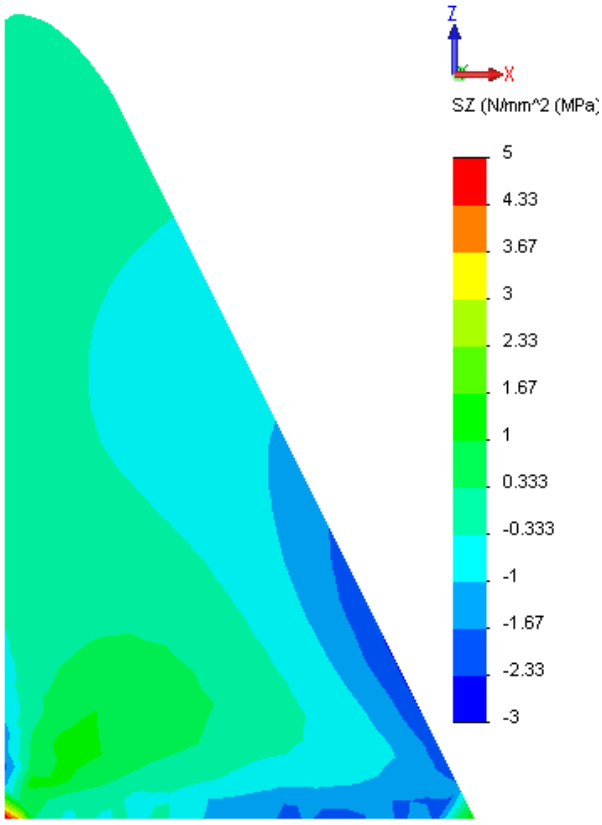

Figure B30: Sc 5 - Crown Cantilever Vertical Stresses

B.4.8. Summary of Displacements

The findings of the above analyses are compared in terms of predicted displacements at the indicated reference points with the equivalent measured values in **Table B5** below:

Table B5: Measured & Predicted Horizontal Displacement Data (mm- July 1993)

Reference Point	**113**	**120**	**212**	**217**	**221**
Measured Values					
Average Maximum Seasonal Variation	*10.5*	*12.1**	*4.3*	*5.9*	*4.5*
Seasonal Variations 1993	*8.0*	*10.5*	*3.2*	*4.5*	*3.5*
Reference Displacements (1993)	*14.5*	*11.7**	*7.65*	*10.1*	*7.5**
Scenario 0 Downstream Displacement	3.45	3.2	3.35	4.2	3.0
Scenario 1 Downstream Displacement	12.7	8.4	8.8	10.1	6.1
Scenario 2 Downstream Displacement	14.3	8.6	9.4	12.4	6.8
Scenario 3 Downstream Displacement	18.1	10.0	11.7	14.4	7.7
Scenario 4 Downstream Displacement	26.1	13.2	15.1	17.3	10.9
Scenario 5 Downstream Displacement	35.3	16.5	20.3	21.3	13.6

The figure marked with "*" are those in which a lower level of confidence is considered to exist.

B.4.9. Discussion of Results

B.4.9.1. General

Reviewing the above results and data, the following two factors must be given consideration:

1. While the induced joint Nos 3, 8, 14 and 17 were modelled as open over their entire height, in reality the instrumentation data recorded at RL 84.25 m confirmed that they did not actually open over the upper section, as the dam was under load by the time the hydration heat had dissipated. In the model, the

temperature drop will cause these induced joints to open and separate and, as each will indicate quite different stiffnesses, the blocks will deflect differentially before meeting together to re-develop arch action. To explain the impact of this effect further; a taller, more flexible block will indicate greater cantilever deflection than an adjacent shorter block under load and they will accordingly not make contact at the crest in the precise same orientation at which they were separated by shrinkage. This is demonstrated in the analyses through differential displacements on either side of the induced joints, particularly in the upper crest; i.e. by a block on one side of a joint indicating greater displacement than the block on the other side. As this separation did not occur in reality, the actual structure will have taken up the arching action more evenly and the predicted differential displacements were consequently not evident on the actual dam structure.

2. When heel tensions are low, the use of an elastic analysis will imply that the downstream crest displacements are over-stated. When the heel tensions are high, however, the elastic analysis will substantially under-estimate the extent of the downstream crest displacements.

B.4.9.2. Measured Displacements

Table B5 lists seasonal displacement variations for 1993 and the average values experienced over the record period from 1993 to 2008 in years when the dam was full year-round. While it is evident that the average annual displacement variations over the full period are greater than those experienced in 1993, the difference is seen primarily in the form of increased upstream movement. In view of the fact that records for displacement in the upper gallery only exist for a full, cooled dam, from August 1992, and no ambiguity is consequently created by behaviour when the dam was empty and heated by hydration, this effect is most evident in these data sets. As discussed under B 3.2.1, grouting of the open sections of the induced joints in late 1993 will have resulted in a situation in which upstream movement of the structure during times of increased temperature will increase, while downstream movement in times of low temperature will not have been decreased. Consequently, it is considered that adopting the average seasonal displacement variation data to establish the structural reference performance of the dam, as opposed to the 1993 data, is conservative.

B.4.9.3. Representivity

Considering the fact that the magnitude of the displacements measured at reference points 120 and 221 are probably exaggerated by higher temperature variations than assumed, the displacements indicated for Scenario 1, or Scenario 2 can be seen to most closely represent the actual displacements measured. Taking into account the level of the heel tensions for Scenarios 3 to 5, it is likely that the predicted displacements are under-stated. In view of the fact that the predicted displacements are already substantially higher than those measured, none of these Scenarios can be considered at all representative of the behaviour of the actual dam structure.

B.4.9.4. Scenario 0

With no temperature drop applied, the arch action can be seen to be even and well developed over the full dam structure, with compressive stresses being strongly defined over the top half of the dam wall. Downstream toe compressions peak locally at 4 MPa and there is no tension at the dam heel. Arch stresses are a maximum of 1 MPa, but the entire section of the dam on the crown cantilever is in compression.

B.4.9.5. Scenario 1

With just an 8°C temperature drop, the arch action can be seen to be substantially compromised, with arching effectively limited to the crest area and stresses being carried much more vertically down into the foundation, while heel tensions start to develop at the base, peaking very locally at 1.5 MPa. As a consequence, the maximum arch stress is increased to 1.5 MPa, although the maximum toe compression stress is not affected.

B.4.9.6. Scenario 2

With a more realistic distribution of temperature drops, the maximum arch stresses in fact reduce, as the total contact area of arching increases. Although the maximum toe compression value does not increase, a greater part of the toe contact area now indicates higher levels of compression stress. Heel tensions have increased, but a large portion of the base remains in compression and again, the extent of the arch action is significantly reduced, with the cantilevers playing a greater role and the stresses being directed more vertically into the foundation.

B.4.9.7. Scenario 3

For a 15°C temperature drop, the extent to which the arch action is compromised simply increases and the heel tension starts to reach a level that would undoubtedly result in cracking and increased tilting of the cantilevers. Tension stress can be seen to cover a more significant part of the dam base.

B.4.9.8. Scenario 4

For a 25°C temperature drop, the toe compressions start increasing and a number of significant tensile stresses develop on the upstream face and over significant portions of the crown-cantilever. It is considered that the structural problems on the prototype structure would start to become evident for the indicated levels of stress and it certainly would not be considered appropriate to design the dam for behaviour of the nature evident.

B.4.9.9. Scenario 5

For a 38°C temperature drop, toe compressions of up to 8 MPa are evident, together with heel tensions of 5 MPa. To develop a realistic assessment of the performance of the structure under such levels of stress, a non-linear analysis with limiting tensile strength would be required.

B.5. CONCLUSIONS

From the analyses presented, it is quite clear that the RCC of Wolwedans Dam did not suffer the reduction in volume that would normally be anticipated in CVC as a result of autogenous shrinkage and creep under early hydration heating. While the analyses demonstrate the significantly deleterious impact of such shrinkage on the structural action of the arch, the comparison of the modelled and measured structural displacements and joint openings allow a single, definitive conclusion. The structural modelling confirms that the RCC of Wolwedans Dam suffered no perceptible volume reduction during the hydration heating and subsequent cooling cycle as a consequence of autogenous shrinkage, or creep.

B.6. REFERENCES

[1] Hattingh LC, Heinz WF & Oosthuizen C. *Joint Grouting of a RCC Arch/Gravity Dam: Practical Aspects*. 2nd International Symposium on Roller Compacted Concrete Dams. Santander, Spain. pp 1037-1051. 1995.

[2] Precise Engineering Surveys. Department of Water Affairs. *Instrumentation Data for Wolwedans Dam. 1990 to 2008*. August 2008.

[3] Structural Research and Analysis Corporation (SRAC). *COSMOSM Finite Element Analysis Program.* General-purpose, modular FE Analysis system. SRAC, a division of SolidWorks Corporation, Dassault Systemes S.A., Paris, France.

[4] United States Army Corps of Engineers. *Gravity Dam Design.* Engineering Manual. EM 1110-2-2200. USACE. Washington. June 1995.

WOLWEDANS DAM

DEFORMATION DISPLACEMENT MEASUREMENTS: 1990 – 2008

Courtesy of Precise Engineering Surveys

Department of Water Affairs

Schoeman Street

Pretoria

South Africa

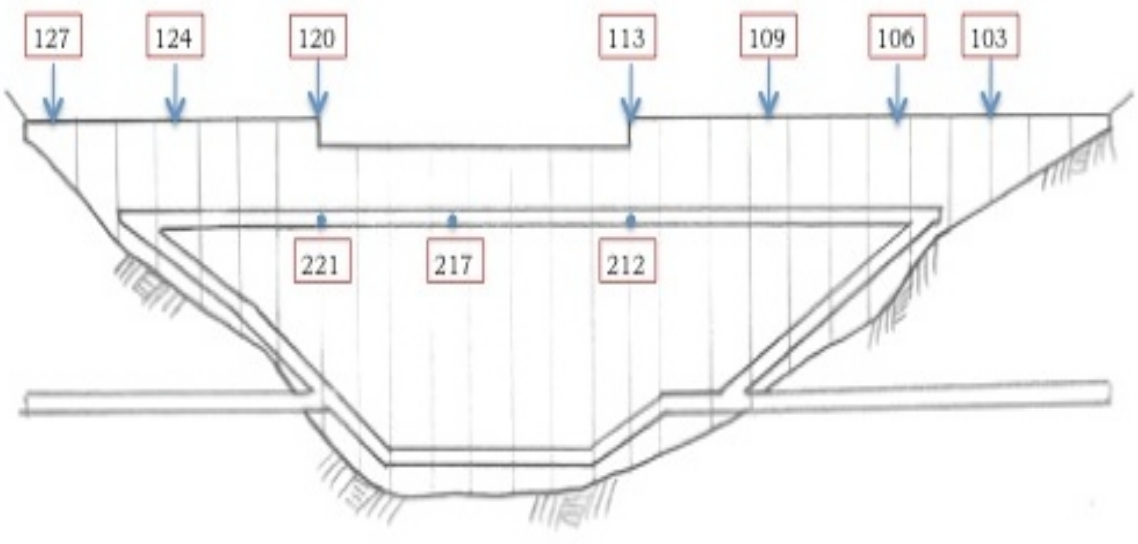

Key to Reference Point Locations (Viewed from Downstream)

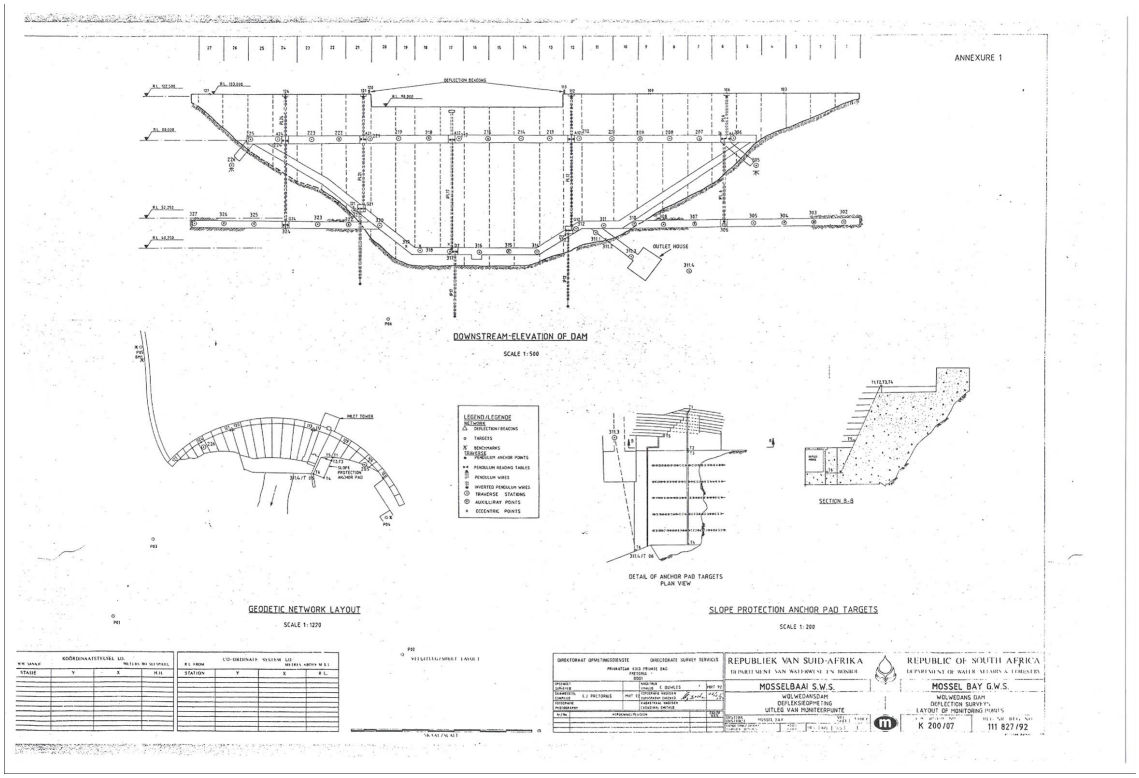

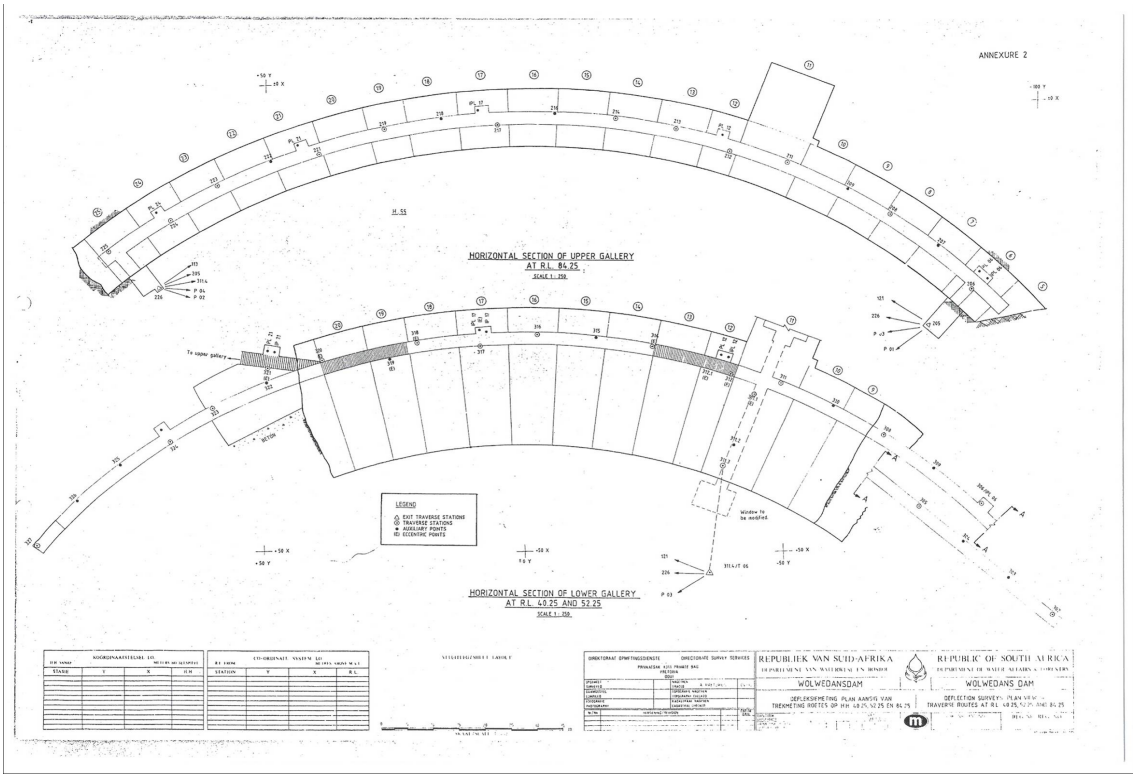

CO-ORDINATE SYSTEM
LOCAL SYSTEM (ON CENTRE OF DAM)

UPSTREAM

- X

RIGHT FLANK + Y **- Y** **LEFT FLANK**

+ X

DOWNSTREAM

VERTICAL DISPLACEMENT: POSITIVE (+) - UPWARD
NEGATIVE (-) - DOWNWARD

PRECISE ENGINEERING SURVEYS

DEFORMATION DISPLACEMENTS

WOLWEDANS DAM

Ref: 07/08/1992

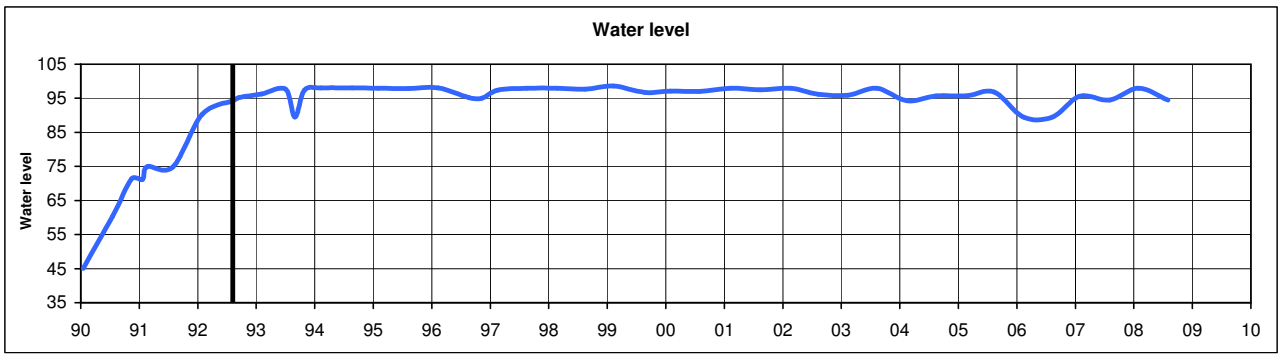

Date	Water Level	P01			P02			P03			P04			P05		
		dy	dx	dz	dy	dx	dz	dy	dx	dz	dy	dx	dz	dy	dx	dz
17/01/1990	45.03	0.7	0.3	0.5	-1.2	-1.2	3.5	0.1	-1.5	0.8	-0.5	0.2	0.0	0.2	-1.1	0.5
18/07/1990	60.30	0.1	0.6	0.4	#N/A	#N/A	1.8	#N/A	#N/A	0.9	#N/A	#N/A	0.0	#N/A	#N/A	1.7
13/11/1990	71.28	-0.2	-0.5	1.9	-1.0	-0.1	1.7	-0.7	-0.7	2.9	-0.5	0.5	0.0	1.1	-0.8	-0.3
22/01/1991	71.15	-0.8	-0.7	-1.2	-0.3	0.3	0.0	-0.6	-0.8	0.3	-0.5	0.8	0.0	1.7	-0.3	0.8
21/02/1991	74.97	-0.4	-0.7	1.6	-0.4	-0.1	1.6	-0.4	-0.5	0.2	-0.6	0.9	0.0	1.5	-0.1	0.0
30/07/1991	74.87	-1.1	-1.0	-1.5	-0.3	0.8	-0.2	-0.6	-0.7	0.1	0.0	0.4	0.0	1.9	-0.3	-0.1
29/01/1992	90.27	-0.3	0.0	1.4	-0.1	0.3	0.6	-0.1	-0.6	1.8	0.5	0.2	0.0	0.2	-0.5	0.6
07/08/1992	94.30	0.0	0.0	0.0	0.0	0.0	0.0	0.0	0.0	0.0	0.0	0.0	0.0	0.0	0.0	0.0
17/09/1992	95.23	-0.1	0.3	0.3	0.2	-0.1	0.2	-0.2	-0.1	0.4	0.3	0.2	0.0	-0.1	-0.4	0.6
03/02/1993	96.22	-0.3	0.4	0.6	0.2	0.1	-2.4	-0.8	0.3	-0.2	0.4	0.4	0.0	-0.2	-0.7	0.7
03/07/1993	97.69	-0.5	0.1	-0.1	0.1	0.4	-0.2	-1.0	0.2	0.6	0.1	-0.7	0.0	0.0	-0.6	1.0
31/08/1993	89.47	-0.1	0.0	0.1	-0.2	0.0	-1.2	-1.1	-0.2	0.8	-0.3	-0.9	0.0	0.1	-0.3	0.3
29/10/1993	97.39	0.3	0.6	1.8	0.2	-0.3	2.6	-0.4	0.4	1.2	0.1	-0.1	0.0	-0.8	-0.1	1.4
09/02/1994	98.07	0.1	1.0	0.4	0.4	-0.3	-0.4	-0.9	0.5	1.2	-0.5	0.4	0.0	-1.0	-0.8	1.1
24/08/1994	98.04	-0.6	0.9	-1.0	0.6	0.1	0.8	0.0	0.4	0.1	-0.4	-0.1	0.0	-0.3	-1.2	1.3
01/02/1995	97.93	-0.4	0.8	0.4	0.4	-0.3	1.2	-0.1	-0.2	1.2	0.2	-0.3	0.0	0.1	-1.2	1.9
09/08/1995	97.90	-0.4	0.6	2.4	0.2	-0.4	0.7	-0.4	0.6	1.4	0.2	-1.5	0.0	0.3	-1.2	1.2
13/02/1996	98.02	0.6	0.8	1.0	-0.8	0.1	1.1	-0.3	0.8	0.5	-0.5	0.8	0.0	-1.8	-1.3	0.2
21/08/1996	95.22	-0.7	0.4	0.9	0.0	1.2	0.3	-1.8	0.7	0.9	-1.5	0.4	0.0	-0.9	-1.3	1.2
12/11/1996	95.05	-0.2	1.2	0.6	0.0	0.4	2.4	-0.7	0.6	0.9	-1.1	0.4	0.0	-1.6	-1.7	1.0
18/02/1997	97.43	0.2	0.1	4.6	-1.0	-0.5	1.5	-3.6	0.0	1.1	-2.4	0.1	0.0	-4.1	-1.5	-0.4
19/08/1997	98.00	-0.3	-0.4	1.7	-1.1	0.6	0.7	-3.2	-0.2	0.9	-2.4	-0.5	0.0	-3.9	-1.6	1.3
26/02/1998	97.92	0.3	0.1	1.7	-1.1	0.8	0.5	-2.4	0.5	0.0	-2.0	0.1	0.0	-1.5	-1.0	0.7
19/08/1998	97.71	-0.3	0.3	2.2	-0.7	1.0	0.7	-2.0	0.9	1.2	-1.8	0.2	0.0	-1.3	-1.5	1.6
10/02/1999	98.64	-0.2	0.7	0.8	0.8	-0.2	0.6	-0.4	0.5	0.5	-0.4	0.3	0.0	-0.2	-0.9	0.3
25/08/1999	96.75	-0.5	0.1	0.9	0.7	0.4	1.4	-1.1	1.1	1.5	-0.5	-0.2	0.0	0.3	-0.3	2.0
02/02/2000	97.11	0.0	0.9	1.3	0.8	-0.6	2.2	-0.2	0.6	-0.5	-0.3	0.2	0.0	-0.6	-0.5	-0.6
02/08/2000	96.99	-0.5	0.3	0.8	0.7	0.1	2.0	-0.7	0.9	0.3	-0.4	0.1	0.0	0.2	-0.5	1.0
08/02/2001	97.93	-0.8	-0.6	-1.0	0.4	0.8	0.8	-0.4	-0.3	-0.2	-0.5	-0.1	0.0	0.9	-0.1	0.0
15/08/2001	97.44	-0.3	0.5	-0.3	0.8	0.0	2.0	-0.3	0.7	-1.0	-0.4	-0.1	0.0	-0.1	-0.4	0.2
20/02/2002	97.99	-0.3	0.7	-0.2	0.6	0.2	0.5	-0.9	1.2	-0.1	0.0	-0.4	0.0	-0.4	-0.5	-0.9
15/08/2002	96.18	-0.8	0.2	-0.4	0.9	0.6	0.7	-0.6	-0.2	0.1	-0.5	-0.2	0.0	0.4	-0.6	0.5
13/02/2003	95.93	-0.7	0.0	0.4	0.7	0.7	0.9	-0.2	0.1	0.7	-0.5	-0.4	0.0	0.5	-0.3	0.9
13/08/2003	98.00	-0.4	1.6	2.0	1.2	-0.2	1.7	-0.6	1.3	1.8	0.1	-0.5	0.0	-1.0	-1.0	0.7
18/02/2004	94.30	-0.3	-0.1	1.8	0.5	0.6	1.1	-1.4	0.3	1.3	-0.6	-0.5	0.0	0.4	0.1	0.8
18/08/2004	95.69	-0.8	0.4	-1.0	1.1	0.8	1.2	-0.9	0.3	0.3	-0.6	-0.7	0.0	0.3	-0.5	0.3
23/02/2005	95.69	-1.0	1.7	1.0	1.5	0.2	2.2	0.0	0.3	0.3	0.2	-0.5	0.0	-0.7	-1.5	0.4
17/08/2005	96.85	-0.3	0.4	-0.5	0.9	0.5	1.3	-1.4	0.1	-0.4	-0.7	-0.7	0.0	0.0	-0.1	0.4
15/02/2006	89.48	-0.2	0.2	-1.8	0.5	0.5	0.6	1.2	-0.8	0.0	-0.4	-0.7	0.0	2.5	-1.9	-0.5
16/08/2006	89.48	0.2	1.8	4.5	1.8	-0.6	1.5	-0.4	1.0	2.0	-0.1	-0.7	0.0	-1.3	-1.4	0.5
01/02/2007	95.60	0.9	1.2	5.6	0.7	-0.1	0.2	-1.2	0.2	1.1	0.4	-0.8	0.0	-0.7	-0.4	-0.2
08/08/2007	94.48	0.3	0.8	3.1	0.8	0.2	1.7	-2.4	0.8	1.4	-0.3	-1.0	0.0	-0.7	0.0	-0.1
05/02/2008	97.91	0.9	1.9	5.2	1.2	-0.7	2.9	-0.4	1.6	1.8	-0.3	-1.0	0.0	-1.7	-0.2	-0.4
06/08/2008	94.48	0.0	1.2	4.5	1.3	0.4	2.3	-2.3	0.8	2.0	-0.6	-1.4	0.0	-0.8	-0.2	0.8

PRECISE ENGINEERING SURVEYS

DEFORMATION DISPLACEMENTS

WOLWEDANS DAM

Ref: 07/08/1992

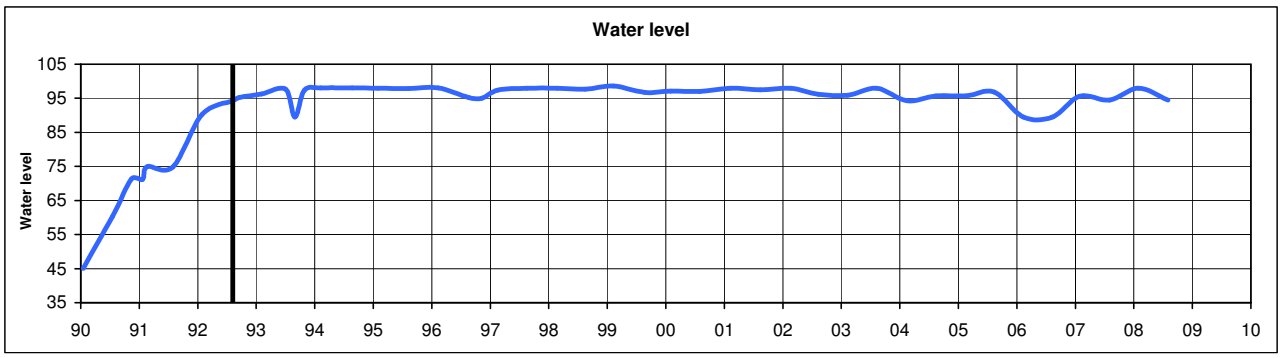

Date	Water Level	P06			P113			P120			R205			R226		
		dy	dx	dz	dy	dx	dz	dy	dx	dz	dy	dx	dz	dy	dx	dz
17/01/1990	45.03	0.3	2.1	4.0	-5.1	-11.5	7.0	3.7	-9.6	6.5	#N/A	#N/A	#N/A	#N/A	#N/A	#N/A
18/07/1990	60.30	#N/A	#N/A	2.9	#N/A	#N/A	1.4	#N/A	#N/A	1.9	#N/A	#N/A	#N/A	#N/A	#N/A	#N/A
13/11/1990	71.28	0.1	1.5	2.6	-2.6	-8.6	2.5	1.0	-8.1	2.0	#N/A	#N/A	#N/A	#N/A	#N/A	#N/A
22/01/1991	71.15	-0.6	0.9	2.1	-3.2	-12.8	3.9	1.9	-11.8	3.9	#N/A	#N/A	#N/A	#N/A	#N/A	#N/A
21/02/1991	74.97	-0.7	0.9	1.7	-3.6	-11.9	3.2	1.8	-11.1	4.3	#N/A	#N/A	#N/A	#N/A	#N/A	#N/A
30/07/1991	74.87	-0.5	0.6	-0.1	-2.0	-4.9	0.3	0.5	-2.9	0.9	#N/A	#N/A	#N/A	#N/A	#N/A	#N/A
29/01/1992	90.27	0.3	0.3	0.6	-1.2	-10.8	3.0	2.6	-12.1	3.1	#N/A	#N/A	#N/A	#N/A	#N/A	#N/A
07/08/1992	94.30	0.0	0.0	0.0	0.0	0.0	0.0	0.0	0.0	0.0	0.0	0.0	0.0	0.0	0.0	0.0
17/09/1992	95.23	0.0	0.1	-0.4	0.5	-0.1	0.5	-0.7	-1.2	0.5	0.3	0.1	0.3	-0.7	-0.1	-0.1
03/02/1993	96.22	0.3	0.1	-0.5	-0.2	-6.2	1.7	2.2	-8.7	1.4	0.8	0.8	-0.3	-0.4	0.5	-0.9
03/07/1993	97.69	0.4	0.1	-0.4	0.9	1.7	0.0	0.2	1.6	0.1	0.0	0.1	-1.1	-0.4	-0.1	-1.5
31/08/1993	89.47	0.2	0.4	-1.0	0.2	-0.7	0.0	0.1	-0.8	0.3	0.3	-0.4	0.0	-0.9	0.5	-0.6
29/10/1993	97.39	0.3	-0.1	-0.6	0.3	-2.7	1.7	0.6	-4.4	1.9	-0.1	0.6	0.0	-0.7	0.3	0.4
09/02/1994	98.07	0.5	0.1	-1.2	-1.5	-7.8	2.3	2.1	-9.4	2.0	-0.4	1.2	0.3	-1.1	1.7	-1.0
24/08/1994	98.04	0.3	0.3	-0.8	-0.3	2.3	0.6	-0.1	1.4	0.5	-0.6	0.8	-0.6	0.0	0.5	-1.0
01/02/1995	97.93	0.0	0.8	-0.9	-0.7	-9.2	2.4	2.8	-11.4	2.4	-0.1	-0.3	0.6	0.5	1.1	-0.1
09/08/1995	97.90	-0.1	1.0	-4.4	0.8	2.0	0.3	0.8	2.2	0.4	-0.2	-0.5	-1.2	0.7	0.3	-2.0
13/02/1996	98.02	2.0	0.6	0.3	-1.8	-8.1	2.1	2.2	-10.4	1.4	-0.8	1.0	-0.4	-0.2	0.7	-1.2
21/08/1996	95.22	1.6	-0.1	0.8	-1.3	3.2	0.2	-0.9	3.1	0.7	-2.0	0.6	-0.7	-0.9	0.5	-1.5
12/11/1996	95.05	1.8	0.3	0.8	-0.7	-2.0	1.3	-0.1	-3.9	1.3	-1.4	1.2	-0.1	-0.9	0.4	-1.2
18/02/1997	97.43	0.6	1.6	2.0	-4.0	-7.8	2.2	-0.1	-9.9	2.1	-2.8	0.7	-0.3	-2.5	0.4	-0.8
19/08/1997	98.00	1.2	1.1	1.5	-2.4	1.8	0.6	-2.1	0.9	0.9	-3.1	0.3	0.0	-2.4	-0.4	-0.7
26/02/1998	97.92	2.3	0.2	1.1	-2.7	-8.0	2.1	1.5	-10.5	2.0	-2.1	0.3	-0.6	-0.8	1.5	-1.1
19/08/1998	97.71	2.3	0.3	1.0	-1.1	3.1	0.8	-1.0	2.9	1.5	-1.8	0.6	-0.2	-0.9	0.9	-0.2
10/02/1999	98.64	3.5	0.3	-0.5	-1.6	-8.1	2.4	2.8	-10.3	2.4	-0.4	1.1	-0.3	0.3	1.6	-0.9
25/08/1999	96.75	2.4	0.7	0.9	0.1	1.9	1.5	0.8	2.3	2.1	-0.6	0.2	-0.2	0.9	1.8	-0.6
02/02/2000	97.11	1.3	1.5	0.0	-1.3	-9.0	2.2	2.8	-11.1	1.3	-0.5	1.0	-0.6	0.6	0.8	-1.8
02/08/2000	96.99	0.7	2.5	-0.1	-0.3	2.9	1.5	0.3	3.5	1.5	-1.2	1.3	0.2	0.1	0.8	-0.3
08/02/2001	97.93	1.1	0.9	-2.5	-1.1	-7.5	2.5	1.9	-9.8	2.3	-0.7	0.9	0.0	0.2	1.3	-1.0
15/08/2001	97.44	1.8	-0.1	-0.7	0.3	3.2	0.3	0.0	2.9	1.0	-0.2	0.9	-0.8	0.0	0.9	-1.3
20/02/2002	97.99	2.4	0.4	-3.0	-0.7	-6.8	1.3	2.3	-8.3	1.1	-0.2	0.8	-1.9	0.7	1.7	-2.4
15/08/2002	96.18	1.8	-0.5	-1.3	0.0	2.0	0.5	-0.1	1.8	1.0	-1.3	0.7	-0.5	-0.2	0.5	-1.3
13/02/2003	95.93	2.0	-0.9	-2.3	-1.6	-11.0	2.1	2.8	-13.2	2.5	-0.8	0.5	-0.3	0.3	0.3	-1.8
13/08/2003	98.00	4.4	1.1	2.1	0.3	4.0	0.2	0.2	4.5	0.7	-0.8	0.6	-0.4	0.4	1.0	-1.2
18/02/2004	94.30	3.5	1.0	1.2	-2.1	-9.6	2.9	2.6	-11.1	2.4	-1.5	0.6	0.3	0.1	0.2	-0.6
18/08/2004	95.69	4.0	-0.7	1.7	0.2	1.6	0.4	0.0	1.5	1.1	-1.6	-0.3	-0.9	0.4	0.0	-1.2
23/02/2005	95.69	4.3	-0.4	1.3	-1.3	-8.9	2.9	2.7	-10.7	2.2	-0.4	0.6	-0.5	0.7	0.4	-1.2
17/08/2005	96.85	3.3	-0.6	-0.1	0.0	2.3	-0.2	-0.4	2.1	0.3	-1.3	0.1	-1.4	-0.1	0.2	-2.1
15/02/2006	89.48	4.3	-2.5	-2.1	-1.3	-11.7	2.3	3.9	-13.2	2.5	-0.3	-0.7	-0.3	1.1	-0.6	-1.7
16/08/2006	89.48	4.7	-0.4	0.6	0.4	2.7	0.1	-0.6	2.6	0.3	0.0	-0.1	0.0	0.0	0.7	-1.2
01/02/2007	95.60	5.3	0.8	1.4	-0.6	-10.6	2.0	3.2	-13.4	2.3	0.5	1.0	-0.1	0.8	0.8	-1.0
08/08/2007	94.48	4.5	0.8	1.3	0.4	2.1	-0.3	0.1	2.9	-0.1	-0.6	0.2	-1.0	0.0	1.2	-1.7
05/02/2008	97.91	5.5	0.1	1.9	0.7	-8.1	1.5	2.4	-10.0	2.1	0.3	-0.3	-0.6	0.3	1.4	-2.0
06/08/2008	94.48	3.7	0.3	0.9	-0.1	2.0	-0.2	-0.3	1.9	1.0	-1.0	0.5	-0.1	-0.5	0.4	-0.9

PRECISE ENGINEERING SURVEYS

DEFORMATION DISPLACEMENTS

WOLWEDANS DAM

Ref: 07/08/1992

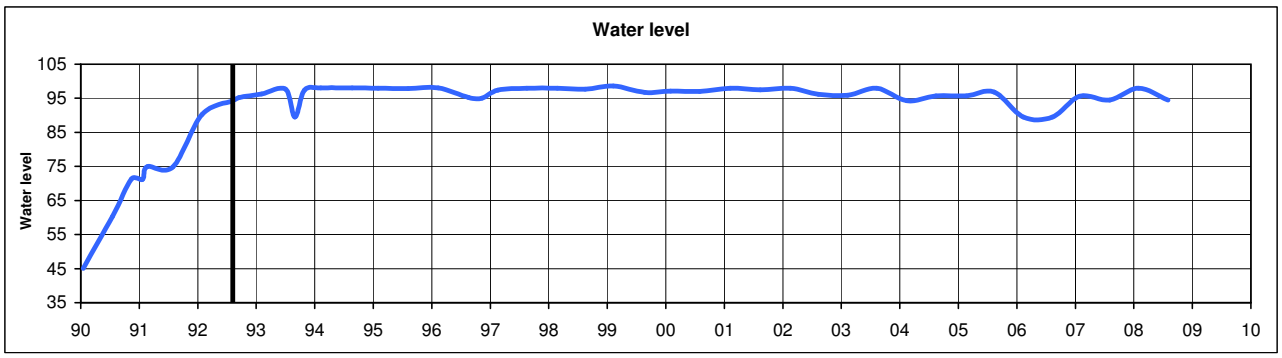

Date	R300	dy	dx	dz
17/01/1990	45.03	#N/A	#N/A	#N/A
18/07/1990	60.30	#N/A	#N/A	#N/A
13/11/1990	71.28	#N/A	#N/A	#N/A
22/01/1991	71.15	#N/A	#N/A	#N/A
21/02/1991	74.97	#N/A	#N/A	#N/A
30/07/1991	74.87	#N/A	#N/A	#N/A
29/01/1992	90.27	#N/A	#N/A	#N/A
07/08/1992	94.30	0.0	0.0	0.0
17/09/1992	95.23	0.0	0.2	0.5
03/02/1993	96.22	0.5	1.1	-0.3
03/07/1993	97.69	-0.4	0.2	-1.0
31/08/1993	89.47	0.1	0.1	0.6
29/10/1993	97.39	-0.3	0.9	0.6
09/02/1994	98.07	-0.7	1.4	0.7
24/08/1994	98.04	-0.8	0.8	-1.1
01/02/1995	97.93	0.3	0.4	0.5
09/08/1995	97.90	-0.2	-0.5	-1.4
13/02/1996	98.02	-0.7	1.3	-0.7
21/08/1996	95.22	-2.1	0.9	-1.3
12/11/1996	95.05	-1.2	1.2	-0.5
18/02/1997	97.43	-2.4	0.6	-0.6
19/08/1997	98.00	-3.3	0.3	0.1
26/02/1998	97.92	-1.7	0.7	-0.8
19/08/1998	97.71	-1.9	0.7	0.4
10/02/1999	98.64	0.0	1.4	-0.4
25/08/1999	96.75	0.1	0.3	0.4
02/02/2000	97.11	0.0	1.3	-2.3
02/08/2000	96.99	-0.7	1.4	-0.1
08/02/2001	97.93	0.0	1.3	-0.4
15/08/2001	97.44	-0.6	1.1	-1.1
20/02/2002	97.99	0.3	1.7	-2.6
15/08/2002	96.18	-0.9	0.8	-0.6
13/02/2003	95.93	0.2	1.2	-1.1
13/08/2003	98.00	-0.2	0.8	-1.4
18/02/2004	94.30	-0.4	0.7	-0.1
18/08/2004	95.69	-0.7	-0.1	-1.3
23/02/2005	95.69	0.4	0.7	-1.0
17/08/2005	96.85	-1.1	0.5	-2.5
15/02/2006	89.48	0.5	-0.3	-0.9
16/08/2006	89.48	-0.1	0.3	-1.5
01/02/2007	95.60	0.9	0.9	-0.3
08/08/2007	94.48	0.2	0.8	-1.2
05/02/2008	97.91	1.1	0.5	-1.4
06/08/2008	94.48	-0.7	0.7	-0.2

PRECISE ENGINEERING SURVEYS

DEFORMATION DISPLACEMENTS

WOLWEDANS DAM

Ref: 07/08/1992

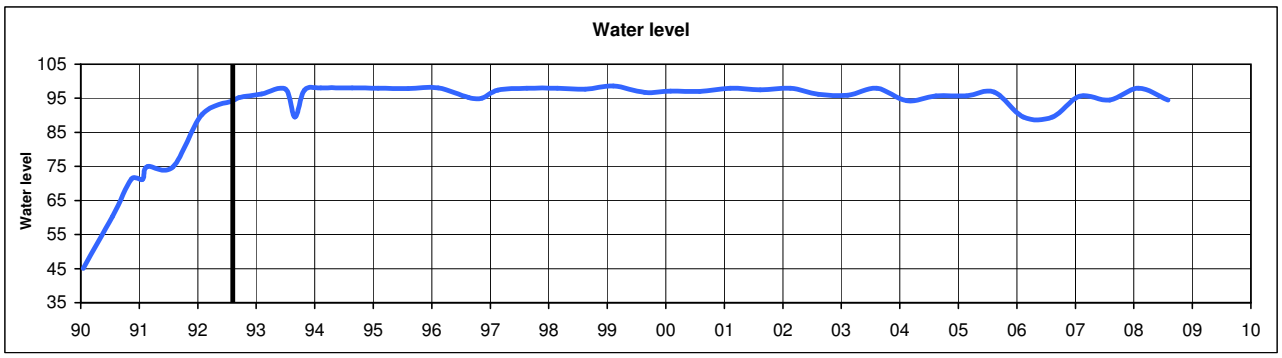

Date	Water Level	103			106			109			112			121		
		dy	dx	dz	dy	dx	dz	dy	dx	dz	dy	dx	dz	dy	dx	dz
17/01/1990	45.03	-3.6	0.3	2.4	-5.8	-2.6	3.9	-6.2	-7.8	5.4	-4.9	-10.7	7.1	4.4	-8.6	6.3
18/07/1990	60.30	#N/A	#N/A	-0.4	#N/A	#N/A	1.1	#N/A	#N/A	1.4	#N/A	#N/A	1.9	#N/A	#N/A	1.7
13/11/1990	71.28	-2.2	0.0	1.4	-3.2	-1.9	2.6	-3.0	-6.3	2.7	-2.4	-7.9	3.1	1.2	-7.3	1.9
22/01/1991	71.15	-3.8	0.0	2.1	-5.2	-3.2	3.6	-5.4	-9.1	4.2	-3.0	-12.0	4.4	2.7	-10.7	3.8
21/02/1991	74.97	-3.5	0.7	1.6	-4.7	-2.7	3.1	-4.5	-8.6	3.6	-3.0	-11.9	3.7	2.8	-10.2	3.9
30/07/1991	74.87	-0.6	0.2	1.0	-0.9	-0.4	1.2	-0.8	-3.8	1.1	-1.7	-5.1	0.9	0.5	-2.8	0.5
29/01/1992	90.27	-3.3	-0.2	0.8	-4.2	-3.4	2.1	-4.1	-8.5	2.5	-1.1	-10.7	2.7	2.6	-10.8	2.2
07/08/1992	94.30	0.0	0.0	0.0	0.0	0.0	0.0	0.0	0.0	0.0	0.0	0.0	0.0	0.0	0.0	0.0
17/09/1992	95.23	-0.4	-0.6	0.9	-0.2	0.0	1.1	0.2	-0.8	1.1	0.4	0.3	1.2	-0.5	-1.2	0.7
03/02/1993	96.22	-2.1	0.1	1.6	-2.9	-2.1	2.3	-2.8	-5.3	2.6	-0.3	-5.5	2.8	2.8	-7.7	1.7
03/07/1993	97.69	-0.2	-1.1	0.6	0.0	-0.2	0.6	0.6	-0.2	0.5	1.0	1.0	0.7	0.9	1.2	-0.1
31/08/1993	89.47	-0.1	-0.7	0.8	-0.1	-0.9	0.9	0.0	-1.4	0.9	-0.3	-0.6	0.9	0.5	-0.9	0.2
29/10/1993	97.39	-0.7	-1.3	1.1	-1.3	-1.6	1.5	-1.2	-2.7	1.9	0.5	-2.0	2.6	0.9	-3.9	2.0
09/02/1994	98.07	-2.9	-0.7	2.1	-4.6	-2.8	2.5	-4.7	-5.7	2.8	-2.0	-6.8	3.2	2.4	-8.5	2.4
24/08/1994	98.04	-0.2	-0.6	-0.2	0.0	0.3	-0.9	0.2	0.5	-1.3	-0.4	1.8	-0.8	0.1	1.4	-1.3
01/02/1995	97.93	-2.9	-2.7	0.6	-4.6	-4.9	0.7	-4.6	-7.8	0.6	-1.1	-8.5	1.1	3.8	-10.4	0.7
09/08/1995	97.90	0.1	-2.5	-0.5	0.7	-0.9	-1.1	1.5	-0.3	-1.2	0.8	1.5	-0.8	1.3	2.0	-1.3
13/02/1996	98.02	-4.1	-1.9	1.7	-5.5	-4.0	1.6	-5.3	-7.2	1.7	-2.1	-7.9	2.1	2.9	-10.2	1.2
21/08/1996	95.22	-1.5	-1.0	-0.8	-1.2	1.0	-1.6	-0.5	1.2	-1.8	-1.3	2.8	-1.4	-1.0	2.9	-1.6
12/11/1996	95.05	-2.9	-0.8	-0.4	-3.4	-1.6	-0.4	-3.0	-2.8	-0.3	-1.4	-2.0	0.0	0.8	-3.6	-0.3
18/02/1997	97.43	-5.4	-1.8	2.1	-6.4	-3.7	2.3	-6.5	-6.3	2.2	-3.9	-7.1	2.4	0.1	-9.6	1.1
19/08/1997	98.00	-2.7	-1.0	-0.4	-2.5	0.0	-0.7	-2.0	0.2	-0.7	-2.0	1.5	-0.3	-1.4	0.6	0.6
26/02/1998	97.92	-4.7	-1.8	1.8	-6.0	-3.8	2.1	-5.8	-6.8	2.4	-2.8	-7.3	3.0	2.0	-9.5	2.3
19/08/1998	97.71	-1.4	-0.3	0.2	-1.3	1.1	0.3	-0.6	1.4	0.9	-1.1	3.0	1.4	-0.7	2.9	1.4
10/02/1999	98.64	-3.8	-0.7	2.4	-4.8	-3.4	2.8	-4.8	-6.7	3.4	-2.2	-8.0	3.9	3.4	-9.7	3.4
25/08/1999	96.75	-0.9	-0.9	1.3	-0.5	0.2	1.5	0.4	0.4	2.0	0.2	1.3	3.0	1.2	2.2	2.8
02/02/2000	97.11	-3.4	-1.9	2.3	-5.0	-4.2	2.7	-5.2	-6.9	3.2	-1.6	-8.3	3.9	4.0	-10.0	2.5
02/08/2000	96.99	-0.1	-0.5	1.3	0.1	1.0	1.4	0.9	1.3	1.9	0.3	2.5	3.0	0.7	3.0	2.1
08/02/2001	97.93	-3.2	-1.4	2.5	-6.5	-4.4	2.6	-4.2	-6.3	3.4	-1.4	-7.3	4.0	3.5	-8.9	3.6
15/08/2001	97.44	-1.1	-1.1	1.2	-0.4	0.8	0.9	0.0	1.1	1.1	-0.1	2.6	1.8	0.4	3.1	1.6
20/02/2002	97.99	-2.4	-2.4	2.3	-3.6	-3.6	2.4	-3.5	-5.3	2.7	-0.7	-5.9	3.1	2.8	-7.8	2.0
15/08/2002	96.18	-0.6	-1.7	1.1	0.0	0.3	1.0	0.6	0.5	1.3	0.2	2.2	1.9	0.3	1.2	1.9
13/02/2003	95.93	-3.9	-2.1	2.4	-5.2	-4.1	2.9	-5.4	-8.5	3.3	-1.9	-9.6	3.8	3.7	-12.4	4.0
13/08/2003	98.00	0.4	-2.2	0.7	0.8	0.5	0.5	1.6	1.4	0.9	0.6	3.2	1.6	0.7	3.4	1.6
18/02/2004	94.30	-4.8	-1.8	2.6	-6.3	-3.9	3.0	-4.6	-7.2	3.5	-2.1	-8.9	4.1	3.3	-11.0	3.7
18/08/2004	95.69	0.3	-2.1	1.3	0.3	-0.3	1.0	1.2	0.0	1.1	0.6	1.5	1.8	1.2	1.1	1.7
23/02/2005	95.69	-2.5	-3.1	2.7	-4.1	-4.4	3.4	-3.8	-7.2	3.9	-0.8	-8.6	4.5	3.6	-9.6	3.5
17/08/2005	96.85	-0.9	0.2	0.9	-0.5	-1.0	0.7	0.8	0.6	1.1	0.3	1.6	1.5	0.0	1.8	1.2
15/02/2006	89.48	-2.7	-3.6	3.0	-4.3	-5.4	3.5	-4.2	-9.3	3.9	-1.0	-10.9	4.1	4.5	-12.4	3.3
16/08/2006	89.48	0.0	-2.1	0.6	0.3	0.4	0.5	0.8	1.0	0.7	0.6	2.5	1.6	1.4	3.2	1.2
01/02/2007	95.60	-3.4	-2.8	2.7	-5.8	-4.6	3.0	-3.4	-4.5	3.5	-0.4	-10.8	3.7	4.9	-11.8	3.6
08/08/2007	94.48	0.7	-1.9	1.4	0.8	0.0	0.9	1.6	0.4	1.0	0.6	1.8	1.4	-0.2	2.4	0.5
05/02/2008	97.91	-0.7	-3.3	1.9	-4.1	-5.4	2.3	-3.3	-7.4	2.8	-0.2	-7.9	3.2	3.1	-9.4	3.4
06/08/2008	94.48	-0.5	-0.7	-0.3	-0.8	-0.1	-0.9	1.1	2.1	-0.7	0.9	1.5	0.2	0.3	1.6	0.8

PRECISE ENGINEERING SURVEYS

DEFORMATION DISPLACEMENTS

WOLWEDANS DAM

Ref: 07/08/1992

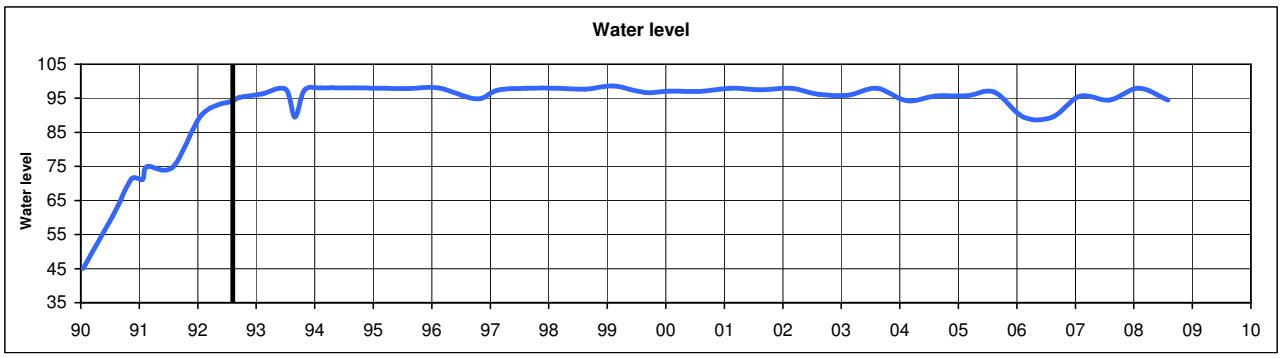

Date	Water Level	124			127		
		dy	dx	dz	dy	dx	dz
17/01/1990	45.03	8.7	-5.2	3.3	2.5	0.6	1.3
18/07/1990	60.30	#N/A	#N/A	0.7	#N/A	#N/A	0.7
13/11/1990	71.28	5.3	-5.3	1.4	0.6	0.3	0.7
22/01/1991	71.15	6.9	-6.4	3.1	2.4	0.4	1.8
21/02/1991	74.97	6.4	-6.0	3.1	1.9	-0.1	1.4
30/07/1991	74.87	-0.1	-0.8	1.0	0.6	0.1	0.4
29/01/1992	90.27	4.9	-4.7	2.9	2.5	0.4	1.1
07/08/1992	94.30	0.0	0.0	0.0	0.0	0.0	0.0
17/09/1992	95.23	0.7	-0.4	0.5	0.1	-0.7	0.5
03/02/1993	96.22	5.0	-3.3	2.5	2.1	0.8	1.6
03/07/1993	97.69	1.6	0.6	-0.1	0.3	-0.3	0.3
31/08/1993	89.47	1.3	-0.4	-0.1	-0.4	-0.3	-0.3
29/10/1993	97.39	3.7	-1.8	1.7	1.1	-0.3	1.1
09/02/1994	98.07	4.9	-3.6	2.8	1.4	0.9	1.7
24/08/1994	98.04	1.3	0.7	-1.1	0.2	0.2	-0.4
01/02/1995	97.93	6.8	-5.6	1.8	3.2	0.5	1.4
09/08/1995	97.90	2.7	0.7	-1.1	1.1	0.2	-0.1
13/02/1996	98.02	6.2	-5.5	1.8	3.0	0.6	1.5
21/08/1996	95.22	0.6	0.6	-1.1	-0.6	-0.4	-0.2
12/11/1996	95.05	4.0	-2.4	-0.1	1.3	-0.1	-0.1
18/02/1997	97.43	3.7	-5.1	1.1	0.3	-0.2	0.1
19/08/1997	98.00	1.0	0.0	-0.2	-0.8	-0.2	-0.1
26/02/1998	97.92	5.0	-4.7	2.6	1.6	0.8	1.5
19/08/1998	97.71	1.6	0.6	1.0	-0.4	0.7	1.2
10/02/1999	98.64	6.4	-5.0	3.6	3.0	0.6	2.3
25/08/1999	96.75	2.6	1.3	2.2	1.0	0.8	2.0
02/02/2000	97.11	6.9	-4.6	2.5	3.2	1.0	1.2
02/08/2000	96.99	2.8	2.0	1.3	1.1	1.0	1.8
08/02/2001	97.93	5.9	-4.1	3.4	2.6	0.4	2.1
15/08/2001	97.44	2.5	1.4	1.2	0.6	1.0	0.8
20/02/2002	97.99	7.2	-3.8	1.9	2.9	2.5	0.5
15/08/2002	96.18	2.2	0.5	1.3	0.4	-0.2	1.5
13/02/2003	95.93	7.1	-5.9	4.3	3.0	-0.2	2.9
13/08/2003	98.00	2.4	1.4	0.9	0.7	0.3	0.7
18/02/2004	94.30	6.6	-5.6	4.0	2.9	0.7	2.8
18/08/2004	95.69	4.5	0.2	1.0	1.6	0.3	0.9
23/02/2005	95.69	7.1	-5.0	3.4	3.9	-0.4	2.2
17/08/2005	96.85	2.9	0.7	0.8	1.3	-0.6	1.0
15/02/2006	89.48	7.7	-6.6	3.3	5.0	-0.6	1.9
16/08/2006	89.48	2.8	1.4	0.6	1.6	0.8	0.8
01/02/2007	95.60	8.7	-6.1	3.6	3.0	0.7	1.8
08/08/2007	94.48	2.3	1.1	-0.5	0.5	0.7	-0.6
05/02/2008	97.91	7.5	-5.3	3.1	3.1	0.4	1.6
06/08/2008	94.48	0.1	2.5	0.2	0.1	-0.1	0.3

PRECISE ENGINEERING SURVEYS

DEFORMATION DISPLACEMENTS

WOLWEDANS DAM

Ref: 07/08/1992

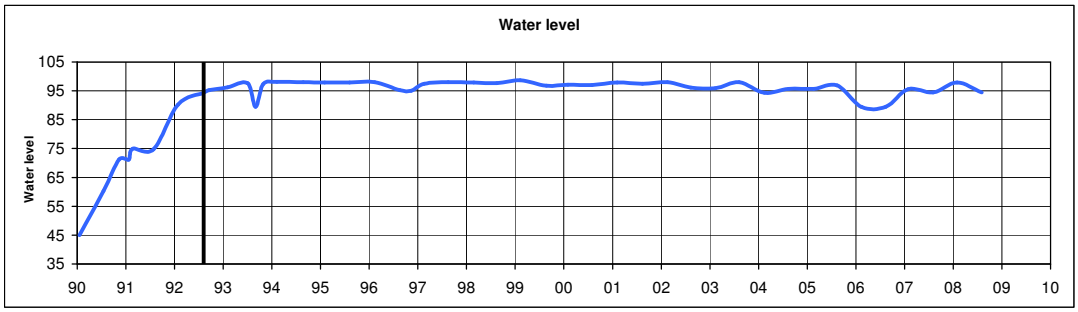

Date		206			207			208			210			211		
		dy	dx	dz	dy	dx	dz	dy	dx	dz	dy	dx	dz	dy	dx	dz
17/01/1990	45.03	#N/A	#N/A	#N/A	#N/A	#N/A	#N/A	#N/A	#N/A	#N/A	#N/A	#N/A	#N/A	#N/A	#N/A	#N/A
18/07/1990	60.30	#N/A	#N/A	#N/A	#N/A	#N/A	#N/A	#N/A	#N/A	#N/A	#N/A	#N/A	#N/A	#N/A	#N/A	#N/A
13/11/1990	71.28	#N/A	#N/A	#N/A	#N/A	#N/A	#N/A	#N/A	#N/A	#N/A	#N/A	#N/A	#N/A	#N/A	#N/A	#N/A
22/01/1991	71.15	#N/A	#N/A	#N/A	#N/A	#N/A	#N/A	#N/A	#N/A	#N/A	#N/A	#N/A	#N/A	#N/A	#N/A	#N/A
21/02/1991	74.97	#N/A	#N/A	#N/A	#N/A	#N/A	#N/A	#N/A	#N/A	#N/A	#N/A	#N/A	#N/A	#N/A	#N/A	#N/A
30/07/1991	74.87	#N/A	#N/A	#N/A	#N/A	#N/A	#N/A	#N/A	#N/A	#N/A	#N/A	#N/A	#N/A	#N/A	#N/A	#N/A
29/01/1992	90.27	#N/A	#N/A	#N/A	#N/A	#N/A	#N/A	#N/A	#N/A	#N/A	#N/A	#N/A	#N/A	#N/A	#N/A	#N/A
07/08/1992	94.30	0.0	0.0	0.0	0.0	0.0	0.0	0.0	0.0	0.0	0.0	0.0	0.0	0.0	0.0	0.0
17/09/1992	95.23	0.5	-0.2	0.4	0.6	-0.1	0.4	0.6	-0.1	0.7	0.6	0.2	0.3	0.6	0.3	0.6
03/02/1993	96.22	-0.6	-0.1	-0.4	-1.0	-0.7	-0.4	-1.1	-1.5	-0.4	-0.6	-1.8	-0.2	-0.4	-2.1	-0.1
03/07/1993	97.69	0.3	-0.6	-0.8	0.5	-0.4	-0.7	0.7	-0.3	-0.8	1.0	0.0	-0.8	1.2	0.2	-0.7
31/08/1993	89.47	0.6	-0.7	0.1	0.8	-0.8	0.0	0.8	-0.7	-0.2	0.8	-0.7	-0.2	0.6	-0.7	-0.1
29/10/1993	97.39	-0.7	0.2	-0.1	-0.4	-0.9	0.0	-0.5	-0.3	0.1	-0.7	-0.8	0.2	-0.3	-0.6	0.5
09/02/1994	98.07	-1.6	0.7	-0.1	-1.9	-1.1	-0.1	-2.3	-1.2	-0.3	-2.4	-2.2	-0.1	-1.8	-2.5	0.0
24/08/1994	98.04	-0.3	0.9	0.1	0.1	0.0	0.1	0.0	0.8	0.1	-0.2	0.4	0.3	0.2	0.7	0.5
01/02/1995	97.93	-1.3	-1.1	0.3	-1.4	-2.8	0.3	-1.4	-2.9	0.1	-1.4	-3.9	0.5	-0.6	-4.0	0.7
09/08/1995	97.90	-0.2	-0.2	-0.7	-1.4	-2.8	0.3	-1.4	-2.9	0.1	-1.4	-3.9	0.5	-0.6	-4.0	0.7
13/02/1996	98.02	-1.8	0.3	-0.7	-2.2	-1.5	-0.6	-2.4	-1.9	-0.6	-2.6	-3.0	-0.3	-2.1	-3.4	-0.1
21/08/1996	95.22	-1.5	0.9	-0.2	-1.1	-0.1	-0.4	-0.9	1.1	-0.4	-1.2	0.5	-0.3	-1.0	1.0	-0.2
12/11/1996	95.05	-1.9	0.9	0.0	-1.6	-0.3	0.1	-1.5	0.5	0.2	-1.7	-0.2	0.5	-1.2	0.0	0.4
18/02/1997	97.43	-3.7	-0.2	-0.7	-3.8	-1.9	-0.8	-3.8	-1.7	-1.0	-4.0	-2.8	-0.3	-3.4	-2.9	-0.4
19/08/1997	98.00	-2.7	0.1	0.1	-2.2	-0.9	0.2	-2.0	0.0	0.8	-2.3	-0.6	0.5	-1.9	-0.3	0.9
26/02/1998	97.92	#N/A	#N/A	-1.2	#N/A	#N/A	-1.2	#N/A	#N/A	0.7	#N/A	#N/A	-0.6	#N/A	#N/A	1.3
19/08/1998	97.71	-1.4	0.4	0.3	-0.8	-0.5	0.3	-0.7	0.4	0.5	-0.7	0.1	0.7	-0.2	0.5	0.7
10/02/1999	98.64	-1.9	0.1	-0.6	-1.9	-1.8	-0.6	-1.8	-1.8	-0.3	-1.9	-3.1	-0.2	-1.2	-3.4	0.4
25/08/1999	96.75	-0.4	0.1	0.1	0.2	-1.0	0.2	0.4	-0.1	0.1	0.1	-0.3	0.3	0.6	0.1	0.1
02/02/2000	97.11	-2.0	0.2	-1.0	-2.2	-1.6	-1.0	-2.3	-1.7	-1.1	-2.4	-2.8	-0.6	-1.8	-3.2	-0.7
02/08/2000	96.99	-0.8	1.5	0.8	-0.3	0.4	0.9	-0.2	1.2	0.9	-0.4	0.8	1.1	0.0	1.1	0.9
08/02/2001	97.93	-2.2	0.0	-0.3	-2.3	-1.8	-0.2	-2.2	-1.8	-0.3	-2.4	-2.7	0.2	-1.7	-2.9	0.2
15/08/2001	97.44	0.0	1.0	-0.5	0.4	0.0	-0.5	0.5	1.0	-0.6	0.1	0.8	-0.3	0.4	1.2	-0.3
20/02/2002	97.99	-0.9	0.2	-2.1	-1.0	-1.5	-2.1	-0.9	-1.4	-2.2	-1.2	-2.1	-1.6	-0.7	-2.2	-1.6
15/08/2002	96.18	-0.8	1.0	-0.1	-0.3	0.0	0.0	-0.3	1.1	-0.1	-0.6	0.8	0.1	-0.3	1.4	1.2
13/02/2003	95.93	-2.1	-0.1	-1.0	-2.3	-2.2	-1.1	-2.4	-2.3	-1.3	-2.6	-3.5	-0.8	-1.9	-3.8	-0.9
13/08/2003	98.00	-0.1	0.7	0.3	0.6	-0.1	0.3	0.7	1.1	0.1	0.4	0.8	0.3	0.7	1.3	0.2
18/02/2004	94.30	-2.9	-0.4	-0.4	-3.0	-2.6	-0.5	-3.0	-3.0	-0.7	-3.2	-4.1	-0.2	-2.4	-4.5	-0.1
18/08/2004	95.69	-1.2	-0.4	-0.5	-0.6	-1.6	-0.6	-0.3	-0.7	-0.7	-0.4	-1.1	-0.5	0.1	-0.7	-0.7
23/02/2005	95.69	-1.7	-0.3	-1.3	-1.9	-2.3	-1.2	-1.9	-2.5	-1.2	-2.1	-3.5	-0.6	-1.4	-3.8	-0.5
17/08/2005	96.85	-0.8	0.4	-0.8	-0.3	-0.8	-0.9	-0.1	0.1	-1.1	-0.2	-0.2	-0.9	0.2	0.2	-1.1
15/02/2006	89.48	-1.7	-1.1	-0.5	-2.1	-3.5	-0.4	-2.2	-3.8	-0.5	-2.5	-5.1	0.1	-1.6	-5.6	0.2
16/08/2006	89.48	0.8	0.2	0.5	1.3	-0.8	0.4	1.2	0.1	0.2	0.8	-0.2	0.4	1.0	0.1	0.3
01/02/2007	95.60	-0.8	-0.1	-0.4	-0.9	-2.3	-0.3	-1.0	-2.6	-0.4	-1.2	-3.7	0.1	-0.6	-4.1	0.2
08/08/2007	94.48	0.4	0.5	0.0	0.9	-0.5	-0.1	1.1	0.7	-0.4	0.8	0.4	-0.2	1.3	0.9	-0.5
05/02/2008	97.91	-0.9	-1.0	-0.4	-1.0	-2.7	-0.3	-0.9	-2.6	-0.4	-1.0	-3.5	0.0	-0.4	-3.6	-0.1
06/08/2008	94.48	-0.5	0.5	0.1	0.0	-0.4	0.2	0.0	0.7	0.0	-0.3	0.4	0.2	0.0	0.8	0.1

PRECISE ENGINEERING SURVEYS

DEFORMATION DISPLACEMENTS

WOLWEDANS DAM

Ref: 07/08/1992

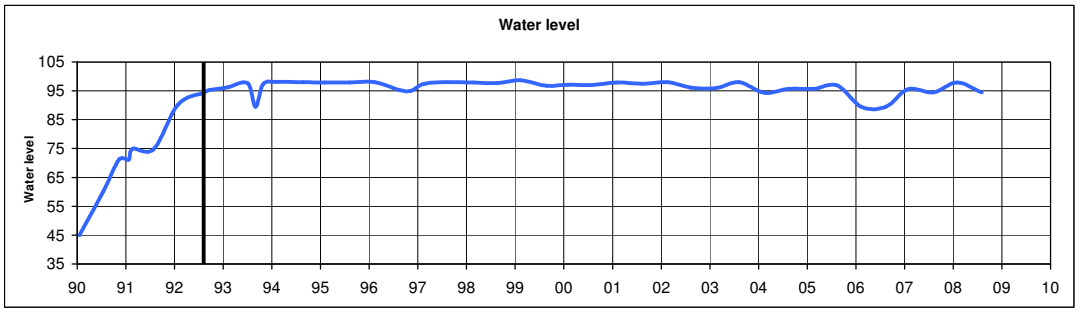

Date	Water Level	212			213			214			216			217		
		dy	dx	dz	dy	dx	dz	dy	dx	dz	dy	dx	dz	dy	dx	dz
17/01/1990	45.03	#N/A	#N/A	#N/A	#N/A	#N/A	#N/A	#N/A	#N/A	#N/A	#N/A	#N/A	#N/A	#N/A	#N/A	#N/A
18/07/1990	60.30	#N/A	#N/A	#N/A	#N/A	#N/A	#N/A	#N/A	#N/A	#N/A	#N/A	#N/A	#N/A	#N/A	#N/A	#N/A
13/11/1990	71.28	#N/A	#N/A	#N/A	#N/A	#N/A	#N/A	#N/A	#N/A	#N/A	#N/A	#N/A	#N/A	#N/A	#N/A	#N/A
22/01/1991	71.15	#N/A	#N/A	#N/A	#N/A	#N/A	#N/A	#N/A	#N/A	#N/A	#N/A	#N/A	#N/A	#N/A	#N/A	#N/A
21/02/1991	74.97	#N/A	#N/A	#N/A	#N/A	#N/A	#N/A	#N/A	#N/A	#N/A	#N/A	#N/A	#N/A	#N/A	#N/A	#N/A
30/07/1991	74.87	#N/A	#N/A	#N/A	#N/A	#N/A	#N/A	#N/A	#N/A	#N/A	#N/A	#N/A	#N/A	#N/A	#N/A	#N/A
29/01/1992	90.27	#N/A	#N/A	#N/A	#N/A	#N/A	#N/A	#N/A	#N/A	#N/A	#N/A	#N/A	#N/A	#N/A	#N/A	#N/A
07/08/1992	94.30	0.0	0.0	0.0	0.0	0.0	0.0	0.0	0.0	0.0	0.0	0.0	0.0	0.0	0.0	0.0
17/09/1992	95.23	0.5	0.3	0.3	0.5	0.3	0.7	0.5	0.4	0.4	0.4	0.5	0.6	0.1	0.4	0.3
03/02/1993	96.22	-0.2	-2.6	0.2	0.1	-3.0	-0.4	0.5	-3.5	-0.4	0.7	-3.6	-0.7	1.0	-3.6	-0.2
03/07/1993	97.69	1.1	0.3	-0.5	1.2	0.5	-0.6	1.3	0.7	-0.6	1.2	0.8	-0.6	1.0	0.9	-0.6
31/08/1993	89.47	0.5	-0.7	-0.2	0.6	-0.7	-0.2	0.6	-0.7	-0.3	0.8	-0.6	-0.4	0.7	-0.6	-0.3
29/10/1993	97.39	-0.2	-0.3	0.6	0.0	-0.7	0.5	0.1	-0.9	0.7	0.3	-1.1	0.8	0.9	-0.9	0.9
09/02/1994	98.07	-1.5	-2.7	0.3	-1.3	-3.8	-0.4	-0.9	-4.1	-0.5	-0.4	-4.3	-0.5	0.4	-4.2	-0.3
24/08/1994	98.04	0.2	1.1	0.7	0.5	0.9	0.9	0.5	1.0	1.4	0.7	1.0	1.2	1.0	1.2	1.1
01/02/1995	97.93	-0.3	-4.2	0.8	0.1	-5.2	0.7	0.7	-5.6	0.7	1.4	-5.7	0.3	2.2	-5.5	1.0
09/08/1995	97.90	-0.3	-4.2	0.8	0.1	-5.2	0.7	0.7	-5.6	0.7	1.4	-5.7	0.3	2.2	-5.5	1.0
13/02/1996	98.02	-1.7	-3.7	0.0	-1.2	-4.7	-0.5	-0.6	-5.3	-0.5	0.0	-5.3	-0.8	0.9	-5.3	-0.1
21/08/1996	95.22	-1.0	1.9	-0.2	-0.9	1.9	0.1	-0.8	2.2	0.1	-0.7	2.7	0.1	-0.3	2.6	0.2
12/11/1996	95.05	-1.0	0.2	0.3	-0.9	-0.2	0.1	-0.8	-0.3	0.2	-0.5	-0.1	0.1	0.2	-0.4	0.3
18/02/1997	97.43	-3.3	-3.0	0.3	-3.0	-4.0	-0.5	-2.5	-4.5	-0.2	-1.9	-4.5	-0.7	-1.2	-4.8	0.2
19/08/1997	98.00	-1.8	0.3	0.4	-2.6	0.5	1.0	-1.9	0.5	0.7	-2.8	1.0	1.3	-2.2	0.8	1.3
26/02/1998	97.92	#N/A	#N/A	-0.3	#N/A	#N/A	1.1	#N/A	#N/A	-0.5	#N/A	#N/A	1.4	#N/A	#N/A	0.7
19/08/1998	97.71	-0.2	1.2	0.7	-1.1	1.7	0.9	-0.4	1.8	1.0	-1.3	2.1	1.2	-1.0	2.2	1.7
10/02/1999	98.64	-0.8	-3.5	0.5	-1.4	-4.2	0.3	-0.3	-4.8	0.0	-0.7	-4.7	0.1	0.4	-4.9	0.3
25/08/1999	96.75	0.8	0.8	0.4	1.1	0.5	0.3	1.2	1.0	0.7	1.6	1.5	0.4	2.0	1.5	0.9
02/02/2000	97.11	-1.5	-3.5	-0.2	-1.0	-4.7	-0.8	-0.5	-5.0	-0.5	0.4	-5.1	-1.0	1.3	-5.3	-0.1
02/08/2000	96.99	0.0	1.8	1.1	0.3	1.5	1.0	0.3	2.0	1.3	0.7	2.5	1.1	0.9	2.4	1.7
08/02/2001	97.93	-1.2	-3.0	0.6	-0.7	-4.1	-0.1	-0.3	-4.3	0.3	0.5	-4.1	-0.1	1.3	-4.2	0.8
15/08/2001	97.44	0.6	1.8	0.0	0.8	1.6	0.0	0.6	2.0	0.6	0.9	2.4	0.2	1.2	2.4	0.6
20/02/2002	97.99	-0.3	-2.1	-1.1	0.1	-3.0	-1.7	0.4	-3.1	-1.4	1.0	-2.9	-1.9	1.7	-3.1	-1.0
15/08/2002	96.18	-0.2	2.0	0.3	0.8	1.6	0.2	0.7	2.1	0.7	0.7	2.7	0.3	0.9	2.5	0.7
13/02/2003	95.93	-1.5	-4.2	-0.5	-1.1	-5.5	-1.2	-0.5	-6.1	-1.0	0.3	-6.1	-1.4	1.2	-6.6	-0.5
13/08/2003	98.00	0.8	2.2	0.5	1.0	2.0	0.6	1.1	2.6	1.1	1.4	3.1	0.7	1.5	3.0	1.0
18/02/2004	94.30	-2.1	-4.8	0.3	-1.5	-6.1	-0.4	-0.9	-6.6	-0.1	-0.1	-6.6	-0.5	0.7	-6.9	0.4
18/08/2004	95.69	0.2	-0.1	-0.4	0.3	-0.3	-0.4	0.4	0.1	0.0	0.7	0.6	-0.3	0.9	0.4	0.2
23/02/2005	95.69	-0.9	-4.1	-0.7	-0.5	-5.3	-1.2	-0.1	-5.6	-1.0	0.6	-5.5	-1.3	1.5	-5.8	-0.3
17/08/2005	96.85	0.2	0.9	-0.8	0.2	0.8	-0.8	0.4	1.4	-0.4	0.8	1.9	-0.7	1.0	1.7	-0.3
15/02/2006	89.48	-1.1	-6.1	-0.2	-0.9	-7.6	-0.9	-0.2	-8.1	-1.9	0.8	-8.1	-2.2	1.9	-8.4	-1.2
16/08/2006	89.48	1.1	0.9	0.6	1.0	0.7	0.6	0.9	1.2	1.0	1.1	1.7	0.7	1.5	1.6	1.1
01/02/2007	95.60	-0.3	-4.6	-0.3	0.0	-5.9	-0.8	0.4	-6.3	-0.6	1.1	-6.2	-1.0	2.1	-6.6	0.0
08/08/2007	94.48	1.3	1.5	-0.2	1.1	1.4	-0.3	1.0	1.9	0.2	1.3	2.4	-0.2	1.4	2.1	0.2
05/02/2008	97.91	-0.1	-3.8	0.3	-0.1	-4.6	-0.3	0.4	-4.6	-0.1	1.0	-4.3	-0.6	1.7	-4.5	0.2
06/08/2008	94.48	0.0	1.4	0.3	0.0	1.2	0.3	-0.2	1.6	0.6	0.0	1.9	0.3	0.3	1.6	0.7

	32	33	34	35	36

PRECISE ENGINEERING SURVEYS

DEFORMATION DISPLACEMENTS

WOLWEDANS DAM

Ref: 07/08/1992

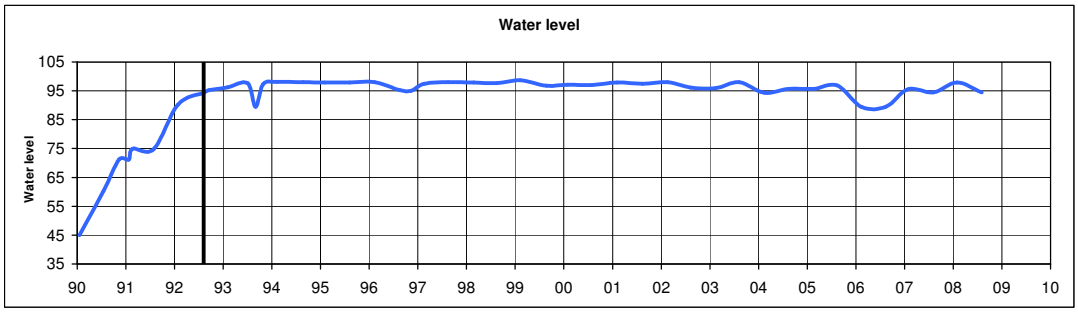

Date	Water Level	218			219			221			222			223		
		dy	dx	dz	dy	dx	dz	dy	dx	dz	dy	dx	dz	dy	dx	dz
17/01/1990	45.03	#N/A	#N/A	#N/A	#N/A	#N/A	#N/A	#N/A	#N/A	#N/A	#N/A	#N/A	#N/A	#N/A	#N/A	#N/A
18/07/1990	60.30	#N/A	#N/A	#N/A	#N/A	#N/A	#N/A	#N/A	#N/A	#N/A	#N/A	#N/A	#N/A	#N/A	#N/A	#N/A
13/11/1990	71.28	#N/A	#N/A	#N/A	#N/A	#N/A	#N/A	#N/A	#N/A	#N/A	#N/A	#N/A	#N/A	#N/A	#N/A	#N/A
22/01/1991	71.15	#N/A	#N/A	#N/A	#N/A	#N/A	#N/A	#N/A	#N/A	#N/A	#N/A	#N/A	#N/A	#N/A	#N/A	#N/A
21/02/1991	74.97	#N/A	#N/A	#N/A	#N/A	#N/A	#N/A	#N/A	#N/A	#N/A	#N/A	#N/A	#N/A	#N/A	#N/A	#N/A
30/07/1991	74.87	#N/A	#N/A	#N/A	#N/A	#N/A	#N/A	#N/A	#N/A	#N/A	#N/A	#N/A	#N/A	#N/A	#N/A	#N/A
29/01/1992	90.27	#N/A	#N/A	#N/A	#N/A	#N/A	#N/A	#N/A	#N/A	#N/A	#N/A	#N/A	#N/A	#N/A	#N/A	#N/A
07/08/1992	94.30	0.0	0.0	0.0	0.0	0.0	0.0	0.0	0.0	0.0	0.0	0.0	0.0	0.0	0.0	0.0
17/09/1992	95.23	0.1	0.3	0.6	-0.2	0.3	0.2	-0.2	0.2	0.1	-0.2	0.3	0.3	-0.4	0.3	0.0
03/02/1993	96.22	1.4	-3.7	-0.7	1.7	-3.3	-0.4	1.8	-2.7	-0.1	2.2	-1.9	-0.3	2.2	-0.9	-0.2
03/07/1993	97.69	1.0	0.8	-0.8	1.0	0.9	-0.9	0.8	0.7	-1.0	0.8	0.7	-1.3	0.9	0.7	-1.4
31/08/1993	89.47	0.8	-0.6	-0.3	0.6	-0.4	-0.4	0.5	-0.4	-0.4	0.6	-0.1	-0.6	0.6	0.3	-0.5
29/10/1993	97.39	0.5	-1.1	1.0	0.3	-0.9	1.0	0.4	-0.6	0.8	0.9	-0.9	0.7	1.4	-0.1	0.6
09/02/1994	98.07	0.5	-4.5	-0.7	0.6	-3.6	-0.5	0.8	-2.5	-0.3	1.5	-2.0	-0.7	1.9	-0.4	-0.7
24/08/1994	98.04	0.8	0.9	1.0	0.5	1.1	0.9	0.5	1.2	0.4	0.9	0.6	-0.1	1.4	1.0	-0.2
01/02/1995	97.93	2.5	-5.6	0.2	2.6	-5.1	0.2	2.9	-3.7	0.6	3.6	-3.0	-0.1	3.8	-1.2	0.2
09/08/1995	97.90	2.5	-5.6	0.2	2.6	-5.1	0.2	2.9	-3.7	0.6	3.6	-3.0	-0.1	3.8	-1.2	0.2
13/02/1996	98.02	1.2	-5.4	-0.6	1.4	-4.9	-0.6	1.6	-3.7	-0.3	2.4	-3.2	-0.9	2.8	-1.5	-0.7
21/08/1996	95.22	-0.6	2.2	0.3	-0.9	2.2	0.2	-0.8	2.2	-0.3	-0.3	1.3	-0.7	0.3	1.4	-0.8
12/11/1996	95.05	0.0	-0.8	0.0	-0.1	-0.6	0.0	0.1	-0.3	-0.1	0.6	-0.6	-0.4	1.2	0.2	-0.5
18/02/1997	97.43	-1.0	-5.2	-0.7	-0.8	-4.6	-0.4	-0.6	-3.6	-0.1	0.1	-3.2	-1.0	0.7	-1.6	-0.6
19/08/1997	98.00	-2.4	0.3	1.7	-2.5	0.5	1.1	-2.1	0.7	0.7	-1.5	0.0	0.8	-0.8	0.3	0.1
26/02/1998	97.92	#N/A	#N/A	1.4	#N/A	#N/A	-0.2	#N/A	#N/A	0.0	#N/A	#N/A	1.3	#N/A	#N/A	-0.4
19/08/1998	97.71	-1.2	1.8	1.7	-1.3	2.0	1.6	-1.0	2.0	1.1	-0.4	1.2	0.8	0.3	1.5	0.5
10/02/1999	98.64	0.8	-5.3	0.0	1.3	-4.6	-0.1	1.9	-3.3	0.2	2.8	-2.8	0.0	3.4	-0.9	-0.2
25/08/1999	96.75	1.8	1.1	0.5	1.6	1.4	0.7	1.8	1.7	0.4	2.4	1.1	0.1	3.0	1.8	-0.1
02/02/2000	97.11	1.6	-5.8	-1.0	1.9	-5.1	-0.9	2.3	-3.9	-0.6	3.1	-3.3	-1.2	3.7	-1.7	-1.4
02/08/2000	96.99	0.6	1.8	1.7	0.5	2.1	1.9	0.6	2.1	1.3	1.0	1.3	0.9	1.5	1.5	0.6
08/02/2001	97.93	1.4	-4.8	-0.1	1.7	-4.1	0.0	2.1	-3.1	0.2	2.9	-2.7	-0.3	3.4	-1.1	-0.3
15/08/2001	97.44	0.9	1.9	0.2	0.6	2.1	0.4	0.7	2.1	0.0	1.3	1.3	-0.4	1.7	1.6	-0.6
20/02/2002	97.99	1.8	-3.6	-1.8	2.0	-3.0	-1.6	2.4	-2.1	-1.4	3.1	-1.8	-1.9	3.7	-0.4	-1.9
15/08/2002	96.18	0.4	2.0	0.3	0.2	2.1	0.5	0.4	2.1	0.2	0.9	1.3	-0.2	1.3	1.5	-0.4
13/02/2003	95.93	1.4	-7.2	-1.5	1.8	-6.6	-1.3	2.3	-5.4	-0.8	3.1	-4.6	-1.3	3.6	-2.6	-1.3
13/08/2003	98.00	1.1	2.5	0.7	0.9	2.7	0.9	1.2	2.7	0.4	1.5	1.8	0.1	2.0	1.9	-0.1
18/02/2004	94.30	1.0	-7.4	-0.5	1.4	-6.6	-0.3	1.9	-5.3	0.1	2.8	-4.6	-0.4	3.5	-2.8	-0.3
18/08/2004	95.69	0.6	0.0	-0.2	0.6	0.3	0.0	1.2	0.4	-0.4	1.8	-0.2	-0.7	2.6	0.2	-0.8
23/02/2005	95.69	1.7	-6.3	-1.0	2.0	-5.6	-0.7	2.3	-4.4	-0.3	3.2	-3.9	-0.7	3.8	-2.2	-0.7
17/08/2005	96.85	0.7	1.1	-0.7	0.6	1.3	-0.5	0.8	1.1	-0.9	1.3	0.2	-1.4	1.9	0.5	-1.6
15/02/2006	89.48	2.4	-8.9	-1.9	3.0	-7.9	-1.8	3.2	-6.6	-1.4	4.3	-5.8	-1.7	4.9	-3.8	-1.5
16/08/2006	89.48	1.0	1.2	0.6	0.9	1.5	0.7	0.8	1.5	0.3	1.2	0.9	-0.1	1.7	1.2	-0.3
01/02/2007	95.60	2.4	-7.1	-0.8	2.9	-6.5	-0.6	3.3	-5.3	-0.2	4.3	-4.3	-0.4	4.7	-2.4	-0.3
08/08/2007	94.48	1.0	1.7	-0.2	0.8	2.0	-0.1	0.7	1.8	-0.5	1.3	1.1	-0.9	1.8	1.5	-1.0
05/02/2008	97.91	1.8	-5.0	-0.6	2.1	-4.1	-0.4	2.1	-3.3	-0.2	3.0	-2.8	-0.6	3.7	-1.3	-0.6
06/08/2008	94.48	0.1	1.1	0.2	0.0	1.2	0.5	0.0	1.0	0.1	0.8	0.3	-0.3	1.4	0.7	-0.5
			37			38										

PRECISE ENGINEERING SURVEYS

DEFORMATION DISPLACEMENTS

WOLWEDANS DAM

Ref: 07/08/1992

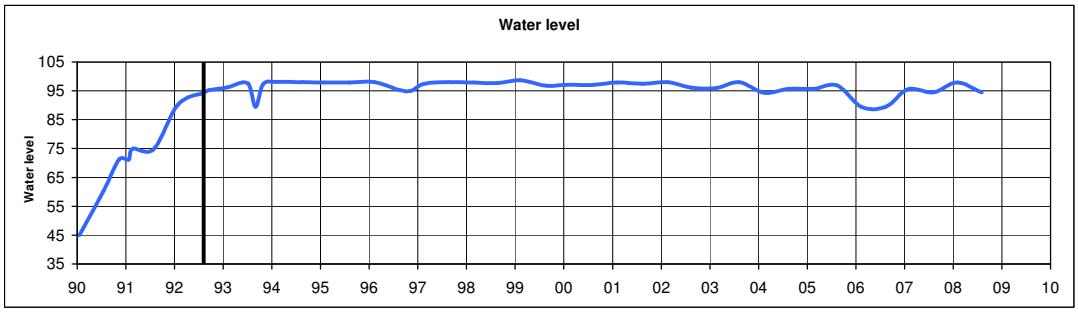

Date	Water Level	224			225		
		dy	dx	dz	dy	dx	dz
17/01/1990	45.03	#N/A	#N/A	#N/A	#N/A	#N/A	#N/A
18/07/1990	60.30	#N/A	#N/A	#N/A	#N/A	#N/A	#N/A
13/11/1990	71.28	#N/A	#N/A	#N/A	#N/A	#N/A	#N/A
22/01/1991	71.15	#N/A	#N/A	#N/A	#N/A	#N/A	#N/A
21/02/1991	74.97	#N/A	#N/A	#N/A	#N/A	#N/A	#N/A
30/07/1991	74.87	#N/A	#N/A	#N/A	#N/A	#N/A	#N/A
29/01/1992	90.27	#N/A	#N/A	#N/A	#N/A	#N/A	#N/A
07/08/1992	94.30	0.0	0.0	0.0	0.0	0.0	0.0
17/09/1992	95.23	-0.3	0.3	-0.1	-0.6	0.3	-0.2
03/02/1993	96.22	2.2	0.1	-0.4	0.7	0.5	-0.7
03/07/1993	97.69	0.9	0.7	-1.5	0.0	0.4	-1.6
31/08/1993	89.47	0.5	0.7	-0.6	-0.2	0.8	-0.6
29/10/1993	97.39	1.1	0.2	0.5	0.3	-0.1	0.6
09/02/1994	98.07	1.4	0.7	-0.6	0.3	1.1	-0.8
24/08/1994	98.04	1.0	1.0	-0.4	0.7	0.5	-0.3
01/02/1995	97.93	3.1	0.2	0.3	2.2	0.8	0.1
09/08/1995	97.90	3.1	0.2	0.3	2.2	0.8	0.1
13/02/1996	98.02	2.3	-0.2	-0.6	1.3	0.2	-1.0
21/08/1996	95.22	0.0	1.3	-0.9	-0.2	0.7	-0.9
12/11/1996	95.05	1.1	0.5	-0.7	0.3	0.3	-0.8
18/02/1997	97.43	0.1	-0.5	-0.4	-1.0	-0.1	-0.6
19/08/1997	98.00	-0.9	0.2	-0.2	-1.4	-0.4	-0.2
26/02/1998	97.92	#N/A	#N/A	-0.3	#N/A	#N/A	-0.8
19/08/1998	97.71	0.1	1.4	0.3	-0.3	0.7	0.2
10/02/1999	98.64	2.9	0.4	-0.2	2.0	1.0	-0.7
25/08/1999	96.75	2.5	1.9	-0.3	1.9	1.6	-0.2
02/02/2000	97.11	3.1	-0.5	-1.4	2.1	0.0	-1.8
02/08/2000	96.99	1.2	1.4	0.4	0.8	0.7	0.4
08/02/2001	97.93	3.0	0.0	-0.3	2.0	0.4	-0.8
15/08/2001	97.44	1.3	1.5	-0.8	0.6	0.7	-0.8
20/02/2002	97.99	3.2	0.7	-1.9	2.2	0.9	-2.3
15/08/2002	96.18	1.0	1.3	-0.7	0.4	0.6	-0.9
13/02/2003	95.93	3.2	-1.2	-1.3	1.9	-0.5	-1.8
13/08/2003	98.00	1.5	1.6	-0.4	1.0	0.9	-0.6
18/02/2004	94.30	2.9	-1.4	-0.1	1.9	-0.8	-0.6
18/08/2004	95.69	2.1	0.2	-1.0	1.8	0.0	-0.9
23/02/2005	95.69	3.4	-1.0	-0.6	2.4	-0.5	-1.1
17/08/2005	96.85	1.6	0.4	-1.7	1.0	-0.2	-1.7
15/02/2006	89.48	4.3	-2.2	-1.4	3.2	-1.4	-1.7
16/08/2006	89.48	1.4	1.2	-0.5	1.0	0.7	-0.5
01/02/2007	95.60	4.1	-1.0	-0.3	3.1	-0.1	-0.7
08/08/2007	94.48	1.3	1.2	-1.2	0.9	0.8	-1.5
05/02/2008	97.91	3.6	-0.1	-0.7	2.5	0.3	-1.1
06/08/2008	94.48	0.9	0.6	-0.7	0.6	0.2	-0.8

PRECISE ENGINEERING SURVEYS

DEFORMATION DISPLACEMENTS

WOLWEDANS DAM

Ref: 07/08/1992

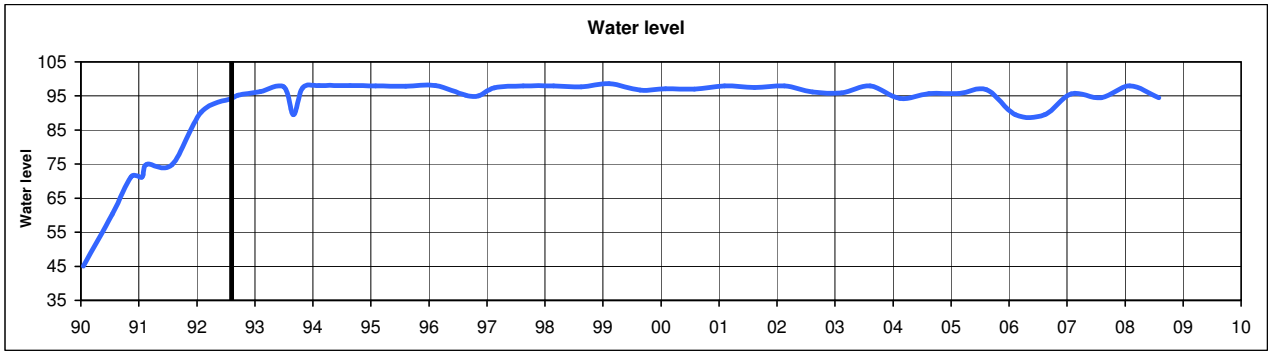

Date	Water Level	301			302			304			305			306		
		dy	dx	dz	dy	dx	dz	dy	dx	dz	dy	dx	dz	dy	dx	dz
17/01/90	45.03	#N/A	#N/A	#N/A	#N/A	#N/A	#N/A	#N/A	#N/A	#N/A	#N/A	#N/A	#N/A	#N/A	#N/A	#N/A
18/07/90	60.30	#N/A	#N/A	#N/A	#N/A	#N/A	#N/A	#N/A	#N/A	#N/A	#N/A	#N/A	#N/A	#N/A	#N/A	#N/A
13/11/90	71.28	#N/A	#N/A	#N/A	#N/A	#N/A	#N/A	#N/A	#N/A	#N/A	#N/A	#N/A	#N/A	#N/A	#N/A	#N/A
22/01/91	71.15	#N/A	#N/A	#N/A	#N/A	#N/A	#N/A	#N/A	#N/A	#N/A	#N/A	#N/A	#N/A	#N/A	#N/A	#N/A
21/02/91	74.97	#N/A	#N/A	#N/A	#N/A	#N/A	#N/A	#N/A	#N/A	#N/A	#N/A	#N/A	#N/A	#N/A	#N/A	#N/A
30/07/91	74.87	#N/A	#N/A	#N/A	#N/A	#N/A	#N/A	#N/A	#N/A	#N/A	#N/A	#N/A	#N/A	#N/A	#N/A	#N/A
29/01/92	90.27	#N/A	#N/A	#N/A	#N/A	#N/A	#N/A	#N/A	#N/A	#N/A	#N/A	#N/A	#N/A	#N/A	#N/A	#N/A
07/08/92	94.30	0.0	0.0	0.0	0.0	0.0	0.0	0.0	0.0	0.0	0.0	0.0	0.0	0.0	0.0	0.0
17/09/92	95.23	-0.7	0.7	0.7	-0.6	0.6	0.7	-0.4	0.3	0.7	-0.2	0.2	0.8	-0.1	-0.1	0.4
03/02/93	96.22	0.1	1.9	-0.5	0.1	1.8	-1.6	0.0	1.4	-1.6	0.0	1.5	-1.4	0.1	1.0	-1.0
03/07/93	97.69	0.2	-0.4	-0.4	0.2	-0.4	-0.9	0.2	-0.6	-0.8	0.0	-0.6	-0.7	0.2	-0.8	-0.7
31/08/93	89.47	-0.4	-1.3	0.8	-0.2	-1.2	0.4	-0.2	-1.1	0.3	0.0	-0.7	0.6	0.2	-0.8	0.5
29/10/93	97.39	0.9	1.7	1.7	0.7	1.5	1.5	0.5	1.2	1.4	0.3	0.9	1.5	0.3	0.5	1.3
09/02/94	98.07	0.2	2.8	0.4	0.3	2.7	0.1	0.0	2.2	0.1	-0.1	1.9	0.3	-0.3	1.6	0.2
24/08/94	98.04	-1.4	0.9	-0.2	-1.0	0.8	-0.9	-1.1	0.4	-0.8	-1.0	0.3	-0.7	-0.9	-0.1	-0.5
01/02/95	97.93	0.2	1.7	-0.3	0.1	1.4	-0.9	-0.1	0.8	-0.6	0.1	0.5	-0.4	0.2	0.0	-0.2
09/08/95	97.90	0.2	1.7	-0.3	0.1	1.4	-0.9	-0.1	0.8	-0.6	0.1	0.5	-0.4	0.2	0.0	-0.2
13/02/96	98.02	-0.5	4.9	-1.6	-0.9	4.3	-2.4	-1.0	3.8	-2.2	-1.2	3.4	-1.9	-1.1	2.7	-1.7
21/08/96	95.22	-4.0	2.0	-0.3	-3.5	2.0	-0.9	-3.4	1.5	-1.0	-3.1	1.4	-0.9	-2.9	0.9	-0.8
12/11/96	95.05	-2.0	2.7	0.3	-2.0	2.5	-0.4	-1.9	2.1	-0.6	-1.8	1.8	-0.5	-1.8	1.2	-0.5
18/02/97	97.43	-0.9	1.7	0.4	-1.3	1.6	-0.5	-1.4	1.1	-0.5	-1.4	0.9	-0.5	-1.3	0.3	-0.2
19/08/97	98.00	-3.1	3.6	1.0	-3.1	3.2	0.6	-3.2	2.7	0.5	-3.1	2.2	0.6	-3.1	1.4	0.4
26/02/98	97.92	#N/A	#N/A	2.1	#N/A	#N/A	3.4	#N/A	#N/A	3.3	#N/A	#N/A	3.4	#N/A	#N/A	1.7
19/08/98	97.71	-1.6	3.4	1.4	-1.4	3.1	0.0	-1.4	2.5	-0.1	-1.4	2.0	-0.1	-1.4	1.3	0.5
10/02/99	98.64	-1.3	3.0	-0.6	-1.3	2.6	-1.2	-1.2	2.1	-1.2	-0.9	1.8	-1.1	-0.6	1.2	-1.2
25/08/99	96.75	0.5	0.4	1.6	0.5	0.2	0.6	0.3	0.1	0.5	0.4	0.1	0.5	0.4	-0.4	0.9
02/02/00	97.11	0.1	3.3	-1.4	-0.1	3.1	-2.5	-0.2	2.7	-2.7	-0.1	2.4	-2.7	-0.1	1.7	-2.2
02/08/00	96.99	-0.6	4.3	1.2	-0.7	3.9	0.2	-0.8	3.4	0.1	-0.8	3.1	0.2	-0.6	2.2	0.7
08/02/01	97.93	-0.9	4.1	0.4	-1.1	3.6	-0.6	-1.1	3.1	-0.7	-1.0	2.7	-0.8	-0.7	1.8	-0.4
15/08/01	97.44	1.5	3.4	-0.2	1.3	3.1	-1.1	0.9	2.7	-1.1	0.8	2.4	-1.0	0.8	1.7	-0.5
20/02/02	97.99	1.3	3.6	-1.7	1.1	3.4	-2.7	0.7	3.0	-2.8	0.6	2.8	-2.8	0.8	2.1	-2.3
15/08/02	96.18	-1.3	3.0	0.3	-1.2	2.8	-0.6	-1.3	2.3	-0.7	-1.1	2.0	-0.7	-0.8	1.2	-0.2
13/02/03	95.93	1.8	4.8	-1.3	1.4	4.5	-2.3	1.0	4.0	-2.4	0.7	3.6	-2.3	0.7	2.8	-1.8
13/08/03	98.00	0.4	3.1	-0.2	0.3	2.9	-1.2	0.1	2.5	-1.3	0.1	2.1	-1.3	0.3	1.4	-0.7
18/02/04	94.30	-0.5	0.0	0.3	-0.6	-0.1	-0.7	-0.5	-0.4	-0.8	-0.4	-0.4	-0.7	-0.2	-0.9	-0.3
18/08/04	95.69	-1.8	1.0	-0.5	-1.7	0.7	-1.5	-1.6	0.1	-1.5	-1.2	-0.3	-1.4	-0.7	-1.1	-1.0
23/02/05	95.69	0.5	1.7	-0.7	0.3	1.5	-1.7	0.1	1.1	-1.8	0.3	0.7	-1.7	0.4	0.1	-1.3
17/08/05	96.85	-1.6	2.2	-0.6	-1.9	2.3	-1.6	-1.9	1.5	-1.8	-1.5	0.9	-1.8	-1.2	-0.1	-1.4
15/02/06	89.48	-0.5	-0.2	-1.1	-0.5	-0.1	-2.2	-0.4	-0.4	-2.3	-0.1	-0.6	-2.3	0.3	-1.2	-1.8
16/08/06	89.48	2.1	0.6	0.0	1.8	0.8	-1.0	1.6	0.6	-1.1	1.6	0.3	-1.1	1.7	-0.5	-0.7
01/02/07	95.60	1.1	-0.4	0.1	1.0	-0.3	-0.9	1.2	-0.5	-1.0	1.3	-0.7	-1.0	1.6	-1.4	-0.6
08/08/07	94.48	0.9	0.9	0.2	0.7	1.1	-0.8	0.6	0.6	-0.9	0.7	0.4	-0.9	0.8	-0.3	-0.4
05/02/08	97.91	0.0	0.8	-1.2	0.0	0.8	-2.3	-0.1	0.3	-2.4	0.2	0.0	-2.4	0.5	-0.8	-2.0
06/08/08	94.48	1.3	1.4	0.6	1.0	1.5	-0.5	1.0	1.1	-0.6	1.0	0.8	-0.6	1.0	0.2	-0.1

PRECISE ENGINEERING SURVEYS

DEFORMATION DISPLACEMENTS

WOLWEDANS DAM

Ref: 07/08/1992

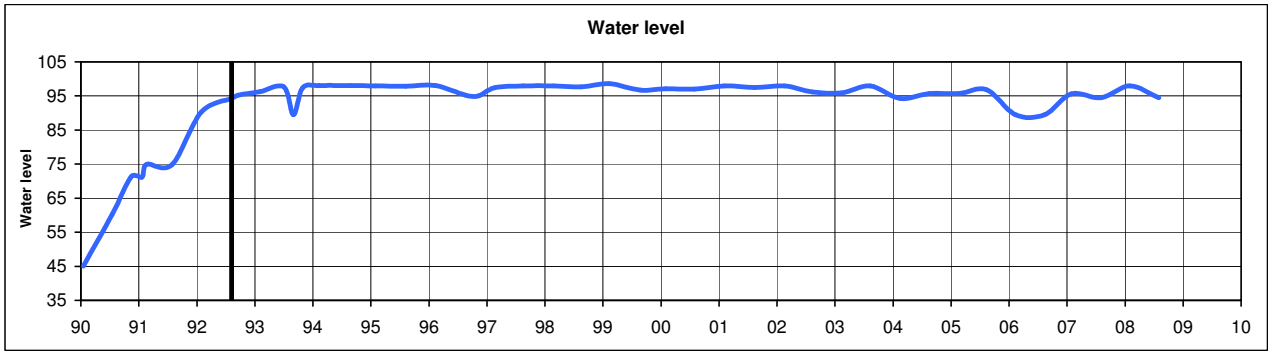

Date	Water Level	307			308			310			311			312		
		dy	dx	dz	dy	dx	dz	dy	dx	dz	dy	dx	dz	dy	dx	dz
17/01/1990	45.03	#N/A	#N/A	#N/A	#N/A	#N/A	#N/A	#N/A	#N/A	#N/A	#N/A	#N/A	#N/A	#N/A	#N/A	#N/A
18/07/1990	60.30	#N/A	#N/A	#N/A	#N/A	#N/A	#N/A	#N/A	#N/A	#N/A	#N/A	#N/A	#N/A	#N/A	#N/A	#N/A
13/11/1990	71.28	#N/A	#N/A	#N/A	#N/A	#N/A	#N/A	#N/A	#N/A	#N/A	#N/A	#N/A	#N/A	#N/A	#N/A	#N/A
22/01/1991	71.15	#N/A	#N/A	#N/A	#N/A	#N/A	#N/A	#N/A	#N/A	#N/A	#N/A	#N/A	#N/A	#N/A	#N/A	#N/A
21/02/1991	74.97	#N/A	#N/A	#N/A	#N/A	#N/A	#N/A	#N/A	#N/A	#N/A	#N/A	#N/A	#N/A	#N/A	#N/A	#N/A
30/07/1991	74.87	#N/A	#N/A	#N/A	#N/A	#N/A	#N/A	#N/A	#N/A	#N/A	#N/A	#N/A	#N/A	#N/A	#N/A	#N/A
29/01/1992	90.27	#N/A	#N/A	#N/A	#N/A	#N/A	#N/A	#N/A	#N/A	#N/A	#N/A	#N/A	#N/A	#N/A	#N/A	#N/A
07/08/1992	94.30	0.0	0.0	0.0	0.0	0.0	0.0	0.0	0.0	0.0	0.0	0.0	0.0	0.0	0.0	0.0
17/09/1992	95.23	0.1	-0.2	0.7	0.0	-0.3	0.5	0.3	-0.1	0.9	0.5	-0.1	0.5	0.6	-0.1	0.6
03/02/1993	96.22	0.1	1.0	-1.4	0.1	0.7	-0.8	0.3	0.6	-0.9	0.5	0.4	-0.8	0.4	0.0	-0.6
03/07/1993	97.69	0.3	-0.6	-0.6	0.4	-0.7	-0.4	0.7	-0.4	-0.3	0.9	-0.5	-0.2	0.9	-0.5	0.0
31/08/1993	89.47	0.4	-0.6	0.4	0.5	-0.6	0.4	0.7	-0.3	0.2	0.8	-0.3	0.3	0.6	-0.3	0.4
29/10/1993	97.39	0.4	0.4	1.5	0.0	0.1	1.4	0.1	0.3	1.3	-0.3	-0.1	1.5	-0.1	-0.6	1.5
09/02/1994	98.07	-0.3	1.3	0.2	-0.6	1.0	0.1	-0.7	0.9	-0.1	-1.1	0.3	0.3	-0.9	-0.4	0.0
24/08/1994	98.04	-0.5	-0.3	-0.8	-0.4	-0.4	-0.6	0.0	-0.3	-1.0	-0.5	-0.6	-0.5	-0.1	-0.8	-0.8
01/02/1995	97.93	0.4	-0.3	-0.5	0.4	-0.7	-0.4	0.7	-0.4	-1.0	0.1	-1.2	-0.7	0.4	-1.7	-0.6
09/08/1995	97.90	0.4	-0.3	-0.5	0.4	-0.7	-0.4	0.7	-0.4	-1.0	0.1	-1.2	-0.7	0.4	-1.7	-0.6
13/02/1996	98.02	-1.1	2.3	-1.9	-1.3	1.6	-1.7	-1.4	1.2	-2.0	-1.5	0.4	-1.8	-1.1	-0.4	-1.9
21/08/1996	95.22	-2.4	0.9	-1.1	-2.4	0.7	-0.9	-1.9	1.3	-0.9	-2.3	0.5	-0.6	-1.8	0.3	-1.0
12/11/1996	95.05	-1.6	1.1	-0.7	-1.8	0.8	-0.7	-1.4	1.2	-1.5	-1.8	0.5	-0.9	-1.4	0.0	-0.9
18/02/1997	97.43	-1.5	0.4	-0.6	-1.7	0.0	-0.5	-1.9	0.4	-0.7	-2.3	-0.4	-0.3	-2.3	-1.0	-0.7
19/08/1997	98.00	-2.8	1.1	0.3	-3.0	0.6	0.0	-2.7	0.8	0.5	-3.2	-0.1	0.6	-2.7	-0.7	0.2
26/02/1998	97.92	#N/A	#N/A	3.2	#N/A	#N/A	1.3	#N/A	#N/A	2.9	#N/A	#N/A	1.6	#N/A	#N/A	0.0
19/08/1998	97.71	-1.3	1.2	-0.3	-1.6	0.8	0.5	-1.4	0.9	0.6	-1.7	0.3	1.0	-1.3	-0.2	0.7
10/02/1999	98.64	-0.4	1.1	-1.3	-0.6	0.8	-1.4	-0.4	1.2	-1.4	-0.8	0.1	-1.2	-0.3	-0.6	-1.2
25/08/1999	96.75	0.6	-0.3	0.3	0.3	-0.4	0.8	0.5	0.2	0.3	0.1	-0.7	1.0	0.6	-0.9	0.7
02/02/2000	97.11	0.0	1.6	-2.8	-0.4	1.1	-2.3	-0.2	1.3	-2.9	-0.6	0.0	-2.2	-0.2	-0.8	-2.3
02/08/2000	96.99	-0.6	2.2	0.1	-0.9	1.8	0.6	-0.6	2.1	0.3	-1.0	1.0	1.0	-0.6	0.5	0.2
08/02/2001	97.93	-0.7	1.7	-1.0	-1.0	1.2	-0.6	-0.7	1.5	-1.1	-1.1	0.3	-0.5	-0.6	-0.5	-0.8
15/08/2001	97.44	0.8	1.6	-0.9	0.3	1.2	-0.5	0.4	1.7	-0.8	-0.2	0.7	-0.1	0.3	0.1	-0.3
20/02/2002	97.99	0.6	1.9	-2.9	0.3	1.5	-2.4	0.4	2.0	-2.9	-0.2	0.9	-2.2	0.3	0.2	-2.3
15/08/2002	96.18	-0.7	1.2	-0.9	-0.9	0.9	-0.3	-0.4	1.3	-0.5	-0.8	0.3	0.3	-0.4	0.0	-0.1
13/02/2003	95.93	0.4	2.5	-2.4	-0.1	2.0	-1.9	-0.1	2.2	-2.6	-0.8	0.8	-1.9	-0.5	-0.1	-2.2
13/08/2003	98.00	0.4	1.3	-1.3	0.0	1.1	-0.7	0.4	1.6	-1.0	-0.2	0.7	-0.2	0.2	0.2	-0.3
18/02/2004	94.30	-0.2	-0.9	-0.9	-0.5	-1.2	-0.5	-0.2	-0.7	-1.1	-0.6	-1.7	-0.5	-0.3	-2.4	-0.6
18/08/2004	95.69	-0.5	-1.0	-1.6	-0.6	-1.3	-1.0	0.0	-0.7	-1.4	-0.5	-1.6	-0.8	0.0	-2.1	-1.0
23/02/2005	95.69	0.5	-0.1	-1.8	-0.3	-0.2	-1.3	0.0	0.3	-1.8	-0.5	-0.9	-1.2	-0.1	-1.6	-1.3
17/08/2005	96.85	-0.8	-0.3	-2.0	-0.8	-0.9	-1.6	-0.1	-0.6	-1.9	-0.1	-1.7	-1.3	0.0	-1.9	-1.6
15/02/2006	89.48	0.5	-1.2	-2.4	0.3	-1.5	-2.0	0.5	-1.1	-2.7	0.1	-2.1	-2.1	0.3	-2.7	-2.3
16/08/2006	89.48	1.6	-0.5	-1.3	1.2	-0.7	-0.8	1.4	-0.1	-1.0	0.9	-1.0	-0.4	0.9	-1.4	-0.6
01/02/2007	95.60	1.6	-1.3	-1.2	1.3	-1.7	-0.8	1.5	-1.1	-1.4	0.9	-2.1	-0.8	1.2	-2.6	-1.1
08/08/2007	94.48	0.8	-0.4	-1.2	0.4	-0.6	-0.7	0.7	0.1	-1.1	0.1	-0.9	-0.5	0.2	-1.2	-0.8
05/02/2008	97.91	0.6	-1.0	-2.7	0.5	-1.3	-2.2	0.9	-0.7	-2.7	0.5	-1.7	-2.1	0.8	-2.0	-2.1
06/08/2008	94.48	0.9	0.2	-0.7	0.5	-0.1	-0.2	0.8	0.5	-0.6	0.1	-0.4	0.1	0.2	-0.7	-0.6

PRECISE ENGINEERING SURVEYS

DEFORMATION DISPLACEMENTS

WOLWEDANS DAM

Ref: 07/08/1992

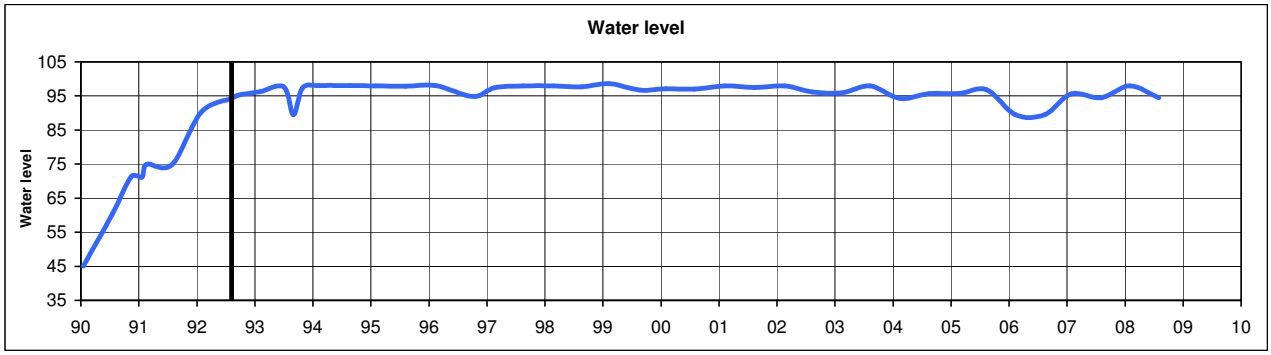

Date	Water Level	50 E313			51 314			52 315			53 316			54 317		
		dy	dx	dz	dy	dx	dz	dy	dx	dz	dy	dx	dz	dy	dx	dz
17/01/1990	45.03	#N/A	#N/A	#N/A	#N/A	#N/A	#N/A	#N/A	#N/A	#N/A	#N/A	#N/A	#N/A	#N/A	#N/A	#N/A
18/07/1990	60.30	#N/A	#N/A	#N/A	#N/A	#N/A	#N/A	#N/A	#N/A	#N/A	#N/A	#N/A	#N/A	#N/A	#N/A	#N/A
13/11/1990	71.28	#N/A	#N/A	#N/A	#N/A	#N/A	#N/A	#N/A	#N/A	#N/A	#N/A	#N/A	#N/A	#N/A	#N/A	#N/A
22/01/1991	71.15	#N/A	#N/A	#N/A	#N/A	#N/A	#N/A	#N/A	#N/A	#N/A	#N/A	#N/A	#N/A	#N/A	#N/A	#N/A
21/02/1991	74.97	#N/A	#N/A	#N/A	#N/A	#N/A	#N/A	#N/A	#N/A	#N/A	#N/A	#N/A	#N/A	#N/A	#N/A	#N/A
30/07/1991	74.87	#N/A	#N/A	#N/A	#N/A	#N/A	#N/A	#N/A	#N/A	#N/A	#N/A	#N/A	#N/A	#N/A	#N/A	#N/A
29/01/1992	90.27	#N/A	#N/A	#N/A	#N/A	#N/A	#N/A	#N/A	#N/A	#N/A	#N/A	#N/A	#N/A	#N/A	#N/A	#N/A
07/08/1992	94.30	0.0	0.0	0.0	0.0	0.0	0.0	0.0	0.0	0.0	0.0	0.0	0.0	0.0	0.0	0.0
17/09/1992	95.23	0.2	0.1	0.5	-0.1	0.3	0.9	0.2	0.3	1.1	0.5	0.4	0.7	0.4	0.4	0.7
03/02/1993	96.22	0.3	0.1	-0.4	0.1	0.2	-0.4	0.3	0.1	-0.6	0.4	0.0	-0.4	0.6	-0.1	-0.4
03/07/1993	97.69	0.8	-0.3	-0.1	0.7	-0.3	0.2	0.9	-0.1	-0.2	0.9	0.0	-0.2	0.8	0.1	-0.3
31/08/1993	89.47	0.5	-0.1	0.3	0.5	0.0	0.5	0.7	0.2	0.2	0.5	0.2	0.3	0.5	0.2	0.3
29/10/1993	97.39	0.4	-0.6	1.3	0.5	-0.4	1.5	0.3	-0.5	1.3	1.3	-0.8	1.1	0.6	-0.6	1.2
09/02/1994	98.07	-0.7	-0.3	0.3	-0.5	0.0	0.2	-0.6	-0.2	-0.3	0.5	-0.5	-0.2	0.0	-0.3	-0.3
24/08/1994	98.04	0.2	-1.2	-0.9	-0.1	-0.4	-0.3	-0.1	-0.5	-0.7	1.0	-0.8	-0.6	0.6	-0.7	-0.6
01/02/1995	97.93	1.0	-1.6	-0.7	0.8	-1.0	-0.5	0.9	-1.3	-0.8	2.0	-1.4	-1.0	1.6	-1.2	-0.9
09/08/1995	97.90	1.0	-1.6	-0.7	0.8	-1.0	-0.5	0.9	-1.3	-0.8	2.0	-1.4	-1.0	1.6	-1.2	-0.9
13/02/1996	98.02	-0.6	-0.2	-2.1	-1.0	0.0	-1.9	-0.8	0.0	-2.1	0.5	-0.8	-2.2	0.2	-0.7	-2.1
21/08/1996	95.22	-1.1	0.2	-1.2	-1.6	0.5	-0.8	-1.5	0.3	-0.9	-0.2	-0.1	-1.1	-0.4	0.1	-1.2
12/11/1996	95.05	-0.7	0.0	-1.2	-1.1	0.2	-0.8	-1.2	0.0	-1.1	0.0	-0.4	-1.2	-0.3	-0.3	-1.3
18/02/1997	97.43	-1.4	-1.3	-1.1	-1.8	-0.5	-0.8	-2.1	-0.7	-1.0	-0.9	-1.0	-1.1	-1.4	-0.9	-1.1
19/08/1997	98.00	-2.2	-0.7	0.0	-2.7	-0.5	0.4	-2.7	-0.5	0.5	-1.4	-1.2	-0.1	-1.7	-1.0	-0.3
26/02/1998	97.92	#N/A	#N/A	0.7	#N/A	#N/A	0.9	#N/A	#N/A	2.8	#N/A	#N/A	0.9	#N/A	#N/A	1.1
19/08/1998	97.71	-0.6	-0.2	0.8	-1.3	0.0	1.0	-1.3	-0.2	0.7	-0.1	-0.6	0.5	-0.5	-0.5	0.3
10/02/1999	98.64	-0.1	-0.7	-1.0	-0.5	0.3	-0.9	-0.4	0.1	-1.0	1.0	-0.2	-1.5	0.7	-0.1	-1.3
25/08/1999	96.75	1.2	-1.1	0.3	1.1	-0.4	0.6	1.2	-0.5	-0.4	2.3	-0.7	-0.1	1.9	-0.4	-0.3
02/02/2000	97.11	0.1	-0.8	-2.3	-0.2	-0.4	-2.3	-0.1	-0.6	-3.1	1.1	-1.1	-2.6	0.6	-1.1	-2.5
02/08/2000	96.99	-0.5	0.4	0.4	-0.8	0.8	0.5	-0.7	0.3	-0.3	0.4	-0.1	0.0	0.2	-0.1	-0.2
08/02/2001	97.93	-0.5	-0.6	-0.6	-0.9	0.0	-0.8	-0.6	-0.4	-1.8	0.8	-0.8	-1.4	0.6	-0.7	-1.7
15/08/2001	97.44	0.4	0.1	-0.3	-0.1	0.4	0.0	-0.2	0.1	-0.8	1.0	-0.3	-0.4	0.6	-0.2	-0.5
20/02/2002	97.99	0.4	0.2	-2.3	0.1	0.6	-2.2	0.3	0.1	-3.0	1.5	-0.3	-2.6	1.4	-0.3	-2.8
15/08/2002	96.18	-0.4	0.0	0.0	-0.7	0.2	0.1	-0.4	0.1	-0.9	0.8	-0.3	-0.5	0.4	-0.1	-0.8
13/02/2003	95.93	0.1	-0.1	-2.3	-0.5	0.2	-2.4	-0.4	-0.5	-3.2	1.0	-1.1	-2.8	0.9	-1.2	-2.8
13/08/2003	98.00	0.7	0.1	-0.5	0.2	0.3	-0.3	0.1	0.0	-1.0	1.1	-0.4	-0.4	0.7	-0.3	-0.4
18/02/2004	94.30	0.6	-2.3	-0.8	0.1	-1.8	-0.6	0.3	-2.0	-1.4	1.4	-2.3	-0.9	1.0	-2.2	-1.0
18/08/2004	95.69	0.4	-2.2	-1.1	-0.3	-1.7	-0.8	0.1	-1.9	-1.6	1.5	-2.3	-1.0	1.2	-2.0	-1.1
23/02/2005	95.69	-0.1	-1.4	-1.5	-0.2	-1.2	-1.3	-0.1	-1.6	-2.2	1.3	-2.0	-1.7	1.0	-1.9	-1.8
17/08/2005	96.85	-0.4	-1.9	-1.3	-0.7	-1.6	-1.0	-0.2	-1.8	-1.7	1.2	-2.1	-1.2	1.2	-1.8	-1.2
15/02/2006	89.48	0.3	-2.4	-2.1	0.0	-2.1	-2.2	0.3	-2.4	-3.1	1.5	-3.0	-2.8	1.5	-2.9	-2.8
16/08/2006	89.48	0.9	-1.4	-0.4	0.6	-1.2	-0.2	0.6	-1.4	-0.9	1.7	-1.7	-0.3	1.3	-1.6	-0.4
01/02/2007	95.60	1.2	-2.4	-0.9	0.9	-2.0	-0.6	1.0	-2.1	-1.7	2.0	-2.7	-1.1	1.8	-2.6	-1.2
08/08/2007	94.48	0.2	-1.2	-0.6	-0.1	-0.9	-0.4	0.1	-0.8	-1.2	1.2	-1.1	-0.5	1.1	-0.7	-1.0
05/02/2008	97.91	0.4	-1.7	-1.8	0.2	-1.3	-1.7	0.4	-1.6	-2.6	1.7	-2.0	-2.0	1.6	-1.9	-2.1
06/08/2008	94.48	0.3	-0.8	-0.7	0.2	-0.4	-0.4	0.0	-0.5	-1.2	1.0	-0.8	-0.7	0.6	-0.6	-0.9

PRECISE ENGINEERING SURVEYS

DEFORMATION DISPLACEMENTS

WOLWEDANS DAM

Ref: 07/08/1992

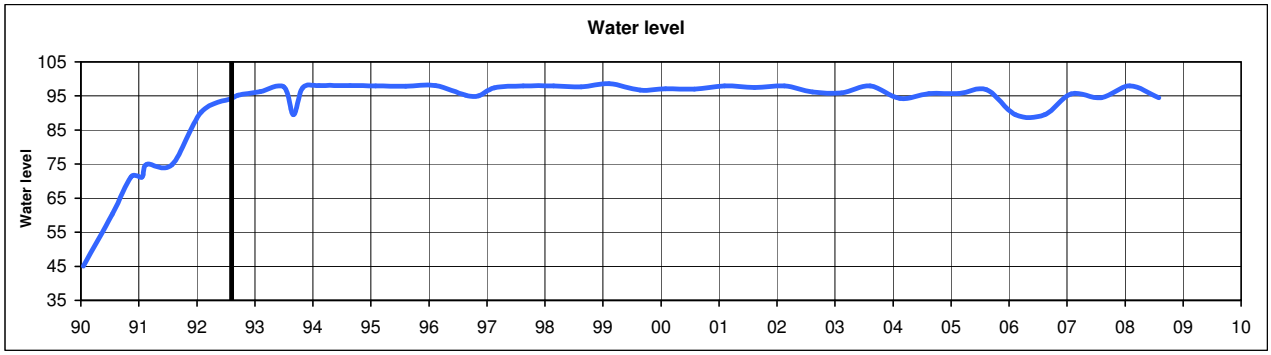

		55			56			57			58			59		
Date	Water Level	318			E319			E319.1			320			321		
		dy	dx	dz	dy	dx	dz	dy	dx	dz	dy	dx	dz	dy	dx	dz
17/01/1990	45.03	#N/A	#N/A	#N/A	#N/A	#N/A	#N/A	#N/A	#N/A	#N/A	#N/A	#N/A	#N/A	#N/A	#N/A	#N/A
18/07/1990	60.30	#N/A	#N/A	#N/A	#N/A	#N/A	#N/A	#N/A	#N/A	#N/A	#N/A	#N/A	#N/A	#N/A	#N/A	#N/A
13/11/1990	71.28	#N/A	#N/A	#N/A	#N/A	#N/A	#N/A	#N/A	#N/A	#N/A	#N/A	#N/A	#N/A	#N/A	#N/A	#N/A
22/01/1991	71.15	#N/A	#N/A	#N/A	#N/A	#N/A	#N/A	#N/A	#N/A	#N/A	#N/A	#N/A	#N/A	#N/A	#N/A	#N/A
21/02/1991	74.97	#N/A	#N/A	#N/A	#N/A	#N/A	#N/A	#N/A	#N/A	#N/A	#N/A	#N/A	#N/A	#N/A	#N/A	#N/A
30/07/1991	74.87	#N/A	#N/A	#N/A	#N/A	#N/A	#N/A	#N/A	#N/A	#N/A	#N/A	#N/A	#N/A	#N/A	#N/A	#N/A
29/01/1992	90.27	#N/A	#N/A	#N/A	#N/A	#N/A	#N/A	#N/A	#N/A	#N/A	#N/A	#N/A	#N/A	#N/A	#N/A	#N/A
07/08/1992	94.30	0.0	0.0	0.0	0.0	0.0	0.0	0.0	0.0	0.0	0.0	0.0	0.0	0.0	0.0	0.0
17/09/1992	95.23	0.3	0.6	0.6	-0.3	0.4	0.4	-0.2	0.4	0.2	-0.4	0.5	0.3	-0.5	0.4	0.6
03/02/1993	96.22	0.8	-0.1	-0.3	0.7	-0.3	-0.4	0.7	-0.3	-0.3	0.8	-0.2	-0.4	0.7	0.2	-0.4
03/07/1993	97.69	0.7	0.2	-0.5	0.6	0.1	-0.6	0.5	0.2	-0.6	0.4	0.3	-0.6	0.4	0.4	-0.7
31/08/1993	89.47	0.3	0.3	0.3	0.3	0.3	0.2	0.4	0.2	0.2	0.4	0.4	0.3	0.2	0.5	0.4
29/10/1993	97.39	0.4	-0.4	1.1	0.3	-0.5	0.9	0.2	-0.6	0.9	0.4	-0.8	0.8	0.1	-0.2	0.8
09/02/1994	98.07	-0.1	0.0	-0.7	-0.2	-0.1	-0.7	-0.1	-0.2	-0.5	0.1	-0.4	-0.7	0.0	0.4	-0.8
24/08/1994	98.04	0.5	-0.6	-0.5	0.3	-0.4	-0.5	0.5	-0.7	-0.5	0.6	-0.9	-0.4	0.5	-0.4	-0.6
01/02/1995	97.93	1.6	-0.8	-0.9	1.1	-0.6	-0.4	1.5	-1.0	-0.8	1.8	-1.1	-0.9	1.5	-0.1	-1.0
09/08/1995	97.90	1.6	-0.8	-0.9	1.1	-0.6	-0.4	1.5	-1.0	-0.8	1.8	-1.1	-0.9	1.5	-0.1	-1.0
13/02/1996	98.02	0.4	-0.5	-2.2	-0.1	-0.3	-1.7	0.4	-0.8	-2.1	0.6	-1.0	-2.1	0.4	-0.1	-2.1
21/08/1996	95.22	-0.4	0.1	-1.4	-0.6	0.3	-1.3	-0.5	-0.1	-1.3	-0.3	-0.4	-1.3	-0.4	0.0	-1.3
12/11/1996	95.05	-0.3	-0.2	-1.4	-0.4	-0.1	-1.3	-0.3	-0.3	-1.3	-0.1	-0.5	-1.2	-0.2	0.0	-1.3
18/02/1997	97.43	-1.5	-0.6	-1.4	-1.8	-0.3	-1.4	-1.7	-0.9	-1.5	-1.2	-1.0	-1.3	-1.8	-0.3	-1.4
19/08/1997	98.00	-1.7	-0.9	-0.5	-1.9	-1.2	-0.4	-1.9	-1.1	-0.4	-1.6	-1.3	-0.3	-1.8	-0.5	0.1
26/02/1998	97.92	#N/A	#N/A	1.0	#N/A	#N/A	1.0	#N/A	#N/A	0.8	#N/A	#N/A	-0.3	#N/A	#N/A	1.5
19/08/1998	97.71	-0.6	-0.3	0.1	-0.9	-0.5	0.2	-0.9	-0.3	0.2	-0.5	-0.6	0.1	-0.5	-0.1	0.1
10/02/1999	98.64	0.9	0.1	-1.5	0.5	0.3	-1.2	0.9	-0.2	-1.5	1.3	-0.4	-1.4	1.2	0.6	-1.2
25/08/1999	96.75	1.9	-0.1	-0.7	1.7	0.3	-0.8	1.8	-0.2	-0.8	1.9	-0.3	-0.6	1.8	0.5	-1.0
02/02/2000	97.11	0.8	-1.0	-2.7	0.7	-1.2	-2.6	0.9	-1.3	-2.7	1.2	-1.5	-2.5	1.1	-0.6	-2.6
02/08/2000	96.99	0.3	0.0	-0.4	0.1	-0.3	-0.2	0.2	-0.4	-0.2	0.6	-0.6	-0.1	0.5	0.0	-0.8
08/02/2001	97.93	0.7	-0.5	-2.0	0.7	-0.8	-1.9	0.7	-0.7	-1.7	1.1	-1.1	-1.9	1.2	-0.2	-2.2
15/08/2001	97.44	0.5	-0.1	-0.6	0.5	-0.3	-0.7	0.4	-0.3	-0.6	0.6	-0.5	-0.5	0.5	0.1	-0.9
20/02/2002	97.99	1.3	-0.2	-3.2	1.4	-0.3	-3.2	1.4	-0.4	-3.2	1.7	-0.7	-3.1	1.5	0.3	-3.3
15/08/2002	96.18	0.2	0.0	-1.0	0.2	-0.1	-1.1	0.1	-0.2	-0.9	0.3	-0.4	-0.9	0.1	0.1	-1.1
13/02/2003	95.93	1.0	-1.1	-3.1	0.9	-1.3	-3.1	1.0	-1.6	-2.9	1.4	-1.9	-3.0	1.2	-1.1	-3.2
13/08/2003	98.00	0.7	-0.2	-0.7	0.6	-0.3	-0.7	0.7	-0.4	-0.6	0.9	-0.6	-0.6	0.9	-0.1	-1.0
18/02/2004	94.30	1.1	-1.8	-1.1	0.9	-2.1	-1.0	0.9	-2.0	-0.9	1.3	-2.3	-1.1	1.1	-1.2	-1.3
18/08/2004	95.69	1.4	-1.8	-1.3	1.3	-1.8	-1.3	1.2	-1.9	-1.1	1.5	-2.1	-1.3	1.7	-1.3	-1.6
23/02/2005	95.69	1.2	-1.7	-2.1	0.9	-1.4	-1.9	1.2	-1.7	-1.9	1.5	-2.1	-1.9	1.4	-1.0	-2.0
17/08/2005	96.85	1.4	-1.6	-1.2	1.0	-1.9	-1.5	0.6	-1.8	-1.6	0.6	-2.0	-1.7	0.8	-1.2	-2.0
15/02/2006	89.48	1.5	-2.8	-3.1	1.5	-2.9	-3.3	1.7	-3.2	-3.0	2.1	-3.4	-2.9	1.8	-2.3	-3.1
16/08/2006	89.48	0.9	-1.4	-0.4	0.8	-1.5	-0.6	0.9	-1.2	-0.5	1.2	-1.4	-0.1	0.7	-0.7	-0.5
01/02/2007	95.60	1.8	-2.3	-1.4	1.8	-2.5	-1.6	2.0	-2.4	-1.3	2.2	-2.5	-1.0	1.8	-1.4	-1.2
08/08/2007	94.48	0.8	-0.5	-1.0	0.7	-0.5	-1.0	0.7	-0.5	-0.8	1.1	-0.7	-0.8	0.8	0.0	-1.1
05/02/2008	97.91	1.4	-1.6	-2.3	1.3	-1.8	-2.3	1.6	-1.6	-2.2	1.8	-1.9	-2.1	1.6	-0.9	-2.3
06/08/2008	94.48	0.4	-0.4	-0.8	0.3	-0.5	-0.8	0.4	-0.6	-0.7	0.6	-0.8	-0.7	0.2	-0.3	-1.0
		60			61			62			63			64		

PRECISE ENGINEERING SURVEYS

DEFORMATION DISPLACEMENTS

WOLWEDANS DAM

Ref: 07/08/1992

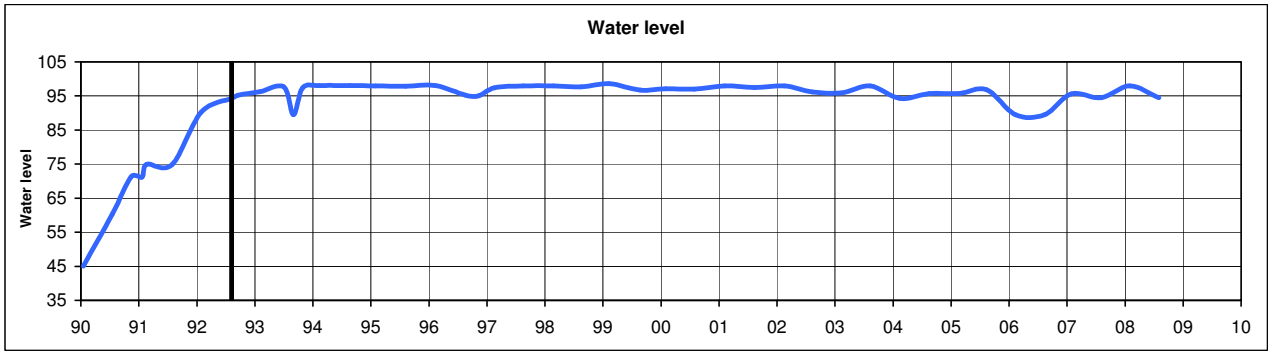

Date	Water Level	322			324			325			326			327		
		dy	dx	dz	dy	dx	dz	dy	dx	dz	dy	dx	dz	dy	dx	dz
17/01/1990	45.03	#N/A	#N/A	#N/A	#N/A	#N/A	#N/A	#N/A	#N/A	#N/A	#N/A	#N/A	#N/A	#N/A	#N/A	#N/A
18/07/1990	60.30	#N/A	#N/A	#N/A	#N/A	#N/A	#N/A	#N/A	#N/A	#N/A	#N/A	#N/A	#N/A	#N/A	#N/A	#N/A
13/11/1990	71.28	#N/A	#N/A	#N/A	#N/A	#N/A	#N/A	#N/A	#N/A	#N/A	#N/A	#N/A	#N/A	#N/A	#N/A	#N/A
22/01/1991	71.15	#N/A	#N/A	#N/A	#N/A	#N/A	#N/A	#N/A	#N/A	#N/A	#N/A	#N/A	#N/A	#N/A	#N/A	#N/A
21/02/1991	74.97	#N/A	#N/A	#N/A	#N/A	#N/A	#N/A	#N/A	#N/A	#N/A	#N/A	#N/A	#N/A	#N/A	#N/A	#N/A
30/07/1991	74.87	#N/A	#N/A	#N/A	#N/A	#N/A	#N/A	#N/A	#N/A	#N/A	#N/A	#N/A	#N/A	#N/A	#N/A	#N/A
29/01/1992	90.27	#N/A	#N/A	#N/A	#N/A	#N/A	#N/A	#N/A	#N/A	#N/A	#N/A	#N/A	#N/A	#N/A	#N/A	#N/A
07/08/1992	94.30	0.0	0.0	0.0	0.0	0.0	0.0	0.0	0.0	0.0	0.0	0.0	0.0	0.0	0.0	0.0
17/09/1992	95.23	-0.2	0.2	0.2	-0.1	0.2	0.3	-0.2	0.1	0.3	-0.2	0.3	0.7	0.0	0.1	0.3
03/02/1993	96.22	0.6	0.4	-0.2	0.6	0.9	-0.1	0.7	1.3	-0.1	0.6	1.9	-0.6	0.6	2.2	-0.2
03/07/1993	97.69	0.8	0.2	-0.7	0.8	0.3	-0.6	0.7	0.3	-0.6	0.6	0.6	-0.6	0.8	0.7	-0.7
31/08/1993	89.47	0.2	0.4	0.4	0.1	0.5	0.5	-0.3	0.4	0.6	-0.5	0.7	0.6	-0.4	0.7	0.6
29/10/1993	97.39	0.3	-0.3	0.8	0.3	-0.1	0.9	0.2	-0.1	1.0	-0.1	0.1	1.2	0.0	0.3	0.9
09/02/1994	98.07	-0.1	0.5	-0.7	-0.2	0.8	-0.6	-0.2	0.9	-0.6	-0.4	1.3	-0.6	-0.3	1.4	-0.7
24/08/1994	98.04	0.7	-0.5	-0.4	0.8	-0.2	-0.3	0.7	-0.1	-0.2	0.7	0.4	-0.4	0.8	0.5	-0.2
01/02/1995	97.93	1.6	-0.2	-1.0	1.6	0.2	-0.9	1.5	0.4	-0.9	1.4	0.9	-1.1	1.4	1.2	-0.9
09/08/1995	97.90	1.6	-0.2	-1.0	1.6	0.2	-0.9	1.5	0.4	-0.9	1.4	0.9	-1.1	1.4	1.2	-0.9
19/08/1997	98.00	-1.3	-0.9	-0.4	-1.1	-0.6	-0.4	-1.0	-0.5	-0.3	-1.1	-0.1	-0.1	-0.9	0.2	-0.3
26/02/1998	97.92	#N/A	#N/A	0.1	#N/A	#N/A	0.1	#N/A	#N/A	0.1	#N/A	#N/A	1.7	#N/A	#N/A	0.0
19/08/1998	97.71	-0.2	-0.1	0.0	-0.2	0.2	0.0	-0.2	0.3	0.1	-0.4	0.8	-0.6	-0.1	1.0	0.1
10/02/1999	98.64	1.4	0.7	-1.4	1.3	1.1	-1.3	1.4	1.3	-1.3	1.2	1.8	-1.3	1.6	2.2	-1.3
25/08/1999	96.75	1.9	0.6	-0.9	1.7	1.0	-0.9	1.6	1.4	-0.9	1.9	1.0	-1.5	1.2	2.4	-0.9
02/02/2000	97.11	1.3	-0.6	-2.4	1.2	-0.1	-2.3	1.3	0.1	-2.3	2.0	-0.5	-2.9	1.4	0.8	-2.3
02/08/2000	96.99	0.7	-0.1	-0.7	0.7	0.2	-0.7	0.8	0.3	-0.8	1.3	-0.3	-1.5	0.5	0.9	-0.8
08/02/2001	97.93	1.5	-0.2	-2.1	1.6	0.4	-2.0	1.6	0.5	-2.0	2.2	0.0	-2.7	1.7	1.4	-2.1
15/08/2001	97.44	0.6	0.0	-0.9	0.5	0.2	-0.8	0.2	0.3	-0.7	0.6	-0.4	-1.4	-0.3	0.7	-0.7
20/02/2002	97.99	1.6	0.3	-3.1	1.4	0.7	-3.0	1.3	0.9	-3.0	1.6	0.4	-3.6	0.9	1.6	-3.0
15/08/2002	96.18	0.2	0.0	-1.1	0.0	0.2	-1.1	-0.3	0.3	-1.2	0.0	-0.3	-1.8	-0.8	0.9	-1.2
13/02/2003	95.93	1.4	-1.2	-2.9	1.3	-0.9	-2.9	1.2	-1.0	-2.9	2.0	-1.7	-3.6	1.6	-0.6	-2.9
13/08/2003	98.00	1.2	-0.3	-1.0	1.1	-0.1	-1.0	1.0	0.0	-0.9	1.5	-0.8	-1.5	0.8	0.4	-0.8
18/02/2004	94.30	1.2	-1.2	-1.1	0.9	-0.7	-1.0	0.8	-0.5	-1.0	1.2	-1.0	-1.6	0.5	0.4	-1.0
18/08/2004	95.69	2.0	-0.9	-1.5	1.8	-0.3	-1.5	1.8	0.3	-1.4	2.4	0.2	-2.0	1.8	2.0	-1.4
23/02/2005	95.69	1.4	-0.9	-1.8	1.2	-0.4	-1.7	1.4	0.0	-1.6	1.9	-0.3	-2.2	1.2	1.1	-1.5
17/08/2005	96.85	1.3	-0.8	-1.9	1.3	-0.1	-1.9	1.5	0.5	-1.8	2.1	0.4	-2.5	1.7	2.1	-1.8
15/02/2006	89.48	2.0	-2.4	-2.8	2.0	-1.8	-2.7	2.1	-1.7	-2.7	2.5	-2.2	-3.3	1.9	-0.9	-2.7
16/08/2006	89.48	0.9	-0.8	-0.5	0.5	-0.4	-0.5	0.4	0.1	-0.5	0.5	-0.3	-1.1	-0.3	1.1	-0.5
01/02/2007	95.60	1.9	-1.2	-1.0	1.6	-0.4	-0.9	1.6	0.1	-1.0	1.9	-0.2	-1.6	1.0	1.4	-1.1
08/08/2007	94.48	1.0	0.1	-1.0	0.9	0.6	-1.0	0.9	0.9	-1.0	1.3	0.7	-1.6	0.4	2.2	-1.0
05/02/2008	97.91	2.0	-0.8	-2.2	1.8	-0.2	-2.2	1.7	0.1	-2.2	2.2	-0.2	-2.8	1.4	1.4	-2.2
06/08/2008	94.48	0.4	-0.3	-0.8	0.3	0.0	-0.7	0.2	0.3	-0.7	0.6	-0.3	-1.3	-0.2	1.1	-0.6

PRECISE ENGINEERING SURVEYS

DEFORMATION DISPLACEMENTS

WOLWEDANS DAM

Ref: 07/08/1992

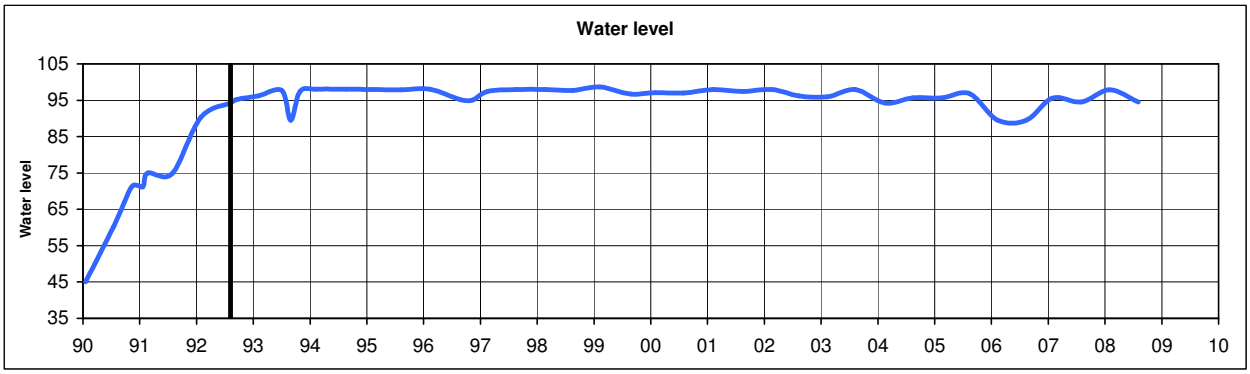

Date	Water Level	T01			T02			T03			T04			T05		
		dy	dx	dz	dy	dx	dz	dy	dx	dz	dy	dx	dz	dy	dx	dz
17/01/1990	45.03	#N/A	#N/A	#N/A	#N/A	#N/A	#N/A	#N/A	#N/A	#N/A	#N/A	#N/A	#N/A	#N/A	#N/A	#N/A
18/07/1990	60.30	#N/A	#N/A	#N/A	#N/A	#N/A	#N/A	#N/A	#N/A	#N/A	#N/A	#N/A	#N/A	#N/A	#N/A	#N/A
13/11/1990	71.28	-1.0	-1.3	2.0	#N/A	#N/A	#N/A	#N/A	#N/A	#N/A	0.8	0.1	2.1	-0.4	-0.6	1.4
22/01/1991	71.15	-1.3	-3.1	2.4	#N/A	#N/A	#N/A	#N/A	#N/A	#N/A	-0.7	0.9	3.9	-0.8	-1.7	2.8
21/02/1991	74.97	-1.1	-2.3	3.0	#N/A	#N/A	#N/A	#N/A	#N/A	#N/A	0.0	1.0	4.6	-0.8	0.0	2.5
30/07/1991	74.87	-0.9	-1.8	1.6	-0.2	-2.5	1.7	1.1	-1.8	2.7	0.4	-2.2	2.8	-1.1	-1.8	2.5
29/01/1992	90.27	0.0	-2.0	2.5	-0.1	-1.3	2.9	-0.3	-0.9	3.9	0.2	0.9	3.1	0.6	-1.8	2.2
07/08/1992	94.30	0.0	0.0	0.0	0.0	0.0	0.0	0.0	0.0	0.0	0.0	0.0	0.0	0.0	0.0	0.0
17/09/1992	95.23	0.0	0.0	0.7	-0.1	-0.1	1.4	0.0	0.1	1.2	0.0	0.1	1.1	-0.2	0.1	0.8
03/02/1993	96.22	0.1	-0.2	1.1	-0.3	0.0	1.4	0.2	0.7	1.5	0.2	2.9	1.5	0.2	0.1	0.6
03/07/1993	97.69	0.4	-1.0	0.8	-0.4	-0.7	0.7	0.3	-0.1	0.9	-0.6	-0.3	-0.5	0.2	-0.4	0.5
31/08/1993	89.47	0.2	-0.6	0.9	0.2	-0.6	1.1	1.3	-0.1	2.1	-0.1	0.3	0.8	0.3	-0.5	1.0
29/10/1993	97.39	0.1	-0.6	2.3	0.1	-0.6	1.9	1.1	-0.1	2.5	-0.1	1.4	2.1	0.1	-0.2	2.1
09/02/1994	98.07	-0.8	0.0	1.5	-1.0	0.3	2.0	-0.7	0.5	2.2	-0.7	2.7	0.6	-0.6	0.2	0.7
24/08/1994	98.04	-1.2	-0.4	-0.3	-0.9	0.1	-0.6	0.1	0.2	0.7	-1.0	-0.2	-1.0	-1.3	-0.4	-0.1
01/02/1995	97.93	-1.7	-1.9	1.0	-2.0	-1.2	1.8	-0.6	-0.6	2.9	-1.6	2.0	1.1	-1.4	-0.6	0.7
09/08/1995	97.90	-0.1	-1.4	-0.7	0.1	-1.7	-1.1	1.5	-1.0	0.0	-0.2	-1.1	-1.1	-0.5	-1.5	-0.8
13/02/1996	98.02	-2.5	-0.4	0.7	-2.6	0.0	1.8	-1.3	0.5	2.5	-2.7	2.9	1.0	-2.1	0.3	-0.1
21/08/1996	95.22	-2.0	-0.5	-0.1	-1.5	-1.1	-0.3	-0.5	0.1	0.8	-2.0	-0.5	-0.8	-2.5	0.0	0.4
12/11/1996	95.05	-2.5	-0.5	0.5	-2.5	-0.2	0.5	-1.3	0.4	1.6	-2.4	1.9	-0.6	-2.5	0.3	0.2
18/02/1997	97.43	-2.7	-1.3	0.5	-2.6	-0.7	1.1	-1.7	-0.6	2.7	-3.7	2.4	0.3	-2.3	-1.0	0.4
19/08/1997	98.00	-2.9	-0.4	0.3	-2.8	-1.2	0.7	-1.4	-0.7	0.8	-2.7	-0.6	-0.3	-3.3	-1.1	0.6
26/02/1998	97.92	-2.3	-1.2	-0.1	-2.3	-1.1	0.8	-1.5	0.0	2.0	-2.8	2.6	0.9	-2.0	-0.9	-0.5
19/08/1998	97.71	-1.5	-0.3	0.9	-1.5	-0.9	1.1	-0.1	-0.6	1.9	-1.7	-0.6	0.2	-2.0	-1.1	1.2
10/02/1999	98.64	-1.4	-1.0	0.4	-2.1	0.0	2.3	-0.5	0.0	2.4	-2.1	3.7	0.8	-1.0	-0.2	0.1
25/08/1999	96.75	-0.6	-0.4	1.6	-0.2	-0.8	0.4	1.1	-0.2	1.5	-0.8	-0.5	0.5	-1.0	-1.1	1.7
02/02/2000	97.11	-1.1	-0.6	0.0	-1.2	0.6	0.3	0.4	0.4	0.7	-1.8	3.2	-0.1	-1.2	0.2	0.1
02/08/2000	96.99	-0.5	0.1	0.9	-0.3	-0.2	0.6	0.9	0.8	1.8	-0.5	0.6	0.3	-0.8	0.1	0.9
08/02/2001	97.93	-1.0	-0.6	0.2	-1.5	0.4	0.8	-0.4	0.5	2.3	-1.7	4.1	0.6	-1.1	0.0	-0.5
15/08/2001	97.44	-0.6	0.2	1.0	-1.0	-0.2	1.5	1.1	0.8	1.7	-1.1	0.2	-0.2	-1.0	-0.1	0.6
20/02/2002	97.99	-0.2	-0.9	-0.4	-0.5	-0.2	0.4	0.8	-0.7	1.6	-0.4	3.1	-0.6	0.2	-0.7	-0.6
15/08/2002	96.18	-0.7	-0.1	1.1	-0.7	0.0	0.6	0.8	0.6	1.5	-0.7	0.2	-0.2	-1.2	0.0	1.1
13/02/2003	95.93	-0.8	-1.6	0.4	-1.3	0.2	1.2	-1.3	0.3	1.8	0.1	4.6	1.2	-1.0	0.8	0.6
13/08/2003	98.00	-0.2	0.1	0.9	0.3	-0.9	-0.3	1.6	0.5	1.1	-0.5	-0.4	-0.6	-0.6	-0.5	1.0
18/02/2004	94.30	-1.9	-0.1	1.6	-1.2	3.4	1.7	-2.5	2.2	2.1	-3.3	3.3	0.0	-0.4	-1.1	-0.7
18/08/2004	95.69	-0.8	-0.2	1.4	-0.4	-0.9	0.9	2.1	-0.4	2.9	-0.8	-0.3	0.2	-1.2	-0.9	0.6
23/02/2005	95.69	0.7	-0.9	1.8	-0.8	-0.4	1.1	0.4	0.7	2.6	-1.3	3.2	1.1	0.0	0.2	0.7
17/08/2005	96.85	-0.9	-0.4	0.3	-0.8	-0.7	0.2	-0.8	-0.6	0.0	-1.5	-1.5	-1.1	-2.2	0.5	0.3
15/02/2006	89.48	0.3	-2.6	0.4	-0.3	-1.3	1.3	1.0	-1.3	2.6	-1.1	2.0	0.9	0.0	-1.2	0.8
16/08/2006	89.48	-0.9	-0.3	-0.3	-0.6	-1.5	-0.2	0.7	-0.4	1.1	0.3	-1.1	0.2	-2.5	-0.4	-0.6
01/02/2007	95.60	0.0	-0.5	0.7	0.0	2.5	1.8	-2.3	3.6	2.2	-1.8	3.7	1.4	-0.3	0.1	0.2
08/08/2007	94.48	-0.2	0.3	0.1	0.4	-1.3	-1.2	1.8	0.3	0.7	-0.5	-0.1	-0.8	-0.5	-0.1	-0.6
05/02/2008	97.91	1.0	-1.4	0.3	0.3	1.6	0.9	-3.2	1.6	1.5	-1.8	3.0	0.5	0.3	-1.0	-0.7
06/08/2008	94.48	0.3	0.3	1.2	0.5	1.5	0.9	-0.4	4.4	2.0	-1.1	1.7	-0.2	-1.4	0.2	1.8

PRECISE ENGINEERING SURVEYS

DEFORMATION DISPLACEMENTS

WOLWEDANS DAM

Ref: 07/08/1992

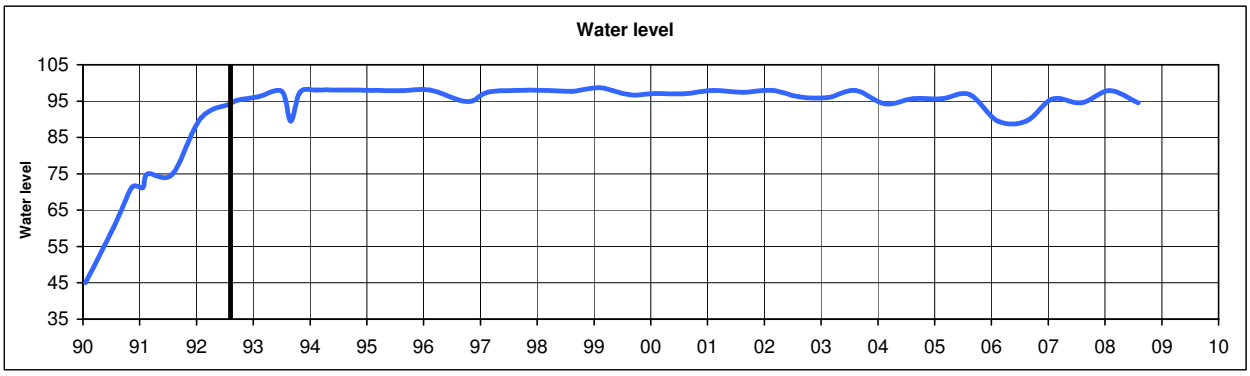

Date	Water Level	T06		
		dy	dx	dz
17/01/1990	45.03	#N/A	#N/A	#N/A
18/07/1990	60.30	#N/A	#N/A	#N/A
13/11/1990	71.28	0.4	0.6	1.5
22/01/1991	71.15	0.2	1.2	1.9
21/02/1991	74.97	-0.3	1.3	2.6
30/07/1991	74.87	-0.8	-1.1	1.8
29/01/1992	90.27	0.5	0.0	1.5
07/08/1992	94.30	0.0	0.0	0.0
17/09/1992	95.23	-0.4	0.8	1.1
03/02/1993	96.22	0.5	2.0	0.0
03/07/1993	97.69	0.1	-0.4	0.2
31/08/1993	89.47	0.2	0.2	0.8
29/10/1993	97.39	0.0	1.3	1.3
09/02/1994	98.07	-0.1	1.9	-0.5
24/08/1994	98.04	-1.0	-0.1	-0.1
01/02/1995	97.93	-1.3	1.2	0.1
09/08/1995	97.90	-0.4	-1.6	-0.5
13/02/1996	98.02	-2.0	2.0	-0.8
21/08/1996	95.22	-2.8	-0.5	1.1
12/11/1996	95.05	-1.8	1.1	-0.8
18/02/1997	97.43	-2.5	1.0	-0.6
19/08/1997	98.00	-3.4	-0.6	1.3
26/02/1998	97.92	-2.2	1.5	0.2
19/08/1998	97.71	-2.1	-1.0	1.5
10/02/1999	98.64	-0.9	2.3	0.1
25/08/1999	96.75	-1.0	-1.1	1.7
02/02/2000	97.11	-0.2	2.1	-1.3
02/08/2000	96.99	-1.7	0.7	3.1
08/02/2001	97.93	-0.2	2.1	-1.6
15/08/2001	97.44	-0.8	-0.1	0.7
20/02/2002	97.99	-0.1	2.4	-1.5
15/08/2002	96.18	-0.9	-0.2	0.9
13/02/2003	95.93	-0.5	2.7	-0.8
13/08/2003	98.00	-0.9	-1.6	0.8
18/02/2004	94.30	-1.0	0.7	-1.2
18/08/2004	95.69	-1.4	-0.4	0.4
23/02/2005	95.69	0.3	2.1	0.1
17/08/2005	96.85	-1.9	-0.6	-0.7
15/02/2006	89.48	0.6	0.9	0.0
16/08/2006	89.48	-2.2	0.8	-0.7
01/02/2007	95.60	0.1	2.0	-0.2
08/08/2007	94.48	-0.7	0.1	0.1
05/02/2008	97.91	1.1	-0.2	-1.4
06/08/2008	94.48	-1.1	-0.2	1.5

PRECISE ENGINEERING SURVEYS

DEFORMATION DISPLACEMENTS

WOLWEDANS DAM

Ref: 07/08/1992

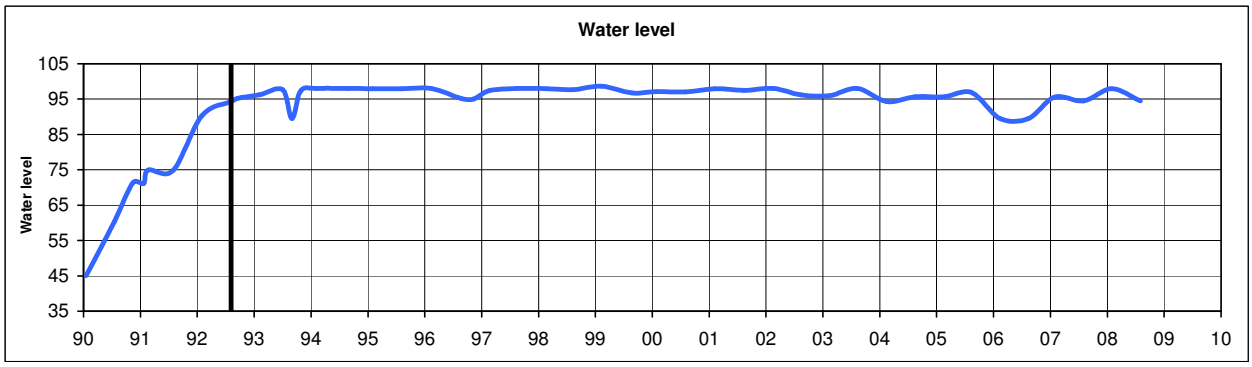

Date	Water Level	PL06		IPL06		PL12		IP12		IPL17	
		dy	dx	dy	dx	dy	dx	dy	dx	dy	dx
17/01/1990	45.03	#N/A	#N/A	#N/A	#N/A	#N/A	#N/A	#N/A	#N/A	#N/A	#N/A
18/07/1990	60.30	#N/A	#N/A	#N/A	#N/A	#N/A	#N/A	#N/A	#N/A	#N/A	#N/A
13/11/1990	71.28	#N/A	#N/A	#N/A	#N/A	#N/A	#N/A	#N/A	#N/A	#N/A	#N/A
22/01/1991	71.15	#N/A	#N/A	#N/A	#N/A	#N/A	#N/A	#N/A	#N/A	#N/A	#N/A
21/02/1991	74.97	#N/A	#N/A	#N/A	#N/A	#N/A	#N/A	#N/A	#N/A	#N/A	#N/A
30/07/1991	74.87	#N/A	#N/A	#N/A	#N/A	#N/A	#N/A	#N/A	#N/A	#N/A	#N/A
29/01/1992	90.27	#N/A	#N/A	#N/A	#N/A	#N/A	#N/A	#N/A	#N/A	#N/A	#N/A
07/08/1992	94.30	0.0	0.0	0.0	0.0	0.0	0.0	0.0	0.0	0.0	0.0
17/09/1992	95.23	0.2	-0.1	0.3	-0.2	0.8	-0.2	0.5	-0.2	0.2	0.2
03/02/1993	96.22	-3.1	-1.8	0.5	0.5	-0.2	-6.0	0.6	0.0	0.1	-0.4
03/07/1993	97.69	0.3	-0.1	0.4	-0.9	1.2	1.0	0.8	-1.0	0.6	-0.1
31/08/1993	89.47	0.4	-0.9	0.3	-0.9	0.7	-1.1	0.4	-0.8	0.6	0.1
29/10/1993	97.39	-2.8	-1.5	-0.2	0.4	-1.1	-1.5	-6.8	2.5	0.2	-0.2
09/02/1994	98.07	-5.6	-2.9	0.0	1.5	-3.2	-6.3	-8.3	4.6	-0.7	0.5
24/08/1994	98.04	-1.2	0.3	-0.4	-0.5	-1.2	2.4	-7.8	3.6	0.2	-0.2
01/02/1995	97.93	-5.6	-5.2	0.3	-0.1	-1.8	-8.0	-6.6	1.3	1.1	-0.8
09/08/1995	97.90	-5.6	-5.2	0.3	-0.1	-1.8	-8.0	-6.6	1.3	1.1	-0.8
13/02/1996	98.02	-6.4	-4.2	-1.1	2.6	-3.2	-7.4	-8.2	2.2	-0.3	-0.5
21/08/1996	95.22	-2.0	0.6	-2.7	0.8	-2.1	3.2	-9.2	3.0	-0.8	0.3
12/11/1996	95.05	-4.6	-1.6	-2.3	1.5	-2.0	-1.3	-8.9	3.2	-0.5	0.1
18/02/1997	97.43	-7.0	-3.1	-2.8	1.4	-4.6	-6.7	-9.3	2.2	-1.9	-0.6
19/08/1997	98.00	-3.4	-0.3	-3.2	1.3	-3.1	1.4	-10.1	2.0	-2.5	-1.3
26/02/1998	97.92	#N/A	#N/A	#N/A	#N/A	#N/A	#N/A	#N/A	#N/A	#N/A	#N/A
19/08/1998	97.71	-1.9	0.1	-1.9	0.9	-1.8	3.4	-6.4	3.9	-1.2	-0.5
10/02/1999	98.64	-5.7	-3.6	-0.9	0.9	-2.7	-6.8	-7.6	3.9	-0.1	-0.2
25/08/1999	96.75	-1.3	-0.2	-0.7	0.0	0.0	1.4	-6.9	3.0	1.2	0.3
02/02/2000	97.11	-6.2	-4.3	-0.7	2.1	-2.6	-7.7	-7.6	3.1	0.5	-0.7
02/08/2000	96.99	-1.3	1.2	-0.8	2.5	-1.1	2.8	-7.7	1.3	0.4	0.2
08/02/2001	97.93	-6.8	-4.6	-0.9	2.1	-2.4	-6.6	-7.8	5.3	0.6	-0.4
15/08/2001	97.44	-0.8	0.4	0.4	2.1	-0.3	2.9	-7.5	3.7	0.7	0.2
20/02/2002	97.99	-4.6	-3.6	0.4	2.4	-1.4	-5.7	-7.3	4.9	1.0	-0.3
15/08/2002	96.18	-1.5	0.3	-1.3	1.4	-0.8	2.6	-8.1	3.8	0.3	-0.3
13/02/2003	95.93	-6.4	-4.2	0.6	2.8	-2.7	-9.2	-7.9	4.4	-0.1	-1.2
13/08/2003	98.00	-0.2	0.6	-0.1	1.8	0.0	3.7	-7.7	5.4	0.6	-0.2
18/02/2004	94.30	-6.6	-4.4	-1.9	-0.1	-3.0	-9.4	-7.7	3.2	0.8	-1.8
18/08/2004	95.69	-1.1	-0.5	-1.2	-0.7	-0.8	0.8	-7.7	2.8	0.5	-2.5
23/02/2005	95.69	-5.6	-4.1	-1.2	1.1	-2.2	-8.2	-5.4	5.0	0.7	-1.8
17/08/2005	96.85	-1.8	-0.6	-1.1	0.1	-0.6	2.0	-8.6	3.1	0.8	-1.9
15/02/2006	89.48	-5.7	-5.0	-0.3	-0.6	-2.4	-10.7	-5.4	3.0	0.9	-3.1
16/08/2006	89.48	0.2	-0.5	0.5	-0.3	-0.2	2.2	-6.9	2.9	0.9	-2.0
01/02/2007	95.60	-5.6	-5.0	0.3	-0.3	-1.5	-9.9	-6.3	2.8	2.0	-2.1
08/08/2007	94.48	-0.2	-0.2	0.5	0.0	0.8	2.4	-7.7	3.4	1.1	-0.4
05/02/2008	97.91	-5.2	-5.2	0.1	-0.3	-0.7	-7.6	-6.7	2.2	1.4	-1.7
06/08/2008	94.48	-1.2	-0.3	1.0	0.5	0.0	1.4	-7.6	4.4	-0.2	-0.5

PRECISE ENGINEERING SURVEYS

DEFORMATION DISPLACEMENTS

WOLWEDANS DAM

Ref: 07/08/1992

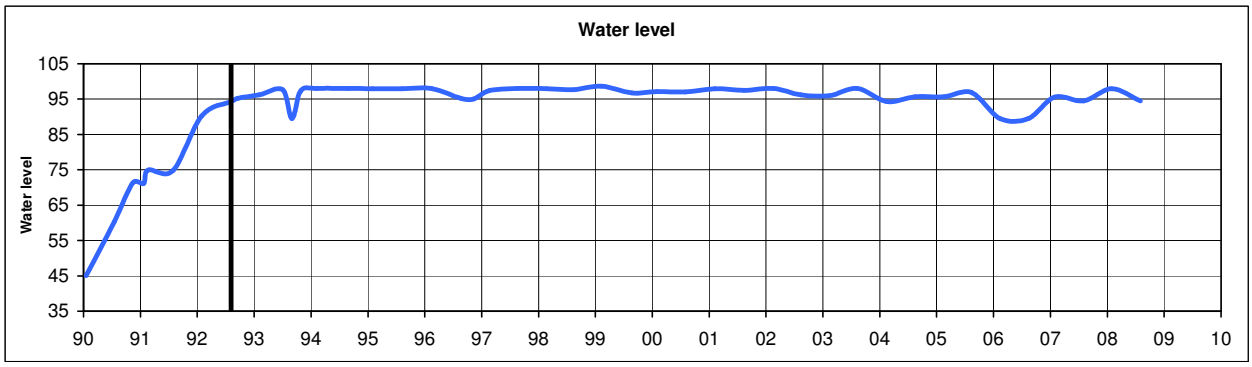

Date	Water Level	IP17		PL21		IP21		PL24	
		dy	dx	dy	dx	dy	dx	dy	dx
17/01/1990	45.03	#N/A	#N/A	#N/A	#N/A	#N/A	#N/A	#N/A	#N/A
18/07/1990	60.30	#N/A	#N/A	#N/A	#N/A	#N/A	#N/A	#N/A	#N/A
13/11/1990	71.28	#N/A	#N/A	#N/A	#N/A	#N/A	#N/A	#N/A	#N/A
22/01/1991	71.15	#N/A	#N/A	#N/A	#N/A	#N/A	#N/A	#N/A	#N/A
21/02/1991	74.97	#N/A	#N/A	#N/A	#N/A	#N/A	#N/A	#N/A	#N/A
30/07/1991	74.87	#N/A	#N/A	#N/A	#N/A	#N/A	#N/A	#N/A	#N/A
29/01/1992	90.27	#N/A	#N/A	#N/A	#N/A	#N/A	#N/A	#N/A	#N/A
07/08/1992	94.30	0.0	0.0	0.0	0.0	0.0	0.0	0.0	0.0
17/09/1992	95.23	0.6	0.2	-0.2	-0.7	-0.3	0.2	0.5	-0.2
03/02/1993	96.22	1.0	0.0	3.1	-7.4	0.1	-1.5	4.6	-3.1
03/07/1993	97.69	1.0	-0.3	0.8	1.4	-0.3	-1.6	0.9	1.1
31/08/1993	89.47	1.4	0.6	1.1	-0.8	-0.2	-1.2	0.9	0.2
29/10/1993	97.39	2.1	0.4	-1.3	-0.2	-0.9	-3.3	2.4	-3.2
09/02/1994	98.07	0.1	1.8	-0.1	-4.6	-2.7	-10.1	3.5	-4.7
24/08/1994	98.04	2.1	1.6	-1.8	5.2	-0.7	-8.2	0.5	-0.5
01/02/1995	97.93	1.8	1.0	1.8	-6.2	-0.5	-9.1	5.7	-6.2
09/08/1995	97.90	1.8	1.0	1.8	-6.2	-0.5	-9.1	5.7	-6.2
13/02/1996	98.02	-0.5	0.6	0.6	-5.8	-1.7	-10.3	4.7	-6.1
21/08/1996	95.22	-1.7	0.3	-3.1	6.5	-2.1	-9.1	-0.7	0.1
12/11/1996	95.05	-0.2	1.4	-1.9	0.1	-1.9	-9.0	2.4	-2.6
18/02/1997	97.43	-1.3	1.1	-1.9	-5.5	-3.5	-8.3	2.2	-5.6
19/08/1997	98.00	-1.7	0.8	-4.2	3.9	-3.5	-10.0	-1.2	-1.6
26/02/1998	97.92	#N/A	#N/A	#N/A	#N/A	#N/A	#N/A	#N/A	#N/A
19/08/1998	97.71	-1.2	0.5	-3.2	6.2	-2.1	-7.2	-0.3	0.2
10/02/1999	98.64	0.5	1.8	1.1	-5.8	-0.4	-5.8	5.2	-5.1
25/08/1999	96.75	2.3	1.5	-0.8	5.9	0.2	-4.8	2.2	0.6
02/02/2000	97.11	0.4	0.8	1.2	-6.0	-0.9	-7.9	5.5	-6.3
02/08/2000	96.99	0.6	2.1	-0.1	6.3	-1.1	-7.6	0.7	0.5
08/02/2001	97.93	0.8	1.6	0.5	-5.2	-0.7	-7.8	5.3	-5.1
15/08/2001	97.44	0.9	1.9	-0.6	6.4	-0.9	-5.4	0.9	0.5
20/02/2002	97.99	1.9	2.4	1.0	-3.5	-0.1	-5.5	5.3	-4.2
15/08/2002	96.18	0.8	1.9	-1.0	5.7	-1.3	-4.9	2.3	-0.9
13/02/2003	95.93	1.3	1.5	1.4	-9.0	0.5	-5.6	5.9	-7.5
13/08/2003	98.00	1.5	1.7	0.4	6.4	-0.4	-6.7	0.8	0.7
18/02/2004	94.30	1.7	0.7	1.1	-7.6	-0.6	-7.4	4.9	-6.4
18/08/2004	95.69	1.7	0.3	-1.6	4.3	-0.1	-7.5	2.0	-0.3
23/02/2005	95.69	1.8	0.7	1.1	-6.3	0.5	-3.4	5.4	-5.7
17/08/2005	96.85	1.4	0.5	-3.0	5.3	-0.3	-5.0	1.2	0.3
15/02/2006	89.48	2.0	-0.3	2.0	-8.4	0.5	-8.8	6.5	-7.2
16/08/2006	89.48	1.8	0.4	-1.9	6.0	-0.3	-6.4	0.9	0.3
01/02/2007	95.60	3.5	1.4	2.5	-9.2	1.1	-6.9	7.1	-6.7
08/08/2007	94.48	1.7	1.2	-1.7	5.7	0.0	-5.9	0.9	0.4
05/02/2008	97.91	2.2	-1.4	1.1	-5.6	0.7	-6.2	5.9	-5.9
06/08/2008	94.48	1.3	0.9	-2.4	4.9	-4.9	-5.9	0.4	0.3

PRECISE ENGINEERING SURVEYS

DEFORMATION DISPLACEMENTS

WOLWEDANS DAM

Ref: 07/08/1992

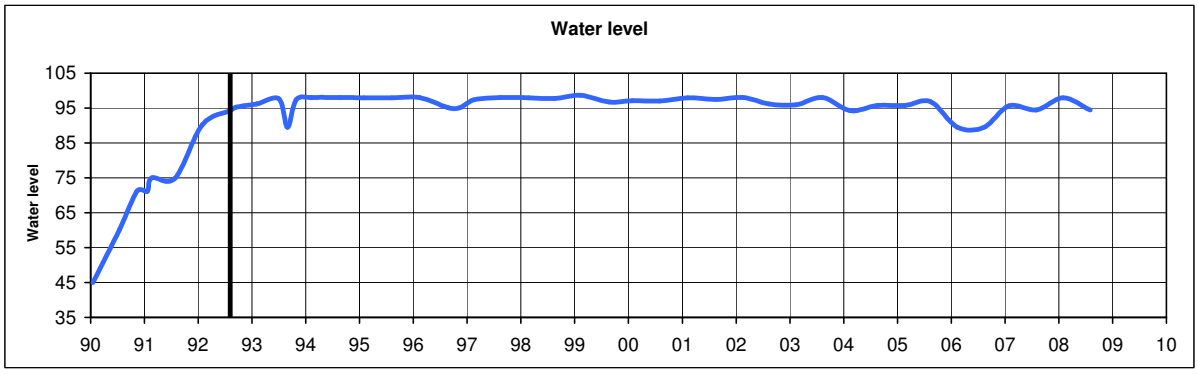

Lower Exit Gallery

Date	Water Level	311.1			311.2			311.3		
		dy	dx	dz	dy	dx	dz	dy	dx	dz
17/01/1990	45.03	#N/A	#N/A	#N/A	#N/A	#N/A	#N/A	#N/A	#N/A	#N/A
18/07/1990	60.30	#N/A	#N/A	#N/A	#N/A	#N/A	#N/A	#N/A	#N/A	#N/A
13/11/1990	71.28	#N/A	#N/A	#N/A	#N/A	#N/A	#N/A	#N/A	#N/A	#N/A
22/01/1991	71.15	#N/A	#N/A	#N/A	#N/A	#N/A	#N/A	#N/A	#N/A	#N/A
21/02/1991	74.97	#N/A	#N/A	#N/A	#N/A	#N/A	#N/A	#N/A	#N/A	#N/A
30/07/1991	74.87	#N/A	#N/A	#N/A	#N/A	#N/A	#N/A	#N/A	#N/A	#N/A
29/01/1992	90.27	#N/A	#N/A	#N/A	#N/A	#N/A	#N/A	#N/A	#N/A	#N/A
07/08/1992	94.30	0.0	0.0	0.0	0.0	0.0	0.0	0.0	0.0	0.0
17/09/1992	95.23	0.3	-0.2	0.4	0.2	0.0	0.6	0.3	0.2	0.2
03/02/1993	96.22	0.4	0.2	-0.8	0.5	0.4	-0.8	0.7	0.8	-0.5
03/07/1993	97.69	0.7	-0.6	-0.2	0.5	-0.3	-0.4	0.3	0.0	-0.5
31/08/1993	89.47	0.7	-0.3	0.2	0.7	-0.1	0.2	0.5	0.0	0.5
29/10/1993	97.39	0.3	-0.6	1.5	0.5	0.0	1.1	1.1	0.3	1.0
09/02/1994	98.07	-0.4	-0.3	0.2	0.1	0.2	0.2	1.1	0.8	0.5
24/08/1994	98.04	0.2	-0.9	-0.6	0.6	-0.3	-1.3	1.0	0.3	-1.1
01/02/1995	97.93	0.8	-1.6	-0.7	1.0	-1.0	-1.0	1.9	-0.1	-0.7
09/08/1995	97.90	0.8	-1.6	-0.7	1.0	-1.0	-1.0	1.9	-0.1	-0.7
13/02/1996	98.02	-0.8	-0.1	-1.8	-0.2	0.3	-1.8	0.8	1.3	-1.7
21/08/1996	95.22	-1.6	0.4	-0.8	-1.2	1.0	-1.1	-0.8	1.2	-1.2
12/11/1996	95.05	-1.1	0.1	-0.8	-0.7	0.7	-1.0	-0.1	1.2	-1.4
18/02/1997	97.43	-1.9	-1.0	-0.3	-1.6	-0.1	-0.5	-0.7	0.4	-0.4
19/08/1997	98.00	-2.6	-0.5	0.6	-2.2	0.1	0.6	-1.3	0.3	0.5
26/02/1998	97.92	#N/A	#N/A	0.1	#N/A	#N/A	3.3	#N/A	#N/A	1.5
19/08/1998	97.71	-1.2	0.0	0.9	-0.8	0.4	0.7	-0.4	0.5	0.9
10/02/1999	98.64	-0.1	-0.4	-1.0	0.5	0.1	-0.8	1.0	0.9	-0.7
25/08/1999	96.75	0.7	-1.0	1.0	0.8	-0.7	0.4	1.3	-0.1	1.0
02/02/2000	97.11	0.1	-0.6	-2.1	1.9	1.9	-2.5	1.4	0.5	-2.0
02/08/2000	96.99	-0.6	0.6	0.8	-0.2	0.8	0.1	0.4	1.5	0.4
08/02/2001	97.93	-0.3	-0.2	-0.4	0.6	0.0	-0.7	1.5	0.8	-0.1
15/08/2001	97.44	0.3	0.3	-0.1	0.7	0.3	-0.9	1.2	0.4	-0.5
20/02/2002	97.99	0.4	0.4	-2.1	1.0	0.6	-2.5	1.7	1.4	-2.0
15/08/2002	96.18	-0.3	0.1	0.3	0.0	0.1	-0.4	0.5	0.3	-0.1
13/02/2003	95.93	-0.5	0.2	-1.8	0.1	0.2	-2.1	0.6	0.9	-1.4
13/08/2003	98.00	0.1	0.4	-0.1	0.3	0.5	-1.2	0.7	0.8	-1.0
18/02/2004	94.30	-0.2	-2.2	-0.3	0.3	-2.2	-0.7	0.9	-1.2	-0.2
18/08/2004	95.69	-0.1	-1.9	-0.6	0.2	-1.8	-1.6	0.7	-1.0	-1.3
23/02/2005	95.69	0.1	-1.3	-1.0	0.9	-0.9	-1.5	1.7	0.1	-1.1
17/08/2005	96.85	0.1	-2.0	-1.3	0.4	-1.5	-2.3	1.0	-0.7	-2.3
15/02/2006	89.48	0.4	-2.6	-1.8	0.7	-2.4	-2.0	1.1	-1.4	-1.3
16/08/2006	89.48	1.1	-1.3	-0.4	1.3	-1.4	-1.4	1.7	-1.2	-1.3
01/02/2007	95.60	1.3	-2.6	-0.7	1.8	-2.3	-1.0	2.4	-1.2	-0.6
08/08/2007	94.48	0.6	-1.2	-0.4	1.0	-1.2	-1.3	1.6	-1.0	-1.0
05/02/2008	97.91	1.0	-2.0	-2.0	1.4	-1.8	-2.6	1.8	-1.0	-2.2
06/08/2008	94.48	0.3	-0.6	0.1	0.4	-0.6	-0.8	0.7	-0.2	-0.6

PRECISE ENGINEERING SURVEYS

DEFORMATION DISPLACEMENTS

WOLWEDANS DAM

Ref: 07/08/1992

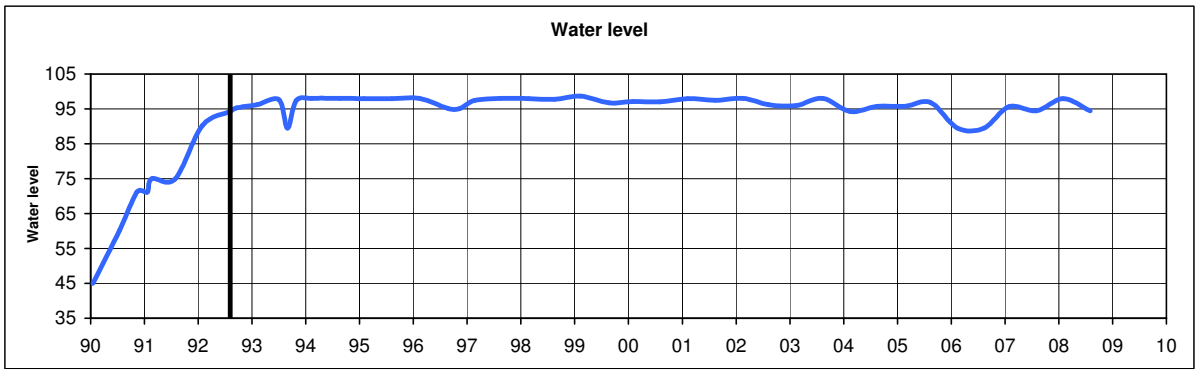

Points on slope left flank of Lower gallery

Date	Water Level	323			323.1		
		dy	dx	dz	dy	dx	dz
17/01/1990	45.03	#N/A	#N/A	#N/A	#N/A	#N/A	#N/A
18/07/1990	60.30	#N/A	#N/A	#N/A	#N/A	#N/A	#N/A
13/11/1990	71.28	#N/A	#N/A	#N/A	#N/A	#N/A	#N/A
22/01/1991	71.15	#N/A	#N/A	#N/A	#N/A	#N/A	#N/A
21/02/1991	74.97	#N/A	#N/A	#N/A	#N/A	#N/A	#N/A
30/07/1991	74.87	#N/A	#N/A	#N/A	#N/A	#N/A	#N/A
29/01/1992	90.27	#N/A	#N/A	#N/A	#N/A	#N/A	#N/A
07/08/1992	94.30	0.0	0.0	0.0	0.0	0.0	0.0
17/09/1992	95.23	-0.6	0.3	0.1	-0.5	0.3	-0.1
03/02/1993	96.22	0.7	-0.2	-0.3	1.1	0.0	-0.6
03/07/1993	97.69	0.4	0.2	-0.6	0.5	0.3	-1.0
31/08/1993	89.47	0.5	0.4	0.4	0.7	0.6	0.0
29/10/1993	97.39	0.1	-0.3	0.8	1.8	0.5	0.6
09/02/1994	98.07	0.2	0.1	-0.6	1.9	0.9	-0.8
24/08/1994	98.04	0.6	-0.4	-0.2	2.0	0.4	-0.2
01/02/1995	97.93	1.8	-0.7	-0.5	3.4	0.1	-0.2
09/08/1995	97.90	1.8	-0.7	-0.5	3.4	0.1	-0.2
13/02/1996	98.02	0.7	-0.6	-1.7	2.5	0.0	-1.4
21/08/1996	95.22	-0.4	0.1	-1.1	1.2	0.9	-1.0
12/11/1996	95.05	-0.2	0.0	-1.0	1.4	0.6	-0.8
18/02/1997	97.43	-1.5	-0.8	-1.2	0.4	-0.1	-1.0
19/08/1997	98.00	-1.6	-0.8	-0.2	0.0	-0.1	-0.1
26/02/1998	97.92	#N/A	#N/A	3.1	#N/A	#N/A	0.5
19/08/1998	97.71	-0.6	0.0	0.2	1.1	0.9	0.4
10/02/1999	98.64	1.3	0.0	-1.2	3.2	0.7	-1.1
25/08/1999	96.75	1.7	0.3	-0.4	3.4	1.3	-0.2
02/02/2000	97.11	1.2	-1.2	-2.2	3.2	-0.4	-2.2
02/08/2000	96.99	0.6	0.0	0.2	2.1	0.8	0.3
08/02/2001	97.93	1.3	-0.6	-1.5	3.1	0.1	-1.3
15/08/2001	97.44	0.5	0.1	-0.3	1.9	1.0	-0.7
20/02/2002	97.99	1.7	-0.1	-2.8	3.5	0.8	-2.6
15/08/2002	96.18	0.3	0.2	-0.7	1.8	1.0	-0.8
13/02/2003	95.93	1.5	-1.5	-2.6	3.2	-0.8	-2.4
13/08/2003	98.00	0.8	0.0	-0.6	2.3	0.9	-0.5
18/02/2004	94.30	1.2	-1.9	-0.8	2.8	-1.1	-0.9
18/08/2004	95.69	1.3	-1.5	-1.1	3.0	-0.4	-1.0
23/02/2005	95.69	1.6	-1.6	-1.6	3.4	-0.7	-1.5
17/08/2005	96.85	0.2	-1.5	-1.9	1.8	-0.4	-1.9
15/02/2006	89.48	2.1	-3.1	-2.7	4.2	-2.2	-2.1
16/08/2006	89.48	0.9	-0.8	-0.1	2.4	0.4	-0.3
01/02/2007	95.60	2.4	-1.9	-0.7	4.1	-0.9	-0.7
08/08/2007	94.48	1.2	0.0	-0.6	2.4	0.8	-0.8
05/02/2008	97.91	2.0	-1.4	-1.6	3.4	-0.4	-1.6
06/08/2008	94.48	0.6	-0.4	-0.6	2.1	0.4	-0.8

PRECISE ENGINEERING SURVEYS

DEFORMATION DISPLACEMENTS

WOLWEDANS DAM

Ref: 07/08/1992

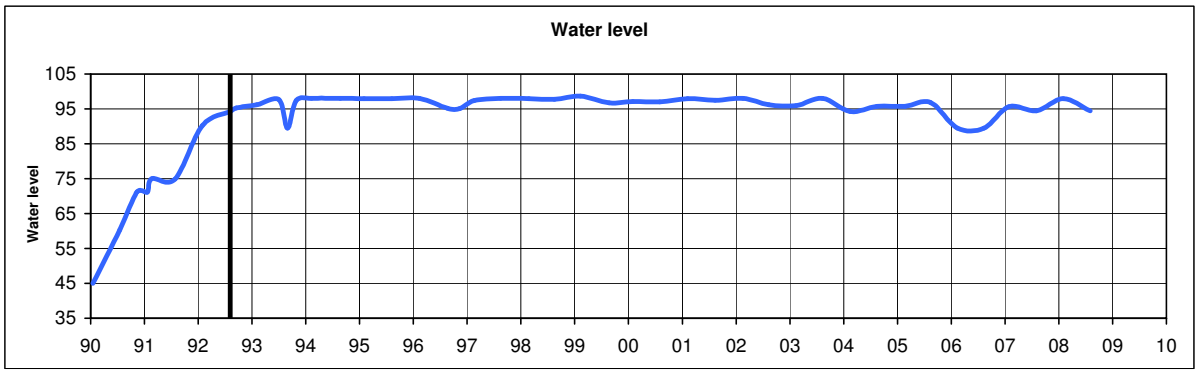

Eccentric points near traverse stations

Date	Water Level	E312			E317		E320			E323		
		dy	dx	dz	dy	dx	dy	dx	dz	dy	dx	dz
17/01/1990	45.03	#N/A	#N/A	#N/A	#N/A	#N/A	#N/A	#N/A	#N/A	#N/A	#N/A	#N/A
18/07/1990	60.30	#N/A	#N/A	#N/A	#N/A	#N/A	#N/A	#N/A	#N/A	#N/A	#N/A	#N/A
13/11/1990	71.28	#N/A	#N/A	#N/A	#N/A	#N/A	#N/A	#N/A	#N/A	#N/A	#N/A	#N/A
22/01/1991	71.15	#N/A	#N/A	#N/A	#N/A	#N/A	#N/A	#N/A	#N/A	#N/A	#N/A	#N/A
21/02/1991	74.97	#N/A	#N/A	#N/A	#N/A	#N/A	#N/A	#N/A	#N/A	#N/A	#N/A	#N/A
30/07/1991	74.87	#N/A	#N/A	#N/A	#N/A	#N/A	#N/A	#N/A	#N/A	#N/A	#N/A	#N/A
29/01/1992	90.27	#N/A	#N/A	#N/A	#N/A	#N/A	#N/A	#N/A	#N/A	#N/A	#N/A	#N/A
07/08/1992	94.30	0.0	0.0	0.0	0.0	0.0	0.0	0.0	0.0	0.0	0.0	0.0
17/09/1992	95.23	0.3	-0.1	0.6	0.3	0.3	-0.6	0.4	0.3	-0.8	0.3	0.1
03/02/1993	96.22	0.3	0.0	-0.6	0.1	-0.2	0.6	-0.3	-0.4	0.6	-0.2	-0.3
03/07/1993	97.69	0.8	-0.5	0.0	0.6	0.1	0.2	0.2	-0.6	0.3	0.2	-0.6
31/08/1993	89.47	0.5	-0.3	0.4	0.6	0.2	0.2	0.3	0.3	0.4	0.4	0.4
29/10/1993	97.39	0.4	-0.6	1.6	0.4	-0.6	0.0	-0.6	1.0	0.4	-0.2	0.5
09/02/1994	98.07	-0.7	-0.3	0.2	-0.6	0.0	-0.1	-0.2	-0.5	0.7	0.3	-1.3
24/08/1994	98.04	0.5	-0.8	-0.7	0.4	-0.7	0.3	-0.8	-0.2	1.0	-0.2	-0.9
01/02/1995	97.93	1.1	-1.7	-0.5	1.3	-1.2	1.4	-1.0	-0.7	2.2	-0.5	-1.2
09/08/1995	97.90	1.1	-1.7	-0.5	1.3	-1.2	1.4	-1.0	-0.7	2.2	-0.5	-1.2
13/02/1996	98.02	-0.4	-0.4	-1.8	0.0	-0.8	0.2	-0.9	-1.9	1.0	-0.5	-2.4
21/08/1996	95.22	-1.2	0.3	-0.9	-0.6	0.1	-0.6	-0.2	-1.1	0.0	0.3	-1.8
12/11/1996	95.05	-0.8	0.0	-0.8	-0.1	-0.5	-0.4	-0.3	-1.0	0.2	0.2	-1.6
18/02/1997	97.43	-1.3	-1.1	-0.6	-1.2	-1.3	-1.9	-1.0	-1.1	-1.0	-0.6	-1.9
19/08/1997	98.00	-2.2	-0.7	0.3	-1.7	-1.6	-2.1	-1.3	-0.1	-1.0	-0.5	-0.9
26/02/1998	97.92	#N/A	#N/A	#N/A	#N/A	#N/A	#N/A	#N/A	#N/A	#N/A	#N/A	#N/A
19/08/1998	97.71	-0.5	-0.2	0.8	-0.5	-1.0	-0.9	-0.4	0.3	-0.3	0.1	-0.5
10/02/1999	98.64	0.5	-0.6	-1.2	0.7	-0.7	0.8	-0.2	-1.2	1.7	0.2	-1.9
25/08/1999	96.75	1.4	-1.0	0.7	1.6	-0.3	1.6	-0.1	-0.5	2.1	0.5	-1.1
02/02/2000	97.11	0.8	-1.0	-2.3	0.8	-1.4	0.8	-1.4	-2.3	1.7	-0.9	-2.8
02/08/2000	96.99	0.2	0.4	0.2	0.4	-0.3	0.2	-0.4	0.1	1.0	0.2	-0.5
08/02/2001	97.93	0.1	-0.5	-0.9	0.8	-0.9	0.8	-0.9	-1.6	1.7	-0.4	-2.1
15/08/2001	97.44	1.0	0.1	-0.3	0.9	-0.4	0.3	-0.3	-0.4	0.9	0.3	-1.0
20/02/2002	97.99	1.0	0.1	-2.4	1.4	-0.7	1.4	-0.5	-2.9	2.1	0.1	-3.4
15/08/2002	96.18	0.2	-0.1	-0.1	0.6	-0.5	-0.1	-0.2	-0.7	0.7	0.4	-1.4
13/02/2003	95.93	0.2	-0.1	-2.2	0.3	-1.3	1.1	-1.7	-2.8	2.0	-1.3	-3.2
13/08/2003	98.00	0.8	0.2	-0.2	1.0	-0.7	0.6	-0.4	-0.5	1.3	0.2	-1.3
18/02/2004	94.30	0.5	-2.4	-0.6	0.8	-2.1	1.0	-2.1	-0.9	1.6	-1.7	-1.5
18/08/2004	95.69	0.7	-2.1	-1.1	1.2	-2.7	1.2	-1.9	-1.1	1.7	-1.3	-1.7
23/02/2005	95.69	0.6	-1.6	-1.3	1.2	-2.3	1.2	-1.9	-1.6	2.0	-1.4	-2.2
17/08/2005	96.85	0.7	-1.9	-1.6	1.3	-2.3	0.3	-1.8	-1.7	0.5	-1.3	-2.8
15/02/2006	89.48	0.9	-2.7	-2.3	1.6	-3.3	1.6	-3.3	-2.7	2.6	-2.8	-3.2
16/08/2006	89.48	1.6	-1.4	-0.6	1.3	-2.2	0.6	-1.3	0.0	1.3	-0.6	-0.8
01/02/2007	95.60	1.9	-2.7	-1.0	1.7	-3.4	1.8	-2.4	-0.8	2.8	-1.7	-1.4
08/08/2007	94.48	0.9	-1.2	-0.8	1.0	-1.6	0.8	-0.5	-0.6	1.6	0.2	-1.3
05/02/2008	97.91	1.5	-2.0	-2.1	1.5	-2.8	1.4	-1.8	-1.8	2.3	-1.2	-2.4
06/08/2008	94.48	1.0	-0.8	-0.7	0.4	-0.7	0.4	-0.6	-0.5	1.0	-0.2	-1.2

PRECISE ENGINEERING SURVEYS

DEFORMATION DISPLACEMENTS

WOLWEDANS DAM

Ref: 07/08/1992

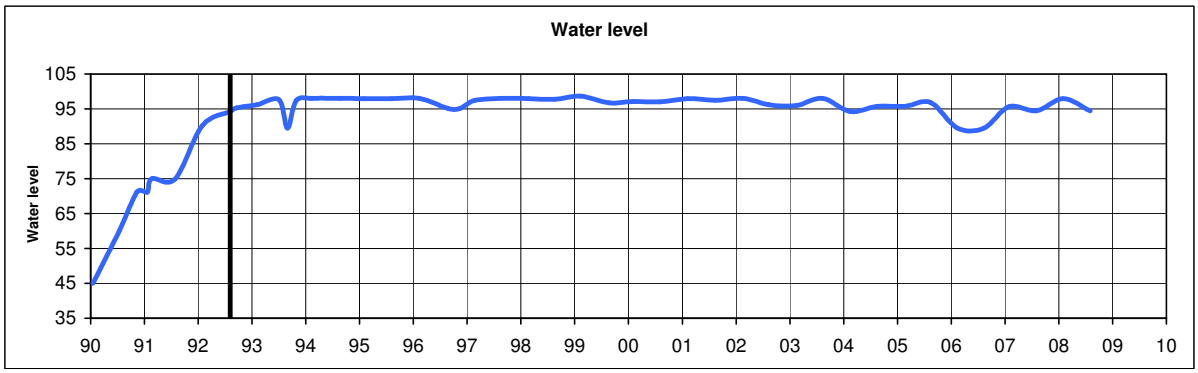

Optical Plummet points

Date	Water Level	E306		E300		
		dy	dx	dy	dx	dz
17/01/1990	45.03	#N/A	#N/A	#N/A	#N/A	#N/A
18/07/1990	60.30	#N/A	#N/A	#N/A	#N/A	#N/A
13/11/1990	71.28	#N/A	#N/A	#N/A	#N/A	#N/A
22/01/1991	71.15	#N/A	#N/A	#N/A	#N/A	#N/A
21/02/1991	74.97	#N/A	#N/A	#N/A	#N/A	#N/A
30/07/1991	74.87	#N/A	#N/A	#N/A	#N/A	#N/A
29/01/1992	90.27	#N/A	#N/A	#N/A	#N/A	#N/A
07/08/1992	94.30	0.0	0.0	0.0	0.0	0.0
17/09/1992	95.23	-0.1	-0.2	0.2	0.2	0.5
03/02/1993	96.22	0.3	0.7	0.7	1.0	-0.3
03/07/1993	97.69	0.3	-0.9	0.1	-0.1	-1.0
31/08/1993	89.47	0.2	-0.8	0.4	0.2	0.6
29/10/1993	97.39	4.1	0.5	-1.6	-3.3	0.7
09/02/1994	98.07	3.9	1.8	-2.0	-3.0	0.6
24/08/1994	98.04	3.3	-0.1	-1.4	-3.9	-1.2
01/02/1995	97.93	4.4	0.1	-0.8	-4.2	0.1
09/08/1995	97.90	4.4	0.1	-0.8	-4.2	0.1
13/02/1996	98.02	3.0	2.7	-1.8	-3.0	-1.1
21/08/1996	95.22	1.4	1.0	-3.0	-3.3	-1.5
12/11/1996	95.05	2.4	1.3	-2.9	-3.0	-1.4
18/02/1997	97.43	2.6	0.6	-3.8	-3.3	-0.7
19/08/1997	98.00	1.1	1.5	-4.1	-3.3	0.0
26/02/1998	97.92	#N/A	#N/A	#N/A	#N/A	#N/A
19/08/1998	97.71	2.7	1.3	-3.3	-3.2	0.3
10/02/1999	98.64	3.5	1.2	-1.9	-2.9	-0.6
25/08/1999	96.75	4.4	-0.3	-1.4	-3.7	0.2
02/02/2000	97.11	4.0	1.9	-1.7	-3.2	-2.3
02/08/2000	96.99	3.6	2.3	-2.5	-2.0	-0.2
08/02/2001	97.93	3.4	1.9	-1.6	-2.9	-0.6
15/08/2001	97.44	4.9	1.8	-1.9	-3.2	-1.3
20/02/2002	97.99	4.9	2.2	-1.5	-1.9	-2.7
15/08/2002	96.18	3.3	1.3	-2.4	-3.1	-1.0
13/02/2003	95.93	4.9	2.8	-2.3	-3.1	-1.4
13/08/2003	98.00	4.5	1.5	-2.1	-2.5	-1.1
18/02/2004	94.30	3.7	-0.8	-2.6	-3.7	-0.2
18/08/2004	95.69	3.3	-1.1	-2.4	-3.8	-1.3
23/02/2005	95.69	4.3	0.2	-1.8	-2.3	-1.2
17/08/2005	96.85	3.0	0.1	-2.2	-3.1	-2.4
15/02/2006	89.48	4.4	-1.2	-2.3	-3.7	-1.2
16/08/2006	89.48	5.5	-0.6	-1.6	-3.7	-1.5
01/02/2007	95.60	5.2	-1.2	-1.0	-0.6	-0.6
08/08/2007	94.48	5.0	-0.3	-1.8	-3.4	-1.2
05/02/2008	97.91	4.7	-0.6	-1.6	-3.2	-1.5
06/08/2008	94.48	5.2	0.2	-2.4	-2.7	-0.1

PRECISE ENGINEERING SURVEYS

DEFORMATION DISPLACEMENTS

WOLWEDANS DAM

Ref: 07/08/1992

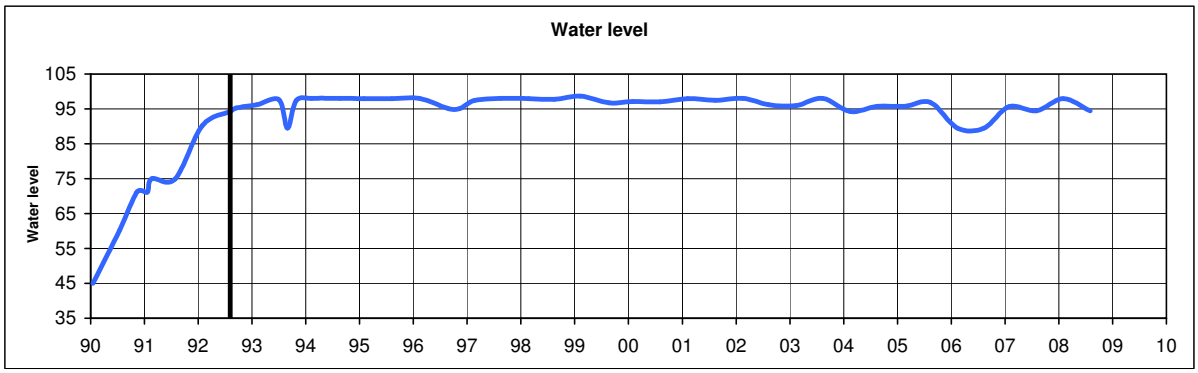

Altrimetric wire weight Lower gallery

Date	Water Level	AW300W
		dz
17/01/1990	45.03	#N/A
18/07/1990	60.30	#N/A
13/11/1990	71.28	#N/A
22/01/1991	71.15	#N/A
21/02/1991	74.97	#N/A
30/07/1991	74.87	#N/A
03/07/1993	97.69	-0.7
31/08/1993	89.47	0.3
29/10/1993	97.39	0.9
09/02/1994	98.07	0.6
24/08/1994	98.04	-1.4
01/02/1995	97.93	-0.6
09/08/1995	97.90	-0.6
13/02/1996	98.02	-1.8
21/08/1996	95.22	-1.8
12/11/1996	95.05	-2.1
18/02/1997	97.43	-0.6
19/08/1997	98.00	0.1
26/02/1998	97.92	-1.3
19/08/1998	97.71	0.3
10/02/1999	98.64	-0.7
25/08/1999	96.75	0.2
02/02/2000	97.11	-2.2
02/08/2000	96.99	-0.2
08/02/2001	97.93	-0.6
15/08/2001	97.44	-1.3
20/02/2002	97.99	-2.7
15/08/2002	96.18	-1.0
13/02/2003	95.93	#N/A
13/08/2003	98.00	#N/A
18/02/2004	94.30	#N/A
18/08/2004	95.69	-1.2
23/02/2005	95.69	-0.4
17/08/2005	96.85	25.9
15/02/2006	89.48	27.0
16/08/2006	89.48	-1.4
01/02/2007	95.60	-0.4
08/08/2007	94.48	-1.2
05/02/2008	97.91	-0.7
06/08/2008	94.48	0.8

APPENDIX C

INSTRUMENTATION LAYOUTS FOR WOLWEDANS DAM AND ÇINE DAM

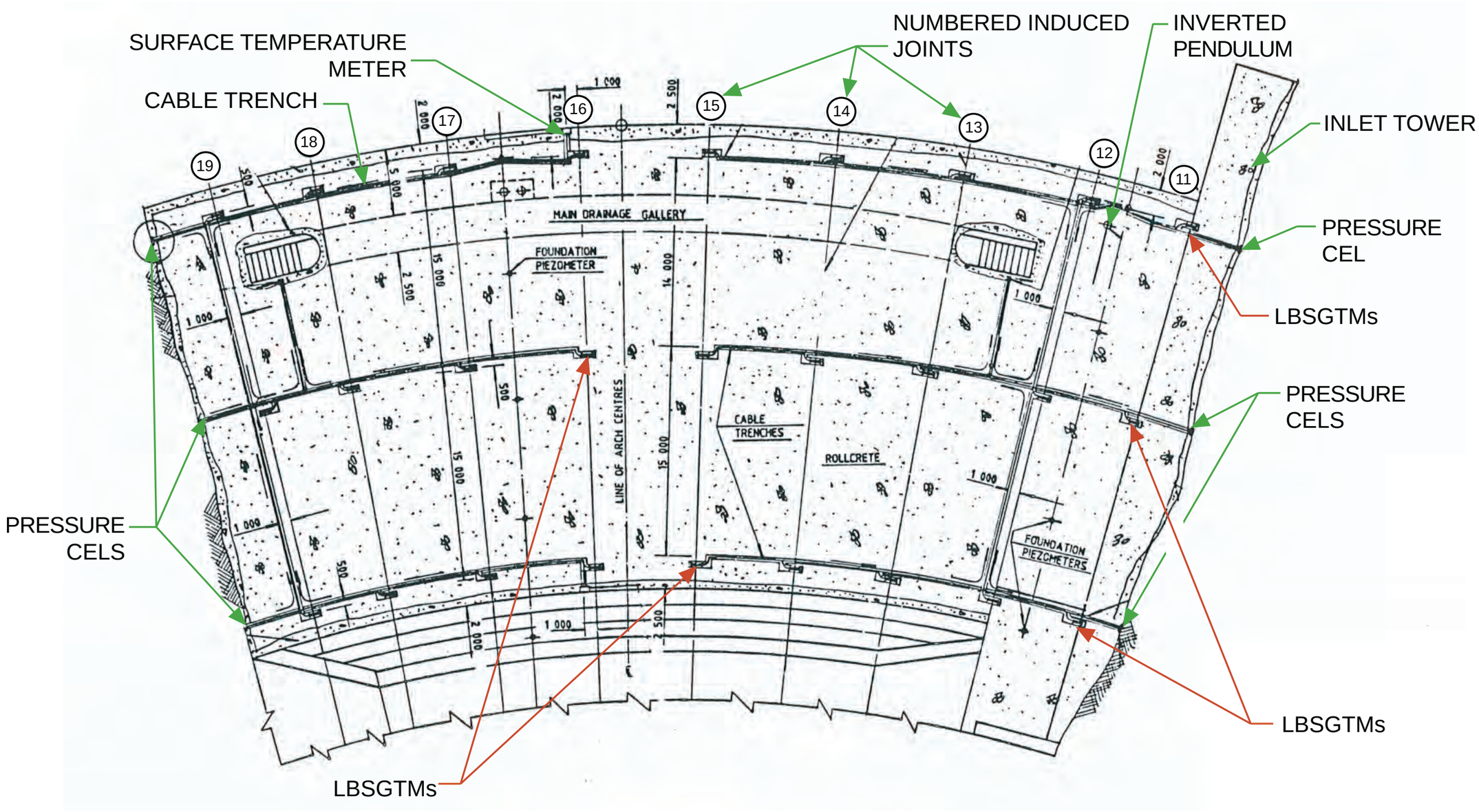

FIGURE C1:

Illustrative Arrangement of Wolwedans Instrumentation at RL 40.25 m – 1st Level[7]
(from 1987/88 Hand Drawn Plans)

FIGURE C1: WOLWEDANS DAM

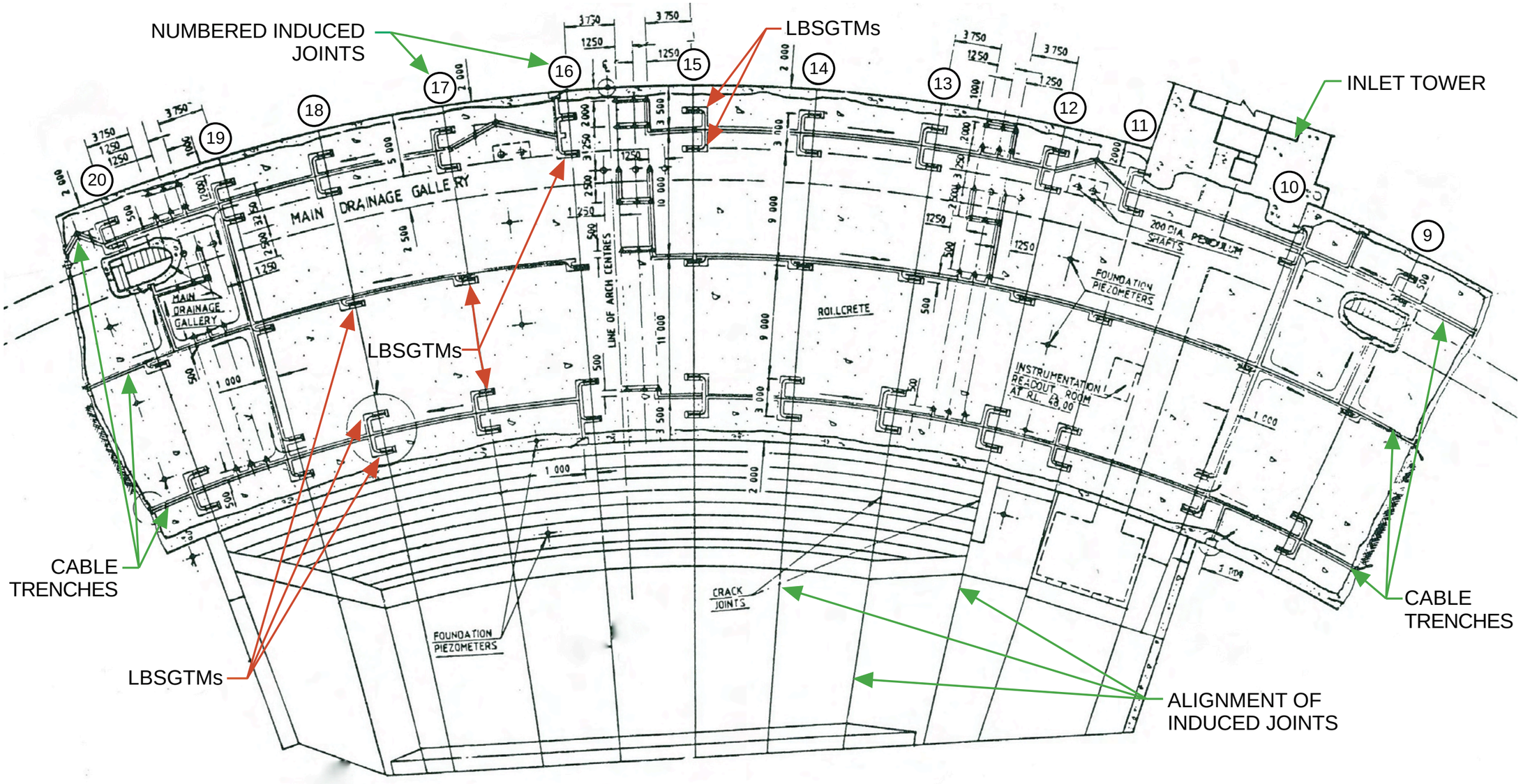

FIGURE C2:

Illustrative Arrangement of Wolwedans Instrumentation at RL 52.25 m – 2nd Level[7]
(from 1987/88 Hand Drawn Plans)

FIGURE C2: WOLWEDANS DAM

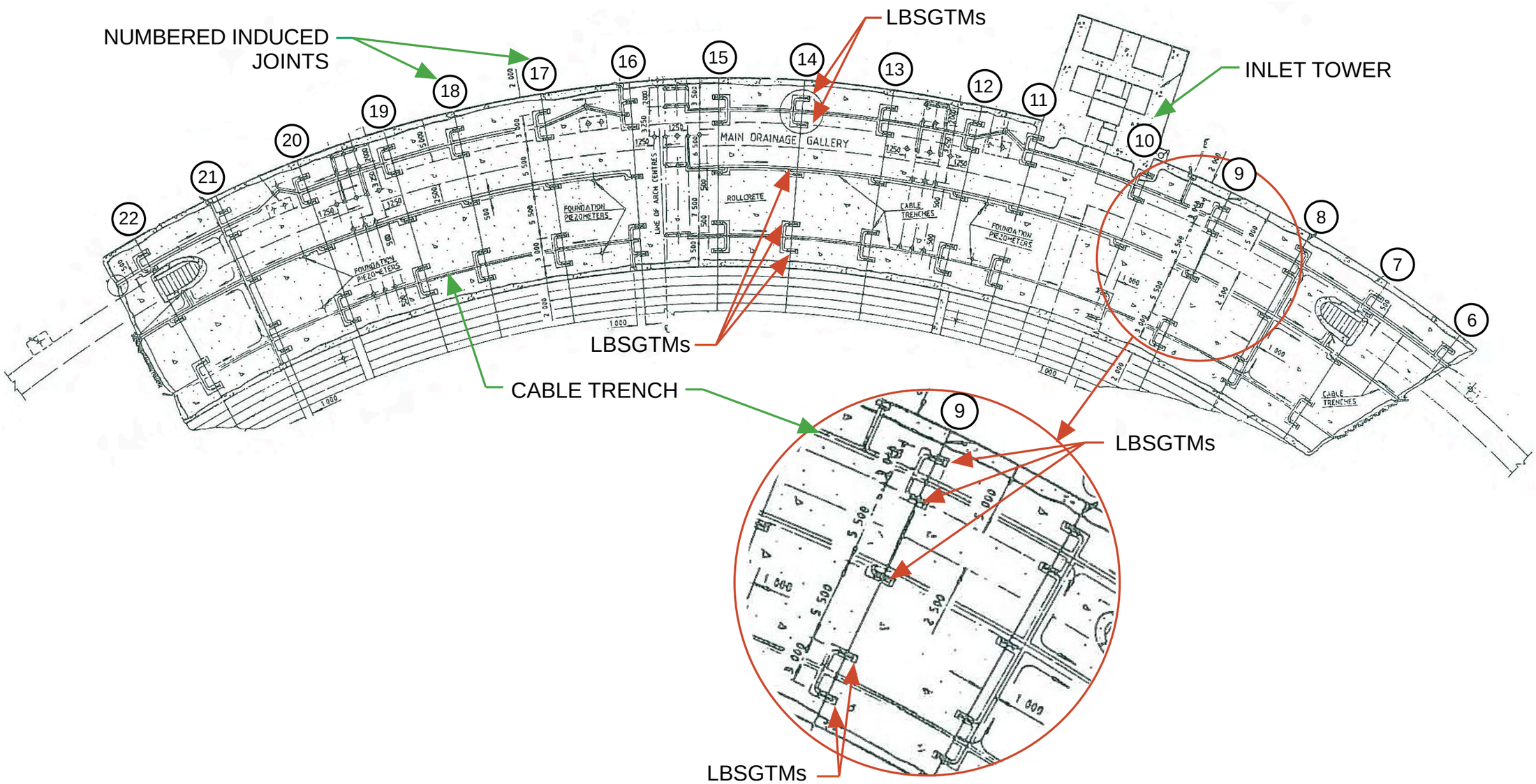

FIGURE C3:

Illustrative Arrangement of Wolwedans Instrumentation at RL 66.25 m – 3rd Level[7]
(from 1987/88 Hand Drawn Plans)

FIGURE C3: WOLWEDANS DAM

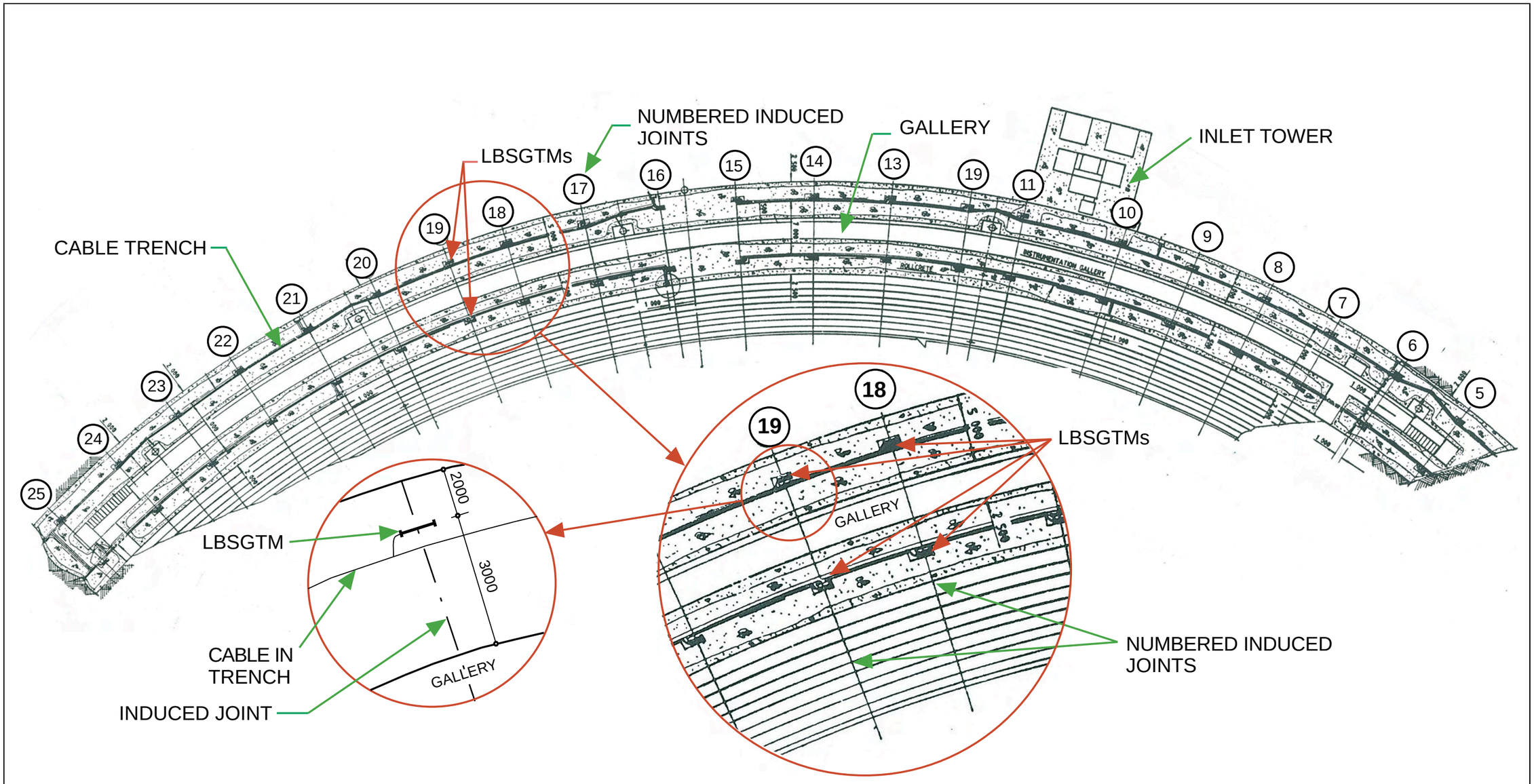

FIGURE C4:

Illustrative Arrangement of Wolwedans Instrumentation at RL 84.25 m – 4th Level[7]

(from 1987/88 Hand Drawn Plans)

FIGURE C4: WOLWEDANS DAM

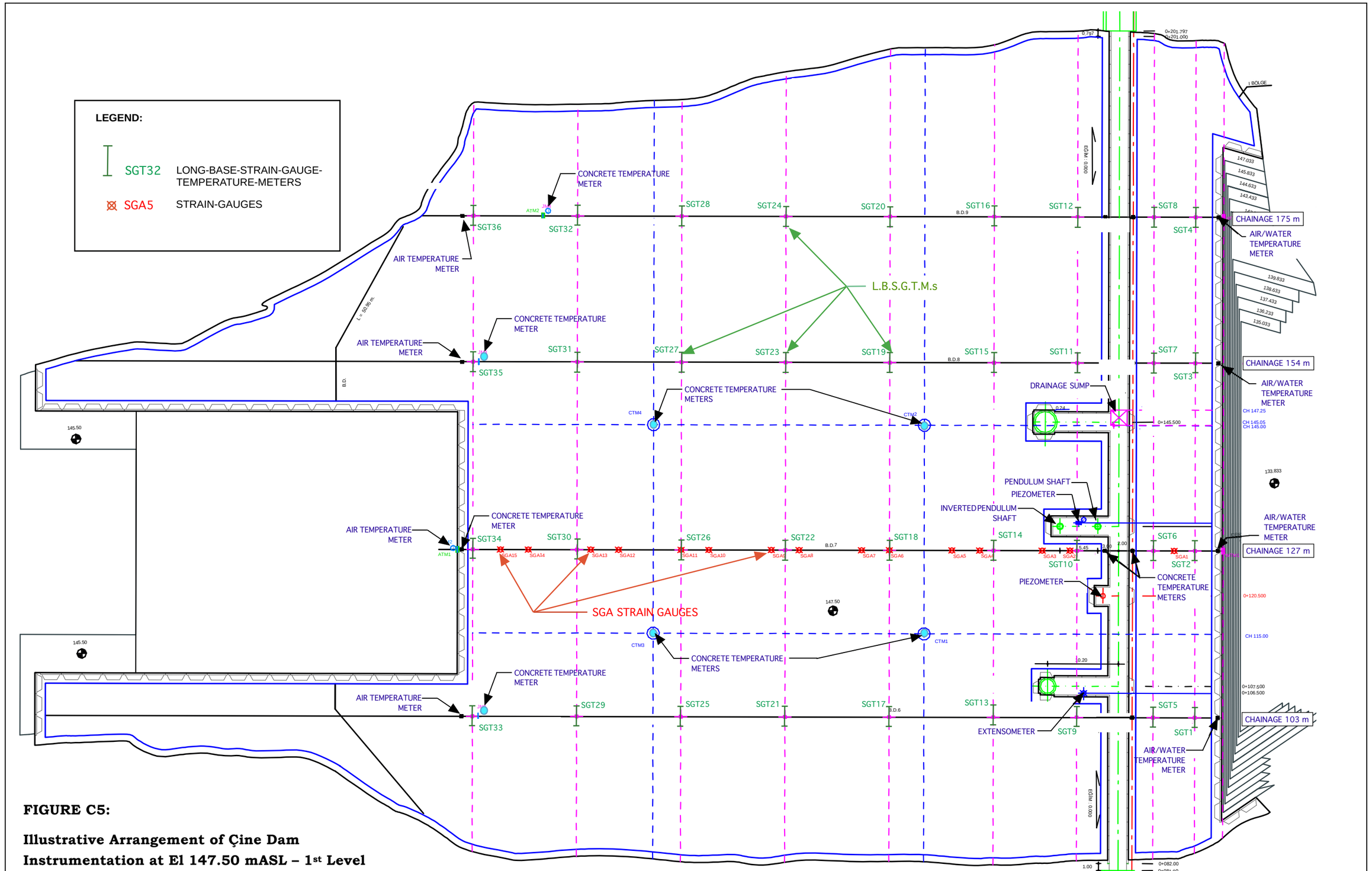

FIGURE C5:

Illustrative Arrangement of Çine Dam Instrumentation at El 147.50 mASL – 1st Level

FIGURE C5: ÇINE DAM

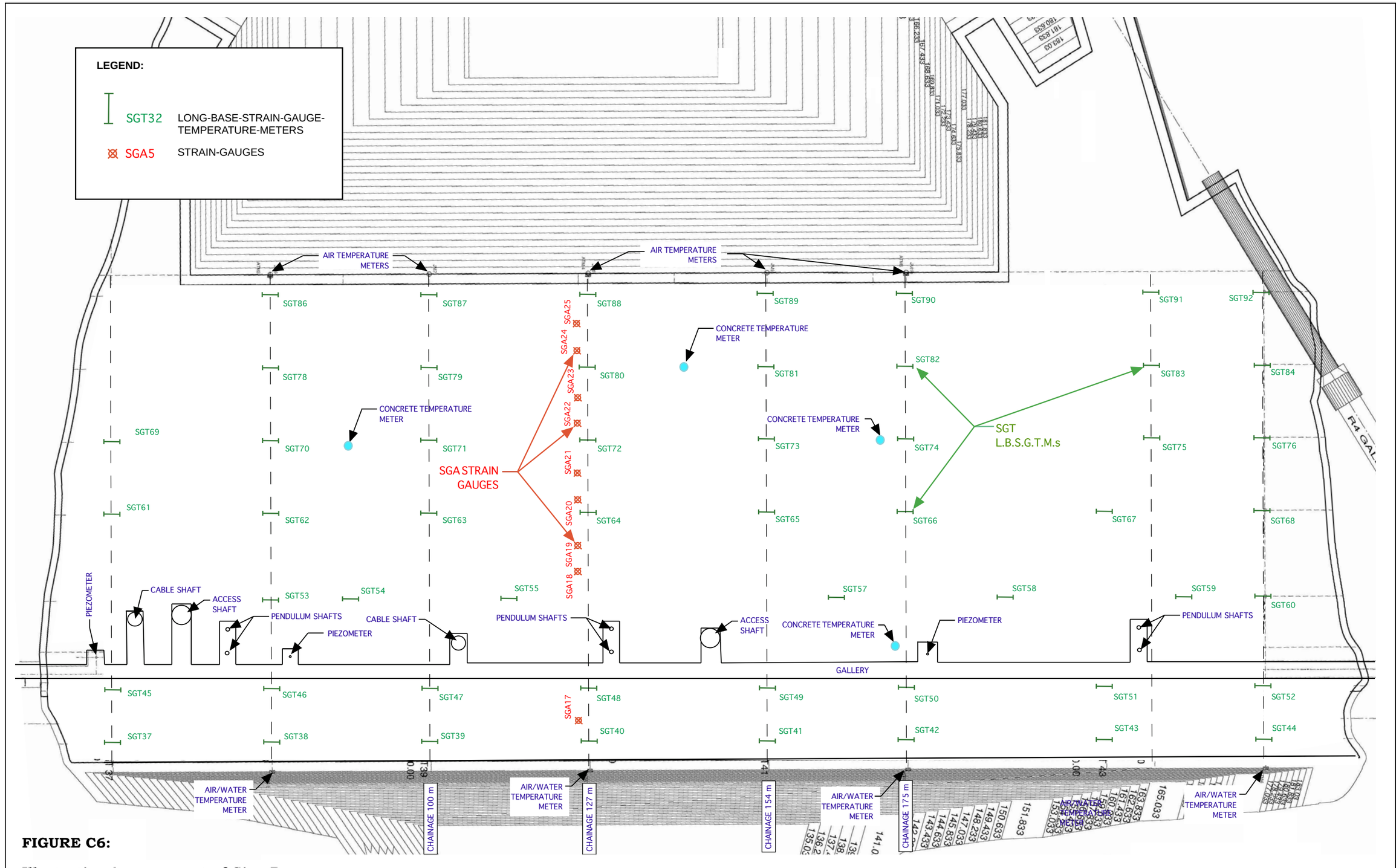

FIGURE C6:

Illustrative Arrangement of Çine Dam Instrumentation at El 185.25 mASL – 2nd Level

FIGURE C6: ÇINE DAM

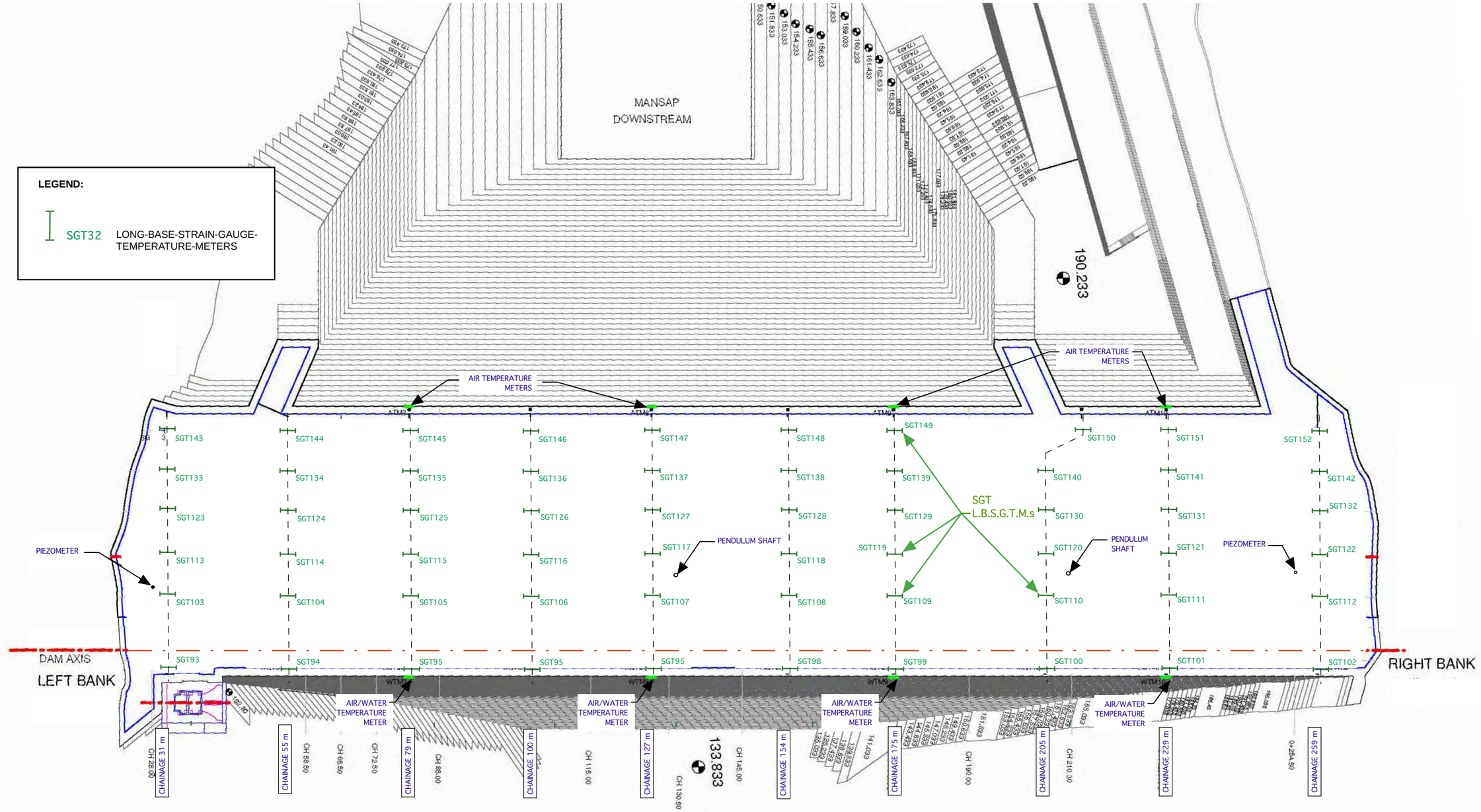

FIGURE C7:

Illustrative Arrangement of Çine Dam Instrumentation at El 208.50 mASL – 3rd Level

FIGURE C7: ÇINE DAM